THE UNIVERSITY
of EDINBURGH

Investigating putative pathogenic mechanisms within a family in which a chromosomal translocation confers risk of major mental illness

Gareth James Briggs

PhD

The University of Edinburgh

2016

Declaration

I declare that, except for where noted, all work contained in this thesis was performed and composed by myself. Where others have contributed to elements of the work, this is clearly stated in the text. No element of this work has been submitted for any other degree or professional qualification.

Gareth J. Briggs

Acknowledgments

The story of this PhD is very long and convoluted, as such I've encountered many people to whom I am hugely grateful for their contributions large and small, which have often produced ripple effects in both the production of the research and the thesis itself.

I'd like to thank Kirsty Millar for her keen critical eye in supervision and the assessing of the thesis as well for her deep knowledgebase of all things DISC. Thanks to Prof. David Porteous who has been inspirational in his professionalism to devoting time to reading chapters as well as supervising the microarray project. Thanks to Prof. Cathy Abbott whose warm encouragement has spurred me to the finish line.

I'd like to thank my bench mate Elise who has been a model of calmness in the face of adversity and became a good friend. It was pleasure to be able to switch from talking about science to talking about food, it was even better when she cooked for me. Thanks to Shaun Mackie who both taught me molecular biology and took me to the pub many, many times and has been on call weekly to aid with thesis queries, of which there has been a multitude. Thanks Fumiaki Ogawa has been a patient and diligent teacher on all things immunocytochemical. Thanks to those who have provided technical troubleshooting and specific training. Paul Perry and Mathew Pearson did a good job teaching me the basics of microscopy. Rob van't Hoff helped greatly in the initial implementation of the luciferase work and found my pidgin Dutch very funny.

I have been very fortunate to maintain contact with Prof. Gordon McEwan at the University of Aberdeen whose unique blend of pragmatic optimism has been a source of inspiration in times of difficulty during the PhD. Additionally I'd like to thank Lucy Foley for her penetrating rationalism and warmth. Together these people gave me faith that times would improve and they did.

My flatties Rosie and Emma have provided many happy memories and eclectic adventures during my stay in Edinburgh. A lot of successful and dark tales of the lab were told over long dinners over beers, in a flat with so much character it was eventually condemned. In particular Rosie has been phenomenally supportive during the production of the thesis, her views on academic writing do's and don'ts and ready availability to help, stretched me.

Thanks to Charlotte MacDonald for being a very accommodating friend, having me stay at short notice during trips to Edinburgh. Her tireless battling to get me reinstated as a student in part enabled this thesis to be produced.

Thanks to Alexander Taxter and Kelly Anderson for technical support and providing a homely retreat for board game days in Aberdeen. Thanks to Gillian Winestone for showing me how to celebrate like a wayward undergrad again during the interim period between the viva and corrections.

Finally, I'd like to extend heartfelt thanks to Eva Steenbergen and my parents, who at distinct phases of the PhD have kept daily life going in the background and have often had to listen to me speak on often incomprehensibly minutiae of the thesis. Thanks for still listening to me even now.

Abstract

In a large Scottish family a high incidence of schizophrenia, bipolar disorder and major depressive disorder co-segregates with a balanced autosomal translocation (t(1;11)(q42.1;q14.3). The translocation disrupts Disrupted-in-Schizophrenia-1 (*DISC1*) and *DISC2* on chromosome 1, and *DISC1FP1* (Disrupted-in-Schizophrenia-Fusion-Partner-1), also known as *Boymaw*, on chromosome 11. *DISC1* is a leading candidate gene for major mental illness and is involved in neurodevelopment and cellular signalling, whilst *DISC2* and *DISC1FP1* are apparently non-coding RNA genes that undergo alternative splicing and that are expressed in the brain. This thesis aimed to investigate putative mechanisms of pathogenesis that may result from the t(1;11), with the hope that pathogenic mechanisms identified in the t(1;11) pedigree might shed light upon mechanisms conferring risk for psychiatric illness in the wider population.

Previous work had identified *DISC1/DISC1FP1* chimeric transcripts in t(1;11)-family derived lymphoblastoid cell lines. The detected transcripts include *CP60* and *CP69* which encode DISC1 aa1-597 plus an additional 60 or 69 amino acids from DISC1FP1, respectively. In this thesis a novel *DISC1/DISC1FP1* transcript, *CP1*, was identified in t(1;11) lymphoblastoid cell lines. The *CP1* transcript encodes DISC1 aa1-597 plus one glycine. A truncated form of DISC1 comprising aa1-597 was previously suggested to be a putative product of the translocation and, as such, has been the focus of multiple studies. The identification of the *CP1* species is of interest as it differs from DISC1 aa1-597, by only a glycine. As glycines are simple uncharged aa's, it is likely that these two DISC species share similar properties.

In vitro exogenous expression of the three DISC1/DISC1FP1 protein species in both COS-7 and primary neuron cultures revealed contrasting cellular phenotypes. CP1 showed a diffuse cellular localisation pattern with cells containing readily visible tubular mitochondria. This is indistinguishable from the staining pattern of DISC1 aa1-597, highlighting the high degree of similarity between these species. CP60 and CP69, however, appeared to be clustered in the perinuclear region of the cell. Initial staining attempts with MitoTracker Red to visualise mitochondria in CP60 and CP69 expressing cells resulted in fewer than 30% of cells being stained. In those that did stain, the mitochondria appeared clustered. The absence of MitoTracker Red staining in mitochondria may be due to the loss of the mitochondrial membrane potential, $\Delta\psi m$. The adoption of a co-staining protocol with antibodies for mitochondrial proteins enabled the visualisation of mitochondrial structure in all of the cells

exogenously expressing CP60 and CP69. All of these mitochondria possessed a clustered morphology, with which CP60 and CP69 expression was substantially co-localised.

To see if MitoTracker staining was perturbed, in t(1;11) lymphoblastoid cell lines, as may occur if the DISC1/DISC1FP1 chimeras are expressed endogenously, the fluorescence of MitoTracker Red staining was investigated by FACS. Pooled analysis of experimental replicates revealed a negative result, with MitoTracker Red staining in t(1;11) lymphoblastoid cell lines not differing from controls. These findings indicate a need for further research using the mitochondrial membrane potential, $\Delta\psi m$ as a metric as this would enable variations in mitochondrial mass to be accounted for.

Prior to my arrival, an expression microarray had been carried out on lymphoblastoid cell line cDNA to assess gene expression differences resulting from the t(1;11). In order to identify putative pathogenic mechanisms, I carried out functional enrichment analysis of the expression array data using multiple analysis programs. Several programs detected dysregulation of the cell cycle and enrichment of altered expression of genes involved in the immune response and inflammation in t(1;11) carriers.

The use of a rare variant investigative paradigm in this thesis furthers understanding of the putative pathogenic mechanisms that might act to increase risk for psychiatric illness in t(1;11) carriers. Moreover, it may aid the biological understanding of the aetiology of psychiatric illness in the general population. As such, improved understanding of the mechanisms of risk in the t(1;11) pedigree may eventually lead to the development of better treatments.

In the intervening time since some of the research for thesis was published, two studies have emerged that may serve to highlight potential mechanisms of pathogenic action mediated by CP60 and CP69 expression. It has recently been observed that WT-DISC1 couples to the adaptor protein TRAK1 and the mitochondrial membrane anchor Miro1, which are part of the mitochondrial transport complex (Ogawa *et al*, 2014; Norkett *et al*, 2016). Furthermore, the exogenous expression of CP60 impairs bidirectional mitochondrial trafficking (Norkett *et al*, 2016). This suggests that CP60 expression may impair interactions with TRAK1 and Miro1. Given the sequence homology between CP60 and CP69, mitochondrial transport deficits also likely arise with CP69 expression. It is therefore possible that the exogenously expressed CP60 and CP69 proteins could be docked on stationary mitochondria, which may contribute to the clustered expression patterns observed.

Lay Summary

In a large Scottish family, high levels of severe mental illness occur along with a rare genetic mutation. This thesis will look at the ways in which the rare mutation may affect the Scottish family. Such research may shed light into how mental illness may occur within the wider population of sufferers.

Previous work has shown that the genetic mutation occurring in the Scottish family is due to changes in chromosome structure. This affects chromosomes 1 and 11. These chromosomes snap and then re-join with the opposite chromosome. Three genes, which are found in the brain, are rearranged due to the mutation. Two of these genes are on chromosome 1 and one is on chromosome 11.

Due to the chromosome structure changes, mutant RNAs have been found in cell lines from the Scottish family. These RNAs contain the genetic code from both a chromosome 1 gene and the chromosome 11 gene. Therefore, any mutant proteins produced would have a mixed genetic background. Two of these mutant RNAs were found previously, a third was detected in Scottish family cell lines in this thesis. The mutant proteins these RNAs code for may be a mechanism of disease in the Scottish family.

To look at possible disease mechanisms, the genetic code for the three mutant RNAs was put into cells to produce proteins. Two of the mutant proteins blocked staining with a dye targeted to the cells power supply centres – the mitochondria. The few mitochondria that stained had an unusual clustered shape, rather than a healthy tube-like shape. Dyeing the surface of the mitochondria lead to the 'invisible' mitochondria being seen. These mitochondria also had a clustered shape. The protein from the newly identified mutant RNA had no effect on mitochondrial shape or staining.

The pattern of staining from the mutant proteins was also looked at. Proteins from the two previously identified mutant RNAs appeared clustered. Protein from the newly identified mutant RNA was spread throughout the cell. The staining patterns of the mutant proteins could be possible disease mechanisms.

Cell lines from the Scottish family were stained with the mitochondrial dye that had shown reduced mitochondrial staining in mutant protein containing cells. This was an indirect means to see if these mutant proteins occurred naturally in Scottish family cell lines. However, no difference was seen in mitochondrial staining. It may be that a more sensitive test is needed.

The genetic mutation in the Scottish family may also effect the switching on and off of genes. This could be due to the rearrangement of the three genes by the mutation or by the three mutant proteins if they naturally occur. RNA levels were measured in cell lines from Scottish family members to calculate gene switching. Computer analysis found alterations to gene activity in the cell cycle, immune function and inflammation. These also represent possible disease mechanisms in the Scottish family.

The understanding of how rare mutations lead to mental illness may lead to the development of better treatment. This may in turn help the other sufferers of mental illness.

Table of contents

List of figures

List of tables

Abbreviations

Genes and proteins

ADAM10	A Disintigrin and Maetalloprotease 10
ADORA2A	Adenosine A2a Receptor
Akt1	V-AKT1 Murine Thymoma Viral Oncogene Homolog 1
APC/C	Anaphase-promoting complex/cyclosome
APOL1	Apolipoprotein L, 1
ATF4	Activating Transcription Factor 4
ATM	Ataxia-telangiectasia Mutated
ATR	ATM-and Rad3-Related
BBS4	Bardet-Biedl Syndrome 4
CACNA1C	Calcium Channel, Voltage-dependent, L Type, Alpha 1C Subunit
CAMDI	Coiled-coil Protein Associated with Myosin II and DISC1
CaMKII	$Ca^{2+/}$Calmodulin-Dependent Protein Kinase II
CCND1	Cyclin D1
CCND2	Cyclin D2
CD14	CD14 Molecule
CD40	Cluster of Differentiation 40
CD40L	Cluster of Differentiation 40 ligand
CDC25A	Cell division cycle 25A
CDC25B	Cell division cycle 25B
CDK5	Cyclin-dependent Kinase 5
CHCM1/CHCHD6	Coiled-coil Helix Cristae Morphology 1/CHCHD6
CHI3L1	Chitinase 3-like 1 (Cartilage Clycoprotein-39)
Chk1	Checkpoint kinase 1
Chk2	Checkpoint kinase 2
CP1	Chimeric Protein 1
CP60	Chimeric Protein 60
CP69	Chimeric Protein 69
CREB	cAMP Response Element-Binding Protein
CVα	Mitochondrial Complex V-alpha Subunit
DISC1	Disrupted-In-Schizophrenia 1

DISC1FP1	Disrupted-In-Schizophrenia 1 Fusion Partner 1 also known as Boymaw
DISC2	Disrupted-In-Schizophrenia 2
DIXDC1	DIX Domain Containing-1
Drp1	Dynamin-1-like Protein
E2F1	E2F Transcription Factor 1
E2F4	E2F Transcription Factor 4
EF-1 alpha	Elongation Factor-1 Alpha
Emi1	Early Mitotic Inhibitor 1
ERBB3	Erb-B2 Receptor Tyrosine Kinase 3
FAN1	FANCD2/FANCI-Associated Nuclease
Fis1	Fission 1
FOXM1	Forkhead Box M1
GBP1	Guanylate Binding Protein 1, Interferon-inducible
GFAP	Glial Fibrillary Acidic Protein
GPAD1	Ganglioside-induced Differentiation-associated Protein 1
Grb2	Growth Receptor Bound Protein 2
GSK3β	Glycogen Synthase Kinase 3 Beta
GST	Glutathione S-transferase (tag)
HA	Influenza Hemagglutinin (tag)
His	Polyhistidine (tag)
hsCRP	Highly Sensitive C-reactive Protein
IFITM1	Interferon Induced Transmembrane Protein 1
IFITM2	Interferon Induced Transmembrane Protein 2
IFITM3	Interferon Induced Transmembrane Protein 3
IFNγ	Interferon Gamma
IGFBP4	Insulin-like Growth Factor Binding Protein 4
IL	Interleukin
IL-12RB2	Interleukin Receptor Beta 2
IL-13RA1	Interleukin 13 Receptor Alpha 1
IL-1RA	Interleukin 1 Receptor Antagonist
IL-21R	Interleukin 21 Receptor
IL-23A	Interleukin Receptor 23 Alpha Subunit p19
IL-27RA	Interleukin Receptor 27 Alpha
IL-4R	Interleukin 4 Receptor

Kal7	Kalirin-7
KIF5A	Kinesin Family Member 5A
LEF	Lymphoid enhancer factor
LIS1	Lissencephaly 1
MBP	Maltose-binding protein (tag)
Mfn1	Mitofusin 1
Mfn2	Mitofusin 2
Miro1	Mitochondrial Rho GTPase 1
mTOR	Mechanistic Target of Rapamycin
NDE1	NudE Neurodevelopment Protein 1
NDEL1	NudE Neurodevelopment Protein 1-Like 1
NFKBIA	Nuclear Factor of Kappa Light Polypeptide Gene Enhancer in B-cells Inhibitor, Alpha
NFKBIE	Nuclear Factor of Kappa Light Polypeptide Gene Enhancer in B-cells Inhibitor, Epsilon
NRG1	Neuregulin 1
OMA1	OPA1 Zinc Metallopeptidase
OPA1	Optic Atrophy 1
p27Kip1	Cyclin-dependent kinase inhibitor 1B
p49/p100	Nuclear Factor of Kappa Light Polypeptide Gene Enhancer in B-cells 2
p57Kip2	Cyclin-dependent kinase inhibitor 1C
PCM1	Pericentriolar Material 1
PDE4	Phosphodiesterase 4
PINK	PTEN-induced kinase 1
PKA	Protein kinase A
PLK1	Polo-like kinase 1
PSD-95	Postsynaptic Density Protein 95
Rac1	Rho GTPase Ras-related C3 Botulinum Toxin Substrate 1
SERPINA3	Serpin Peptidase Inhibitor, Clade A (Alpha-1 Antiproteinase, Antitrypsin), Member 3
sICAM-1	Soluble Intercellular Adhesion Molecule-1
sIL-2R	Soluble Interleukin -2 Receptor
sIL-6R	Soluble Interleukin -6 Receptor
sTNFR1	Soluble Tumour Necrosis Factor Receptor-1

TAZ	Tafazzin
TCF	T-cell factor
TFDP1	E2F Dimerization Partner 1
TFDP2	E2F Dimerization Partner 2
TGF-β	Transforming Growth Factor Beta
TNFRSF1B	Tumour Necrosis Factor Receptor Superfamily Member 1B
TNFRSF8	Tumour Necrosis Factor Receptor Superfamily Member 8
TNFRSF9	Tumour Necrosis Factor Receptor Superfamily Member 9
TNF-α	Tumour Necrosis Factor Alpha
TNIK	TRAF2 and NCK Interacting Kinase
TRAK1	Trafficking Protein, Kinesin Binding 1
TRX	Thioredoxin (tag)
TSNAX	Translin Associated Factor X
ΔN597	DISC1 aa326-597
ΔNCP69	N-terminal deleted CP69 (DISC1 aa326-597 and 69 aa from DISC1FP1)

Units

°C	Degree centigrade
b	Base (nucleic acid)
AU	Arbitrary units
Da	Dalton
g	Gram
l	Litre
m	Metre
M	Molar (mols per litre)
mol	Mols
rpm	Revolutions per minute
V	Volt
n	Nano ($x10^{-9}$)
μ	Micro ($x10^{-6}$)
m	Milli ($x10^{-3}$)
k	Kilo ($x10^{3}$)
M	Mega ($x10^{6}$)

Amino acids

A	Alanine
C	Cysteine
D	Aspartic acid
E	Glutamic acid
F	Phenylalanine
G	Glycine
H	Histidine
I	Isoleucine
K	Lysine
L	Leucine
M	Methionine
N	Asparagine
P	Proline
Q	Glutamine
R	Arginine
S	Serine
T	Threonine
V	Valine
W	Tryptophan
Y	Tyrosine

Nucleotides

A	Adenine
C	Cytosine
G	Guanine
T	Thymidine

Anatomical regions

ACG	Anterior cingulate gyrus
CA	*cornu ammonis*
CNS	Central nervous system

DLPFC	Dorsolateral prefrontal cortex
FC	Frontal cortex
PFC	Prefrontal cortex
PSD	Post-synaptic density

Chemical compounds and biomolecules

ADP	Adenosine diphosphate
AMPA	α-amino-3-hydroxy-5-methyl-4-isoxazolepropionic acid
APP	Amyloid precursor protein
ATP	Adenosine triphosphate
cAMP	Cyclic adenosine monophosphate
CCCP	Carbonyl cyanide m-chlorophenylhydrazone
cDNA	Complementary DNA
CO2	Carbon dioxide
D2	Dopamine receptor D2
DA	Dopamine
DABCO	1,4-diazabicyclo[2.2.2]octane
DAPI	4',6-diamidino-2-phenylindole
DAT	Dopamine transporter
dH2O	Deionised water
DMSO	Dimethyl sulfoxide
DNA	Deoxyribonucleic acid
dNTP	Deoxyribonucleotide triphosphate
DOPA	3,4-dihydroxyphenylalanine
EDTA	Ethylenediaminetetraacetic acid
ENU	*N*-ethyl-*N*-nitrosourea
FCCP	Carbonyl cyanide-4-(trifluoromethoxy)phenylhydrazone
FITC	Fluorescein isothiocyanate
GABA	γ-Aminobutyric acid
$GABA_A$ receptor	γ-Aminobutyric acid A receptor
GDP	Guanosine diphosphate
GluN2A	Glutamate receptor, ionotropic, N-Methyl D-Aspartate 2A
GluR1	Glutamate receptor, ionotropic, AMPA 1
GTP	Guanosine-5'-triphosphate

mRNA	Messenger RNA
MTT	3-(4,5-Dimethylthiazol-2-yl)-2,5-diphenyltetrazolium
NAD dehydrogenase	Nicotinamide adenine dinucleotide dehydrogenase
NF-κB	Nuclear factor kappa-light-chain-enhancer of activated B cells
NKCC1	Na-K-Cl cotransporter
NMDA	N-methyl-D-aspartate
NMDAR	N-methyl-D-aspartate receptor
PBS	Phosphate buffered saline
PCP	Phencyclidine
PDVF	Polyvinylidene difluoride
PE	Phycoerythrin
PML	Promyelocytic leukemia bodies
Poly I:C	Polyinosinic:polycytidylic acid
RNA	Ribonucleic acid
rRNA	Ribosomal ribonucleic acid
SAP	Shrimp alkaline phosphatase
SDS	Sodium dodecyl sulphate

Other abbreviations

31p-MRS	31P-magnetic resonance spectroscopy
3-D	Three dimensional
ANOVA	Analysis of variance
BAC	Bacterial artificial chromosome
bp	basepairs
BLAST	Basic Local Alignment Search Tool
BSA	Bovine serum albumin
CD-CV	Common disease-common variant
CD-RV	Common disease-rare variant
CNV	Copy number variation
DDR	DNA damage response signalling network
der	Derived
DIV	Days in vitro
DMEM	Dulbecco Modified Eagle’s minimum essential Medium
DSM-5	Diagnostic and Statistical Manual of Mental Disorders, Fifth Edition

DZ	Dizygotic
E	Embryonic
EBV	Epstein–Barr virus
ERP	Event related potential
EST	Expressed sequence tag
ETC	Electron transport chain
FACS	Fluorescence-activated cell sorting
FSL	Flinders-sensitive rat line
FST	Forced swim test
G_1 phase	Gap 1 phase
GEO	Gene expression omnibus
GMFI	Geometric mean fluorescence intensity
GO	Gene ontology analysis
GOI	Genes-of interest
GOTree	Gene ontology tree machine
GWAS	Genome-wide association
hCMV	Human cytomegalovirus
HGNC	HUGO Gene Nomenclature Committee
ICD-10	10th revision of the International Statistical Classification of Diseases and Related Health Problems
IPA	Ingenuity pathway analysis
iPSC	Induced pluripotent stem cells
KEGG	Kyoto encyclopaedia of genes and genomes
LI	Latent inhibition
LOD	Logarithm of odds
mEPSC	Miniature excitatory postsynaptic current
MHC	Major histocompatibility complex
MITO	MitoTracker Red
M-Phase	Mitotic phase
MRI	Magnetic resonance imaging
MSD	Merck Sharpe and Dohme
MSigDB	Molecular Signatures Database
Mw	Molecular weight
MZ	Monozygotic
NCBI	National Center for Biotechnology Information

NEB	New England Biolabs
NLS	Nuclear localisation signal
ns	Not significant
OR	Odds ratio
ORF	Open reading frame
OXPOS	Oxidative phosphorylation
P	Postnatal
PBMC	Peripheral blood monocytes
PCR	Polymerase chain reaction
PPI	Prepulse inhibition
PSB	Protein sample buffer
RIPA	Radio immuno precipitation assay
RNAi	RNA interference
ROS	Reactive oxygen species
RPMI	Roswell Park Memorial Institute Medium
RT-PCR	Reverse transcription polymerase chain reaction
SD	Standard deviation
SF-rich	Serine-phenylalanine-rich motif of DISC1
SNP	Single nucleotide polymorphism
SOC	Super optimal broth with catabolite repression
t(1;11)	Translocation between chromosomes 1 and 11 (in the DISC1 family)
TAE	Tris-Acetate-EDTA
TCA	Tricarboxylic acid cycle
TST	Tail suspension test
UCSC	University of California, Santa Cruz
UV	Ultra-violet
YLD	Years of life lived with disability
WT	Wild type

Chapter 1 - Introduction

1.1 Psychiatric illness

1.1.1 The impact of psychiatric illness

Mental illness represents a challenge in the 21st century due to the burden of disease, rising economic costs and requirement of better treatments (Collins *et al*, 2011). The economic burden of mental illness globally is predicted to more than double within 20 years, from an estimated US$ 2.5 trillion in 2010 rising to US$ 6.0 trillion by 2030 (Bloom *et al*, 2012). Combined, mental health and substance abuse problems account for 22.9% of the global years of life lived with disability (YLD). For the neuropsychiatric disorders of depression, schizophrenia and bipolar disorder which are described in the following section, the YLD as a proportion of the total mental health and substance abuse disorders is 42.5%, 7.9% and 7.4%, respectively. These mental disorders therefore contribute greatly to the global burden of disease (Whitehead 2013).

The prevalence of these mental illnesses, is the proportion of people with a disorder at a given time point and those individuals and the people that suffered from the disorder up until the given time point. The lifetime prevalence of suffering from an episode of major depressive disorder ranges from 5.5% to 14.6% depending on the country surveyed (Bromet *et al*, 2011). For schizophrenia the lifetime prevalence is 0.4% (Eaton *et al*, 2011). The lifetime prevalence for bipolar disorder type I is 0.6% and for bipolar disorder type II is 0.4% (Merikangas *et al*, 2011).

A greater understanding of the brain from basic science research is needed for the effective treatment of mental illnesses, including depression, schizophrenia and bipolar disorder. The knowledge gained by investigating the molecular pathogenesis of mental illnesses could potentially be translated to develop novel diagnostic tools and therapies. This approach may reduce both the high disease and economic burdens caused by mental illness (Insel & Landis, 2013).

1.1.2 Major depressive disorder, bipolar disorder and schizophrenia

Diagnosis of a mental illness requires assessment by a psychiatrist. For diagnosis purposes mental illnesses are clearly categorised in diagnostic manuals. In the UK the ICD-10 is the commonly used diagnostic manual for mental illness whereas the USA favours the DSM-5.

Major depressive disorder

Major depressive disorder is also known as unipolar depression. The ICD-10 states the major depressive disorder is a mood disorder that can be primarily characterised by lowered mood and a reduction in interest or pleasure, which cumulates in fatigue and a reduction in levels of activity (WHO, 1992). Furthermore, depressed individuals may possess the following symptoms: lowered self-esteem; a pessimistic worldview; impaired concentration; a persistence of guilt; feelings of uselessness and impairments to sleep and appetite (WHO, 1992). Increased severity of depression is indicative of a heightened likelihood of suicidal ideation being present (WHO, 1992).

Bipolar Disorder

This is a mood disorder and was formerly known as manic depression. The ICD-10 specifies that sufferers of this syndrome must experience two or more instances of disturbance to their mood and activity levels that include both an episode of depression and an episode of hypomania or mania (WHO, 1992). Hypomania entails a moderate heightening of mood and activity level (WHO, 1992). Affected individuals suffer impairments in daily function arising from the development of interests in novel social and economic pursuits. Behaviourally, social inhibition is reduced and talkativeness increases, a mild impairment in concentration is also frequently present. In Mania the symptomology of hypomania is exacerbated. Mood is exuberant and activity levels are abnormally elevated (WHO, 1992). Sufferers experience a loss of social inhibition and regularly engage in the impulsive undertaking of detrimental social and economic actives to excess. Behaviour is frequently grandiose and may deteriorate to aggression, speech becomes rapid-fire, both concentration and attention are significantly impaired and the need for sleep is severely diminished. Severe prolonged mania potentially leads to development of psychosis, which may be comprised of hallucinations and grandiose, persecutory or religious delusions (WHO, 1992).

Schizophrenia

Schizophrenia is a complex heterogeneous syndrome characterised by disturbances in cognition, perception and emotion (WHO, 1992). These alterations are partially classified as positive and negative symptoms. The positive symptoms are additional to normal experience and include delusions and hallucinations. The ICD-10 lists a variety of delusions potentially occurring in schizophrenia (WHO, 1992). This includes: delusions of control; the belief in thought insertion or broadcasting; delusions of irrelevant everyday stimuli having special meaning and delusions that are contrary to cultural norms, for example, holding the belief that one can control the climate. Hallucinations are principally auditory but can encompass any sensory modality (WHO, 1992). In comparison, the negative symptoms are subtractive to normal experience (WHO, 1992). These include a marked reduction in speech, apathy and the blunting of emotions. The persistence of negative emotions may lead to social withdrawal (WHO, 1992). Schizophrenia is also associated with cognitive defects including working memory and attention.

1.1.3 The genetic contribution to psychiatric illness

Twin, family and adoption studies are supportive of a role of genetics in the aetiology of schizophrenia (Cardno & Gottesman, 2000; Craddock *et al*, 2005; Sullivan *et al*, 2003) bipolar disorder (Craddock *et al*, 2005; Smoller & Finn, 2003) and major depressive disorder (Kendler *et al*, 2006; Sullivan *et al*, 2000). A review of the literature by Cardno & Gottesman (2000) regarding twin studies and schizophrenia, observes concordance rates for monozygotic (MZ) twins of 41-65% and concordance rates of 0-28% for dizygotic (DZ) twins. A higher concordance of MZ/DZ twins is suggestive of a genetic cause to an illness. The heritability estimate for schizophrenia, the amount of phenotypic variations between individuals that can be ascribed to genetic variation, was estimated to be approximately 80-85% (Cardno & Gottesman, 2000). Similarly, a meta-analysis of schizophrenia twin studies estimates heritability to be 81% (Sullivan *et al*, 2003). Reviewing the genetic epidemiology of bipolar disorder Smoller & Finn (2003) found the concordance rate of MZ twins to be 38.5-62%, while for DZ twins this was 8-9.1%, with heritability estimated at 59-87%. In a study from the Swedish national twin register into the hereditability of major depressive disorder Kendler *et al.*, (2006) performed analysis with respect to gender. The correlation of female MZ twins for occurrence of lifetime major depressive disorder was 0.44, for male MZ twins this was 0.31 while in female DZ twins a correlation of 0.16 was identified, for male DZ twins this was 0.11 and for male-female DZ twins the correlation was 0.11, hereditability of major depressive disorder was estimated to be 38% (Kendler *et al*, 2006). The hereditability estimate of Kendler

et al., (2006) closely resembles a hereditability estimate of 37% identified by Sullivan *et al.*, (2000) from the meta-analysis of twin studies studying the genetics of major depressive disorder. The evidence from twin studies clearly demonstrates a genetic cause to major psychiatric illness, however, that neither the concordance rate of MZ twins nor the estimation of hereditability are 100% in these studies indicates that there is a proportion of phenotypical variance that is dependent upon the influence of environmental factors (Craddock *et al*, 2005; Smoller & Finn, 2003; Sullivan *et al*, 2000).

Adoption studies are able to provide evidence of the genetic transmission of a disorder. This is shown if the illness of an adoptee proband shows greater occurrence in biological relatives over adoptive relatives. For adoptees with chronic schizophrenia a 10-fold higher prevalence of the disorder were observed in biological relatives than controls (Kety *et al*, 1994). Wender *et al.*, (1986) observed an 8-fold increase in unipolar depression in the biological relatives of the affected adoptees. The study by Wender *et al.*, (1986) also suggests evidence for a genetic basis for bipolar disorder under the guise of major mood disorders. However, when compiling this category, the proband or the relatives were considered affected if they had bipolar disorder or unipolar depression**.**

The identification that a genetic contribution underpins major psychiatric illness from the observations of twin, family and adoption studies has led to numerous studies that have attempted to identity candidate genes. However, genetic heterogeneity, loosely defined traits and incomplete penetrance has impeded the identification of specific genetic rick factors (Burmeister *et al*, 2008). In the ongoing quest for identifying genes associated with major psychiatric illness, two non-mutually exclusive hypotheses have been pursued. The common disease-common variant hypothesis (CD-CV hypothesis) proposes that the variation in complex traits such as those evident in psychiatric illnesses, arises from the contribution of 100s or 1000s of common variants - polygenicity, of low penetrance that occur at appreciable frequencies within the population (Gibson, 2012; Schork *et al*, 2009). The CD-CV hypothesis has been investigated using large scale genome-wide association studies (GWAS) that characterise 100,000s of single nucleotide polymorphisms (SNPs) from populations of cases and controls (Gershon *et al*, 2011). Recently a schizophrenia GWAS identified 108 associated loci, 83 of which were novel findings (Consortium, 2014). Several of these SNPs were associated with genes with a role in glutamatergic neurotransmission and associations were also identified with the dopamine receptor D_2 (D_2). In two separate bipolar disorder GWAS (Ferreira *et al*, 2008; Sklar *et al*, 2011), SNPs have been associated with the gene *Calcium Channel, Voltage-dependent, L Type, Alpha 1C Subunit* (*CACNA1C*), this concordance

suggests a role for *CACNA1C* in this disorder. In comparison to schizophrenia or bipolar disorder studies GWAS of major depressive disorder has met with limited success (Flint & Kendler, 2014). A recent GWAS mega-analysis failed to identify any SNP associations at genome wide significance (Ripke *et al*, 2013b).

The contrasting school of thought to the CD-CV hypothesis is the common disease rare variant hypothesis (CD-RV hypothesis), whereby multiple rare variants of moderately high penetrance contribute to psychiatric illness (Gibson, 2012; Schork *et al*, 2009). The CD-RV hypothesis assumes genetic heterogeneity, whereby mutations in different genes affect different individuals and families (Mitchell & Porteous, 2011). The CD-RV hypothesis has until recently been pursued mostly by linkage, small family and single case studies. The t(1;11) pedigree which has multiple individuals affected by major mental illness co-segregating with a balanced translocation (Blackwood *et al*, 2001) that disrupts *Disrupted-In-Schizophrenia 1* (*DISC1*), *Disrupted-In-Schizophrenia 2* (*DISC2*) (Millar *et al*, 2000b) and *Disrupted-In-Schizophrenia 1 Fusion Partner 1* (*DISC1FP1*) also known as *Boymaw* (Eykelenboom *et al*, 2012; Zhou *et al*, 2010; Zhou *et al*, 2008), is an example of a rare variant that has been identified in a family study and will be discussed further later in this chapter. Recent advances in technology have allowed rare variants such as CNVs (Copy number variations), point mutations and small insertions and deletions (indels) to be analysed by microarray and next generation sequencing. Case control and family studies have repeatedly found the enrichment of CNVs in individuals with schizophrenia with the loci for CNVs being spread throughout the genome (Malhotra & Sebat, 2012). Generally, CNV studies into schizophrenia implicate genes associated with neuronal function that possibly act on synaptic activity and neurodevelopment (Malhotra & Sebat, 2012). *De novo* (non-inherited) CNVs have been identified that occur with 8-fold greater frequency in sporadic schizophrenia than healthy controls (Xu *et al*, 2008). The role of CNVs in bipolar disorder is controversial with inconsistencies occurring between studies (Craddock & Sklar, 2013). However, the data suggests a role for CNVs in a sub-type of bipolar disorder with an early age of onset (Craddock & Sklar, 2013). Furthermore, few schizophrenia loci appear to be shared with bipolar disorder (Malhotra & Sebat, 2012). The investigation into CNVs as mediators of depression has produced mixed and contradictory results, though this represents an emerging field and presently few studies have been published (O'Dushlaine *et al*, 2014; Rucker *et al*, 2013; Rucker *et al*, 2015).

Major psychiatric disorders may not necessarily 'breed true', whereby relatives to a proband with a psychiatric illness may be at risk from suffering from another psychiatric disorder as

well as being at risk from suffering the same disorder. For example, the risk of major depressive disorder to a relative of a proband with bipolar disorder was increased approximately 2-fold compared to controls, in comparison the risk to relatives of suffering bipolar disorder was increased approximately 9-fold (Merikangas & Yu, 2002). In a twin study where the proband was diagnosed with bipolar disorder, the heritability estimate was increased when compared to a broad concordance measure in which the co-twin suffered from either unipolar depression or bipolar disorder over a narrow concordance whereby the co-twin was diagnosed with bipolar disorder (McGuffin *et al*, 2003). Another twin study highlights the underlying common genetic contributions to the psychotic disorders schizophrenia, bipolar disorder and schizoaffective disorder, which were identified along with disorder specific genetic contributions (Cardno *et al*, 2002). The co-aggregation of bipolar disorder and schizophrenia has been identified in a large scale Swedish family study, whereby first degree relatives of probands with schizophrenia were found to have increased risk of bipolar disorder and vice versa (Lichtenstein *et al*, 2009). GWAS may have detected some of the common genes underpinning these observations, shared loci have been identified for autism spectrum disorder, attention deficit-hyperactivity disorder, bipolar disorder, major depressive disorder, and schizophrenia (Consortium, 2013). Additionally, GWAS by Purcell *et al.*, (2009b) observed common SNPs that were present in both schizophrenia and bipolar disorder cases.

1.1.4 The environmental contribution to psychiatric illness

1.1.4.1 Schizophrenia

A role for an environmental contribution to the aetiology of major mental illness is evidenced by the observation that neither the concordance for MZ twins nor the hereditability estimates for these disorders are 100% (Craddock *et al*, 2005; Smoller & Finn, 2003; Sullivan *et al*, 2000). Environmental risk factors for schizophrenia have been identified that occur at various instances in throughout development from preconception to adulthood (Opler *et al*, 2013; Schmitt *et al*, 2014; Sullivan, 2005). Furthermore, both place of birth and season of birth are risk factors for schizophrenia, with urbanicity and winter having the greatest effect size, respectively (Sullivan, 2005). At preconception, an environmental risk factor for schizophrenia is paternal age, with advanced paternal age conferring the greatest risk of producing offspring with schizophrenia (Brown *et al*, 2002; Malaspina *et al*, 2001; Sipos *et al*, 2004). This research generated the following results regarding advanced parental age being predictive of schizophrenia in offspring, per 10 year increase in paternal age: the risk of

schizophrenia is 1.89 (Brown *et al*, 2002); the rate of schizophrenia is 1.45 (Malaspina *et al*, 2001) and the hazard ratio is 1.47 (Sipos *et al*, 2004). These analyses are adjusted with respect to maternal age. Nominal results were observed in separate analyses focussing on maternal age that adjusted for paternal age (Malaspina *et al*, 2001; Sipos *et al*, 2004).The effect of advanced paternal age is believed to be due to the increased generation of *de novo* mutations in sperm with increased age (Brown *et al*, 2002; Malaspina *et al*, 2001).

Epidemiological studies have highlighted maternal immune activation during the prenatal period as a possible means of conferring the risk of schizophrenia to the foetus (Brown & Derkits, 2010). The exposure *in utero* to pathogens resulting in infection may propagate an altered and deleterious neurodevelopment trajectory by common or novel pathways. Several pathogens have been positively associated with the risk of developing schizophrenia following maternal immune activation including: herpes simplex virus type-2 (Buka *et al*, 2008), influenza (Mednick *et al*, 1994) and the parasite *T.gondii* (Mortensen *et al*, 2007). Prenatal malnutrition is also a risk factor for schizophrenia. Retrospective studies into both the Dutch Hunger Winter of 1944–1945 (Hoek *et al*, 1998; Susser *et al*, 1996; Susser & Lin, 1992) and the Chinese famine of 1959–1961 (St Clair *et al*, 2005; Xu *et al*, 2009) identify that subjects in gestation during these periods as having an elevated risk of schizophrenia.

Perinatal obstetric complications show small effects sizes with schizophrenia (Cannon *et al*, 2002). These include complications during delivery such as asphyxia or emergency caesarean section and abnormal foetal growth and development such as low birth weight and reduced head circumference. Furthermore, the effects of labour-delivery problems have been related to schizophrenia associated alterations in brain structure (McNeil *et al*, 2000).

Cannabis use is a component cause in the liability to schizophrenia (Henquet *et al*, 2005). In adolescence, the age at which cannabis use occurs is important for the later development of schizophrenia symptomology (Arseneault *et al*, 2002). Early cannabis use aged 15 is a greater risk factor for developing schizophrenia than cannabis use at age 18. Additionally, the risk of conferring schizophrenia due to cannabis use is dependent on the number of times cannabis is smoked, with high frequency users having the greatest risk (Zammit *et al*, 2002).

1.1.4.2 Affective disorders

For affective disorders stressful life events is a risk factor that is seen to be predictive to susceptibility to both depression (Kendler *et al*, 1999; Mazure, 1998; Tennant, 2002) and bipolar disorder (Brietzke *et al*, 2012; Weiss *et al*, 2015). Additionally, life stressors are one of the strongest predictors of relapse in bipolar disorder (Altman *et al*, 2006). The exposure to childhood maltreatment has been associated with increased risk of developing depression that has poorer long-term outcomes (Nanni *et al*, 2012), while childhood trauma that is inclusive of abuse has been frequently associated with bipolar disorder (Etain *et al*, 2008). It has been suggested that the occurrence of this childhood trauma may be instrumental to early perturbations of neurodevelopment that result in bipolar disorder.

Preterm birth has been observed to be an obstetric complication that is linked to affective disorders. A study using the Swedish medical birth register, found that births of less than 32 weeks gestation were 2.9 times likely to develop a depressive illness and 7.4 times likely bipolar disorder, in comparison to term births (Nosarti *et al*, 2012). A recent study on Finnish sufferers of bipolar disorder has identified birth by caesarean section as an obstetric complication associated with bipolar disorder (Chudal *et al*, 2014). However, in comparison to schizophrenia, research studies into obstetric complications in bipolar disorder have suffered from methodological problems due to the small scale of the studies and issues with defining the complications (Scott *et al*, 2006).

The relationship between maternal immune activation and bipolar disorder has been investigated, regarding infections from herpes simplex virus types 1 & 2, cytomegalovirus, *T.gondii*, influenza and febrile cold (Mortensen *et al*, 2003; Mortensen *et al*, 2011; Stöber *et al*, 1997). However, the limited number of studies attempted in this field have produced negative results. Likewise a cohort study by Pang *et al.,* (2009) failed to find an association between depression and prenatal viral infection. In contrast, an increase in the number of individuals that develop major depressive disorder following gestational exposure to influenza has been detected by Machon *et al.,* (1997).

Cannabis use is also an environmental risk factor for bipolar disorder. A dose dependent effect of cannabis use and the onset of bipolar symptomology has been identified by Lagerberg *et al.,* (2014) whereby higher rates of cannabis use may result in earlier illness onset. The long term use of cannabis in the general population may lead to the symptoms of mania in a dose dependent manner, with increased frequency of cannabis use increasing manic symptoms (Henquet *et al*, 2006). Furthermore, in established bipolar disorder the co-occurrence of a

cannabis usage disorder is associated with a greater frequency of both manic/hypomanic and depressive episodes (Lev-Ran *et al*, 2013).

Tobacco smoking is also an environmental risk factor in bipolar disorder. In comparison to nonsmokers with bipolar disorder, affected smokers show higher morbidity, with an earlier age of onset, poorer functioning, increased co-morbidity, a greater number of episodes and a broader array of symptoms (Baek *et al*, 2013; Ostacher *et al*, 2006; Waxmonsky *et al*, 2005). Furthermore, increased levels of tobacco smoking are correlated with greater severity of psychotic symptoms in bipolar disorder (Corvin *et al*, 2001). Tobacco smoking in bipolar disorder is also associated with a history of suicide attempts, OR 1.5-2.3 (Baek *et al*, 2013; Ostacher *et al*, 2006; Waxmonsky *et al*, 2005). Moreover, it is possible the smoking status in bipolar disorder may be predictive of future suicide risk. In line with this, affected smokers show a greater incidence of suicide attempts in the 9-month period following initial suicidal ideation assessment, than nonsmokers with bipolar disorder, OR 5.25 (Ostacher *et al*, 2009).

Alcohol represents a significant environmental risk factor for bipolar disorder, with the co-morbidity of alcohol use disorder and bipolar disorder commonly occurring (Farren *et al*, 2012). Alcohol use disorder has been associated with a poorer longitudinal outcome in bipolar disorder via a destabilisation of the illness, with increased frequency of mood switching and number of episodes occurring (Rakofsky *et al*, 2013). Similarly, using the criteria of alcohol abuse or dependence, co-occurring with bipolar disorder, worse functional outcomes, earlier age of onset, increased severity of depressive symptoms and a severe increase in the number of suicide attempts have been observed (Cardoso *et al*, 2008). Moreover, meta-analysis identifies an elevated incidence of suicide attempts in individuals with bipolar disorder comorbid with alcohol use disorder compared to sufferers of bipolar disorder without alcohol use disorder, OR 1.72 (Carrà *et al*, 2014).

1.2 Disrupted-in-Schizophrenia 1 (DISC1)

1.2.1 The t(1;11) pedigree

In 1968 a cytogenetic investigation into boys being allocated to Scottish borstals identified an 18 year old boy with a balanced translocation between chromosome 1 and a C group chromosome (Jacobs *et al*, 1970). This chromosome abnormality was examined in four generations of the pedigree.

20 years later, the initial pedigree studied by Jacobs *et al.,* (1970) was identified from records in the MRC Cytogenetics Registry, Edinburgh and by follow-up reports from GPs as having multiple family members that had been referred to psychiatric services (St Clair *et al*, 1990). The interest in the potential relationships between the chromosomal translocation, now identified as a balanced t(1;11) (q43p21), with mental illness prompted the characterisation of the psychiatric disorder in the t(1;11) pedigree by structured interviews with psychiatrists. The t(1;11) was established as co-segregating with mental illness. 49% of translocation carriers had a psychiatric diagnosis, including several incidences of major mental illness, with sufferers of major depressive disorder, schizophrenia and schizoaffective disorder identified (St Clair *et al*, 1990). In contrast, the karyotypically normal family members were found to suffer from only minor mental disorders.

An in depth clinical follow-up of the t(1;11) pedigree 10 years after St Clair *et al.,* (1990) identified 87 family members, 37 of whom carry the translocation (Blackwood *et al*, 2001). Within the translocation carriers, seven had schizophrenia, one had bipolar disorder and ten suffered from major depressive disorder. Following this, the linkage of the t(1;11) to schizophrenia generated a logarithm of odds (LOD) score of 3.6. If the incidences of bipolar disorder and major depressive disorder are also included, the linkage of the t(1;11) to major mental illness produces an LOD score of 7.1 . These results indicate that the t(1;11) is linked to the instances of major mental illness seen in the t(1;11) pedigree and it is most likely that the translocation is the aetiological mechanism precipitating these disorders.

Members of the t(1;11) pedigree have been assessed using the p300 event related potential (ERP) as a means to identify possible deficits in cognition that may be conferred by the translocation (Blackwood *et al*, 2001). The p300 ERP occurs following the presentation of a random 'oddball' stimulus that may be visual, auditory or somatosensory and is seen as a measure of selective attention and working or short term memory (Blackwood, 2000). Deficits in the p300 ERP have been seen to be a trait marker for schizophrenia (Blackwood, 2000). In the t(1;11) pedigree the performance of translocation carriers, including those that did not exhibit major mental illness was seen to be impaired and similar to individuals with schizophrenia. This performance differed from non-translocation carrying t(1;11) pedigree members and healthy controls (Blackwood *et al*, 2001). The results of the p300 ERP findings on the t(1;11) pedigree indicate the translocation may intrinsically induce cognitive deficits. Given that p300 ERP testing establishes impairments to memory and attention in t(1;11) carriers, future neuropsychiatric assessment of the pedigree could focus on the further investigation of cognitive deficits associated with the translocation.

An aetiological mechanism by which the translocation could propagate the major mental illness observed in the t(1;11) carriers was thought to be via the interruption of genes spanning the chromosome 1 and chromosome 11 breakpoints. Therefore in the periods between the publication of St. Clair *et al.,* (1990) and Blackwood *et al.,* (2001), a series of studies focussed on both the fine-mapping of the translocation and aimed to identify genes that may be affected by the potential gene disruption at these locations (Devon *et al*, 1997; Evans *et al*, 1995; Fletcher *et al*, 1993; Millar *et al*, 1998; Muir *et al*, 1995; Semple *et al*, 2001). Following these efforts the breakpoint was confirmed as being located at 1q42.1 and 11q14.3.

1.2.2 The identification of genes at the t(1;11) breakpoints

At the chromosome 1 breakpoint two novel genes were observed to be interrupted by the translocation: *Disrupted-in-Schizophrenia 1 (DISC1) and Disrupted-in-Schizophrenia 2 (DISC2)* (Millar *et al*, 2000b). The t(1;11) breakpoint lies in intron 8 between exons 8 and 9 of *DISC1* (Millar *et al*, 2001) (see figure 1.2A). DISC1 was found to be comprised of 13 exons and identified as being a protein coding gene encoding an 854aa species (Millar *et al*, 2001; Millar *et al*, 2000b). DISC1 has been observed to be expressed in multiple brain regions (Chubb *et al*, 2008). In t(1;11)-family derived lymphoblastoid cell lines, the levels of *DISC1* are reduced by approximately 50% in comparison to karyotypically normal controls (Millar *et al*, 2005b). This is evidence of the haploinsufficiency of DISC1 that may occur in t(1;11) carriers as a mechanism of pathogenesis.

DISC2 has been identified as brain expressed non-coding RNA and is located antisense to *DISC1* (see figure 1.2A), encompassing a single exon that overlaps with *DISC1* exon 9 (Millar *et al*, 2001; Millar *et al*, 2000b). Given the antisense proximity of *DISC2* to *DISC1* and that *DISC2* is a non-coding RNA, it is possible that *DISC2* may function as a negative regulator of *DISC1* transcription (Chubb *et al*, 2008), however further studies are required to establish this.

At the chromosome 11 breakpoint, initial research found no evidence of genes immediately in the proximity of the 11q14.3 region (Devon *et al*, 1997; Millar *et al*, 1998; Semple *et al*, 2001). However, a brain expressed non-coding RNA named *Disrupted-in-Schizophrenia Fusion Partner 1 (DISC1FP1)* (Eykelenboom *et al*, 2012) also known as *Boymaw* (Zhou *et al*, 2010; Zhou *et al*, 2008) has been identified to span the chromosome 11 breakpoint (see figure 1.2A). Furthermore, a recent study suggests that *Boymaw* may actually a protein coding gene that is targeted to the mitochondria (Ji *et al*, 2015). Alternative splices of this species have been proposed to be able to splice with *DISC1* at the t(1;11) breakpoints (Zhou *et al*, 2008) and have since been identified as being capable of generating chimeric transcripts with *DISC1*

(Eykelenboom *et al*, 2012). The topic of *DISC1/DISC1FP1* chimeric transcripts will be covered in greater detail in section 1.2.10.

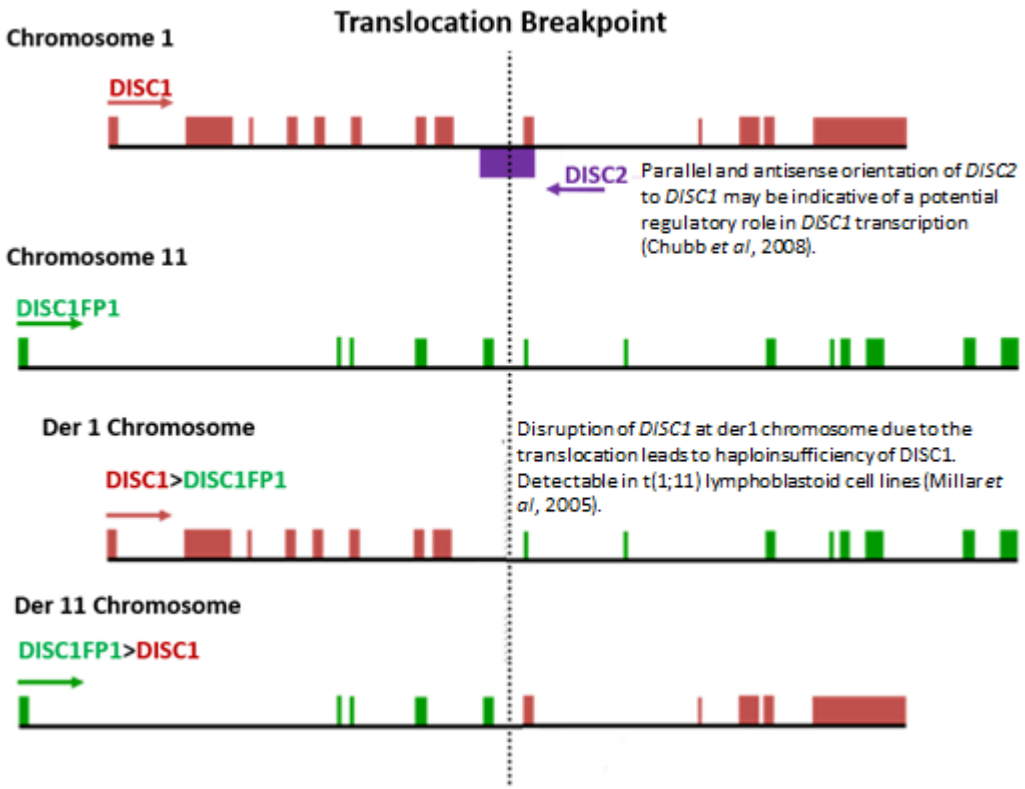

Figure 1.2.A: Relative locations of *DISC1*, *DISC2* and *DISC1FP1* to the translocation breakpoint on both normal and derived chromosomes. Dashed vertical line indicates translocation breakpoint, exons: *DISC1* (red), *DISC2* (Purple), *DISC1FP1* (Green). Arrows denote direction of transcription.

1.2.3 DISC1 protein structure

Western blotting in conjunction with use of antibodies targeted to different epitopes on DISC1 protein has resulted in the detection of multiple isoforms of human DISC1. Frequently a DISC1 species of ~100 kDa protein has been observed and this is presumed to be the translation product of the Long (L)-isoform of DISC1 (Soares *et al*, 2011). This isoform encodes all 13 of the exons originally identified in the DISC1 gene (Millar *et al*, 2000b). Furthermore additional DISC1 proteins have been detected, this includes, but is not exclusive to: 71, 70-85, 75, 80, 98, 150 and 200kDa species (James *et al*, 2004; Sawamura *et al*, 2005;

Soares *et al*, 2011). It is possible that the DISC1 protein species detected as running between 71-75 kDa may represent the translation of a short DISC1 transcript, the S-isoform (Chubb *et al*, 2008; Taylor *et al*, 2003). The 150 and 200kDa species may arise from the homodimerization of 75 and 100 kDa species, respectively. Such an occurrence is likely given that DISC1 is capable of self-associating (Kamiya *et al*, 2005). The correct assignment of other DISC1 protein isoforms to known DISC1 transcripts may be encumbered due to post-translational modifications, which could impact upon the molecular weight a given species migrates at.

The full length 854aa DISC1 protein represents a unique protein, in that there is no significant similarity between its aa sequence and that of known proteins (Millar *et al*, 2000b). Conservation of *DISC1* has been studied in multiple vertebrate species with orthologues identified in mammals, fish and birds (Bord *et al*, 2006; Chubb *et al*, 2008; Ma *et al*, 2002; Taylor *et al*, 2003). Outside of primate species the conservation of DISC1 is relatively poor (Bord *et al*, 2006; Chubb *et al*, 2008). For example the mouse *Disc1* gene has a 60% identity with full-length *DISC1* (Ma *et al*, 2002). This reduction in conservation may be indicative that *DISC1* is a gene that has undergone rapid evolution in primates (Bord *et al*, 2006). Additionally, *DISC1* orthologues have been identified within invertebrates, plants and algae (Sanchez-Pulido & Ponting, 2011).

At present no 3-D crystal structure of full-length DISC1 has been produced. Investigations into structural information regarding DISC1 have primarily focused on bioinformatics approaches and additionally the biophysical characterisation of DISC1 (Chubb *et al*, 2008; Soares *et al*, 2011). In silico analysis suggests that full length DISC1 can be divided into two domains based on overall structural differences, an N-terminal 'head' region comprising aa1-350 that is of low complexity and a more structurally diverse C-terminal region encompassing aa351-854 (Millar *et al*, 2000; Soares *et al*, 2011) (see figure 1.2.B). The N-terminal is frequently predicted to fold into a 'globular domain' in that this region contains amino acids that fail to fold into a set 3-D structure (Soares *et al*, 2011). As a disordered protein structure, it is likely that the N-terminal region will adopted a folded protein structure upon interaction with another protein (Fink, 2005). The N-terminal sequence is also poorly conserved (Taylor *et al*, 2003). However, within the N-terminal there are two motifs that are notably well conserved, an arginine-rich nuclear localisation signal comprising aa35-44 (Ma *et al*, 2002; Taylor *et al*, 2003) and a serine and phenylalanine-rich (SF-rich) motif of unknown function spanning aa206-217 (Taylor *et al*, 2003) (see figure 1.2.B). The use of structural prediction programs suggests that the C-terminal region contains several α-helices, a minimum of four

coiled coils at aa347-393, aa452-499, aa603-680 and aa805-828 (see figure 1.2.B), while some of the coiled coils leucine zipper motifs may be present at aa458-486, aa607-628, aa808-829 (Chubb *et al*, 2008; Soares *et al*, 2011).

DISC1 has been found to form complexes of varying molecular weights via self-interaction. The identification of DISC1 species of 200-250kDa, led Brandon *et al.*, (2004) to infer that that these proteins were complexes of smaller DISC1 isoforms. A subsequent study by Kamiya *et al.*, (2005) identified a DISC1 self-association region at aa403-504 using domain mapping. Biophysical characterisation of DISC self-association has been further investigated using C-terminal fragments of DISC (Leliveld *et al*, 2008; Leliveld *et al*, 2009). DISC1 was observed to exist in complexes as either dimers, oligomers or multimers (Leliveld *et al*, 2008). The characterisation also revealed that the third coiled coil domain facilitates dimerisation and the fourth coiled coil domain promotes multimerisation (Leliveld *et al*, 2009).

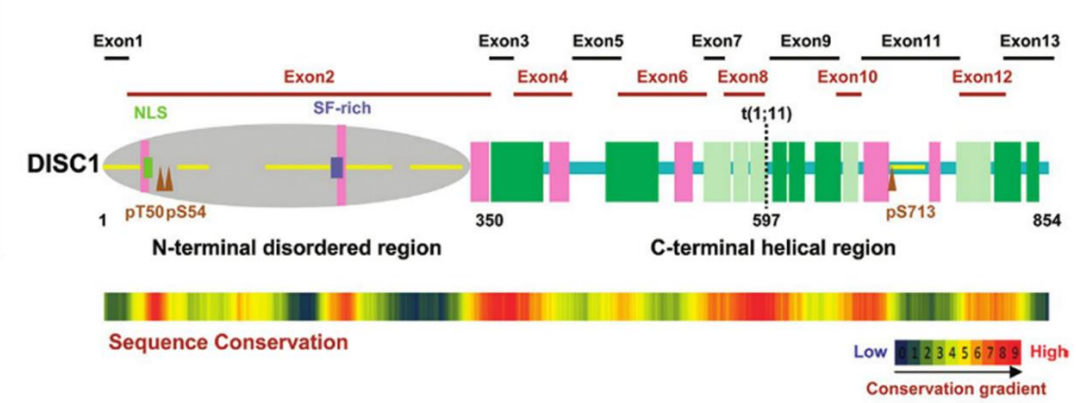

Figure 1.2.B: Full-length DISC1 aa854 protein structure and conservation. Adapted from Soares *et al.*, (2011). The figure visualises the secondary structure, coiled-coils (green), regular α-helixes (pink), ambiguous helixes (light green). The nuclear localisation signal (NLS) and serine-phenylalanine-rich (SF-rich) motif are highlighted. Brown triangles represent phosphorylation sites. Dashed vertical band represents the translocation breakpoint at DISC1 aa597. Beneath the structure is a band detailing orthologue conservation of the DISC1 sequence.

1.2.4 *DISC1* tissue expression and subcellular protein distribution

The analysis of *DISC1* expression in adult derived tissues observes strong mRNA expression in the brain, heart and placenta with weaker expression evident in the kidney and pancreas (Millar *et al*, 2000b). While in foetal tissues, *DISC1* expression at the mRNA level has been found in the brain, heart, kidney, limb and spleen. Similarly, DISC1 protein can be detected in foetal tissue, with greatest prominence in the kidney and is also observed in the brain, heart, liver and limb (James *et al*, 2004). The expression of *DISC1* mRNA in multiple brain regions was highlighted by Millar *et al.*, (2000b), including the amygdala, caudate nucleus, corpus callosum, hippocampus, substantia nigra, subthalmic nucleus, thalamus and the whole brain. The levels of *DISC1* transcripts have been found to be higher in the embryonic period and undergo a gradual decline in the postnatal period (Nakata *et al*, 2009). DISC1 protein expression is highly prominent within a subset of granule cells within the dentate gyrus of the hippocampus, a lower level of DISC1 expression is also detected in areas *cornu ammonis* 1-3 (CA1-3) of the hippocampus (James *et al*, 2004). Using post-mortem brain tissue, modest increases in the levels of DISC1 have been identified in the hippocampus of individuals with schizophrenia compared to heathy controls (Lipska *et al*, 2006b). An increase in DISC1 immunoreactivity has also been observed post-mortem in the fronto-parietal white matter of sufferers of paranoid schizophrenia compared to healthy controls or individuals with undifferentiated schizophrenia (Bernstein *et al*, 2015). In contrast, the post-mortem levels of a 75-85kDa DISC1 species detected in the orbitofrontal cortex of individuals with major depressive disorder, bipolar disorder and schizophrenia, did not differ from controls (Sawamura *et al*, 2005). Additionally, in post-mortem hippocampal and dorsolateral prefrontal cortex (DLPFC) tissue, no alterations in *DISC1* variant mRNA levels were detected between sufferers of schizophrenia and healthy controls (Lipska *et al*, 2006b).

Two studies have addressed *DISC1* tissue expression in primates. Austin *et al.*, (2003) assayed mRNA levels in several brain areas of the adult African green monkeys, finding high expression in the dentate gyrus and lateral septum and lower expression in the amygdala, cerebellum, cortex, and interpeduncular nucleus. Bord *et al.*, (2006), studied both mRNA and protein levels of DISC1 in the rhesus monkey, observing the highest expression in the hippocampus as well as high expression in the frontal, occipital, parietal and temporal lobes and lower expression in the cerebellum. Both of these studies therefore support a notion for high DISC1 expression in the hippocampus or hippocampal sub-regions.

Rodents show the highest expression of *Disc1* mRNA in the heart, with expression also detected in the brain, kidney, skeletal muscles and testis (Ma *et al*, 2002; Ozeki *et al*, 2003).

In line with this, DISC1 protein in the rat is found most prominently within the heart as well as in the brain, kidney liver, skeletal muscles and thymus (Ozeki *et al*, 2003). Rodent *Disc1* mRNA expression is observed in specific brain areas including, the granule cell layer of the dentate gyrus where expression is notably high, as well as in the amygdala, brainstem, cerebellum, corpus callosum, cortex, hippocampus, hypothalamus and olfactory bulb (Ma *et al*, 2002; Miyoshi *et al*, 2004; Osbun *et al*, 2011; Schurov *et al*, 2004). Similarly, in the rat, DISC1 protein has been found to have high expression in the cortex, hippocampus and olfactory bulb, with lower expression observed in the cerebellum (Ozeki *et al*, 2003) The expression levels within the mouse brain of an 100 kDa isoform of DISC1 have been observed to peak at E13.5, a period of intense neurogenesis and cell migration and also at P35 onwards to 6 months, a time point that is analogous to puberty (Schurov *et al*, 2004). Further studies in rodents have observed a gross postnatal peak in *Disc1* mRNA (Austin *et al*, 2004; Honda *et al*, 2004) or protein (Kuroda *et al*, 2011) followed by a gradual decline. In contrast, *Disc1* mRNA levels in the hippocampus has been found to be high at all developmental stages and is detectable from E14, peaking at P21, with *Disc1* mRNA levels remain prominent into adulthood (Austin *et al*, 2004). These observations suggest a role of *Disc1* in the patterning and connecting of hippocampal neurons during development. Supporting this notion, is the finding that mouse DISC1 is observed to localise in the dentate gyrus to regions where granule cell progenitors occur (Meyer & Morris, 2008). Within the subgranular zone of the dentate gyus, DISC1 co-localises with the cell cycle marker Ki67, highlighting the proliferation occurring in this region.

In summary, both *DISC1* and *Disc1* have been detected in multiple CNS and non-CNS tissues. The hippocampus and hippocampal sub-regions often show the most prominent expression of *DISC1* and *Disc1*, this of relevance to the consideration of *DISC1* as a candidate gene for schizophrenia, given multiple studies associate the hippocampal formation with this disorder (Tamminga *et al*, 2010).

1.2.5. DISC1 sub-cellular distribution

DISC1 has been observed to localise to multiple subcellular compartments, this is reviewed in Chubb *et al.*, (2008), Soares *et al.*, (2011) and Thomson *et al*., (2013), a summary of the main findings adapted from Soares *et al.*, (2011) is presented in table 1.2.A. The compartmentalisation of DISC1 to a variety of sub-cellular locations is in line with the notion that DISC1 participates in wide assortment of cellular functions that are mediated by multiple protein-protein interactions in discrete cellular compartments (Bradshaw & Porteous, 2012;

Brandon *et al*, 2009; Thomson *et al*, 2013) (1.2.A). The targeting of DISC1 to subcellular locations may be facilitated by interactions with binding partners or via signalling peptides structurally located within DISC1 (Soares *et al*, 2011; Thomson *et al*, 2013). The localisation of DISC1 to the centrosome will be further covered in section *1.2.7 DISC1 in neurodevelopment, plasticity and cellular signalling*, whilst localisation of DISC1 to the mitochondria will be further covered in *1.2.11 DISC1 and mitochondrial function.*

Cellular location	Details and associated functions of DISC1	References
Aggresome	DISC1 aggregates recruited to the aggresome for degradation.	(Atkin *et al*, 2012)
Centrosome	Involved in the recruitment of kendrin, dynein and dynactin subunits, LIS1, NDEL1, PCM1, ninein and CAMDI to the centrosome. Also interacts with PDE4B, PDE4D, NDE1 and BBS4. These interactions include those both important for microtubule aster formation, neurite outgrowth and neuronal migration.	(Bradshaw *et al*, 2009; Bradshaw *et al*, 2008; Fukuda *et al*, 2010a; Kamiya *et al*, 2005; Kamiya *et al*, 2008; Kamiya *et al*, 2006; Miyoshi *et al*, 2004; Morris *et al*, 2003; Shimizu *et al*, 2008)
Cilia	Found at the base of primary cilia and appears to regulate their formation and/or maintenance. Knock-down of endogenous DISC1 leads to marked reduction of primary cilia. Other DISC1 interactors found at the base of primary cilia include BBS4 and PCM1.	(Marley & von Zastrow, 2010)
Cytoskeleton	Seen along both actin filaments and microtubules. Expression of DISC1 aa1-597 leads to a disorganised microtubule network	(Kamiya *et al*, 2005; Miyoshi *et al*, 2003; Morris *et al*, 2003)

Golgi apparatus	Seen in association with the membrane structures of the golgi apparatus in hippocampal neurones and astrocytes. May participate in vesicle movement from the Golgi apparatus	(Kuroda *et al*, 2011)
Growth Cones	Found here in the hippocampus and is involved in the recruiting proteins including LIS1, NDEL1, 14-3-3ε and girdin via kinesin-based transport along the cytoskeleton. Also important for axonal elongation.	(Enomoto *et al*, 2009; Miyoshi *et al*, 2003; Shinoda *et al*, 2007; Taya *et al*, 2007)
Membranes	Found in membrane fractions where it interacts with APP, which is important in cortical precursor formation.	(Brandon *et al*, 2005; Ozeki *et al*, 2003; Young-Pearse *et al*, 2010)
Mitochondria	Found at mitochondria present on microtubules and regulates trafficking. Can cause mitochondria to form 'ring' structures. Interacts with mitofilin within the mitochondria and is required for correct electron transport chain, monoamine oxidase and Ca^{2+} activity. 37W variant results in clustered peri-nuclear mitochondria. Associates with TRAK1 and Miro1 as part of the mitochondrial transport complex. Promotes anterograde mitochondrial movement. Localises with ATF4 at mitochondria.	(Atkin *et al*, 2011; Brandon *et al*, 2005; James *et al*, 2004; Malavasi *et al*, 2012; Millar *et al*, 2005a; Ogawa *et al*, 2014; Ozeki *et al*, 2003; Park *et al*, 2010)

Nucleus	Found at the chromatin, promyelocytic leukemia (PML) bodies and outer layers of the nuclear membrane. Represses ATF4 transcriptional activity and transcription of N-cadherin and alters sleep homeostasis in *Drosophila*. DISC1 variants 37W and 607F independently disrupt DISC1 nuclear targeting	(Hattori *et al*, 2010; James *et al*, 2004; Kirkpatrick *et al*, 2006; Malavasi *et al*, 2012; Sawamura *et al*, 2008)
Synapse	Seen at the post-synaptic density along with PDE4 and NDE1. Interacts with and inhibits TNIK here, leading to degradation of key synaptic proteins. Also affects spine formation through modulation of PSD-95/Kal7/Rac1 complexes here.	(Bradshaw *et al*, 2008; Clapcote *et al*, 2007; Hayashi-Takagi *et al*, 2010; Kirkpatrick *et al*, 2006; Wang *et al*, 2011)

Table 1.2.A: Subcellular localisation of DISC1. Adapted from Soares *et al.,* (2011). DISC1 rare variant 37W and common variant 607F arise from R37W and the L607F substitutions, respectively and are further detailed in section 1.2.11 DISC1 and mitochondrial function.

1.2.6. DISC1 binding partners

Multiple large-scale yeast-two hybrid studies have been implemented that have identified numerous DISC1 interactors (Brandon *et al*, 2004; Camargo *et al*, 2006; Millar *et al*, 2003; Miyoshi *et al*, 2004; Morris *et al*, 2003; Ozeki *et al*, 2003; Shinoda *et al*, 2007; Taya *et al*, 2007). At present more than 200 potential DISC1 interactors have been identified, for a minority of these species the interaction with DISC1 has been further validated by co-immunoprecipitation, GST-pulldown or co-localisation studies. In some instances domain mapping has been pursued to identify protein-protein interactions using deletion mutants, which can confirm a specific protein binding region or abolish protein binding. Alternatively, peptide arrays have also been used for fine mapping of interaction sites. The use of both of these processes to identify novel interactions with DISC is reviewed in Soares *et al.*, (2011).

The DISC1 interactome study by Camargo *et al.*, (2006) combined yeast-2-hybrid screening with bioinformatics analysis, characterising pathway and functional roles of putative DISC1 interactors. 289 potential interactors were identified 34 of which were identified as high confidence interactors. Gene ontology analysis (GO) on these species identified that DISC1 interactors can be associated with functions involved in cytoskeletal organisation and biogenesis, mRNA/protein synthesis, cell cycle/division, intracellular transport and signal transduction processes.

The number of DISC1 interactors coupled with the extensive expression of DISC1 at the cellular and tissue level has led to the proposal that DISC1 is a 'hub' protein. A number of DISC1 interactors have been independently associated with psychiatric illness, these findings establish networks linked to psychopathology within which DISC1 functions as a hub (Bradshaw & Porteous, 2012).

A search of NCBI PubMed in June 2015 for DISC1 in title/abstract retrieves 500+ papers. The sizeable nature of the DISC1 literature puts a comprehensive review of DISC1 interactors and their functions beyond the scope of this thesis. The following section *1.2.7 DISC1 in neurodevelopment, plasticity and cellular signalling* will cover material on several interactors of note.

1.2.7 DISC1 in neurodevelopment, plasticity and cellular signalling

In eukaryotes the centrosome is the major microtubule organising centre of the cell and establishes and coordinates microtubule arrays to other intracellular structures during cell division (Dehay & Kennedy, 2007). The centrosome is essential for the regulation of the cytoskeleton and the maintenance of polarisation. In addition to being a hub for the microtubule array the centrosome also provides signalling for neuronal guidance. Together these centrosomal mechanisms enable neurogenesis, neuronal migration and differentiation to occur efficiently (Higginbotham & Gleeson, 2007).

Several studies have observed the localisation of DISC1 to the centrosome, here DISC1 interacts with various proteins that are established as being involved in centrosome mediated facets of neurogenesis. This includes Bardet-Beidel Syndrome 4 Protein (BBS4), kendrin (also known as pericentrin), lissencephaly 1 (LIS1), NudE Neurodevelopment Protein 1-Like 1 (NDEL1) (Bradshaw *et al*, 2009; Brandon *et al*, 2004; Kamiya *et al*, 2008; Millar *et al*, 2003; Miyoshi *et al*, 2004; Morris *et al*, 2003; Shinoda *et al*, 2007). Subsequently, a role for DISC1 in the recruitment and anchoring of several of these proteins at the centrosome has been identified. For example, centrosomal DISC1 interacts with kendrin which facilitates microtubule network formation (Shimizu *et al*, 2008). Furthermore, DISC1 and the DISC1 interactor BBS4 act synergistically in the recruitment of Pericentriolar Material 1 (PCM1) to the centrosome (Kamiya *et al*, 2008). Knockdown of each of these protein species results in neuronal migration deficits.

DISC1 is a constituent of the dynein motor complex which facilitates retrograde movement along the axon (Kamiya *et al*, 2005). DISC1 is required for the stabilisation and localisation of the dynein complex at the centrosome in conjunction with LIS and NDEL, thus maintaining microtubule organisation and dynamics. DISC1 is also involved in anterograde transport via interactions with the motor protein kinesin-1 (KIF5A) and Growth Receptor Bound Protein 2 (Grb2), which transport the NDEL1/LIS1/14-3-3ε complex to the distal axon and this process is required for axonal elongation (Shinoda *et al*, 2007; Taya *et al*, 2007).

DISC1 participates in the maintenance of the neural progenitor pool (Mao *et al*, 2009). Neural progenitor proliferation can be regulated by the binding and inhibition of Glycogen Synthase Kinase 3 Beta (GSK3β) by DISC1 which prevents GSK3β autophosphorylation (Mao *et al*, 2009). Within the canonical Wnt signalling pathway GSK3β phosphorylates β-catenin, which is then targeted for destruction, preventing downstream gene activation by β-catenin that would otherwise mediate neuronal proliferation (Wu & Pan, 2010). Knockdown of DISC1 increases both phospho-β-catenin and GSK3β autophosphorylation as well as reducing

proliferation, whist overexpression of DISC1 acts with opposite effects (Mao *et al*, 2009). The DISC1-GSK3β interaction therefore stabilises the cellular pool of β-catenin allowing gene transcription to occur and promotes proliferation. The co-regulation of Wnt-GSK3β/β-catenin signalling and neural progenitor proliferation has been observed to occur via the interaction of DIX Domain Containing-1 (DIXDC1) with DISC1 (Singh *et al*, 2010). This interaction has been found to function in an additive fashion. Furthermore, these Wnt-GSK3β/β-catenin signalling findings are of interest regarding the treatment of bipolar disorder, as lithium chloride is a potent inhibitor of GSK3β and one of the most successful drug treatments to combat this disorder (Klein & Melton, 1996).

A switch in DISC1 phosphorylation governs the transition from the regulation of the proliferation of mitotic progenitor cells to the maintenance of the migration of post-mitotic neurones (Ishizuka *et al*, 2011). The switch is facilitated by phosphorylation at S713 in DISC1 and S710 in mouse DISC1. The absence of phosphorylation at DISC1 S710 positively regulates Wnt-GSK3β/β-catenin signalling, with both WT-DISC1 and phospho-dead mutant DISC1 A710 capable of rescuing downstream β-catenin signalling following DISC1 knockdown, but phospho-mimic mutant DISC1 E710 is unable to do so. Furthermore GSK3β binding is enhanced with phospho-dead mutant DISC1 A710 but not phospho-mimic mutant DISC1 E710 (Ishizuka *et al*, 2011). In contrast, the expression of the phospho-mimic mutant DISC1 E710 results in enhanced DISC1/BBS binding and increased localisation of these interacting species at the centrosome. A previous study has highlighted the importance of DISC1 interacting with BSS proteins and identified a role for these protein complexes at the centrosome in regulating neural migration so promoting cortical development (Kamiya *et al*, 2008). Further evidence supporting DISC1 pS710 as a molecular switch in neurodevelopment are rescue experiments following the knockdown of WT-DISC1. Proliferation deficits could only be rescued by WT-DISC1 or phospho-dead mutant DISC1 A710 whereas migration deficits could be rescued by WT-DISC1 or phospho-mimic mutant DISC1 E710 (Ishizuka *et al*, 2011).

Neural migration is also affected by the interaction of DISC1 with DIXDC1. This appears to be dependent on the phosphorylation of DIXDC1 by Cyclin-dependent Kinase 5 (CDK5) which regulates NDEL binding and promotes the formation of a DIXDC1/DISC1/ NDEL complex (Singh *et al*, 2010).

A role for DISC1 in the maturation and integration of neurones is in the hippocampus has been highlighted by DISC1 complexing with girdin (also known as KIAA1212) (Enomoto *et al*, 2009; Kim *et al*, 2009). This interaction is known to inhibit signalling through the

serine/threonine kinase V-Akt1 Murine Thymoma Viral Oncogene Homolog 1 (Akt1), whereas the overexpression of girdin alone potentiates Akt1 signalling (Kim *et al*, 2009). The knockdown of DISC1 in the adult mouse hippocampus produces neuronal morphological abnormalities that closely resemble the effects of either girdin overexpression or the expression of a constitutively active form of Akt1. These morphological deficits can be ameliorated following treatment with rapamycin, an inhibitor of the Akt1 effector, Mechanistic Target of Rapamycin (mTOR) (Kim *et al*, 2009). Together these results suggest that DISC1, girdin and Akt1 exist in a pathway within the adult hippocampus, regulating neuronal morphology. However, a parallel study by Enomoto *et al.*, (2009) addressing DISC1/girdin interaction and the effects on neuronal maturation in the dentate gyrus, observed that the morphological abnormalities present with girdin knockdown could not be rescued by constitutively active Akt1, implying that girdin acts downstream of Akt1.

Hippocampal maturation by DISC1 has also been identified to require signalling by the γ-aminobutyric acid $_{A}$ ($GABA_{A)}$ receptor to activate depolarization via the Na-K-Cl cotransporter NKCC1 (Kim *et al*, 2012). In adult-borne neurones in the dentate gyrus, the knockdown of DISC1 produces multiple neuronal deficits including accelerated dendrite growth. The knockdown of either NKCC1 or the $GABA_A$ receptor subunit $_{\gamma 2}$ are capable of rescuing DISC1 knockdown solely with respect to the dendritic growth deficits. The knockdown of NKCC1 or $GABA_A$ receptor subunit $_{\gamma 2}$ co-occurring with DISC1 knockdown also attenuates the increased Akt1 signalling that is evident with DISC1 knockdown alone (Kim *et al*, 2012). These findings suggest that DISC1 together with GABA signalling act synergistically to modulate the Akt1/mTOR pathway and regulate dendritic growth in adult neurogenesis. DISC1 knockdown or the exposure of mice to maternal deprivation stress individually have no effect on neuronal morphology. However, when the genetic and environmental insults are combined, a synergistic effect is noted with the early-postnatal dentate gyrus neurones bearing the same deficits as seen with DISC1 knockdown in adult-borne neurones (Kim *et al*, 2012). For the maternal stress/DISC1 knockdown neuronal deficits to be apparent in early-postnatal neurogenesis, depolarisation via GABA signalling appears to be required, as knockdown of NKCC1 rescues the majority of the morphological defects. Likewise, Akt1-mTOR signalling is involved in early-postnatal neurogenesis to produce the neuronal deficits following maternal stress/DISC1 knockdown as rapamycin could rescue the neuronal morphology. These findings indicate a conserved mechanism between DISC1, GABA signalling and the Akt1/mTOR pathway in the maintenance of neurogenesis with regard to early-postnatal neurones exposed to stress and adult-borne neurones within the dentate gyrus (Kim *et al*, 2012).

Recently further evidence has emerged regarding DISC1 signalling, the mTOR pathway and neuronal maturation. In adult mice, the selective knockdown of DISC1 in proliferating neural progenitors within the dentate gyrus induces a variety of dendritic abnormalities as well as cognitive and behavioural disturbances, with mice exhibiting a depression/anxiety-like phenotype (Zhou *et al*, 2013). Treatment of these animals with the mTOR inhibitor rapamycin rescued the neuronal abnormalities, reducing the number of primary dendrites and mispositioned neurones as well as ameliorating the cognitive and behavioural defects.

In addition to functional roles in regulating neuronal proliferation, migration and maturation, DISC1 is also known to participate in specific synaptic transmission and plasticity events which underpin the cellular basis of learning and memory (Hayashi-Takagi *et al*, 2010; Wang *et al*, 2011; Wei *et al*, 2014). Multiple studies on primate, human and rodent brain tissue samples and neurons have detected an enrichment of DISC1 expression within the post-synaptic density (PSD) (Bradshaw *et al*, 2008; Hayashi-Takagi *et al*, 2010; Kirkpatrick *et al*, 2006; Paspalas *et al*, 2013; Wang *et al*, 2011). The PSD is an electron and protein dense region of the postsynaptic neuron containing a network of signalling and structural molecules and is typically located at the tip of dendritic spines (Sheng & Kim, 2011). TRAF2 and NCK Interacting Kinase (TNIK) has been identified as a regulator of the actin cytoskeleton is enriched in the PSD and also binds to DISC1 (Wang *et al*, 2011). The kinase activity of TNIK is negatively regulated by DISC1. Studies that inhibit TNIK activity with a peptide designed to mimic DISC1 binding suggest that the interaction between these two molecules promotes degradation of synaptic proteins including, the α-amino-3-hydroxy-5-methyl-4-isoxazolepropionic acid (AMPA) receptor regulatory protein stargazin, the AMPA receptor subunit glutamate receptor, ionotropic, AMPA 1 (GluR1), and the scaffold protein and Postsynaptic Density Protein 95 (PSD-95) (Wang *et al*, 2011). Furthermore the interaction of TNIK with the DISC1 mimetic peptide reduces AMPA receptor miniature excitatory postsynaptic current (mEPSC) frequency and amplitude. Together these data suggest DISC1 may negatively regulate AMPA signalling at the PSD via interaction and inhibition of TNIK.

A signalosome between DISC1, the GDP/GTP exchange factor kalirin-7 (Kal7) and the Rho GTPase Ras-related C3 Botulinum Toxin Substrate 1 (Rac1) which regulates dendritic spine size has been identified (Hayashi-Takagi *et al*, 2010). Mechanistically the signalosome functions whereby DISC1 binds to and anchors Kal7, preventing both the access of Rac1 to Kal7 and subsequent Rac1 activation. The activity dependent stimulation of N-methyl-D-aspartate receptors (NMDAR) results in Kal7 release from DISC1 and access to Rac1 enabling the regulation of spinal morphology by activated Rac1 (Hayashi-Takagi *et al*, 2010).

DISC1 knockdown has been observed to result in an increase in NMDAR currents predominantly mediated by effects of glutamate receptor, ionotropic, N-Methyl D-Aspartate 2A (GluN2A) subunits (Wei *et al*, 2014). Likewise, the GluN2A subunits are also identified to be elevated by DISC1 gene silencing. These findings are thought to be underpinned by increased Protein kinase A (PKA) signalling. This may be mediated by the inhibition of the enzyme Phosphodiesterase 4 (PDE4), due to DISC1 knockdown. In the absence of DISC1 silencing, PDE4 has been observed to be sequestered by DISC1and then released in an active state, in response to elevated cellular cyclic adenosine monophosphate (cAMP) (Millar *et al*, 2005b; Murdoch *et al*, 2007). Active PDE4 then hydrolyses cAMP, resulting in the downstream reduction of PKA levels and cAMP Response Element-binding Protein (CREB) signalling. Wei *et al.*, (2014) suggest that following DISC1 silencing and subsequent PDE4 inhibition CREB is phosphorylated due to elevated levels of PKA. CREB then translocates to the nucleus to promote gene transcription of GluN2A, which then results in altered NMDAR signalling. This indicates a role of DISC1 and signalling downstream of DISC1 in the maintenance of NMDAR function. The results of the studies into TNIK, Kal7 and the NMADR have highlighted the role of DISC1 in glutamatergic neuronal transmission (Hayashi-Takagi *et al*, 2010; Wang *et al*, 2011; Wei *et al*, 2014). This is highly relevant to schizophrenia research as glutamatergic hypofunction is a known mechanism of pathogenesis in this disorder (Coyle, 2012).

In addition to the PSD, DISC1 has also been detected at the perisynaptic and extrasynaptic regions of dentritic spines of pyramidal neurones within layers II/III of the prefrontal cortex (PFC) (Paspalas *et al*, 2013). DISC1, PDE4 and dopamine receptor D_1 co-localise here with hyperpolarisation activated cyclic nucleotide gated channels (HCN), which regulate neuronal network firing. A cAMP signalplex is proposed by Pasapalas *et al.*, (2013) to dynamically regulate HCN channel gating. This would arise due to the close proximity of DISC1 and PDE4B, which together can modulate cAMP signalling (Millar *et al*, 2005b; Murdoch *et al*, 2007) along with co-localisation of D_1, activation which elevates cAMP levels, at the HCN channels.

Perturbations to dopamine (DA) signalling are of relevance to schizophrenia research given that the dopaminergic hypothesis proposes deficits in dopaminergic signalling at the synapse as a mechanism of pathogenesis with this disorder (Howes & Kapur, 2009). The knockdown of DISC1 in pyramidal neurones of the mouse PFC during early development results in reduced extracellular levels of DA, deficits in the maturation of axon terminals within the dopaminergic projection and a hypersensitivity to methamphetamine that are observed

postnatally (Niwa *et al*, 2010). Methamphetamine is a stimulant that acts upon the dopaminergic system and can induce schizophrenia-like symptoms (Robinson & Becker, 1986).

DA receptors D_1, D_2, and D_5 are targeted to primary cilia (Marley & von Zastrow, 2010). The knockdown of DISC1 in primary striatal neurons or cultured NIH3T3 cells reduces the number of primary cilia. This highlights a potential relationship between DISC1 and dopaminergic signalling.

The 100P mice contain ENU induced point mutations to DISC1 that cause amino acid changes (L100P) and result in a schizophrenia-like phenotype (Clapcote *et al*, 2007). When 100P mice are treated with the dopaminergic stimulant amphetamine, they display defects across a range of cognitive-behavioural assays in comparison to wild type controls (Lipina *et al*, 2010). The cognitive and behavioural impairments in 100P mice can be rescued following treatment with the typical antipsychotic haloperidol. A D_2/DISC1 complex has been identified that is dependent on D_2 activation (Su *et al*, 2014). The complex has been observed to be increased in post-mortem brain tissue from sufferers of schizophrenia and 100P mice. D_2/DISC1 complex formation reduces the phosphorylation of GSK3β at serine 9, which increases the availability of the GSK3β active site favouring GSK3β pathway upregulation. Su *et al.,* (2014) developed an interfering peptide to disrupt the D_2/DISC1 interaction and prevent the modulation of GSK3β phosphorylation. The interfering peptide also proved capable of rescuing the schizophrenia-like behaviours of the 100P mice. Evidence of dopaminergic dysfunction in DISC1 C-terminal truncated mice is detailed in section 1.2.9.

1.2.8 *In vitro* overexpression of DISC1 aa1-597 in cultured cells

The concept of a dominant-negative truncated DISC1 species encoded by the DISC1 ORF proximal to the t(1;11) was first proposed by Millar *et al.,* (2000). Consequently several laboratories have investigated the functional properties of the species that could potentially be encoded, DISC1 aa1-597. The existence of DISC1 aa1-597 as a mechanism of pathogenesis within the t(1;11) pedigree is non-mutually exclusive to the haploinsufficiency of DISC1 (Millar *et al*, 2005b). *In vitro*, the overexpression of DISC1 aa1-597 along with DISC1 causes the dominant-negative redistribution of DISC1, from a punctate localisation to the diffuse cytoplasmic distribution typical of DISC1 aa1-597 expression. This phenomenon is a due to a self-association domain located in DISC1 aa403-504 that is retained in DISC1 aa1-597 (Kamiya *et al*, 2005). As such, when DISC1 is co-expressed with DISC1 aa1-597, the anchoring of the dynein motor protein by DISC1 to the centrosome is perturbed. The

overexpression of DISC1 aa1-597 in COS-7 cells can also produce a lariat or 'ring' shaped mitochondrial morphology, in a subset of transfected cells (Millar *et al*, 2005a).

Complementary to the structural mitochondrial alterations due to the overexpression of DISC1 aa1-597 that were reported by Millar *et al.*, (2005a), is research showing that DISC1 aa1-597 overexpression is detrimental to mitochondrial function. The overexpression of a mouse equivalent of DISC1 aa1-597 alters mitochondrial bioenergetics, reducing both NADPH dehydrogenase activity (respiratory chain complex I) and ATP levels (Park *et al*, 2010). Regarding neuronal-like cellular functions, the expression of DISC1 aa1-597 *in vitro* impairs neurite outgrowth in PC12 cells with both transient transfection (Ozeki *et al*, 2003) and inducible DISC1 aa1-597 (Pletnikov *et al*, 2007). DISC1 aa1-597 also inhibits axon elongation in hippocampal cultures (Taya *et al*, 2007). DISC1 has been identified as negatively regulating oligodendrocyte differentiation, in contrast the exogenous expression of DISC1 aa1-597 promotes oligodendrocyte differentiation (Hattori *et al*, 2014) The *in vitro* expression of DISC1 aa1-597 has a multitude of deleterious effects that could perturb normal cell functioning. However at present endogenous DISC1 aa1-597 has not been detected.

1.2.9. DISC1 C-terminal truncated mouse models

1.2.9.1 Neuronal transgene expression in C-terminal truncated DISC1/*Disc1* models

Three transgenic mouse models have been created that express human DISC1 aa1-597 neuronally (Hikida *et al*, 2007; Niwa *et al*, 2013; Pletnikov *et al*, 2008) (see table 1.2.B). Two of these transgenic models use a Ca^{2+}/Calmodulin-dependent Protein Kinase II (CaMKII) promoter to drive human DISC1 aa1-597 transgene expression. In the Hikida *et al*, (2007) murine model, referred to as the DN-DISC1 mouse, the transgene is constitutively active. In contrast, the ΔhDISC1 mouse (Pletnikov *et al*, 2008), uses an inducible induction system. This is due to the incorporation of a Tet-off system that regulates the CaMKII promoter activity. Most recently, the third mouse line, expressing a human DISC1 aa1-597 transgene, has been generated. The DISC1-DN-Tg-PrP mouse line uses a prion promoter to express truncated DISC1 (Niwa *et al*, 2013). The use of a prion promoter, as opposed to the CaMKII promoters used in previous DISC1 aa1-597 models (Hikida *et al*, 2007; Pletnikov *et al*, 2008), appears to produce a transgene expression profile with greater similarity to endogenous DISC1 expression (Niwa *et al*, 2013).

A transgenic mouse model has been produced that expresses a truncated Disc1 species (Shen *et al,* 2008) (see table 1.2.B). The *Disc1$_{tr}$* mice express two copies of Disc1 exons 1-8, from a mouse BAC, with the truncated expression driven by endogenous promoters (Shen *et al,* 2008). This is important when making comparison to murine transgenic models that express DISC1 aa1-597 using constitutively active CaMKII (Hikida *et al,* 2007) and prion promoters (Niwa *et al,* 2013) or an inducible CaMKII promoter (Pletnikov *et al,* 2008). Beyond this intrinsic difference in promoter expression and the use of truncated mouse DISC1 as opposed to DISC1 aa1-597, the *Disc1$_{tr}$* is conceptually very similar to the DISC1 1-597 mouse models.

1.2.9.2 Behavioural alterations associated with C-terminal truncated DISC1/Disc1 models

The NMDA receptor hypofunction theory of schizophrenia (or glutamatergic hypofunction theory) proposes that alterations to NMDA receptor function in neurodevelopment and the consequential disruption to neuronal structure and function underpin the pathogenesis of schizophrenia (Coyle, 2012). The NMDA receptor antagonists, MK-801, phencyclidine (PCP) and ketamine, have been used to investigate and validate components of this theory in human and animal models and subsequently these compounds are now used to pharmacologically model schizophrenia-like behaviour (Bubeníková-Valešová *et al*, 2008). The ΔhDISC1 male mice show an increase in locomotor activity following treatment with MK-801 that is significantly higher than the increase that is observed in control mice (Ayhan *et al,* 2011). This observed hyperlocomotion may be regarded as a greater propensity to psychosis-like behaviour in the context of the antagonism of NMDA receptor activity (Bubeníková-Valešová *et al,* 2008).

Behavioural assays	LI (attention)				Y
	PPI (sensori-motor gating)	Y 74dB/n	/n	/y¥ 78 & 86 dB	
	Morris Water Maze (spatial learning and memory)	N	Y♀/n		
	Fear conditioning	/y			
	Y-maze (working memory)	N/y	/n		
	TST immobility				Y
	FST immobility	Y		/y¥	Y
	Elevated plus-maze (anxiety)	N	/y		
	Abnormal social interaction	/y(- CL,Hal)	Y♂/y♂		
	MK-801 induced hyperactivity	/y(+ CL,Hal)			
	Open field locomotor activity	Y	Y♂/y♂	/y¥	N
Dopaminergic dysfunction	Amphetamine hyperactivity	Y♂/y	Y♂	/y¥	
	Dopamine	Excel meth↑♂ excel BL ↓♂ D_2↑♂ DAT↑♂	FC♂↓ DA HC♀→ DA DOPAC♂↓	[Excel DA ↓FC¥] [excel mth N FC] ↓FC DA	
	T. hydroxylase			/↓FC¥	
Histology/ morphology	Interneurones	↓PV/↓PV	↓ PV→CR		↓PV
	LV vol	↑L†	↑/→	→	↑
	Primary neurite outgrowth		↓		↓
	Corpus Callosum				↓
	Total cortex vol		↓		↓
	Total brain vol		→		↓♂
	Promoter	CaMKII constituative	Tet-off CaMKII inducible	Prion constituative	BAC endogenous
	Transgene	human DISC1 aa 1-597			Exons 1-8
		DN-DISC	ΔhDISC1	DISC1-DN-Tg-PrP	*Disc1*$_{tr}$

Table 1.2.B: The featured histological, dopaminergic and behavioural characteristics of C-Terminal truncated DISC1 and *Disc1* transgenic mouse models. Left hand side of / denotes conventional genetic model, right hand side of / denotes gene-environment model.

Key to table 1.2.B.

L†	Left lateral ventricle increase, reverts at 3 months old
¥	ameliorated by treatment with the glucocorticoid antagonist RU38486
-	No response to drug treatment
+	Positive response to drug treatment
♂	Male
♀	Female
↑	Increase
↓	Decrease
→	No change
BAC	Bacterial artificial chromosome
CaMKII	Ca^{2+}/calmodulin activated kinase II
CL	Clozapine
CR	Calretinin
dB	Decibels
D_2	Dopamine receptor D_2
DA	Dopamine
DAT	Dopamine active transporter
dB	Decibels
DN	Dominant negative
DOPAC	3,4-Dihydroxyphenylacetic acid
Excel BL	Extracellular baseline dopamine
Excel DA	Extracellular dopamine
Excel mth	Extracellular dopamine following methamphetamine challenge
FC	Frontal cortex
Hal	Haliperidol
HC	Hippocampus
LI	Latent inhibition
LV	Lateral ventricles
N	Tested on given behavioural assay but did not show significant change lower case denotes this in gene environment model
PPI	Prepulse inhibition
PV	Parvalbumin
Y	Shows significant change, lower case is significant change in gene environmental model
T. Hydroxylase	Tyrosine Hydroxylase

The open field activity is a general measure of the locomotor activity and has been frequently used in the testing of anxiolytic compounds, whereby the increased activity of the mouse is seen to represent the animals level of stress (Prut & Belzung, 2003). However, how the measurement of locomotor activity varies between mouse lines and specific protocols can impair inter-experimental comparison (Stanford, 2007). Open field activity is observed to be increased in the DN-DISC1 and male ΔhDISC1 mice (Hikida *et al*, 2007; Pletnikov *et al*, 2008), suggesting that these mice have an anxiety-like behavioural phenotype.

Forced swim test (FST) deficits are observed in two of the models expressing DISC1 aa1-597 (Hikida *et al*, 2007; Pletnikov *et al*, 2008) and are also seen in the *Disc1*$_{tr}$ mice (Shen *et al*, 2008). This assay measures the amount of time a mouse spends immobile following immersion in a water filled tube. In a similar behavioural assay, the tail suspension test (TST), mice are

hung by their tails and the time the animal spends immobile is recorded. Both female ΔhDISC1 (Ayhan *et al*, 2011) and the *Disc1*$_{tr}$ mice (Shen *et al*, 2008) show an increased time immobile during tail suspension. These assays have been described in papers as 'depression tests' (Shen *et al*, 2008); as a means to 'test depression-like behaviours' (Ayhan *et al*, 2011); or assays that 'may parallel anhedonia seen in schizophrenia' (Hikida *et al*, 2007). However, both the FST and TST were developed as rapid means to screen antidepressant effects within pharmaceutical animal trials. Due to the inherent "black box" design of these tests, their validity as measures of depression-like behaviour is contentious (Nestler & Hyman, 2010).

Functional impairments in cognition are associated with schizophrenia (Green *et al*, 2000) and are now thought to be core features of the illness (Keshavan *et al*, 2011). Deficits in spatial learning memory had been detected in the female ΔhDISC1 mice following Morris water maze trials (Pletnikov *et al*, 2008). Regarding psychiatric illness, the meta-analysis of working memory studies assessing the task performance in schizophrenia groups, identifies defects to this cognitive system. Within these analyses, a domain specific impairment to visuospatial working memory is also identified (Forbes *et al*, 2009; Lee & Park, 2005). The degree of impairment in verbal and spatial working memory task performance in both individuals with bipolar disorder and those with schizophrenia is similar (Glahn *et al*, 2006). However, the spatial working memory deficits seen in bipolar disorder are specific to those patients with history of psychosis (Glahn *et al*, 2006). Therefore, it may be that the repeated occurrence of psychosis impairs this cognitive function or that the impairment represents underlying aberrant neurodevelopment associated with psychosis proneness. The investigation of working memory problems within depression has produced mixed results. This appears to be the consequence of methodological problems and measured deficits actually originating from non-specific effects. It remains possible that working memory impairment *per se* is simply associated with mental illness (Gotlib & Joormann, 2010).

The *Disc1*$_{tr}$ mice have impaired latent inhibition (LI) (Shen *et al*, 2008). Latent inhibition occurs when prior exposure to a stimulus, such as an acoustic tone, later has the effect of inhibiting the association between the noise and an unconditioned stimulus, such as a food pellet (Arguello & Gogos, 2006). LI is believed to be a measure of attention. In relation to schizophrenia, reduced LI is seen in unmedicated patients and this can be ameliorated by antipsychotic medication. In line with this, in mouse models, LI phenomena are reduced by dopaminergic agonism and are increased with dopaminergic antagonism (Lubow, 2005).

In the initial characterisation, the DN-DISC1 mice possess an impairment in prepulse inhibition (PPI) that was identified at 74dB (Hikida *et al*, 2007). The PPI assay is a measure

of sensorimotor gating. It is the attenuation of startle response to a loud noise, whereby before the delivery of the loud noise the subject is exposed to an initial pre-pulse stimulus of low intensity noise. PPI results when the low intensity noise diminishes the following response to the loud noise. As such, PPI is seen as a measure of the ability to gate superfluous sensory data (Arguello & Gogos, 2006). PPI deficits have been repeatedly identified in individuals with schizophrenia and there is a degree of cross species similarity between rodent and human PPI results. However, impairment in PPI is not specific to sufferers of schizophrenia although the bulk of research into PPI has predominantly focussed on schizophrenia (Swerdlow *et al*, 2008). Compared to schizophrenia, relatively few studies have been conducted into PPI in bipolar disorder. Abnormal PPI performance has been investigated in eurhythmic bipolar patients and shows sexual dimorphism, in which the PPI response is increased in females and decreased in males (Gogos *et al*, 2009). Interestingly, the PPI impairment that is detected in bipolar patients that are suffering from acute mania with psychosis and individuals with schizophrenia do not differ significantly (Perry *et al*, 2001).

The male ΔhDISC1 mice show evidence of abnormal murine social interaction and have an increase in aggressive behaviours (Ayhan *et al*, 2011; Pletnikov *et al*, 2008). Such aberrant behaviours may be seen as analogous to deficits in social cognition which are frequently seen as a core symptom of schizophrenia (Couture *et al*, 2006).

1.2.9.3 Histopathology & morphology of C-terminal truncated DISC1/*Disc1* models

The DN-DISC1 (Hikida *et al*, 2007), ΔhDISC1 (Pletnikov *et al*, 2008) and $Disc1_{tr}$ (Shen *et al*, 2008) mice all possess enlarged lateral ventricles. This gross anatomical abnormality is the most common pathophysiological feature detected in sufferers of schizophrenia in magnetic resonance imaging (MRI) studies (Shenton *et al*, 2001). Unusually, in the DN-DISC1 mice, the lateral ventricular abnormality reverts to normal by three months of age (Hikida *et al*, 2007). Furthermore, enlarged lateral ventricular phenotype in the ΔhDISC1mice appears to be dependent on postnatal transgene expression (Ayhan *et al*, 2011). In the ΔhDISC1 mice, the lateral ventricular observations may partly be accounted for by a reduction in the arborisation of primary neurones that is observed (Pletnikov *et al*, 2008). Unusually, when the DISC1-DN-Tg-PrP transgene is expressed alone, in the absence of environmental stress modelling, lateral ventricular enlargement is absent. This could possibly be a consequence of the use of a prion promoter in this model (Niwa *et al*, 2013).

The number of GABAergic parvalbumin-positive interneurones in the PFC is reduced in the *Disc1*$_{tr}$ (Shen *et al*, 2008), ΔhDISC1 (Ayhan *et al*, 2011) and DN-DISC1 mice (Hikida *et al*, 2007). Parvalbumin-positive interneurones and the consequential altering of neuronal inhibition have been associated with schizophrenia. In particular, with the presence of cognitive deficits (Lewis *et al*, 2012; Lewis *et al*, 2005). In the *Disc1*$_{tr}$ model, the parvalbumin staining is also observed to be reduced in the hippocampus (Shen *et al*., 2008).

The *Disc1*$_{tr}$ (Shen *et al*, 2008) mice also possess a partial agenesis of the corpus callosum, the largest fibre tract in the brain, which connects both hemispheres. The meta-analysis of MRI studies concerning schizophrenia and the corpus callosum observes the reduction of callosal fibres is seen in patients with schizophrenia (Arnone *et al*, 2008).

Total cortex volume is seen to be reduced in both the *Disc1*$_{tr}$ (Shen *et al*, 2008) and the ΔhDISC1 mice (Ayhan *et al*, 2011). Reduced cortical thickness is apparent in schizophrenia (Rimol *et al*, 2012) and is even detected in first episode sufferers (Schultz *et al*, 2010). In bipolar disorder, a subgroup of patients show evidence of reduced cortical thickness that is specific to the frontal lobes (Rimol *et al*, 2012). The *Disc1*$_{tr}$ (Shen *et al*, 2008) mice additionally possess a reduction in total brain volume that is specific to the male mice. Meta-analysis of MRI publications reveals that total brain volume is frequently decreased in cases of first episode schizophrenia (Steen *et al*, 2006) and that, over time, the loss of brain volume in individuals with schizophrenia occurs at an increased rate compared to controls (van Haren *et al*, 2008).

Additionally, in both the ΔhDISC1 (Pletnikov *et al*, 2008) *Disc1*$_{tr}$ mice (Shen *et al*, 2008), reduced neurite outgrowth is evident in primary neurone cultures. This is an autonomous cell mechanism that is thought to partially explain the gross anatomical anomalies that are seen in these mouse models.

1.2.9.4 Dopaminergic alterations in C-terminal truncated DISC1/*Disc1* models

The dopaminergic hypothesis of schizophrenia has been central to psychiatric research for decades. A current iteration of this hypothesis involves alterations to dopaminergic function at the synapse which cumulates in the induction of psychosis within vulnerable individuals predisposed by both genetic and environmental risk factors (Howes & Kapur, 2009). The assessment of the impact of methamphetamine treatment on the locomotion of mice in the open field is seen as a measure of psychosis-like behaviour. This concept originates from clinical findings that chronic amphetamine users would frequently go on to develop psychosis

and other symptoms of schizophrenia whilst positive symptoms of schizophrenia are exacerbated by amphetamine use. Subsequently, the treatment of rodents with amphetamine is observed to elicit behavioural hyperactivity and stereotypy which is seen to be a model of possible dopaminergic dysfunction in schizophrenia (Robinson & Becker, 1986). The augmentation of hyperlocomotion is observed in both male DN-DISC1 (Jaaro-Peled *et al*, 2013) and ΔhDISC1 (Ayhan *et al*, 2011) mice following treatment with methamphetamine and d-amphetamine respectively. In the male ΔhDISC1 mice, the levels of DA and DOPAC, a DA metabolite, are decreased in the frontal cortex (FC). The reduced DA levels in the FC may contribute to the augmentation of locomotion following amphetamine treatment (Ayhan *et al*, 2011).

Converging evidence that includes neuroimaging, autoradiography and molecular biology, detects evidence of dysfunction within the dopaminergic system of the DN-DISC mice. In the striatum, the levels of D_2 receptors and the DA transporter (DAT) are increased while baseline DA levels are reduced (Jaaro-Peled *et al*, 2013). Within the striatum, in populations with schizophrenia, a small, but significant, increase in D_2 receptor levels is frequently observed (Brunelin *et al*, 2013). For DAT, with a role in the reuptake of DA at the synapse, the majority of studies have found no evidence of abnormal DAT density in schizophrenia. However, in addition to this, there is evidence that the DAT density may be increased in major depressive disorder (Brunswick *et al*, 2003; Laasonen-Balk *et al*, 1999).

1.2.9.5 Gene-environment interactions in C-terminal truncated DISC1 models

The DN-DISC1 (Hikida *et al*, 2007) and the ΔhDISC1 (Pletnikov *et al*, 2008) mouse models have been used to simulate gene-environment effects on neurodevelopment. This involved the injection of neonatal DN-DISC1 mice with poly I:C in the early postnatal period (Ibi *et al*, 2010; Nagai *et al*, 2011) or the exposure of mice *in utero* to poly I:C in parallel with prenatal transgene activation in the ΔhDISC1 mice (Abazyan *et al*, 2010). The administration of poly I:C, an inflammatory agent, mimics viral infection, and is commonly used in animal models of schizophrenia (Meyer & Feldon, 2012). It is thought that prenatal viral infection as an environmental factor has a role in the aetiology of schizophrenia by perturbing neurodevelopment (Brown & Derkits, 2010).

The DISC1-DN-Tg-PrP mouse (Niwa *et al*, 2013) has primarily been used in a gene-environment paradigm to investigate the effects of stress isolation in adolescence as an

environmental factor in conjunction with a genetic risk - the expression of hDISC1 aa-1-597 - on dopaminergic function.

1.2.9.6 Behavioural alterations associated with gene-environment C-terminal truncated DISC1 models

The male ΔhDISC1/poly I:C mice have increased locomotor activity and spend less time in the open arms of the elevated plus-maze (Abazyan *et al*, 2010). These behavioural alterations are indicative of increased anxiety-like behaviours (Prut & Belzung, 2003; Walf & Frye, 2007). In itself, anxiety can be a mental illness and anxiety disorders often occur comorbid with schizophrenia (Achim *et al*, 2011), bipolar disorder (Keller, 2005) and depression (Kessler *et al*, 2005). Furthermore, the male ΔhDISC1/poly I:C mice show evidence of abnormal social interaction and spend a significant time immobile in the forced swim test (Abazyan *et al*, 2010). The abnormal social interaction may be evidence of deficits in social cognition, a core feature of schizophrenia (Couture *et al*, 2006), while the forced swim test is a "black box" test used to trial susceptibility to antidepressant drugs (Nestler & Hyman, 2010).

The DN-DISC1/poly I:C mice have multiple behavioural deficits. Cognition is affected, including hippocampus-dependent fear memory and short term memory deficits. Social interaction is also reduced and the DN-DISC1/poly I:C mice show more aggressive behaviours (Ibi *et al*, 2010; Nagai *et al*, 2011). The social interaction abnormalities are not rectified following the administration of the antipsychotics, clozapine and haloperidol (Nagai *et al*, 2011). This finding is relevant to schizophrenia, in that, negative symptoms in affected individuals, such as social withdrawal, are less responsive to treatment with both first generation antipsychotics, including haloperidol, or second generation antipsychotics, such as clozapine (Tandon *et al*, 2010). Conversely, when a pharmacological challenge, using the NMDAR antagonist MK-801, is applied to the DISC1/poly I:C to induce NMDA receptor hypofunction and pharmacologically model schizophrenia (Bubeníková-Valešová *et al*, 2008), these mice have a greater susceptibility to MK-801 induced hyperactivity than controls (Ibi *et al*, 2010; Nagai *et al*, 2011). The augmentation of locomotion seen in the DISC1/poly I:C can be ameliorated by treatment with antipsychotics. This observation reflects that the positive symptoms of schizophrenia, which are seen as additional to normal experience and are responsive to treatment with antipsychotics (Tandon *et al*, 2010), such behaviours can be seen to be psychosis-like (Bubeníková-Valešová *et al*, 2008).

The DN-DISC1/poly I:C mice display reduced performance in the Y-maze, a behavioural assay that assesses spatial working memory function (Ibi *et al*, 2010). This observation highlights a deficit to working memory resulting from truncated DISC1 expression. Additionally, the DN-DISC1/poly I:C mice have an impairment in fear conditioning (Ibi *et al*, 2010). This behavioural learning and memory paradigm involves associative learning of an unconditioned stimulus such as a tone with a fear inducing conditioned stimulus, e.g. electric shock. Typically, the fear conditioning model is used to study the amygdala molecular pathways and synaptic plasticity mechanisms involved in the learning of fearfulness (Johansen *et al*, 2011). The fear conditioning behavioural assay, performed by the DN-DISC1/poly I:C mice, is contextual (Ibi *et al*, 2010) and as such would involve hippocampal signalling to enable the processing of fear memories (Lee *et al*, 2004). The insights resulting from fear conditioning studies may be translatable to the investigation of anxiety disorders (Johansen *et al*, 2011).

In the DISC1 aa1-597 expression by social isolation gene environment paradigm that was initiated by Niwa *et al*, (2013), the mice showed deficits in PPI and FST, as well as hyperlocomotion at both basal levels and following methamphetamine treatment. These behavioural abnormalities are indicative of sensorimotor impairment (Arguello & Gogos, 2006) and positive symptoms of schizophrenia (i.e. psychosis) (Robinson & Becker, 1986), as well as the increased immobility in FST which could be indicative of antidepressant responsiveness (Nestler & Hyman, 2010). Following treatment with the glucocorticoid antagonist RU38486, all of these behavioural defects are ameliorated (Niwa *et al*, 2013). This occurs as stress activates glucocorticoids which in turn increase DA levels leading to psychosis-like behaviour (Corcoran *et al*, 2003).

1.2.9.7 Histopathology & morphology of C-terminal truncated DISC1 gene-environment models

Unusually, it appears that the poly I:C treatment, in conjunction with the transgene expression, may attenuate the enlargement of the lateral ventricles (Abazyan *et al*, 2010) compared to the enlargement seen with expression of the transgene alone in the ΔhDISC1 mice (Pletnikov *et al*, 2008).

1.2.3.8 Dopaminergic alterations in C-terminal truncated DISC1 gene-environment models

Following the isolation stress, the DISC1-DN-Tg-PrP mice show a range of perturbations to DA function as well as elevated glucocorticoid levels (Niwa *et al*, 2013) (see table 1.2.B). The majority of these alterations to measures of dopaminergic function within this gene-environment paradigm can be ameliorated following the treatment of the mice with RU38486, a glucocorticoid antagonist. Specifically, the alterations to the dopaminergic system with the DISC1-DN-Tg-PrP/social stress mice are isolated to both the FC and nucleus accumbens. Of the two brain regions, it is the dopaminergic impairment tractable to the FC which is associated with epigenetic modification of the tyrosine hydroxylase promoter by increased methylation. Tyrosine hydroxylase is of fundamental importance to dopaminergic neurotransmission as this enzyme converts tyrosine into DOPA prior to DOPA being synthesised into DA by DOPA decarboxylase (Rang *et al*, 2003). This modification occurs via the mesocortical pathway which projects between the ventral tegmental area and the FC. This methylation of the tyrosine hydroxylase promoter, specific to the mesocortical pathway, is reduced when the mice are treated with the glucocorticoid antagonist, RU38486. It is proposed by Niwa *et al*, (2013) that the DISC1-DN-Tg-PrP gene environment paradigm used is a model of psychotic depression.

1.2.3.9 Expression of truncated DISC1 species in glial cells

The ΔhDISC1 mouse model has also been used to investigate oligodendrocyte development in relation to the expression of DISC1 aa1-597 (Katsel *et al*, 2011) (see table 1.2.C). Perturbation to myelination and abnormalities to oligodendrocytes are detectable in schizophrenia (Flynn *et al*, 2003; Tkachev *et al*, 2003). In 12 month old ΔhDISC1 mice, oligodendrocyte lineage genes are strongly upregulated in both the FC and the white matter. In line with this finding, genes related to glial progenitor cells and oligodendrocytes show a strong trend to upregulation at E15. Upregulation at P1 is markedly reduced from the levels of E15 but the trend is still that of a statistically significant increase in gene expression. These early developmental alterations are thought to be underpinned by a dysregulation of cell cycle genes. This is interpreted by Kastel *et al*, (2011) to be causative to an increase in the proliferation of oligodendrocyte precursors in the absence of differentiation at E15 followed by a premature increase in differentiation at P1. The expression of the neuregulin signalling genes, *Erb-B2 Receptor Tyrosine Kinase 3* (*ERBB3*), *ERBB4* and *Neuregulin 1* (*NRG1*) are also altered. These three genes show a trend towards upregulation in the forebrain in early neurodevelopment and white matter at 12 months. NRG1 signalling may underpin the

oligodendrocyte abnormalities seen in the ΔhDISC1 mouse model, given that NRG1 signalling can promote the myelination of oligodendrocytes (Taveggia *et al*, 2008). Overall, the Katsel *et al,* (2011) manipulation of the ΔhDISC1 mouse line indicate a possible role for DISC1 in the proliferation and differentiation of oligodendrocytes that may relate to clinical observations seen in schizophrenia.

A novel adaption to study the effects of expression of human DISC1 aa1-597 in a mouse is the ΔC-hDISC1 mouse line (see table 1.2.C). In these transgenic mice, human DISC1 aa1-597 can be expressed in astrocytes via an inducible Glial Fibrillary Acidic Protein (GFAP) promoter (Ma *et al*, 2012). Such a model enables the investigation of truncated DISC1 expression along with theories of NMDA hypofunction (Coyle, 2012). This is because astrocytes contain serine racemase, the enzyme which synthesises D-serine, a potent NMDAR co-agonist (Wolosker *et al*, 1999). The selective expression of DISC1 aa1-597 transgene is associated with both a reduction in D-serine in adult ΔC-hDISC1 mice that had the transgene induced throughout their life span. These mice displayed abnormalities in both MK-801 induced hyperactivity in the open field and to MK-801 facilitated PPI. The administration of exogenous D-serine rectified the locomotion abnormalities in male and female ΔC-hDISC1 mice and partially ameliorated the PPI response in male mice (Ma *et al*, 2012). The work of Ma *et al*, (2012), highlights how glial mediated glutamatergic neurotransmission can be altered following the expression of DISC1 aa1-597.

Gene expression	ERBB4		↑FB [P1, 12MO]
	ERBB3		↑FB [E15, 12MO] ↓FB [P1] ↑WM [12MO]
	NRG1		↑FB [E15, 12MO] ↑WM [12MO]
	OLG lineage genes		Trend upregulation [12MO]
	OLG related genes		Trend upregulation [E15, P1]
	Cell cycle		Trend dysregulation
Behavioural assays	MK-801 induced hyperactivity	Y^{ds}	
	MK-801 impaired PPI	Y, $p4^{ds}$ & p8, ♂	
Molecular dysfunction	D-Serine	↑Ctx [P21] ↓Ctx [P0] ↓P.Ast	
	SR	↓P.Ast ↓FB	
Mouse model	Promoter	Tet-off GFAP	Tet-off CaMKII
	Transgene	human DISC1 aa 1-597	
	Model name	ΔC-hDISC1	ΔhDISC1

Table 1.2.C: Characteristics of DISC1 C-terminal truncated transgenic models and their effect on glia.

Key to table 1.2.B.

12MO	12 Months old
♂	Male
↑	Increase
↓	Decrease
CaMKII	Ca^{2+}/calmodulin activated kinase II
Ctx	Cortex
^{ds}	Ameliorated by D-serine treatment
E15	Embryonic day 15
FB	Forebrain
GFAP	Glial fibrillary acidic protein
p	Prepulse intensity above background level of 70 dB
P0	Postnatal day 0
P1	Postnatal day 1
P21	Postnatal day 21
P.Ast	Primary Astrocytes
SR	Serum racemase
WM	White matter
Y	Shows significant change

1.2.10 DISC1/DISC1FP1 chimeras to date

Following the isolation of the *DISC1FP1* gene (Eykelenboom *et al*, 2012) also known as *Boymaw* at 11q14.3 (Zhou *et al*, 2010; Zhou *et al*, 2008), a novel mechanism of pathogenesis was proposed whereby *DISC1* may fuse with *DISC1FP1* to produce abnormal chimeric transcripts. This had the potential to produce both der1 and der11 aberrant protein species. Since this initial observation 3 *DISC1/DISC1FP1* chimeric transcripts have been identified in t(1;11)-family derived lymphoblastoid cell lines (Eykelenboom *et al*, 2012). The der 1 *DISC1/DISC1FP* transcripts of Chimeric Proteins 60 and 69 (*CP60*) and (*CP69*) arise from the splicing of exon 8 of *DISC1* to exon 4 of the *DISC1FP1* ESTs CK000409 or BU599486, respectively (Eykelenboom *et al*, 2012) (see figure 1.2.C). CP60 encodes DISC1 aa1-597 plus an additional 60aa from *DISC1FP1* whilst CP69 encodes DISC1 aa1-597 plus a further 69 aa from *DISC1FP1*. It is possible that CP60 and CP69 could be expressed endogenously in the t(1;11) family under the *DISC1* promoter and that the novel protein structure of these species may confer gain of function or dominant negative effects that are functionally different to the established roles of DISC1. As such putative pathogenic mechanisms of CP60 and CP69 require further investigation.

The third *DISC1/DISC1FP1* transcript identified by Eykelenboom *et al.,* (2012) is a der 11 species and is produced by the splicing of *DISC1FP1* exon 2 to *DISC1* exon 8. In the der 11 transcript multiple stop codons are present and the only significant ORF is internal and

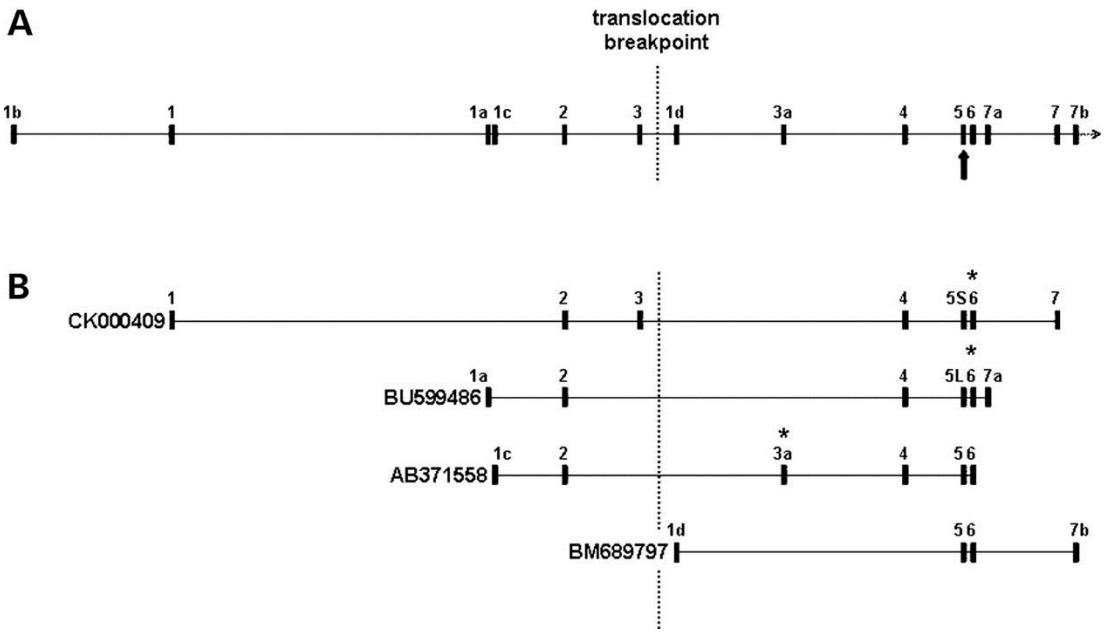

Figure 1.2.C: Schematic of *DISC1FP1* (not to scale). (A) Genomic structure of *DISC1FP1* denoting exons, arrow indicates alternatively spliced exon 5, vertical dashed line demarks translocation breakpoint. (B) *DISC1FP1* ESTs: CK000409 encodes CP60 and BU599486 encodes CP69 which comprise DISC1 aa1-597 plus an additional 60 or 69aa from DISC1FP1, respectively. The investigation into species encoded by AB371558, will be a component of this thesis. Asterisks indicate predicted stop codons. Adapted from Eykelenboom *et al.,* (2012).

---

encodes aa669–854 of the DISC1 C-terminus, which would suggest it is unlikely that this transcript would be expressed endogenously. Interestingly, a transgenic mouse model has been produced that expresses DISC1 aa671–852 in the forebrain (Li *et al*, 2007). These animals had a schizophrenia-like phenotype that includes deficits to working memory and reduced dendritic complexity.

Since the identification of the three *DISC1/DISC1FP1* transcripts by Jennifer Eykelenboom another *DISC1FP1* EST, AB371558 has been identified (see figure 1.2.B.). Further investigation is needed to detect possible der 1 and der 11 *DISC1/DISC1FP1* transcripts that may be produced by the fusing of AB371558 with *DISC1*.

1.2.11 DISC1 and mitochondrial function

Several studies highlight the importance of DISC1 on mitochondrial function. 71 kDa and 75 kDa isoforms of DISC1 have been isolated in the mitochondrial fraction (James *et al*, 2004) and DISC1 co-localises with mitochondria in cell lines (James *et al*, 2004; Millar *et al*, 2005) and primary cortical neurons (Brandon *et al*, 2005). Further studies have also been performed that suggest DISC1 is located on the inside of the outer mitochondrial membrane (James *et al*, 2004; Park *et al*, 2010). Additionally investigations by Ramsey *et al*., (2011) and Paspalas *et al*., (2013) observe DISC1 at the mitochondria but fail to give precise details of localisation. A recent study by Ogawa *et al.,* (2014) indicates that DISC1 is also located on the outside of the mitochondria as a component of the mitochondrial transport complex. Within this complex DISC1 interacts with the milton homolog, Trafficking Protein, Kinesin Binding 1 (TRAK1) an adaptor protein, as well the mitochondrial membrane anchor Mitochondrial Rho GTPase 1 (Miro1). The variant R37W is an ultra-rare DISC1 mutation that has been identified in an individual with schizophrenia (Song *et al*, 2008) and within a Scottish family. Here, DISC1 R37W occurs in two sufferers of major depressive disorder and one of generalised anxiety (Thomson *et al*, 2014). The cellular expression of DISC1-37W is associated with the redistribution of DISC1 and the formation of clustered peri-nuclear mitochondria (Ogawa *et al*, 2014). These effects are likely mediated via an increased association DISC1-37W shows for TRAK1. Furthermore, an uncoupling effect of DISC1-37W on TRAK1-Miro1 interaction was also observed

Given the association of DISC1 with the mitochondrial transport complex, Ogawa *et al*,. (2014) assessed the effect of DISC1 on mitochondrial movement. While DISC1 promotes anterograde mitochondrial movement, DISC1-37W has no effect on anterograde transport. A previous study by Atkin *et al.,* (2011) noted an increase in total mitochondrial movement. Methodological differences likely underpin the lack of concordance of this result with the observations of Ogawa *et al.,* (2014). Interestingly, Atkin *et al.,* (2011) also observed that the common DISC1 variant DISC1 607F (L607F) proved incapable of fully rescuing DISC1 knockdown, with mitochondria in cells expressing DISC1 607F showing reduced movement.

Mitofilin is a protein important to the maintenance of cristae morphology, knockdown of mitofilin impairs the mitochondrial inner membrane formation of cristae, promotes apoptosis and reduces proliferation (John *et al*, 2005). DISC1 has been identified as interacting with mitofilin and has suggested a role of DISC1 in regulating mitochondrial bioenergetics (Park *et al*, 2010). The knockdown of either mouse DISC1 or mitofilin results in the reduction of

cellular adenosine triphosphate (ATP) and NADH dehydrogenase (complex I), as well as Ca^{2+} buffering. Similar bioenergetic results are seen with the expression of truncated mouse DISC an orthologue of DISC1 aa1-597. This perturbation of mitochondrial bioenergetics caused by a reduction in mouse DISC1 levels can be partially rescued by the overexpression of mitofilin, supporting a notion of common mitochondrial functions between the two proteins. Additionally, a role of DISC1 in the stability of mitofilin is indicated by the observation that the knockdown of mouse DISC1 promotes mitofilin ubiquitination. DISC1 has also been identified to interact with the inner mitochondrial membrane protein Coiled-coil Helix Cristae Morphology 1/CHCHD6 (CHCM1/CHCHD6) (An *et al*, 2012). The established functional effects of CHCM1/CHCHD6 bear similarity to observations for mitofilin (John *et al*, 2005; Park *et al*, 2010). Deficits in CHCM1/CHCHD6 affect cristae morphology, ATP levels as well as O_2 consumption (An *et al*, 2012). However, functional mitochondrial effects of DISC1-CHCM1/CHCHD6 interactions have not been characterised.

1.3 Mitochondria

1.3.1 The mitochondrial membrane potential, Δψm

This section serves to introduce background material on the mitochondrial membrane potential, Δψm, which will feature in chapters 4 and 5, as such the information here may aid in the interpretation of subsequent data. The proton gradient generated by respiratory chain activity in the inner mitochondrial membrane gives rise to both the mitochondrial membrane potential, Δψm and a pH gradient (Chen, 1988). In combination with the pH gradient, the mitochondrial membrane potential, Δψm contains the energy to produce torque via proton movement that drives the synthesis of ATP by F_0F_1ATPase activity. The quantitative measurement of the mitochondrial membrane potential, Δψm in primary cultured rat cortical neurons by Gerencser *et al.,* (2012), identifies a value of −139 mV at rest. This mitochondrial membrane potential, Δψm was found to vary between −108 mV and −158 mV due to demands on ATP biosynthesis, and Ca^{2+}mediated metabolic activation.

In the intrinsic apoptotic pathway, the mitochondrial membrane potential, Δψm has frequently been observed to be dissipated (Ly *et al*, 2003). However, the specific details regarding the sequence in which this pathway activation occurs is unclear. Depending on the cell systems and apoptotic stimuli used, the loss of the mitochondrial membrane potential, Δψm may take place in early apoptosis or arise in late apoptosis following the activation of signalling pathways. Furthermore, the relationship between cytochrome *c*, an inner membrane protein

released from mitochondria during apoptosis (Liu *et al*, 1996) and the mitochondrial membrane potential, Δψm is also uncertain (Ly *et al*, 2003). It has been suggested that mitochondrial membrane potential, Δψm dissipation accompanies cytochrome *c* release (Heiskanen *et al*, 1999) and is a principle requirement for this to occur (Yoshino *et al*, 2001). However, cytochrome *c* release has also been observed to be independent of mitochondrial membrane potential, Δψm loss (Goldstein *et al*, 2005) or may occur prior to this event (Goldstein *et al*, 2000). Methodological differences may account for these conflicting results.

The mitochondrial membrane potential, Δψm also has a role in mitochondrial fission-fusion dynamics. Collapse of the mitochondrial membrane potential, Δψm by the ionophore carbonyl cyanide *m*-chlorophenylhydrazone (CCCP) leads to the fragmentation of mitochondria and an inhibition of fusion (Ishihara *et al*, 2003; Legros *et al*, 2002). This mitochondrial fragmentation occurs due to the impairment of mitochondrial inner membrane fusion (Malka *et al*, 2005). Specifically, fusion is impaired by the proteolytic inactivation of the fusion protein Optic Atrophy 1 (OPA1) by OPA1 Zinc Metallopeptidase (OMA1), a process which is dependent on the loss of the mitochondrial membrane potential, Δψm (Ehses *et al*, 2009; Head *et al*, 2009).

1.3.2 Mitochondrial morphology

Mitochondria are dynamic organelles capable of altering their shape due to changing environmental and metabolic demands (Benard & Rossignol, 2008). Underpinning the ability of the mitochondrial network to rapidly alter its structure, is the fission-fusion dynamics of the mitochondrial membranes (Chan, 2006). Primarily, the fission-fusion machinery is composed of Dynamin-1-like Protein (Drp1) and Fission 1 (Fis1) which mediate membrane fission (Mozdy *et al*, 2000; Smirnova *et al*, 2001), whereas inner membrane fusion is facilitated by OPA1 and outer membrane fusion is promoted by mitofusin 1 (Mfn1) and mitofusin 2 (Mfn2) (Song *et al*, 2009). The functional relationship between fission and fusion must be managed to maintain an optimal mitochondrial network structure, dominance of unrestrained fission will ultimately lead to fragmentation of mitochondria whereas maintained fusion will lead to elongation of the mitochondrial network (Chan, 2006). For example, Drp1 null-mutant cells (Ishihara *et al*, 2009) or Drp1 knockdown cells (Youle & van der Bliek, 2012) possess elongated tubular networks of mitochondria with fission being absent. In contrast, the knockdown of OPA1 induces mitochondrial fragmentation (Ishihara *et al*, 2006), likewise Mfn1 and Mfn2 null-mutant cells (Koshiba *et al*, 2004) display a mitochondrial network that is fully fragmented with a total absence of fusion.

Mitochondrial bioenergetics influence the morphology of the mitochondrial network (Benard & Rossignol, 2008). Westermann *et al.*, (2012) proposes a model to explain the role of fission-fusion dynamics in regard to respiratory demand. Under basal conditions the mitochondrial network undergoes constant remodelling due to cycles of dynamic fusion and fission, with the mitochondria neither being fully fused nor fully fragmented. At extremes of respiratory activity the mitochondrial morphology adapts to cope with demands. High energy demand may result in the hyperfusing of the mitochondrial network to allow maximal ATP production whereas low energy demand may give rise to fragmentation of the mitochondrial network and mitochondria existing in a resting state. Furthermore, mitochondrial network fragmentation is frequently observed following the impairment of oxidative phosphorylation (OXPHOS) by the use of chemical inhibitors to specific electron transport chain (ETC) complexes, or the use of uncoupling agents to collapse the membrane potential, $\Delta\psi m$ (Benard & Rossignol, 2008). It may also be that compromised mitochondrial function in general promotes fragmentation. A RNA interference (RNAi) screen in *C.elegans* identified that of 719 genes associated with mitochondria function, knockdown of ~80% of genes resulted in mitochondrial fragmentation and in only 3.5% of cases, elongation was observed (Ichishita *et al*, 2008). It appears that the impairing of OXFOS or perhaps broader mitochondrial function leads to a morphological shift towards fragmentation. However, the exact signalling methods to initiate the changes in fission-fusion dynamics in relation to the bioenergetics are at present poorly understood

Processes of autophagy involve alterations to mitochondrial morphology. Mitophagy is a means to ensure the quality control of mitochondria enabling the removal of compromised or excess mitochondria (Kanki & Klionsky, 2010). The fragmentation of the mitochondrial network is observed to occur before the onset of mitophagy (Gomes & Scorrano, 2008; Twig *et al*, 2008). In part this is a prerequisite for the mitochondria to be able to fit inside the autophagosome prior to degradation (Gomes & Scorrano, 2013). Mitochondria are selected for mitophagy following a process of fission-fusion events that leaves a sub-population of mitochondria with a low membrane potential, $\Delta\psi m$ and reduced levels of OPA1 (Twig *et al*, 2008). These organelles display abnormal bioenergetic processes. The mitophagy of the degraded aberrant mitochondria is observed to be dependent on Drp1 to initiate the structural fragmentation.

Macroautophagy is the principle pathway of autophagy and is a less selective process than mitophagy, involving the generalised elimination of proteins and organelles within the cell to maintain homeostasis and cell survival (Yang & Klionsky, 2010). The induction of macroautophagy results in the elongation of the mitochondrial network which spares the

mitochondria from degradation. The initiation of unbalanced fusion is responsible for this elongation, which results from the inhibition of the fission protein Drp1 due to the serum starvation used to initiate the macroautophagy (Gomes *et al*, 2011). The sparing of the elongated mitochondria in macroautophagy is likely a consequence of this highly fused mitochondrial network being too large to be engulfed by the autophagosome (Gomes & Scorrano, 2013).

1.3.3 Mitochondrial trafficking in neurones

The long range transport of mitochondria is required to maintain a sufficient supply of ATP and regulate intracellular Ca^{2+} by buffering within the highly specialised morphology of the neurone (Lin & Sheng, 2015). The trafficking of mitochondria within the cell is driven by motor proteins that depend on ATP hydrolysis to move along the microtubule network (Hirokawa *et al*, 2010). Kinesin-1 motor proteins generate anterograde movement from the soma to the distal region, conversely dynein motor proteins facilitate retrograde movement from distal regions towards the soma. Kinesin-1 and dynein both form trafficking motor complexes with the mitochondrial membrane anchor Miro1 which interacts with the mitochondrial outer membrane as well as the adaptor protein milton, which links Miro1 to the given motor protein (Schwarz, 2013). Mitochondrial respiration appears to be the principle source of ATP for the motor proteins, as the blocking of respiration rapidly abolishes mitochondrial transport, therefore mitochondria likely fuel their own motility (Zala *et al*, 2013). The motility of mitochondria within neurons is often complex and dynamic, with mitochondria moving over long distances then pausing and sometimes changing direction, showing bi-directional movement (Sheng, 2014). In cultured hippocampal neurones it has been observed that ~20-30% of mitochondria are motile within the axon, some of this population moves to and from the synaptic bouton, while the remaining ~ 70-80% of axonal mitochondria remain stationary (Kang *et al*, 2008). Stationary mitochondria may become motile again following metabolic or synaptic changes (Sheng, 2014). Furthermore, there are twice as many motile mitochondria within the axon than the dendrites (Overly *et al*, 1996).

Mitochondrial trafficking dynamics are proportional to the level of neuronal activity that is occurring within the cell (MacAskill & Kittler, 2010). For example, the rise in intracellular adenosine diphosphate (ADP) at the synapse due to metabolic activity may result in an increase in the targeting of mitochondria to this region via trafficking (Mironov, 2007). This is likely to supply the localised demand for further ATP. Mitochondria may also be trafficked to the synapse following increases in intracellular Ca^{2+} levels there (Lin & Sheng, 2015). However,

the exact mechanisms as to how energy consumption or Ca^{2+} increases result in mitochondrial trafficking to the synapse are not fully clear and are the subject of ongoing research.

1.3.4 Mitochondrial function in psychiatric illness

1.3.4.1 Major depressive disorder

Evidence from cellular based studies suggests a role of mitochondrial dysfunction in major depressive disorder. Gardiner *et al.,* (2003) found a reduction in the mitochondrial ATP production rate and in the ratios of the electron transport chain (ETC) respiratory complexes I+III/IV as well as II+III/IV, in muscle cells obtained from sufferers of major depressive disorder displaying somatisation. These sufferers had common features of both depression and mitochondrial disorders. Karabatsiakis *et al.,* (2014) observed lowered levels of respiration, ATP turnover related respiration and OXPHOS coupling efficiency in peripheral blood monocytes (PBMCs) from patients with major depressive disorder versus healthy controls. Furthermore, a correlation between the severity of the depression and the intensity of the respiratory dysfunctions was noted. The mitochondrial membrane potential, $\Delta\psi m$ was found to be increased in platelets from sufferers of major depressive disorder in comparison to healthy controls (Moreno *et al,* 2013). In another study using platelets to monitor mitochondrial function in depression, Hroudová *et al.,* (2013) detected reductions in the respiratory rate following complex I inhibition and in the maximal capacity of the ETC in depressed patients showing partial remittance. However, no differences were observed between depressed patients in the absence of remittance compared to healthy controls. Overall, these studies suggest a generalised deficit in respiration may occur in peripheral cells in sufferers of major depressive disorder that is possibly underpinned by abnormal functioning in some of the ETC complexes.

Animal models suggest that mitochondrial abnormalities may in part mediate the pathogenesis of depression. Chronic mild stress can be used as an experimental model of depression. In rats subjected to this paradigm, reduced activity of the mitochondrial respiratory chain complexes I, III and IV was identified in both the cerebellum and the cortex (Rezin *et al,* 2008). Further work by the same group identified increased reactive oxygen species (ROS) as measured by increased levels of superoxide in the hippocampus, PFC and cortex following chronic mild stress (Lucca *et al,* 2009). Inducing depression via chronic mild stress in mice, Gong *et al.,* (2011) found impaired mitochondrial respiratory function in the hippocampus, hypothalamus and cortex. The mitochondrial membrane potential, $\Delta\psi m$ was also observed to be reduced in

these brain areas. Additionally, mitochondrial morphology appeared altered, with evidence of abnormalities to the mitochondrial cristae and membranes apparent. Mitochondrial abnormalities have also been identified in the Flinders-sensitive rat line (FSL), which possess a genetic predisposition to depression-like behaviours (Chen *et al*, 2013). Within the CA1 of the hippocampus of the FSL rats, a reduced number of mitochondria were present, these mitochondria also had a greater volume than that of matched controls. It was possible to rectify the mitochondrial deficit in the FSL rats following treatment with the antidepressant imipramine, which increased the number of mitochondria.

1.3.4.2 Bipolar disorder

Studies using post-mortem brain tissue have identified associations between bipolar disorder and mitochondrial impairment. Post-mortem analysis of the PFC of sufferers of bipolar disorder reveals reduced mitochondrial size in comparison to healthy controls (Cataldo *et al*, 2010). The study of post-mortem PFC brain tissue from bipolar patients has also identified a reduction in the activity levels of respiratory complex I activity (Andreazza *et al*, 2010). This may be associated with the increased levels of oxidative damage to proteins that was likewise observed in the tissue sections. Gene expression micro-array analysis of the post-mortem PFC from bipolar individuals has revealed downregulation to components of the ETC (Sun *et al*, 2006). This included genes encoding subunits of respiratory complexes I, IV and V (F_1F_0 ATP synthase). Overall these post-mortem studies indicate that within the PFC of bipolar individuals there may be deficits to respiratory complexes, the dysfunction of which may have downstream effects mediating oxidative damage, perturbing mitochondrial function.

Animal models highlight a role of mitochondrial dysfunction that suggest an involvement with the presentation of mania. The pharmacological modelling of mania can be induced by the treatment of animals with amphetamines. In rats treated with amphetamines, the activity of respiratory complexes I, II, III and IV was reduced in the PFC, striatum and hippocampus (Valvassori *et al*, 2010). Treatment with the mood stabiliser valproic acid was capable of ameliorating all of the respiratory complex deficits measured. In a similar mania model Fery *et al.*, (2006) found an increase in oxidative stress markers within the hippocampus, striatum and cortex. Recently, Valvassori *et al.*, (2014) observed a reduction in tricarboxylic acid cycle (TCA) enzyme activity within the FC, hippocampus and striatum of rats following treatment with amphetamine. The TCA enzyme reduction was inversely correlated with the degree of hyperlocomotion evident, a mania-like feature of the rat model.

1.3.4.3 Schizophrenia

There is evidence that the distribution and number of mitochondria are altered in schizophrenia. Examination of post-mortem brains from individuals with schizophrenia revealed an average 26-30% reduction in mitochondrial density per synapse quantified, specific to the striatum, versus healthy controls (Somerville *et al*, 2011a). Similarly, an average 37% decrease in mitochondrial density was observed per synapse quantified, in the putamen and caudate nucleus of schizophrenia patients (Somerville *et al*, 2011b). Deficits in the mitochondria number has also been found to occur within oligodendrocytes in both the PFC and caudate nucleus in post-mortem brain tissue from sufferers of schizophrenia (Uranova *et al*, 2001). It is possible that these regionalised reductions in mitochondria could impinge upon localised synaptic signalling and myelination in individuals with schizophrenia.

Multiple studies have identified an association between schizophrenia and perturbations to cellular energy generation. Using a proteomics, metabolomics and transcriptomics approach to analysing the post-mortem PFC from patients with schizophrenia Prabakaran *et al.,* (2004) found downregulation of metabolic pathways. This included components of glycolysis, oxidative phosphorylation (OXPHOS) and ATP synthesis alongside the upregulation in ROS associated pathways. In line with the possibility of impairments of OXPHOS in schizophrenia, reductions is the activity levels of respiratory complexes have been identified in post-mortem brain tissue from individual with schizophrenia, occurring to complex IV within the FC and temporal cortex and to complexes I and III in the temporal cortex and basal ganglia (Maurer *et al*, 2001). Complex I activity has also been found to be reduced in peripheral blood monocytes form individuals with schizophrenia in comparison to healthy controls (Gubert *et al*, 2013). *In vivo,* 31p-MRS neuroimaging has identified reductions to ATP in patients with schizophrenia specific to the basal ganglia (Fujimoto *et al*, 1992) and the frontal lobes (Volz *et al*, 2000).

A recent study provides some evidence that mitochondrial dynamics is altered in schizophrenia. Reduced mitochondrial network connectivity was identified in patient derived lymphoblastoid cell lines from individuals with schizophrenia (Rosenfeld *et al*, 2011). Such an observation suggests that a shift in mitochondrial dynamics to favour fission has occurred. In line with this, OPA1 levels were found to be lowered in both lymphoblastoid cell lines and post-mortem brain tissue from patients with schizophrenia (Rosenfeld *et al*, 2011).

Animal models of schizophrenia highlight mitochondrial dysfunction. The facilitation of social isolation rearing in rats produces a neurodevelopmental model of schizophrenia, in these animals cortico-straital abnormalities in ATP are evident (Möller *et al*, 2013). A reduction in

ATP in the FC was observed which may underpin negative schizophrenia-like symptomology in the social isolation model, while conversely ATP levels in the striatum were increased, that could perhaps in part explain positive symptoms observed. Mitochondrial complex activity has been investigated within a pharmacological model of schizophrenia using ketamine in rats (De Oliveira *et al*, 2011). Mitochondrial complex activity was monitored in the striatum, hippocampus, PFC at three time point's post-ketamine injection. In each of the brain regions tested, some degree of abnormal mitochondrial complex activity was detected within the total time course. It was thought these respiratory chain alterations impacting on brain energy status may be linked to the hyperlocomotor abnormalities that are also evident in this rat model.

1.4 Summary

From the introduction, it can be seen that the field of psychiatric genetics is making useful progress towards understanding these complex disorders. One clear message however is that psychiatric disorders are more complex and heterogeneous than is perhaps suggested by the over-simplified DSM and ICD categorizations. On the other hand, it is also becoming evident that the underlying biology transcends these boundaries, with findings being applicable to multiple disorders. The example of DISC1 may be rare in terms of genetic origin, but the biological insights that have emerged, point to convergences on biological processes that are generally held to relate directly to mental illness across the spectrum from schizophrenia to major depressive disorder.

1.5 Aims

The t(1;11) co-segregates with multiple instances of major mental illness in a large Scottish family. Until the identification of the chimeric *DISC1/DISC1FP1* transcripts *CP60* and *CP69* by Jennifer Eykelenboom, the only mechanism of pathogenesis proposed for the t(1;11) family was a model invoking the haploinsufficiency of DISC1. However it is possible that the t(1;11) is associated with additional potential mechanisms of pathogenesis including the expression of aberrant DISC1/DISC1FP1 chimeric proteins, which could possess a dominant-negative or gain of function effect. Recently a further *DISC1FP1* EST has been identified: AB371558. This suggests that other *DISC1/DISC1FP1* chimeric transcripts may exist.

It is of interest to observe how the addition of amino acids from DISC1FP1 to DISC1 aa1-597 will affect the function and localisation of chimeric DISC1/DISC1FP1 proteins given the established studies into DISC1 aa1-597 *in vitro* and *in vivo*. To investigate this, the der 1 DISC1/DISC1FP1 chimeric species will be exogenously expressed in cell lines as well as mouse primary cortical neurones and characterised. This will include the analysis of cellular expression and investigation into the mitochondrial phenotype of these species. Characterisation of mitochondrial expression is of interest given that DISC1 has been frequently localised to the mitochondria and has established roles in mitochondrial function, while DISC1 mutants have been associated with mitochondrial dysfunction.

If mitochondrial pathology is induced by the exogenous expression of DISC1/DISC1FP1 chimeric proteins it is possible that evidence of such a deficit can also be detected in t(1;11)-family derived cell lines. The staining of lymphoblastoid cell lines with Mitotracker Red and subsequent detection of fluorescence will give a proxy indication as to the integrity of the mitochondrial membrane potential, $\Delta\psi m$ in these cells.

It is currently unknown as to whether the t(1;11) confers an alteration to gene expression, although this seems possible given the established roles and sub-cellular localisations of DISC1 not to mention any potential roles of DISC1FP1 or DISC2. Recently t(1;11) lymphoblastoid cells were assayed on a gene expression microarray by Merck Sharp and Dohme. Consequently, these data will be analysed by gene ontology and pathway analysis programs, using over representation analysis. Further putative mechanisms of pathogenesis may be uncovered following data analysis with multiple functional enrichment programs.

Overall this study aims to identify putative pathogenic mechanisms within the t(1;11) family which may be translatable to the mechanisms of psychiatric illness in the general population.

The aims of this thesis were as follows:

- To identify novel *DISC1/DISC1FP1* transcripts that arise from the splicing of *DISC1* and the *DISC1FP1* EST AB371558.
- To characterise the exogenously expressed DISC1/DISC1FP1 proteins.
- To investigate mitochondrial fluorescence in t(1;11) lymphoblastoid cell lines.
- To perform gene ontology and pathway analysis on t(1;11) microarray data.

Chapter 2 - Materials and Methods

2.1 Bioinformatics

2.1.1 Identification of EST AB371558 chromosomal co-ordinates

Sequence data and chromosomal location of the *DISC1/DISC1FP1* EST AB371558 was acquired from UCSC genome browser.

2.1.2 Translation predication

The Sequence Manipulation Suite's Translation tool was used to translate nucleotide sequences into protein open reading frames.

2.1.3 Sequence comparison

For the initial analysis of BigDye sequencing traces for cloning data, FinchTV software was used. Following this, BLAST (bl2seq) was used to align two given nucleic acid sequences.

2.1.4 Restriction enzyme mapping

To map a nucleotide sequence for the presence of restriction sites that are substrates for commercially available restriction enzymes, NEBcutter was used.

2.1.5 Gene enrichment analysis for t(1;11) microarray data

For the analysis of the microarray gene enrichment data, the WEB-based Gene Set Enrichment Analysis Toolkit (WebGestalt) (Wang *et al*, 2013; Zhang *et al*, 2005) software was used. All data was analysed using hypergeometric statistical analysis.

2.1.6 Generation of genes of interest lists for t(1;11) microarray data

The initial microarray analysis of t(1;11) lymphoblastoid cDNA was performed by Miguel Camargo of Merck Sharp & Dohme. Following this initial round of analysis, the t(1;11) microarray dataset was then filtered to isolate genes showing differential expression that had both a fold change of +/- 1.3 and a $p \leq 0.05$. Such a cut-off was used as it is the threshold for reliable detection. This filtering process created the initial t(1;11) Genes of Interest List (GOI). The original GOI list was then subjected to a second filtering process; this stage removed non-neuronally expressed genes present in the lymphoblastoid cDNA from the dataset. The aim of the second round of filtering was to create a GOI list with an expression profile that was more in line with a post-mortem brain tissue derived GOI list than the initial original unfiltered GOI

list. Underpinning this filtering is the observation that gene expression in the blood can significantly differ from that found in the brain using gene expression microarray analysis (Cai *et al*, 2010; Sullivan *et al*, 2006). In order to create the second gene list the original unfiltered GOI list was analysed using Ingenuity Pathway Analysis (IPA) and the GOI list was then filtered by nervous system and CNS cell line expression creating a neuronally filtered GOI list that contained only neuronally expressed genes. The filtering of both of the GOI lists produced, was performed in collaboration with Ruth Boxall, a PhD student under the supervision of David Porteous.

In the generation of both reference and genes of interest lists for WebGestalt analysis a minority of gene names needed altering to synonyms or prior names to be accepted by WebGestalt. This entailed both the consultation of NCBI gene, GeneCards and the use of the HGNC list search tool.

The microarray study was conducted by Merck Sharp & Dohme using a proprietary in house Rosetta chip based analysis. As such a limitation of this study is that the raw data was not available. Consequently, for data analysis it was not possible to align the results directly with other public domain data as is widely practiced using the Illumina chips**.**

2.1.7 Web pages of online programs

BLAST http://blast.ncbi.nlm.nih.gov/

GeneCards http://www.genecards.org/

HGNC list search http://www.genenames.org/hgnc-searches

NCBI Gene http://www.ncbi.nlm.nih.gov/gene

NEBcutter http://tools.neb.com/NEBcutter2/

Sequence Manipulation Suite http://www.bioinformatics.org/sms2/

UCSC Genome Browser http://genome.ucsc.edu/

WebGestalt http://bioinfo.vanderbilt.edu/webgestalt/

2.2. Materials

2.2.1 Reagents

Below are listed the details of the chemical reagents used in the production of this thesis. The source of each chemical reagent is stated alongside, in brackets. Where relevant, the buffer that a reagent is suspended in is stated.

- Agar (BD Bioscience)
- Agarose (Invitrogen) made up using TAE buffer
- Ampicillin (Sigma) made up using TAE buffer
- Bromophenol blue (Sigma)
- BSA (Sigma) made up using PBS
- DABCO (Sigma)
- DAPI (Sigma)
- DMSO (Sigma)
- D-PBS (Invitrogen)
- Dried milk powder (Marvel) made up using PBS
- EDTA (Sigma) made up in dH_2O
- Ethanol (Fischer) dH_2O used to dilute as needed
- FACS Sheath Solution (BD Biosciences)
- Formalin (Sigma) made up using PBS
- Glycerol (Promega)
- Glycogen (Sigma)
- Isoproponol (Fischer)
- Kanamycin (Sigma)
- Magnesium chloride solution, PCR grade (Invitrogen)
- Methanol (Fischer)
- Mowiol (Sigma)
- NP-40 (Sigma)
- Orange G (Sigma)
- Phenol/chloroform/isoamyl alcohol (Invitrogen)
- Protease Inhibitor Cocktail (Roche) made up in dH_2O
- SDS (Fischer) made up in dH_2O
- Sodium Azide (Sigma) made up in dH_2O

- Sodium Chloride (Fischer) made up in dH_2O
- Sodium Deoxycholate (Fischer) made up in dH_2O
- Tris (Fischer)
- Tris-HCL (Fischer)
- TRIS-SDS Running Buffer
- Tryptone (BD Biosciences)
- TWEEN-20 (Sigma)
- X-Gal (Invitrogen)
- Yeast Extract (BD Bioscences)

2.2.2 Solutions and buffers

Below are listed the buffers and solutions that are used in the techniques detailed within the methods chapter.

L Agar/ampicillin/kanamycin

50 g	Tryptone
25 g	Yeast Extract
50 g	Sodium Chloride

Up to 5l with dH_2O

Adjust the pH to 7.2. Pour into a bottle with 1.5g of Agar/100ml of medium. Stored at 4℃. Prior to usage, melt in a microwave, when cool enough to touch add ampicillin or kanamycin to 50ng/ml. Use immediately.

L Broth/ampicillin/kanamycin

50 g	Tryptone
25 g	Yeast Extract
50 g	Sodium Chloride

Up to 5l with dH_2O

Adjust the pH to 7.2. Stored at 4℃. Prior to use, add ampicillin or kanamycin to 50ng/ml

Membrane wash buffers

The basic membrane wash buffer used was prepared as follows:

100 ml	10xPBS
10 ml	TWEEN-20
Up to 1l with	dH_2O

Membrane wash buffers were kept at room temperature.

Mowiol mounting solution

7.5 g	Mowiol
10 ml	Glycerol
25 ml	dH_2O

Solution then incubated overnight at room temperature.

50 ml	Tris-HCL(pH 8.5)

Solution then heated to 100℃ for 20 min and allowed to cool.

1.75 g	DABCO

Solution then stored at -20℃, with working stock stored at 4℃.

PBS-Triton lysis buffer

5 ml	10x PBS
5 ml	10% Triton X-100
Up to 50 ml	dH_2O
1 tablet	Protease inhibitor cocktail

Buffer stored at 4℃ prior to addition of the protease inhibitor tablet. Following tablet addition, buffer stored at -20℃.

Protein sample buffer

6.25 ml	1M Tris (pH 6.8)
10 ml	Glycerol
10 ml	20% SDS
13.75 ml	dH_2O
1 ml	0.1% Bromophenol blue

Solution stored at room temperature.

RIPA lysis buffer

2.5 ml	1M Tris-HCl (pH 7.5)
2.5 ml	3M Sodium Chloride
0.5 ml	NP-40
2.5 ml	10% Sodium deoxycholate
250 ul	20% SDS
Up to 50 ml	dH_2O
1 tablet	Protease Inhibitor Cocktail

Buffer stored at 4℃ prior to addition of the protease inhibitor tablet. Following tablet addition, buffer stored at -20℃.

2.3 Cell Culture

2.3.1 Cell line maintenance

Both the lymphoblastoid and COS-7 cell lines were cultured in a Galaxy S incubator (scientific laboratory supplies), at 37°C and 5% CO_2. All of the cell culture was carried out in an Envair Bio2+ Class II Safety Cabinet following containment level 1 measures.

The COS-7 cells were grown in in Cellstar T25 or T75 flasks (Greiner Bio-One) and split at 80-90% confluence. To split a COS-7 culture, the media was aspirated and the cells washed twice in PBS (Invitrogen), following this 5mls of TrypLE Express (Invitrogen) was applied to the cells. The COS-7 cells were then incubated at 37°C and 5% CO_2 for 2-5 minutes until the cells detached from the basal membrane. The suspension was then centrifuged at 1,000rpm for 10 minutes and the supernatant removed. The cell pellet was then resuspended in 1ml of pre-warmed media (see table 2.3.A). For the generation of Western Blot lysates, the suspended

Cell line	Source	Medium	Serum
COS-7	ECACC	DMEM	10% foetal calf serum
KK	(Millar *et al*, 2005b)	RPMI	10% foetal calf serum

Table 2.3.A: Media in which cell lines were cultured: all media was supplied by Invitrogen. The ECACC, is the European Collection of Cell Cultures.

cell volume was diluted with prewarmed media (see table 2.3.A) to enable cells to be aliquoted in 10mls media (see table 2.3.A) per 10cm tissue culture dish (Iwoki) at a density of $2.5x10^6$ cells per plate. For immunocytochemistry, 12 well Costar plates (Corning), each well containing a 16mm sterile glass cover slip (VWR) were seeded with $0.5\text{-}1x10^5$ COS-7 cells in 1ml of media (see table 2.3.A). The cells seeded for Western Blot or immunocytochemistry were grown overnight, then transfected.

The lymphoblastoid cell lines were initially grown in Cellstar T25 flasks (Greiner Bio-One) and fed three times weekly. For feeding, 2/3 of the conditioned media was aspirated and replaced with pre-warmed media (see table 2.3.A). Following feeding, flocculations of cultured lymphoblastoid cell lines were agitated by gentle pipetting to promote cell growth. At confluence, a portion of conditioned media was aspirated and the lymphoblastoid cell flocculation's disrupted by pipetting. Then 4/5 of the cells suspended in the media were transferred to a T75 flasks (Greiner Bio-One). The T25 and T75 flasks containing lymphoblastoid cell lines were then refilled with prewarmed media (see table 2.3.A). Prior to the harvesting of lymphoblastoid cell lines for use in FACS analysis, confluent flasks were first fed with 10ml of pre-warmed media (see table 2.3.A) for three consecutive days. For cell counting a 20ul sample of the suspended cells was injected into a counting chamber (Nexcelom Bioscience) and analysed by a Cellometter Auto T4 Cell Counter (Nexcelom Bioscience). Following this, four samples of each culture, each containing $1x10^6$ cells were aliquoted into 15ml Falcon tubes and centrifuged at 500rpm for five minutes. The supernatant was then removed and the cell pellet was resuspended in 1ml of the conditioned media specific to the cell line. The resuspended cells were then aliquoted into 12-well dishes generating four wells per plates of the same cell line each with $1x10^6$ cells in lml of media (see table 2.3.A) and placed in the incubator at 37°C and 5% CO_2 for 20 minutes, prior to MitoTraker Red treatment.

2.3.2 Transfection of plasmids into eukaryotic cells

To transfect plasmid DNA into cells for the exogenous expression of protein, Lipofectamine 2000 (Invitrogen) was used in conjunction with Opti-MEM (Invitrogen) as per manufacturer's instructions. The amount of plasmid DNA transfected was: 2µg per well 12-well plate, 5.6µg per 10cm dish. The cells were incubated with the transfection media at 37 °C and 5% CO_2 for 4-6 hours. The transfection media was aspirated and replaced with prewarmed media (see table 2.3.A). The transfected cells were harvested 18-24 hours later. The plasmids used in this thesis are listed in table 2.3.B.

Plasmid	Protein	Tag	Source
pcDNA 3.1(+)	Empty vector	None	Invitrogen
pcDNA 3.1(+) FLAG	Empty vector	FLAG	Fumiaki Ogawa
pcDNA 3.1(+) FLAG-DISC1	DISC1	FLAG	Nick Brandon[1] (Brandon *et al*, 2004)
pDEST40	Empty vector	HIS	Novagen
pETG20a	Empty vector	TRX	Novagen
pETG30a	Empty vector	GST	Novagen
pETG40a	Empty vector	MBP	Novagen

Table 2.3.B: Pre-existing plasmid constructs used in the production of this thesis. [1]Pfizer Neuroscience, Groton, Connecticut, USA.

2.3.3 Drug treatment

For mitochondrial staining 1mM MitoTracker Red (Invitrogen) was diluted 1:20 in DMSO into 50µM aliquots that were then snap frozen on dry ice for future use. For immunocytochemistry MitoTracker Red was used at 1:1000 to a final concentration of 50nM in 2ml of media per well. Following the addition of MitoTracker Red, the cells were returned to the incubator for 30 minutes and maintained at 37°C and 5% CO_2. The 12-well plate containing the MitoTracker stained cells was then wrapped in aluminium foil between the entire cell fixation and blocking steps to prevent the loss of MitoTracker florescence due to excitation of the fluorescent probe by ambient light.

For the initial FACS analysis with lymphoblastoid cell lines, the end concentration of MitoTracker Red was 50nM in 1ml of media (see table 2.3.A). Following the addition of MitoTracker Red or sham DMSO treatment, the cells, were returned to the incubator for 45 minutes and maintained at 37°C and 5% CO_2. To determine an optimal incubation time for the staining of lymphoblastoid cell lines with 50nM MitoTracker Red, incubation times of 60, 45, 30 and 15 minutes were tested. In the generation of experimental data the incubation time was 15 minutes, in the presence of 30nM MitoTracker Red. Prior to FACS analysis the MitoTracker Red treated lymphoblastoid cells were centrifuged at 500rpm, the supernatant removed and the pellet resuspended in warm PBS. The cells in solution were then passed through a BD Falcon 100µM Cell Strainer (BD Biosciences) into a FACS tube. All samples were then kept wrapped in aluminium foil to prevent excitation of the probe by ambient light.

2.4 Protein-related methods

2.4.1 Antibodies

A variety of antibodies were used in this project. Details of the antibodies and the conditions under which they were used, are shown in table 2.4.A.

Name in text	Specificity	Species	Source	Conditions (WB)	Conditions (ICC)	Notes
R47	DISC1 (N-term)	Rabbit	Custom	1:1000 Overnight Coldroom	N/A	Fraction (8)
FLAG (M2)	FLAG (N-term)	Mouse	Invitrogen	1:1000 2 hours	1:100,000 1 hour – COS-7 2 hours–primary neuronal	
FLAG (Poly)	FLAG (N-term)	Rabbit	Invitrogen	N/A	1:5000 1 hour – COS-7 2 hours–primary neuronal	
CVα	CVα	Mouse	Mitoscience/Abcam	N/A	1:3000 1 hour – COS-7 2 hours–primary neuronal	
Cytochrome *c*	Cy *c*	Mouse	Mitoscience/Abcam	N/A	1:2000/1:30001 hour – COS-7 2 hours–primary neuronal	
Pig-anti-rabbit	Rabbit Ig	Pig	Dako	1:3000 30 mins	N/A	Secondary
Rabbit-anti-mouse	Mouse Ig	Rabbit	Dako	1:2000 30 mins	N/A	Secondary
Alexa-Flour 488 Goat-anti-mouse	Mouse Ig	Goat	Invitrogen	N/A	1:2000 1 hour	Secondary Fluorescent 488 nm
Alexa-Flour 594 Goat-anti-mouse	Mouse Ig	Goat	Invitrogen	N/A	1:2000 1 hour	Secondary Fluorescent 544 nm
Alexa-Flour 488 Goat-anti-rabbit	Rabbit Ig	Rabbit	Invitrogen	N/A	1:2000 1 hour	Secondary Fluorescent 488 nm

Alexa-Flour 647 Chicken-anti-mouse	Mouse Ig	Chicken	Invitrogen	N/A	1:2000 1 hour	Secondary Fluorescent 647 nm

Table 2.4.A: A list of all of the antibodies used in this thesis and the conditions under which they were used. WB refers to western blotting and ICC refers to immunocytochemistry, whilst species refers to the species in which the antibody was raised.

2.4.2 Cell lysates

2.4.2.1 Production of cell lysates and processing of the cell pellet

Cells were cultured for lysis on 10cm dishes to 75-90% confluence. Cell media was then aspirated and the cells washed with 10mls of 4℃ PBS. This was then aspirated and between 500 and 1000ul of lysis buffer (either PBS-Triton or RIPA) was applied to the culture dish. The dish was rotated so that the lysis buffer covered all of the adherent cells. Following this a cell scraper was used to mechanically detach the cells from the culture dish and the whole cell lysate was then transferred to an eppendorf.

Two methods of pellet processing were used in order to extract exogenously expressed CP60 and CP69 protein for Western blot analysis and were adapted from a protocol by Keryer-Bibens *et al.,* (2006), with additional input from the Millar group senior postdoc Shaun Mackie. These experiments aimed to determine if the chimeric proteins were isolated in the membrane fraction.

Condition 1: The whole cell lysate was placed on a rotary wheel at 20-30rpm for 2 hours at 4°C and then spun at 13,000rpm by centrifuge for 30 minutes. The soluble protein lysate was then separated from the insoluble pellet fraction by pipette, snap frozen on dry ice and stored at -20 or -70℃. The pellet was then resuspended in 20µl buffer by pipette. An ultrasonic probe then applied sonication to the pellet solution in the eppendorf in an attempt to disrupt proteins in the solution. The ultrasonic probe was set on drive with 3x 10 second bursts of sonication administered. During operation of the sonicator the eppendorf containing the pellet in solution, was packed in ice within a beaker to minimise possible protein degradation occurring due to sonication during sample processing. The solubilised pellet was then combined with an equal volume of 2x Protein sample buffer (PSB) and heated to 100°C for 5 minutes on a hotblock.

Condition 2: The whole cell late was solubilised on a rotary wheel at 20-30rpm for 2 hours at 4°C. The eppendorf containing the whole cell lysate was then subjected to 10 minutes of sonication in an ultra-sonic bath. The sonication was used in an attempt to disrupt proteins in the cell lysate. The disrupted whole cell lysate was then spun at 13,000rpm by centrifuge for 30 minutes. Following this, the soluble protein lysate was then separated from the insoluble pellet fraction by pipette, snap frozen on dry ice and stored at -20 or -70℃. The pellet was then resuspended in 50µl RIPA and combined with an equal volume of 2x PSB. The pellet in PSB was then vortexed for 1 minute, heated to 100°C for 5 minutes on a hotblock, vortexed for 1 minute and heated to 100°C for 5 minutes. This cycle of heating and vortexing was thought to

be a means of fractionating insoluble proteins from the pellet into solution. Cell pellet fractions were typically stored at -20 or -70℃.

However, in retrospect it should be noted that these methods simply isolate CP60 and CP69 to a fraction that is insoluble by RIPA alone. Future studies could be implemented to determine which specific sub-cellular compartments these chimeric species partition to. Such a suitable fractionation protocol to partition proteins to multiple sub-cellular compartments is provided by Rockstroh *et al.,* (2010).

2.4.2.2 Measuring the protein concentration of cell lysates

The concentration of protein lysates was determined using the BioRad protein assay. This used 25ul of each of 6 BSA protein standards with concentrations ranging from 0-1mg/ml that increased in 0.2mg/ml increments. 2.5ul of protein lysate sample were made up to 25ul using dH_2O. To each sample and standard, 125ul of reagent A and 1ml of reagent B was added. The reactions were left to incubate at room temperature for 25 minutes. The absorbance readings of the reactions was then taken at 750nm using an Ultrospec 3000 optical reader (Pharmacia Biotech). The 750nm readings from the protein standards were then used to plot a standard curve of protein concentration versus absorbance. The interpretation of the standard curve then enabled the determination of the protein concentration for the sample protein lysates.

2.4.3 Western blotting

2.4.3.1 Sample preparation

Prior to Western analysis the cell lysates were combined with an equal volume of PSB. This sample was then heated to 100°C for 5 minutes on a hotblock. The heating of the solution aimed to both denature the proteins and disrupt the interactions between proteins in the solution.

2.4.3.2 Invitrogen system

Western blotting firstly involves the process of electrophoresis to drive the movement of proteins through the gel with the distance moved being dependent on the molecular weight (Mw) of the given protein species. The Western blotting method used is the Invitrogen system. Pre-cast 7% Tris-Acetate gels (Invitrogen) were used for gel electrophoresis and were held in a XCell Surelock gel tank. The experimental samples and All Blue Marker (Bio-Rad) where

then loaded and the gel immersed in 400ml 1x NuPage Tris-Acetate SDS Running Buffer (Invitrogen). The gel electrophoresis was performed for 90 minutes at 150V using a Power Pac 3000 (BioRad).

Following this, a 500ml of 1X NuPage Transfer Buffer (Invitrogen) containing 20% methanol was made up. A PDVF membrane (Invitrogen) was briefly immersed in methanol, then soaked along with five sponge pads in NuPage Transfer Buffer /20% methanol for ~5 minutes prior to transfer. Upon completion of the gel electrophoresis the gel casing was opened and the gel aligned with the membrane. Two sponge pads were then put into the transfer chamber with the gel and then membrane, followed by three sponges. When two gels were transferred at once, a sponge was used to separate the gels with two sponges either side. The transfer chamber was then closed, inserted back into the XCell tank. The transfer chamber was then surrounded with H_20 to dissipate heat as the transfer electrophoresis was active. The transfer ran for 60 minutes at 30V using a Power Pac 3000 (BioRad). The membrane was then washed three times in dH_20 over 5 minutes and then in blocking buffer for 30 minutes at room temperature or overnight in at 4°C.

2.4.3.3 Immunostaining

Following blocking, the membrane was incubated with the primary antibody in blocking buffer. This process took between 1-2 hours at room temperature or overnight in at 4°C, depending on the primary antibody used. The membrane was then washed three times over 15 minutes with wash buffer. After this the membrane was incubated with a secondary antibody in blocking solution for 30 minutes at room temperature. The membranes was then washed three times over 15 minutes in wash buffer and then with PBS. For both antibody incubations and the washes, the immersed membranes were rocked at ~15rpm. Details of both the primary and secondary antibody incubation times are given in table (see table 2.4.A). The membrane was then placed on cling film to air dry.

For development of the membrane onto photosensitive film (Scientific Laboratory Supplies), 5ml of ECL Plus (Amersham) development reagent was applied to the air-dried membrane for ~5 minutes. The ECL Plus was then removed from the membrane and the membrane was then exposed to photosensitive film in order to visualise the antibody binding to a given protein species. The time period for the exposure to the film ranged from 1 second to 16 hours. The exposed photosensitive film was then developed using an Amersham Hyperprocessor.

2.4.4 Immunocytochemistry

2.4.4.1 Cell fixation

Prior to the addition of antibodies to cells exogenously expressing protein, the cells were fixed and permeabilized. Fixation terminates biochemical reactions but preserves protein-protein interactions. Permeabilisation results in protein epitopes potentially being accessible for the binding of primary antibodies.

The cells were washed twice with warm PBS (Gibco), each PBS wash was aspirated from the well. Following this the cells were fixed with 0.5mls of 3.7% formaldehyde (Sigma) per well, and left at room temperature for 10 minutes. A second series of two PBS washes was then applied. The cells were then permeabilized with 0.5mls of chilled methanol per well. The 12-well plate was then placed in the -20°C freezer for 5 minutes, following this, the cells were washed twice in PBS.

2.4.4.2 Immunostaining

Each well received 1ml of blocking solution PBS/3% BSA vol/wt and was rocked at 25-30rpm at room temperature for 30 minutes. All further immunostaining was carried out at room temperature. Following blocking, the primary antibodies were applied to the fixed and permeabilized cells in 450µl PBS/ 3% BSA vol/wt. The 12-well plate was rocked at 25-30rpm 1 hour for COS-7 immunostaining and for 2 hours for primary neuron immunostaining. The concentrations of the primary and secondary antibodies used in immunocytochemistry are shown in table 2.4.A. Three washes of PBS/ 3% BSA were then applied to the cells to remove unbound primary antibody. The fluorescent conjugated secondary antibodies were then applied in 400µl PBS/3% BSA and incubated for 1 hour and rocked at 25-30rpm 1 hour. During this period the 12-well plate was wrapped in aluminium foil to prevent the loss of secondary antibody florescence due to excitation of the fluorescent probe by ambient light. Three washes of PBS/3% BSA were then applied to the cells to remove unbound secondary antibody. The coverslips were then mounted onto slides using mowiol mounting medium with 250ng/µl DAPI. The immunocytochemistry slides were then kept wrapped in aluminium foil at 4°C.

2.4.4.3 Microscopy

Fluorescence Microscopy was performed on a Zeiss Axioskop 2 MOT epifluorescence microscope with Image J software used for image processing. This was used for the visualisation of immunocytochemistry for both qualitative analysis and for optimisation of antibody staining. The fluorescence microscopy can visualise dual colour fluorescence in the Green (FITC) and Red (Texas Red) spectra. The integrity of staining following immunocytochemistry was checked on the fluorescence microscope and images were then acquired using confocal microscopy on the Zeiss LSM510. The use of confocal microscopy enabled the acquisition of optical sections of the immunocytochemically stained cells that were of greater resolution than images produced by fluorescence microscopy. The LSM510 also allowed a greater number of fluorescent conjugated antibodies to be used within an experiment, in particular, conjugated antibodies that fluoresced in the far red (Cy-5) spectrum. This enabled the implementation of a triple-staining protocol.

2.4.4.4 Qualitative analysis of immunocytochemistry

Qualitative analysis of immunocytochemistry on COS-7 cells exogenously expressing FLAG-tagged: CP60, CP69, WT-DISC1 and DISC1 aa1-597 was used to characterise the cellular expression pattern and the Mitotracker Red staining associated with CP60 and CP69 protein. All of the plasmids were transfected into COS-7 cells under blinding with three experimental replicates produced. Based on previous observation of these DISC species, the cellular phenotype categories for the gross anti-FLAG staining used, were: punctate; diffuse and clustered. The Mitotracker Red staining categories firstly addressed whether the mitochondria were stained and secondly, if so, was the mitochondrial network tubular or clustered. Fluorescence microscopy was used to qualitatively categorise the cells. For each cell assessed, first the cellular phenotype, the ant-FLAG staining was observed using the Green (FITC) channel and the morphology noted, then the Red (Texas Red) channel used to visualise mitochondrial network staining with Mitotracker Red. For the qualitative analysis a random field was used to select cells. Per experiment one cover slip per DISC species was produced, with 20 fluorescing cells analysed per cover slip in a single session. Each cover slip was analysed three times and the results from each experimental replicate set of coverslips then averaged. This gave 60 cells counted per transfected DISC species. When all qualitative data was acquired, the blinding was removed and the data plotted in Microsoft Excel.

2.5 Molecular biology methods

2.5.1 Primers

Details of all of the oligonucleotide primers used in this thesis may be found in table 2.5.A. Primer-blast (http://www.ncbi.nlm.nih.gov/tools/primer-blast/) was frequently used to design primers.

2.5.2 PCR reactions

2.5.2.1 RT-PCR to amplify CP1

The RT-PCR to detect the CP1 transcript used the following reaction mix:

Forward primer	50pmol
Reverse primer	50pmol
GoTaq green master mix (Promega)	25 µl
cDNA	1 µl
dH_2O	to 50 µl

RT-PCR thermal cycle:

95°C 2min

95°C 30s
60°C 30s
72°C 30s* } x35 cycles

72°C 4min

4°C for ever

* Extension step, 30s is the time required for extension of DNA products <500bp GoTaq Green PCR.

Purpose	Name	Direction	Sequence
Untagged pcDNA3.1(+) DISC1 aa1-598	WT DISC 1 Eco	5’	GATCGAATTCGCCACCATGCCAGGCGGGGGTCCTCAGGGCGCC
	DISC1 598 Not1	3’	GATCGCGGCCGCTTATCCTGATATGGCATGCATTTTGGCTTCAAG
FLAG pcDNA3.1(+) DISC1 aa1-597	FLAG DISC1	5’	GATCGAATTCGCCGCCATGGATTACAAG GATGACGACGATAAG
	DISC1 597 Not1	3’	GATCGCGGCCGCCTATGATATGGC ATGCATTTTGGCTTCAAG
FLAG pcDNA3.1(+) DISC1 CP1	FLAG DISC 1	5’	GATCGAATTCGCCGCCATGGATTACAAGGATGACGACGATAAG
	DISC1 598 Not1	3’	GATCGCGGCCGCTTATCCTGATATGGCATGCATTTTGGCTTCAAG
FLAG pcDNA3.1(+) CP69	DISC1 Eco Start	5’	GATCGAATTCCCAGGCGGG GGTCCTCAG GGC
	FTL 69 Not1	3’	GATCGCGGCCGCTTAGGAGAA ATATATCAGTCTACCAGAAAATATTC
FLAG pcDNA3.1(+) CP60	DISC1 Eco Start	5’	GATCGAATTCCCAGGCGGGGGTCCTCAGGGC
	FTS 60 Not1	3’	GATCGCGGCCGCCTACCAGAA AATATTCTTTTGGAGTCTCCAATG
3’primers to confirm start codon in sequence and frame of ΔNCP69	Trunc69R80	3’	AGCAGACAATCACGCAGC
	Trunc69R160	3’	CTGCTTTATCATAATCATCG
5’ Primers to confirm stop codon presence in ΔNCP69	Trunc69F100	5’	GTTCTGGGTTTTAGCTATCTG
	Trunc69F200	5’	ACCACCGATCGTAGTCTGG
Mutagenesis Primers for ΔN597	FMutTrunc69	5’	AAATGCATGCAATTAGCTAATAAGGCACCACCGATCGTAGTCTG
	RMutTrunc69	3’	CAGACTACGATCGGTGGTGCCTTATTAGCTAATTGCATGCATTT
Primers to sequence the insert region of ΔNCP69	F1T69	5’	TCATCACCACCACGATTATG
	F2T69	5’	GATACCCATACACCGCTGC
	F3T69	5’	AACGTATTAAAAGCCTGAATC
	R1T69	3’	CCTGCAGGGCTTTGCTAAC
	R2T69	3’	ACTTTTTGCAGACGCCAATG
	DISC1NF	5’	AAGGAGCCTCCAGGAAAGAA

RT-PCR to detect CP1 species	ABFUS1C	3’	CAAGAAATGCCAAAGTGAGTTC
	pETG-Seq 20F	5’	GGTTCTGGTTCTG
	pETG-Seq 30F	5’	CGACCATCCTCC
	pETG-Seq 40F	5’	GCGCAGACTCC
	pETG-Seq R	3’	GTGGTGGTGCTC
	pDEST14 Seq F	5’	CGTAGAGGATCGAG
	pDEST14 Seq R	3’	CGGGCTTTGTTAGC

Table 2.5.A: Details of all of the primers used in this thesis.

2.5.2.2 Pfu Ultra II fusion PCR

For the generation of FLAG-tagged constructs of CP1, CP60 and CP69, the standard PCR thermal cycle conditions detailed in section 2.1.2.1 were used in conjunction a high fidelity polymerase. This enabled open reading frames to be amplified that were flanked 5' and 3' restriction sites. Here the * extension step 30s is sufficient for DNA products <2kb, with the following reaction mix:

Forward primer	50pmol
Reverse primer	50pmol
Pfu Ultra II Fusion HS DNA polymerase (Aglient Technologies)	1µl
Template (5-0.1ng)	1µl
dNTPS	1.25µl
10x Buffer (Aglient Technologies)	5µl
dH_2O	to 50µl

For the generation of the CP60 and CP69 inserts an additional 0.75µl and 1.5µl of 50mM MgCl (Sigma) was added to the PCR reaction.

2.5.2.3 Touchdown PCR

To amplify a 597 insert a touchdown PCR thermal cycle was used in conjunction with the Pfu Ultra II fusion reaction mix (see section 2.1.2.2). The touchdown PCR initially progresses through a thermal cycle and has an annealing temperature that decreases by 1°C per cycle. After 9 cycles an annealing temperature of 55°C is initiated and maintained for 19 cycles.

Touchdown PCR thermal cycle:

95°C 2min

95°C 20s

65°C 20s - 1°C per cycle } x9 cycles

72°C 30s

95°C 20s

55 °C 20s } x19 cycles

72°C 30s

72°C 3min

4°C for ever

2.5.2.4 BigDye sequencing PCR

To sequence the PCR products generated, the BigDye Terminator v3.1 Ready Reaction Mix (Life Technologies) was used. The reactions were either assembled in eppendorfs or 96 well plates. The reaction mix used was as follows:

Primer	1µl (3.2pmol)
5x Sequencing Buffer	1.5µl
2.5x Ready reaction Mix	1µl
Template (PCR product)	1µl
dH_2O	5.5µl

BigDye Terminator v3.1 PCR thermal cycle:

96°C 1min

96°C 10s

50°C 5s } x24 cycles

60°C 4min

4°C for ever

2.5.2.5 Site-directed mutagenesis PCR

A QuickChange Lightning site-directed mutagenesis kit (Agilent Technologies) was used to insert a double stop codon into the sequence of ΔNCP69. This generated an open reading frame that encoded ΔN597. The reaction mix used is as follows:

Forward primer	1.25µl (125ng)
Reverse primer	1.25µl (125ng)
Template (300ng)	3µl
dNTPS (Agilent Technologies)	1µl
10x Buffer (Agilent Technologies)	5µl
Quick solution (Agilent Technologies)	1.5µl
dH_2O	to 50µl
Then QuikChange Lightning enzyme (Agilent Technologies)	1 µl

Site-Directed Mutagenesis thermal cycle:

95°C 2min

95°C 20s
60°C 10s
68°C 2min 30s
} x18 cycles

68°C 5min

4°C for ever

2.5.3 Sequencing PCR products and plasmids

The BigDye Terminator v.3.1 cycle sequencing kit (Invitrogen) was used to sequence both plasmids and DNA amplified by PCR. This protocol required further PCR reactions to be performed on the initial sample of DNA prior to sequencing (see section 2.1.2.2) This BigDye PCR used a single 5' or 3' primer to bind to and amplify regions of DNA. When amplifying

regions of DNA ~>300bp, sets of primers were designed that would create partially overlapping chromatogram reads from the products of separate BigDye reactions.

The BigDye sequencing reactions were carried out in either 96-well plates or eppendorfs. Following generation of the PCR product on the thermal cycler, each eppendorf had 2.5µl of 125mM EDTA added and 30µl of 100% ethanol. The tubes were then vortexed briefly and left to incubate at room temperature for 15 minutes. The sequencing reaction was then centrifuged at 13,000 at 4°C for 20 minutes and again, for 2 minutes. After each centrifugation the supernatant was then removed by pipette. 30µl of 70% ethanol added and the sequencing reaction which was then centrifuged at 13,000 at 4°C for 5 minutes and again, for 2 minutes. After each centrifugation the supernatant was then removed by pipette. The eppendorfs were then dried at 37°C to remove and residual ethanol for 2-3 minutes.

The BigDye PCR reactions were analysed by Agnes Gallacher (Medical Research Council Human Genetics Unit). The Sequence chromatograms traces were visualised using FinchTV v.1.3.1 software (http://www.geospiza.com/Products/finchtv.shtml). BLAST was used to align nucleotide sequences (http://blast.ncbi.nlm.nih.gov/Blast.cgi). The Sequence manipulation suite (http://www.bioinformatics.org/sms2), Translate application was used to convert nucleotide sequences into amino acid sequences; The ORF Finder application was used to identify ORF's within a nucleotide sequence.

2.5.4 Purification of PCR products

The QIAquick PCR purification kit (Qiagen) was used to purify both the DISC1 ORF's generated by PCR also the *CP1* transcript amplified by RT-PCR. The PCR purification removed contaminants from the PCR product which may have otherwise impaired the actions of T4 DNA ligase (Roche) or the TOPO-TA cloning, respectively. The purified PCR products were eluted into dH_2O or 10mM Tris·Cl, pH 8.5 (Quiagen).

2.5.5 Making and running agarose gels

To prepare agarose gels, TAE buffer and the required mass of powdered agarose were combined and heated using a microwave until the agarose melted. The agarose gels produced are described by wt/vol; a 1% agarose gel made with 70ml TAE contained 0.7g of powdered agarose. SYBR Safe DNA Gel Stain (Life Technologies) was added to the warm agarose gel to enable DNA detection. 1% agarose gels were used to detect linear DNA >500bp and

contained SYBR Safe at a final dilution of 1:10,000, 2% agarose gels were used to detect linear DNA <500bp and contained SYBR Safe at a final dilution of 1:3,333. The warm agarose gel was poured into a casing tray and a comb inserted into the liquid. The gel cooled at room temperature for 10+ minutes.

The electrophoresis tank (Applied Biosciences) was filled with TAE. The agarose gel was then submerged in the tank, the comb removed and the DNA product loaded into the wells. 2% agarose gels were ran with a 50bp ladder (Invitrogen); 1% agarose gels were ran with a 1kb DNA Ladder (Invitrogen) and a λHindIII DNA Ladder (Invitrogen). The gel electrophoresis was ran at 50-100V for 30-90 minutes. The linear DNA that had migrated through the agarose gel was visualised and photographed using an Uvidoc light box.

2.5.6 cDNA production

The cDNA used in this thesis was produced by Jennifer Eykelenboom. The RT-PCR product sequenced in section 3.2 uses lymphoblastoid cDNA from cell lines, KK107 for the t(1;11) family member and KK47 for the karyotype control.

2.5.7 Culture of bacteria transformed with plasmid constructs

2.5.7.1 Transformation of bacteria with plasmid constructs

To transform the FLAG-tagged constructs into cells, the following process was used: DH5α chemically competent *E. coli* were thawed on ice, then 5µl of the ligation reaction was added to 50µl of the DH5α cells and mixed gently. The DH5α cells were then incubated on ice for 30 minutes. The DH5α cells were heat shocked at 42°C for 20 seconds and then placed on ice for two minutes. 400µl of room temperature SOC media (Sigma) was added to the cells. The cells were then incubated at 37°C in an Innova 4300 incubator shaker (New Brunswick Scientific) at 225rpm for one hour.

Following the initial incubation, a bacterial cell spreader was used to spread 50-150ul of the bacterial culture per L Agar/ampicillin plate. The agar plates were then incubated for 16-22 hours at 37°C and 5% CO_2 in a Plus II incubator (Gallencamp), by which time bacterial colonies were typically visible.

Molecular biology kits recommended specific cells for transformation of constructs. The TOPO-TA (Invitrogen) cloning of the CP1 RT-PCR product, used TOP10 chemically

competent E. coli (Invitrogen). The sight directed mutagenesis reactions used XL10-Gold ultracompetent cells (Aglient). The protocol for each of these competent cell types is similar to that covered above for the DH5α cells. The bacterial cultures for the site directed mutagenesis to generate ΔN597 used L Agar/ kanamycin plates, given the destination vector mutated encoded ampicillin resistance.

2.5.7.2 Blue/white screening of transformed bacteria

The pCR 2.1-TOPO vector that the CP1 ORF was TOPO-TA cloned into can be blue/white screened using L Agar/x-gal plates. The x-gal is a substrate for β-galactosidase. In the presence of functional β-galactosidase, the hydroxylation of x-gal results in blue colonies. However β-galactosidase requires the LacZα peptide to function. The LacZα gene which is encoded in the pCR 2.1-TOPO vector is disrupted, as a result of the insertion of the CP1 ORF within the TOPO vector cloning cassette. The screening process therefore enables the identification of *E. coli* colonies where the insert and TOPO vector have recombined (white) Vs colonies containing TOPO vector only (blue).

The transformed TOPO-TA bacterial cultures were spread onto L Agar plates that had been pretreated with 40ul of x-gal. The L Agar/x-gal plates were then incubated for 16-22 hours at 37°C and 5% CO_2 in a Plus II incubator by which time both blue and white bacterial colonies were typically visible.

2.5.7.3 Amplification of plasmid constructs

Single transformed bacterial colonies form the L Agar/ampicillin or L Agar/kanamycin plates could be picked to grow larger bacterial cultures. These large bacterial cultures were grown in L-broth media with the appropriate antibiotic, ampicillin or kanamycin, for 16-18 hours at 37°C in an Innova 4300 incubator shaker at 200rpm. Small cultures of bacteria were pelleted by centrifugation at 13,000rpm for 1-2 minutes using a bench top centrifuge. The bacterial pellets were then lysed and the DNA prepped using the QIAprep Spin Miniprep Kit (Qiagen) as per manufacturer's instructions. For larges bacterial cultures of 200mls, the bacteria were isolated using centrifugation at 5,000rpm at 4°C for 10 minutes using an Avanti J-201 centrifuge. The bacterial pellets were then lysed and the DNA prepped the Plasmid Maxiprep Kit (Qiagen) or Endofree Plasmid Maxiprep Kit (Qiagen). The plasmid DNA was eluted into TE buffer pH 7.5 and stored either at 4°C or -20°C.

2.5.7.4 Measuring plasmid DNA concentration

A NanoDrop 1000 spectrophotometer was used to measure plasmid DNA concentration. Prior to the analysis of plasmid DNA, the NanoDrop 1000 first took a blank read from 1µl of dH_2O then from the buffer the plasmid was solubilised in e.g. TE buffer. 1µl of plasmid DNA was then analysed and the concentration in ng/µl of the plasmid DNA calculated. The 260/280nm and 260/230nm absorbance ratios were also calculated by the Nanodrop. Both ratios can inform how free of protein contaminates the plasmid DNA is. For the 260/280 read-out a ratio of 1.8 indicates DNA that is free of impurities. A 260/230nm absorbance >2.0 was indicative of DNA containing impurities.

2.5.8 Cloning techniques

2.5.8.1 Site-directed mutagenesis

The insertion of additional nucleotides into DNA sequence was performed using a QuikChange Lightning Site-Directed Mutagenesis Kit (Agilent Technologies). 5' and 3' primer pairs that encoded the additional nucleotides and existing regions of the plasmid ORF were used in the site directed mutagenesis PCR reaction (see section 2.5.2.5). Following the site-directed mutagenesis PCR, 2µl of DpnI was added to the PCR product, which was immediately incubated at 37°C for five minutes. The DpnI enzyme digested the unmodified template plasmid. The mutated plasmid DNA was then transformed into *E. coli* (see section 2.5.7.1) and the bacteria cultured and then DNA isolated (see section 2.5.7.3). The mutated plasmid ORF was confirmed by sequencing (see section 2.5.3)

2.5.8.2 Restriction digests

Restriction enzymes were used to digest both vector and insert DNA at given restriction sites to created 'sticky' ends for ligation of vector and insert. The FLAG-tagged plasmids created in this thesis all contain EcoR1 and Not1 restriction sites.

Restriction enzyme nucleotide cleavage sites.

EcoRI	5'G^AATTC	3'CTTAA^G
Not1	5'GC^GGCCGC	3'CGCCGG^CG

Insert Digest

PCR product 55µl

EcoR1 (Roche) 4µl

Not1 (Roche) 4µl

10x buffer H (Roche) 10µl

Incubated overnight at 37°C

Vector Digest

Vector DNA 3µl (3ng)

EcoR1 2µl

10x buffer H 5µl

dH_2O 40µl

The digestion reaction was incubated for 37°C for two hours. Then, 2µl Not1 was added to the digest, which was then incubated a further two hours at 37°C.

The restriction digest products were analysed on agarose gels (see section 2.1.5) to confirm DNA digestion.

2.5.8.3 Phenol–chloroform extraction

Phenol–chloroform extraction was used to remove proteins and lipids from the DNA product following restriction digest and prior to ligation. 100µl digest product and 100µl phenol/chloroform/isoamyl alcohol were briefly vortexed, then centrifuged at 13,000rpm for two minutes. 70µl of the aqueous phase was extracted to an eppendorf. 40µl of EB buffer (Qiagen) was then added to the Phenol–chloroform, briefly vortexed, and then centrifuged at 13,000rpm for two minutes. 60µl was then extracted from the aqueous phase and combined with the initial extraction, to give a total volume of 130µl extracted.

Following the phenol-chloroform extraction the DNA in the extraction product was precipitated. To the extraction product 2x of 100% ethanol and 1:10 3M pH5.2 sodium acetate were added. Extraction products containing DNA inserts received an additional 1ul of

20mg/ml Glycogen. The solution was then precipitated at -20°C for two hours then centrifuged at 13,000rpm for 30 minutes. The supernatant was removed and 100µl of 70% ethanol added, then centrifuged at 13,000rpm for five minutes. The supernatant was removed and the DNA pellet dried at 37°C for five minutes. The DNA pellet was then resuspended in dH_2O or 10mM Tris·Cl, pH8.5 (Quiagen).

2.5.8.4 SAP treatment

SAP treatment of the vector DNA prior to ligation, removes phosphates groups which have the potential to detrimentally affect the ligation of the insert to the vector. The SAP treatment was performed on the vector DNA following ethanol precipitation. The SAP reaction mixture was as follows:

Vector DNA	10ul (100ng/ul)
SAP Buffer (USB)	8.5ul
SAP Phosphatase (USB)	1.5µl

The reaction was incubated at 37°C for 30 minutes and then incubated at 65°C for 10 minutes.

2.5.8.5 Ligation reaction

A rapid DNA ligation Kit (Roche) was used to ligate the insert DNA to the linear plasmid DNA via complimentary restriction sites. The ligation reaction mixture was as follows:

Insert DNA	4µl
Plasmid DNA	1µl (50ng)
1xBuffer (Roche)	5µl
2xBuffer (Roche)	10µl
T4 Ligase (Roche)	1µl

The ligation reaction was incubated at room temperature for one hour prior to transformation into DH5α cells (see section 2.5.7.1).

2.5.8.6 Gateway cloning

Gateway cloning was used to move both ΔNCP69 and ΔNCP597 ORFs from a pENTR221 donor vector backbone and into a tagged destination vector. The gateway cloning used the Gateway LR Clonase II enzyme kit (Invitrogen) and the reaction was as follows:

Donor vector containing ORF	1µl (100ng)
Destination vector	1µl (150ng)
TE Buffer	6µl
LR Clonase (Invitrogen)	2µl

Vortex LR Clonase reaction twice briefly, centrifuge briefly. Incubate the LR Clonase reaction at 25°C for 25 minutes. Add 1µl of Proteinase K (Invitrogen) to each tube, vortex. Incubate LR Clonase reaction at 37°C for one hour. The LR Clonase reaction was then transformed into DH5α cells (see section 2.5.7.1).

2.5.8.7 TOPO cloning

The CP1 PCR product was TOPO-TA (Invitrogen) cloned to generate sufficient DNA to sequence. The reaction mix was as follows:

PCR product	2µl
Salt Solution (Invitrogen)	0.5µl
TOPO vector (Invitrogen)	0.5µl

The reaction was mixed gently and incubated at room temperature for five minutes, then transformed (see section 2.1.7.1).

2.6 FACS analysis

FACS analysis was performed using a FACSCalibur flow cytometer (BD Biosciences) using an argon laser (488nm). The cytometer parameters set for measurement were: Forward scatter (FSC), Side scatter (SSC), FL1 (FITC 530 nm emission bandpass), FL2 (PE 585 nm emission bandpass). BD FACSFlow Sheath Fluid (BD Bioscience) was used as the sheath fluid for FACS analysis.

Data analysis was performed using CellQuest software (BD Biosciences). Prior to data acquisition, presaved instrument settings specific to the cell line assayed, COS-7 or lymphoblastoid, were loaded into CellQuest. All FACS analysis was graphed as dot plots. For each FACS analysis, 10,000 events were measured and displayed on a dot plot, with the GMFI measured for the gated events. The use of a dot plot over a histogram enabled the visualisation of individual events that have high fluoresce.

The control cells were ran by FACS analysis firstly using the FSC Vs. SSC parameters, which measure the cell size and cell complexity, respectively. Following this the FL1 Vs. FL2 parameters were used to acquire the baseline fluorescence of the control cells. A subjective gate was drawn in either the FL1 or FL2 region to measure the fluorescing cells. For the measurement of the geometric mean fluorescence intensity (GMFI) of the COS-7 cells expressing exogenous GFP, the subjective gate was drawn in the FL1 region. In the quantification of Mitotracker Red fluorescence in stained lymphoblastoid cell lines, a subjective gate drawn was the FL2 region. The fluorescing cells were then analysed by FACS and the percentage of cells gated and the populations GMFI acquired. The FSC Vs. SSC was then measured for the given fluorescing cell line being assayed.

2.7 t(1;11) gene expression microarray protocol

Karyotype control and t(1;11) lymphoblastoid cells lines were cultured concurrently. RNA was then prepared from these cell lines by colleagues at the University of Edinburgh using a RNAeasy kit (Qiagen), followed by treatment with TurboDNA-free (Ambion). This total RNA was provided to Merck Sharpe and Dohme (MSD) as collaborators for the purposes of a collaborative research agreement under a materials transfer agreement. MSD then performed cDNA synthesis and subsequent quality control. Samples were then run on a Rosetta/Merck Human 44k 1.1 dual channel microarray platform (GEO platform identifier: GPL4372). This is a proprietary ink jet array created by Rosetta under contract to MSD, containing 39,302 probes. The resulting data was analysed by MSD's proprietary Rosetta Resolver gene

expression analysis software.

`

Chapter 3 - Initial investigations into DISC1/DISC1FP1 chimeras

3.1 Introduction

The t(1;11) pedigree are a large Scottish family with members that suffer from major depressive disorder, schizophrenia and bipolar disorder (Blackwood *et al*, 2001). In the pedigree, a balanced autosomal t(1;11) co-segregates with these mental illnesses, meaning that only translocation carriers within the pedigree are affected by these psychiatric diseases. There are t(1;11) carriers who are unaffected by illness. However, these individuals share cognitive deficits in common with affected t(1;11) carriers. Two genes, *DISC1* and the antisense encoded *DISC2* gene, are located at 1q42 and are disrupted as a consequence of the t(1;11) (Millar *et al*, 2000b). The gene *DISC1FP1*, also known as *Boymaw*, is located at 11q14.3. Here the *DISC1FP1* ESTs CK000409 and BU599486 span the t(1;11) breakpoint region. With genes identified as being disrupted at both 1q42 and 11q14.3, it was proposed that chimeric *DISC1/DISC1FP1* transcripts may be produced from the derived chromosomes 1 and 11 (Zhou *et al*, 2008).

The majority of the work that comprises this chapter is also included in Eykelenboom *et al*., (2012). In this study, *DISC1FP1* was also disrupted by the translocation and was cryptically spliced to *DISC1* generating *DISC1/DISC1FP1* transcripts that were detected by RT-PCR in t(1;11) lymphoblastoid cell lines. Two der 1 chimeric transcripts were detected, *CP60* and *CP69*, transcripts that encode DISC1 aa1-597 plus an additional 60 and 69 novel amino acid originating from *DISC1FP1* (Eykelenboom *et al*, 2012). A single novel der 11 transcript has also been detected. However, this species possesses an internal ORF of DISC1 aa669–854, and encodes a distal DISC1 C-terminus fragment (Eykelenboom *et al*, 2012; Zhou *et al*, 2010; Zhou *et al*, 2008). Given this it was decided to investigate the exogenous expression of CP60 and CP69 as these der 1 species are aligned to use the endogenous *DISC1* promoter. Importantly, if CP60 and CP69 were expressed endogenously (Eykelenboom *et al*, 2012; Zhou *et al*, 2008) it is possible that the presence of the additional amino acids from DISC1FP1 would confer aberrant function to CP60 and CP69 protein. This may produce gain of function or dominant negative effects that are functionally different to the established roles of DISC1.

Since the detection of the three *DISC1/DISC1FP1* chimeric transcripts (Eykelenboom *et al*, 2012), a further *DISC1FP1* EST, AB371558 has been identified, which spans the t(1;11)

`

breakpoint region at 11q14.3. This raises the possibility that further novel *DISC1/DISC1FP1* transcripts may be present in t(t1;11) lymphoblastoid cells as a consequence of *DISC1* being spliced to AB371558. The detection of other novel chimeric transcripts would add greater complexity to possible mechanisms of pathogenesis in the t(1;11) pedigree. This chapter will cover the use of RT-PCR on t(1;11) lymphoblastoid cell lines to detect a *DISC1*/AB371558 transcript.

The detection of the chimeric transcripts in t(1;11) lymphoblastoid cell lines (Eykelenboom *et al*, 2012), furthers the investigation into the pathophysiology underlying the high incidence of major mental illness observed in translocation carriers (Blackwood *et al*, 2001). It is important to build upon the discovery of the chimeric transcripts by expressing and characterising chimeric DISC1/DISC1FP1 protein species to look for possible pathophysiological mechanisms. Presently the single transgenic mouse model encoding chimeric DISC1/DISC1FP1 protein species expresses only CP60 and the C-terminus DISC1 fragment (Ji *et al*, 2014), whilst post mortem t(1;11) brain tissue is not available. Therefore, to characterise DISC1/DISC1FP1 protein, investigations will focus on *in vitro* expression of constructs encoding the chimeric species.

This chapter will also look at the exogenous expression of CP60 and CP69 and the subsequent Western blot analysis of the respective chimeric protein species. In this chapter the basic characterisation of exogenously expressed CP60 and CP69 protein by Western blot will be addressed. This aims to (1) determine the protein fraction each chimeric protein is isolated in; (2) validate each protein species predicted molecular weight; (3) detail the cell lysate processing methods used. Research published since the investigations in this thesis were completed, has isolated an exogenously expressed der 1 chimera protein in the lysate pellet fraction by Western analysis, this was identified as exogenously expressed CP60 protein (Ji *et al*, 2014; Zhou *et al*, 2010).

Expanding on the initial investigations into the exogenous expression of DISC1/DISC1FP1 protein required the generation of further chimeric constructs. The development of FLAG-tagged chimeric constructs would enable the immunolabeling of exogenously expressed protein using commercial FLAG antibodies, removing the requirement for N-terminal DISC1 antibodies. The method development of der 1 chimeric FLAG-tagged construct generation and that of relevant controls is covered in this chapter. The method development for construct generation required to perform biophysical characterisation of the additional 69 aa encoded by

`

DISC1FP1 in the species CP69, will also feature. The biophysical investigation itself was conducted by Nicholas Bradshaw and Dinesh Soares (Eykelenboom *et al*, 2012).

3.2 Detection of the *DISC1*/AB371558 chimeric transcript *CP1*

3.2.1 *In silico* predictions of *DISC1* and AB371558 chimeric transcripts

AB371558, like BU599486 and CK000409 is an EST specified by *DISC1FP1* that in karyotypically normal genomes spans the region of the t(1;11) breakpoint at 11q14.3. In t(1;11) carriers, it is possible that AB371558 and *DISC1* fuse, producing both der 1 and der 11 *DISC1/DISC1FP1* chimeric transcripts and that these chimeric transcripts could be detected by RT-PCR. Prior to carrying out RT-PCR, sequences of the possible der 1 and *DISC1*/AB371558 and der 11 AB371558/*DISC1* chimeric transcripts were generated.

The putative der 1 *DISC1*/AB371558 chimeric transcript is encoded by *DISC1* exons 1-8 proximal to the translocation breakpoint which are spliced to exon 3a of AB371558 distal to the breakpoint. This gives an *in silico* predicted ORF encoding DISC1 aa1-597 plus a glycine (see figure 3.2.A). The glycine at aa598 is encoded by nucleotides from both *DISC1* and AB371558. Importantly DISC1 aa598 is also a glycine, although a different codon is used (Eykelenboom *et al*, 2012). Following on from the nomenclature used for *CP60* and *CP69*, the putative chimera was named *CP1*, given this chimeric transcript derives a single amino acid as a consequence of the fusion of *DISC1* and AB371558. RT-PCR of t(1;11) lymphoblastoid cell lines needed to be performed to detect this novel der 1 species, CP1, which at the level of amino acid sequence coding is indistinguishable from DISC1 aa1-598.

In silico predictions of the der 11 AB371558/*DISC1* transcript, encoded by the splicing of AB371558 to exons 1c-2 to *DISC1* exons 9-13, show only an internal open reading frame that encodes a C-terminus DISC1 fragment as detected by Eykelenboom *et al.* (2012) (see figure 3.2.B). As the der 11 product would replicate the RT-PCR results of Jennifer Eykelenboom, the next section will focus on the detection of the *CP1* transcript.

`

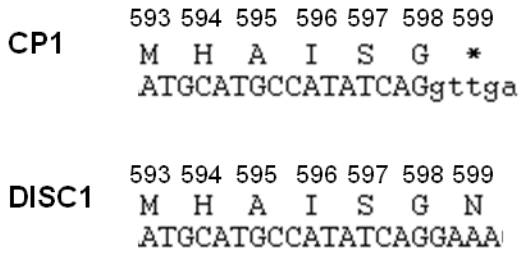

Figure 3.2.A: Predicted sequence of the der 1 *DISC1*/AB371558 chimera *CP1*. This is a consequence of splicing of exons 1-8 of *DISC1* proximal to the t(1;11) to the exons 3a-6 *DISC1FP1* EST AB371558 distal to the breakpoint. The resulting CP1 transcript encodes the same amino acid sequence as DISC1 up to aa1-598 before terminating at a stop codon. Note that aa598 in *CP1* and *DISC1* is a glycine, though with different codon usage. For clarity these sequences start at aa593 (top line), and show amino acids (middle line), and nucleotides (bottom line). Upper case nucleotide *DISC1* ORF, lower case neucleotide AB371558 ORF.

LSPREMCFSPSTMIVGPPQPH*NAFMK*GPGIEETPKGETEV*KSKKSGCGSRQKKRTAN

I*KSLRRTPQGNHFWTAKDLTEEIRSLTSEREGLEGLLSKLLVLSSRNVKKLGSVKEDYN

RLRREVEHQETAYETSVKENTMKYMETLKNKLCSCKCPLLGKVWEADLEACRLLIQSL

QLQEARGSLSVEDERQMDDLEGAAPPIPPRLHSEDKRKTPLKVLEEWKTHLIPSLHCAG

GEQKEESYILSAELGEKCEDIGKKLLYLEDQLHTAIHSHDEDLIQSLRRELQMVKETLQA

MILQLQPAKEAGEREAAASCMTAGVHEAQA*

Figure 3.2.B: Predicted sequence of the der 11 AB371558/*DISC1* chimera. This is a consequence of splicing of exons 1c-2 AB371558 proximal to the translocation breakpoint, to *DISC1* exons 9-13 distal to the breakpoint. This transcript only possesses an internal ORF of DISC1 aa669-854 (blue text), and was first identified by Eykelenboom *et al.* (2012).

`

3.2.2 Detection of the *CP1* transcript by RT-PCR

RT-PCR was performed on t(1;11) lymphoblastoid cell lines to detect the *CP1* transcript. This was a similar method to that used by Eykelenboom *et al.*, (2012) to identify the *DISC1/DISC1FP1* transcripts *CP60* and *CP69*. In the RT-PCR reaction to amplify *CP1*, the forward primer used was complimentary to *DISC1* exon 7 and the reverse primer to exon 3a of AB371558 (see figure 3.2.C.i).

A cDNA template from t(1;11) lymphoblastoid cell lines was used to detect a *CP1* band, (T). No PCR product is detected in the negative control (N) and normal karyotype control (K) (see figure 3.2.C.ii). The *CP1* chimeric transcript product was verified by sequencing. The region of RT-PCR product that was analysed by sequencing spanned the der 1 t(1;11) breakpoint region and contains both *DISC1* and AB371558 coding sequence and encodes a stop codon (see figure 3.2.C.iii). The *CP1* transcript encodes the same amino acid sequence as DISC1 aa1-598. However, the codon usage for aa598, a glycine differs between the two species. *CP1* uses the codon GGT while DISC1 uses GGA. The sequencing results match the *in silico* prediction (see figure 3.2.A). This establishes the existence of a third *DISC1/DISC1FP1* transcript detected in t(1;11) lymphoblastoid cells.

The chimeric transcript, *CP1*, is a comparable species to DISC1 aa1-597. The DISC1 aa1-597 ORF has been expressed *in vitro* (Brandon *et al*, 2005; Hattori *et al*, 2014; Kamiya *et al*, 2005; Millar *et al*, 2005a; Morris *et al*, 2003; Ozeki *et al*, 2003; Pletnikov *et al*, 2007; Taya *et al*, 2007) and *in vivo* (Hikida *et al*, 2007; Niwa *et al*, 2013; Pletnikov *et al*, 2008) within the field of DISC1 research as a potential C-terminal DISC1 truncated protein that may have been transcribed from the proximal der 1 chromosome.

`

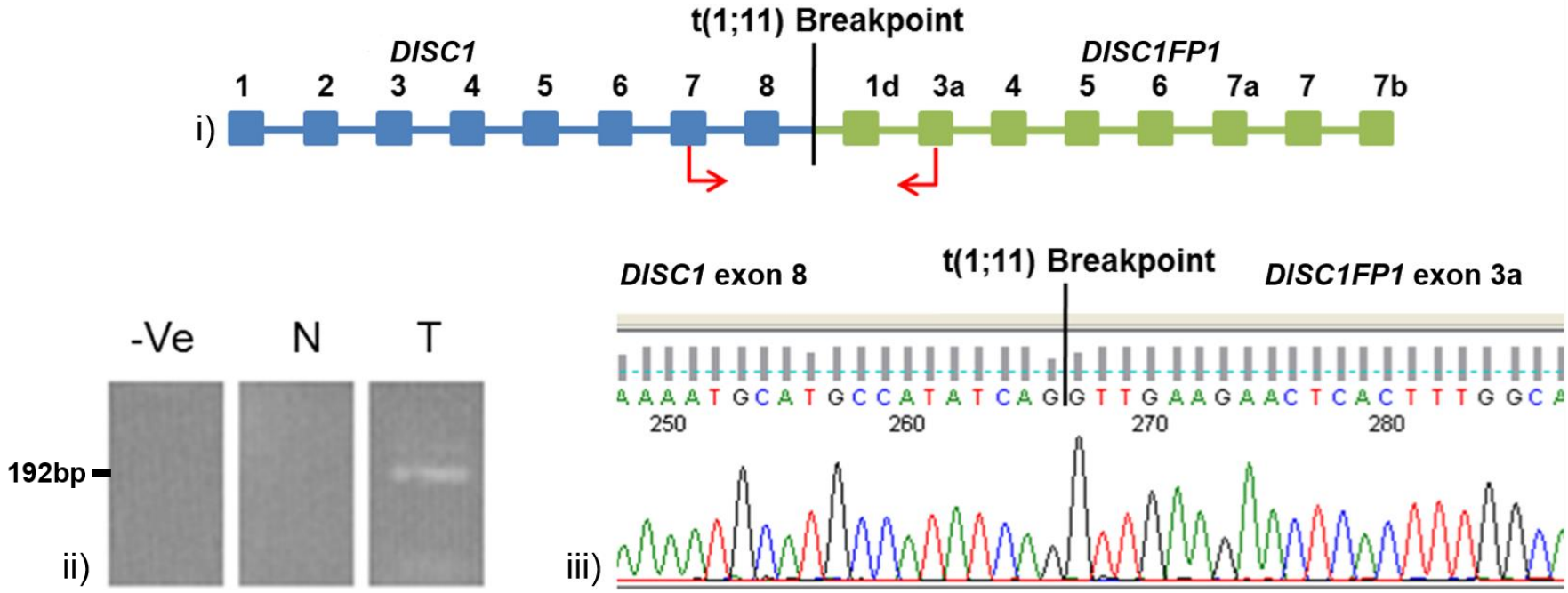

Figure 3.2.C: Detection of the *CP1* transcript in t(1;11) lymphoblastoid cell lines. i): RT-PCR primer location (red arrows). ii): Detection of the *CP1* transcript by RT-PCR. (T) is a t(1;11) cell line, (N) is a normal karyotype control, (-Ve) is negative control. iii): Sequence chromatogram spanning t(1;11) breakpoint confirming *CP1* transcript amplification.

`

3.3 Detection of exogenously expressed CP60 and CP69 protein by Western blot

3.3.1 Exogenously expressed CP60 and CP69 protein is detected in the pellet fraction

In order to exogenously express and characterise CP60 and CP69 proteins, untagged ORF*s* encoding these two species were synthesized in a pcDNA3.1(+) vector backbone by GENEART. The untagged CP60 and CP69 constructs were transiently transfected into COS-7 cells and both the cell lysate and pellet fraction were analysed by Western blot. The blots were probed with the antibody, R47, which has an epitope in the N-terminal of DISC1 located at aa191-202 (James *et al*, 2004). The R47 antibody is capable of detecting exogenously expressed DISC1 aa1-597 in the cell lysate fraction (Millar *et al*, 2005b). This is important given that the CP60 and CP69 transcripts encode DISC1 aa1-597 plus an additional 60 and 69 aa from DISC1FP1, respectively. R47, therefore, seems suitable for the detection of these der 1 chimeric protein species.

The COS-7 cell lysates were produced using both PBS-Triton and the more potent lysis buffer, RIPA, as the optimal lysis buffer to isolate exogenously expressed CP60 and CP69 protein was not known. Pre-experimental data suggested that these chimeric proteins could not be detected in the lysate with overnight exposures (see annex A2). Probing with the R47 antibody, both CP60 and CP69 proteins are only detected in the cell pellet, at a molecular weight of ~75kDa (see figure 3.3.A) irrespective of the potency of the lysis buffer used. These observations are comparable with the predicted molecular weights of CP60 and CP69, 72kDa and 73kDa respectively. In contrast, full-length wild-type FLAG-DISC1 was detected in both the cell lysate and pellet fractions, at a molecular weight of ~100kDa. This is as expected for FLAG-DISC1.

3.3.2 An alternate pellet processing method to detect exogenously expressed CP60 and CP69 protein

An alternative method of processing the cell pellet for Western analysis was carried out. This was performed as it was unusual to detect the exogenously expressed CP60 and CP69 protein in the cell pellet (see section 3.3.1). It was a possibility that an alternative method of processing the cell pellet may have detected other protein species in the cell pellet, or was more efficient at solubilising the pellet. The pellet processing method used in section 3.3.1 involved repeated

`

sonication with an ultrasonic probe to disrupt the cell pellet. A second pellet processing method was devised; this involved use of an ultrasonic bath to disrupt the pellet followed by repeated cycles of heating and vortexing to solubilise the pellet in PSB. Both pellet processing methods were used on RIPA COS-7 cell lysates exogenously expressing either CP60 or CP69.

The use of the ultrasonic bath pellet processing method on COS-7 cell lysates exogenously expressing CP60 and CP69 protein, mirrors the results of an ultrasonic probe processing method (see figure 3.3.B). Again CP60 and CP69 proteins are only detected in the pellet fraction, at approximately 75kDa irrespective of the processing method used on the COS-7 pellet fractions. FLAG-DISC1 is detected in both cell lysate and pellet fractions. These results are indistinguishable from the previous RIPA or PBS-Triton cell pellet blots detecting exogenously expressed CP60 and CP69 (figure 3.3.A).

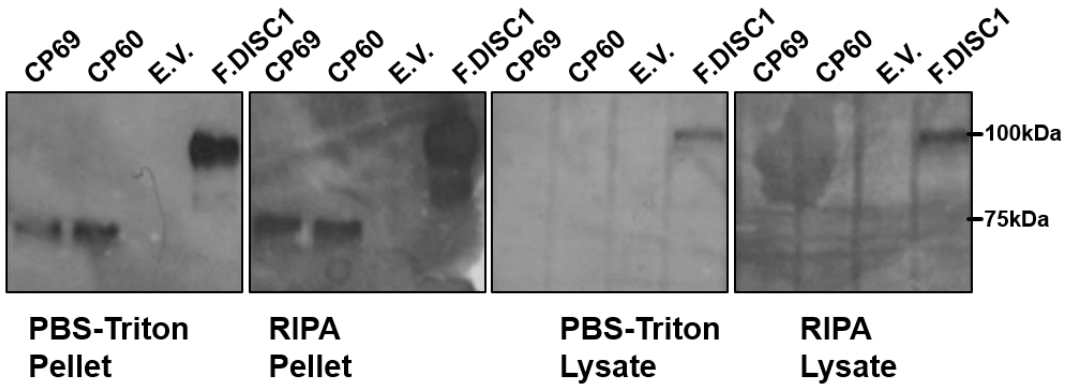

Figure 3.3.A: Detection of CP60 and CP69 protein in the pellet fraction. Western blotting detects exogenously expressed untagged CP60 and CP69 protein in COS-7 cells in the cell pellet at ~75kDa using the N-terminal DISC1 antibody R47 (1:1000). In these experiments no CP60 or CP69 protein is detected in the cell lysate. This observation is seen with both PBS-triton and RIPA lysis buffers and follows the transient transfection (24hr) of untagged pcDNA3.1(+), FLAG-DISC1 pcDNA3.1(+), CP60 pcDNA3.1(+) and CP69 pcDNA3.1(+) constructs into COS-7 cells. In comparison to CP60 and CP69, FLAG-DISC1 is seen in both the supernatant and pellet fractions at ~100kDa. E.V. is the empty vector condition, pcDNA3.1(+).

`

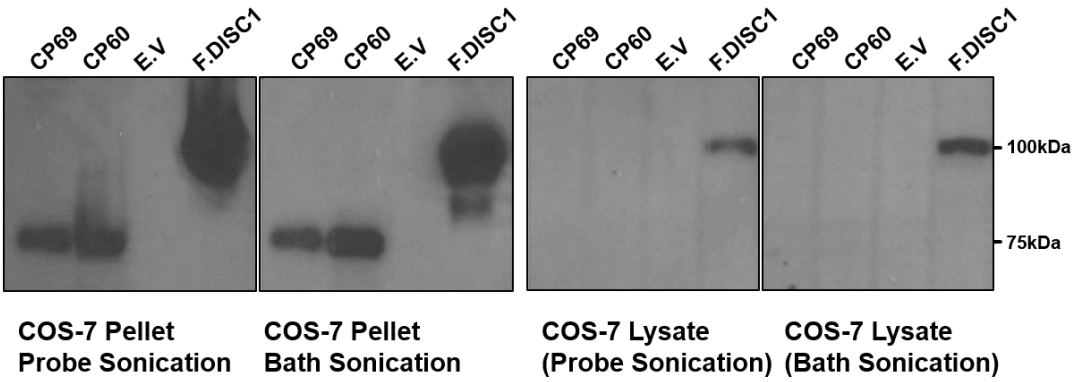

Figure 3.3.B: An alternate pellet processing method to detect exogenous CP60 and CP69 protein. Western blotting detects exogenously expressed untagged CP60 and CP69 protein is COS-7 cells in the cell pellet at ~75kDa using the N-terminal DISC1 antibody R47 (1:1000). This is following the use of bath sonication and probe sonication methodologies to disrupt the cell pellet. Detection of the chimeric protein in these two methodologies is highly similar. In these experiments, no CP60 or CP69 protein is detected in the cell lysate. In comparison, FLAG-DISC1 is seen in both the supernatant and pellet fractions at ~100kDa. E.V is the empty vector condition, pcDNA3.1(+).

The exogenously expressed CP60 and CP69 protein is detectable in the pellet fraction with the DISC1 N-terminal antibody R47. This contrasts with the DISC1 aa1-597 species, which, when exogenously expressed, can be detected in the cell lysate by the R47 antibody (Millar *et al*, 2005b). It may be that the additional 60 and 69 novel amino acids from DISC1FP1 interact with DISC1 aa1-597 also encoded in the chimeric species, resulting in the detection of CP60 and CP69 protein in the pellet fraction. The further characterisation of these chimeric protein species may reveal potential molecular pathophysiology mechanisms relating to the major mental illness seen in the t(1;11) pedigree (Blackwood *et al*, 2001). A range of chimeric constructs were designed for exogenous expression to enable immunocytochemistry and biophysical characterisation of CP60 and C69 protein species. This construct generation is covered in sections 3.4 and 3.5.

`

3.4 Generation of DISC/DISC1FP1 constructs for mammalian expression

3.4.1 Rationale for der 1 DISC1/DISC1FP construct production for expression in mammalian cell lines

To further investigate exogenously expressed DISC1/DISC1FP1 protein, several tagged constructs needed to be produced. Tagged CP1, CP60 and CP69 constructs would aid the detection of these exogenously expressed species in cell lines *in vitro* using immunofluorescence. Without the addition of peptide or protein tags, the DISC1/DISC1FP1 species can only be detected by N-terminal DISC1 antibodies such as R47 (James *et al*, 2004) of which there are limited stocks. Therefore, it was decided to use N-terminal FLAG-tags (Einhauer & Jungbauer, 2001) upstream of the chimeric ORF in the generation of further DISC1/DISC1FP1 constructs. This would enable the expressed FLAG-tagged der 1 species to be detected using commercial FLAG antibodies.

The possibility of endogenous der 1 protein expression in t(1;11) lymphoblastoid cell lines also needed to be investigated. In these experiments Western blotting would be used to analyse cell lysates and pellets from both t(1;11) lymphoblastoid cell lines and cell lines exogenously expressing the extant untagged DISC1/DISC1FP1 species. The resulting protein bands detected with N-terminal DISC1 antibodies would then be compared to see if the t(1;11) lymphoblastoid cell lysates and pellets provide evidence of endogenously expressed der 1 chimeric protein (Eykelenboom *et al*, 2012). An untagged CP1 construct needed to be generated for these experiments. This construct would be expressed in parallel with the existing untagged CP60 and CP69 constructs.

A FLAG-tagged DISC1 aa1-597 construct also needed to be generated for use as both a control, and to provide comparison with the exogenous expression of CP1. This was required because all of the DISC1/DISC1FP1 transcripts partially encode DISC1 aa1-597 (Eykelenboom *et al*, 2012), and CP1 encodes DISC1 aa1-598 (see section 3.2.2). At an early stage in method development, a pEF1 FLAG-DISC1 aa1-597 construct had been proposed. The Elongation Factor-1 Alpha (EF-1 alpha) promoter in the pEF1a vector produces less off-target lentiviral transduction into neurones (Jakobsson *et al*, 2003) than the hCMV promoter, which is found in pcDNA3.1(+) DISC1/DISC1FP constructs. This was initially seen as a means of delivering the der 1 chimeric species to neurone cultures *in vitro*. The idea was abandoned after single pEF1a construct pEF1 FLAG-DISC1 aa1-597 was generated; this will be detailed in the following section.

`

As the initial untagged CP60 and CP69 constructs from GENEART were housed in a pcDNA3.1(+) vector backbone, it was decided to use this vector to house the additional DISC1/DISC1FP1 constructs and controls. Figure 3.4.A shows cartoons of all the constructs generated, illustrating tagging, DISC1 and DISC1FP1 components.

3.4.2 DISC1/DISC1FP construct generation for expression in mammalian cell lines

A breakdown of the protocols used for cloning these constructs and their order of implementation is detailed in figure 3.4.B. The inserts for both the DISC1/DISC1FP1 constructs and the DISC1 aa1-597 constructs were produced by PCR (see figure 3.4.Ci-Hi). All of these inserts had 5' EcoR1 and 3' Not1 restriction sites flanking the ORF, which were incorporated into the primer pair design. The addition of FLAG-Tags to ORFs was a consequence of the FLAG ORF being derived from either the initial template, or from the final vector.

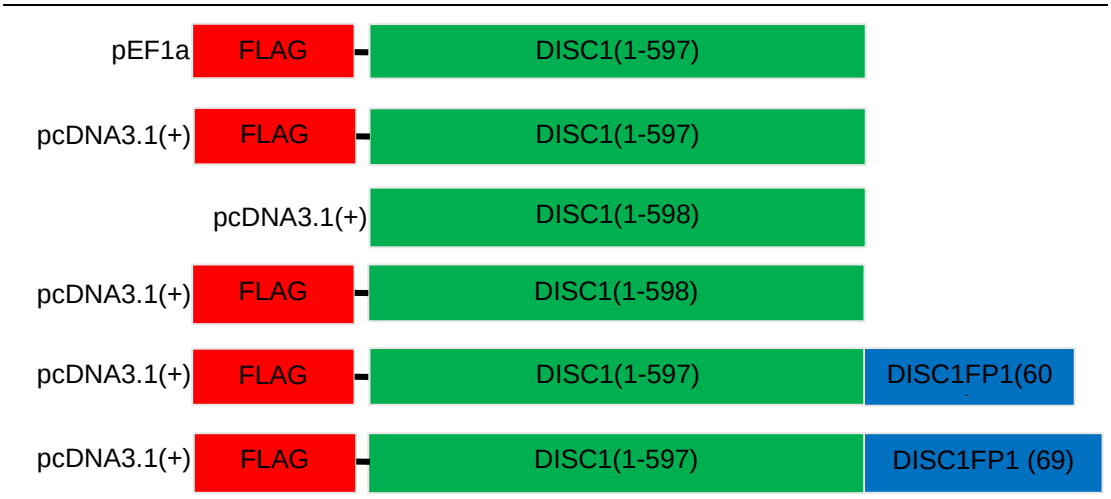

Figure 3.4.A: Cartoon depicting der 1 DISC1/DISC1FP and DISC1 aa1-597 constructs produced for expression in mammalian cell lines. Top to bottom: pEF1a-FLAG-DISC1-aa1-597, pcDNA3.1(+)-FLAG-DISC1-aa1-597, untagged pcDNA3.1(+)-CP1; pcDNA3.1(+)-FLAG-CP1; pcDNA3.1(+)-FLAG-CP60, pcDNA3.1(+)-FLAG-CP69. N-terminal FLAG-tag (red), *DISC1* ORF (green), *DISC1FP1* ORF (blue).

`

Following amplification of the insert, both vector and insert underwent restriction digestion with EcoR1 and Not1 to create sticky ends. The resultant vectors then underwent phenol-chloroform extraction to remove the by-products of the restriction digests and were then concentrated by ethanol precipitation. Prior to ligation, vectors were SAP treated to remove phosphates. The vectors and inserts were then ligated, and the ligation products transformed into *E.coli*. The bacteria were then cultured, lysed and plasmid DNA preps produced. The putative plasmid DNA was then digested using EcoR1/Not1 restriction digests to isolate the insert from the vector, and analysed by gel electrophoresis (see figure 3.4.Cii-Hii). Plasmid preparations that released inserts approximate to the predicted size of the ORF in question were then sequenced (see figure 3.4.Ciii-iv-Hiii-iv).

It should be noted that the template for both the untagged and FLAG-tagged CP1 constructs was pcDNA 3.1 (+) DISC1. The CP1 transcript itself encodes DISC1 aa1-598. However the constructs generated use the codon GGA for the glycine at aa598 as is found in DISC1. The CP1 transcript identified by RT-PCR (see section 3.2.2) has the codon GGT, which also codes for glycine.

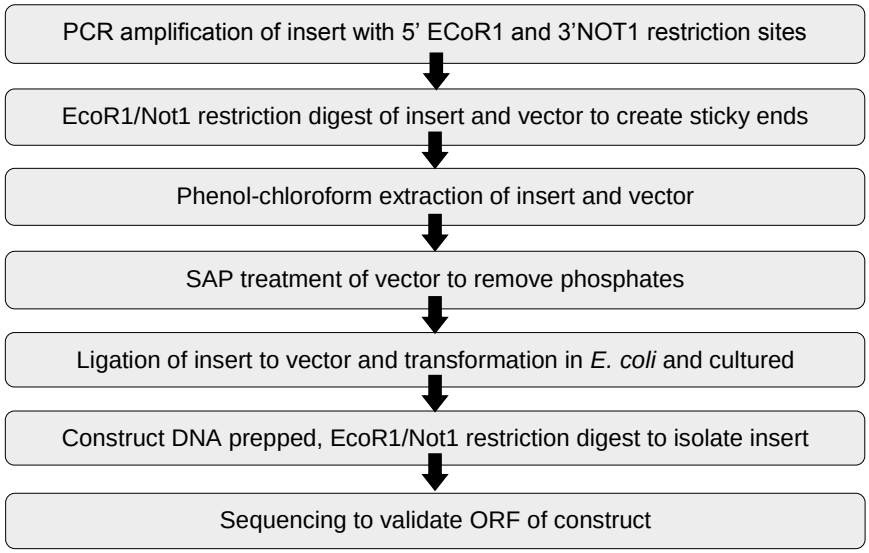

Figure 3.4.B: Cloning procedure for generating DISC1/DISC1FP1 constructs for expression in mammalian cell lines. The flow diagram shows an approximation of the steps taken to generate the following constructs: pEF1α-FLAG-DISC1 aa1-597, pcDNA3.1(+)-FLAG-DISC1 aa1-597, untagged pcDNA3.1(+)-CP1; cDNA3.1(+)-FLAG-CP1; pcDNA3.1(+)-FLAG-CP60, pcDNA3.1(+)-FLAG-CP69.

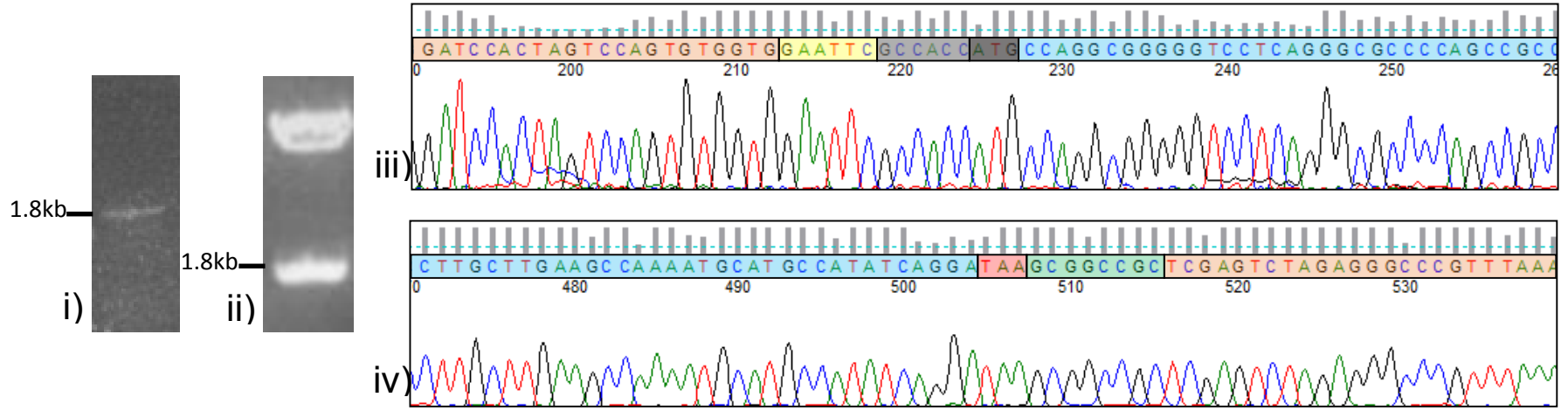

Figure 3.4.C: Creation of the pcDNA3.1(+)-CP1 construct. i) PCR band of EcoR1-DISC1 aa1-598-Not1 product. ii) EcoR1/Not1 restriction digest confirming the DISC1 aa1-598 insert (lower band). Linearized vector (upper band). iii) 5' sequence chromatogram of pcDNA3.1 (+) DISC1 aa1-598. iv) 3' sequence chromatogram of pcDNA3.1 (+) DISC1 aa1-598. Chromatogram key: Cloning cassette (pale pink), EcoR1 site (yellow), Kozak sequence (light grey), Methionine (dark grey), *DISC1* ORF (blue), Stop codon (pink), Not1 site (green).

`

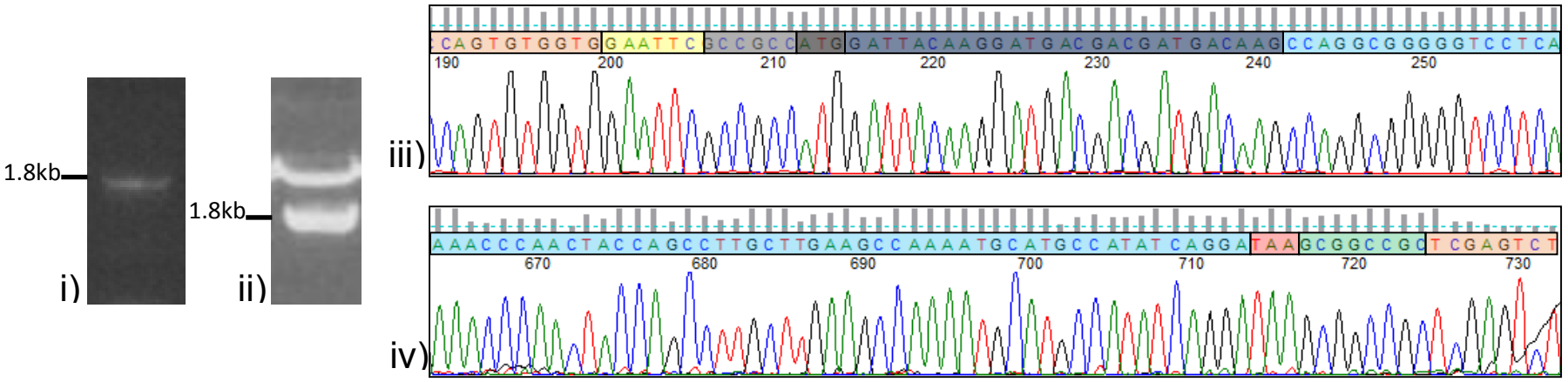

Figure 3.4.D: Creation of the pcDNA3.1(+)-FLAG-CP1 construct. i) PCR band of EcoR1-FLAG-DISC1 aa1-598-Not1 product. ii) EcoR1/Not1 restriction digest confirming the FLAG-DISC1 aa1-598 insert (lower band). Linearized vector (upper band). iii) 5' sequence chromatogram of pcDNA3.1 (+) FLAG-DISC1 aa1-598. iv) 3' sequence chromatogram of pcDNA3.1 (+) FLAG-DISC1 aa1-598. Chromatogram key: Cloning cassette (pale pink), EcoR1 site (yellow), Kozak sequence (light grey), Methionine (dark grey), FLAG-tag (dark blue), *DISC1* ORF (blue), Stop codon (pink), Not1 site (green).

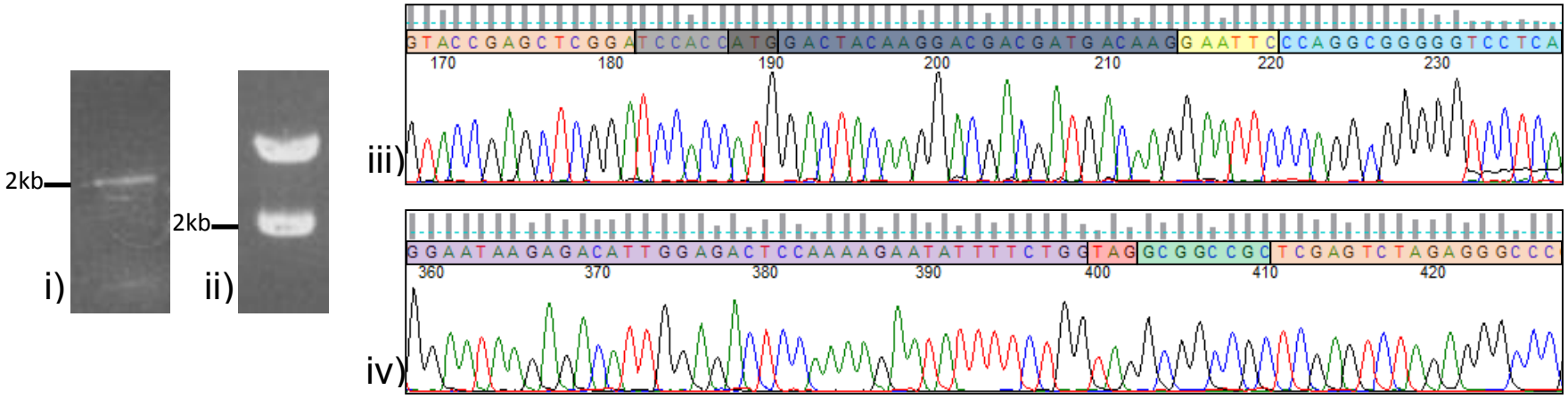

Figure 3.4.E: Creation of the pcDNA3.1(+)-FLAG-CP60 construct. i) PCR band of EcoR1-FLAG-CP60-Not1 product. ii) EcoR1/Not1 restriction digest confirming the FLAG-CP60 insert (lower band). Linearized vector (upper band). iii) 5' sequence chromatogram of pcDNA3.1 (+) FLAG-CP60. iv) 3' sequence chromatogram of pcDNA3.1 (+) FLAG-DISC1 CP60. Chromatogram key: Cloning cassette (pale pink), EcoR1 site (yellow), Kozak sequence (light grey), Methionine (dark grey), FLAG-tag (dark blue), *DISC1* ORF (blue), Stop codon (pink), Not1 site (green).

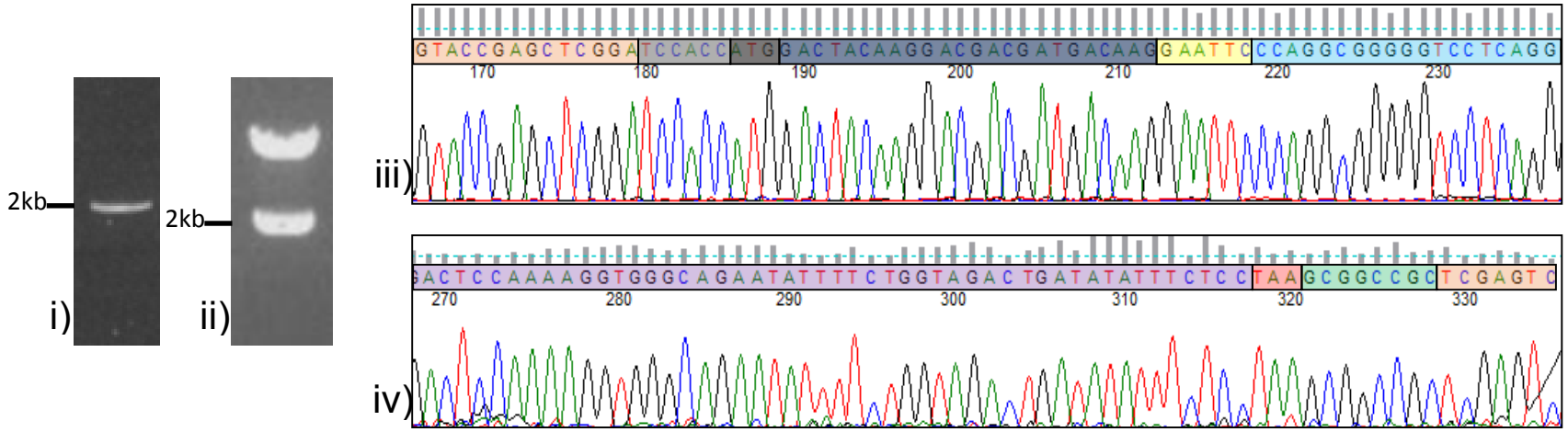

Figure 3.4.F: Creation of the pcDNA3.1(+)-FLAG-CP69 construct. i) PCR band of EcoR1-FLAG-CP69-Not1 product. ii) EcoR1/Not1 restriction digest confirming the FLAG-CP60 insert (lower band). Linearized vector (upper band). iii) 5' sequence chromatogram of pcDNA3.1 (+) FLAG-C69. iv) 3' sequence chromatogram of pcDNA3.1 (+) FLAG-DISC1 CP69. Chromatogram key: Cloning cassette (pale pink), EcoR1 site (yellow), Kozak sequence (light grey), Methionine (dark grey), FLAG-tag (dark blue), *DISC1* ORF (blue), Stop codon (pink), Not1 site (green).

`

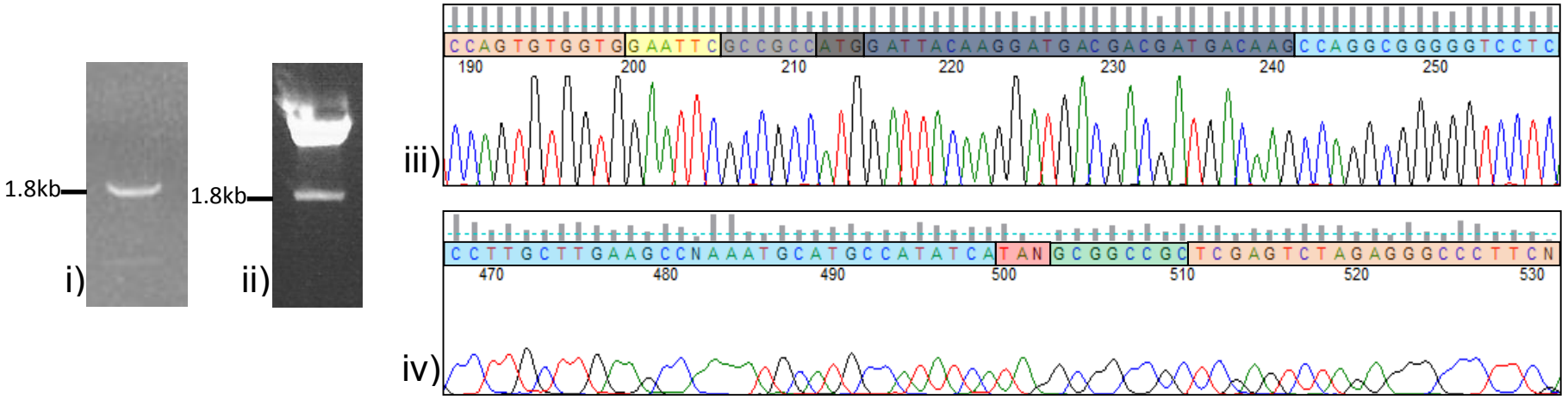

Figure 3.4.G: Creation of the pEF1α-FLAG-DISC1 aa1-597 construct. i) PCR band of EcoR1-FLAG-DISC1 aa1-597-Not1 product. ii) EcoR1/Not1 restriction digest confirming the FLAG-DISC1 aa1-597 insert (lower band). Linearized vector (upper band). iii) 5' sequence chromatogram of pEF1a FLAG-DISC1 aa1-597. iv) 3' sequence chromatogram of pEF1a FLAG-DISC1 aa1-597. Chromatogram key: Cloning cassette (pale pink), EcoR1 site (yellow), Kozak sequence (light grey), Methionine (dark grey), FLAG-tag (dark blue), *DISC1* ORF (blue), Stop codon (pink), Not1 site (green).

`

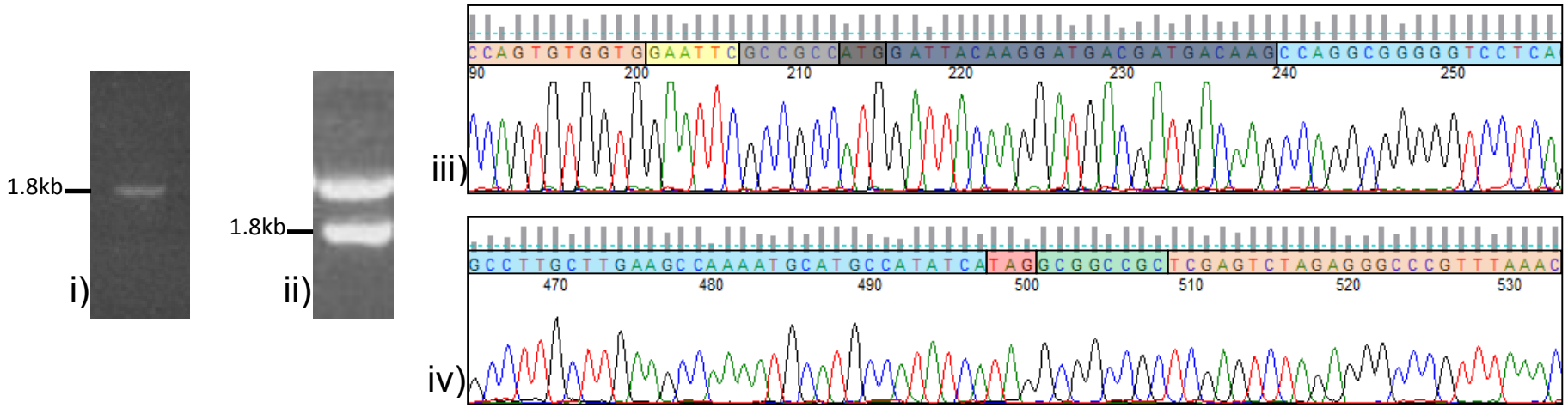

Figure 3.4.H: Creation of the pcDNA3.1(+)-FLAG-DISC1 aa1-597 construct. i) PCR band of EcoR1-FLAG-DISC1 aa1-597-Not1 product. ii) EcoR1/Not1 restriction digest confirming the FLAG-DISC1 aa1-597 insert (lower band). Linearized vector (upper band). iii) 5' sequence chromatogram of pcDNA3.1 (+) FLAG-DISC1 aa1-597. iv) 3' sequence chromatogram of pcDNA3.1 (+) FLAG-DISC1 aa1-597. Chromatogram key: Cloning cassette (pale pink), EcoR1 site (yellow), Kozak sequence (dark green), Methionine (dark grey), FLAG-tag (dark blue), *DISC1* ORF (blue), Stop codon (pink), Not1 site (green).

`

As the nucleotide coding in question is synonymous there should be no issue with this difference in nucleotide use. In total the der 1 DISC1/DISC1FP constructs for expression in mammalian cell lines produced were: untagged pcDNA3.1(+)-CP1, pcDNA3.1(+)-FLAG-CP1, pcDNA3.1(+)-FLAG-CP60, pcDNA3.1(+)-FLAG-CP69, pEF1α-FLAG-DISC1 aa1-597, pcDNA3.1(+)-FLAG-DISC1 aa1-597.

3.5 Generation of der 1 DISC1/DISC1FP constructs for expression in *E.coli*

3.5.1 Production of ΔNCP69 constructs for expression in *E.coli*

Exogenously expressed CP60 and CP69 are predominantly located in the pellet fraction. This observation suggests that the addition of 60 or 69 novel aa from DISC1FP1 spliced to DISC1 aa1-597 produces abnormal protein species. A biophysical approach was proposed to investigate the possibility of structural changes induced by the extra DISC1FP1 aa's. An N-terminal truncated species encoding DISC1 aa326-597 and 69 aa from DISC1FP1, with codon usage optimised for bacterial expression was synthesised by GENEART, named pENTRΔNCP69. The N-terminal head region is absent as the protein structure there is predicted to be highly disordered (Soares *et al*, 2011) and is believed to be the reason that DISC1 is difficult to purify. Only CP69 was chosen as the model for the DISC1/DISC1FP1 N-terminal truncate as CP60 and CP69 have high sequence homology.

For bacterial expression, the ΔNCP69 insert needed to be housed in bacterial expression vectors that also encoded protein tags to enable affinity purification of expressed protein. The ΔNCP69 insert was sub-cloned into four bacterial expression vectors using gateway cloning (see figure 3.5.A). Following the gateway cloning, the putative constructs were transformed and DNA prepared. PCR was then performed with vector specific primers on the four ΔNCP69 constructs to confirm construct generation (see figure 3.5.B). PCR was then used to verify that the ΔNCP69 insert was in frame and that the insert ORF was error free. This produced pDST14-HIS-ΔNCP69; pETG20a-TRX-ΔNCP69; pETG30a-GST-ΔNCP69 and pETG40a-MBP-ΔNCP69 constructs for bacterial expression.

`

3.5.2 Production of MBP-ΔN597 construct for expression in *E.coli*

To discern the contribution of the novel 69 aa from DISC1FP1 to ΔNCP69 protein characteristics, a DISC1 aa326-597 construct for bacterial expression needed to be produced (see figure 3.5.A). Site directed mutagenesis was performed using the pENTRΔNCP69 construct as a template to insert a double stop codon, TAATAA, after DISC1 aa597. This produced a pENTRΔN597 construct with an ORF optimised for bacterial expression that encoded DISC1 aa326-597. The choice of double stop codon rather than a single, was a precautionary measure to ensure that translation terminated and no ΔNCP69 protein was produced (see figure 3.5.C). Initially all four bacterial expression vectors were going to be produced and protein expression tests carried out to select the most promising construct/tag combination. As the MBP-ΔNCP69 protein proved to produce the largest quantities of purified protein, it was decided to only fully sequence the pETG40a-MBP- ΔN597 construct.

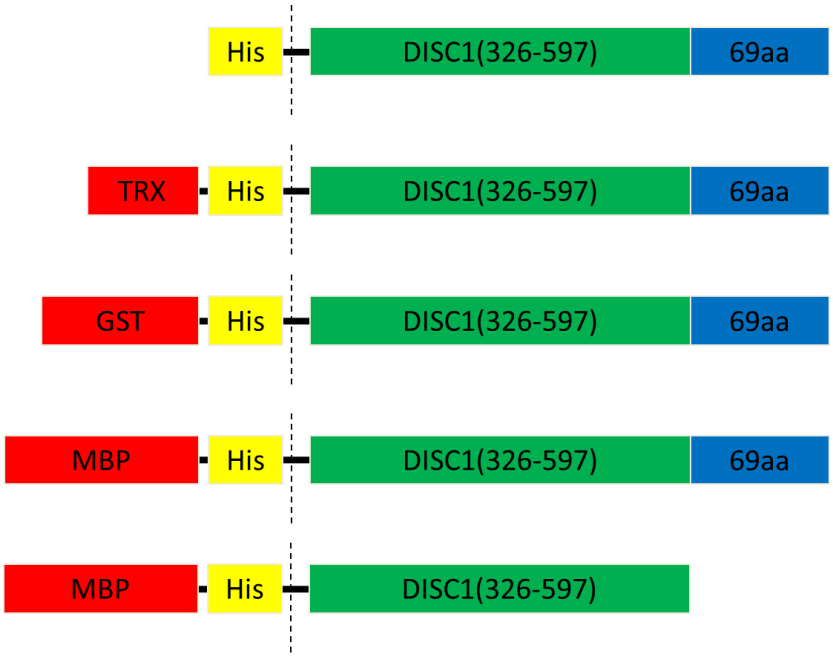

Figure 3.5.A: Cartoon depicting ΔNCP69 and ΔN597 constructs for bacterial expression. Top to bottom: pDST14-HIS-ΔNCP69; pETG20a-TRX-ΔNCP69; pETG30a-GST-ΔNCP69; pETG40a-MBP-ΔNCP69 and pETG40a-MBP-ΔN597. Dashed vertical line represents cleavage point whereby the protein tag can be separated from the protein of interest. Protein tags (red), 6xHis peptide tag (yellow), *DISC1* ORF (Green), *DISC1FP1* ORF (blue). Figure adapted from Nicholas Bradshaw.

`

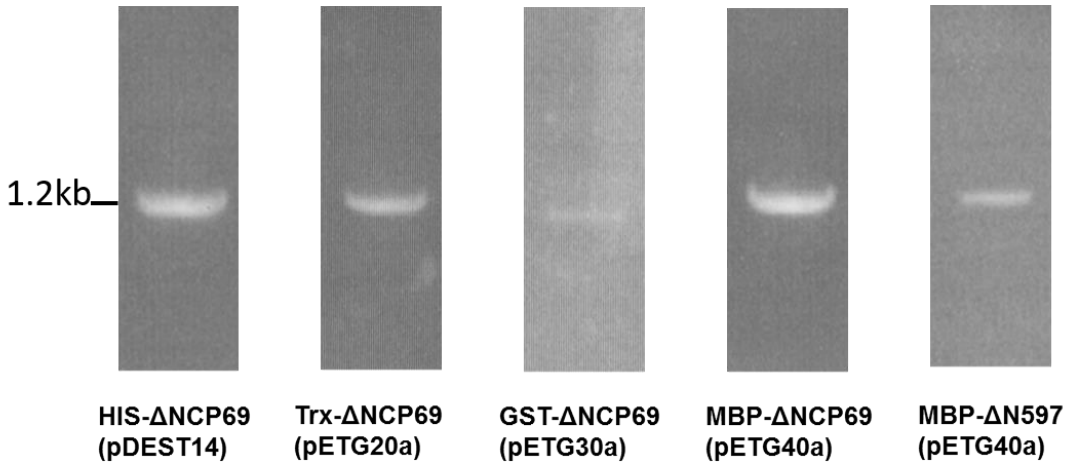

Figure 3.5.B: Generation of tagged ΔNCP69 and ΔN597 in bacterial expression vectors. This is the PCR product using vector specific primers following gateway sub-cloning of pENTRΔNCP69 and pENTRΔN597 into tagged destination vectors. Top row details tagged insert, bottom row, brackets, is the bacterial expression vector.

The PCR product confirming the pETG40a-MBP-ΔN597 construct generation is shown in figure 3.5.A. It would have been possible to introduce a double stop codon upstream of the aa326 in the MBP-ΔNCP69 construct using site directed mutagenesis, to create expression of the MBP tag only. This could have been used to remove the signal associated with the MBP protein from the biophysical experiments.

The biophysical experiments contrasting MBP-ΔNCP69 and MBP-ΔN597 protein were carried out by Dinesh Soares and Nicholas Bradshaw (Eykelenboom *et al*, 2012). This work addressed how the additional 69 aa confer altered protein structure over DISC1 aa 1-597. Dynamic light scattering indicates that MBP-ΔNCP69 produces protein species of greater size than MBP-ΔN597. The MBP-ΔNCP69 species also exhibit a higher melting point than MBP-ΔN597, indicative of greater stability. Far-UV circular dichroism spectra were ascertained to provide insight into the secondary structure of the protein species. MBP-ΔNCP69 was identified as containing 1.4-1.8 more α-helices with a reduced incidence of β-strands than that observed for MBP-ΔN597. These results suggest that the addition of a novel 69 aa to DISC1 aa1-597 results in larger protein assemblies being formed that exhibit increased stability and possess a specific secondary structure variation (Eykelenboom *et al*, 2012).

`

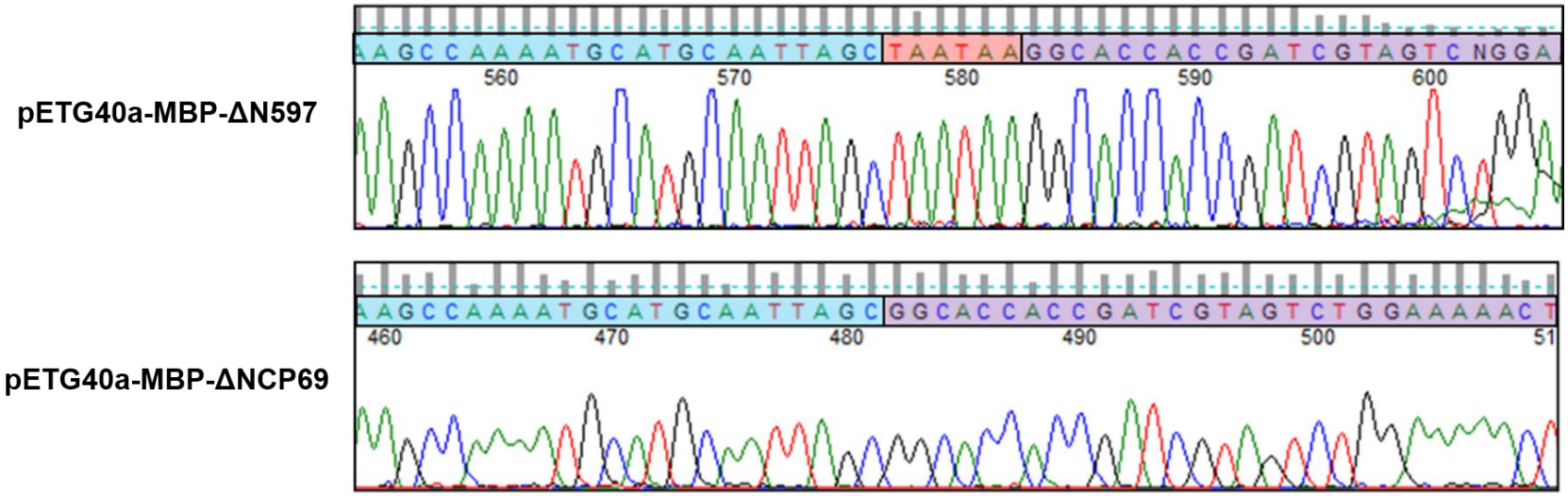

Figure 3.5.C: Generation of pETG40a-MBP-ΔN597. Sequence chromatogram of pETG40a-MBP-ΔN597 depicting the double stop codon TAATAA (top), that were introduced by site directed mutagenesis to the donor vector. This is contrasted with the pETG40a-MBP-ΔNCP69 sequence chromatogram depicting the DISC1 and DISC1FP1 ORF in the same region (bottom). The presence of the stop codons in pETG40a-MBP-ΔN597 terminate transcription following DISC1 aa597, resulting in the encoding of the N-terminal truncated DISC1 species MBP-ΔN597. Chromatogram key: *DISC1* ORF (blue), *DISC1FP1* ORF (Purple), Stop codon (pink).

`

3.6 Discussion

3.6.1 Relevance of the *CP1* transcript to the field

Canonically, in DISC1 research, DISC1 aa1-597 has been investigated both *in vitro* (Brandon *et al*, 2005; Hattori *et al*, 2014; Kamiya *et al*, 2005; Millar *et al*, 2005a; Morris *et al*, 2003; Ozeki *et al*, 2003; Pletnikov *et al*, 2007; Taya *et al*, 2007) and *in vivo* (Hikida *et al*, 2007; Niwa *et al*, 2013; Pletnikov *et al*, 2008) as a C-terminal truncated DISC1 species that may have been produced as a result of the t(1;11) from the proximal der 1 chromosome, that possesses novel pathogenic properties. However, there is no evidence that a DISC1 transcript encoding DISC1 aa1-597 exists, although the *CP1* transcript, if translated in t(1;11) carriers would give a protein that differs from DISC1 aa1-597 by only a single glycine at aa598 (Eykelenboom *et al*, 2012). Therefore, a summary of the behavioural and histological evidence from the *in vivo* expression of C-terminal truncated DISC and *Disc1* species in transgenic models will be covered in the following section in relation to the potential phonotypes that could be produced by CP1 if it is expressed *in vivo*. The high degree of sequence homology between DISC1 aa1-597 and the CP1 species, means that the C-terminal truncated DISC1/Disc1 models may be informative as to CP1 mechanisms of pathogenesis *in vivo* as they are almost hypothetical CP1 transgenic models.

3.6.2 C-terminal truncated DISC1/*Disc1* mouse models may give insight into the effects of CP1 protein expression *in vivo*

This discussion section summarises the findings of key papers on C-terminal truncated DISC1/*Disc1* mouse models (see introduction) as a means to see how such models could be informative as to what phenotypes would be produced by the expression of an endogenous CP1 species *in vivo*. This is given that the *CP1* transcript essentially encodes DISC1 aa1-598 (Eykelenboom *et al*, 2012). Assuming that the glycine at aa598 is uncharged and that it makes little or no difference to the expressed CP1 protein structure in comparison to DISC1 aa1-597. Then, at the very least, CP1 expression *in vivo* could bare great similarity to the human DISC1 aa1-597 mice models, ΔhDISC1 (Pletnikov *et al*, 2008) and DN-DISC1 (Hikida *et al*, 2007). Based on the common functions between these two models, CP1 expression *in vivo* might be expected to produce a histological profile of lateral ventricular enlargement and a reduction in parvalbumin-positive interneurones in the PFC as well as behavioural abnormalities in open field locomotor activity, a degree of amphetamine hyperactivity and increased forced swim test (FST) immobility.

`

Ultimately, in relation to the high incidence of major mental illness in the t(1;11) pedigree (Blackwood *et al*, 2001), some qualification must be made as to how similar to major mental illness the phenotype of such a hypothetical endogenous expression of CP1 *in vivo* would be. Regarding the common findings between ΔhDISC1 (Pletnikov *et al*, 2008) and DN-DISC1 (Hikida *et al*, 2007) mice that may feature in such an expression of CP1 *in vivo*, lateral ventricular enlargement is the most common observation in individuals with schizophrenia seen in MRI studies (Shenton *et al*, 2001). The reduction in parvalbumin-positive staining interneurones in these mouse models is in line with observed deficiencies in parvalbumin-positive neuronal sub-populations in individuals with schizophrenia (Lewis *et al*, 2012; Lewis *et al*, 2005). Therefore, the two common histological findings from the DN-DISC1 (Hikida *et al*, 2007) and ΔhDISC1 (Pletnikov *et al*, 2008) mice that could possibly be seen with CP1 expression *in vivo* can be seen to be schizophrenia-like. The common behavioural observations between these models possess a broader spectrum of phenotypes. In the hyperlocomotion in the open field, the activity measured is relative to the level of stress the animal is undergoing. As such, this test is seen to be a measure of anxiety-like behaviour (Prut & Belzung, 2003). In contrast, the use of amphetamines in the open field can be seen to be a model of psychosis-like behaviour (Robinson & Becker, 1986). However, the FST is not a measure of a depression-like behaviour phenotype *per se* but a screen for sensitivity to antidepressant compounds. Therefore, from the ΔhDISC1 (Pletnikov *et al*, 2008) and DN-DISC1 (Hikida *et al*, 2007) models it can be inferred that the expression of CP1 *in vivo* could possibly produce a schizophrenia/anxiety-like phenotype.

However, there is a caveat in deriving a possible *in vivo* CP1 expression phenotype from the ΔhDISC1 (Pletnikov *et al*, 2008) and DN-DISC1 (Hikida *et al*, 2007) models. Both of these transgenic models use a CaMKII promoter and, as such, do not recapitulate endogenous expression. The *Disc1*$_{tr}$ mice though, express truncated *Disc1* endogenously from a BAC (Shen *et al*, 2008). Fortunately, this is the most comprehensively histologically phenotyped model, and, along with the ΔhDISC1 (Pletnikov *et al*, 2008) and DN-DISC1 (Hikida *et al*, 2007) models, also has the schizophrenia-like morphology of lateral ventricle enlargement and a reduction in parvalbumin-positive interneurones. This makes it more likely that the endogenous expression of CP1 protein *in vivo* could produce these aberrations than from the evidence of the ΔhDISC1 (Pletnikov *et al*, 2008) and DN-DISC1 (Hikida *et al*, 2007) models alone. It is possible that the expression of CP1 *in vivo* could also produce some of the other anatomical abnormalities seen in the *Disc1*$_{tr}$ mice (Shen *et al*, 2008).

`

Though included in this discussion, the DN-DISC1/poly I:C (Ibi *et al*, 2010; Nagai *et al*, 2011) or ΔhDISC1/poly I:C (Abazyan *et al*, 2010) mouse models may not translate directly to the investigation of CP1 in the pathogenesis of mental illness in the t(1;11) family. This is because it would seem unlikely that the pedigree have all succumbed to a viral infection around birth. However, these models are informative as to the prospect of gene-environment interactions and the resulting phenotypical changes over expression of the transgene alone. Conversely, the gene-environmental interaction by Niwa *et al*., (2013) of isolation stress and humanised DISC1 aa1-597 expression is perhaps more likely a model to translate to the possibility of CP1 *in vivo* expression within the t(1;11) pedigree. It would seem feasible that, in their development, members of the t(1;11) pedigree have been exposed to stress as an environmental insult. This suggests that CP1 *in vivo* expression could possibly produce a range of dopaminergic dysfunctions, as seen in Niwa *et al.*, (2013), provided the expression was against a background of stress within translocation carriers.

It is possible that *in vivo* expressed CP1 would affect glia. The exogenous expression of CP1 could, like that of human DISC1 aa1-597, induce abnormal oligodendrocyte proliferation and differentiation (Katsel *et al*, 2011), albeit with the use of an endogenous, as opposed to a CaMKII, promoter. An endogenous CP1 species could also possibly perturb the function of serine racemase to synthesise D-serine causing glutamatergic dysfunction in astrocytes, as this has been observed for DISC1 aa1-597, expressed under a GFAP promoter (Ma *et al*, 2012). However, it would be a prerequisite that CP1 *in vivo* was expressed endogenously in astrocytes.

In summary, it seems possible that the endogenous expression of CP1 *in vivo* would, at the very least, induce a histological phenotype that is schizophrenia-like and would involve the features of enlarged lateral ventricles and a reduction in parvalbumin-positive interneurones. Such expression of CP1 could likely also include other features that have been identified in the ΔhDISC1 (Pletnikov *et al*, 2008) DN-DISC1 (Hikida *et al*, 2007) and *Disc1*$_{tr}$ mice (Shen *et al*, 2008). It is also equally possible that the expression of CP1 *in vivo* may have an effect on the proliferation and differentiation of oligodendrocytes (Katsel *et al*, 2011) as well as glutamatergic function as facilitated by astrocytes (Ma *et al*, 2012). Lastly, the possibility remains that CP1 expression could produce further phenotypic change if expressed in t(1;11) carriers against an environmental insult such as stress, which in Niwa *et al*, (2013) produces a range of dopaminergic dysfunctions.

`

3.6.3 Detection of exogenously expressed CP60 and CP69 protein in the cell pellet

It is surprising to find the CP60 and CP69 protein isolated in the pellet fraction. The cell pellet typically contains high molecular weight structures including: polymerised microtubules, hydrophobic membrane structures and fragmented membranes. This suggests that CP60 and CP69 protein may possess novel aberrant properties and warrants further investigation, and may be informative to the pathogenesis of major mental illness in the t(1;11) pedigree (Blackwood *et al*, 2001).

The observation that the exogenously expressed CP60 and CP69 chimeric proteins are isolated in the cell pellet is in agreement with two published reports that have emerged in the time since these experiments were completed. Zhou *et al*, (2010) detected protein in the cell pellet, from the expression of the DB7 construct that encodes CP60 in HEK293 cells. Here the chimeric protein was tagged with HA at the C-terminus. A repeat of this experiment carried out in both HEK293 and COS-7 cells again detected low levels of CP60 protein specifically in the pellet fraction (Ji *et al*, 2014). The expression of CP60 both *in vitro* and *in vivo* has been associated with a decrease in the reduction of MTT and a reduction in both translation and rRNA levels. Furthermore, converging lines of evidence suggest that the CP60 species undergoes degradation once expressed (Ji *et al*, 2014) which may partly explain why CP60 and CP69 are only observed in the pellet fraction in the Western blotting in this chapter.

3.6.4 Conclusions from the biophysical characterisation of MBP-ΔNCP69

MBP-ΔNCP69 produces large stable protein assemblies with a greater proportion of α-helices than MBP-ΔN597 (Eykelenboom *et al*, 2012). The addition of the extra 69 novel aa from DISC1FP1 to DISC1 aa326-597 results in the alteration of the structure of aa326-597. It is likely that this is also the case for CP60 given the high degree of homology between CP60 and CP69. It is possible therefore that CP60 and CP69 protein possess novel properties that differ from either the CP1 or DISC1 aa1-597 species due to these biophysical findings. These results may also in part explain the isolation of CP60 and CP69 in the pellet as a consequence of altered protein structure.

This chapter has highlighted that CP1, CP60 and CP69 may possess novel properties that could result in protein behaviour that differs from that of WT-DISC1. The next chapter will focus on the *in vitro* expression of three DISC1/DISC1FP1 species CP1, CP60 and CP69 in both

`

COS-7 cell lines and primary cortical neuron cultures in order to characterise potential pathogenic properties of DISC1/DISC1FP1 proteins.

`

Chapter 4 - The detection of overexpressed DISC1/DISC1FP chimeric proteins by immunofluorescence

4.1 Introduction

The existence of *DISC1/DISC1FP1* chimeric transcripts adds further complexity to the mechanism of pathogenesis of mental illness in t(1;11) carriers. Prior to the detection of the *DISC1/DISC1FP1* transcripts (Eykelenboom *et al*, 2012), haploinsufficiency of DISC1 was proposed as the mechanism of pathogenesis of mental illness in t(1;11) carriers (Millar *et al*, 2005b). The discovery of *DISC1/DISC1FP1* transcripts raises the possibility of additional pathogenic mechanisms. This requires that the *DISC1/DISC1FP1* transcripts that have been detected are translated into aberrant proteins in t(1;11) carriers. Presently, post-mortem neuronal t(1;11) tissue is not available to investigate endogenous expression of DISC1/DISC1FP1 chimeric proteins. It is possible, however, to look at the *in vitro* expression of FLAG-tagged: CP1, CP60, and CP69 in both COS-7 cells and primary mouse cortical neurones using immunofluorescence. COS-7, a monkey kidney cell line, was initially chosen for use in immunocytochemistry specifically due to the large size of these cells. The sizable cell body and organelles in COS-7 cells make any changes due to the mis-localisation of exogenous proteins readily visible. The use of neurones when investing phenotypes or potential pathogenic properties of the proteins pertaining to mental illness was essential, with any findings in COS-7 cells hopefully replicating those observed in neurones.

Previous immunofluorescence experiments to detect exogenously expressed DISC1 have shown a predominantly punctate localisation, whereas the expression of exogenous DISC1aa1-597 displayed a predominantly diffuse staining pattern (Brandon *et al*, 2005; Millar *et al*, 2005a; Morris *et al*, 2003; Ozeki *et al*, 2003). The *CP1* open reading frame is highly similar to that of DISC1 aa1-597, differing only by the addition of a glycine at aa598 (Eykelenboom *et al*, 2012). It therefore seems reasonable to assume that the localisation of expressed CP1 protein will closely resemble that of DISC1 aa1-597 rather than full length DISC1, and may likewise produce a diffuse staining pattern. It seems unlikely that the presence of an additional glycine, a neutral amino acid, will alter protein expression greatly.

`

It is likely that expressed CP60 and CP69 will differ from CP1 expression. This is due to the additional 60 and 69 amino acids from DISC1FP following DISC1 aa1-597 in CP60 and CP69, respectively. Zhou *et al.*, (2010) expressed the DB7 construct, that corresponds to CP60, in a rat neuronal-like cell line and observed a punctate staining pattern, rather than the diffuse staining of DISC1 aa1-597, with localisation present in the cytoplasm and neuronal periphery.

In this chapter, immunofluorescence was utilised as a technique to characterise the expression of FLAG-tagged CP1, CP60 and CP69 protein, in both COS-7 cells and mouse primary cortical neurones. The characterisation of these exogenously expressed abnormal chimeric DISC1/DISC1FP1 proteins may provide additional insight into the pathogenesis of the major mental illness seen in t(1;11) carriers. The majority of the immunofluorescence work in this chapter is published in Eykelenboom *et al.*, (2012).

4.2 When expressed in COS-7 cells, CP60 and CP69 are targeted to mitochondria where they induce extreme dysfunction

4.21 Exogenous CP60 or CP69 localise as perinuclear clusters in COS-7 cells

In order to investigate any possible pathophysiological properties of CP60 and CP69, the localisation patterns of FLAG-CP60, FLAG-CP69, FLAG-DISC1 aa1-597 and full-length FLAG-DISC1 were investigated after overexpression in COS-7 cells. The cells were then immunostained with anti-FLAG (M2) antibody in the presence of the mitochondrial dye, MitoTracker Red. When stained with anti-FLAG antibody, overexpressed CP60 or CP69 protein localises as perinuclear clusters (see figure 4.2.A-B). In figure 4.2.A, **a-c** depict increasing levels of CP60 protein expression. Such variation in expression can also be seen for CP69 (data not shown). There is no apparent difference in the localisation pattern between CP60 and CP69. The clustered localisation pattern of exogenously expressed CP60 or CP69 differs from the localisation of overexpressed WT-DISC1, which displays a predominantly punctate pattern. In contrast DISC1 aa1-597, is diffusely expressed throughout the cytoplasm. CP60 and CP69 encode DISC1 aa1-597 fused to 60 or 69 novel aa, respectively, from DISC1FP1 (Eykelenboom *et al*, 2012). The difference in localisation observed from the expression of DISC1 aa1-597 versus that of either CP60 or CP69 therefore arises as a consequence of the addition of these novel DISC1FP1 derived aa's. These results suggest that

`

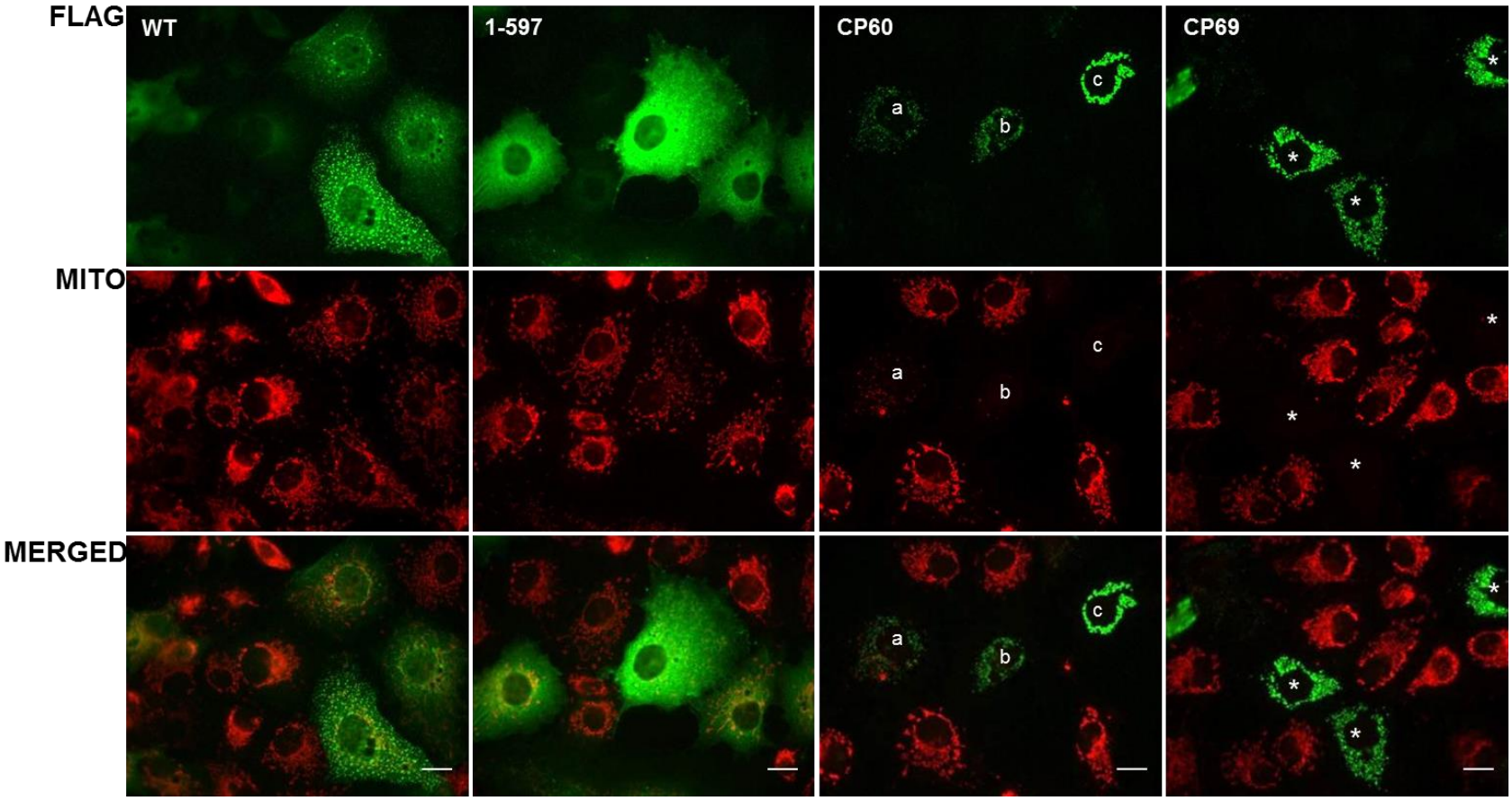

Figure 4.2.A: Expression of exogenous CP60 and CP69 in COS-7 cells. Immunostaining: FLAG (green) and MitoTracker Red. Lower case a-c demarks increasing expression of CP60 protein; asterisks denote expression of CP69 protein. CP60 and CP69 localise as clusters and COS-7 cells expressing these chimeras often do not stain with MitoTracker Red. Scale bar represents 10μM.

`

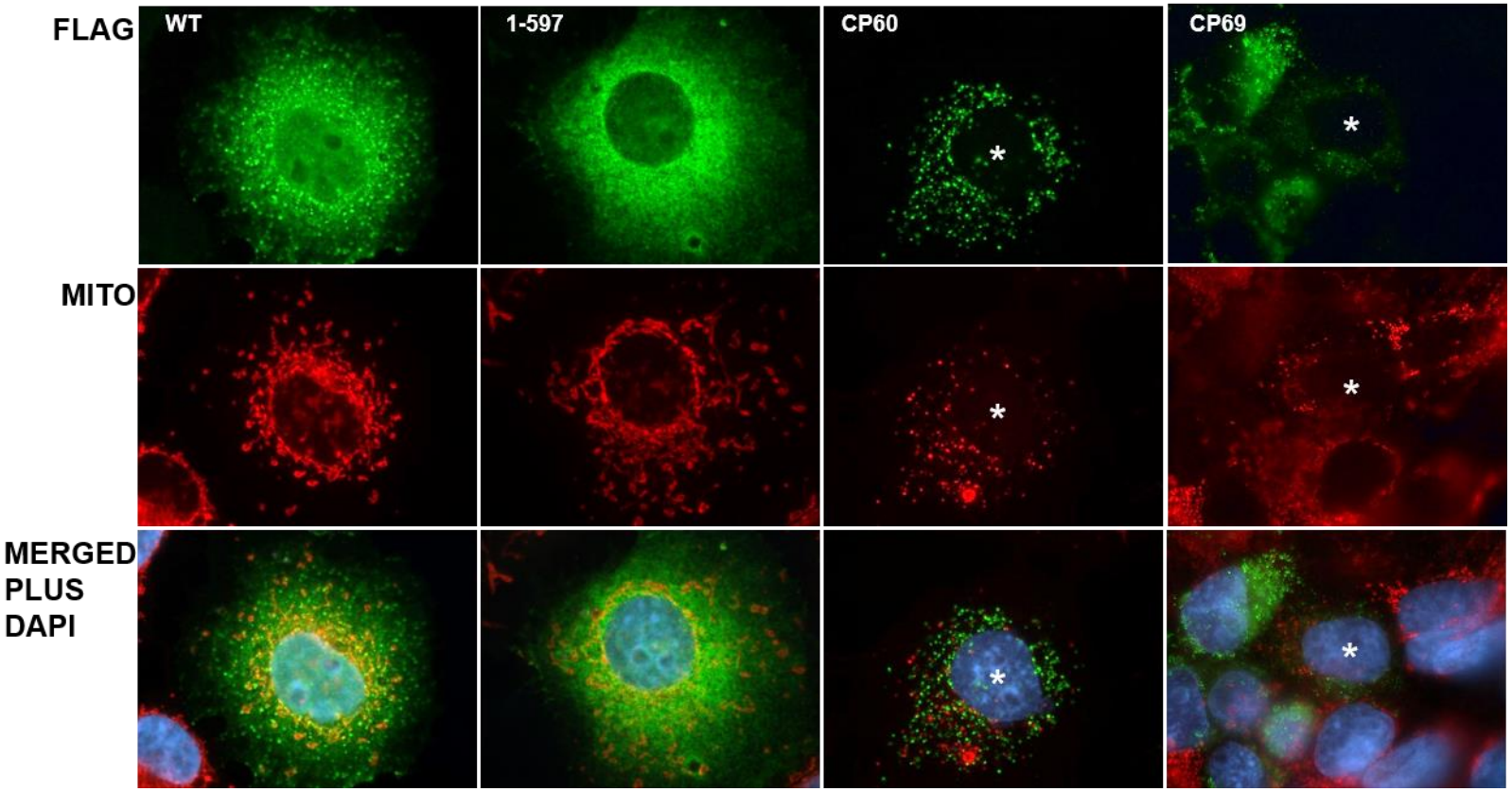

Figure 4.2.B: Clustered MitoTracker Red staining is evident in a subpopulation of COS-7 cells exogenously expressing CP60 and CP69. Immunostaining: DAPI (blue) FLAG (green) and MitoTracker Red.

`

CP60 and CP69 proteins may have novel properties differing from other DISC1 species (Eykelenboom *et al*, 2012).

This initial immunofluorescence evidence indicated that exogenously expressed CP60 and CP69 proteins localise in a novel manner, as clusters. Additional experiments, using qualitative analysis of overexpressed CP60 and CP69 protein in COS-7 cells, were needed to determine how consistently this novel localisation pattern was observed, and indeed if the localisation of CP60 and CP69 differed.

4.2.2 Exogenous CP60 or CP69 impair MitoTracker Red uptake

DISC1 is known to be targeted to the mitochondria (James *et al*, 2004; Millar *et al*, 2005a; Norkett *et al*, 2016; Ogawa *et al*, 2014; Park *et al*, 2010) and the expression of DISC1 aa1-597 in COS-7 cells induces the formation of 'ring' mitochondria in a sub-population of transfected cells (Millar *et al*, 2005a). It is therefore plausible that the expression of exogenous CP60 or CP69 may produce a mitochondrial phenotype detectable by immunofluorescence.

In the majority of COS-7 cells expressing exogenous CP60 or CP69, the staining of mitochondria by MitoTracker Red was absent **(**see figure 4.2.A). In contrast, cells overexpressing WT-DISC1 or DISC 1 aa1-597, MitoTracker Red displayed stained tubular mitochondria. However, a sub-population of CP60 and CP69 expressing cells were stained, displaying clustered mitochondria (see figure 4.2.B).

MitoTracker Red is a dye that fluoresces upon entering respiring cells where it is sequestered by the mitochondria. The staining of mitochondria by MitoTracker dyes can be influenced by both oxidative stress and changes in the mitochondrial membrane potential, $\Delta\psi m$ (Buckman *et al*, 2001). The absence of MitoTracker Red staining seen in COS-7 cells expressing CP60 and CP69 may be due to impairment in the uptake of MitoTracker due to alterations in the mitochondrial membrane potential, $\Delta\psi m$. This observation suggests that the expression of CP60 and CP69 produces mitochondrial dysfunction. Further investigation using qualitative analysis of overexpressed CP60 and CP69 protein in COS-7 cells was needed to determine how frequently MitoTracker staining was absent, and how often clustered mitochondria were visible.

`

4.2.3 Qualitative analysis of the localisation of expressed exogenous CP60 and CP69

To further characterise the expression pattern of CP60 and CP69 protein, a blinded counting paradigm was adopted. Three independent immunofluorescence experiments were performed under blinding. Again, these were performed by transfecting FLAG-CP60, FLAG-CP69, FLAG-DISC1 aa1-597 and FLAG-WT-DISC1 into COS-7 cells, immunostaining with anti-FLAG (M2) antibody and then mitochondrial staining with MitoTracker Red 24hrs post-transfection. Using fluorescence microscopy, the expression pattern of the anti-FLAG staining was tallied as either 'punctate', 'diffuse' or 'clustered'. These categories of expression pattern represented the observed WT-DISC1, DISC1aa1-597 and CP60 or CP69 protein localisation seen previously (see figure 4.2.A-B). In total, the expression pattern of anti-FLAG immunostaining of 60 transfected cells was categorized per construct.

It may be that when a greater population of transfected cells were observed and characterised, that the expression pattern of overexpressed CP60 and CP69 protein may have been more heterogeneous than initial observations suggested. It was possible that a variety of localisation patterns could be present. For example, Brandon *et al.,* (2005), identified three different expression patterns for the exogenous expression of WT-DISC1 or DISC1 aa1-597 in HeLa cells. The WT-DISC1 expression was primarily observed as punctate but diffusely distributed or aggregated staining was also evident, while the DISC1 aa1-597 expression pattern was predominantly diffuse with some cells observed to be aggregated or punctate.

Figure 4.2.C collates the data for fluorescence staining patterns. The predominant expression pattern of CP60 and CP69 in COS-7 cells was evident as perinuclear clustering and this expression pattern, like those of the other DISC1 species, was highly uniform. The clustered phenotype was seen in 99% and 97% of CP60 and CP69 overexpressing cells, respectively. In 99% of WT-DISC1 overexpressing cells the expression pattern was characterised as punctate. Likewise, 99% of DISC1 aa1-597 overexpressing cells were noted as having a diffuse cytoplasmic distribution. The predominant WT-DISC1 and DISC1 aa1-597 expression patterns observed were similar to previously published qualitative observations (Brandon *et al*, 2005; Millar *et al*, 2005a).

The overexpression of CP60 and CP69 protein produces a novel clustered perinuclear cellular expression pattern, with no significant difference between CP60 and CP69 localisation observed. The similarity of expressed CP60 and CP69 protein in COS-7 cells reflects the

`

homology between CP60 and CP69. The perinuclear clustering of exogenously CP60 or CP69 *in vitro* may be indicative of a role of these chimeras in the pathogenesis of major mental illness in the t(1;11) pedigree**.**

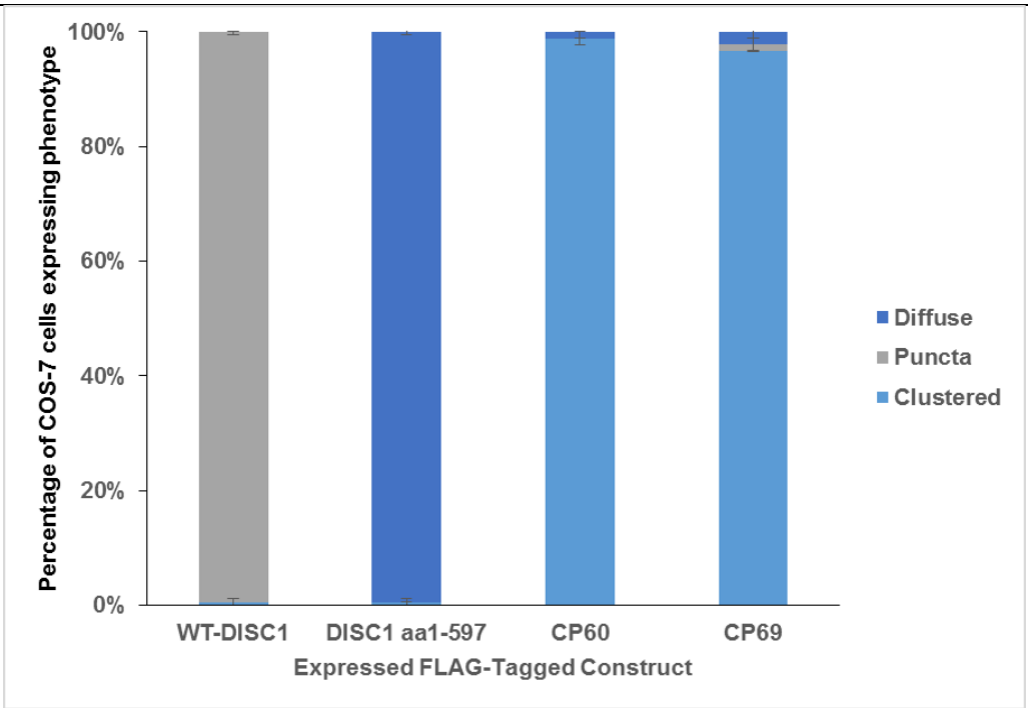

Figure 4.2.C: Qualitative analysis of the expression pattern of overexpressed CP60 and CP69 protein in COS-7 cells. CP60 and CP69 show a clustered expression pattern in COS-7 cells. In contrast the predominant expression of WT-DISC1 and DISC1 aa1-597 was characterised as punctate, and as being diffusely distributed throughout the cytoplasm, respectively. The phenotyping involved blinded counting of 60 COS-7 cells per construct. The COS-7 cells were visualized by anti-FLAG immunostaining. Data are ± SD and from n=3 independent experiments.

4.2.4 Qualitative analysis of MitoTracker Red staining in COS-7 cells expressing CP60 and CP69

It was possible to investigate the staining of mitochondria using MitoTracker Red, in COS-7 cells expressing CP60 and CP69 and using the same data collation/fluorescence paradigm as in figure 4.2.C. In conjunction with the anti-FLAG expressed protein characterisation, the

`

presence or absence of MitoTracker Red staining was noted. Mitochondrial staining and mitochondria shape were analysed, appearing tubular or clustered. Tubular staining was descriptive of the typical mitochondrial structural organisation observed with the overexpression of WT-DISC1 and DISC1 aa1-597 (see figure 4.2.A-B). Clustered mitochondrial staining described the structure of mitochondria seen in COS-7 cells expressing exogenous CP60 or CP69 when MitoTracker Red staining was visible (see figure 4.2.B). Importantly, the absence of mitochondrial staining was also noted.

Less than 30% of the COS-7 cells expressing exogenous CP60 and CP69 stain with MitoTracker Red (see figure 4.2.D). The MitoTracker staining data was analysed with One-way ANOVA, $p=0.0001$, followed by paired Bonferroni post-tests. The COS-7 cells overexpressing exogenous WT-DISC1 predominantly show punctate staining in combination with a tubular mitochondrial morphology and combined, these staining patterns differ significantly from the other DISC1 species expressed. Difference in the % of cells exhibiting punctate anti-FLAG staining and tubular mitochondria vs cells expressing WT-DISC1, WT-DISC1 vs DISC1 aa1-597, $p<0.001$, WT-DISC1 vs CP60, $p<0.001$, WT-DISC1 vs CP69, $p<0.001$. Similarly, with DISC1 1-597 the diffuse cellular staining along with the detection of tubular mitochondria is prominent with DISC1 aa1-597 expression and significantly differs from other expressed species. Difference in % of cells exhibiting diffuse DISC1 staining and tubular mitochondria vs cells expressing DISC1 aa1-597, DISC1 aa1-597 vs WT-DISC1 vs, $p<0.001$, DISC1 aa1-597 vs CP60, $p<0.001$, DISC1 aa1-597 vs CP69, $p<0.001$. The principal effect of CP60 and CP60 exogenous expression is clustered cellular staining coupled with clustered MitoTracker staining, although as noted previously the latter is frequently absent. The staining that is evident differs significantly from that of WT-DISC1 and DISC1 aa1-597. Interestingly the staining pattern differs significantly between CP60 and CP69, CP69 is observed to show greater mitochondrial staining (see figure 4.2D). Difference in the % of cells exhibiting clustered DISC1 staining and clustered mitochondria vs cells expressing CP60 or CP69, WT-DISC1 vs CP60, $p<0.001$, CP60 vs DISC1 aa1-597, $p<0.001$, CP60 vs CP69, $p<0.001$, CP69 vs WT-DISC1, $p<0.001$, CP69 vs DISC1 aa1-597, $p<0.001$.In summary the overexpression of CP60 or CP69 in COS-7 impairs mitochondrial staining with MitoTracker Red. The mitochondria that do stain are clustered, and differ from the tubular mitochondria seen in COS-7 cells expressing exogenous WT-DISC1 and DISC1 aa1-597. The clustered mitochondria may possess novel pathophysiological properties. Alterations in mitochondrial structure can give rise to changes in the bioenergetic activity of mitochondria and vice versa

`

(Benard & Rossignol, 2008). Given this link between mitochondrial structure to function, the bioenergetics of clustered mitochondria may differ from tubular mitochondria.

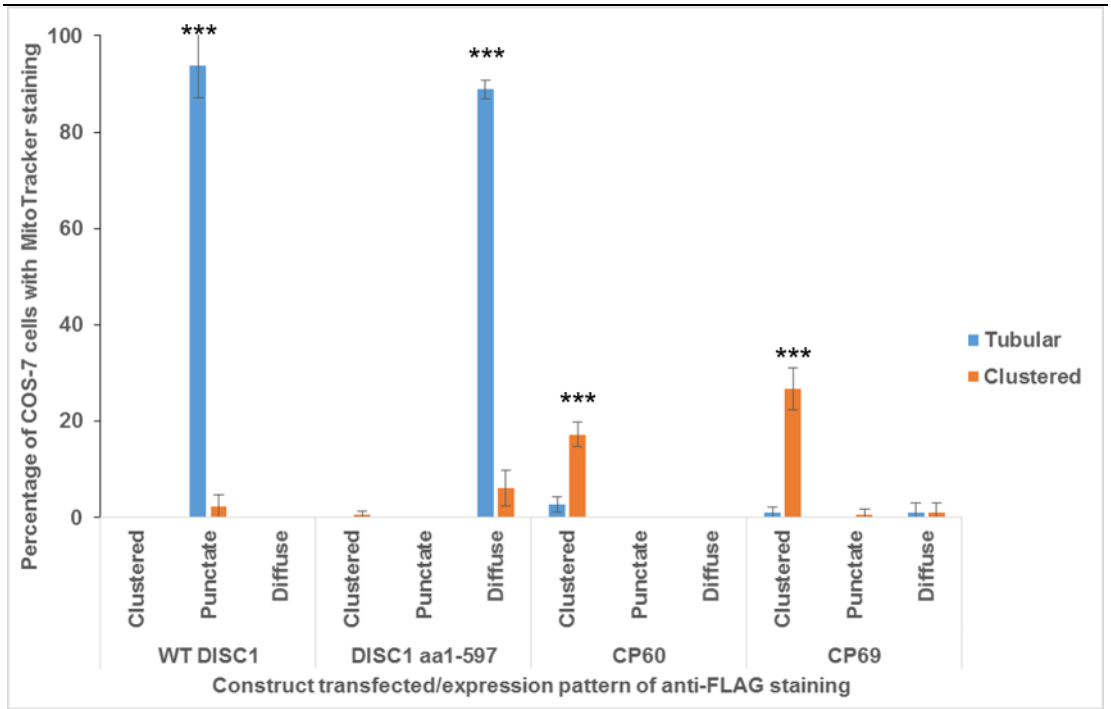

Figure 4.2.D: Qualitative analysis of MitoTracker Red staining of mitochondria in COS-7 cells expressing exogenous CP60 and CP69. The mitochondria of COS-7 cells expressing exogenous CP60 and CP69 frequently do not show MitoTracker Red staining. When staining is present in cells expressing CP60 and CP69, mitochondria appear fragmented. One-way ANOVA, p=0.0001, paired Bonferroni post-tests: difference in % of cells exhibiting punctate anti-FLAG staining and tubular mitochondria vs cells expressing WT-DISC1, WT-DISC1 vs DISC1 aa1-597, p<0.001 (***), WT-DISC1 vs CP60, p<0.001, WT-DISC1 vs CP69, p<0.001. Difference in % of cells exhibiting diffuse DISC1 staining and tubular mitochondria vs cells expressing DISC1 aa1-597, DISC1 aa1-597 vs WT-DISC1 vs, p<0.001, DISC1 aa1-597 vs CP60, p<0.001, DISC1 aa1-597 vs CP69, p<0.001. Difference in % of cells exhibiting clustered DISC1 staining and clustered mitochondria vs cells expressing CP60 or CP69, WT-DISC1 vs CP60, p<0.001, CP60 vs DISC1 aa1-597 , p<0.001, CP60 vs CP69, p<0.001, CP69 vs WT-DISC1, p<0.001, CP69 vs DISC1 aa1-597, p<0.001. The mitochondrial staining of 60 anti-flag stained cells was quantified per construct. Data are ± SD and from n=3 independent experiments.

`

The large pool of COS-7 cells overexpressing CP60 and CP69 that do not stain with MitoTracker Red needed to be visualised. The existence of mitochondrial structures had to be verified by some other means. An alternative mitochondrial dye or immunostaining targeted to mitochondrial protein were two possibilities. If this was carried out in conjunction with MitoTracker Red staining, mitochondria that did not stain could be visualised alongside those that take up MitoTracker.

4.3 Expression of CP1 in COS-7 cells

4.3.1 Expression of pcDNA DISC1 aa1-597 in COS-7 cells

The initial immunofluorescence expression and characterisation of CP60 and CP69 was performed comparing the expression pattern of a FLAG-DISC1 aa1-597 construct with a pEF1a backbone (see figures 4.2.A-D). However, the other constructs: FLAG-WT-DISC1; FLAG-CP60; FLAG-CP69, used in these experiments had a pcDNA3.1(+) backbone. At the time the initial FLAG-CP1 expression experiments where to be performed, a FLAG-tagged DISC1 aa1-597 construct was produced that had been cloned into a pcDNA3.1(+) backbone. There is no apparent difference between the pEF1a or pcDNA3.1(+) FLAG DISC1 aa1-597 cellular expression or mitochondrial morphology seen in transfected COS-7 cells as visualised by anti-FLAG and MitoTracker Red immunofluorescence (see figure 4.3.A). Both constructs express diffusely throughout the cytoplasm and show tubular mitochondria. The diffuse cytoplasmic staining of expressed DISC1 aa1-597 in COS-7 cells mirrors previous research (Brandon *et al*, 2005; Kamiya *et al*, 2005; Millar *et al*, 2005a). The use of the pcDNA3.1(+) vector for FLAG-DISC1 aa1-597 expression, seemed prudent given that FLAG-CP1 also possessed a pcDNA3.1(+) vector backbone.

4.3.2 Expressed CP1 is indistinguishable from DISC1 aa1-597 in COS-7 cells

The CP1 open reading frame differs from that of DISC1 aa1-597 only by the coding of a single aa, a glycine at position 598 (Eykelenboom *et al*, 2012). Amino acid 598 in the translated DISC1 open reading frame is also a glycine. Therefore, CP1 is essentially DISC1 aa1-598. The initial immunofluorescence with the overexpression of CP1 was performed alongside the

`

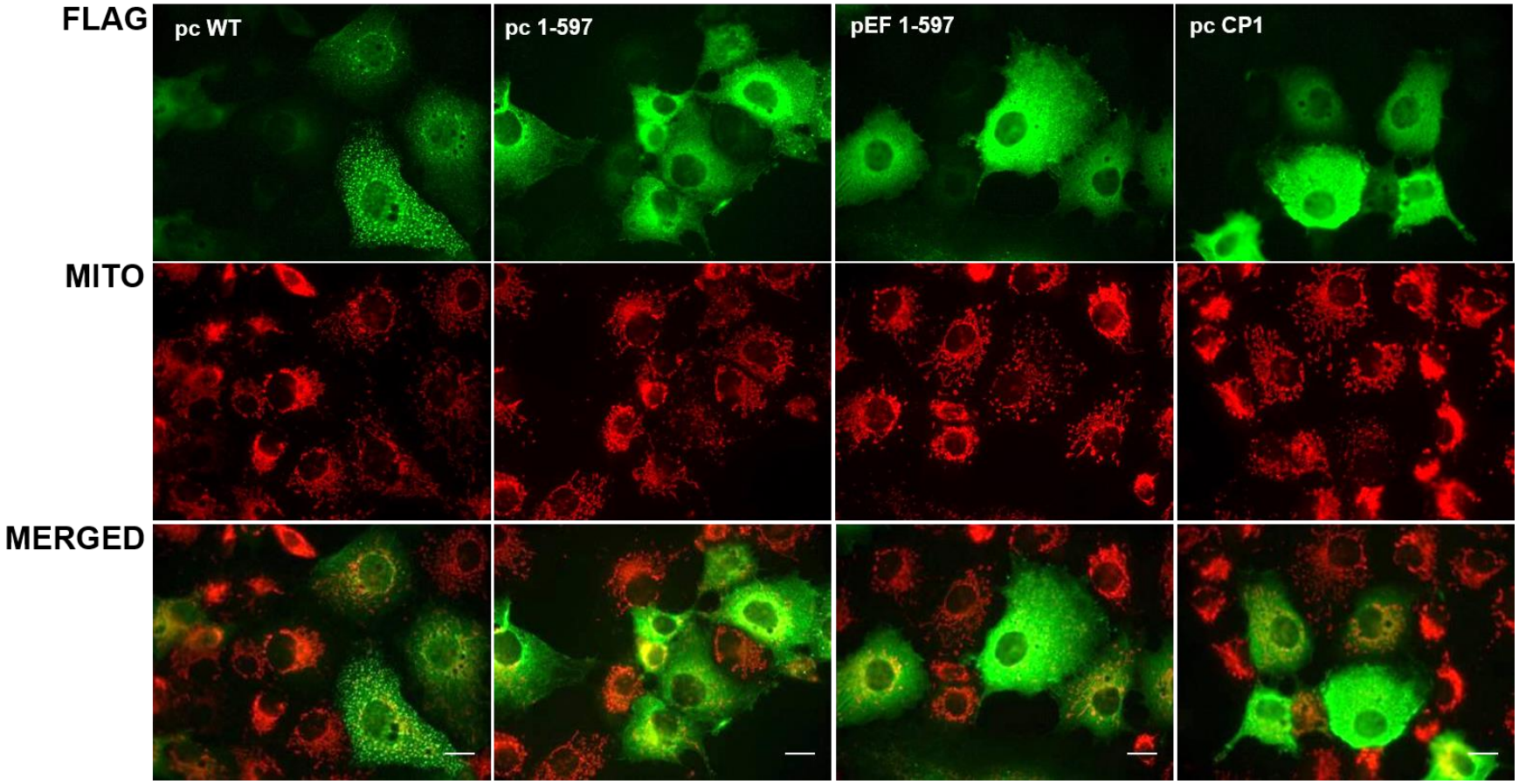

Figure 4.3.A: Expression of exogenous FLAG-tagged DISC1 aa1-597 in pcDNA 3.1(+) (pc) and pEF1a (pEF) vectors; and FLAG-tagged CP1 in pcDNA 3.1(+), in COS-7 cells. Immunostaining: FLAG (green); mitochondrial detection, MitoTracker Red. Scale bar represents 20μM.

`

overexpression of DISC1 aa1-597. It was predicted, given that the overexpressed proteins only differ by a single glycine, that the observed staining would be extremely similar.

The exogenous expression of CP1 in COS-7 cells, produces diffuse cytoplasmic anti-FLAG staining and the mitochondria stain with MitoTracker Red, appearing tubular (see figure 4.3.A). These observations are indistinguishable from both the anti-FLAG and mitochondrial staining seen in COS-7 cells overexpressing DISC1 aa1-597. This is not surprising, given the extremely high degree of sequence homology between the two species. Importantly, the CP1 expression differs from the other two DISC1/DISC1FP1 chimeras, CP60 and CP69, which show clustered anti-FLAG staining and frequently inhibit MitoTracker dye uptake (see figure 4.2.A). The differences in CP1 and CP60 and CP69 protein expression patterns may be indicative of alternate and independent molecular mechanisms of pathogenesis. This initial immunofluorescence needed to be followed up with the expression of all three der 1 DISC1/DISC1FP1 chimaeras utilising multiple mitochondrial markers.

4.4 Expression of CP1, CP60 and CP69 in COS-7 cells with multiple mitochondrial markers

4.4.1 Optimization of mitochondrial antibodies for a triple staining immunofluorescence protocol in COS-7 cells

To further investigate the mitochondrial phenotype seen in COS-7 cells expressing CP60 or CP69, double immunofluorescence staining was conducted using anti-Flag in conjunction with either MitoTracker Red or the mitochondrial targeted antibodies, anti-CVα or anti-cytochrome *c*. This was an optimisation protocol before conducting a triple staining immunofluorescence experiments with anti-FLAG, MitoTracker Red and CVα or cytochrome *c* staining. The aim was to visualise the mitochondria that could not otherwise be seen with MitoTracker Red in cells transfected with CP60 or CP69.

Mitochondrial Complex V-alpha Subunit (CVα) is a subunit of ATP synthase and is located within the inner portion of the mitochondrial membrane (Nakamoto *et al*, 2008). Given the location of CVα protein, anti-CVα staining should give a gross visualization of mitochondrial structure. Cytochrome *c* is a mitochondrial protein, located in the inter membrane space, that effluxes from mitochondria in cells undergoing apoptosis (Liu *et al*, 1996; Yang *et al*, 1997). If the cytochrome *c* staining differed markedly from the CVα staining, for example by an

`

efflux of cytochrome *c* from a population of cells overexpressing CP60 or CP69, then this could possibly be an indicator of apoptosis occurring as a consequence of aberrant protein expression.

The overexpression of CP60 or CP69 impairs mitochondrial staining with the dye MitoTracker Red (see figure 4.4.A). However, the mitochondria in cells overexpressing CP60 or CP69 can be alternately visualised with antibodies to CVα or cytochrome *c* (see figures 4.4.B and 4.4.C respectively). These mitochondria appear clustered, similar in shape to the CP60 and CP69 anti-FLAG expression pattern. Comparing the CVα and cytochrome *c* stained images, it does not appear that CP60 or CP69 expression causes efflux of cytochrome *c* from the mitochondria. It was suspected that the CP60 and CP69 expressing cells may be prone to apoptosis. Two observations suggested that apoptosis may be occurring, firstly the mitochondrial membrane potential, $\Delta\psi m$ had collapsed in many cells, which is associated with apoptosis (Ly *et al*, 2003). Secondly, the mitochondrial clustering that is evident bears resemblance to the fission prompted fragmentation of the mitochondrial network that occurs in apoptosis (Martinou & Youle, 2011). A possible interpretation of the absence of cytochrome *c* efflux may indicate that the COS-7 cells overexpressing CP60 and CP69 are undergoing a pathology that is independent of apoptosis, or that precedes apoptosis. For example, an alternative to apoptosis occurring may be mitophagy mediated by the PTEN-induced Kinase 1 (PINK1)-parkin pathway, this mechanism targets depolarised mitochondria and results in the promotion of fission within the mitochondrial network (Gomes & Scorrano, 2013; Van Laar & Berman, 2013). These are optimisation experiments and are not intended to correlate the mitochondrial dysfunction evident by impaired MitoTracker staining with staining from antibodies targeted to the mitochondria. This is the aim of the triple staining immunofluorescence experiment with multiple mitochondrial markers.

The observations show that the population of mitochondria in cells overexpressing CP60 and CP69 can be visualised and show a clustered morphology when stained with anti-CVα and anti-cytochrome *c* (see figures 4.4.B and 4.4.C, respectively). This enabled the development of a triple staining immunofluorescence paradigm, that would use anti-FLAG, MitoTracker Red and either anti-CVα and anti-cytochrome c, to visualise the mitochondria in COS-7 cells overexpressing CP60 or CP69 that show impaired MitoTracker Red uptake.

`

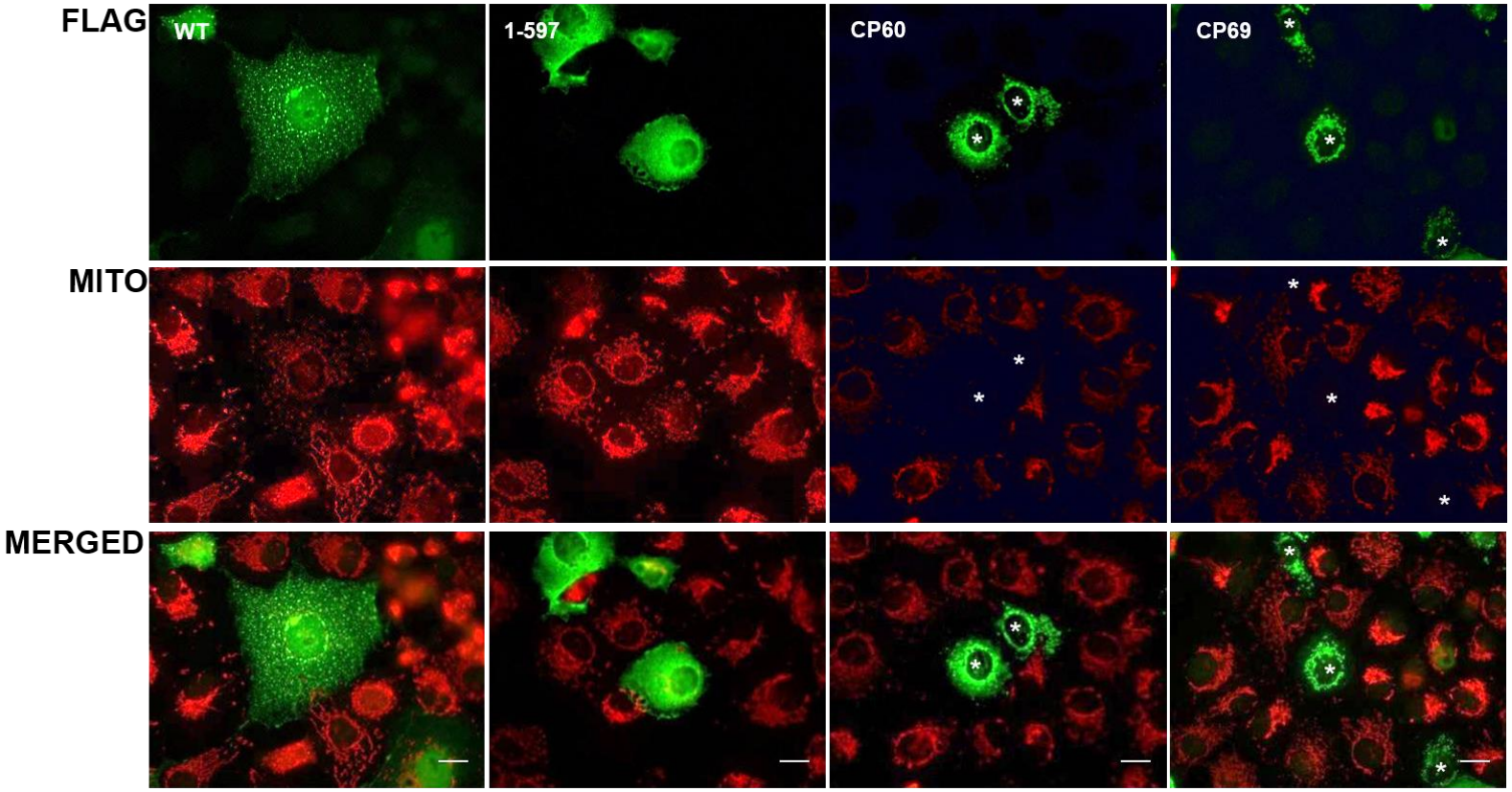

Figure 4.4.A: Optimisation for triple staining with multiple mitochondrial markers I: MitoTracker Red staining. Expression of exogenous FLAG-tagged CP1, CP60, and CP69 in COS-7 cells. Immunostaining: FLAG (green); mitochondrial detection, MitoTracker Red. Asterisks indicate cells transfected with CP60 or CP69. Scale bar represents 20μM.

`

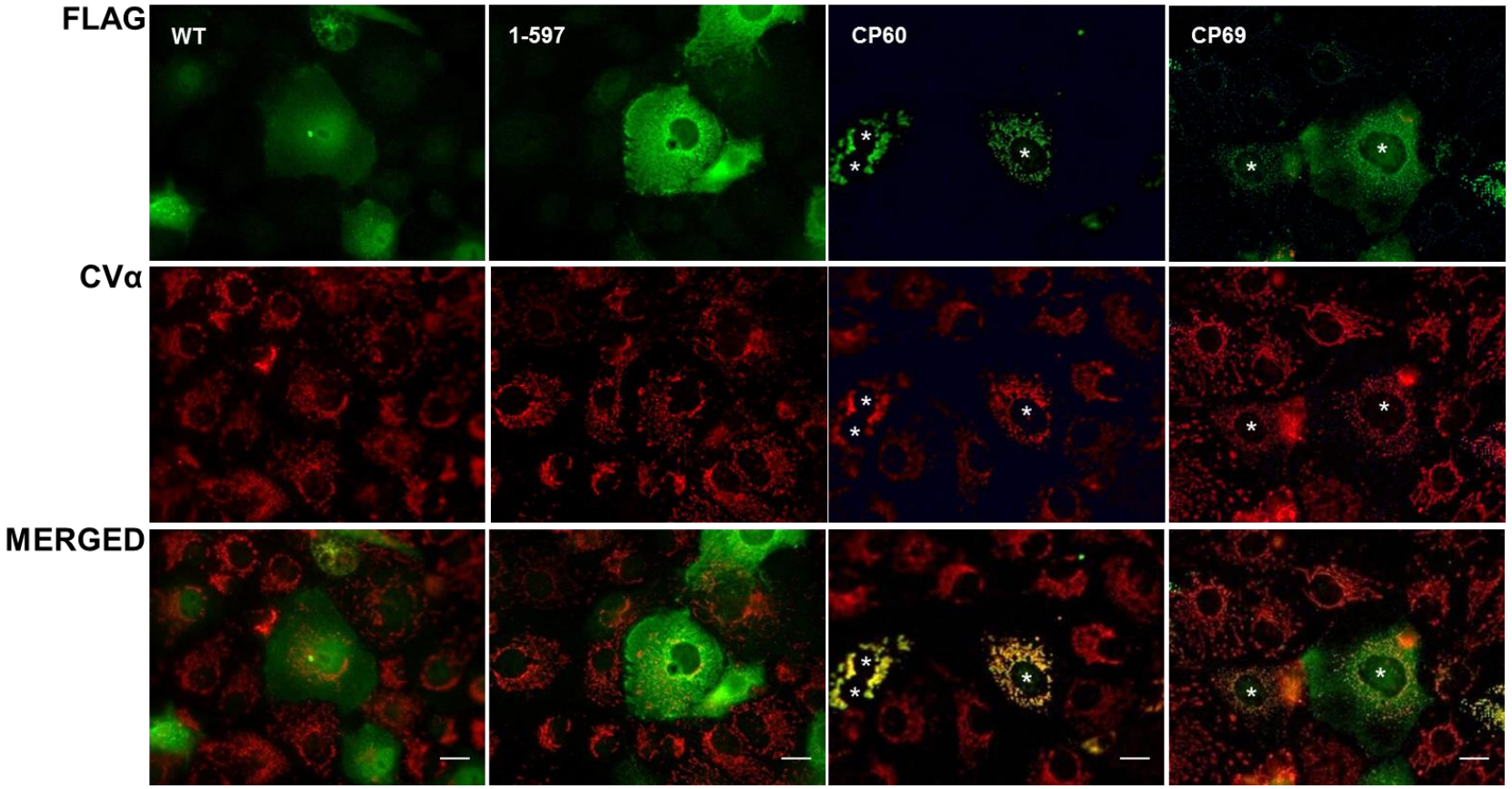

Figure 4.4.B: Optimisation for triple staining with multiple mitochondrial markers II: anti-CVα staining. Expression of exogenous FLAG-tagged CP1, CP60, and CP69 in COS-7 cells. Immunostaining: FLAG (green); mitochondrial detection, anti-CVα (red). Asterisks indicate cells transfected with CP60 or CP69. Scale bar represents 20μM.

`

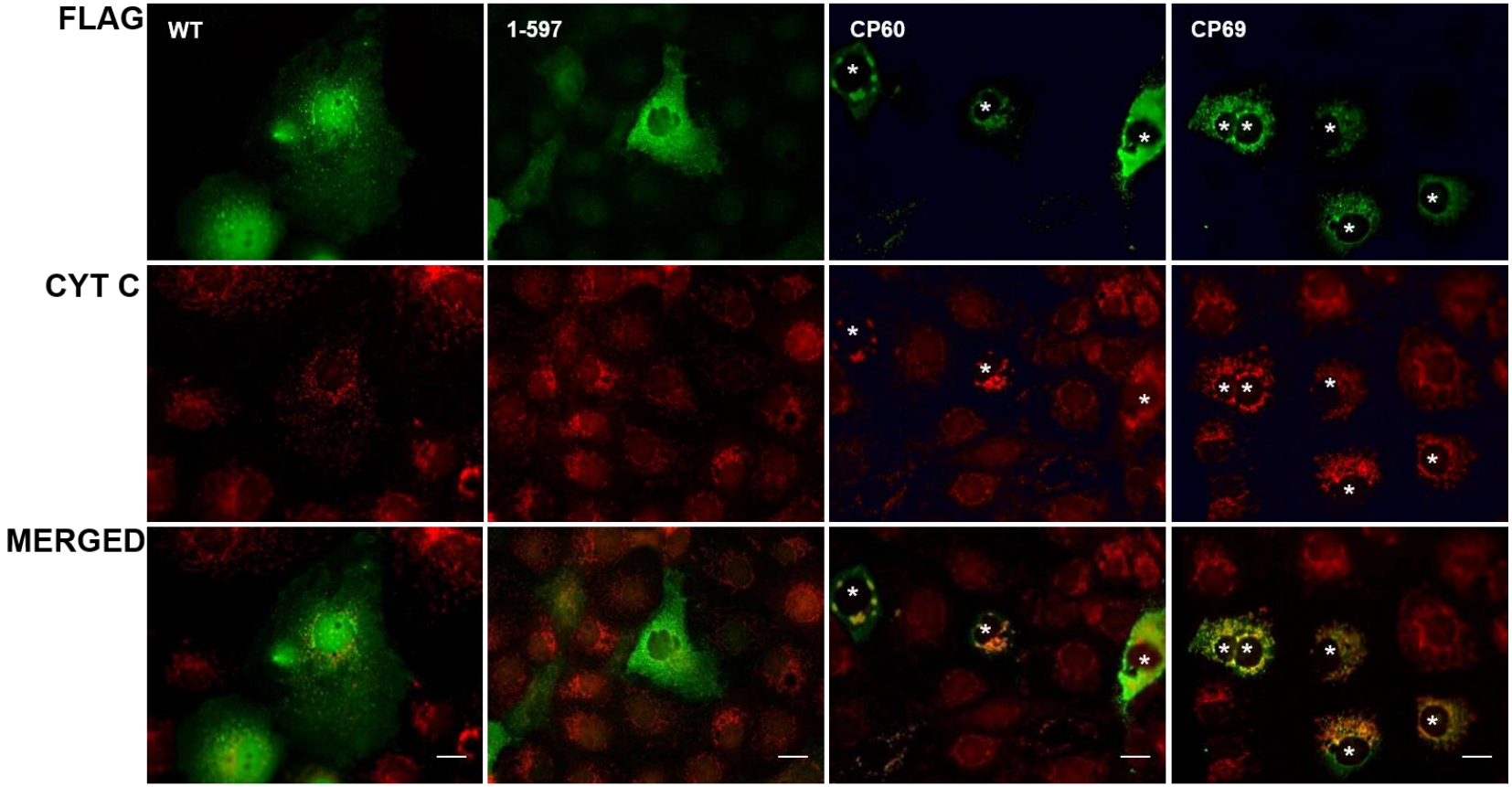

Figure 4.4.C: Optimisation for triple staining with multiple mitochondrial markers III: anti-cytochrome *c* staining. Expression of exogenous FLAG-tagged CP1, CP60, and CP69 in COS-7 cells. Immunostaining: FLAG (green); mitochondrial detection, anti-cytochrome *c*, CYT C, (red). Asterisks indicate cells transfected with CP60 or CP69. Scale bar represents 20μM.

`

4.4.2 Expression of exogenous der 1 DISC1/DISC1FP1 chimeras in COS-7 cells visualised with multiple mitochondrial markers

The triple staining immunofluorescence protocol was designed to investigate the cellular expression and mitochondrial morphology of CP1, CP60 and CP69. This involved staining with anti-FLAG, MitoTracker Red and an antibody targeted to the mitochondrial protein, either anti-cytochrome *c* or anti-CVα.

In terms of cellular expression pattern and mitochondrial structure, CP1 and DISC1 aa1-597 display very similar behaviour, while CP60 and CP69 are also similar to one another (see figures 4.4.D and 4.4.E). As previously seen, the mitochondria in the majority of cells expressing CP60 or CP69 do not stain with MitoTracker Red. However, the co-staining with anti-cytochrome *c* or anti-CVα visualises these mitochondria. The perturbation of MitoTracker dye uptake appears to be dose dependent. The COS-7 Cells labelled **a-c** in figure 4.4.E show that the increase in both CP60 and CP69 protein expression is accompanied by a decrease in observed MitoTracker Red staining. The reduction or absence of MitoTracker staining is most likely indicative of a detrimental alteration to the mitochondrial membrane potential, $\Delta\psi m$, which MitoTracker Red dye activity is sensitive to (Buckman *et al*, 2001) with increasing doses of CP60 or CP69 correlating with greater mitochondrial dysfunction. These abnormal clustered mitochondria are likely to have altered biogenetic properties. It seems unlikely though that the mitochondrial dysfunction is part of an apoptotic process, given that the there is no evidence of an efflux of cytochrome *c* from the mitochondria. The visualisation of cytochrome *c* in the cytoplasm may be observed by immunocytochemistry following the promotion of apoptosis (Lagna *et al*, 2006). However, here the anti-cytochrome *c* and anti-CVα staining both reveal similar patterns.

`

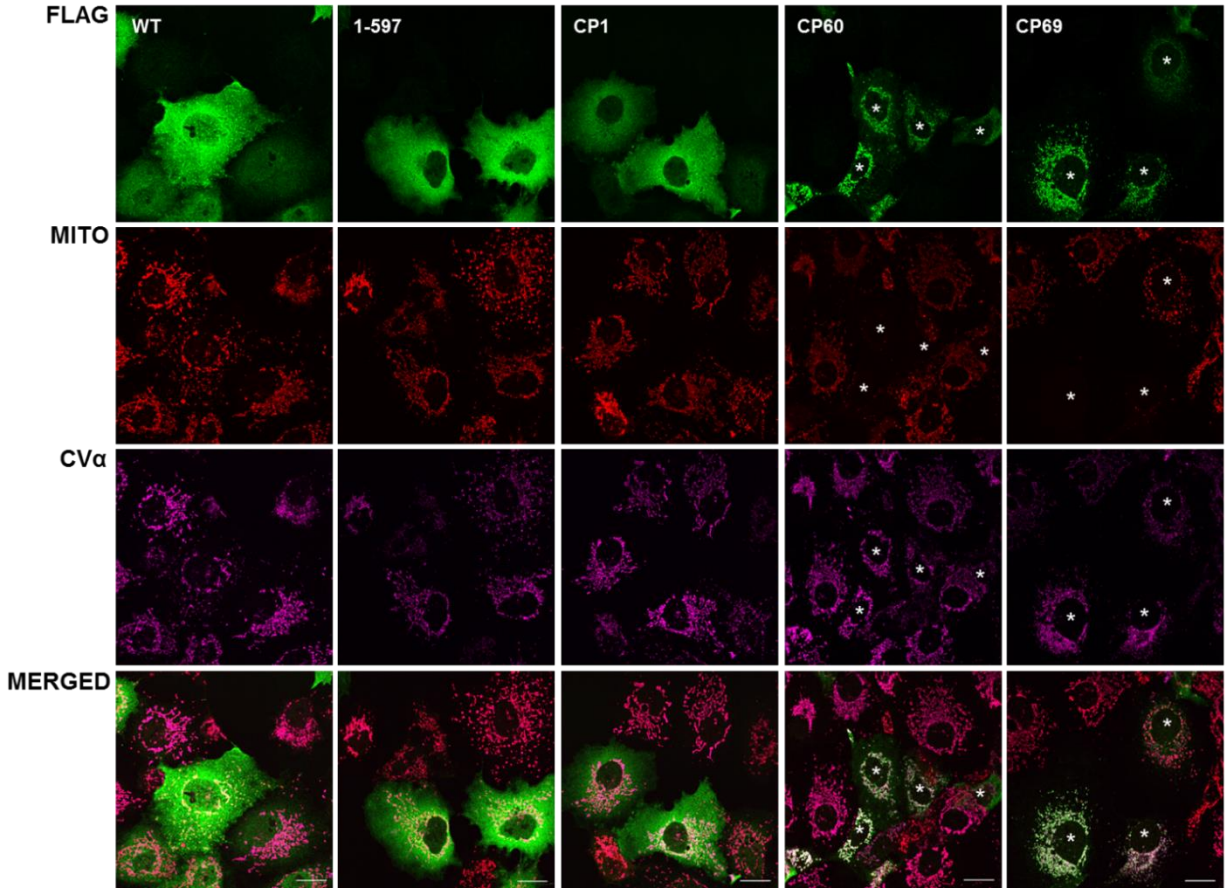

Figure 4.4.D: Expression of exogenous FLAG-tagged CP1, CP60, and CP69 in COS-7 cells with multiple mitochondrial markers I. Immunostaining: FLAG (green); mitochondrial detection, MitoTracker Red and anti-CVα (pink). Scale bar represents 20μM.

`

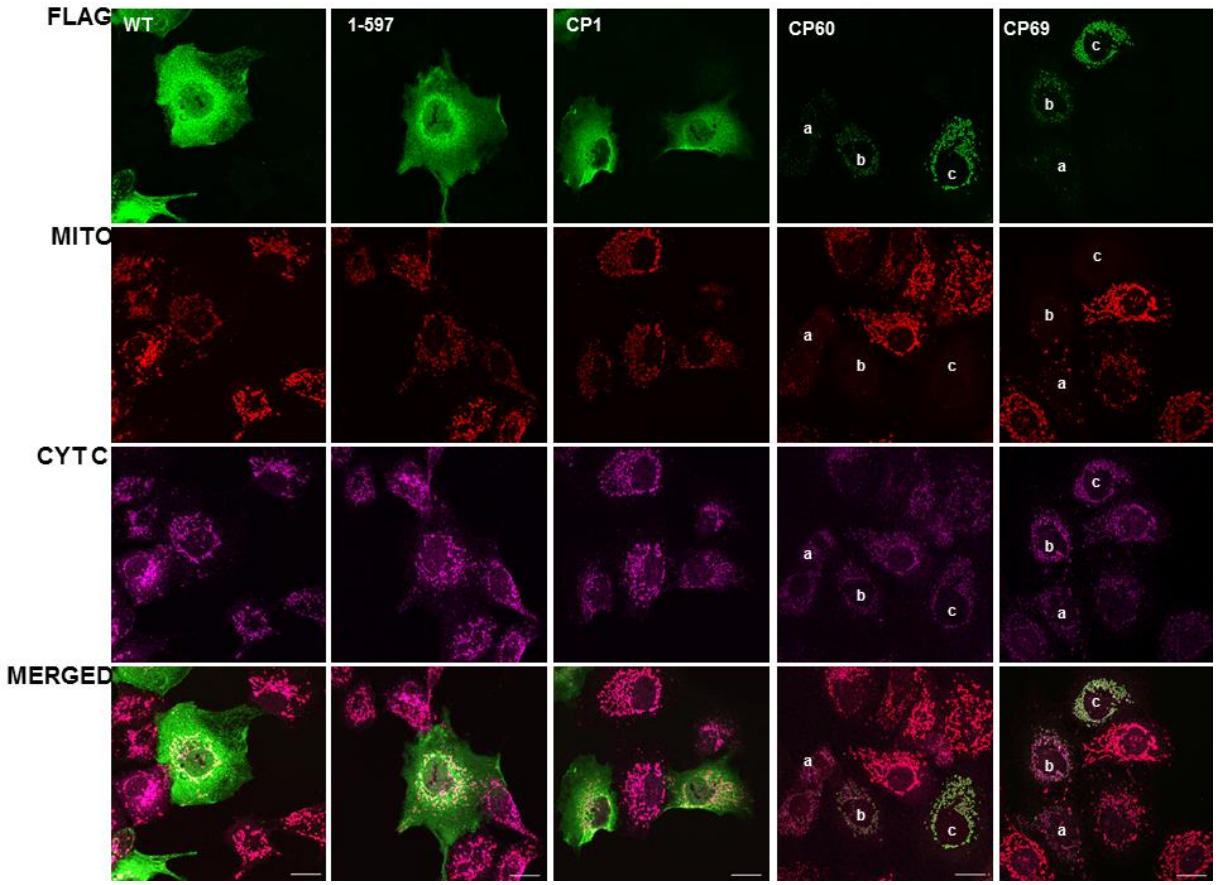

Figure 4.4.E: Expression of exogenous FLAG-tagged CP1, CP60, and CP69 in COS-7 cells with multiple mitochondrial markers II. Immunostaining: FLAG (green); mitochondrial detection, MitoTracker Red and anti-cytochrome *c* (pink). Scale bar represents 20μM. Text a-c represents low to high chimeric protein expression.

`

4.4.3 Initial Expression of exogenous of DISC1/DISC1FP1 chimeras in primary mouse cortical neurones

To investigate the potential role for the DISC1/DISC1FP1 chimeras in major mental illness, it was necessary that CP1, CP60, and CP69 were expressed in a more relevant disease model/culture system, primary cultured neurones. It seemed likely CP1 would express in neurones in a similar way to DISC1 aa1-597 given the high similarity between the two species, and previous observations from COS-7 cells (see figure 4.3.A). DISC1 aa1-597 has been overexpressed in human NT2N neurones (Morris *et al*, 2003) and primary mouse cortical neurones (Brandon *et al*, 2005) and is observed to be diffusely distributed throughout the cytoplasm. A construct that encodes CP60 has been overexpressed in a rat neuronal-like cell line HCN-B27. The expression pattern is described as appearing punctate and is visible throughout cytoplasm and neuronal processes (Zhou *et al*, 2010). A more clustered staining pattern is seen in primary neurones from the DISC1-Boymaw mouse which expresses CP60 (Ji *et al*, 2014). Given the previous observations of both CP60 and CP69 expression in COS-7 cells, and the great degree of sequence homology between the two chimeras, it seemed likely that the expression of these two species would be indistinguishable from one another.

The DISC1/DISC1FP1 chimeras were overexpressed in C57BL/6 mouse primary cortical neurones at 11 days *in vitro* (see figure 4.4.F). The chimeric proteins were visualised with the same dual staining paradigm as had been used for the initial COS-7 based experiments. Anti-FLAG detection was used to visualise chimeric protein localisation and MitoTracker Red to stain mitochondrial structures and visualised with fluorescence microscopy. The overexpressed CP60 and CP69 cellular expression pattern were indistinguishable from one another and were similar to those seen by Ji *et al.*, (2014) when expressing CP60 from the DB7 gene in primary neurones from the DISC1-Boymaw mouse model. It should be noted that the Ji *et al*., (2014) paper came out after these experiments were completed and published. The clustered anti-FLAG staining localises predominantly to the cell soma, with little expression in peripheral neuronal processes. Importantly, there is evidence of mitochondrial dysfunction as indicated by the frequent absence of MitoTracker Red staining in the cell soma. The CP1 anti-FLAG staining appears diffuse throughout the cell soma and larger processes, with MitoTracker Red staining observed in the same regions. In this experiment, the DISC1 aa1-597 and the WT-DISC1 fluorescence for both anti-FLAG and MitoTracker Red are markedly similar to CP1 staining.

`

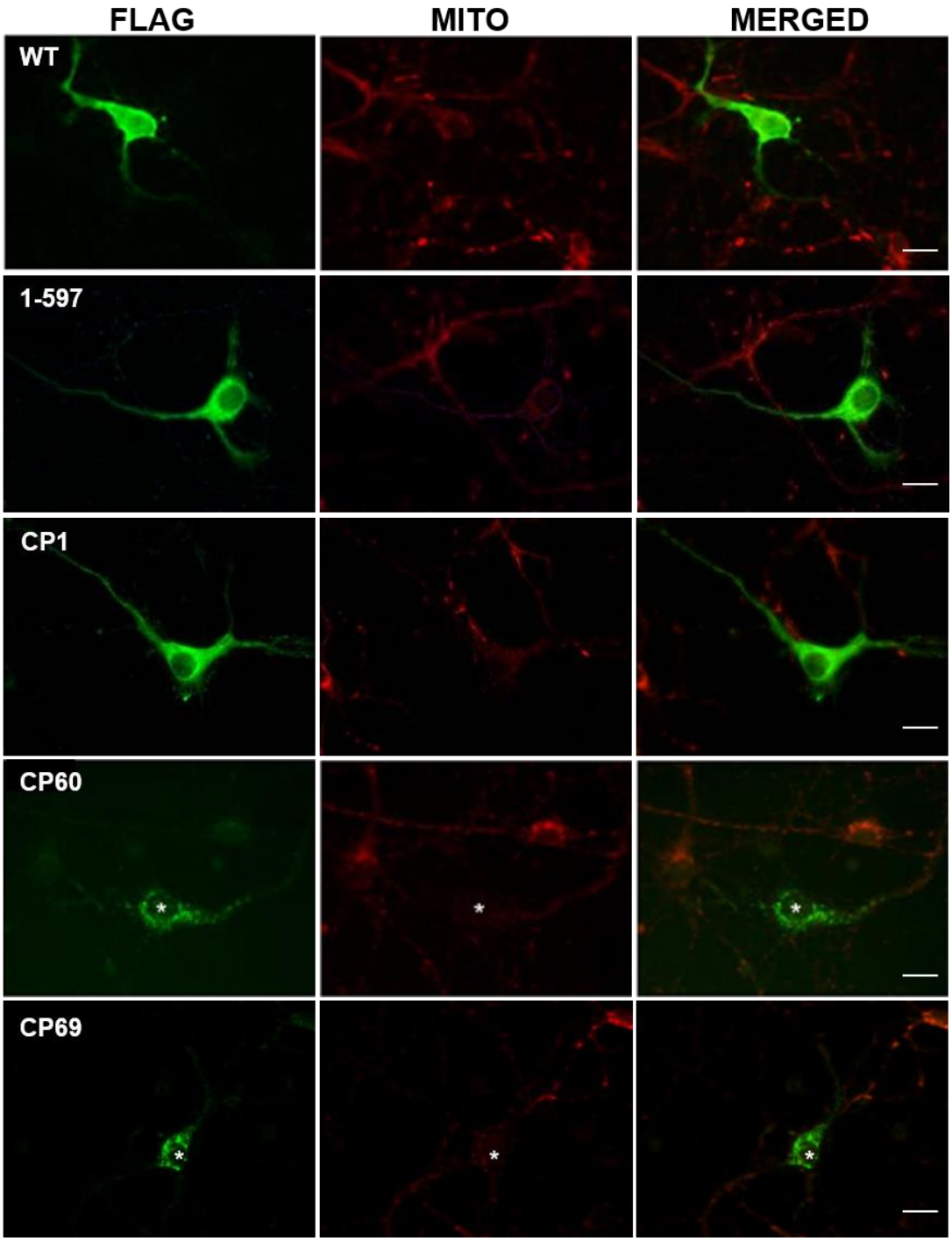

Figure 4.4.F: Expression of exogenous FLAG-tagged CP1, CP60, and CP69 in cultured C57BL/6 primary mouse cortical neurones (11 DIV). Immunostaining: FLAG (green); mitochondrial detection, MitoTracker Red. Asterisks indicate cells transfected with CP60 or CP69. Scale bar represents 10μM. In this experiment all of the neuronal culture, transfections and cell staining were performed by Fumiaki Ogawa.

`

4.4.4 Expression of exogenous of der 1 DISC1/DISC1FP1 chimeras in primary cultured neurones visualised with multiple mitochondrial markers

To further investigate the mitochondria in primary cortical neurones overexpressing CP1, CP60 or CP69, the mitochondrial structure needed to be visualised by a means other than MitoTracker Red, which was frequently absent in cells overexpressing CP60 and CP69. This was achieved by using the triple staining paradigm that had been initially carried out on COS-7 cells (see figures 4.4.D and 4.4.E). The triple staining involved anti-FLAG and MitoTracker Red staining in the presence an antibody targeted to mitochondrial protein, either cytochrome *c* or CVα, and was visualised with confocal microscopy.

The der 1 DISC1/DISC1FP1 chimeras were overexpressed in CD1 primary cortical neurones at five days *in vitro* (see figures 4.4.G and 4.4.H). Of primary importance in these two experiments was that the mitochondria in neurones overexpressing CP60 or CP69 that do not stain with MitoTracker Red can be seen when they are co-stained with either anti-cytochrome *c* or anti-CVα. These mitochondria appear clustered, co-localising with the clustered anti-FLAG staining in the CP60 or CP69 overexpressing cells. The anti-FLAG staining itself is largely confined to the soma with little peripheral staining evident. This indicates that the degree of mitochondrial dysfunction, initially observed in COS-7 cells, is also fully apparent in primary cortical neurones when either CP60 or CP69 are overexpressed.

In the CD1 neurones, the WT-DISC1 overexpression staining appears punctate with mitochondria in the soma and large processes. The CP1 overexpression staining is diffuse throughout the cell body with similar peripheral mitochondrial staining to WT-DISC1. The DISC1 aa1-597 staining pattern is highly similar to that seen for the overexpression of CP1.

The immunofluorescence co-staining for either cytochrome *c* or CVα does not substantially differ in the pattern of mitochondrial protein visualised for any of the der 1 DISC1/DISC1FP1 chimeric overexpressed proteins. This would suggest apoptosis by way of the intrinsic apoptotic pathway (Elmore, 2007), whereby cytochrome *c* effluxes from the mitochondria, does not occur in any of the DISC1/DISC1FP1 overexpressing neurones. Alternatively it may be that the apoptotic process occurring is not advanced enough to be detectable. This observation is particularly important with regard to neurones overexpressing either CP60 or CP69, given the mitochondrial dysfunction evident in these transfected neurones.

`

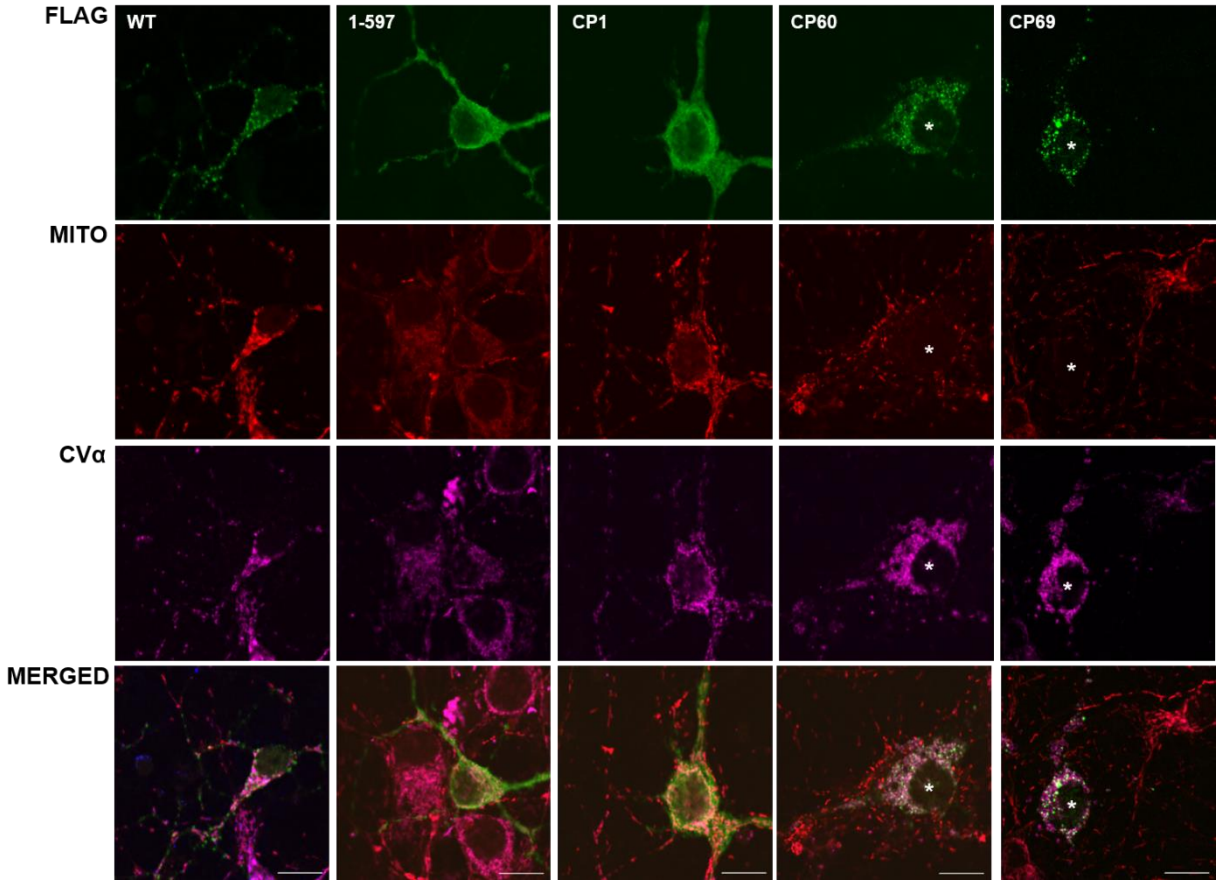

Figure 4.4.G: Expression of exogenous FLAG-tagged CP1, CP60, and CP69 in cultured CD1 primary mouse cortical neurones (5 DIV) with multiple mitochondrial markers I. Immunostaining: FLAG (green); mitochondrial detection, MitoTracker Red and anti-CVα (pink). Asterisks indicate cells transfected with CP60 or CP69. Scale bar represents 10μM. In this experiment, all of the neuronal culture and transfections were performed by Fumiaki Ogawa.

`

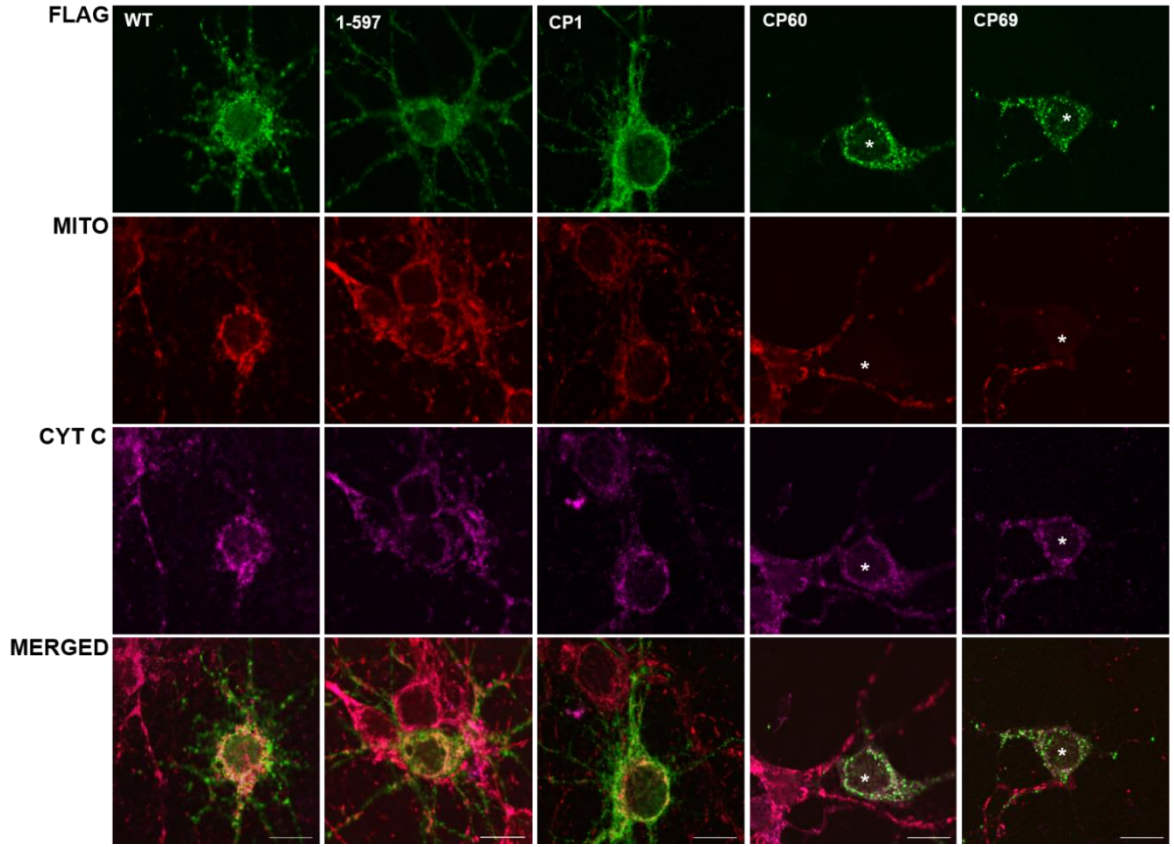

Figure 4.4.H: Expression of exogenous FLAG-tagged CP1, CP60, and CP69 in cultured CD1 primary mouse cortical neurones (5DIV) with multiple mitochondrial markers II. Immunostaining: FLAG (green); mitochondrial detection, MitoTracker Red and anti-cytochrome *c* (pink). Asterisks indicate cells transfected with CP60 or CP69. Scale bar represents 10μM. In this experiment, all of the neuronal culture and transfections were performed by Fumiaki Ogawa.

`

The 129S6/SvEv mouse line carries a mutation that results in both a frame shift and the premature termination of *Disc1* open reading frame (Koike *et al*, 2006). This results in a truncated abnormal DISC1 protein species being produced. The use here of both CD1 and C57BL/6 primary cultures that produce converging results, eliminates any concern arising from the use of the CD1 mouse line for immunofluorescence some of which may contain the same mutation as 129S6/SvEv mice.

The observations from the immunofluorescence on the overexpression of CP1, CP60 or CP69 in primary cortical neurones co-stained for multiple mitochondrial markers mirror the conclusions from the COS-7 immunofluorescence. CP1 expression is markedly similar to DISC1aa1-597, localising diffusely throughout the cytoplasm. This is unsurprising given the sequence homology between the two species. The overexpression of CP60 and CP69 protein showed a perinuclear clustered expression pattern that co-localises with clustered mitochondria. These clustered mitochondria have altered membrane potentials as evidenced by an inability to take up the mitochondrial dye, MitoTracker Red. This represents a novel molecular pathogenic mechanism. Taken together, the results suggest that, if the DISC1/DISC1FP1 chimeric protein is expressed in t(1;11) carriers, they could contribute to major mental illness via multiple pathogenic mechanisms.

4.5 Discussion

4.5.1 CP1 protein expression

The CP1 immunofluorescence staining is extremely similar to that of DISC1 aa1-597. This is unsurprising given the open reading frame for CP1 differs from DISC1 aa1-597 by a single glycine at position 598 (Eykelenboom *et al*, 2012). CP1 is C-terminal truncated DISC1 aa1-598. As a truncated species, CP1 will lack DISC1 aa599-854 for protein binding. Looking at important DISC1 interactors, DISC1 aa1-597 is capable of binding PDE4B (Millar *et al*, 2005b), although a further PDE4B binding site is present in DISC1 aa611-650 (Murdoch *et al*, 2007). This may give CP1 altered PDE4 interaction properties compared to DISC1. However, the DISC1 novel variant, DISC1 LΔ78T9, which possesses a slightly longer ORF than CP1, shows only very weak binding to PDE4B (Newburn *et al*, 2011). DISC1 has been shown to bind to and inhibit GSK3β (Mao *et al*, 2009) and an exogenously expressed short DISC1 splice variant, encoding DISC1 aa1-347 alone, is capable of binding GSK3β (Newburn *et al*, 2011). Therefore, it would be expected that CP1 protein would interact with GSK3β.

`

However, a direct NudE Neurodevelopment Protein 1 (NDEL1)/NUDEL and CP1 interaction would not occur, as NDEL1/NUDEL requires DISC1 aa727-845 to bind (Soares *et al*, 2011).

Prior to the detection of the chimeric transcripts in t(1;11) patient lymphoblastoid cell lines (Eykelenboom *et al*, 2012), DISC1 aa1-597 was examined in many laboratories as a novel species that could possibly be derived from the proximal der1 translocated chromosome 1 in t(1;11) carriers. A comparison of *in vivo* DISC1 aa1-597 expression in mouse models and the possible consequences of CP1 expression *in vivo* is summarised in chapter 3 (see section 3.6.2). Furthermore, a number of putative pathogenic mechanisms resulting from CP1 exogenous expression *in vitro* may be proposed based on the high degree of homology shared with DISC1 aa1-597 and the established research on this species (see chapter 1). CP1 is therefore likely capable of redistributing DISC1 to a diffuse cytoplasmic expression pattern (Kamiya *et al*, 2005). This dominant-negative mechanism would be mediated by a self-association domain at DISC1 aa403-504. CP1 exogenous expression may also induce mitochondrial pathology distinct from that of CP60 and CP69. Firstly CP1 overexpression could result in morphological alterations to mitochondria, inducing the formation of 'ring' or lariat shaped mitochondria in a subpopulation of transfected cells (Millar *et al*, 2005a). Secondly the expression of CP1 could possibly perturb mitochondrial bioenergetics, potentially reducing both cellular ATP and NADPH dehydrogenase (complex 1) levels. It is also likely that CP1 expression could impair both neurite outgrowth in PC12 cells (Ozeki *et al*, 2003; Pletnikov *et al*, 2007) and axonal elongation in hippocampal cultures (Taya *et al*, 2007). The expression of CP1 in oligodendrocytes would likely result in the promotion of differentiation which is converse to the action of DISC1 expression which negatively regulates oligodendrocyte differentiation (Hattori *et al*, 2014).

4.5.2 CP60 and CP69 protein expression

CP60 and CP69 are indistinguishable when overexpressed and visualised by immunofluorescence in both COS-7 cells and mouse primary cortical neurones. The clustered expression pattern for these chimeric species bares similarity to the findings of a study that has emerged since the work in this thesis was completed and published. Ji *et al.*, (2014) observed a clustered CP60 staining pattern with the exogenous expression of the DB7 construct in primary neurone cultures. The clustered expressed protein localisation and the induction of putative pathogenic mechanisms of mitochondrial dysfunction of CP60 and CP69 are distinct from the mitochondrial morphology and expression patterns of overexpressed WT- DISC1, DISC1 aa1-597 and CP1 *in vitro*.

`

Proteomics has been used to ascertain differences between DISC1 aa1-597 and CP69 protein. This approach used the expression of N-terminally truncated proteins MBP-ΔN597 and MBP-ΔNCP69 (Eykelenboom *et al*, 2012), as the N-terminus of DISC1 is disordered and difficult to express *in vitro* and purify in sufficient quantities for biophysical analysis (Soares *et al*, 2011). The MBP-ΔNCP69 protein had altered structure and formed larger protein assemblies that exhibited greater thermal stability than the MBP-ΔN597 protein (Eykelenboom *et al*, 2012). This indicates that the additional protein structure from the 69 novel aa from DISC1FP1 alters the interaction with DISC1 aa326-597 differently to that seen with MBP-ΔN597 protein alone. The observations from MBP-ΔNCP69 expression translate to CP60, given the high degree of sequence homology between CP60 and CP69. Furthermore, the production of large protein assemblies and alterations to the secondary structure seen due to the novel DISC1FP1 aa's present in MBP-ΔNCP69 (Eykelenboom *et al*, 2012) may be evidence of the biophysical alterations that contribute to the abnormal CP60 and CP69 clustered protein expression pattern with overexpression. An interpretation of the 'clustering' phenomenon observed in the immunocytochemistry is that that the large protein assemblies and secondary structure alterations occur to such an extent so as to promote the formation of CP60 and CP69 aggregates. However, further biochemical testing is needed for definitive conformation of aggregation. DISC1 aggregation has been associated with a reduction in the number of mitochondria being transported within the neurone, suggesting that aggregation impacts on the regulation of mitochondrial transport (Atkin *et al*, 2012). Furthermore, aberrant DISC1 detergent insoluble protein aggregates have been detected in post mortem brain tissue from subjects diagnosed with depression, bipolar disorder and schizophrenia (Leliveld *et al*, 2008; Leliveld *et al*, 2009).

That the expressed CP60 and CP69 protein is indeed clustered or aggregated *per se* is open to interpretation. It is possible that the apparent clustered localisation is an artefact of these species being transported along with the mitochondria in a defective manner, given that DISC1 could be trafficked with mitochondria as it is associates with components of the mitochondrial trafficking machinery (Ogawa *et al*, 2014). Alternatively, in line with the biophysical data (Eykelenboom *et al*, 2012) large protein assemblies of CP60 and CP69 could potentially bind to the outside of the mitochondria, where DISC1 has been observed to complex with Miro1 and TRAK1 (Ogawa *et al*, 2014), where these chimeric species may form clusters or aggregates. To be able to suggest that the aberrant CP60 and CP69 protein formed aggregates would require evidence these species may be involved in aggresomal pathways as occurs with full-length DISC1 aggregates (Atkin *et al*, 2012). Further research is needed to characterise

`

the exogenously expressed CP60 and CP69 protein to establish their specific cellular and molecular properties as a putative mechanism of pathogenesis in the t(1;11) pedigree, aside from the observed effects in promoting mitochondrial dysfunction.

In light of the aberrant protein produced from CP60 and CP69 exogenous expression, future work could look at whether these species show enhanced binding to overexpressed DISC1, via its self-association regions, by co-immunoprecipitation. This could be performed by co-expressing FLAG tagged CP60 or CP69 with Myc or HA-tagged DISC1. The relative co-immunoprecipitation of mutant and wild-type DISC1 would be detected by Western blotting combined with densitometry analysis. The biophysical data indicate that the CP60 and CP69 proteins may exhibit increased self-association (Eykelenboom *et al*, 2012). It is possible that this would extend to altered binding to full-length DISC1. Immunofluorescence could be used in parallel, to look at chimeric protein co-expression with wild-type DISC1. This work would be a precursor to investigating how DISC1 binding partners are affected by the potential protein clustering or aggregation that may be induced by CP60 and CP69 overexpression. It would also be of interest to see how comparable the interactions with DISC1 binding partners are between CP60, CP69 and CP1. This would both possibly discover novel putative pathogenic mechanisms and build on the protein structural findings.

The CP60 and CP69 protein is targeted to the mitochondria within cells. Structurally, the mitochondria appear clustered, co-localising with the overexpressed CP60 and CP69 protein. Targeting to mitochondria and the alteration of mitochondrial morphology has been observed with several other DISC species *in vitro*. The addition of GFP-tags to full length DISC1 induces mitochondrial targeting, while the expression of DISC1 aa1-597 can produce 'ring' or lariat shaped mitochondria (Millar *et al*, 2005a). A DISC1 missense mutation has been identified that alters mitochondrial morphology. R37W is an ultra-rare DISC1 mutation identified in one individual of a cohort of individuals diagnosed with schizophrenia (Song *et al*, 2008). The DISC1 R37W mutation has also been observed in members of a Scottish family, two of whom suffered major depressive disorder and one that suffered from generalised anxiety disorder (Thomson *et al*, 2014). The expression DISC1-37W induces mitochondrial clustering (Ogawa *et al*, 2014). The novel protein species resulting from CP60 and CP69 exogenous expression may alter some of the protein interactions that occur between the encoded DISC1 aa1-597 of these proteins and mitochondria, and/or intermediary species. DISC1 has been shown to interact with the mitochondrial protein, mitofilin (Park *et al.*, 2010). Mitofilin is important in cristae morphology (John *et al*, 2005). DISC1 stabilises mitofilin, maintaining mitochondrial function. However, the expression of a truncated form of mouse

`

DISC1, analogous to the DISC1 aa1-597 sequence, is sufficient to bind with mitofilin and impairs mitochondrial bioenergetic function. The interaction between mitofilin and mouse DISC1 occurs inside the mitochondria (Park *et al*, 2010). DISC1 has been shown to associate with the mitochondrial transport machinery on the outside of the mitochondria (Ogawa *et al*, 2014). It seems likely that CP60 and CP69 would also maintain such associations given both these species encode the motif required for interacting with TRAK1, the adaptor protein around which mitochondrial trafficking complexes are built. The possibility therefore exists for CP60 and CP69 to localise both inside the mitochondria potentially perturbing bioenergetic processes, and to affect trafficking mechanisms on the outside of the mitochondria.

Functionally, the mitochondria show a dose dependent alteration to the mitochondrial membrane potential, $\Delta\psi m$, which is demonstrated by the impairment in the uptake of the fluorescent mitochondrial dye, MitoTracker Red. The labelling of cultured neurones by MitoTracker Red can be impaired by the application of the metabolic inhibitor Carbonyl cyanide-4-(trifluoromethoxy)phenylhydrazone (FCCP), which depolarises the mitochondrial membrane potential, $\Delta\psi m$ (Buckman *et al*, 2001). The mitochondrial clustering induced by CP60 and CP69 expression may be mechanistically associated with the alteration in membrane potential, $\Delta\psi m$. However, it should be noted that the fragmentation of mitochondria has been associated with abolished, increased, or unchanged mitochondrial membrane potential, $\Delta\psi m$, following experimental manipulation (Benard & Rossignol, 2008). Functionally, the mitochondrial membrane potential, $\Delta\psi m$ has been associated with direction of neuronal transport. In neurones, mitochondria with high membrane potential predominantly travel in the direction of the growth cone, whilst those with a low membrane potential predominantly travel towards the cell body (Miller & Sheetz, 2004). If CP60 and CP69 induced a low mitochondrial membrane potential $\Delta\psi m$ this could possibly explain the abundance of CP60 and CP69 protein at the cell body in transfected neurone cultures. Impaired mitochondrial transport due to altered DISC1 expression has been previously detected using live cell-imaging (Atkin *et al*, 2011; Ogawa *et al*, 2014). It is possible that live cell-imaging could be used to test a hypothesis that CP60 and CP69 expression depolarize the mitochondrial membrane potential $\Delta\psi m$, and this, in turn, would favour net mitochondrial movement towards the cell body. This could be tested by using inducible CP60 and CP69 expression constructs. Cells could be stained with JC-1, a dye that can indicate the mitochondrial membrane potential, $\Delta\psi m$, with live cell imaging used pre- and post-induction of expression of CP60 or CP69, to capture changes in mitochondrial motility and JC-1 staining due to the aberrant proteins.

`

Given more time it would have been of interest to implement additional tests to investigate mitochondrial dysfunction due to the exogenous expression of der 1 chimeric proteins. The quantification of an absolute mitochondrial membrane potential, $\Delta\psi m$ for each species would enrich the interpretation of the immunocytochemistry data. A suitable method is provided by Gerencser *et al*., (2012), which measures the dynamics of a mitochondrially permeable fluorescent probe operating under a voltage clamp. The determination of the activity of mitochondrial respiratory chain complexes I–IV associated with DISC1/DISC1FP1 protein expression would also be beneficial and could be facilitated by single-wavelength spectrophotometry (Spinazzi *et al*, 2012). The findings could be compared with the diverse array of established research on respiratory complex deficits in major mental illness (see section 1.3.4). Additionally, the immunofluorescence paradigm discussed in this chapter could be adopted to investigate signs of mitochondrial apoptosis (Tait & Green, 2010). The COS-7 cells could be cultured for a longer time, 36 hours, to enhance the window of opportunity for apoptosis to occur and then be co-stained for caspases.

4.5.3 Endogenous der 1 DISC1/DISC1FP1 chimeras

The exogenous expression of CP1, CP60 and CP69 in both the COS-7 cell lines and mouse primary cortical neurones shows pathogenic mechanisms that may arise from the consequences of altered cellular expression patterns and mitochondrial toxicity. There is no evidence of endogenous chimeric protein expression at the present time. To date, the der 1 chimeric transcripts are detectable in t(1;11) cell lines, though at low levels (Eykelenboom *et al*, 2012). The CP60 and CP69 transcripts may not be translated, due to a splice site downstream of the stop codon, which suggests these transcripts may be targeted for nonsense mediated decay. However, the transcripts are readily detected so, conversely, may be translated (Eykelenboom *et al*, 2012).

Western blot analysis to detect endogenous chimeric proteins in t(1;11) lymphoblastoid cell lysates failed to detect endogenous expression of CP1, CP60 or CP69 protein. This involved the analysis of lysates expressing exogenous untagged CP1, CP60 and CP69 in parallel with t(1;11) lymphoblastoid cell lysates. The exogenously expressed CP1, CP60 and CP69 contained protein bands specific to each respective chimeric species. These chimera-specific bands were not detected in the t(1;11) lysate, when probed with N-terminal DISC1 antibodies (Eykelenboom *et al*, 2012). The possibility remains that DISC1/DISC1FP proteins may have been present at low levels in the t(1;11) lymphoblastoid lysates which were beyond the threshold of detection for the N-terminal DISC1 antibodies used.

`

Endogenous expression of CP1, given the phenotypes of DISC1 aa1-597 transgenic mice, may produce a phenotype similar to schizophrenia (see chapter 3). The expression of endogenous CP60 and CP69 would likely produce mitochondrial impairment even with low levels of expression. It is possible that CP60 and CP69 overexpression produces an alteration in mitochondrial network dynamics that results in the generation of clustered mitochondria. CP1 expression likely produces 'ring' or lariat like mitochondria (Millar *et al*, 2005a) which could also represent changes in the mitochondrial network. It is also interesting to observe that the DISC1-37W mutant (Ogawa *et al*, 2014) alters mitochondrial dynamics. Mutations to proteins involved in mitochondrial fission and fusion dynamics generally produce illness and disablement that is distinguishable from mental illness. Optic atrophy results from certain mutations to OPA1, (Delettre *et al*, 2000; Hudson *et al*, 2008). Mutations to Mfn2 and the mitochondrial fission protein Ganglioside-induced Differentiation-associated Protein 1 (GPAD1) produce Charcot-Marie-Tooth disease which is associated with peripheral nerve degeneration, muscular atrophy and sensory impairment. Charcot-Marie-Tooth type 2A is caused by mutations to the mitochondrial fusion protein, Mfn2, resulting in altered axonal degradation and regeneration. Charcot-Marie-Tooth type 4 is caused by mutations to GAPD1, producing axonal demyelination (Liesa *et al*, 2009). Given the severity of the symptoms associated with mutations in mitochondrial fission and fusion proteins, if CP60 and CP69 were expressed endogenously, and they influence fission/fusion, the t(1;11) carriers could be expected to have a more heterogeneous phenotype. However, the major mental illness seen in t(1;11) carriers displays no unique features (Eykelenboom *et al*, 2012)

Alternatively, in contrast to the fission-fusion dysfunction of the neurodegenerative diseases discussed above, it may be that the effects of CP60 and CP69 expression are more subtle. These species may possibly mediate pathogenesis by impinging on the mitochondrial trafficking machinery. As mentioned previously, full-length DISC1 binds with both Miro1 and TRAK1 as part of the mitochondrial transport complex (Ogawa *et al*, 2014) and is involved in mitochondrial trafficking (Atkin *et al*, 2011; Ogawa *et al*, 2014). Mutations to the mitochondrial transport machinery can have detrimental effects on mitochondrial trafficking. In *Drosophila* mutation of dMiro1 results in build-up of a pool of mitochondria in the cell body (Guo *et al*, 2005). Similar observations are also seen in *Drosophila* studies with mutants of the TRAK1 orthologue milton, again mitochondria accumulate in the soma and are absent from the axon and synaptic processes (Stowers *et al*, 2002). Regarding DISC1 mutations and mitochondrial trafficking, the DISC1-37W variant does not promote anterograde mitochondrial movement and thus serves to impair anterograde movement mediated by

`

endogenous DISC1 (Ogawa *et al*, 2014). Additionally, the expression of the disease associated DISC1 607F polymorphism (L607F) is associated with a reduction in the number of mobile mitochondria (Atkin *et al*, 2011). Given this evidence it would seem feasible that CP60 and CP69 could affect mitochondrial transport as a putative mechanism of pathogenesis in the t(1;11) pedigree. The TRAK1 binding site that is affected by the 37W mutilation (Ogawa *et al*, 2014), would be retained in the DISC1/DISC1FP chimeras.

The above proposals imply that the der 1 chimeras could mediate mitochondrial pathogenesis via altered fission-fusion dynamics or by abnormal mitochondrial trafficking. Since this thesis was initially submitted, evidence has emerged that observed that the exogenous expression of CP60 causes deficits to both mitochondrial transport and mitochondrial fusion (Norkett *et al*, 2016) (i.e. pathogenic insults to these processes can co-occur). It is suggested these the impairments are mediated by dominant negative effects of CP60 on TRAK1-Miro1 and Mfn1/Mfn2, respectively. Given the high degree of structural homology between CP60 and CP69 it is extremely likely that these potential mechanisms of pathogenesis may also occur with CP69 expression.

Findings from the DISC1-Boymaw mouse (Ji *et al*, 2014) are in line with the observation that the t(1;11) family do not show immediate evidence of mitochondrial fission-fusion based neurodegenerative disease, This model contains both the BD13 and DB7 fusion genes knocked-in, ORFs that correspond to those of DISC1/DISC1FP1 chimeric transcripts, encoding the C-terminal DISC1 fragment and CP60, respectively. The *in vivo* expression of these proteins produces a phenotype that includes reduced translation in both the hippocampus and primary neurones as well as reduction in rRNA levels in the hippocampus and cortex. Ketamine mediated hyperlocomotion was increased in the male mice as was a measure of PPI. The mice also displayed altered erythropoiesis and a decrease in the reduction of MTT. Taken together, these phenotypes do not immediately seem to relate to the mitochondrial pathophysiology seen with the *in vitro* expression of CP60 or CP69. However, Ji *et al.*, (2014) used a theoretical model to explain the translation and rRNA deficits around the MTT assay findings and the observation that NADPH oxidoreductase function in the MTT assay was reduced with CP60 expression. The model of cellular signalling features NADPH oxidoreductase upstream of the transcription and rRNA dysregulation. It is proposed that mitochondrial oxidoreductase activity could impair ATP production and that this functional outcome is compatible with the observations that there is an impairment in the mitochondrial membrane potential, $\Delta\psi m$ seen with CP60 and CP69 expression *in vitro*. The findings from the DISC1-Boymaw mouse (Ji *et al*, 2014) indicate that the end phenotypes produced by CP60

`

and the highly similar species CP69 may be more complex than that of a direct extrapolation from the *in vitro* phenotypes (Eykelenboom *et al*, 2012). It may be the case that the differences in phenotype noted are underpinned by the contrasting methods in protein expression. The overexpression *in vitro* is a potent method of protein expression, whereas the transgenic expression may be more subtle, and thus mediate different effects.

Comparing the symptoms of mitochondrial disorders to those of psychiatric disorders is one way to address whether the mental illness in t(1;11) carriers could be associated with mitochondrial dysfunction. What if mitochondrial dysfunction is associated with major mental illness in itself? For mood disorders, such as depression and bipolar disorder, a growing and converging body of evidence exists for mitochondrial abnormalities. These include: mutations to mitochondrial DNA, alterations to Ca^{2+} signalling and reductions in the levels of ATP in the brain (Manji *et al*, 2012). Research into schizophrenia has shown reduced mitochondrial density post-mortem; associated reductions to the neuropil; brain region-specific alteration of mitochondrial gene expression; and NADH dehydrogenase activity (Manji *et al*, 2012; Park *et al*, 2010). It may be possible in the future to carry out a non-invasive test on t(1;11) carriers such as neuroimaging to detect ATP levels in the brains of t(1;11) carriers and test the hypothesis regarding mitochondrial dysfunction and exogenous der 1 chimera expression.

At the present time, post-mortem brain tissue is not available from a t(1;11) carrier, to probe for evidence of endogenous chimeric protein expression. However, t(1;11) induced pluripotent stem cells (iPSC's) have been generated. This could be an avenue for future investigation into the possible expression of endogenous der 1 chimeric proteins. These t(1;11) iPSC's could be differentiated down a number of neural pathways to produce a variety of post-mitotic neurone types, from which endogenous CP1,CP60 and CP69 protein expression could be investigated. The der 1 DISC1/DISC1FP1 immunofluorescence paradigm detailed in this chapter could be replicated on endogenous DISC1 species in the iPSC neurones along with Western blot analysis to try to detect endogenous CP1, CP60 and CP69. This Western blotting and immunofluorescence would entail the use of custom peptide antibodies that were targeted to epitopes specific to each chimeric protein. Mitochondrial function could be measured in iPSC and t(1;11) lymphoblastoid cells by looking at cellular and mitochondrial ATP levels, measuring the mitochondrial membrane potential, $\Delta\psi m$ and addressing mitochondrial toxicity.

A possible explanation for the lack of appreciable mitochondrial disease in the t(1;11) pedigree and the inability to detect endogenous chimeric proteins is that these species may be subject to temporal clearance and aggregation. Acting concert, this may result in the rapid degradation

`

of chimeric proteins. Firstly, recent evidence has emerged that a small boymaw protein may be expressed via an internal ORF (Ji *et al,* 2015). This species appears to be subject to proteasomal degradation under basal conditions and is upregulated in response to a variety of stressors. Importantly, 59 of the 63 aa's in this boymaw protein are also present in CP60 and hence the majority will also be present in CP69. This implies that due to the DISC1FP1 aa's present in these chimeric species CP60 and CP69 may be subject to stress dependent regulation and could be targeted for rapid proteasomal degradation.

Secondly, evidence of the potential for the aggregation of these chimeras arises from biophysical experiments expressing the epitope tagged truncate MBP-ΔNCP69 (Eykelenboom *et al,* 2012). High molecular weight assemblies and an altered secondary structure were observed with the expression of MBP-ΔNCP69 in comparison to MBP-ΔN597. These findings may be indicative of a potential for aggregation in the CP69 species and are therefore are also likely to be present with CP60 expression. Furthermore, the immunocytochemistry of exogenously expressed CP60 and CP69 presented in this chapter displays a clustered cellular phenotype which may actually be the occurrence of aggregation. However, definitive biochemical testing of these species is needed to confirm this view. If indeed CP60 and CP69 do form aggregates, the potential exists that these species would be capable of depleting endogenous DISC1. The sequestering of DISC1 from the cytoplasm has been noted by both WT-DISC1 aggregates (Atkin *et al,* 2012) as well as aggregated mutant DISC1 species with truncations to the distal C-terminus (Wen *et al,* 2014). Were CP1 to be exogenously expressed, this species could also be depleted by such a mechanism and be absorbed by CP60 or CP69 aggregates. The underlying interactions would presumably be mediated by interactions of the DISC1 self-interaction-domain (Kamiya *et al,* 2005), which all of the der 1 chimeric species contain.

Thirdly, these aggregates and the additional species bound within them may be targeted to aggrisome and subsequently be degraded by the autophagic pathway, as is the case for WT-DISC1 aggregates (Atkin *et al,* 2012). In summary, by incorporating several lines of evidence the preceding text suggests a potential hypothesis as to why der 1 chimeric species have not been isolated endogenously. Succinctly, this is as follows: CP60 and CP69 may be stress regulated, then subject to rapid degradation, yet when present these species may aggregate depleting WT-DISC1 and CP1 from the cytoplasm, in turn these chimeric aggregates would also be degraded by cellular surveillance. Further experiments on t(1;11) derived cell lines could be implemented to test this hypothesis. This would entail the culturing of these cells in the presence of stressors and proteasomal inhibitors similar to the methodology used by Ji *et*

`

al., (2015) to investigate the small boymaw protein. To test the specific aggregation of CP60 and CP69, the protocols followed Atkin *et al.*, (2012) to study WT-DISC aggregation could be employed.

Prior to the identification of the der 1 DISC1/DISC1FP1 fusion transcripts, the established pathogenic mechanism as a consequence of the t(1;11) was believed to be haploinsufficiency of DISC1 (Millar *et al*, 2005b). The possibility of aberrant DISC1 protein species as a pathogenic mechanism does not preclude that of haploinsufficiency as a co-occurring pathogenic insult. The existence of endogenous fusion proteins may seem unlikely, given the paucity of the transcripts (Eykelenboom *et al*, 2012). However, the transcripts still can be readily detected. Given the pleiotropic effect of the chimeras and that the mitochondrial dysfunction induced by CP60 and CP69 overexpression is apparent at low level expression, low level of exogenous fusion expression would likely be pathogenic. The novel mechanisms of molecular pathogenesis proposed by the der 1 DISC1/DISC1FP1 chimeras warrant further research. The next chapters will investigate whether MitoTracker Red uptake is impaired in t(1;11) lymphoblastoid cells.

`

Chapter 5 - FACS analysis of MitoTracker Red fluorescence in t(1;11) lymphoblastoid cell lines

5.1 Introduction

When the chimeric species, CP60 and CP69, are overexpressed in COS-7 cells and primary cortical neurones, mitochondrial staining by MitoTracker Red is impaired (see chapter 4). The uptake of MitoTracker Red dye, a cationic molecule, into mitochondria is dependent on the mitochondrial membrane potential, $\Delta\psi m$ (Poot *et al*, 1996). Therefore, if CP60 and CP69 protein is expressed endogenously in translocation lymphoblastoid cell lines, it is possible that an impairment of the staining of the mitochondria in these cells by MitoTracker Red dye may occur.

It is also likely that the CP1 species perturbs mitochondrial function. This chimeric species is highly similar to DISC1 aa1-597, with CP1 encoding DISC1 aa1-598. The overexpression of the murine equivalent to DISC1 aa1-597 protein downregulates mitofilin *in vitro* (Park *et al*, 2010). Mitofilin is an inner membrane mitochondrial protein involved in the morphology of cristae and the knockdown of this protein results in the mitochondrial membrane potential, $\Delta\psi m$ becoming increasingly negative (John *et al*, 2005). Therefore, it is possible that CP1 overexpression would hyperpolarise the mitochondrial membrane potential, $\Delta\psi m$. This would be consistent with the presence of MitoTracker Red staining from immunocytochemistry data with CP1 overexpression (see chapter 4). The DISC1-mitofilin interaction and expression could also be a mechanism that explains the altered mitochondrial staining seen with the exogenous expression of CP60 and CP69. These species also encode DISC1 aa1-597 (Eykelenboom *et al*, 2012; Zhou *et al*, 2008), and it is possible that the additional 60 and 69 novel amino acids in these aberrant species could possibly confer an altered protein-protein interaction with mitofilin. This might explain the abolition of the mitochondrial membrane potential, $\Delta\psi m$ observed with the overexpression of these aberrant protein species *in vitro*.

At present, endogenously expressed DISC1/DISC1FP1 protein species have not been detected by Western blotting of t(1;11) lymphoblastoid cell lysates with N-terminal DISC1 antibodies (Eykelenboom *et al*, 2012). However, it may be that endogenously expressed chimeric protein species are present in t(1;11) lymphoblastoid cell lines below the threshold of the detection of the Western analysis used to date (Eykelenboom *et al*, 2012).

`

FACS analysis can be used to measure the fluorescence intensity of MitoTracker Red stained lymphoblastoid cell lines (Pendergrass *et al*, 2004; Poot *et al*, 1996; Xu *et al*, 2005). With regard to mitochondrial dysfunction, mitochondrial poisons have been observed to decrease MitoTracker fluorescence in stained lymphoblastoid cell lines using flow cytometry. This includes: CCCP, an uncoupler of the electron transport chain and inhibitor of mitochondrial complexes, the complex II inhibitor, antimycin, and the complex IV inhibitor, sodium azide. However, the treatment of lymphoblastoid cells with rotenone, a complex 1 inhibitor, did not affect the fluorescence intensity of MitoTracker Red staining (Poot *et al*, 1996). Additionally, MitoTracker fluorescence alterations can be detected in patient cell lines. Barth syndrome is a rare multi-factorial disease caused by mutations in the gene *Tafazzin* (*TAZ*) which encodes an inner mitochondrial membrane phospholipid (Gonzalvez *et al*, 2013). FACS analysis of Barth syndrome patient derived lymphoblastoid cell lines, incubated with MitoTracker Red, detected increased MitoTracker fluorescence, indicative of mitochondrial pathology (Xu *et al*, 2005). Given this data, it was decided to use FACS analysis as a means to investigate if the MitoTracker Red fluorescence intensity of t(1;11)-family derived lymphoblastoid cell lines differs from that of karyotypically normal family controls. If CP1, CP60 and CP69 are endogenously expressed in translocation cell lines, it is possible that these aberrant proteins will alter the mitochondrial membrane potential, $\Delta\psi m$ and therefore detectably alter MitoTracker Red fluorescence.

This chapter will focus on both the development of the FACS analysis protocol and the subsequent experiments used to quantify the MitoTracker Red fluorescence intensity in translocation lymphoblastoid cell lines.

5.2 FACS analysis performed

This section will briefly cover FACS parameters that will be discussed in the following optimisation and experimentation section and gives typical examples of the data captured. To measure the baseline fluorescence, a sham (DMSO) treated lymphoblastoid cell line sample was assayed by FACS and captured by FL1 vs FL2 parameters, the FITC 530 nm and PE 585 nm emission fluorescence detector settings. Following the establishment of the sham samples fluorescence signal, a subjective gate, R1, was drawn to isolate cells with increased FL2 fluorescence. These would be MitoTracker Red stained cells. The FACS analysis was then performed with the fluorescing cells. All data were displayed as FL1vs FL2 dot plots (see figure 5.2.A). The, geometric mean fluorescent intensity (GMFI), was collected for each of the parameters along with the percentage of cells gated in the R1 region. The GMFI is the log-

`

normal mean florescence intensity and is appropriate here as events were displayed on log-log dot-plots.

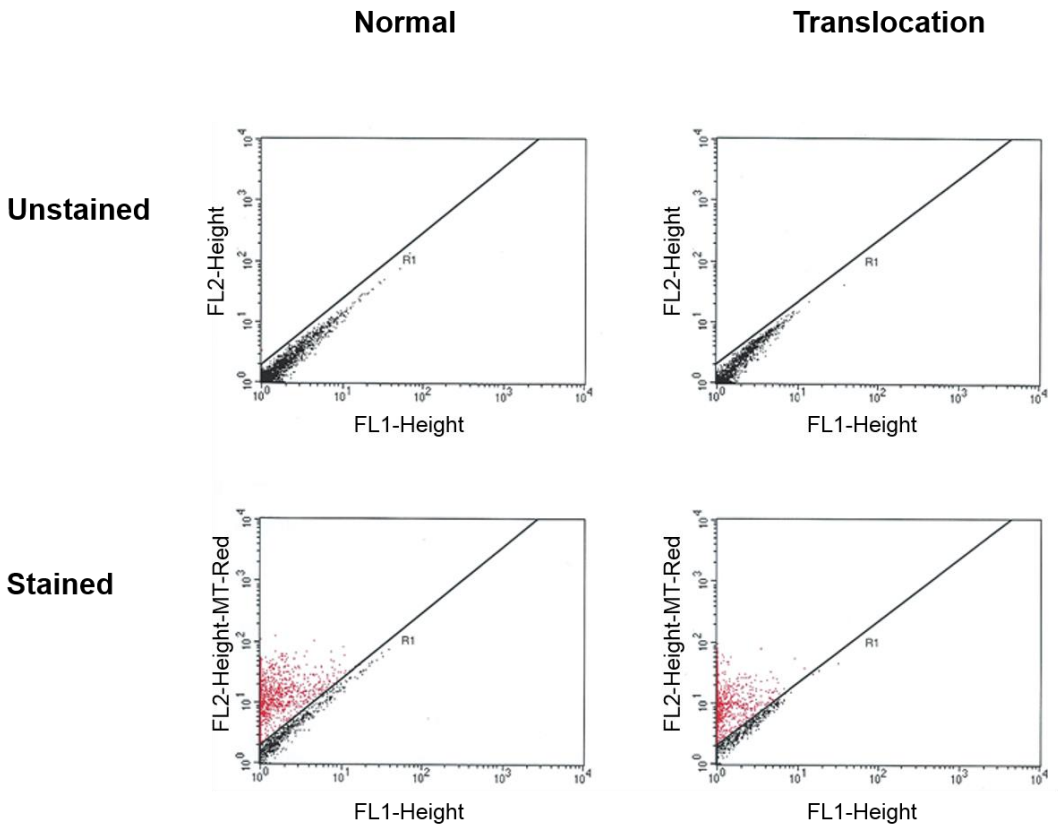

Figure 5.2.A: MitoTracker Red fluorescence in t(1;11) lymphoblastoid cell lines detected by FACS analysis. Unstained sham (DMSO) treated: normal karyotype control and translocation lymphoblastoid cell lines (top), MitoTracker Red stained cells (bottom). R1 region is a subjective gate drawn to detect MitoTracker Red fluorescing cells following the measurement of baseline fluorescence of unstained cells. MitoTracker Red stained fluorescing cells were then detected in the R1 gated region. Normal GMFI =7.17; % MitoTracker Red fluorescing cells gated = 80.00. Translocation GMFI = 5.23; % cells MitoTracker Red fluorescing cells gated = 82.60. Dot plots here depict typical examples of FACS analysis. Black dots depict unstained cell events, red dots depict MitoTracker Red cell events. 10,000 events recorded per dot plot. The dot-plots displayed are representative examples of the FACS analysis performed.

In parallel with the reading of lymphoblastoid cells' MitoTracker fluorescence by FL1 vs FL2 parameters, the populations of both MitoTracker Red stained and unstained cells were also

`

analysed using FSC vs SSC parameters. The data were then displayed on dot plots (see figure 5.2.B). The FSC (forward scatter) is a measure of cell size, while SSC (side scatter) is a measure of the complexity and granularity of a cell. This analysis was a precautionary measure to guard against the possibilities of treatment effects falling outside of the expected fluorescence occurring in the MitoTracker Red incubated cells, or the cell lines assayed showing signs of apoptosis (Koopman *et al*, 1994). Importantly, the FSC vs SSC dot plots for the MitoTracker Red stained cells or sham (DMSO) controls did not show any appreciable differences (see figure 5.2.B, other cell line data not shown).

5.3 MitoTracker Red incubation time optimisation for lymphoblastoid cell line fluorescence

Prior to the generation of experimental FACS data, optimisation trials were carried out to determine how MitoTracker Red fluorescence varied with the length of incubation in lymphoblastoid cells lines. It was possible that MitoTracker staining of lymphoblastoid cells was highly sensitive to variations in incubation time or produced saturation effects which might have negatively affected the generation of FACS data.

For the optimisation results covered here, and following experimental data, all of the lymphoblastoid cell lines that were analysed by FACS were unfixed. The fixing of cells stained with MitoTracker Red has been observed to impact both the resolution and fluorescence detected by FACS analysis (Gilmore & Wilson, 1999). For the optimisation, three different lymphoblastoid cell lines (under blinding) were incubated with MitoTracker Red for either: 15, 30, 45 or 60 minutes or were incubated in parallel with sham (DMSO) treatment. Following this, the lymphoblastoid cells were analysed by FACS using FL1 vs FL2 analysis (see section 5.2).

Across all three cell lines assayed, the GMFI showed the trend of increasing with incubation time in the MitoTracker Red dye. However, this increase in GMFI between each 15 minute time point across all cell lines was not significant, as analysed by One-way ANOVA, $F(3,8)=0.442$, $p=0.729$. The percentage of MitoTracker Red fluorescing cells gated showed no clear trend with increasing incubation time with the MitoTracker stain. Although there appeared to be intra-experimental trends in the proportion of the MitoTracker Red fluorescing cells detected which were specific to each cell line, in the technical replications (see table 5.3.A). It should be noted that for each incubation time point, a new subjective gate was drawn

`

to capture MitoTracker fluorescing lymphoblastoid cell lines. It is, therefore, possible that cell line specific gating frequencies are observed here.

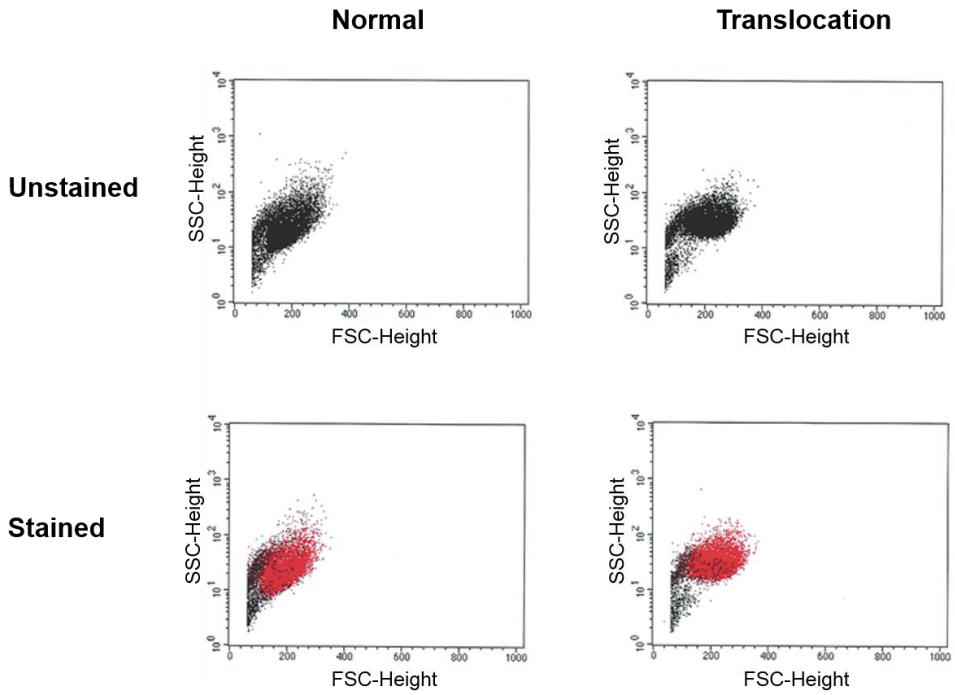

Figure 5.2.B: FSC vs SSC in MitoTracker Red stained t(1;11) lymphoblastoid cell lines detected by FACS analysis. Top: FSC vs SSC analysis of sham (DMSO) treated, normal karyotype control (left) and translocation lymphoblastoid cell lines (right). Bottom: FSC vs SSC analysis of the MitoTracker Red treated cells. Unstained cells with low SSC and FSC values are observed in both translocation and normal cell lines. Black dots depict unstained cell events, red dots depict MitoTracker Red cell events. 10,000 events recorded per dot plot.

`

Lymphoblastoid cell line genotype	MITO incubation time (Min)	% of MITO fluorescing cells gated	GMFI (AU)
Translocation 1	60	85.9	10.1
	45	87.3	10.0
	30	87.4	9.9
	15	87.4	9.7
Translocation 2	60	89.6	10.6
	45	90.0	10.6
	30	89.3	10.5
	15	91.1	10.5
Normal	60	84.4	10.4
	45	84.8	10.5
	30	87.0	10.4
	15	87.3	10.1

Table 5.3.A: Optimisation of the MitoTracker Red incubation time for lymphoblastoid cell lines for FACS analysis. One-way ANOVA shows no effect of treatment time on GMFI, p=0.729. The proportion of MitoTracker Red fluorescing cells gated appears to show consistency within each of the t(1;11)-family derived and normal karyotype control lymphoblastoid cell lines. All three cell lines assayed were under blinding. FACS analysis per cell line recorded 10,000 events using FL1 vs FL2 analysis (see figure 5.2.A).

Following this optimisation, it was decided to use a 15 minute incubation time using 30nM MitoTracker Red dye. This reduction from the concentration of MitoTracker dye was introduced to prevent saturation of the lymphoblastoid cell lines. The incubation with lymphoblastoid cell lines with 30nM MitoTracker Red has been previously observed to be sufficient for FACS analysis to determine MitoTracker fluorescence (Lee *et al*, 2010).

`

5.4 FACS analysis of MitoTracker Red fluorescence in translocation lymphoblastoid cell lines

5.4.1 Background on statistical analysis of experimental replicates of MitoTracker Red staining of translocation cell lines assayed by FACS

Before the statistical analysis of the FACS data to determine fluorescence intensity of the MitoTracker staining in t(1;11)-family derived lymphoblastoid cell lines, it is relevant that the experimental protocol is explained in the context of the replications performed. In this section, the individual experimental replicates were analysed. The analysis of the pooled experimental replicate dataset will be covered in section 5.4.4 onwards. In total, three experimental replicates were performed, each containing three translocation and three normal karyotype control lymphoblastoid cell lines. In an individual experimental replicate, two technical replicates were assayed per cell line. Each of these technical replicates contained a MitoTracker Red treatment and a sham (DMSO) treatment. The same lymphoblastoid cell lines were used across the three experimental replicates. This used the growing of new cell cultures between experiments. For clarification, the protocol for a single experimental replication is shown in figure 5.4.A.The three experimental replicates were carried out in order to have the minimum number of replicates required for generating a pooled experimental dataset that could be statistically analysed. However no *a priori* power tests were performed to determine if the use of three replicates is sufficient for statistical analysis.

The reasoning to analyse the three experimental replicates separately is as follows. As each lymphoblastoid cell line comes from a unique individual, there will be background effects between all cell lines. Due to this independence, each cell line could, therefore, be classed as a single experimental unit (Lazic, 2010). Additionally, these cell lines were cultured in separate tissue culture flasks, although within the same incubator. Therefore, there is a level of independence in these individual experimental replicates that is beyond that seen in a single flask of cells that are split six times into tissue culture dishes and assigned equally into treatment or control groups, which would possess an n=1 (Cumming *et al*, 2007). As a consequence, it is proposed that the individual experimental replicates can be analysed as n=3. This is also taking into account that the internal technical replicates of repeating the MitoTracker FACS analysis twice per cell line are simply pseudo replicates measuring the same individual cell line (Cumming *et al*, 2007; Lazic, 2010).

`

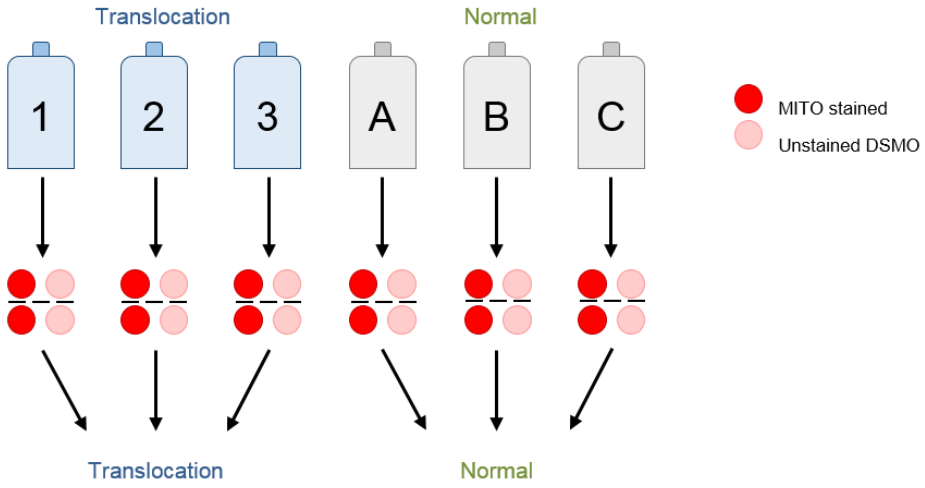

Figure 5.4.A: Cartoon depicting the generation of an experiment replicate in the FACS analysis of MitoTracker Red fluorescence in t(1;11)-family derived lymphoblastoid cell lines. Flasks of translocation (blue) and normal karyotype controls (green) were cultured, with 3 different lymphoblastoid cell lines assayed per genotype. This is illustrated by the use of numbers for translocation cell lines and capitalised letters for normal cell lines. Per individual cell line, two technical replicates of 30nM MitoTracker Red and sham (DMSO) treatments were analysed by FACS to quantify MitoTracker GMFI. Following FACS analysis, these technical replicates were averaged by cell line and the GMFI by genotype was then statistically analysed. Consequently, (n=3) per experimental replicate.

5.4.2 MitoTracker Red GMFI in translocation lymphoblastoid cell lines as statistically analysed per experimental replicate

The treatment of lymphoblastoid cells with MitoTracker Red showed inconsistent results regarding genotype and the detected fluorescence. One of the three experimental replicates showed reduced MitoTracker staining in translocation lines (see figure 5.4.B). There was no significant difference in the MitoTracker Red GMFI between translocation and normal karyotype controls in experimental replicate 1, Student's unpaired two-tailed *t*-test, $t(4)=0.43$, $p=0.69$. There was also no significant difference in the MitoTracker Red GMFI between the translocation and normal karyotype controls in experimental replicate 2, Student's unpaired two-tailed *t*-test, $t(4)=0.37$, $p=0.73$. However, for experimental replicate 3 there was a highly significant difference in the MitoTracker Red GMFI translocation and normal karyotype, Student's unpaired two-tailed *t*-test $t(4)=11.29$, $p<0.001$. In experimental replicate 3, the

`

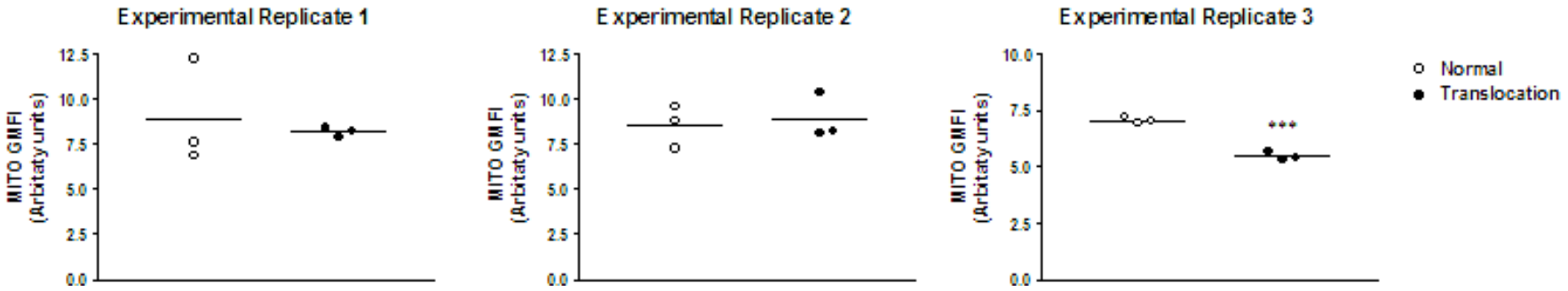

Figure 5.4.B: MitoTracker Red GMFI in t(1;11)-family derived lymphoblastoid cell lines by experimental replicate. Each experimental replicate compares FACS derived GMFI between translocation and normal karyotype control lymphoblastoid cell lines, (n=3, with two technical replicates per cell line). The horizontal line represents mean MGFI by genotype. Experimental replicate 3 shows a significant reduction in translocation MGFI, Student's unpaired two-tailed *t*-test, df 4, *** p <0.001. The same analysis on experimental replictes 1 & 2, p = ns, respectively. 10,000 events recorded per dot plot.

`

GMFI in translocation cell lines is significantly lower than normal karyotype controls.

It is unusual that in experimental replicates 1 and 2 the MitoTracker GMFI results parallel each other, yet experimental replicate 3 shows highly significant reduction in translocation lymphoblastoid cell line GMFI (see figure 5.4.B). It is important to note that these experiments are displayed in order of completion. Each experimental replicate of FACS analysis was performed three to four weeks apart to enable the growth of new cell cultures. Therefore, a possible explanation for the inconsistency between the GMFI data for experimental replicates may be the effect of practice in performing the experiment, with performance of the experiment improving with replications here. Another explanation could be that the cells in experimental replicates 1 and 2 were not confluent enough to express the translocation product at a level that would have impaired MitoTracker Red staining, in contrast with the cells in experimental replicate 3 which may have been fully confluent. Alternatively, there may have been more generalised cell culture differences and treatment differences between the experimental replicates. Another possibility is that the percentage of MitoTracker Red fluorescing cells that were gated differs across experimental replicates, in such a manner as to bias the GMFI analysis. This is the topic of the next section. Finally, the three experiments' GMFI data needs to be pooled and analysed to determine if the significant reduction in translocation GMFI seen with experimental replicate 3 is retained or abolished. This will be covered in section 5.4.5.

5.4.3 Proportion of lymphoblastoid cells showing MitoTracker Red fluorescence by genotype per experimental replicate

Analysis of the gating by genotype within an experimental replicate will inform if there is a significant difference in the number of MitoTracker stained cell events between translocation and control lymphoblastoid cell lines. Such differences could explain the lack of agreement in the experimental replicate MitoTracker Red GMFI results (see section 5.4.2). When interpreting the gating data, it is important to remember that the GMFI is calculated from both the numbers of fluorescing cells gated and the fluorescence intensity of that gated sub-population. The following statistical analysis is performed on each of the three individual experimental replicates to compare the proportion of lymphoblastoid cells displaying MitoTracker Red fluorescence between the translocation and normal karyotype control genotypes. The sub-populations of lymphoblastoid cells with MitoTracker fluorescence do not differ by genotype in each of the three experimental replicates analysed (see figure 5.4.C).

`

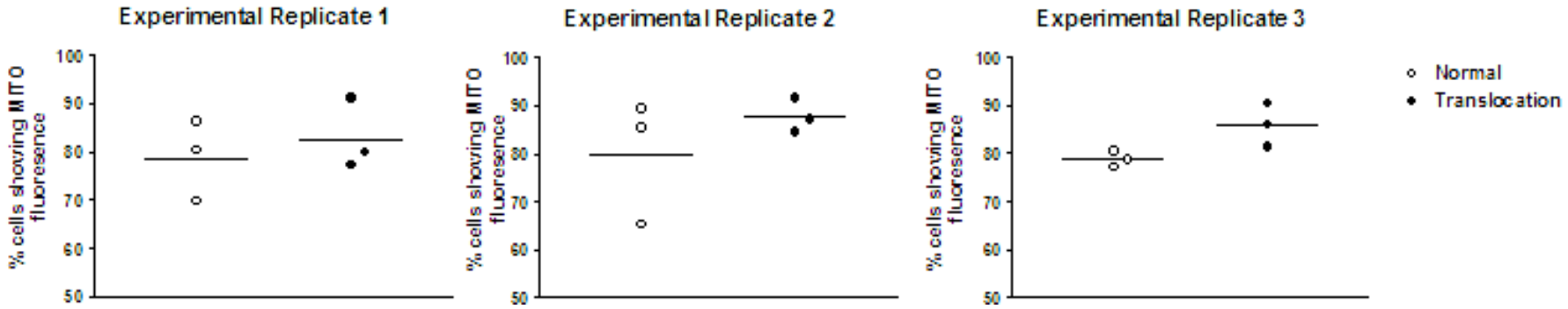

Figure 5.4.C: Proportion of lymphoblastoid cells showing MitoTracker Red fluorescence by genotype per experimental replicate. Each experimental replicate compares the percentage of MitoTracker Red fluorescing cells gated for translocation and normal karyotype control lymphoblastoid cell lines, (n=3, with two technical replicates per cell line) per experimental replicate by genotype. The horizontal line represents mean percentage cells fluorescing with MitoTracker Red by genotype. Student's unpaired two-tailed *t*-test, df 4,p = ns for each experimental replicate, respectively. 10,000 events recorded per dot plot.

`

There was no significant difference in the proportion of MitoTracker Red fluorescing cells gated between translocation and normal karyotype controls in experimental replicate 1, Student's unpaired two-tailed *t*-test, t(4)=0.61, p=0.58 There was no significant difference in the proportion of MitoTracker Red fluorescing cells gated between translocation and normal karyotype controls in experimental replicate 2, Student's unpaired two-tailed *t*-test, t(4)=1.00, p=0.37. There was no significant difference in the proportion of MitoTracker Red fluorescing cells gated between translocation and normal karyotype controls in experimental replicate 3, Student's unpaired two-tailed *t*-test t, t(4)=2.58, p=0.06, this is however, a of a trend towards significance.

It is interesting that for experimental replicate 3 there is an increase in proportion of translocation cell events with MitoTracker staining that are gated compared to controls and that the difference is approaching significance. This suggests that, although the GMFI for experimental replicate 3 is reduced in translocation lymphoblastoid cell lines (see section 5.4.1), this fluorescence measure is drawn from a larger (although not significantly different) population of cells compared to the karyotype control data. This would appear to support, rather than contradict, the observation that translocation cell GMFI is significantly reduced for experimental replicate 3.

5.4.4 Background on statistical analysis of pooled experimental replicate data of MitoTracker Red staining of translocation cell lines assayed by FACS

The pooling of the FACS data from the three experimental replicates raises further questions regarding cell culture data analysis. If each lymphoblastoid cell line is taken to be an experimental unit, then repeating the experiment with the same cell lines may be seen as using the same individuals (Lazic, 2010). However, this is not an entirely accurate depiction of what has occurred experimentally. In performing the three experimental replications pooled here, the cell lines used are from the same six individuals, but the cell cultures per single experiment were grown three to four weeks apart, being clones of the same cell line. Due to this, multiple potential stochastic environmental and experimental events could have occurred that introduce novel intra- and inter-experimental variability. This can be seen as a degree of biological independence that is not possible within a single experimental replicate. Therefore, the pooling of the data of the three experimental replicates may be seen to be a more robust analysis to determine if MitoTracker Red fluorescence is impaired in translocation lymphoblastoid cell

`

lines. Although it is understood that the hypothesis being tested is not analysing the ability to accurately culture cells within and between experiments.

The pooled experimental data are also analysed with a two-tailed *t*-test. The pooling of the three experimental replicates has n=3 (Cumming *et al*, 2007) as this is the number of different lymphoblastoid cell lines per genotype in the experimental replicate dataset.

5.4.5 MitoTracker Red GMFI in translocation lymphoblastoid cell lines as statistically analysed by pooled mean of experimental replicates

The pooled t(1;11)-family derived MitoTracker Red fluorescence lymphoblastoid data are shown in figure 5.4.D. For the pooled experimental data there was no significant difference in the MitoTracker Red GMFI between translocation and normal karyotype controls, Student's unpaired two-tailed *t*-test t(4)=0.64, p=0.56. The pooling of the experimental data does not support a reduction in the MitoTracker Red GMFI in translocation cell lines. This contrasts with the analysis of the experimental replicates individually in which experimental replicate 3 had a reduction in the GMFI in translocation lymphoblastoid cell lines (see section 5.4.2).

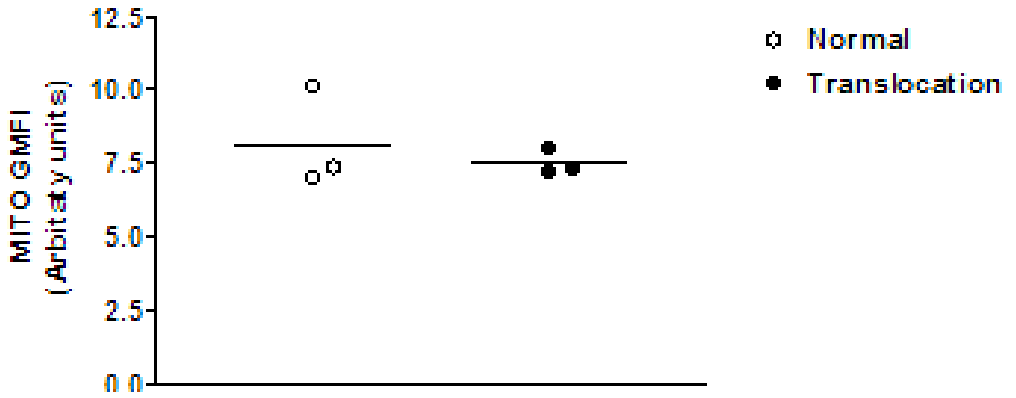

Figure 5.4.D: MitoTracker Red GMFI in t(1;11)-family derived lymphoblastoid cell lines by mean experimental replicate data. Each circle represents the mean lymphoblastoid GMFI by genotype from an experimental replicate, derived by FACS analysis (see figure 5.4.B). The horizontal line represents mean GMFI by genotype. n=3 independent experimental replicates, with two technical replicates per cell line. Student's unpaired two-tailed *t*-test, df 4, p=0.56. FACS analysis of cell population: 10,000 events recorded per dot plot.

`

5.5 Discussion

5.5.1 Disagreement in the MitoTracker Red GMFI data in translocation cell lines between experimental replicates

The analysis of the MitoTracker Red GMFI data in t(1;11) derived lymphoblastoid cell lines shows disagreement between the experimental replicates when they are analysed separately. While one FACS replicate displays a highly significant reduction in the MitoTracker Red GMFI in translocation lymphoblastoid cells, the other two replicates show no difference in MitoTracker GMFI by genotype. The individual experimental replicates discussed have been analysed as independent experiments as it is believed they fulfil the criteria according to the experimental design used (Cumming *et al*, 2007; Lazic, 2010). This encompasses three individual patient cell lines per genotype. However, it would be expected that the experimental result was consistent with repeated analysis. The subsequent analysis of the pooled data of all three experimental replicates detects no difference in MitoTracker GMFI.

The single experimental replicate that has a significant reduction in MitoTracker Red, a mitochondrial membrane potential, $\Delta\psi m$ dependent dye (Poot *et al*, 1996), is supportive of the *in vitro* observations with the overexpression of chimeric protein species. The exogenous expression of CP60 and CP69 in COS-7 cells and primary neurone cultures results in impaired mitochondrial staining from MitoTracker Red due to the abolition of the mitochondrial membrane potential, $\Delta\psi m$ (see chapter 4). However, why only a single significant reduction in MitoTracker GMFI in translocation cell lines is observed across replications remains unexplained. It is possible to speculate that the result may, alternatively, be the consequence of experimental error or a product of a practice effect on performing the FACS analysis. The latter view is supported as this replicate was the final FACS analysis of the three performed. Irrespective of these possible explanations, the disparity in the lymphoblastoid MitoTracker GMFI data is not the result of significant differences in the proportion of the sub-population of lymphoblastoid cells displaying MitoTracker Red fluorescence between genotype conditions.

Given the disagreement in the data regarding the MitoTracker fluorescence in translocation lymphoblastoid cell lines, the following discussion sections will focus on alternative measurements of MitoTracker Red fluorescence and of the mitochondrial membrane potential, $\Delta\psi m$, within these cells. This would aim to further characterise the translocation lymphoblastoid cell lines for evidence supportive of endogenous chimeric protein species and characterise exogenously expressed CP1 protein.

`

5.5.2 The measurement of MitoTracker Red fluorescence and the measurement of the mitochondrial membrane potential, (Δψm)

The use of MitoTracker Red alone is suitable for generating data on the intensity of fluorescence in patient lymphoblastoid cells with mitochondrial dysfunction (Xu *et al*, 2005). This analysis used GMFI as the measure of MitoTracker fluorescence. However, MitoTracker Red GMFI is not a direct measure of the mitochondrial membrane potential Δψm, merely a consequence of abnormal mitochondrial membrane potential, Δψm (Pendergrass *et al*, 2004; Poot & Pierce, 2001; Poot *et al*, 1996). The quantification of the mitochondrial membrane potential, Δψm itself, resulting from endogenous or exogenous DISC1/DISC1FP1 chimeric protein expression, is of greater interest to contextualise the observed mitochondrial pathophysiology than the quantification of the effects of these physiological changes upon MitoTracker dye uptake and florescence.

The determination of the mitochondrial membrane potential Δψm in a population of cells using a mitochondrial membrane potential, Δψm dependent dye, such as MitoTracker Red, requires that both the cellular fluorescence and the mitochondrial mass of the fluorescing cells is known. Differences in the mitochondrial mass within cells would impact upon MitoTracker Red fluorescence as cells with greater mitochondrial mass would fluoresce more (Poot & Pierce, 2001). It remains possible that the mitochondrial mass varies both within the individual cell lines and between control and t(1;11) lymphoblastoid populations, given the mitochondrial clustering observed with the exogenous expression of CP60 and CP69 *in vitro* (see chapter 4). To counter any possible bias arising from such variations and to derive the mitochondrial membrane potential, Δψm, it is possible to use a membrane potential insensitive dye such as MitoTracker Green in conjunction with a membrane potential sensitive dye (*here* MitoTracker Red) during FACS analysis. The ratio of the MitoTracker Red fluorescence to the MitoTracker Green fluorescence produces a normalised mitochondrial membrane potential, Δψm value (Pendergrass *et al*, 2004; Poot & Pierce, 1999; Poot & Pierce, 2001).

Given the disagreement in the results here measuring MitoTracker Red in translocation cell lines, it would be seem prudent to perform pilot experiments to detect the mitochondrial membrane potential, Δψm. From this work *a priori* power tests could be used to calculate the number of independent experimental replicates required to detect an effect of the translocation on the mitochondrial membrane potential, Δψm by MitoTracker Red/MitoTracker Green fluorescence.

`

A ratiometric approach to correct for mitochondrial mass was not used initially as it was inferred that even with low levels of CP60 and CP69 expression in t(1;11) lymphoblastoid cell lines that MitoTracker Red fluorescence would be significantly impaired. This was thought to be irrespective of these species potential to induce mitochondrial clustering, given that the clustered mitochondria frequently do not show MitoTracker Red fluorescence (see chapter 4). However, with hindsight the potentially low levels of endogenously expressed CP60 and CP60 may not be potent enough to abolish MitoTracker Red staining, merely to partly reduce the fluorescence. The magnitude of this effect in turn will be compromised by the size of the clustered mitochondria affected. Therefore the measurement of mitochondrial membrane potential, Δψm is a preferable metric to MitoTracker Red fluorescence alone.

5.5.3 Future work to investigate the effect of DISC1/DISC1FP1 chimeric protein on the mitochondrial membrane potential, Δψm

Despite the negative result for the pooled GMFI data, the use of FACS analysis to calculate the mitochondrial membrane potential, Δψm is an ideal way to further characterise the functional consequences of exogenous CP1 protein expression. The aim for future studies would be to determine the mitochondrial membrane potential, Δψm value for CP1 in comparison to DISC1 aa1-597 The hypothesis could focus on what is known of the interactions between the murine equivalent of DISC1 aa1-597 and mitofilin (Park *et al*, 2010) For the FACS analysis of CP1, given that this species is highly similar to DISC1 aa1-597, it is likely to downregulate mitofilin expression *in vitro* (Park *et al*, 2010) which, consequently, might hyperpolarise the mitochondrial membrane potential, Δψm (John *et al*, 2005). Further analysis of the mitochondrial membrane potential, Δψm in CP60 and CP69 expressing cells may not be required. This is because these species abolish the mitochondrial membrane potential, Δψm in the COS-7 cell lines and primary cortical neurons in the majority of expressing cells as evidenced by an impairment in MitoTracker Red staining (see chapter 4).

If the proposed further FACS analysis, to determine the mitochondrial membrane potential, Δψm in translocation lymphoblastoid cell lines and exogenous expression of der 1 chimeric proteins in cell lines was initiated, the use of further statistical measures would be beneficial. The dot plots used in this chapter to display FSC vs SSC and FL1 vs FL2 data are saturated by events so that the displayed data are seen as solid blocks of colour, whereby a single dot may also represent more than one event at that given fluorescence intensity (see figures 5.2.A and 5.2.B). This output limits interpretation of FACS data. If quartile contour plots were used to display the events, the comparison of experimental data both within and between genotypes

`

assayed would have had greater utility. Quantile contour plots separate the events by contours so that the location of the cell density is visualised (Herzenberg *et al*, 2006). In the analysis of the MitoTracker Red fluorescence in translocation cell lines the use of quantile contour plots could be utilised to determine if sub-populations of cells displayed reduced MitoTracker fluorescence within the overall population of fluorescing cells.

In terms of adopting the MitoTracker Red FACS experimental protocol, Further cell lines from t(1;11) family members could be added to the experimental run to increase sample size per experiment. This would be a means to get a more accurate estimation of the translocation cell line mitochondrial membrane potential, $\Delta\psi m$. Alternatively, the sample size of n=3 by genotype could be kept and a full biological replicate of the experiment could be performed, as a robust measure of experimental reproducibility (Lazic, 2010). This would entail either lymphoblastoid cell lines from a different n=3 of t(1;11) family members being used in experimentation or lymphoblastoid cell lines from the same individuals but different clones (Cumming *et al*, 2007). These experimental modifications are a response to the inconsistent data generated in the measurement of MitoTracker Red GMFI in translocation lymphoblastoid cell lines.

`

Chapter 6 - Functional enrichment analysis of t(1;11) gene expression microarray data

6.1 Introduction

A further means to investigate the high incidence of major mental illness in the t(1;11) pedigree (Blackwood *et al*, 2001) is to use pathway analysis to identify biological processes and functions impacted by changes in gene expression that arise as a result of the translocation. Presently no post-mortem brain tissue is available from t(1;11) carriers therefore all of the cDNAs assayed for this analysis are derived from t(1;11)-family derived-lymphoblastoid cell lines that have been transformed by the Epstein–Barr virus (EBV). This study was implemented by Merck Sharp & Dohme, using a proprietary in house Rosetta chip. Consequently, a limitation is that the raw data was not available for alignment of the results with public domain data as is possible with Illumina chips.

There are several ways by which the t(1;11) could influence gene transcription. Firstly, DISC1 is subject to haploinsufficiency due to the translocation (Millar *et al*, 2005b). This would reduce the levels of DISC1 available to interact with binding partners and likely cause disruption to pathways in which DISC1 had a role in transcription. DISC1 has been observed to interact with Activating Transcription Factor 4 (ATF4) and ATF5 (Morris *et al*, 2005), transcription factors that have roles in stress response (Ameri & Harris, 2008) and nervous system development (Greene *et al*, 2009), respectively. DISC1 localises with ATF4 in the nucleus and inhibits ATF4 transcriptional activity at basal levels of cAMP (Malavasi *et al*, 2012), whilst conversely augmenting the transcriptional repression of ATF4 at elevated levels of cAMP (Sawamura *et al*, 2005). PDE4D9 transcription is repressed by a DISC1 and ATF4 regulated transcriptional repression complex, which undergoes dynamic regulation by cAMP signaling (Soda *et al*, 2013). Here, haploinsufficiency of DISC1 could lead to increased levels of PDE4D9 following loss of transcriptional repression due to a reduction in DISC1 levels, leading to fewer DISC1/ATF4 complexes. In contrast to ATF4, little is known regarding DISC1/ATF5 functional interactions.

The binding of DISC1 to ATF4 and ATF5 represent downstream mechanisms of action affecting transcription, upstream mechanisms within pathways are also likely to occur. The knockdown of DISC1 has been demonstrated to result in the upregulation of GluN2A expression, mediated by increased PKA and CREB signaling Wei *et al.*, (2014). The authors propose that the expression of WT DISC1 modulates PDE4 signaling which acts to directly

`

reduce cellular levels of PKA, impinging on the downstream CREB signaling and subsequently downregulating the transcription of GluN2A. The knockdown of DISC1 by Wei *et al.,* (2014) could somewhat recapitulate an effect of haploinsufficiency of DISC, the interpretation being that half normal levels of DISC1 could lead to a partial upregulation of GluN2A. A further example of an upstream mechanism of gene expression regulation by DISC1, is GSK3β/DISC1 binding and the resulting inhibition of GSK3β (Mao *et al,* 2009). This promotes the stabilisation of β-catenin which translocates to the nucleus and participates in downstream gene activation via interaction with the T-cell factor/lymphoid enhancer factor (TCF/LEF) transcription factors. The haploinsufficiency of DISC1 may lead to greater levels of unbound GSK3β, which could phosphorylate β-catenin, targeting it for proteasomal degradation and so reducing the downstream activity of TCF/LEF mediated gene transcription.

Due to *DISC2* being a ncRNA and its antisense and parallel orientation to *DISC1* (Millar *et al,* 2000b) it has been proposed that this species may potentially function as a negative regulator of *DISC1* mRNA levels (Chubb *et al,* 2008; Millar *et al,* 2000b,). Following this rationale, as a consequence of the t(1;11), such negative regulation of *DISC1,* could be impinged upon by the haploinsufficiency of *DISC2*. However, given the paucity of data on *DISC2* it is difficult to predict what the functional effects of haploinsufficiency of *DISC2* would be. It may be the case that *DISC2* haploinsufficiency has a nominal overall effect. This is as it co-occurs against background of DISC1 haploinsufficiency and the half normal levels of each species may negate any detriment in function. Additionally, it is unknown if *DISC1FP1* as a ncRNA (Eykelenboom *et al,* 2012; Zhou *et al,* 2010; Zhou *et al,* 2008), has any roles in transcriptional regulation, although this remains a possibility.

DISC1/DISC1FP1 proteins could potentially impact upon gene transcription. This is assuming the chimeric transcripts are translated (Eykelenboom *et al,* 2012). The possibility then arises for aberrant protein-protein interactions to occur. The chimeric species could bind WT-DISC1 via the DISC1 self-interaction domain (Kamiya *et al,* 2005) or with DISC1 interactors directly. This may be detrimental to the function of pathways associated with transcription in which DISC1 participates. Furthermore, a small American pedigree has been identified in which single instances of schizophrenia and schizoaffective disorder co-occur with a 4bp frameshift mutation at the distal region of *DISC1* exon 12 (Sachs *et al,* 2005). This rare mutation is predicted to encode a truncated DISC1 species as a consequence of the frameshift introducing 9 abnormal aa's followed by a premature stop codon. Transcriptional analysis on forebrain neurons derived from iPSC's generated from the American pedigree and analysed using RNA-seq and RT-PCR, revealed large-scale gene dysregulation (Wen *et al,* 2014). The differentially

`

expressed genes were associated with synaptic fiction as well as major mental illness. Dysregulation also occurred to the transcript levels of multiple DISC1 interactors. The authors propose that the mutant species of DISC1 studied may induce transcriptisomal dysregulation as a common disease mechanism. The findings of Wen *et al.*, (2014) may be highlighting the effects of mechanisms action that impinge upon gene expression similar to those proposed above for the DISC/DISC1FP1 chimeras. Overall the study by Wen *et al.*, (2014) serves as an example that mutations to DISC1 can mediate alterations to transcription, which then brings to the fore the implications of endogenous DISC1/DISC1FP1 protein expression on transcription. However, further research is needed into the impact of mutant DISC1 species binding on transcription,

In this chapter two 'genes-of interest' (GOI) lists will be analysed by functional enrichment programs. The first list, referred to as the unfiltered list is derived from the genes showing differential expression with a fold change cut-off of +/- 1.3, significant at $p \leq 0.05$ (see methods). This is a commonly used threshold for asserting expression differences. The second GOI list referred to as the neuronally filtered list, is the unfiltered GOI list with non-neuronally expressed genes removed (see methods). This was performed to generate a GOI list that was more brain-like and less blood like. Regarding this decision, the benefits and caveats of using blood as a proxy or surrogate for post-mortem brain tissue in gene expression microarray analysis will be covered in greater depth in the following section 6.2 *The analysis of blood versus brain in gene expression microarray studies.*

In the interpretation of the t(1;11) lymphoblastoid cDNA microarray data, gene set analysis programs within the WEBGestalt suite of programs (Wang *et al*, 2013) will be used to analyse both the unfiltered and neuronally filtered GOI lists in parallel. The results of these analysis will be presented sequentially allowing for comparison between the results of these differing GOI lists. The programs used will include: 1) GOTree, to look at gene ontology (Zhang *et al*, 2004) 2) Pathway Commons analysis (Cerami *et al*, 2011), 3) KEGG Analysis (Kanehisa *et al*, 2008) and 4) Wikipathways Analysis (Pico *et al*, 2008) to look at pathway enrichment, 5) Disease Enrichment Analysis (Jourquin *et al*, 2012) to determine at the enrichment of particular disease states relating to the GOI lists 6) Cytogenetic Band Analysis to see if genes are enriched to specific chromosomal loci and 7) Transcription Factor Target Analysis to see if gene sets associated with specific transcription factor motifs are enriched. All of these programs use over representation analysis in the calculation of gene enrichment. This method detects the number of differentially expressed genes within a given pathway or category

`

(Khatri *et al*, 2012). The results of these analysis aimed to further the knowledge into the pathogenesis of the major mental illness that is seen in the t(1;11) pedigree.

6.2 The analysis of blood versus brain in gene expression microarray studies

Blood is frequently used as a proxy or surrogate for brain tissue in gene transcription studies of neuropsychiatric disorders such as schizophrenia, bipolar disorder and major depressive disorder. In contrast to the CNS, blood can be collected via non-invasive methods that are easy to implement (de Jong *et al*, 2012). Additionally blood samples can be drawn at different stages of illness and from large numbers of subjects. The collection of such blood samples can be carried out under standardised controlled conditions using replicable blood processing protocols alongside well regulated sample preservation methods resulting in the harvesting of higher quality blood mRNA than that from post-mortem brain tissue (Jasinska *et al*, 2009). In contrast the harvesting of brain tissue must take place from post-mortem brain collections. This severely limits the number of subjects per study. Likewise, the limited number of lymphoblastoid cell lines assayed in this study is a potential caveat. The use of brain tissues also introduces confounding factors, such as: post-mortem interval, the pH of brain tissue, the quality of mRNA extracted, the age of subjects, and the length of the agonal state, each of which can affect gene expression. (Lipska *et al*, 2006a).

The applicability of blood-based expression findings to the central nervous system (CNS) has been the subject of several studies. The correlation between transcripts from blood versus from brain tissue has been found to be weak (Cai *et al*, 2010) or moderate (Sullivan *et al*, 2006). The gene expression of putative schizophrenia candidate genes also shows variation. 24% of schizophrenia candidate genes are identified as having co-expression in peripheral blood mononuclear cells with cerebellum tissue (Rollins *et al*, 2010) whereas Sullivan *et al*., (2006) identifies a 50% co-expression with a separate set of schizophrenia candidate genes between whole blood and post-mortem brain tissue from multiple brain regions. Additionally Sullivan (2006) identified multiple similarities in gene ontology between whole blood and CNS tissues, this includes: transcription factor activity, apoptosis, G-protein coupled receptor activity, cytokine activity, DNA replication and kinase activity. The disparities in the estimates of the similarities between gene expression between blood and brain likely arise due to methodological differences between studies, such as array types, the brain regions that tissue was sampled from and the post-array data analysis methods used. It is apparent though from

`

such evidence that blood is not identical to brain but bears a degree of similarity to brain, which may make blood a useful tissue to use as a proxy or surrogate to brain. Furthermore, it is important to consider that when looking at between-group differences in gene expression, the differences observed may still be informative as to the pathophysiology of illness irrespective of whether the sample mRNA assayed originates from blood or from brain. This is relevant even if blood only has a limited degree of similarity to brain. Additionally, it is important to note that the brain is structured with heterogeneous regionalised variations in glial and neuronal populations and, therefore, to simply call tissue originating from the brain post-mortem "brain tissue" does not reflect the degree of variation present within the brain.

One factor that might contribute towards correlation in gene expression levels between the blood and the brain is that both tissues are affected by circulating factors such as neurotransmitters and hormones. For example, the levels of Brain-derived Neurotrophic Factor (BDNF) in the blood and in brain tissue are observed to be similar in several mammal species (Klein *et al*, 2011). Furthermore, leukocytes possess an array of hormone and neurotransmitter receptors and in turn also produce hormones and neurotransmitters that are also common to brain tissue for use in bi-directional communication in the immune response (Blalock & Smith, 2007).

This study measured gene expression in lymphoblastoid cell lines. In addition to the caveats that exist when comparing blood to brain, it is important to consider the effects of immortalisation of gene expression. Following transformation by the EBV, large gene expression differences are apparent between peripheral blood mononuclear cells and lymphoblastoid cell lines. However, Rollins *et al*, 2010 reported a 62% transcript commonality between the cell lines. Moreover, the effects of EBV transformation of lymphoblastoid cell lines on gene dysregulation appear to show little inter-subject variability and are specifically distributed throughout the genome. EBV transformation-induced changes in gene expression should have little effect on between-group comparisons, apart from when the effect of the transformation masks an illness-related expression difference.

`

6.3 Functional enrichment analysis of the t(1;11) gene expression microarray

6.3.1 Comparing gene number in GOI and reference lists

The initial, unfiltered microarray data mapped to 10,923 genes. After applying the criteria for differential expression (a fold change of +/- 1.3 and $p \leq 0.05$), 1,010 genes remained and compose the unfiltered GOI list. Therefore, for the unfiltered t(1;11) microarray data ~9.2% of the genes from the reference set are differentially expressed at the levels of the cut-offs. The reference list from the neuronally filtered GOI list contains 9462 genes and the neuronally filtered GOI list itself contains 889 genes. Therefore for the neuronally filtered data ~9.4% of the genes from the reference list are differentially expressed at the level the cut-offs. Additionally the neuronally filtered reference list contains ~13% fewer genes than the unfiltered reference list and the neuronally filtered GOI list contains ~12% fewer genes than the unfiltered GOI list.

6.3.2 Cytogenetic band analysis

Cytogenetic Band Analysis (http://bioinfo.vanderbilt.edu/webgestalt/analysis.php) was applied to the t(1;11) GOI lists. This analysis measures whether the GOI list is enriched for given chromosomal loci and aimed to exclude the possibility that loci other than the t(1;11) were responsible for mediating the differential expression changes observed. For the Cytogenic Band Analysis a significance level of $p<0.05$ was applied.

The cytogenetic band analysis of the dysregulated genes in both the unfiltered GOI list and the neuronally filtered GOI list, fails to detect significant gene enrichment to specific chromosome loci. Using cytogenetic band analysis to derive the top 10 chromosomal loci per list, the unfiltered GOI list data has an adjusted $p=0.60$ (see table 6.3A) while the neuronally filtered GOI list has an adjusted $p=0.42$ (see table 6.3B). These p-values correspond to all of the chromosomal loci analysed per top 10 analyses.

The results indicate no other significant loci are involved in the differential expression. However, it should be noted that this analysis is not sufficient to be able to exclude additional gene specific effects fixed by the t(1;11), such as the possibility that additional genes and SNPs in the vicinity of the der 1 and 11 loci may be inherited along with the t(1;11). Sullivan (2013) has speculated that a 'hitchhiking' effect analogous to this potential inherence mechanism may occur in the pathoetiology of the t(1;11). Furthermore, random effects that are significantly

`

partitioned between t(1;11) carriers and non-carriers are not able to be accounted for in this analysis. For example, background genetic variation present in a sub-set of t(1;11) carriers could modulate the phenotype of major mental illness by acting additively of synergistically with the pathophysiological effects of the t(1;11). This may in part account for the spectrum of major mental illness observed in the t(1;11) pedigree, in conjunction with the contribution of non-shared environmental effects.

Chromosome Position	Observed	Expected	Ratio	p-value
18q12	6	2.48	2.42	6.05E-01
10q11	6	2.48	2.42	6.05E-01
13q22	4	1.38	2.9	6.05E-01
5q	51	34.82	1.46	6.05E-01
14q21	6	2.57	2.33	6.05E-01
3p26	4	1.1	3.63	6.05E-01
12p13	12	6.71	1.79	6.05E-01
16q13	4	1.29	3.11	6.05E-01
5q33	6	2.66	2.25	6.05E-01
10q	39	26.82	1.45	6.05E-01

Table 6.3.A: Cytogenetic Band Analysis for the unfiltered GOI list. Top 10 most significant results displayed. Observed and expected are measures of the number of genes and ratio is the observed number of genes/expected number of genes.

`

Chromosome Position	Observed	Expected	Ratio	p-value
2q34	3	0.56	5.35	4.24E-01
5q	46	31.88	1.44	4.24E-01
3p26	4	1.03	3.89	4.24E-01
10q21	6	2.06	2.92	4.24E-01
10q11	6	1.78	3.38	4.24E-01
10q	35	23.19	1.51	4.24E-01
12p13	11	5.14	2.14	4.24E-01
8p11	7	2.8	2.5	4.55E-01
16q13	4	1.12	3.57	4.55E-01
14q21	6	2.34	2.57	4.55E-01

Table 6.3.B: Cytogenetic Band Analysis for the neuronally filtered GOI list. Top 10 most significant results displayed. Observed and expected are measures of the number of genes and ratio is the observed number of genes/expected number of genes.

6.3.3 GOTree Analysis

Gene ontology tree machine, GOTree, is a web based gene ontology analysis (GO) program. In GOTree, GO categories are arranged hierarchically with the GO annotation being highly specific and precisely defined relating to a given set of co-regulated genes. GOTree output comprises three different categories to describe data on these gene products: (1) *biological process* (2) *molecular function* and (3) *cellular component* (Zhang *et al*, 2004). (http://bioinfo.vanderbilt.edu/webgestalt/analysis.php). For the GOTree analysis a significance level of $p<0.05$ was applied.

The GOTree analysis highlights GO categories exclusively associated with the cell cycle. This is irrespective of whether the output is generated using the unfiltered or the neuronally filtered GOI lists. The GO categories in the GOTree output are primarily found in the categories of biological process and cellular component (see tables 6.3.C and 6.3.D). Figure 6.3.A displays the cell cycle phases in conjunction with the associated GO categories. It is clear from this diagram that M-phase has numerous GO categories whereas S-phase only has 3, interphase has 2, and G_2 has 3 shared transitional phases with M-phase. This would seem to suggest that differential gene expression in the t(1;11) microarray data results in the dysregulation of the cell cycle and predominantly within the M-phase. However, it is possible that within the GO annotation database, there is greater coverage of GO categories for M-phase as opposed to, for

`

example, interphase due to research bias. It may then be prudent to simply acknowledge that all of the phases of the cell cycle, bar G_1 show an enrichment in GO annotation.

The S-phase GO categories are solely concerned with DNA based processes, in line with S-phase being principally involved with DNA replication (Alberts *et al*, 2008). The M-Phase includes GO categories that are fundamental components of mitosis and cytokinesis. This includes multiple GO categories pertaining to the kinetochore, which is a centromericaly located macromolecular structure that acts as a hub to link microtubules to chromosomes. As such the kinetochore is consequently involved in force generation that segregates chromosomes during mitosis (Cheeseman, 2014). Strongly associated with the kinetochore is the Ndc80 complex, which also receives a GO annotation associated with M-phase. The Ndc 80 complex is involved in the anchoring of microtubules directly to the kinetochore (Wilson-Kubalek *et al*, 2008). A range of studies in both cultured cell lines and primary neurones identify DISC1 as being localised at the centrosome (Bradshaw *et al*, 2008; Kamiya *et al*, 2005; Kamiya *et al*, 2008; Miyoshi *et al*, 2004; Morris *et al*, 2003). In this GOTree analysis the centrosome appears as an enriched category.

GO Term	Observed	Expected	Ratio	p-value
cell cycle phase	136	64.01	2.12	2.31E-15
M phase	95	39.21	2.42	5.83E-14
cell cycle	183	102.17	1.79	5.83E-14
nuclear division	79	29.89	2.64	7.60E-14
mitosis	79	29.89	2.64	7.60E-14
mitotic cell cycle	126	60.93	2.07	7.86E-14
cell cycle process	150	78.23	1.92	7.86E-14
M phase of mitotic cell cycle	80	30.76	2.6	8.16E-14
organelle fission	79	31.62	2.5	1.30E-12
cell division	79	35.46	2.23	8.17E-10
microtubule-based process	66	29.12	2.27	2.36E-08
regulation of cell cycle process	70	32.58	2.15	7.16E-08
condensed chromosome	38	13.04	2.91	2.70E-07
chromosome segregation	35	11	2.98	3.49E-07
spindle	47	18.94	2.48	3.59E-07
cytoskeletal part	124	74.42	1.67	3.59E-07
condensed chromosome kinetochore	25	7.04	3.55	4.82E-07
microtubule cytoskeleton	105	60.62	1.73	4.82E-07
condensed chromosome, centromeric region	26	7.52	3.46	4.82E-07
mitotic prometaphase	26	7.5	3.47	1.31E-06

`

chromosome, centromeric region	35	12.94	2.7	1.52E-06
regulation of cell cycle	95	53.73	1.77	2.21E-06
regulation of G2/M transition of mitotic cell cycle	13	2.21	5.88	4.43E-06
sister chromatid segregation	19	4.61	4.12	4.99E-06
kinetochore	27	9.04	2.99	5.75E-06
microtubule cytoskeleton organization	47	20	2.29	6.16E-06
cytoskeleton	152	103.63	1.47	1.14E-05
mitotic sister chromatid segregation	18	4.42	4.07	1.28E-05
microtubule	46	21.7	2.12	2.21E-05
DNA replication	46	20.86	2.21	2.37E-05
spindle pole	23	7.9	2.91	5.81E-05
G2/M transition of mitotic cell cycle	29	10.76	2.69	6.20E-05
spindle organization	21	6.82	3.08	0.0002
cell cycle checkpoint	43	20.28	2.12	0.0002
regulation of mitotic cell cycle	48	23.64	2.03	0.0002
interphase	59	31.72	1.86	0.0002
regulation of cell cycle arrest	44	21.91	2.01	0.0005
chromosomal part	64	38.35	1.67	0.0008
regulation of microtubule cytoskeleton organization	17	5.29	3.22	0.0009
interphase of mitotic cell cycle	56	31.14	1.8	0.0009
DNA packaging	23	8.75	2.63	0.001
DNA metabolic process	95	61.99	1.53	0.001
cell cycle arrest	54	29.99	1.8	0.0011
microtubule motor activity	15	3.85	3.9	0.0011
condensin complex	5	0.57	8.76	0.0012
negative regulation of G2/M transition of mitotic cell cycle	7	1.06	6.62	0.0015
regulation of mitosis	19	6.73	2.82	0.0017
negative regulation of cell cycle	59	34.31	1.72	0.0017
regulation of nuclear division	19	6.73	2.82	0.0017
negative regulation of cell cycle process	21	7.88	2.66	0.0017
chromosome condensation	10	2.21	4.52	0.0017
condensed nuclear chromosome kinetochore	4	0.38	10.51	0.0022
condensed chromosome outer kinetochore	6	0.95	6.31	0.0025
DNA conformation change	27	11.92	2.27	0.0027
attachment of spindle microtubules to kinetochore	8	1.54	5.2	0.003
cytoskeleton organization	76	48.73	1.56	0.003
chromosome	70	45.68	1.53	0.0044
microtubule organizing center	58	36.16	1.6	0.0044
condensed nuclear chromosome, centromeric region	6	1.14	5.25	0.0083
non-membrane-bounded organelle	293	250.28	1.17	0.0093
intracellular non-membrane-bounded organelle	293	250.28	1.17	0.0093

`

cytoplasmic microtubule	8	2.19	3.66	0.0146
Ndc80 complex	3	0.29	10.51	0.0146
condensed nuclear chromosome outer kinetochore	3	0.29	10.51	0.0146
motor activity	18	6.57	2.74	0.0151
centrosome	45	28.36	1.59	0.0187
spindle microtubule	10	3.43	2.92	0.0224
midbody	15	6.76	2.22	0.0345
cytosol	196	164.25	1.19	0.036

Table 6.3.C: GOTree Analysis of the unfiltered GOI list. Observed and expected are measures of the number of genes and ratio is the observed number of genes/expected number of genes. Biological process (Black), Cellular component (Red), Molecular function (Green).

GO Term	Observed	Expected	Ratio	p-value
cell cycle phase	131	60.78	2.16	2.06E-15
M phase	91	37.18	2.45	8.23E-14
mitotic cell cycle	123	58.37	2.11	8.23E-14
cell cycle process	144	74.07	1.94	9.63E-14
mitosis	77	28.99	2.66	9.63E-14
M phase of mitotic cell cycle	78	29.67	2.63	9.63E-14
nuclear division	77	28.99	2.66	9.63E-14
cell cycle	173	96.51	1.79	1.08E-13
organelle fission	77	30.63	2.51	1.71E-12
cell division	76	34.19	2.22	2.08E-09
microtubule-based process	62	27.45	2.26	9.28E-08
regulation of cell cycle process	66	30.82	2.14	2.24E-07
chromosome segregation	35	11.56	3.03	2.24E-07
condensed chromosome	37	12.6	2.94	3.37E-07
spindle	45	18.04	2.49	8.26E-07
cytoskeletal part	115	69.3	1.66	1.37E-06
condensed chromosome, centromeric region	25	7.25	3.45	1.37E-06
microtubule cytoskeleton organization	47	19.65	2.39	1.58E-06
condensed chromosome kinetochore	24	6.87	3.49	1.59E-06
sister chromatid segregation	19	4.43	4.29	2.42E-06
mitotic prometaphase	25	7.42	3.37	4.07E-06
regulation of G2/M transition of mitotic cell cycle	13	2.22	5.87	4.13E-06
regulation of cell cycle	90	50.95	1.77	4.22E-06
mitotic sister chromatid segregation	18	4.24	4.25	5.56E-06
microtubule cytoskeleton	96	56.89	1.69	6.42E-06

`

chromosome, centromeric region	33	12.6	2.62	8.18E-06
G2/M transition of mitotic cell cycle	29	10.5	2.76	3.45E-05
kinetochore	25	8.78	2.85	3.74E-05
cytoskeleton	140	95.93	1.46	3.74E-05
spindle pole	23	7.64	3.01	3.74E-05
spindle organization	21	6.45	3.25	8.06E-05
interphase	58	30.34	1.91	8.97E-05
DNA replication	42	19.55	2.15	1.00E-04
regulation of mitotic cell cycle	46	22.35	2.06	1.00E-04
cell cycle checkpoint	41	19.46	2.11	3.00E-04
interphase of mitotic cell cycle	55	29.76	1.85	4.00E-04
microtubule	41	20.52	2	0.0004
DNA packaging	23	8.48	2.71	6.00E-04
regulation of microtubule cytoskeleton organization	17	5.2	3.27	7.00E-04
regulation of cell cycle arrest	42	21	2	8.00E-04
chromosomal part	61	36.27	1.68	0.0009
cell cycle arrest	52	28.7	1.81	1.20E-03
condensin complex	5	0.57	8.73	0.0012
negative regulation of G2/M transition of mitotic cell cycle	7	1.06	6.61	1.60E-03
negative regulation of cell cycle	57	32.75	1.74	1.60E-03
chromosome condensation	10	2.22	4.51	0.0019
attachment of spindle microtubules to kinetochore	8	1.44	5.54	0.002
regulation of mitosis	18	6.26	2.88	0.002
regulation of nuclear division	18	6.26	2.88	0.002
condensed nuclear chromosome kinetochore	4	0.38	10.48	0.0022
condensed chromosome outer kinetochore	6	0.95	6.29	0.0024
cytoskeleton organization	73	46.33	1.58	0.0029
regulation of microtubule-based process	18	6.45	2.79	0.0029
mitotic spindle organization	11	2.79	3.94	0.0029
DNA conformation change	26	11.37	2.29	0.0029
chromosome	67	43.34	1.55	0.0043
microtubule organizing center	55	34.17	1.61	0.0043
microtubule motor activity	13	3.4	3.83	0.0066
intracellular non-membrane-bounded organelle	278	235.58	1.18	0.0073
non-membrane-bounded organelle	278	235.58	1.18	0.0073
condensed nuclear chromosome, centromeric region	6	1.15	5.24	0.0073
centrosome	44	26.82	1.64	0.0105
Ndc80 complex	3	0.29	10.48	0.0144
condensed nuclear chromosome outer kinetochore	3	0.29	10.48	0.0144
spindle microtubule	10	3.44	2.91	0.0229

`

midbody	15	6.49	2.31	0.0235
motor activity	16	5.85	2.74	0.0265
cytoplasmic microtubule	7	2.1	3.33	0.0466

Table 6.3.D: GOTree Analysis of the neuronally filtered GOI list. Observed and expected are measures of the number of genes and ratio is the observed number of genes/expected number of genes. Biological process (Black), Cellular component (Red), Molecular function (Green).

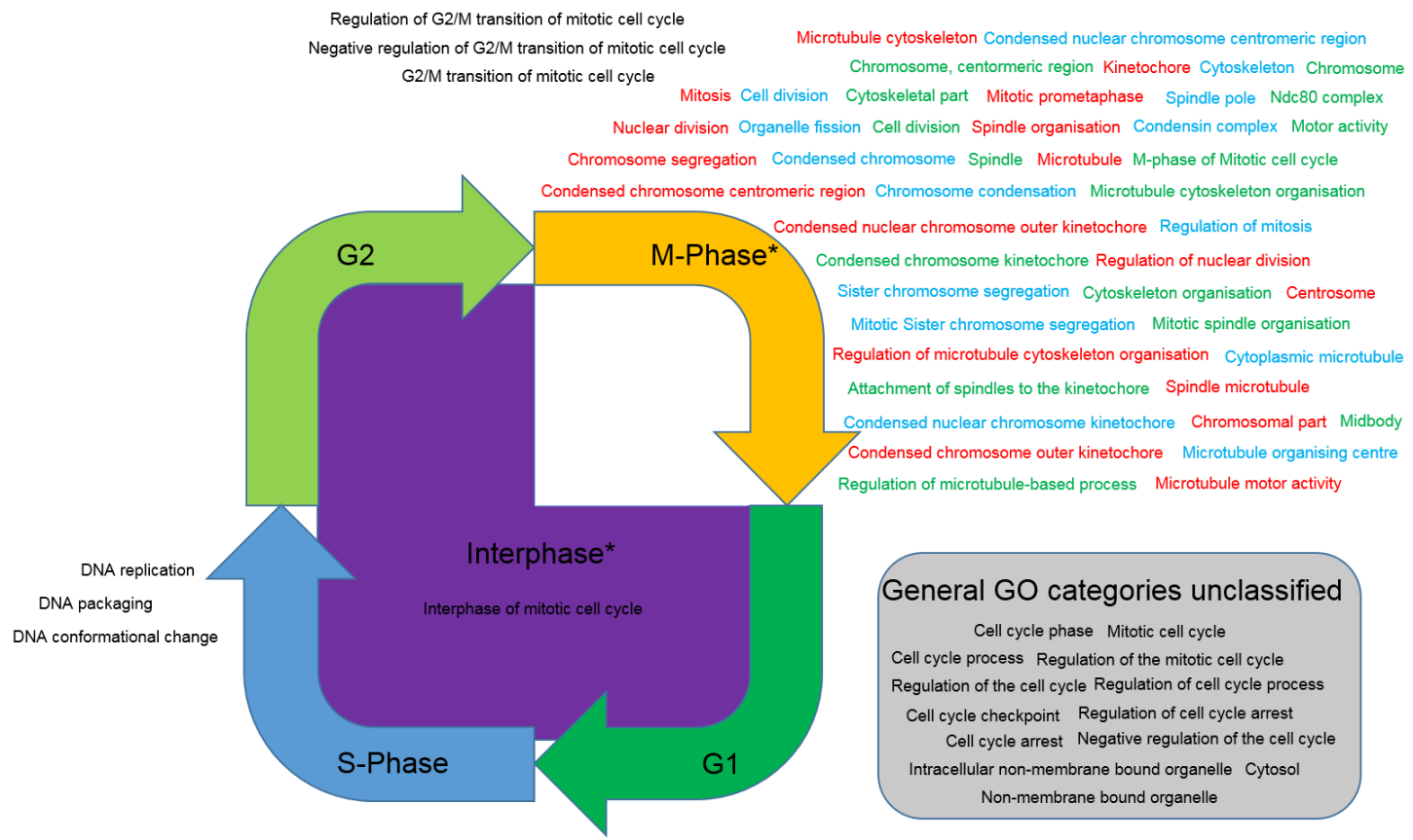

Figure 6.3.A: GO categories from the GOTree analysis of the t(1;11) microarray data and their relation to the cell cycle. Asterisk indicates cell cycle component is also a GO annotation. GO annotations associated with cell cycle phases using Alberts *et al*., (2008). To ease identification GO categories associated with M-Phase have been coloured red, blue and green.

`

The DISC1 interactome dataset is derived from the findings of yeast-two hybrid screens to identify DISC1 binding partners. The specific molecular and cellular properties of novel DISC1 interactors identified in the DISC1 interactome dataset has been characterised by GO (Camargo *et al*, 2006). GO analysis of the members of the DISC1 interactome shares common features with the analysis carried out on differentially expressed genes identified in carriers of the t(1;11) translocation. For biological processes this includes: microtubule-based process, mitosis, M-phase of the mitotic cell cycle, nuclear division, M-phase, mitotic cell cycle, chromosome segregation, sister chromatid cohesion, mitotic sister chromatid segregation and regulation of mitosis. The cellular component categories shared are: kinetochore, spindle pole, microtubule, spindle microtubule, chromosome, centrosome, condensed chromosome. The common molecular function categories are: motor activity and molecular motor activity (Camargo *et al*, 2006). Therefore from the DISC1 interactome dataset, DISC1 can be linked to proteins that have roles in cell cycle dynamics, in particular M-phase. The concordance between the DISC1 interactome dataset and the t(1;11) microarray data suggests that the molecular processes DISC1 interactors may be involved in (Camargo *et al*, 2006) are in turn dysregulated in t(1;11) lymphoblastoid cell lines. It is possible that the interactions of DISC1 with binding partners identified in the interactome dataset is impaired due to haploinsufficiency within the t(1;11)-family derived lymphoblastoid cell lines (Millar *et al*, 2005b) and that this is where the similarity in GO results originates from.

There was very little difference between the GO categories highlighted using either the unfiltered or neuronally filtered GOI lists. The differences that occur between the two GOI lists in the GOTree analysis of the t(1;11) microarray data come from the p-value ranking of the GO categories and even then, there are marked similarities in the p-values of the highly significant GO categories.

6.3.4 Pathway Commons Analysis

Pathway Commons is a web based pathway analysis program that uses multiple publicly available pathway databases (Cerami *et al*, 2011) (http://www.pathwaycommons.org/about/ , http://bioinfo.vanderbilt.edu/webgestalt/analysis.php). For the Pathway Commons analysis a significance level of $p<0.05$ was applied.

The Pathway Commons analysis of the t(1;11) microarray data is both supportive and yet different to the GOTree analysis of the data set. In the Pathway Commons data set, like the GOTree ontology, mitosis features strongly in the pathways generated, however the Pathway

`

Commons analysis is broader in the scope of the pathways produced, with mitosis being a fraction of the cell cycle pathways detected and additionally non-cell cycle pathways are highlighted, that are primarily immunological as well as pathways that may be said to be auxiliary to the cell cycle (see tables 6.3.E and 6.3.F). In line with the GOTree analysis there was little difference in the analysis of the unfiltered GOI list data and analysis using the neuronally filtered GOI data.

In summary, the mitotic cell cycle is the most significant pathway by three orders of magnitude. Mitosis is also highlighted as within M-phase, Mitotic M-M/G_1 phases, Mitotic prometaphase, G_2/M checkpoints, the G_2/M transition, Mitotic G_2-G_2/M phases, Mitotic G_1-G_1/S phases, G_2/M DNA replication checkpoint and the mitotic spindle checkpoint pathways are detected. S-phase is present by way of the DNA replication pathway, which is the fourth most significant result and by G_1/S-specific transcription. G_1 phase is represented in the data by pathways specifying transitions in the cell cycle. Mitotic M-M/G_1 phases, G_1/S-specific transcription, G_0 and early G_1, Mitotic G_1-G_1/S phases. G_2 phase is represented in the data by checkpoints and transition phases. G_2/M checkpoints, G_2/M DNA damage checkpoints, G_2M transition. Additionally, cell cycle checkpoints appears as a pathway in its own right.

Pathway	Observed	Expected	Ratio	p-value
Cell Cycle, Mitotic	70	25.54	2.74	1.13E-12
Polo-like kinase signalling events in the cell cycle	32	8.54	3.75	4.67E-09
PLK1 signalling events	31	8.27	3.75	6.27E-09
DNA Replication	55	21.68	2.54	8.59E-09
M Phase	39	12.77	3.05	1.41E-08
Mitotic M-M/G1 phases	49	20.03	2.45	2.42E-07
Mitotic Prometaphase	27	8.18	3.3	1.20E-06
Signalling by Aurora kinases	25	7.62	3.28	4.23E-06
FOXM1 transcription factor network	14	2.85	4.92	1.18E-05
G2/M Checkpoints	16	3.77	4.25	1.65E-05
Aurora B signalling	14	3.03	4.62	2.50E-05
Cyclin B2 mediated events	6	0.55	10.89	3.16E-05
G1/S-Specific Transcription	8	1.1	7.26	8.62E-05
Chromosome Maintenance	17	4.87	3.49	1.00E-04
Kinesins	9	1.56	5.76	2.00E-04
G0 and Early G1	9	1.65	5.44	4.00E-04
Activation of ATR in response to replication stress	13	3.31	3.93	4.00E-04
G2/M DNA damage checkpoint	11	2.48	4.44	4.00E-04

`

Cyclin A/B1 associated events during G2/M transition	7	1.01	6.93	4.00E-04
E2F mediated regulation of DNA replication	10	2.2	4.54	8.00E-04
Cell Cycle Checkpoints	23	9.92	2.32	3.00E-03
G2/M Transition	18	7.26	2.48	5.80E-03
Nucleosome assembly	8	1.93	4.15	7.10E-03
ATM pathway	40	22.69	1.76	7.10E-03
Chk1/Chk2(CDS1) mediated inactivation of Cyclin B:CDK1 complex	4	0.46	8.71	7.10E-03
Aurora A signalling	14	5.05	2.77	7.10E-03
Deposition of New CENPA-containing Nucleosomes at the Centromere	8	1.93	4.15	7.10E-03
E2F transcription factor network	14	5.14	2.72	8.80E-03
Mitotic G2-G2/M phases	18	7.53	2.39	8.80E-03
Mitotic G1-G1/S phases	23	11.3	2.04	1.45E-02
Phosphorylation of Emi1	7	1.65	4.23	1.45E-02
IL-12-mediated signalling events	17	7.35	2.31	1.60E-02
Fanconi anaemia pathway	11	4.04	2.72	0.033
Extension of Telomeres	8	2.48	3.23	0.0402
CD40/CD40L signalling	12	4.78	2.51	0.0402
Telomere Maintenance	9	3.03	2.97	0.0409
Telomere C-strand (Lagging Strand) Synthesis	7	2.02	3.46	0.0455
Reelin signalling pathway	7	2.02	3.46	0.0455
G2/M DNA replication checkpoint	3	0.37	8.16	0.0476
Mitotic Spindle Checkpoint	6	1.56	3.84	0.048

Table 6.3.E: Pathway Commons Analysis for the unfiltered GOI list. Observed and expected are measures of the number of genes and ratio is the observed number of genes/expected number of genes.

Pathway	Observed	Expected	Ratio	p-value
Cell Cycle, Mitotic	69	25.24	2.73	1.64E-12
Polo-like kinase signalling events in the cell cycle	32	8.41	3.8	2.55E-09
PLK1 signalling events	31	8.13	3.81	3.40E-09
DNA Replication	54	21.32	2.53	1.17E-08
M Phase	38	12.62	3.01	3.42E-08
Mitotic M-M/G1 phases	48	19.73	2.43	3.81E-07
Signalling by Aurora kinases	25	7.57	3.3	3.83E-06
Mitotic Prometaphase	26	8.23	3.16	4.88E-06
FOXM1 transcription factor network	14	2.9	4.83	1.36E-05
G2/M Checkpoints	16	3.74	4.28	1.36E-05

`

Aurora B signalling	14	3.09	4.54	3.02E-05
Cyclin B2 mediated events	6	0.56	10.7	3.45E-05
G1/S-Specific Transcription	8	1.12	7.13	9.63E-05
Activation of ATR in response to replication stress	13	3.27	3.97	4.00E-04
Chromosome Maintenance	16	4.77	3.36	4.00E-04
G2/M DNA damage checkpoint	11	2.52	4.36	5.00E-04
Cyclin A/B1 associated events during G2/M transition	7	1.03	6.81	5.00E-04
G0 and Early G1	9	1.68	5.35	5.00E-04
E2F mediated regulation of DNA replication	10	2.24	4.46	9.00E-04
Kinesins	8	1.5	5.35	1.20E-03
Cell Cycle Checkpoints	22	9.72	2.26	5.70E-03
G2/M Transition	18	7.2	2.5	5.70E-03
Aurora A signalling	14	4.96	2.83	7.90E-03
Mitotic G2-G2/M phases	18	7.48	2.41	7.90E-03
E2F transcription factor network	14	5.14	2.72	9.00E-03
Nucleosome assembly	8	1.96	4.07	9.00E-03
Chk1/Chk2(Cds1) mediated inactivation of Cyclin B:Cdk1 complex	4	0.47	8.56	9.00E-03
Deposition of New CENPA-containing Nucleosomes at the Centromere	8	1.96	4.07	9.00E-03
Mitotic G1-G1/S phases	23	11.31	2.03	1.52E-02
IL-12-mediated signalling events	16	6.73	2.38	1.57E-02
ATM pathway	38	22.44	1.69	1.57E-02
Phosphorylation of Emi1	7	1.68	4.16	1.57E-02
CD40/CD40L signalling	12	4.58	2.62	0.0286
Extension of Telomeres	8	2.43	3.29	0.0352
Telomere C-strand (Lagging Strand) Synthesis	7	1.96	3.57	0.0395
TCR signalling in naïve CD8+ T cells	16	7.57	2.11	0.0497
G2/M DNA replication checkpoint	3	0.37	8.02	0.0497
Reelin signalling pathway	7	2.06	3.4	0.0497

Table 6.3.F: Pathway Commons Analysis for the neuronally filtered GOI list. Observed and expected are measures of the number of genes and ratio is the observed number of genes/expected number of genes.

`

As well as highlighting pathways that detail the four cell cycle phases, the Pathway Commons analysis brings up pathways that occur within the cell cycle. This data does not appear in the GOTree ontology. Polo-like kinase signalling events in the cell cycle and PLK1 signalling events are the second and third most significant pathways in the analysis. Polo-like kinase/PLK1 signalling is involved in the maturation and separation of the centrosomes and importantly, in the regulation of the assembly of functional bipolar spindles. These processes take place from G_2 to M-phase respectively. Additionally Polo-like Kinase 1 (PLK1) has a role in the recovery of the cell following DNA damage being detected at the G_2 checkpoint and also is involved in the signalling for cohesin removal from sister chromatids (Van De Weerdt & Medema, 2006).

Signalling by Aurora kinases and Aurora A and Aurora B signalling also appears in the Pathway Commons analysis. The Aurora kinases contribute to the cell cycle to aid the dynamics of mitosis. Aurora A kinase functions to aid centrosome maturation from G_2 to M-phase and to control the formation of the bipolar spindle apparatus. Aurora A is required from the correct localisation and function of other proteins in the development of the spindle. Aurora B kinase has a variety of cell cycle roles including: sister chromatid cohesion and the destabilisation of incorrect microtubule attachments to the spindle pole and the disassembly of the mitotic spindle in telophase (Vader & Lens, 2008).

The activation of ATR in response to stress appears in the Pathway Commons analysis as does the ATM pathway. Ataxia-telangiectasia Mutated (ATM) and ATM-and Rad3-Related (ATR) are the principle transducing kinases within the DNA damage response (DDR) signalling network. The DDR is associated with cell cycle checkpoints and functions to maintain genomic viability in DNA damaged cells or destroy cells with highly damaged genomes by apoptosis. The actions of ATM focus on double stranded DNA breaks, whereas ATR has a wider scope of function, also delaying with DNA lesions that may prevent replication (Marechal & Zou, 2013). Additionally in the Pathway Commons analysis Chk1/Chk2 (CDS1) mediated inactivation of Cyclin B: CDK1 complex features. The effector kinases of ATM is Checkpoint Kinase 2 (Chk2) and for ATR is Chk1. All of these kinases within the DDR are active at the DNA damage checkpoints within the cell cycle at G_1, G_2 and S-phase (Kastan & Bartek, 2004).

The phosphorylation of Emi1 is a highly specific pathway that is enriched in the Pathway Commons analysis. Early Mitotic Inhibitor 1 (Emi1) also known as FBX05 is a protein responsible for the temporal regulation of the anaphase-promoting complex/cyclosome

`

(APC/C) during interphase (Di Fiore & Pines, 2008). The phosphorylation on Emi1 by PLK1 results in the degradation of Emi1 (Hansen *et al*, 2004; Moshe *et al*, 2004).

Transcription factors appear in the Pathway Commons analysis. Forkhead Box M1 (FOXM1) protein is a transcription factor that is required for entry into G_1, G_2 and mitosis (Costa, 2005). FOXM1 -/- mice show a reduction in PLK1 and Aurora B kinases. This indicates FOXM1 expression is required for the expression of these cell cycle proteins (Krupczak-Hollis *et al*, 2004).

The E2F transcription factor network also appears in the Pathway Commons analysis as does E2F mediated regulation of DNA replication. The E2F family of transcription factors are involved in the regulation of the cell cycle. Sub-groups of the E2F family have roles in the progression through the cell cycle, cell cycle exit and differentiation, and transcriptional repression, respectively (Attwooll *et al*, 2004). Interestingly the E2F transcription factors E2F Transcription Factor 1 (E2F1) and E2F4 appear as the principle transcription factor bindings sites highlighted in the Transcription Factor Target Analysis.

In the Pathway Commons analysis, pathways that are primarily associated with the immune system also appear. Interlukin-12 (IL-12)-mediated signalling events is present. IL-12 is secreted by dendritic cells and matures naive T-cells into Th1 cells as part of the adaptive immune response (Macatonia *et al*, 1995). Within the immune response IL-12 signalling can also modify the function of other immune cell types such as enhancing the cytotoxic abilities of natural killer cells and cytotoxic T lymphocytes as well as bringing about the production of the cytokine INF-$^{\gamma}$ (Trinchieri, 2003).

CD40/CD40L signalling is listed in the Pathway Commons analysis. Cluster of Differentiation 40 (CD40) and Cluster of Differentiation 40 Ligand (CD40L) are respectively, a receptor and ligand that are frequently associated with the adaptive immune response although are present in a variety of cell types. CD40 and CD40L function in a co-stimulatory capacity often secondary to other receptor based signalling mechanisms and are important in the activation of naive T cells, B-cells and macrophages (Schönbeck & Libby, 2001).

Interestingly four pathways appear on the Pathway Commons analysis that have been researched as part of investigations into the pathophysiology of major mental illness. Kinesins are motor proteins that facilitate anterograde transport along microtubules and are important in both intracellular transport (Hirokawa *et al*, 2009) and within spindle dynamics during mitosis (Wittmann *et al*, 2001). DISC1 has been observed to interact directly with Kinisin-1

`

(KIF5A), whereupon DISC functions axonally as a cargo-receptor for the localisation of the cargo complex NDEL/LIS/14-3-3ε (Taya *et al*, 2007). Additionally, in mitochondrial fractionations, the DISC1 disease associated structural variant 37W (R37W) (Song *et al*, 2008; Thomson *et al*, 2014) has been observed to have a two-fold greater association to kinesin within than WT-DISC1 (Ogawa *et al*, 2014).

Reelin is a glycoprotein with a multifunctional role in brain development. During embryonic development reelin has a role in neuronal migration (D'Arcangelo, 2014). Postnatally reelin is involved in the development of apical dendrites and dendritic spines and in adulthood reelin functions to modulate synaptic plasticity with reelin enhancing long term potentiation (D'Arcangelo, 2014). Reelin has been associated with a number of neurodevelopmental diseases including schizophrenia, bipolar disorder, major depressive disorder and autism as well as with neurodegeneration via Alzheimer 's disease (Folsom & Fatemi, 2013). For example, reelin levels have been observed to be reduced within the PFC in post-mortem brain studies from patients with schizophrenia and bipolar disorder (Guidotti *et al*, 2000), while the serum levels of reelin isoforms in the blood of patients with schizophrenia, bipolar disorder and major depressive disorder is markedly altered in isoform composition compared to controls (Fatemi *et al*, 2001). There is a connection between reelin signalling and DISC1. An epistatic interaction has been identified between the reelin SNP rs580884 and the DISC1 SNP rs3738401 in a neurogenomics study focusing on using an MRI derived intermediate phenotype of schizophrenia to identify gene interactions. The epistasis is associated with a reduction in cerebral tissue and with an increase in ventricular brain ratio (Andreasen *et al*, 2011). It is possible that the reelin pathway dysregulation in the t(1;11) microarray data set is highlighting another means to contribute to the high level of major mental illness seen in the t(1;11) pedigree. However, it should be heeded that the p-value for this finding is just significant at $p<0.05$ at $p=0.0455$ and this pathway is several orders of significance less than the bulk of the cell cycle focussed results.

Fanconi Anaemia is an autosomal recessive or X-linked disorder. Sufferers of this disease present a wide clinical phenotype due to the accumulation of spontaneous DNA damage arising from DNA interstrand crosslinking. Bone marrow failure is central to the disease along with congenital abnormalities and cancer is frequently seen. As such the Fanconi Anaemia pathway is proposed to be a means of maintaining genomic stability with research into the pathway encompassing amongst others, the fields of DNA repair, oncogenesis and the ubiquitination of protein (Moldovan & D'Andrea, 2009). The t(1;11) family do not appear to have the symptoms of Fanconi Anaemia however the presence of this disease pathway in the

`

t(1;11) microarray analysis may simply highlight an enrichment of genes within the canonical Fanconi Anaemia pathway. Mutations is the gene FANCD2/FANCI-Associated Nuclease 1 (FAN1) which is part of the Fanconi Anaemia pathway is associated with both schizophrenia and autism (Ionita-Laza *et al*, 2014). It is hypothesised that as FAN1 is involved in DNA repair the mutations may cause pathophysiological abnormalities by mediating aberrant DNA repair.

In addition to the pathways listed above telomere functions also appear as a pathway within Pathway Commons analysis. Regarding the cell cycle, the passage of a cell through repeated cell cycles increases telomere length (Marcand *et al*, 2000). The pathway data may therefore be highlighting gene enrichment to telomere pathways arising from changes to telomere maintenance due to an overall cell cycle disruption in the t(1;11) lymphoblastoid cell lines. Furthermore, the shortening of telomeres has been associated with depression (Hartmann *et al*, 2010; Wikgren *et al*, 2012).

6.3.5 KEGG Analysis

KEGG pathway analysis is a web based pathway analysis program whereby the pathway maps are annotated from the databases of the Kyoto Encyclopaedia of Genes and Genomes (Kanehisa *et al*, 2008). (http://www.genome.jp/kegg/ ,http://bioinfo.vanderbilt.edu/webgestalt/analysis.php). For the KEGG pathway analysis a significance level of $p<0.05$ was applied.

In the KEGG analysis the cell cycle is the most significantly enriched pathway for both of the GOI lists analysed (see tables 6.3.G and 6.3.H). The second most enriched pathway is progesterone-mediated oocyte maturation, this pathway maps gene dysregulation downstream of progesterone signalling extracellularly and includes both signal transduction and the MAPK signalling pathways. The progesterone-mediated oocyte maturation pathway is predominantly upstream of the cell cycle and completely upstream of meiosis I and II. As such the enrichment of the progesterone modulated oocyte pathway can be seen as a precursor to oocyte maturation that includes cell cycle components. If taken superficially as an enrichment of progesterone mediated signalling the progesterone-mediated oocyte maturation pathway may be associated with major mental illness. Progesterone treatment has been observed to increase both the levels of BDNF protein and mRNA (Kaur *et al*, 2007). In sufferers of schizophrenia the serum levels of BDNF commonly show sexual dimorphism, however as to which sex has the higher serum level depends on the experimental methodologies and selection criteria used (Jindal *et al*, 2010; Xiu *et al*, 2009). It is suggested that the variation in serum BDNF levels seen in

`

schizophrenia is partially dependent on sex steroid hormones such as progesterone (Hill, 2012).

The third most enriched pathway, oocyte meiosis, maps all of the meiotic cell cycle as well as condensed aspects of progesterone mediated oocyte maturation. As such, within oocyte meiosis prophase I occurs followed by germinal vesicle breakdown, meiosis I, interkinesis and meiosis II. Each of these steps in meiosis includes genes that are dysregulated. The pathway enrichment of oocyte meiosis can be taken as further evidence of cell cycle dysregulation within the differentially expressed genes from the t(1;11) lymphoblastoid cell lines of the original unfiltered and neuronally filtered GOI lists.

In the KEGG analysis the only difference between the GOI lists was the order of magnitude of the significance of the pathway enrichment. Both the unfiltered GOI list and the neuronally filtered GOI list analysis brought up the same 3 enriched pathways.

KEGG Pathway	Observed	Expected	Ratio	p-value
Cell cycle	25	9.46	2.64	7.00E-04
Progesterone-mediated oocyte maturation	18	6.25	2.88	2.10E-03
Oocyte meiosis	18	7.26	2.48	1.01E-02

Table 6.3.G: KEGG Analysis for the unfiltered GOI list. Observed and expected are measures of the number of genes and ratio is the observed number of genes/expected number of genes.

KEGG Pathway	Observed	Expected	Ratio	p-value
Cell cycle	24	9.44	2.54	2.10E-03
Progesterone-mediated oocyte maturation	17	6.08	2.8	5.10E-03
Oocyte meiosis	17	7.11	2.39	2.52E-02

Table 6.3.H: KEGG Analysis for the neuronally filtered GOI list. Observed and expected are measures of the number of genes and ratio is the observed number of genes/expected number of genes.

`

6.3.6 Wikipathways Analysis

Wikipathways is a web based pathways analysis program whereby the curation of pathway data is mediated by the community (Pico *et al*, 2008). (http://bioinfo.vanderbilt.edu/webgestalt/analysis.php,http://www.wikipathways.org/index.php/WikiPathways). In the Wikipathways analysis a significance level of $p<0.05$ was applied.

The pathway enrichment in the Wikipathways analysis of Cell cycle and DNA replication (see tables 6.3.I and 6.3.J) is in agreement with results from GOTree, KEGG pathways analysis and the Pathway Commons analysis. The enrichment of the integrated Cancer pathway may be a by-product of the overall enrichment of cell cycle data within this analysis, given that the cell cycle and cancer are virtually synonymous. Such a pathway enrichment need not necessarily suggest that the t(1;11) pedigree have an increased susceptibility to cancer following this result, rather that the differentially expressed data pertaining to the cell cycle is dysregulated to a sufficient degree to produce this enrichment.

The use of the different GOI lists in this analysis produces little difference in terms of final pathway enrichment. The analysis of the neuronal filtered GOI list over the original unfiltered GOI list merely produces a difference in the rankings of the enriched pathways.

Wikipathway	Observed	Expected	Ratio	p-value
Cell cycle	22	8.82	2.49	5.50E-03
DNA Replication	12	3.86	3.11	1.89E-02
Integrated Cancer pathway	3	0.28	10.89	3.36E-02

Table 6.3.I: Wikipathways Analysis for the unfiltered GOI list. Observed and expected are measures of the number of genes and ratio is the observed number of genes/expected number of genes.

`

Wikipathway	Observed	Expected	Ratio	p-value
DNA Replication	12	3.74	3.21	1.25E-02
Cell cycle	21	8.7	2.42	1.25E-02
Integrated Cancer pathway	3	0.28	10.7	3.33E-02

Table 6.3.J: Wikipathways Analysis for the neuronally filtered GOI list. Observed and expected are measures of the number of genes and ratio is the observed number of genes/expected number of genes.

6.3.7 Transcription Factor Target Analysis

To see if the dysregulated genes from the t(1;11) microarray data were targeted by specific transcription factors, Transcription Factor Target Analysis was performed (http://bioinfo.vanderbilt.edu/webgestalt/analysis.php). The gene sets for Transcription Factor Target Analysis are curated by MSigDB (Liberzon *et al*, 2011) (http://www.broadinstitute.org/gsea/msigdb/genesets.jsp?collection=TFT). For the Transcription Factor Target Analysis a cut-off of $p<0.05$ was applied.

The transcription factor gene sets that are identified are targeted by either the E2F1 transcription factor or the E2F1 and E2F4 transcription factors in conjunction with a dimerization partner or refer to a transcription factor motif for which a specific transcription has yet to be identified (see tables 6.3.K and 6.3L)

The dysregulated genes in the gene sets V$E2F1_Q6 and V$E2F1_Q3, have a promoter region between 2kb downstream or upstream of the transcription start site encoding a TTTSGCGS motif and NKTSSCGC motif, respectively and are both targets for E2F1.

In the gene sets V$E2F1DP2_01 and V$E2F1DP1_01 the dysregulated genes highlighted have a promoter region between 2kb downstream or upstream of the transcription start site encoding both TTTSSCGC and TTTCSCGC motifs. These dysregulated genes are targeted by E2F1 transcription factor in a heterodimer along with the transcription factors E2F Dimerization Partner 2 (TFDP2) and E2F Dimerization Partner 1 (TFDP1), respectively. Likewise the gene sets V$E2F4DP1_01 and V$E2F4DP2_01 have respective motifs of TTTSGCGC and TTTCSCGC. The dysregulated genes in these gene sets are targeted by E2F4 heterodimer containing either TFDP1 or TFDP2, respectively, that interacts with the tumour suppressor's p107 and p130.

`

Transcription Factor	Transcription Factor Gene Set	Observed	Expected	Ratio	p-value
E2F1	hsa_V$E2F1_Q6	34	16.54	2.06	2.15E-02
E2F1	hsa_V$E2F1_Q3	31	16.26	1.91	2.24E-02
E2F1 & TFDP2	hsa_V$E2F1DP2_01	31	15.89	1.95	2.24E-02
Unknown	hsa_V$E2F_Q6	31	16.17	1.92	2.24E-02
E2F4 p107/p130 & TFDP1	hsa_V$E2F4DP1_01	31	16.17	1.92	2.24E-02
E2F1 & TFDP1	hsa_V$E2F1DP1_01	31	15.89	1.95	2.24E-02
Unknown	hsa_V$E2F_02	31	15.98	1.94	2.24E-02
E2F4 p107/p130 & TFDP2	hsa_V$E2F4DP2_01	31	15.89	1.95	2.24E-02
Unknown	hsa_V$E2F_Q4	31	16.44	1.89	2.65E-02
Unknown	hsa_GATTGGY_V$NFY_Q6_01	99	72.75	1.36	4.78E-02

Table 6.3.K: Transcription Factor Target Analysis for the unfiltered GOI list. Observed and expected are measures of the number of genes and ratio is the observed number of genes/expected number of genes.

The gene sets V$E2F_Q6, V$E2F_02, V$E2F_Q4 and GATTGGY_V$NFY_Q6_01 again target the dysregulated genes promoter region at plus or minus 2kb from the transcription start site. These gene sets contain the respective motifs of TTTSGCGS TTTSGCGC, TTTSGCGS and GATTGGY. However, these transcription factor binding sites do not match any known transcription factors.

For the dysregulated genes within the gene sets associated with E2F1 and E2F4, a strong trend in the downregulation of gene expression is revealed when they were searched for within the microarray data (data not shown). In line with this the gene expression of E2F1 and E2F4 is also downregulated (data not shown).

`

Transcription Factor	Transcription Factor Gene set	Observed	Expected	Ratio	p-value
Unknown	hsa_V$E2F_02	30	15.33	1.96	2.38E-02
E2F4 p107/p130 & TFDP2	hsa_V$E2F4DP2_01	30	15.24	1.97	2.38E-02
E2F4 p107/p130 & TFDP1	hsa_V$E2F1DP1_01	30	15.24	1.97	2.38E-02
Unknown	hsa_V$E2F1_Q6	33	15.99	2.06	2.38E-02
E2F1 & TFDP2	hsa_V$E2F1DP2_01	30	15.24	1.97	2.38E-02
E2F1 & TFDP1	hsa_V$E2F4DP1_01	30	15.52	1.93	2.97E-02
E2F1	hsa_V$E2F_Q6	30	15.71	1.91	3.40E-02
Unknown	hsa_V$E2F_Q4	30	15.99	1.88	3.72E-02
E2F1	hsa_V$E2F1_Q3	29	15.52	1.87	4.63E-02

Table 6.3.L: Transcription Factor Target Analysis for the neuronally filtered GOI list. Observed and expected are measures of the number of genes and ratio is the observed number of genes/expected number of genes.

E2F1 and E2F4 are thought to have contrasting roles in the cell cycle. The overexpression of E2F1 propagates the movement of quiescent cells through G_0 into S-phase (Johnson *et al*, 1993). The overexpression of E2F1 is also associated with both p53-dependent (Kowalik *et al*, 1995; Qin *et al*, 1994) and independent apoptosis (Nahle *et al*, 2002). Recent advances in the understanding of E2F1 function within the cell cycle have led to a dual role of E2F1 being proposed within oncogenesis. Classically E2F1 has been seen as a tumour suppressor participating in apoptosis following the detection of damage to DNA. However, recent research suggests that E2F1 may function within a tumour progression signalling pathway, whereby the activity of E2F1 promotes oncogenesis (Engelmann & Putzer, 2012).

Whereas E2F1 is seen as an activator E2F, E2F4 is seen as a repressor that is associated with differentiation and growth suppression. For example, in oncogenesis E2F4 appears to function as a tumour suppressor (Crosby & Almasan, 2004). In the cell cycle, E2F4 is important in the

`

establishing of G_2 arrest following DNA damage, preventing cell cycle progression into M-phase (Plesca *et al*, 2007).

A role of E2F4 in differentiation is supported by evidence from animal models of E2F4 -/- transgenic mice. These animals are of reduced size and display evidence of altered cellular development to multiple cell lines, especially hematopoietic cell types, as well as possessing craniofacial abnormalities (Humbert *et al*, 2000; Rempel *et al*, 2000).

The use of the differing unfiltered GOI and neuronal filtered GOI lists makes little difference in terms of the number of genes that appear in the gene sets, the analysis results are produced from essentially the same set of common set of 29-34 genes bar the result for hsa_GATTGGY_V$NFY_Q6_01 in the unfiltered GOI list . However the ranking of the significance of the gene set results differs markedly between the unfiltered GOI and the neuronal filtered GOI list analysis. The results for both analysis compliment the theme in the t(1;11) microarray data analysis of there being a dysfunction in the cell cycle occurring.

6.3.8 Disease Association Analysis

Disease Association Analysis is a web based program supported by Gene List Derived Automatically for You, which associates disease terms to gene lists of interest using PubMED sources (Jourquin *et al*, 2012). (http://bioinfo.vanderbilt.edu/glad4u, http://bioinfo.vanderbilt.edu/webgestalt/analysis.php). For the Disease Association Analysis a significance level of $p<0.05$ was applied.

Aneuploidy is the most significant result for both the unfiltered and filtered GOI lists (see tables 6.3.M and 6.3.N). Aneuploidy is the condition whereby a cell exists that has either gained or lost one or more chromosomes resulting in the cell no longer containing the normal chromosome number for the given species. As such aneuploidy is associated with a variety of distinct disease pathologies. Aneuploidy arises due to abnormalities in the recombination of chromatids during either meiosis I or II, which commonly includes the premature separation of sister chromatids (Nagaoka *et al*, 2012). Cell and tissue specific aneuploidy is also characteristic of cancer. In cancer the genomic instability propagated by aneuploidy can lead to deficits in cell function mediated by alterations to the transciptosome and the proteome (Gordon *et al*, 2012).

`

Disease	Observed	Expected	Ratio	p-value
Aneuploidy	27	8.91	3.03	1.00E-04
Cancer or viral infections	75	46.94	1.6	1.31E-02
Hodgkin Disease	22	9.19	2.39	2.90E-02

Table 6.3.M: Disease Association Analysis for the unfiltered GOI list. Observed and expected are measures of the number of genes and ratio is the observed number of genes/expected number of genes.

Disease	Observed	Expected	Ratio	p-value
Aneuploidy	26	8.79	2.96	3.00E-04
Immune System Diseases	47	25.34	1.85	1.03E-02
Bronchiolitis	20	8.13	2.46	0.0329
Bronchitis	20	8.51	2.35	0.0395
Cancer or viral infections	70	45.72	1.53	0.0395

Table 6.3.N: Disease Association Analysis for the neuronally filtered GOI list. Observed and expected are measures of the number of genes and ratio is the observed number of genes/expected number of genes.

However, it is extremely unlikely that the t(1;11) pedigree suffer from aneuploidy, such an occurrence would have been detected during the initial cytogenetic karyotyping of the t(1;11) pedigree (St Clair *et al*, 1990). It is possible that aneuploidy may be intrinsic to the lymphoblastoid cell lines assayed on the microarray. If lymphoblastoid cell lines are cultured for long periods of time, e.g. over 180 population doubling levels, they can immortalise gaining strong telomerase activity and aneuploidy. In this context immortalisation refers to the long-lifespan of such cells in culture rather than the process of the EBV transformation of the cell lines (Sugimoto *et al*, 2004). Although, as this is differential expression data such an explanation would require that only the t(1;11) lymphoblastoid cell lines assayed were immortalised and the control cell lines not. A more likely explanation is that aneuploidy is arising in the disease association due to a) the enrichment of cell cycle processes in general or b) due to the DNA damage and repair mechanisms associated with the translocation.

`

Immune system diseases is also broad category for gene enrichment to occur in. The vast majority of the genes in this category are associated with immune function. This result may therefore reflect the dysregulation of immune function within Disease Association Analysis. The dysfunction of the immune system is fundamental to the pathophysiology of schizophrenia. The detrimental effects of immune dysfunction may occur at various points in neurodevelopment throughout the individual's lifespan. This is evidenced by data from GWAS, post-mortem transcriptome studies, the study of peripheral biomarkers and animal models of maternal immune activation (Michel *et al*, 2012). Kinney *et al*., (2010), goes so far as to propose a unifying hypothesis on schizophrenia that focuses of vulnerabilities within the development of the immune system and its function in contrast to a neurodevelopmental hypothesis of schizophrenia.

Cancer and viral infections is a broad category for gene enrichment to occur in. Multiple genes contributing to this result are either oncogenes or genes fundamental to cell cycle function. This result may arise from the wide scale enrichment of cell cycle pathways and ontology within this chapter and so the occurrence of this result probably reflects the involvement of cell cycle dysregulation in cancer within the Disease Association Analysis. It may also be the case that this classifier refers to instances where viruses act as cancer agents in oncogenesis (White *et al*, 2014). In the analysis of the neuroanally filtered GOI list cancer and viral infections just passes the significance level of $p<0.05$.

Hodgkin's disease also known as Hodgkin lymphoma is a form of cancer that originates from B-cells and is highly common in occurrence for a lymphoma (Küppers *et al*, 2012). The occurrence of Hodgkin disease in the Disease Association Analysis appears to be primarily due to the presence of multiple genes associated with immune function being dysregulated. A secondary contribution to Hodgkin's disease being highlighted comes from the presence of several Hodgkin's disease specific genes and from genes that may be exclusive to the unfiltered GOI list that pertain to B-cell mediated processes.

Bronchitis is the transitory inflammation of the large airways of the lung associated with coughing in the absence of pneumonia. Pathologically the inflammation originates due to the infection of the epithelium of the bronchi (Wenzel & Fowler III, 2006). Bronchiolitis is a respiratory infection that occurs in young children and affects the small airways of the lung. Pathologically the inflammation originates from the infection of respiratory tract epithelium (Smyth & Openshaw, 2006). Both the bronchitis and bronchiolitis results in the Disease Association Analysis originate from the same set of dysregulated genes. The highlighting of

`

these two results should not be interpreted as the t(1;11) pedigree having an enhanced susceptibility to respiratory diseases, rather that immune response, in particular inflammation is possibly altered in the t(1;11) lymphoblastoid cell lines assayed. Alterations in inflammation are thought to have a role in schizophrenia in adults (Kirkpatrick & Miller, 2013) while prenatal inflammation is itself a risk factor for schizophrenia (Miller *et al*, 2013). In the analysis of the neuroanally filtered GOI list both bronchitis and bronchiolitis just pass the significance level of $p<0.05$.

6.4 Discussion

The functional enrichment analysis of t(1;11) gene expression microarray data possess several limitations. The samples sizes are small and only technical replicates as opposed to sample replicates were performed. The lymphoblastoid cell lines used are at best likely to have a moderate correlation in transcript expression to that of post-mortem brain tissue (Cai *et al*, 2010; Sullivan *et al*, 2006). No comparison with either fresh whole blood or fractionated blood has been performed, had this been done, confounding factors induced by EBV transformations of lymphoblastoid cell lines could possibly be identified. Regarding the data analysis, the over-representation analysis based programs used do not accept fold change data nor do they account for relationships that may exist between genes (Khatri *et al*, 2012). Furthermore, it is extremely likely that the databases that support the pathway analysis and ontology programs are biased towards cancer-related processes, including the cell-cycle. As a consequence of this further experimental work is required to determine whether the translocation has an effect on the cell-cycle or whether this finding reflects an intrinsic bias of pathway analysis programs. Additionally, multiple enrichment categories analysed are only marginally significant and as such may not replicate.

6.4.1 Cell cycle dysregulation

Looking at the output of multiple pathway analysis programs, there is clear evidence for alterations to the cell cycle and DNA replication in translocation carriers. Several of the functional enrichments also suggest that the translocation might affect immune function and inflammation.

The involvement of aberrant cell cycle function in the pathogenesis of psychiatric illness is supported by the literature. Gene expression microarray analysis of the anterior cingulate gyrus

`

(ACG) using post-mortem brains of individuals with schizophrenia detects alterations to the cell cycle and categories associated with cell cycle using Ingenuity Pathway Analysis (IPA), by both network analysis and the analysis of molecular and cellular functions (Katsel *et al*, 2008). The pattern of cell cycle dysregulation within the ACG suggests an over activity of the cell cycle possibly incurring the re-entry of cells into the cell cycle. Genes associated with G_1 activation, *Cyclin D1* (*CCND1*) and *Cyclin D2* (*CCND2)* are upregulated. Whereas genes associated with the downregulation of the cell cycle such as *Cyclin-dependent Kinase Inhibitor 1B* (*$p27^{Kip1}$*) and *Cyclin-dependent Kinase Inhibitor 1C* (*$p57^{Kip2}$*) are downregulated. Overall this would suggest a progression from G_1 to S-phase readily occurs in the ACG in schizophrenia. Additionally, genes associated with S-phase are also upregulated, suggesting that S-phase is also active (Katsel *et al*, 2008).

Olfactory epithelial biopsies have been used to study the relationship between schizophrenia and the cell cycle (Fan *et al*, 2012; Féron *et al*, 1999; McCurdy *et al*, 2006). Féron *et al.,* (1999) observed that the number of non-neuronal cells in mitosis in biopsies from patients with schizophrenia is two and a half times that for control cell biopsies. This has been replicated by comparing patients with schizophrenia to patients with bipolar I disorder as well as healthy controls. Again, the same proportional increase in mitosis for the cell biopsies from schizophrenia patients is seen, with no difference between bipolar individuals and controls (McCurdy *et al*, 2006). This is suggestive of an increased rate of proliferation occurring in schizophrenia. It is possible that the enrichment of mitosis categories in the GOTree and Pathway Commons analysis may have been highlighting such an enhancement of mitosis. However, it is equally possible that these enrichments may be highlighting a deficit in mitosis. Further experimentation is required to determine the underpinnings of the mitotic dysregulation in the t(1;11)-family derived lymphoblastoid cell lines.

Gene expression microarray analysis of the olfactory epithelial biopsies from individuals with schizophrenia reveals enrichments relating to the cell cycle, in both DNA recombination and the positive regulation of cell proliferation, by GO (McCurdy *et al*, 2006). Furthermore, olfactory neurosphere-derived cells from patients with schizophrenia show altered cell cycle dynamics, with patient cells observed to spend a greater amount of time in $S/G_2/M$-phases as opposed to G_1. Interestingly, the cell cycle phase of the patient olfactory neurosphere-derived cells was two hours ahead of the control cell lines and in line with this the total length of the cell cycle was two hours shorter in the patient cell lines versus those of controls (Fan *et al*, 2012). A future experiment, that would enrich the current data on cell cycle dysregulation in the t(1;11) pedigree, would be to use FACS as performed by Fan *et al.*,(2012) to determine the

`

length of time t(1;11)-family derived lymphoblastoid cell lines spent in particular cell cycle phases. This would add a temporal aspect to the interpretation of the pathway analysis data.

Regarding DISC1 function in relation to the cell cycle, the knockdown of mouse DISC1 in neural progenitors in the ventricular zone/sub-ventricular zone, results in a 2-3 fold increase in the number of progenitor cells exiting the cell cycle. In addition to this, altered differentiation is apparent (Mao *et al*, 2009). This is interesting as the t(1;11)-family derived lymphoblastoid cell lines assayed on the microarray have been shown to have half normal levels of DISC1protein expression (Millar *et al*, 2005b). It is possible that this may have the same premature cell cycle exit effect as the reduction of DISC1 induced by RNAi as performed by Mao *et al*., (2009). The expression of DISC1 aa1-597 in the inducible ΔhDISC1 mouse model results in the dysregulation of several cell cycle genes that are associated with the differentiation of oligodendrocyte precursor cells (Katsel *et al*, 2011). The DISC1/DISC1FP1 species *CP1* encodes DISC1 aa1-598. If expressed endogenously in the t(1;11)-family derived lymphoblastoid cell lines, CP1 could result in the same dysregulation of cell cycle genes observed by Katsel *et al.*, (2011). However, CP1 protein has not been detected in the t(1;11) lymphoblastoid cell line by Western blot, although the species may be present below the threshold of detection (Eykelenboom *et al*, 2012).

Multiple studies, in both cultured cell lines and primary neurones identify DISC1 as being localised at the centrosome (Bradshaw *et al*, 2008; Kamiya *et al*, 2005; Kamiya *et al*, 2008; Miyoshi *et al*, 2004; Morris *et al*, 2003). The centrosome features as a highlighted GO category in GOTree. In eukaryotes the centrosome functions as the major microtubule organising centre within the cell, whereupon the centrosome establishes and coordinates microtubule arrays to other intracellular structures during mitosis (Bettencourt-Dias & Glover, 2007). Several DISC1 interactors exist that are also centrosomal proteins, this includes: various BSS proteins, Coiled-coil Protein Associated with Myosin II and DISC1 (CAMDI), LIS1, NDE1, NDEL1, PCM1 and pericentrin (Brandon *et al*, 2004; Camargo *et al*, 2006; Fukuda *et al*, 2010b; Kamiya *et al*, 2008; Miyoshi *et al*, 2004; Ozeki *et al*, 2003; Shinoda *et al*, 2007). These proteins typically have roles with centrosomally mediated effects that contribute to neurodevelopment (Thomson *et al*, 2013). However, it may be that these centrosomal proteins also have roles in the cell cycle and so perhaps could in part explain some of the dysregulation of the cell cycle that is seen in the t(1;11) microarray analysis. For example, the importance of LIS1 in the cell cycle is highlighted in a series of experiments using mouse embryonic fibroblasts from LIS1 knockout mice that display a variety of mitotic defects (Moon *et al*, 2014). This includes: misaligned and unattached chromosomes during metaphase, the

`

misegregation of chromosomes during anaphase, the presence of additional centromeres, abnormal mitotic spindle positioning and orientation and a reduction in the targeting of LIS1 to kinetochores. It is possible that DISC1 at the centrosome binds LIS1 during the typical mitotic activity of LIS1. If this is the case such an interaction may be reduced in the t(1;11)-family derived lymphoblastoid cell lines due to haploinsufficiency (Millar *et al*, 2005b). It may be then that reduced DISC1/LIS1 binding results in the propagation of mitotic deficits similar to those observed by Moon *et al.*,(2014). Future research into cell cycle dysregulation during mitosis in the t(1;11) family derived lymphoblastoid cell line could involve immunocytochemistry at the various stages of mitosis. This would use antibodies targeting DISC1 and DISC1 interactors that are located at the centrosome as well as visualising the kinetochore, the chromosomes and the α-tubulin of the mitotic spindle. The aim of this series of experiments would be to see what is actually occurring during the mitotic stages and to identify any aberrant function arising via reductions in the endogenous levels of DISC1 due to haploinsufficiency.

Recent research identifies PDE4D9 as being active during mitosis, modulating the levels of both cAMP and PKA via the hydrolysis of cAMP. Inhibition of PDE4D9 results in the dysregulation of cell cycle transition with accelerated progress from S-phase to G_2/M phase observed, alongside a rapid G_2/M transition into a lengthened G_1 phase (Sheppard *et al*, 2014). PDE4D9 is transcriptionally repressed by an ATF4/DISC1 complex. The loss of function of either component of the transcriptional repression complex results in an increase in PDE4D9 transcription (Soda *et al*, 2013). It is possible that some of the cell cycle dysregulation detected by pathway analysis and GO may arise from alterations to PDE4D9 transcription and function, due to the t(1;11)-family derived lymphoblastoid cell lines assayed on the microarray being haploinsufficient for DISC1 (Millar *et al*, 2005b). The effects of haploinsufficiency of DISC1 on PDE4D9 may be two-fold. Firstly the transcriptional repression by the DISC1/ATF4 complex may be reduced, with half normal levels of DISC1 present, leading to an abundance of PDE4D9. Secondly there will be a reduction in the interactions between DISC1 and PDE4D9. This will be a reduction in the sequestering of PDE4D9 in a low activity state, as occurs between DISC1 and other PDE4s (Millar *et al*, 2005b; Murdoch *et al*, 2007). Overall the haploinsufficiency would engender a greater amount of PDE4D9 in cells that would in turn be more actively hydrolysing cAMP and, therefore, reducing PKA levels, actions that will have downstream signalling effects throughout the cell cycle.

Multiple categories of G_1 transitions appear in the Pathway Commons analysis. The length of G_1 phase exerts influence on the mode of cell division and cell fate within the cell cycle. Short

`

G_1 phases favour proliferative cell divisions, whereby neuronal cells re-enter the cell cycle. Long G_1 phases favour differentiated divisions whereby differentiated cells exit the cell cycle (Calegari & Huttner, 2003). The lengthening of G_1 phase to provide a pool of differentiated cells is of particular importance in mid-late corticogenesis (Dehay & Kennedy, 2007). Therefore it is possible that in the t(1;11)-family derived lymphoblastoid cell lines that G_1 phase has an altered phase length from that of control cell lines. This could lead to an alteration in the stoichiometry in the maintenance of proliferative/differentiated pools of cells which could impact on upstream corticogenesis. The length of G_1 phase could be investigated in the future using time-lapse video microscopy.

It may be that the enrichment of G_2 phase pathways that is observed in the Pathway Commons analysis, reflects processes in cell cycle dysregulation that may have shortened or lengthened this phase. G_2 phase length has also been associated with the differential production of proliferating cells and differentiated cells. The knock-down of the positive cell cycle regulator Cell Division Cycle 25B (CDC25B) results in the lengthening of G_2 phase and favours the production of neural progenitors. Conversely at basal levels of CDC25B, when co-expressed with Cell Division cycle 25A (CDC25A), G_2 phase is shorter and neurogenesis occurs with the production of differentiated cells occurs (Peco *et al*, 2012). . It is possible that G_2 phase length alteration could be the precipitant of a process that may occur in the brains of the t(1;11) pedigree, that alters the balance in the production of proliferating versus differentiating cells during neurogenesis.

GoTree and multiple pathway analysis programs identify DNA replication, which specifically occurs in S-phase, as being enriched for genes showing differential expression in carriers of the t(1;11) translocation The length of S-phase has also been observed to vary with the cell type emerging from the cell cycle. Proliferating apical and basal progenitors have been seen to spend a longer time in S-phase than apical and basal progenitors that differentiate into post-mitotic neurones. It is inferred from this that the progenitors that are retained in the proliferating pool engage in a lengthier S-phase transition to ensure greater DNA quality control (Arai *et al*, 2011). It is possible that the length of S-phase varies in the t(1;11) lymphoblastoid cell lines assayed which may affect cell fate determination as to whether cells emerge from the cell cycle as progenitors or as differentiated cells. 31L mice contain ENU induced point mutations that cause amino acid changes (Q31L) to DISC1 and result depression-like phenotype (Clapcote *et al*, 2007). 31L mice have been observed to possess a deficit in proliferating cells in the hippocampus as evidenced by reduced number of neurospheres and intermediate progenitor cells (Chandran *et al*, 2014). It is possible that this

`

mutation to *Disc1* may induce cell cycle abnormalities that share underpinnings with the biological pathway deficits observed in this study.

The widespread dysregulation of M-phase and in particular mitosis evident in the GOTree and Pathway Commons analysis may represent a process that could impact upon intrinsic cell asymmetry within neural stem cell populations within the t(1;11) pedigree. Cell asymmetry arises when a stem cell divides into phenotypically different daughter cells in terms of cell size and macromolecular continent. The asymmetry between the daughter cells results in differential cell fate determination. During mitosis the positioning of the mitotic spindle (asymmetric rather than centred) and the asymmetric accumulation of cell fate determinants within the dividing cell specify for asymmetrical as opposed to symmetrical cell division (Neumüller & Knoblich, 2009). It is possible that the dysregulation of mitosis in the t(1;11)-family derived lymphoblastoid cell represents mechanisms by which intrinsic asymmetrical division in the brain could be perturbed. This could result in the final daughter cell phenotypes being fundamentally altered from those occurring in a normal developmental pathway in the absence of cell cycle dysregulation.

Translating the blood based t(1;11) microarray data on cell cycle dysregulation to the actual functions of the brain in the t(1;11) pedigree may not be clear cut. It may be inappropriate to take a view with a single global brain based dysfunction in the cell cycle from the data. For example Benes *et al.*, (2009) examined both bipolar and schizophrenia post-mortem brain samples from the *strata oriens* of the hippocampus and site specific deficits were apparent between the CA2/3 and CA1 regions in cell cycle gene expression. The site specific deficits were both within and between groups, suggesting that even within very local regions of the brain there can be differences in the cell cycle dysregulation associated with pathophysiology. As such an appropriate future experiment would be to run gene expression microarray analysis on multiple brain areas from post-mortem t(1;11) brain tissue to further elaborate on the cell cycle dysfunction regarding regional brain deficits.

6.4.2 Immune function and inflammation enrichment

Multiple genome wide association studies have found associations between the major histocompatibility complex (MHC) and schizophrenia (Consortium & 2, 2012; Consortium, 2011; Hamshere *et al*, 2012; Lencz *et al*, 2013; Purcell *et al*, 2009b; Ripke *et al*, 2013a; Shi *et al*, 2009; Stefansson *et al*, 2009; Yue *et al*, 2011). The MHC locus at 6p21.32-p22.1 contains more than 160 protein coding genes and is key to both the susceptibility and fighting of disease,

`

being integral to the adaptive, innate and autoimmune responses (Traherne, 2008). Key to the MHC is the ability to discern what is 'self' from 'non-self'(Richard & Brahm, 2012).

The findings of expression microarray and RNA-seq studies also demonstrate links between immunity and inflammation responses and schizophrenia. The enrichment of genes involved in the immune response has been highlighted by GO in a post-mortem brain FC microarray study, with the genes *Serpin Peptidase Inhibitor, Clade A* (*Alpha-1 Antiproteinase, Antitrypsin*), *Member 3* (*SERPINA3*), *Interferon Induced Transmembrane Protein 2* (*IFITM2*), *Interferon Induced Transmembrane Protein 3* (*IFITM3*) and *Guanylate Binding Protein 1, Interferon-inducible* (*GBP1*) that are related to inflammatory process being upregulated (Saetre *et al*, 2007). A post-mortem brain microarray study specific to the PFC observed a >50% upregulation in genes involved in chaperone or immune function, totalling 10 genes. Of these, five genes were identified as being involved in immune function and appear to co-regulate expression. These genes are *SERPINA3, IFITM3*, *Interferon Induced Transmembrane Protein 1* (*IFITM1*), *Chitinase 3-like 1 (Cartilage Glycoprotein-39)* (*CHI3L1*) *and CD14 Molecule* (*CD14*) (Arion *et al*, 2007). Conversely in a microarray study of the superior temporal cortex, the downregulation of 70 genes associated with immune function was observed (Schmitt *et al*, 2011). While dysregulation of the expression of immune function associated genes has been observed in a PFC microarray study (Garbett *et al*, 2008). GO identifies significant enrichment in the humoral response following the expression microarray study using post-mortem DLPFC tissue and the subsequent analysis of shared genes between both individuals with schizophrenia and those with bipolar disorder (Shao & Vawter, 2008). In a peripheral blood monocyte microarray study the functional annotation by IPA using genes differentially expressed in subjects with schizophrenia reveals enrichment of immune function. Of the IPA annotations of the functions of the differentially expressed genes, 37% were observed to be involved with immune and inflammation processes. This included infectious disease; inflammatory response; respiratory and infectious disorder and inflammatory and immune response (Gardiner *et al*, 2013). Using RNA-seq to analyse post mortem hippocampal tissue, enrichment mapping reveals a cluster of predominantly upregulated genes that are categorised as having biological involvement in defence response; immune response and inflammatory response. Within the same hippocampal dataset from individuals diagnosed with schizophrenia, the mRNA of the genes *Adenosine A2a Receptor* (*ADORA2A*); *Apolipoprotein L, 1* (*APOL1*), *Insulin-like Growth Factor Binding Protein 4* (*IGFBP4*), *IFITM1, IFITM2* and *IFITM3* that are involved in inflammation and the immune response were all significantly increased (Hwang *et al*, 2013). Focusing on the post-mortem

`

DLPFC using RNA-seq, Fillman *et al.,* (2012) found the IPA category "inflammatory response" to be significantly enriched, due to the increased expression of the *interleukins* (*IL*), *IL-6, IL-8* which are proinflammatory and anti-inflammatory cytokines and SERPINA3. Taken together the results of these microarray and RNA-seq studies suggest a role of immune and inflammatory dysfunction that is detectable in tissues acquired from adults with schizophrenia.

Microarray array studies also implicate immunity and inflammation in the pathophysiology of major depressive disorder and bipolar disorder, although the area is less well studied than schizophrenia. In a microarray study using post-mortem PFC tissue from subjects that had suffered from depression, significant enrichment in the cytokine pathway was identified. This was due to the upregulation in expression of the interleukins *1α (IL-1α), IL-2, IL-3, IL-5, IL-8, IL-9, IL-10, IL-12A, IL-13, IL-15, IL-18*, as well as that of *Interferon Gamma* (*IFNγ*) and *Lymphotoxin α,* (cytokines with roles in the immune and inflammatory responses), suggesting a role for inflammation in the aetiology of depression (Shelton *et al*, 2010)**.** Microarray analysis of the PFC and orbitofrontal cortex from individuals diagnosed with bipolar disorder has shown a significant upregulation in the expression of genes associated with the immune response (Ryan *et al*, 2006).

Alterations to immune function can be identified in first episode drug-naive schizophrenia patients (Cazzullo *et al*, 2001; Herberth *et al*, 2014). Taken together, these findings suggest that observations of altered immune function in schizophrenia cannot be entirely attributed to medication effects and may represent a primary pathogenic mechanism. The cytokine profile in both first episode and acutely relapsed schizophrenia patients has been compared by meta-analysis of immune system dysfunction. This reveals that the cytokine dysregulation between both patient populations is similar and can be grouped into both state and trait markers. IL-1β, IL-6, and Transforming Growth Factor Beta (TGF-β), a cytokine with roles in immunity, are identified as state markers and are detectable at high concentrations during acute episodes of illness and are reduced when patients have reached a stable baseline following antipsychotic treatment. IL-12, IFN-γ, Soluble IL-2 Receptor (sIL-2R) and Tumour Necrosis Factor Alpha (TNF-α) a proinflammatory cytokine with roles in immunity, are trait makers and as such are continually associated with schizophrenia even following antipsychotic medication (Miller *et al*, 2011). Such changes in immune function may have effects on the symptomology of schizophrenia. Severe impairments in cognition have been associated with inflammation in schizophrenia. These deficits can be ameliorated following treatment with anti-inflammatory drugs (Ribeiro-Santos *et al*, 2014). Negative symptoms of non-affective psychosis have been

`

associated with increased concentrations of IL-6 (Garcia-Rizo *et al*, 2012; Kim *et al*, 2000). The structure of the brain may be influenced by cytokine levels. Increased levels of IL-6 in first episode psychosis patients have been associated with a reduction in the volume of the left hippocampus (Mondelli *et al*, 2011).

Inflammation and cytokine activity has been identified as a mechanism of pathogenesis in depression (Miller *et al*, 2009). Inflammation interacts with the vast majority of disease domains associated with depression including neurotransmitter metabolism, endocrine function and neuroplasticity. The meta-analysis of cytokine immune dysregulation in major depressive disorder identifies higher concentrations of IL-6 and TNF-α, to be associated with the illness (Dowlati *et al*, 2010). Altered levels of cytokines and other inflammatory markers may influence the symptomology of depression. Regarding cognitive function and inflammation in depression, increased Highly Sensitive C-reactive Protein (hsCRP) a marker for inflammation, is associated with lower psychomotor speed. However, increased levels of IL-6 in patients was not associated with any cognitive effects above baseline measurements (Krogh *et al*, 2014). Sleep disturbance is common in major depressive disorder and, interestingly, high concentrations of nocturnal levels of IL-6 and Soluble Intercellular Adhesion Molecule-1 (sICAM-1) have been associated with sleep disturbances at night in individuals suffering from major depressive disorder (Motivala *et al*, 2005). Cytokines may have an effect on brain morphology. High IL-6 levels have also been observed to be linked to low hippocampal volumes in patients with major depressive disorder (Frodl *et al*, 2012).

The meta-analysis of cytokine prevalence in bipolar disorder identifies elevations in the concentrations of a number of inflammatory mediators. This includes: IL-4, IL-6, IL-10, sIL-2R, Soluble IL-6 Receptor (sIL-6R), TNF-α, Soluble TNF Receptor-1 (sTNFR1) and IL-1 Receptor Antagonist (IL-1RA) (significant in mania only) (Modabbernia *et al*, 2013). In bipolar disorder, the level of immune dysfunction including the concentrations of cytokines may be related to the phase or stage in the illness. In a study addressing the differences in cytokine levels between early stage and late stage bipolar disorder Kauer-Sant'Anna *et al.,* (2009) observed that TNF-α, IL-6 and IL-10 concentrations were increased in the early stages of bipolar disorder, within 3 years of the first manic episode, yet only TNF-α and IL-6 levels were elevated in the late stage of the illness, 10 years after diagnosis with bipolar disorder. Additionally IL-6 levels show a significant reduction between the early and late stages of bipolar disorder. It is suggested that such changes in endogenous cytokine levels may be of use as markers of disease progression in bipolar disorder. Analysis of the discrete phases of bipolar disorder: mania, depression and eurythmia, reveals specific episodic profiles for

`

cytokine elevation. Brietzke *et al*., (2009) has shown that mania is associated with increased levels of IL-2, IL-4 and IL-6. In depression, only IL-6 is increased, while eurythmic patients show no abnormalities in cytokine levels versus healthy controls. In contrast, Ortiz-Domínguez *et al.*, (2007) has shown elevated levels of IL-4 and TNF-α in mania coupled with low levels of IL-2 and in depression measured elevated levels of IL-6 and TNF-α compared to healthy controls. When comparing cytokine levels in the depressed phase and the manic phase, the manic phase was found to be associated with elevated IL-4 and reduced IL-1β and IL-6 concentrations whilst these cytokine levels were reversed in the depressed phase. O'Brien *et al*., (2006) has reported no phasic difference between manic and depressed sufferers of bipolar disorder and has found increased TNF-α and IL-8 concentrations in both conditions. Taken together, these studies provide tentative support for the notion that cytokine levels are altered in a phase-specific manner in bipolar disorder. However, a lack of consistency between studies makes it difficult to determine the precise nature of these changes. This may due to the effects of sample sizes, medication effects or other methodological differences.

Maternal immune activation is a risk factor for schizophrenia. The prenatal exposure of the foetus to infectious agents such as influenza, the intracellular parasite *T. gondii* and the Herpes simplex virus type 2 has been observed to increase the risk of schizophrenia in multiple epidemiological birth cohort studies (Brown & Derkits, 2010). Two hypotheses exist regarding maternal immune activation. The first sees the action of unique effects specific to the infectious agent producing aberrant neurodevelopment. The second, more prominent hypothesis, sees the action of a single common or common mechanisms that act to perturb neural development. The action of maternal immune activation coupled with an underlying genetic susceptibility in the foetus is proposed to result in an altered developmental trajectory being pursued in the fetal brain. This may result in aberrant cell division, migration patterns and axonal pathfinding occurring following an initial acute immune response. It is suggested that these developmental alterations are driven by an residual 'immune scar' of chronic inflammation that lasts throughout life (Horváth & Mirnics, 2014). The *in utero* elevation of cytokines, which is part of the immune response mechanism to infections agents, has also been associated with schizophrenia. The elevation of IL-8 during the second trimester of pregnancy, has been observed in mothers whose offspring later develop schizophrenia (Brown *et al*, 2004). Increased TNF-α levels have also been detected at birth in mothers whose offspring later develop psychosis as adults (Buka *et al*, 2001).

DISC1 transgenic mouse models have used poly I:C, an inflammatory agent that mimics viral infection (Meyer & Feldon, 2012) to model maternal immune activation in gene-environment

`

studies (Abazyan *et al*, 2010; Ibi *et al*, 2010; Lipina *et al*, 2013; Nagai *et al*, 2011). 100P mice contain *N*-ethyl-*N*-nitrosourea (ENU) induced point mutations that cause amino acid changes (L100P) to DISC1 and possess a schizophrenia-like phenotype (Clapcote *et al*, 2007) In 100P mice the induction of maternal immune activation via poly I:C exposed pregnant dams results in an exacerbation in schizophrenia-like behaviours, with deficits in prepulse inhibition (PPI) and latent inhibition (LI) becoming apparent in offspring. In contrast the poly I:C generated Q31L mice do not show any behaviours that are not shared with wild type controls. Interestingly the PPI and LI defects in the L100P mice can be ameliorated following treatment with anti-IL-6, an antibody that targets IL-6 (Lipina *et al*, 2013). The ΔhDISC1 inducible DISC1 aa1-597 mice model (Pletnikov *et al*, 2008) has been used to model maternal activation with pregnant dams injected with poly I:C (Abazyan *et al*, 2010). The ΔhDISC1/poly I:C mice feature a depression/anxiety-like phenotype with a dysregulation in cytokine levels being apparent. Abnormal brain morphology was observed, with decreased volumes in the right periaqueductal grey matter and right amygdala and a reduced spine density in the dentate gyrus. It's noteworthy that in a study by Abazyan *et al.,* (2010) that evidence of cytokine dysregulation was also seen when the DISC1 aa1-597 transgene was expressed solely, suggesting that DISC1 aa1-597 alone can influence endogenous cytokine levels. The constitutively active DN-DISC1 model that expresses DISC1 aa1-597 (Hikida *et al*, 2007) has also been used in the gene-environment modelling of maternal immune activation. This method used poly I:C injected into neonates (Ibi *et al*, 2010; Nagai *et al*, 2011). The DN-DISC1/poly I:C mice possessed a wide array of deficits including an impairments in novel object recognition, fear memory, short-term memory, social interaction and an augmentation to MK-801 induced hyperactivity. Additionally parvalbumin-positive neuron staining was observed to be reduced (Ibi *et al*, 2010). Further investigations using the DN-DISC1/poly I:C paradigm highlighted how the model produced schizophrenia-like responses to antipsychotic medication treatment across a range of behavioural assays (Nagai *et al*, 2011). Overall the poly I:C gene-environment modelling maternal immune activation using DISC1 transgenic mice demonstrated how the poly I:C treatment was capable of modulating the phenotype of the mice at both the behavioural and anatomical level.

Regarding the t(1;11) pedigree, maternal immune activation may serve to modulate the penetrance of the translocation, in that translocation carriers that are exposed to maternal immune activation would exhibit a more severe mental illness phenotype. Maternal immune activation could partly explain the immune system dysfunction and inflammation observed in the microarray analysis. However, it seems unlikely that all of the translocation carriers with

`

schizophrenia suffered from maternal exposure to infectious agents. It remains possible though that maternal immune activation may have been a contributing factor to a few of the cases of schizophrenia in the t(1;11) pedigree, Such an occurrence may have led to 'immune scarring' and long term gene dysregulation (Horváth & Mirnics, 2014) the latter of which may be detectible by expression microarray analysis. However, it must be stressed that maternal immune activation would be unlikely to account for all of the incidences of schizophrenia in the t(1;11) pedigree. Another explanation for the prevalence of immunity and inflammation associated processes in the pathway analysis of the microarray data could come from the endogenous presence of the DISC1/DISC1FP1 species CP1 in the lymphoblastoid cell lines. *CP1* encodes DISC1 aa1-598 and is as such highly similar to DISC1 aa1-597, which has been shown to cause cytokine dysregulation (Abazyan *et al*, 2010). To date, however, expression of the CP1 protein has not been identified in t(1;11) lymphoblastoid cell lines. It is, however, possible that the species may be present at levels below the limits of detection of Western blotting (Eykelenboom *et al*, 2012). As such the exact origin and mechanism of action for the immune and inflammation responses highlighted in the t(1;11) microarray require further investigation. One potential future experiment could be to generate a humanised translocation mouse model and expose it to poly I:C *in utero* with a view to characterising the immunological disturbances and effects on behavioural and neuroanatomical phenotypes versus untreated translocation mice.

From the Disease Association Analysis, three categories of genes involved with inflammation and immune function emerged. Interleukins are a class of cytokines that can mediate both proinflammatory and anti-inflammatory functions within the immune system. Genes involved in interleukin signalling, including *Interleukin 4 Receptor* (*IL-4R*), *Interleukin Receptor Beta 2* (*IL-12RB2*) *Interleukin 13 Receptor Alpha 1* (*IL-13RA1*), *Interleukin 21 Receptor* (*IL-21R*), *Interleukin Receptor 23 Alpha Subunit p19* (*IL-23A*) and *Interleukin Receptor 27 Alpha* (*IL-27RA*), contribute to disease categories found to be enriched in the functional enrichment analysis. These interleukin receptors mediate both pro-inflammatory and anti-inflammatory responses by signal transduction. The tumour necrosis factor superfamily also appears in the Disease Association Analysis with *Tumour Necrosis Factor Receptor Superfamily Member 1B* (*TNFRSF1B*), *Tumour Necrosis Factor Receptor Superfamily Member 8* (*TNFRSF8*), *Tumour Necrosis Factor Receptor Superfamily Member 9* (*TNFRSF9*) are all present in the functional enrichment analysis. The tumour necrosis factor superfamily are involved in mediating the pro-inflammatory response in both acute immune responses and the chronic immune responses of inflammatory disease (Aggarwal *et al*, 2012). Nuclear factor kappa-

`

light-chain-enhancer of activated B cells (NF-κB) is a transcription factor protein complex which has dual roles in both the immune and inflammatory responses (Tak & Firestein, 2001). Within the significant Disease Association Analysis results, an NF-κB subunit appears, *Nuclear Factor of Kappa Light Polypeptide Gene Enhancer in B-cells 2* (*p49/p100*). In addition, two kinases that modulate NF-κB activity appear. These are *Nuclear Factor of Kappa Light Polypeptide Gene Enhancer in B-cells Inhibitor, Alpha* (*NFKBIA*); and *Nuclear Factor of Kappa Light Polypeptide Gene Enhancer in B-cells Inhibitor, Epsilon* (*NFKBIE*). The Disease Association Analysis results do not include any of the interleukins identified as significant by meta-analyses of cytokine expression in schizophrenia (Miller *et al*, 2011), bipolar disorder (Modabbernia *et al*, 2013), or major depressive disorder (Dowlati *et al*, 2010). However, in the Pathway Commons analysis a pathway for IL-12-mediated signalling events was found to be statistically enriched. IL-12 is seen as a trait marker for schizophrenia that can be detected even when individuals are taking antipsychotic medication and is present in a meta-analysis of cytokine alterations in schizophrenia (Miller *et al*, 2011). In contrast to IL-12 being associated with schizophrenia the Disease Association Analysis highlights immune function and inflammation by the enrichment of interleukin associated genes and those involved in the tumour necrosis superfamily and NF-κB signalling, that are not directly identified with major mental illness by meta-analysis.

The medication status of the members of the t(1;11) pedigree whose lymphoblastoid cell lines were assayed here is unknown. Medication could theoretically have affected gene expression in lymphocytes in a manner that was preserved beyond EBV transformation. For example the drug lithium, commonly used to treat bipolar disorder has been observed to promote the repair of double strand DNA breaks in hippocampal neurons (Yang *et al*, 2009). It may be that t(1;11) pedigree members taking lithium may derive some degree of neuroprotection from the cell cycle dysregulation seen in this analysis. Alternatively the observation of cell cycle dysregulation may originate from the use of drugs such as lithium that affect the cell cycle. Regarding medication and immune function, the use of various antipsychotics on drug-naive schizophrenia patients has been shown to be associated with the levels of CD19+ (B)- and CD3+ (T)-lymphocytes returning to the baseline levels of heathy controls (Maino *et al*, 2007). It is therefore possible that the antipsychotic medication that the t(1;11) carriers receive may confer some immunoprotective effects. Conversely, it may be that the antipsychotic drugs taken by the t(1;11) carriers could possibly be the source of the immune function and inflammatory dysregulation observed in the t(1;11) microarray data.

`

6.4.3 Outcome of using unfiltered versus the neuronally filtered GOI lists

The analysis of the t(1;11) expression microarray data involved the use of both an unfiltered GOI list and a neuronally filtered GOI list. It was thought that the neuronally filtered GOI list may differ markedly from the unfiltered GOI list in terms of functional enrichment across analysis programs and may function as a more brain-like as opposed to blood based GOI list. However, only the Disease Enrichment Analysis had enrichment in multiple immune and inflammation disease categories specific to the neuronally filtered GOI list (See section 6.3.8). The differences in enrichment between the two GOI lists across programs was otherwise nominal. The use of the neuronally filtered GOI list as a more brain-like GOI list is also intrinsically misleading. It is explicit that the filtering to remove non-neuronal genes from the original GOI list is purely subtractive. There is no means to add in neuronal genes to the neuronally filtered GOI list that are absent in the lymphoblastoid cDNA. It is also possible that the use of the neuronally filtered GOI list may be an impediment when trying to compare results with other EBV-lymphoblastoid studies into major mental illness. Given these caveats it may be preferable to focus on the unfiltered GOI list results which are for the cell cycle highly similar to the neuronally filtered data but place less emphasis on immune function and inflammation in the pathogenesis of the t(1;11) pedigree.

Taking into account both the limitations of this gene enrichment study and the need for further replication, the GOI based approach detailed here is nevertheless a means that offers some promise in the identification of plausible biological pathways of relevance to psychopathology.

`

Chapter 7 - Final Discussion

7.1 Summary of findings

In this study I have looked at the t(1;11) pedigree, a family with a well characterised balanced autosomal translocation, which co-segregates with instances of bipolar disorder, schizophrenia and major depressive disorder (Blackwood *et al*, 2001). I have attempted to functionally characterise the t(1;11) for further putative mechanisms of pathogenesis. These mechanisms may exist in parallel to, or may in part be dependent upon, another potential mechanism of pathogenesis, the haploinsufficiency of DISC1 that has been identified in t(1;11) lymphoblastoid cell lines (Millar *et al*, 2005b). The search for cellular processes that may be perturbed so as to contribute to pathogenesis in the t(1;11) pedigree has involved both the exogenous expression of DISC1/DISC1FP1 chimeras in COS-7 cells and primary cortical neurone cultures as well as the functional enrichment analysis of a t(1;11)-family derived lymphoblastoid gene expression microarray data.

In this final chapter a summary of the findings of this thesis will be addressed, as well as future work and caveats and the wider relevance of this work to the field.

7.2 Identification of a novel *DISC1/DISC1FP1* transcript arising from the splicing of *DISC1* to the *DISC1FP1* EST AB371558 in lymphoblastoid cell lines

The transcripts for two der 1 *DISC1/DISC1FP1* chimeras, *CP60* and *CP69* that encode DISC1 aa1-597 plus an additional 60 and 69 novel aa from DISC1FP1 have been isolated in t(1;11)-family derived lymphoblastoid cell lines (Eykelenboom *et al*, 2012). The identification of a further *DISC1FP1* EST, AB371588 leads to the possibility that other der1 and der 11 chimeric *DISC1/DISC1FP1* species may arise due to the t(1;11). These novel chimeric species may be detectable as transcripts in t(1;11)-family derived lymphoblastoid cell lines. Using RT-PCR on t(1;11) lymphoblastoid cell lines a novel *DISC1/DISC1FP1* chimeric species named *CP1* has been identified. The *CP1* species is a der 1 chimeric species that is produced by the fusing of chromosome 1 where *DISC1* is located, to chromosome 11 that encodes the *DISC1FP1* EST AB371588, as a result of the translocation. The *CP1* species encodes the der 1 *DISC1* ORF proximal to the translocation which encompasses DISC1 aa1-597 plus an additional amino acid encoded by *DISC1* and AB371588. The additional aa in CP1 that is not present in

`

DISC1 aa1-597 is a glycine, which is a simple uncharged aa. Additionally, DISC1 aa598 is also a glycine, so the *CP1* transcript can be seen to encode DISC1 aa1-598. Given the simple uncharged nature of the glycine encoded at aa598 by *CP1*, it would seem likely that exogenously expressed CP1 protein would behave similarly to exogenously expressed DISC1 aa1-597 protein.

DISC1 aa1-597 has been the subject of extensive research as a dominant negative truncated species as a possible mechanism of pathogenesis in the t(1;11) pedigree. DISC1 aa1-597 has been studied *in vitro* (Brandon *et al*, 2005; Hattori *et al*, 2014; Kamiya *et al*, 2005; Millar *et al*, 2005a; Morris *et al*, 2003; Ozeki *et al*, 2003; Pletnikov *et al*, 2007; Taya *et al*, 2007) and *in vivo* (Hikida *et al*, 2007; Niwa *et al*, 2013; Pletnikov *et al*, 2008). This theory is seen as an alternative though not mutually exclusive explanation of pathogenesis seen in the t(1;11) pedigree to that of the haploinsufficiency of DISC1 (Millar *et al*, 2005b) The identification of endogenous CP1 protein would likely result in the studies into DISC1 aa1-597 being fully accepted into the cannon of DISC1 research relating to the t(1;11) pedigree, such is the similarity between the CP1 and DISC1 aa1-597 species. It may be possible to predict what phenotypic features CP1 would produce when expressed *in vivo* from the features evident in the DN-DISC1 (Hikida *et al*, 2007) and ΔhDISC1 (Pletnikov *et al*, 2008), DISC1 aa1-597 mouse models. Common to both of these models are the features of enlarged lateral ventricles and a reduction in parvalbumin-positive interneurons, therefore, it would be reasonable to predict that a similar phenotype may arise from the *in vivo* expression of CP1 in the human brain.

The corresponding der 11 species resulting from AB371588/*DISC1* cryptic splicing has been previously identified (Eykelenboom *et al*, 2012) and so was not studied here. This transcript contains an ORF encoding a C-terminal DISC1 truncate.

The potential for further novel *DISC1/DISC1FP1* chimeric species exists. Translin-Associated Factor X (TSNAX) plays a role in the neuronal binding and trafficking of RNA (Li *et al*, 2008). The *TSNAX* gene is located upstream of *DISC1*and the intragenic splicing of *TSNAX* to *DISC1* creates several *TSNAX/DISC1* transcripts. (Millar *et al*, 2000a). The majority of the *TSNAX/DISC1* transcripts encode novel exons that insert premature stop codons, separating the *TSNAX* and *DISC1* ORFs (Millar *et al*, 2000a). However, one of the transcripts amplified from *TSNAX* exon 4 is spliced directly to exon 2 of *DISC1* conserving the ORF. Therefore this transcript encodes a potential TSNAX/DISC1 chimeric protein. Furthermore this ORF has been identified as extending to exon 13 of *DISC1* (Millar *et al*, 2000a). In translocation cell

`

lines it is possible that the *DISC1* ORF in this *TSNAX/DISC1* transcript could also splice with *DISC1FP1,* giving rise to the possibility of a *TSNAX/DISC1/DISCFP1* transcripts Interestingly, the *TSNAX/DISC1* transcript with the read-through ORF has been identified in brain tissue (Millar *et al*, 2000a). A later study by Nakata *et al.,* (2009) identifies several *TSNAX/DISC1* transcripts that start at *TSNAX* exon 1. However, these transcripts all include premature stop codons in the ORF that would interrupt the production of a *TSNAX/DISC1* chimeric protein.

More promising for the production of additional der 1 chimeric species are the alternative splice variants of *DISC1* that have been identified in foetal brain tissue (Nakata *et al*, 2009). The *DISC1* alternative splice variant transcripts that could potentially produce novel der 1 *DISC1/DISC1FP1* chimeric species, including: DISC1Δ5Δ6 (lacking exons 5 and 6 and terminating at exon 13); DISC1Δ7Δ8* (lacking DISC1 exons 7 and 8 terminating at exon 9); DISC1Δ7Δ8Δ9 (lacking exons 7-9 terminating at exon 10); DISC1Δ7Δ8Δ9 (lacking exons 7-9 terminating at exon 11); DISC1Δ8 (lacking exon 8 terminating at exon 9) and DISC1Δ8 (lacking DISC1 exon 8 terminating at exon13. Novel der 1 *DISC1/DISC1FP1* chimeric species produced by the cryptic splicing of the ORF of these *DISC1* splice variants to *DISC1FP1* may confer additional aberrant functions and altered protein behaviour arising through the absence of specific *DISC1* exons. Additionally, it is apparent from the work of Nakata *et al.,* (2009) that the various *DISC1* alternatively spliced transcripts would encode a variety of novel der 11 *DISC1/DISC1FP1* transcripts. However it is likely that these species would encode N-terminal truncates of the der 11 *DISC1* ORF of varying length, analogous to the potential der 11 *DISC1* C-terminal truncate detailed in Eykelenboom *et al.*, (2012). This is because on the der11 the *DISC1FP1* ESTs spliced to *DISC1* produce ORFs with multiple upstream stop codons present and the only feasible ORF is internal to the *DISC1* component of the chimeric transcript. To date these experiments to identify der 1 or der 11 *DISC1/DISC1FP1* chimeras produced by *DISC1* alternative spliced variants have not been attempted.

7.3 The exogenous expression of DISC1/DISC1FP1 species in order to characterise possible pathogenic mechanisms operating within the t(1;11) pedigree

Chimeric transcripts encoding *CP60* and *CP69* have been detected in t(1;11)-family derived lymphoblastoid cell lines (Eykelenboom *et al*, 2012) and, until now, both CP60 and CP69 protein have not been studied *in vitro*. Protein products corresponding to the DISC1/DISC1FP1 chimeric species CP60 and CP69 are both isolated in the insoluble pellet

`

fraction and absent in the lysate fraction when assayed by Western blot, in contrast to FLAG-DISC1 which appears in both fractions. It is possible that the localisation of CP60 and CP69 protein to the pellet fraction is indicative of these species possessing novel aberrant properties. Biophysical characterisation of MBP-ΔNCP69, an N-terminal truncated species encoding DISC1 aa326-597 and 69 aa from DISC1FP1, provides further insight into CP60 and CP69 protein. In this species the DISC1 N-terminus is absent as it is predicted to be highly disordered and is known to be difficult to purify (Soares *et al*, 2011). A series of biophysical experiments have compared MBP-ΔNCP69 expression to that of a species encoding DISC1 aa326-597, MBP-ΔN597. From this it is revealed that the addition of a novel 69 aa to DISC1 aa1-597 results in the formation of larger protein assemblies that show increased thermal stability and have a unique secondary structure (Eykelenboom *et al*, 2012). It is possible that the protein assemblies and the secondary structure variation detected confer altered protein behaviour that results in localisation of CP60 and CP69 protein to the pellet.

Qualitative analysis of exogenously expressed FLAG-CP60 and FLAG-CP69 in COS-7 cells using fluorescence microscopy and immunocytochemistry reveals these species to possess a predominantly clustered expression pattern. This is discernible from the punctate expression pattern of FLAG-WT-DISC1 and the diffuse expression pattern of FLAG-DISC1 aa1-597. In contrast, separate immunocytochemistry experiments show that the CP1 species, encoding DISC1 aa1-598, which is extremely similar to DISC1 aa1-597, has the same diffuse expression pattern as DISC1 aa1-597. Therefore the additional novel 60 and 69 DISC1FP1 aa of CP60 and CP69, respectively, confer an altered and novel cellular localisation pattern to these chimeric species.

Qualitative analysis of MitoTracker Red staining aimed to phenotype the mitochondrial morphology of mitochondria in COS-7 cells exogenously expressing the DISC11/DISC1FP1 chimeras CP60 and CP69. In this analysis fewer than 30% of the cells counted expressing FLAG-CP60 and FLAG-CP69 species are visibly stained with MitoTracker dye. In contrast ~95% of the cells expressing either FLAG-WT-DISC1 or DISC1 aa1-597 show mitochondrial staining. The mitochondria in FLAG-CP60 and FLAG-CP69 expressing cells that showed MitoTracker fluorescence displayed a similar clustered morphology to that seen for expression pattern of exogenous FLAG-CP60 and FLAG-CP69. In comparison to this, in both FLAG-WT-DISC1 and FLAG-DISC1 aa1-597 expressing cells, mitochondria were readily visible with MitoTracker Red staining and possess a tubular morphology. A separate, immunocytochemistry experiment in which CP1 was expressed in COS-7 cells and compared to WT-DISC1 and DISC1 aa1-597 exogenous expression has shown that the expression of this

`

DISC1/DISC1FP1 chimeric species is associated with mitochondria that stain with MitoTracker Red and are tubular in appearance. This result is unsurprising given the very high degree of similarity between DISC1 aa1-597 and the CP1 chimeric species.

In order to visualise mitochondria that do not stain with MitoTracker Red, co-staining with antibodies for CVα, a mitochondrial subunit, and for Cytochrome *c*, an inner mitochondrial membrane protein, was attempted in both COS-7 cells and primary cortical neurones. This enabled the visualisation of clustered mitochondria in cells expressing exogenous CP60 and CP69 that did not otherwise show MitoTracker Red fluorescence. It is inferred that the mitochondrial dysfunction evident in cells expressing exogenous CP60 and CP69 likely occurs due to an impairment in the mitochondrial membrane potential, Δψm. This is because MitoTracker Red staining is impaired by the collapse or depolarisation of the membrane potential, Δψm (Buckman *et al,* 2001).

The DISC1/DISC1FP1 chimeras CP1, CP60 and CP69 could potentially be pleiotropically pathogenic. Given the extremely high similarity in the expression of CP1 to DISC1 aa1-597, it is very likely that mechanisms of pathogenesis that have been established for DISC aa1-597 would also result from CP1 expression both *in vivo* and *in vitro* (see previous section). Importantly all three chimeric transcripts encode a DISC1 self-association domain at DISC1 aa403-504 (Kamiya *et al,* 2005). Therefore, CP1, CP60 and CP69 could interact with endogenous DISC1, potentially in a dominant negative manner and additionally form complexes with each other. For CP60 and CP69, both the clustering of the expressed protein and the induced mitochondrial dysfunction are potential mechanisms of pathogenesis. The clustering of the expressed protein may have an effect on the localisation of endogenous DISC1 and/or DISC1 interactors by binding WT-DISC1, it may also be that the clustered protein could potentially form aggregates that are pathogenic. This is as endogenous DISC1 is capable of pathogenic aggregation (Atkin *et al,* 2012). The mitochondrial clustering and the apparent collapse of the mitochondrial potential, Δψm could have a variety of detrimental effects including: the reduction of cellular ATP levels, the disruption of mitochondrial transport, the production of deficits in synaptic signalling, the impairment of action potential generation in neurones and cause generalised deficits in cell growth and development.

`

7.4 Further investigation of the molecular dysfunction resulting from the DISC1/DISC1FP1 chimeric species: FACS analysis of mitochondrial fluorescence in t(1;11) lymphoblastoid cell lines

Given that CP60 and CP69 show impaired staining with the fluorescent mitochondrial dye MitoTracker Red it was proposed to investigate the fluorescence of MitoTracker Red in t(1;11) –family derived lymphoblastoid cell lines. At present the DISC1/DISC1FP1 chimeric proteins have not been isolated in t(1;11) lymphoblastoid cell lines (Eykelenboom *et al*, 2012), but it may be that these species are below the threshold of detection. It is possible that FACS analysis of MitoTracker Red fluorescence in t(1;11)-family derived lymphoblastoid cell lines may be able to detect a reduction in MitoTracker Red fluorescence as a consequence of endogenous DSIC1/DISC1FP1 expression. Such an occurrence might suggest the existence of endogenous DISC1/DISC1FP1 expression. In this series of experiments the experimental replicates of MitoTracker Red stained t(1;11) lymphoblastoid cell lines versus karyotype controls show enough biological independence to justify statistical analysis as separate experiments of n=3. This is due to the biological independence of the three t(1;11) lymphoblastoid cell lines per replicate and the independence in conditions between the cultured flasks of cells (Cumming *et al*, 2007; Lazic, 2010). One of the three experimental replicates performed on the t(1;11) lymphoblastoid cell lines showed a significant reduction in MitoTracker Red fluorescence in comparison to karyotypically normal controls. However, when the three experimental replicates are pooled and analysed as one data set the MitoTracker Red fluorescence in t(1;11) lymphoblastoid cell lines was not found to be significantly different from karyotype controls.

It is possible that the single positive result from an experimental replicate is the result of a practice effect given this experimental replicate was the final series of experimental replicates assayed. It is also possible that the negative result from the pooled data that detects no significant difference in MitoTracker Red fluorescence between t(1;11) lymphoblastoid cell line and karyotype controls is in fact a true result. Further work needs to be done regarding MitoTracker Red florescence and t(1;11) lymphoblastoid cells perhaps using the determination of the mitochondrial membrane potential, $\Delta\psi m$.

`

7.5 Analysis of t(1;11) gene expression microarray data using functional enrichment programs

The assessment of t(1;11)-family derived lymphoblastoid cell lines by gene expression microarray aimed to identify putative pathogenic mechanisms operating within the t(1;11) pedigree via differential gene expression and subsequent analysis by functional enrichment programs. The original unfiltered GOI list was filtered to remove blood specific non-neuronal genes creating a neuronally filtered GOI list that was putatively more brain based. The reasoning behind this being that blood based gene expression can be significantly different to that of brain based gene expression (Cai *et al*, 2010; Rollins *et al*, 2010; Sullivan *et al*, 2006). Lymphoblastoid cell lines were used in the microarray analysis rather than neuronal material as at the time this was the only (t;1;11) material available. As such, the two GOI lists, filtered and unfiltered, were analysed for functional enrichment in parallel.

In the functional enrichment analysis the enrichment of both the cell cycle and immune function and inflammation are highlighted in multiple instances and may serve as novel putative pathogenic mechanisms within the t(1;11) pedigree. The GOTree analysis features an enrichment for a wide variety of categories that are associated with M-phase, that in particular are components of mitosis. In Pathways Commons analysis a broad spectrum of pathways are enriched. This expands upon the cell cycle category enrichments seen in GOTree by highlighting enrichments in all four cell cycle phases, S-phase, G_2-phase, M-phase and G_1-phase, each occurring several times. Importantly the mitotic cell cycle is the most significantly enriched pathway for both GOI lists. In Pathways Commons analysis pathways that have associations with DISC1 are enriched, including the reelin signalling pathway (Andreasen *et al*, 2011) and kinesins (Ogawa *et al*, 2014; Taya *et al*, 2007). Immune function pathways are also enriched in the Pathways Commons analysis, of particular note is the appearance of IL-12-mediated signalling. This cytokine appears to be of relevance to inflammation and immunity in schizophrenia as a trait marker (Miller *et al*, 2011)

The results of the investigation of the t(1;11) microarray data using both KEGG and Wikipathways pathway analysis also focus heavily on cell cycle dysregulation, with the cell cycle pathway enriched in both programs. Disease Association Analysis identifies enrichment pertaining to diseases. Hodgkin's disease appears on the unfiltered GOI analysis and this disease pathway is identified as principally containing genes with a role in immune function. The remaining analysis of the neuronally filtered GOI list has a strong emphasis on immune function and inflammation with the enrichment of bronchitis, bronchiolitis and immune system diseases occurring. Of all of the analysis performed the Disease Association Analysis has the

`

greatest differences in the outputs between the unfiltered GOI list and the neuronally filtered GOI list. For all other functional analysis programs these two lists produce markedly similar results with slight differences in the rankings of p-values for enriched categories.

The dysregulation of the cell cycle evident in the t(1;11) microarray analysis may produce multiple forms of pathogenesis that could in part explain the high incidence of major mental illness in the t(1;11) pedigree. Given that M-phase and specifically the enrichment of mitosis occurs, it is possible that the basal rate of proliferation is altered in t(1;11) lymphoblastoid cell lines which could impact on neurodevelopment and adult brain function if this also occurs, for example, in neural progenitors. There is evidence that neural precursor deficits which could arise from impaired neuronal proliferation, may be associated with depression. The transgenic inhibition of neurogenesis in adult mice reduces the number of precursor cells within the hippocampus and produces a depression-like phenotype (Snyder *et al*, 2011). In humans, evidence from post mortem brain tissue in elderly sufferers of depression, has detected reductions in neuronal precursors within the hippocampus (Lucassen *et al*, 2010). Interestingly, post-mortem examination on brain samples from sufferers of major depressive disorder who underwent antidepressant treatment, reveals a greater number of neuronal progenitors within the dentate gyrus, compared to unmediated sufferers (Boldrini *et al*, 2012; Boldrini *et al*, 2009). This increase in the number of neuronal progenitors was correlated with an increase in dentate gyrus size. In the case of the t(1;11) perigee if alterations to the neural progenitors or neuronal precursors occurred this could consequently reduce the number of newly borne neurones. Given the nature of the genetic insult in the t(1;11) pedigree, this detriment to neurogenesis could potentially occur throughout development.

The alterations to S-phase, G_2-phase, and G_1-phase may be indicative of changes to the length of these phases that has been shown to influence the differential production of proliferating and differentiated cells within the brain (Arai *et al*, 2011; Dehay & Kennedy, 2007; Peco *et al*, 2012). However, at present using pathway analysis alone it is impossible to determine specific spatial or temporal alterations to cell cycle phases. Regarding DISC1 function, DISC1 localises to the centrosome (Bradshaw *et al*, 2008; Kamiya *et al*, 2005; Kamiya *et al*, 2008; Miyoshi *et al*, 2004; Morris *et al*, 2003) which is an enriched category within GOTree. Within the cell cycle it is possible that the binding of DISC1 with DISC1 interactors that possess roles in the cell cycle may be reduced by the haploinsufficiency of DISC1 that occurs in t(1;11) lymphoblastoid cell lines (Millar *et al*, 2005b). This may result in abnormalities in cell cycle mechanisms that affect the dynamics of mitosis. Additionally, the expression of DISC1 aa1-597 in the ΔhDISC1 mouse line results in the dysregulation of several cell cycle genes that are

`

involved in the differentiation of oligodendrocyte precursor cells (Katsel *et al*, 2011). It is possible that the expression of the DISC1/DISC1FP1 species CP1 that is virtually indistinguishable from DISC1 aa1-597 may also affect cell cycle gene expression.

The occurrence of immune function and inflammation associated categories in the functional analysis of the t(1;11) microarray data, highlight these processes as putative mechanisms of pathogenesis in the t(1;11) pedigree. Members of the t(1;11) pedigree have been diagnosed as suffering from schizophrenia, depression or bipolar disorder, all three of these disorders have been linked to immune dysfunction. The meta-analysis of studies into the relationship between mental illness and immunity identify roles for elevated cytokine levels in schizophrenia (Miller *et al*, 2011) depression (Dowlati *et al*, 2010) and bipolar disorder (Modabbernia *et al*, 2013). For schizophrenia an immune function related process that has been identified as a mechanism of pathogenesis is maternal immune activation. This is an established risk factor for schizophrenia and arises due to the foetus being exposed prenatally to infectious agents (Brown & Derkits, 2010). Maternal immune activation has been studied using gene environment modelling on DISC1 transgenic mice (Abazyan *et al*, 2010; Ibi *et al*, 2010; Lipina *et al*, 2013; Nagai *et al*, 2011). The use of the inflammatory agent poly I:C in such modelling frequently modulates the phenotype of the transgenic mice. In 100P mice the prenatal exposure to poly I:C results in the exasperation of a schizophrenia-like phenotype (Lipina *et al*, 2013). Likewise in the DN-DISC mouse line neonatal exposure to poly I:C results in the production of a schizophrenia-like phenotype (Ibi *et al*, 2010; Nagai *et al*, 2011). The maternal immune activation of ΔhDISC1 mice produces a depression/anxiety-like phenotype (Abazyan *et al*, 2010). Additionally the expression of DISC1 aa1-597 in ΔhDISC1 mice alone has been observed to dysregulate the levels of cytokines (Abazyan *et al*, 2010). Therefore the expression of the DISC1/DISC1FP1 species CP1 which is highly similar to DISC1 aa1-597 may also induce the dysregulation of the levels of cytokines.

Maternal immune activation within the t(1;11) pedigree could serve to modulate the phenotype of mental illness by the penetrance of the translocation. However it is unlikely to have occurred with such frequency in the t(1;11) pedigree to explain all of the instances of schizophrenia. At present it requires further investigation to identify the specific molecular underpinning of the enrichment in immune function and inflammation related categories in the t(1:11) gene expression microarray data.

Following the analysis of both the unfiltered and neuronally filtered GOI lists it appears that the unfiltered GOI list may have more utility. This is as the neuronally filtered GOI list is a

`

limited surrogate for a brain derived GOI list. Focusing on data derived from the unfiltered GOI list would only reduce the number of categories that show immune function association and have little effect on the impact of cell cycle dysregulation.

Figure 7.5.A. displays the main putative mechanisms of pathogenesis that have been investigated in this thesis, that are reviewed in this chapter so far, including the cell cycle dysfunction and enrichment of immune function and inflammation evident in the t(1;11) microarray data. The results of the exogenous expression of the DISC1/DISC1FP1 chimeras are also depicted.

7.6 Caveats

To date the DISC1/DISC1FP1 chimeras have only been identified as transcripts. Efforts to identify endogenous DISC1/DISC1FP1 chimeric protein using the DISC1 N-terminal antibody R47 in t(1;11)-family derived lymphoblastoid cell lines have produced a negative result (Eykelenboom *et al*, 2012). The exogenous expression of CP1, CP60 and CP69 in this study indicates these species are likely to have pluripotent mechanisms of pathogenesis. However the endogenous expression of DISC1/DISC1FP1 chimeras must be supported with experimental data in order for these species to be considered a mechanism of pathogenesis within the t(1;11) pedigree. It remains possible that the DISC1/DISC1FP1 chimeras are expressed below the detection threshold of the Western blotting used so far (Eykelenboom *et al*, 2012) and that even at low levels of expression these species could produce detrimental cellular effects. Further research is needed to try to detect these species endogenously in tissue from the t(1;11) pedigree.

In the dysregulation of the cell cycle that is highlighted by multiple pathways analysis programs in the t(1;11) gene expression microarray analysis the various cell cycle phases are enriched and in particular mitosis within M-phase is altered. However the use pathway analysis alone cannot give spatial, temporal or mechanistic data relating to the dysregulation occurring in these phases. As such it is impossible to determine if a given phase has been seen to lengthen or shorten due to differential gene expression. Further research is needed into determining the specific changes that occur to the cell cycle phases to enable more accurate predictions to be made on the phenomena of cell cycle dysregulation within t(1;11) lymphoblastoid cell lines.

`

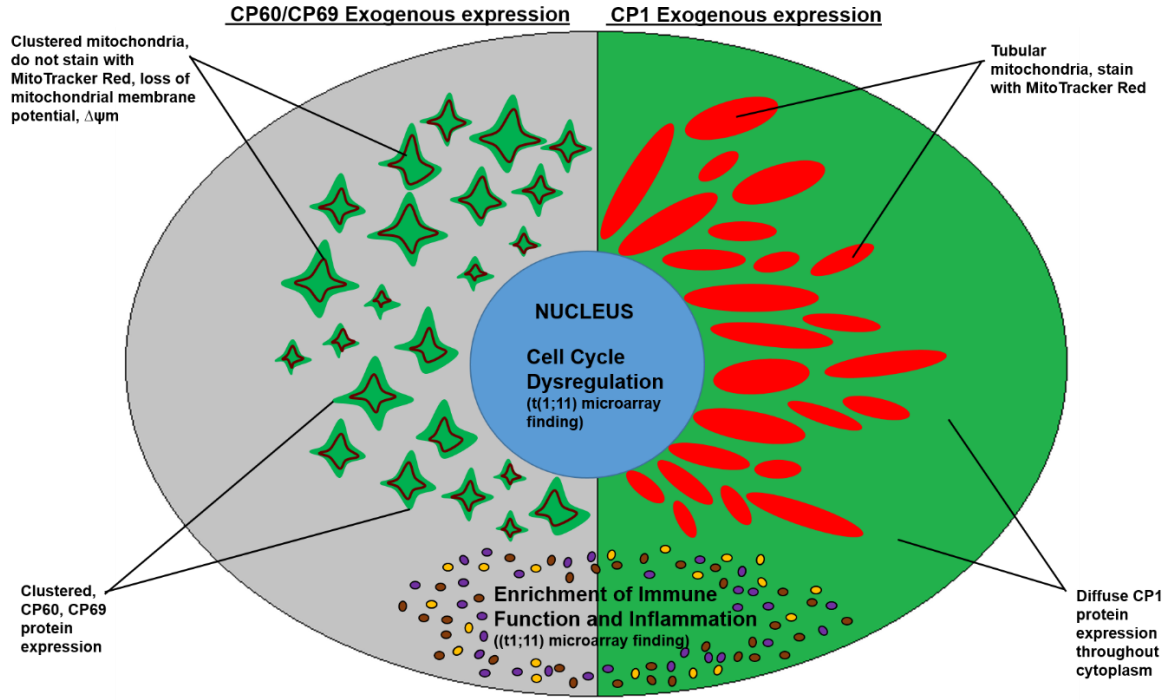

Figure 7.5.A: Putative pathogenic mechanisms that may possibly operate in the t(1;11) pedigree. The effects of exogenous expression of CP60 or CP69 (left), the effects of exogenous CP1 expression (right). DISC1/DISC1FP1 protein (green). Cellular effects derived from functional enrichment analysis of the t(1;11) gene expression microarray as labelled. Dysregulated cytokines (brown, orange and purple ovals).

`

The highlighting of cell cycle dysregulation in functional enrichment analysis could possibly be the result of an intrinsic bias in the pathway enrichment and ontology programs. This is as the databases that support these programs have the tendency to over-represent cancer processes including the cell cycle. Ideally a series of experiments would be implemented to validate the notion of intrinsic cell cycle dysregulation within t(1;11)-derived cell lines.

The use of t(1;11) lymphoblastoid cell lines as a surrogate for neural material in the t(1;11) gene expression microarray may have resulted in a narrower spectrum of enriched pathways being highlighted than would occur had t(1;11) post-mortem brain tissue or iPSC-derived neural material been assayed. The main findings from this work that the cell cycle is dysregulated and that immune function and inflammation is enriched do not represent brain specific pathways *per se*. It is likely that the absence of brain specific pathways in the functional enrichment analysis of the t(1;11) microarray data arises due to the underlying differences in transcript expression between blood and brain (Cai *et al*, 2010; Sullivan *et al*, 2006) rather than as a limitation of the analysis programs used.

7.7 Future work

In order to determine if the DISC1/DISC1FP1 chimeras are expressed endogenously, the ideal experiment would involve post-mortem brain tissue from the t(1;11) pedigree. At present such tissue is not available. However, neural precursors and neurones have been developed from t(1;11)-derived iPSC's. The use of iPSC-derived neurones to investigate neuropsychiatric illness represents a paradigm shift over previous studies, being a more disease relevant model than patient lymphoblastoid cell lines. When assayed with peptide antibodies with epitopes specific to the chimeras, these t(1;11) iPSC's may be a promising avenue of investigation to detect DISC1/DISC1FP1 species endogenously. It is possible that iPSC's driven down a neural differentiation pathway may possess a greater level of expression of the chimeras than that of t(1;11) lymphoblastoid cell lines. In the intervening time since this thesis was initiated, these experiments have been carried out. *DISC1*/*DISC1FP1* chimeric transcripts have been identified in iPSC-derived neurones, but as yet endogenous chimeric proteins have not been detected (JK Millar personal communication).

The work of Nakata *et al.,* (2009) on the identification of alternative DISC1 splice variants suggests that it should be possible to identify additional novel der 1 and der 11 *DISC1/DISC1FP* species *in vitro*. Further RT-PCR on t(1;11)-family derived lymphoblastoid cell lines should be pursued to comprehensively isolate and catalogue the transcripts of these

`

putative chimeras. However, such an investigation should be mindful of the possibility that some of these transcripts may well be transcription errors, as possibly evidenced by the occurrence of premature stop codons within many of these species.

The interaction between DISC1 and the DISC1/DISC1FP1 chimeras could be characterised. Firstly co-immunoprecipitation of WT-DISC1 with CP1, CP60 or CP69 could be performed and analysed by densitometry to address the effect of the DISC1 self-association domain (Kamiya *et al*, 2005) on the binding between these species. It is possible that the additional 60 and 69 aa in CP60 and CP69, respectively, confer altered binding properties with WT-DISC1 to these chimeras. Secondly, immunocytochemistry could be used to investigate how the cellular and mitochondrial phenotypes of the DISC1/DISC1FP1 chimeras present when co-expressed with exogenously expressed WT-DISC1. It is possible dominant-negative effects may be present due to chimeric species expression or that WT-DISC1 may in part ameliorate the pathogenic effects of the chimeras. Finally, the process of characterising interaction of DISC1 interactors with the DISC1/DISC1FP1 chimeras by co-immunoprecipitation and immunocytochemistry could be implemented. This would aim to establish whether further pathogenic interactions occur due to co-expression alongside the chimeric species.

At present, it is unknown if/how CP60 and CP69 expression affects mitochondrial motility. Given the observation the CP60 and CP69 are associated with a reduction in the mitochondrial membrane potential, $\Delta\psi m$, it is possible that the expression of these chimeras would lead to a net movement of mitochondria towards the cell body. This is because there is evidence that mitochondrial movement in the direction of the cell body is favoured by a low membrane potential, $\Delta\psi m$ (Miller & Sheetz, 2004), although this remains controversial. Mitochondrial movement in relation to mitochondrial membrane potential, $\Delta\psi m$ perturbations could be assessed using inducible CP60 and CP69 expression constructs. Cells could be stained with JC-1, a dye which is mitochondrial membrane potential, $\Delta\psi m$ sensitive. Live cell imaging could be performed both pre- and post-induction of expression of the chimeric proteins, to visualise resulting alterations to mitochondrial motility and JC-1 staining.

The mitochondrial mass of cells needs to be corrected for the FACS analysis of t(1;11) lymphoblastoid cell lines stained with MitoTracker Red in order to determine if the negative result in this series of experiments is a true negative. A future experiment could use co-staining with MitoTracker Green, given this dye is non-mitochondrial membrane potential, $\Delta\psi m$ dependent, as a means to identify mitochondrial mass (Pendergrass *et al*, 2004). The ratio of MitoTracker Red: MitoTracker Green fluorescence could then be used to derive the

`

normalised mitochondrial membrane potential, Δψm which is a more robust metric as opposed to that of MitoTracker Red fluorescence alone. In addition to the study of t(1;11) lymphoblastoid cell lines, the mitochondrial membrane potential, Δψm for exogenously expressed CP1 and DISC1 aa1-597 could also be calculated. This work would further characterise the exogenous expression of DISC1/DISC1FP1 chimeras and aid in the interpretation of established immunocytochemistry data.

Regarding the (1;11) microarray, the gene expression changes need to be validated via quantitative RT-PCR. Quantitative measurement of t(1;11) lymphoblastoid cell line protein should also be implemented. This could be achieved by Western blotting and reverse phase protein lysate microarray, when high quality antibodies for species can be found. A mass spectrometry based quantitative proteomics approach could be pursued when suitable antibodies are unavailable.

The specific temporal alterations that may occur to the cell cycle phases highlighted in the analysis of the t(1;11) microarray, could also be investigated. A suitable approach would be to use live cell imaging or FACS analysis to determine the lengths of S-phase, G_2-phase, M-phase and G_1-phase as well as the total cell cycle length in comparison to karyotypically normal controls.

To follow up the t(1;11) microarray result of cell cycle dysfunction, immunofluorescence could be used to detect expression of DISC1 at the centrosome with co-staining of DISC1 interactors within t(1;11) lymphoblastoid cells as well as the visualisation of the kinetochore and the α-tubulin of the mitotic spindle. Specifically, this would aim to investigate if the haploinsufficiency of DISC1 in the t(1;11) lymphoblastoid cells (Millar *et al*, 2005b) causes dysfunction of DISC1 at the centrosome which could in turn possibly perturb cell cycle dynamics.

To investigate the possibility of maternal immune activation as a means to modify the penetrance of the t(1;11), a humanised translocation mouse model could be generated and mice could be treat with the inflammatory agent poly I:C when pregnant. The resulting offspring could be characterised using a range of neurobehavioral assays to determine how maternal immune activation effects the resulting phenotype in comparison to translocation mice that were not exposed to poly I:C *in utero*. It is possible that poly I:C exposed translocation mice would express a unique mental illness-like phenotype as a result of the neonatal activation of inflammatory and immune function pathways.

`

Microarray analysis of t(1;11)-derived iPSC's differentiated down neuronal pathways could be performed as a means to validate the findings of the t(1;11) lymphoblastoid cell line gene expression microarray. Additionally, it is possible that (1;11)-derived neurones would also show novel pathway enrichment to brain specific categories as well as the possible enrichment to the cell cycle, immune function and inflammation.

7.8 Relevance of this thesis to the field

This thesis has investigated the putative pathogenic mechanisms that may result from the t(1;11). Further work is required to build upon and replicate the findings of this study (see section 7.7). However, the results presented in this thesis demonstrate the utility of a family-based approach to investigating the aetiology of major mental illness. Although the t(1;11) is unique to the pedigree studied here, it is possible that the putative mechanisms of pathogenesis identified in this family might also represent risk mechanisms in unrelated sufferers of schizophrenia, bipolar disorder and major depressive disorder. Studies of Alzheimer's disease set a precedent for the use of a family study methodology to identify rare mutations in pedigrees that in turn highlight pathogenic mechanisms, which represent a risk mechanism in ill, non-mutation carrying individuals (Cruchaga *et al*, 2012; Kim *et al*, 2009). For example rare mutations in A Disintegrin and Metalloprotease Domain 10 (ADAM10), a cell surface protein, confer reduced α-secretase activity and increase amyloid-β levels (Kim *et al*, 2009). Possible examples of putative pathogenic mechanisms from this study that may share common pathways and therefore may be translatable to the general population of sufferers with major mental illness are as follows:

The characterisation of DISC1 CP60 and CP69 revealed a clustered mitochondrial phenotype and loss of the mitochondrial membrane potential, $\Delta\psi m$. These observations are supportive of previous studies that establish DISC1 as being predominantly localised to the mitochondria (James *et al*, 2004) and of DISC1 mutants (Millar *et al*, 2005a; Ogawa *et al*, 2014) having involvement in mitochondrial dysfunction as a possible pathophysiological mechanism in major mental illness. It may be that the mitochondrial dysfunction triggered by CP60 and CP69 acts upon common mitochondrial pathways that have been found to be perturbed in individuals neuropsychiatric disorders (Manji *et al*, 2012). Disturbance of mitochondrial pathways has been found to produce defects in synaptic plasticity and alterations to long-term cellular resilience.

Pathway analysis of the t(1;11) microarray highlights an enrichment in immune function and inflammation. It is possible that the t(1;11) pedigree with its broad spectrum of psychiatric

`

phenotypes that has functional enrichment in cytokine abnormalities, may share common biological origins with other studies into major mental illness, immune function and inflammation. It may be that the potential cytokine dysfunction in the t(1;11) pedigree operates within mechanisms of pathogenesis in common with the findings of research into the meta-analysis of immune dysregulation in bipolar disorder (Modabbernia *et al*, 2013), schizophrenia (Miller *et al*, 2011) and major depressive disorder (Miller *et al*, 2009).

Family studies are able to detect rare variants with large effect sizes; in comparison GWAS permits the identification of common sequence and copy number variants, so far with small effect sizes in the field of psychiatry. Family studies and GWAS thus both have a role in identifying genetic variants (Lee *et al*, 2012) within populations, albeit with specificities as to how frequently occurring and how large an effect size a given variant has. A rare variant, such as the t(1;11) would not be detected by GWAS analysis of a large, unrelated population and would contribute to the 'missing hereditability' (Manolio *et al*, 2009). In a family study, the investigation of a relatively homogenous population leads to the enrichment of the variant therefore changes in gene expression arising as a result of the t(1;11) that may be more easily detectable and attributable to the translocation. Moreover, a family-based approach mitigates the issue of population stratification, which plagues GWASs. Additionally, there will also be greater homogeneity with respect to shared environmental effects

In this study, the effects of the t(1;11) translocation were assessed by comparing carriers and non-carriers of the translocation. Translocation carriers were not segregated by clinical diagnosis. The reasoning behind this is that this study sought to address mechanisms of putative pathogenesis within the t(1;11) pedigree that are common to the various psychiatric diagnoses observed in the family. Furthermore, there is epidemiological evidence for aetiological overlap between bipolar disorder and schizophrenia (Lichtenstein *et al*, 2009) as well as evidence from GWAS regarding shared loci between psychiatric disorders (Consortium, 2013; Purcell *et al*, 2009a). By studying all t(1;11) carriers together, regardless of diagnosis, this study has attempted to identify the common biological mechanisms that act upstream of clinically distinct psychiatric disorders. Were the t(1;11) microarray data to be segregated by diagnosis, which would only be possible for schizophrenia and major depressive disorder as a bipolar sample size is too small, it might be the case that differential effects in the enrichment of immune function and inflammation may be apparent. For example, individuals with schizophrenia (Miller *et al*, 2011) may show an altered profile of cytokine enrichment compared to sufferers of major depressive disorder (Dowlati *et al*, 2010). It is also possible that differences in immune function an inflammation by diagnosis could be mediated

`

my variation in the MHC locus. The MHC locus has frequently been enriched in schizophrenia GWAS (Consortium & 2, 2012; Consortium, 2011; Hamshere *et al*, 2012; Lencz *et al*, 2013; Purcell *et al*, 2009b; Ripke *et al*, 2013a; Shi *et al*, 2009; Stefansson *et al*, 2009; Yue *et al*, 2011) and has not shown significant enrichment in GWAS Mega-analysis for major depressive disorder (Ripke *et al*, 2013b). Additionally, a recent schizophrenia GWAS detected the enrichment of immune function enhancers as causal variants, with greatest enrichment occurring to B-cell lineages expressing CD19 and CD20 (Consortium, 2014). This finding was present even when the MHC locus was removed from analysis by filtering. However the analysis of t(1;11) pedigree associated data by diagnosis is beyond the scope of this thesis, but could be focus for future research. In addition to this, it is possible that the varying presentations of psychiatric illness in the t(1;11) pedigree are in part the result of different environmental contributions in conjunction with the genetic insult. It would be impossible to mimic these deleterious environmental influences in lymphoblastoid cell lines or iPSC's.

7.9 Relevance of this thesis to other studies into DISC1/DISC1FP1 chimeric species

Regarding studies by others into the pathophysiology of DISC1/DISC1FP1 chimeras, firstly, two studies that have emerged since the experiments in this thesis were completed, that also observe that the CP60 species localises predominantly to the pellet fraction in Western blotting (Ji *et al*, 2014; Zhou *et al*, 2010). Secondly, a transgenic mouse model that expresses both CP60 and the der 11 C-terminal DISC1 truncate has been devised (Ji *et al*, 2014). This mouse model predominantly shows deficits in translation and a reduction in rRNA levels as well as a decrease in the reduction of MTT. It could be hypothesised from the *in vitro* expression of CP60 that the resultant mitochondrial dysfunction may have made this species embryonically lethal *in vivo*. The transgenic mice may be viable due to the *in vivo* expression of CP60 being markedly lower than the *in vitro* overexpression, therefore producing damaging but not fatal molecular and cellular insults. However, alternatively it may be that the phenotype of these animals is modulated by the co-expression of the C-terminal DISC1 truncate. Additionally, at present this mouse model has not been directly phenotyped for mitochondrial pathologies, so the observations from the *in vitro* findings of clustered mitochondria and an inferred loss of the mitochondrial membrane potential, $\Delta\psi m$, observed in this study cannot as yet be confirmed *in vivo*. Although, the authors suggest that the decrease in the reduction of MTT and associated reduction in NADPH oxidoreductase function has the potential to be associated with a reduction in cellular ATP. The authors theorise that this could be comparable to the effects of

`

the loss of the mitochondrial membrane potential, Δψm observed with the exogenous expression of CP60 and CP69 *in vitro* as seen in Eykelenboom *et al.,* (2012).

Recently it has been observed that an internal ORF in *Boymaw* encodes a 7kDa protein (Ji *et al*, 2015). 59 of the 63aa in this species are present in CP60. Importantly, the Boymaw protein exhibits mitochondrial targeting, which may account for part of the mechanism of mitochondrial pathogenesis mediated by CP60 and CP69.

7.10 Final Comments

The study of the t(1;11) pedigree permits investigation into the mechanisms by which a rare genetic lesion increases risk for a spectrum of psychiatric conditions. In this thesis, putative pathogenic mechanisms have been identified that might contribute to the high incidence of mental illness seen in the t(1;11) pedigree. These mechanisms include mitochondrial dysfunction, abnormal cellular protein localisation, perturbation of the cell cycle and dysregulation of immune function and inflammation. Further work is now required to extend the present results. It is essential that efforts are made to ascertain the presence of chimeric protein species in t(1:11) tissue. The putative pathogenic mechanisms identified in this thesis may also contribute to the onset of schizophrenia, bipolar disorder and major depressive disorder in individuals who do not possess the translocation. Therefore the study into the molecular pathogenesis within the t(1;11) pedigree may be informative as to mechanisms of psychiatric illness in the general population. Ultimately, the work presented in this thesis may result in improved understanding of the aetiology of these conditions, which in turn might lead to improvements in treatment.

`

References

Abazyan B, Nomura J, Kannan G, Ishizuka K, Tamashiro KL, Nucifora F, Pogorelov V, Ladenheim B, Yang C, Krasnova IN, Cadet JL, Pardo C, Mori S, Kamiya A, Vogel MW, Sawa A, Ross CA, Pletnikov MV (2010) Prenatal interaction of mutant DISC1 and immune activation produces adult psychopathology. *Biological psychiatry* **68:** 1172-1181

Achim AM, Maziade M, Raymond É, Olivier D, Mérette C, Roy M-A (2011) How prevalent are anxiety disorders in schizophrenia? A meta-analysis and critical review on a significant association. *Schizophrenia bulletin* **37:** 811-821

Aggarwal BB, Gupta SC, Kim JH (2012) Historical perspectives on tumor necrosis factor and its superfamily: 25 years later, a golden journey. *Blood* **119:** 651-665

Alberts B, Johnson A, Lewis J, Raff M, Roberts K, Walter P (2008) *Molecular Biology of the Cell*, 5th edn. New York, NY: Garland Science.

Altman S, Haeri S, Cohen LJ, Ten A, Barron E, Galynker II, Duhamel KN (2006) Predictors of relapse in bipolar disorder: a review. *Journal of Psychiatric Practice®* **12:** 269-282

Ameri K, Harris AL (2008) Activating transcription factor 4. *The international journal of biochemistry & cell biology* **40**: 14-21

An J, Shi J, He Q, Lui K, Liu Y, Huang Y, Sheikh MS (2012) CHCM1/CHCHD6, novel mitochondrial protein linked to regulation of mitofilin and mitochondrial cristae morphology. In *J Biol Chem* Vol. 287, pp 7411-7426. United States

Andreasen NC, Wilcox MA, Ho B-C, Epping E, Ziebell S, Zeien E, Weiss B, Wassink T (2011) Statistical epistasis and progressive brain change in schizophrenia: an approach for examining the relationships between multiple genes. *Molecular psychiatry* **17:** 1093-1102

Andreazza AC, Shao L, Wang J-F, Young LT (2010) Mitochondrial complex I activity and oxidative damage to mitochondrial proteins in the prefrontal cortex of patients with bipolar disorder. *Archives of general psychiatry* **67:** 360-368

Arai Y, Pulvers JN, Haffner C, Schilling B, Nüsslein I, Calegari F, Huttner WB (2011) Neural stem and progenitor cells shorten S-phase on commitment to neuron production. *Nature communications* **2:** 154

Arguello PA, Gogos JA (2006) Modeling madness in mice: one piece at a time. *Neuron* **52:** 179-196

Arion D, Unger T, Lewis DA, Levitt P, Mirnics K (2007) Molecular evidence for increased expression of genes related to immune and chaperone function in the prefrontal cortex in schizophrenia. *Biological psychiatry* **62:** 711-721

Arnone D, McIntosh A, Tan G, Ebmeier K (2008) Meta-analysis of magnetic resonance imaging studies of the corpus callosum in schizophrenia. *Schizophrenia research* **101:** 124-132

Arseneault L, Cannon M, Poulton R, Murray R, Caspi A, Moffitt TE (2002) Cannabis use in adolescence and risk for adult psychosis: longitudinal prospective study. *Bmj* **325:** 1212-1213

`

Atkin TA, Brandon NJ, Kittler JT (2012) Disrupted in Schizophrenia 1 forms pathological aggresomes that disrupt its function in intracellular transport. *Human molecular genetics* **21:** 2017-2018

Atkin TA, MacAskill AF, Brandon NJ, Kittler JT (2011) Disrupted in Schizophrenia-1 regulates intracellular trafficking of mitochondria in neurons. *Mol Psychiatry* **16:** 122-124

Attwooll C, Denchi EL, Helin K (2004) The E2F family: specific functions and overlapping interests. *The EMBO journal* **23:** 4709-4716

Austin C, Ky B, Ma L, Morris J, Shughrue P (2004) Expression of Disrupted-In-Schizophrenia-1, a schizophrenia-associated gene, is prominent in the mouse hippocampus throughout brain development. *Neuroscience* **124:** 3-10

Austin CP, Ma L, Ky B, Morris JA, Shughrue PJ (2003) DISC1 (Disrupted in Schizophrenia-1) is expressed in limbic regions of the primate brain. *Neuroreport* **14:** 951-954

Ayhan Y, Abazyan B, Nomura J, Kim R, Ladenheim B, Krasnova IN, Sawa A, Margolis RL, Cadet JL, Mori S, Vogel MW, Ross CA, Pletnikov MV (2011) Differential effects of prenatal and postnatal expressions of mutant human DISC1 on neurobehavioral phenotypes in transgenic mice: evidence for neurodevelopmental origin of major psychiatric disorders. *Mol Psychiatry* **16:** 293-306

Baek JH, Eisner LR, Nierenberg AA (2013) Smoking and suicidality in subjects with bipolar disorder: results from the National Epidemiologic Survey on Alcohol and Related Conditions (NESARC). *Depression and anxiety* **30**: 982-990

Benard G, Rossignol R (2008) Ultrastructure of the mitochondrion and its bearing on function and bioenergetics. *Antioxidants & redox signaling* **10:** 1313-1342

Benes FM, Lim B, Subburaju S (2009) Site-specific regulation of cell cycle and DNA repair in post-mitotic GABA cells in schizophrenic versus bipolars. *Proceedings of the National Academy of Sciences* **106:** 11731-11736

Bernstein H-G, Jauch E, Dobrowolny H, Mawrin C, Steiner J, Bogerts B (2015) Increased density of DISC1-immunoreactive oligodendroglial cells in fronto-parietal white matter of patients with paranoid schizophrenia. *European archives of psychiatry and clinical neuroscience*: 1 10

Bettencourt-Dias M, Glover DM (2007) Centrosome biogenesis and function: centrosomics brings new understanding. *Nature Reviews Molecular Cell Biology* **8:** 451-463

Blackwood D (2000) P300, a state and a trait marker in schizophrenia. *The Lancet* **355:** 771-772

Blackwood DH, Fordyce A, Walker MT, St Clair DM, Porteous DJ, Muir WJ (2001) Schizophrenia and affective disorders--cosegregation with a translocation at chromosome 1q42 that directly disrupts brain-expressed genes: clinical and P300 findings in a family. *American journal of human genetics* **69:** 428-433

Blalock JE, Smith EM (2007) Conceptual development of the immune system as a sixth sense. *Brain, behavior, and immunity* **21:** 23-33

`

Bloom DE, Cafiero E, Jané-Llopis E, Abrahams-Gessel S, Bloom LR, Fathima S, Feigl AB, Gaziano T, Hamandi A, Mowafi M. (2012) The global economic burden of noncommunicable diseases. Program on the Global Demography of Aging.

Boldrini M, Hen R, Underwood MD, Rosoklija GB, Dwork AJ, Mann JJ, Arango V (2012) Hippocampal angiogenesis and progenitor cell proliferation are increased with antidepressant use in major depression. *Biological psychiatry* **72:** 562-571

Boldrini M, Underwood MD, Hen R, Rosoklija GB, Dwork AJ, Mann JJ, Arango V (2009) Antidepressants increase neural progenitor cells in the human hippocampus. *Neuropsychopharmacology* **34:** 2376-2389

Bord L, Wheeler J, Paek M, Saleh M, Lyons-Warren A, Ross CA, Sawamura N, Sawa A (2006) Primate disrupted-in-schizophrenia-1 (DISC1): high divergence of a gene for major mental illnesses in recent evolutionary history. *Neuroscience research* **56:** 286-293

Bradshaw NJ, Christie S, Soares DC, Carlyle BC, Porteous DJ, Millar JK (2009) NDE1 and NDEL1: multimerisation, alternate splicing and DISC1 interaction. *Neuroscience letters* **449:** 228-233

Bradshaw NJ, Ogawa F, Antolin-Fontes B, Chubb JE, Carlyle BC, Christie S, Claessens A, Porteous DJ, Millar JK (2008) DISC1, PDE4B, and NDE1 at the centrosome and synapse. *Biochemical and biophysical research communications* **377:** 1091-1096

Bradshaw NJ, Porteous DJ (2012) DISC1-binding proteins in neural development, signalling and schizophrenia. In *Neuropharmacology* Vol. 62, pp 1230-1241. England: 2011 Elsevier Ltd

Brandon N, Handford E, Schurov I, Rain J-C, Pelling M, Duran-Jimeniz B, Camargo L, Oliver K, Beher D, Shearman M (2004) Disrupted in Schizophrenia 1 and Nudel form a neurodevelopmentally regulated protein complex: implications for schizophrenia and other major neurological disorders. *Molecular and Cellular Neuroscience* **25:** 42-55

Brandon NJ, Millar JK, Korth C, Sive H, Singh KK, Sawa A (2009) Understanding the role of DISC1 in psychiatric disease and during normal development. *The Journal of Neuroscience* **29:** 12768-12775

Brandon NJ, Schurov I, Camargo LM, Handford EJ, Duran-Jimeniz B, Hunt P, Millar JK, Porteous DJ, Shearman MS, Whiting PJ (2005) Subcellular targeting of DISC1 is dependent on a domain independent from the Nudel binding site. *Molecular and cellular neurosciences* **28:** 613-624

Brietzke E, Mansur RB, Soczynska J, Powell AM, McIntyre RS (2012) A theoretical framework informing research about the role of stress in the pathophysiology of bipolar disorder. *Prog Neuropsychopharmacol Biol Psychiatry* **39:** 1-8

Brietzke E, Stertz L, Fernandes BS, Kauer-Sant'Anna M, Mascarenhas M, Escosteguy Vargas A, Chies JA, Kapczinski F (2009) Comparison of cytokine levels in depressed, manic and euthymic patients with bipolar disorder. *Journal of affective disorders* **116:** 214-217

`

Bromet E, Andrade LH, Hwang I, Sampson NA, Alonso J, de Girolamo G, de Graaf R, Demyttenaere K, Hu C, Iwata N (2011) Cross-national epidemiology of DSM-IV major depressive episode. *BMC Medicine* **9:** 90

Brown AS, Derkits EJ (2010) Prenatal infection and schizophrenia: a review of epidemiologic and translational studies. *The American journal of psychiatry* **167:** 261-280

Brown AS, Hooton J, Schaefer CA, Zhang H, Petkova E, Babulas V, Perrin M, Gorman JM, Susser ES (2004) Elevated maternal interleukin-8 levels and risk of schizophrenia in adult offspring. *American Journal of Psychiatry* **161:** 889-895

Brown AS, Schaefer CA, Wyatt RJ, Begg MD, Goetz R, Bresnahan MA, Harkavy-Friedman J, Gorman JM, Malaspina D, Susser ES (2002) Paternal age and risk of schizophrenia in adult offspring. *American Journal of Psychiatry* **159:** 1528-1533

Brunelin J, Fecteau S, Suaud-Chagny MF (2013) Abnormal striatal dopamine transmission in schizophrenia. *Current medicinal chemistry* **20:** 397-404

Brunswick DJ, Amsterdam JD, Mozley PD, Newberg A (2003) Greater availability of brain dopamine transporters in major depression shown by [99mTc] TRODAT-1 SPECT imaging. *American Journal of Psychiatry* **160:** 1836-1841

Bubeníková-Valešová V, Horáček J, Vrajova M, Höschl C (2008) Models of schizophrenia in humans and animals based on inhibition of NMDA receptors. *Neuroscience & Biobehavioral Reviews* **32:** 1014-1023

Buckman JF, Hernandez H, Kress GJ, Votyakova TV, Pal S, Reynolds IJ (2001) MitoTracker labeling in primary neuronal and astrocytic cultures: influence of mitochondrial membrane potential and oxidants. *J Neurosci Methods* **104:** 165-176

Buka SL, Cannon TD, Torrey EF, Yolken RH, Disorders CSGotPOoSP (2008) Maternal exposure to herpes simplex virus and risk of psychosis among adult offspring. *Biological psychiatry* **63:** 809-815

Buka SL, Tsuang MT, Torrey EF, Klebanoff MA, Wagner RL, Yolken RH (2001) Maternal cytokine levels during pregnancy and adult psychosis. *Brain, behavior, and immunity* **15:** 411-420

Burmeister M, McInnis MG, Zöllner S (2008) Psychiatric genetics: progress amid controversy. *Nature Reviews Genetics* **9:** 527-540

Cai C, Langfelder P, Fuller TF, Oldham MC, Luo R, van den Berg LH, Ophoff RA, Horvath S (2010) Is human blood a good surrogate for brain tissue in transcriptional studies? *BMC genomics* **11:** 589

Calegari F, Huttner WB (2003) An inhibition of cyclin-dependent kinases that lengthens, but does not arrest, neuroepithelial cell cycle induces premature neurogenesis. *Journal of cell science* **116:** 4947-4955

`

Camargo L, Collura V, Rain J, Mizuguchi K, Hermjakob H, Kerrien S, Bonnert T, Whiting P, Brandon N (2006) Disrupted in Schizophrenia 1 Interactome: evidence for the close connectivity of risk genes and a potential synaptic basis for schizophrenia. *Molecular psychiatry* **12:** 74-86

Cannon M, Jones PB, Murray RM (2002) Obstetric complications and schizophrenia: historical and meta-analytic review. *American Journal of Psychiatry* **159:** 1080-1092

Cardno AG, Gottesman II (2000) Twin studies of schizophrenia: from bow-and-arrow concordances to star wars Mx and functional genomics. *American journal of medical genetics* **97:** 12-17

Cardno AG, Rijsdijk FV, Sham PC, Murray RM, McGuffin P (2002) A twin study of genetic relationships between psychotic symptoms. *The American journal of psychiatry* **159:** 539-545

Cardoso BM, Sant'Anna MK, Dias VV, Andreazza AC, Ceresér KM, Kapczinski F (2008) The impact of co-morbid alcohol use disorder in bipolar patients. *Alcohol* **42**: 451-457

Carrà G, Bartoli F, Crocamo C, Brady KT, Clerici M (2014) Attempted suicide in people with co-occurring bipolar and substance use disorders: systematic review and meta-analysis. *Journal of affective disorders* **167**: 125-135

Cataldo AM, McPhie DL, Lange NT, Punzell S, Elmiligy S, Nancy ZY, Froimowitz MP, Hassinger LC, Menesale EB, Sargent LW (2010) Abnormalities in mitochondrial structure in cells from patients with bipolar disorder. *The American journal of pathology* **177:** 575-585

Cazzullo C, Sacchetti E, Galluzzo A, Panariello A, Colombo F, Zagliani A, Clerici M (2001) Cytokine profiles in drug-naive schizophrenic patients. *Schizophrenia research* **47:** 293-298

Cerami EG, Gross BE, Demir E, Rodchenkov I, Babur Ö, Anwar N, Schultz N, Bader GD, Sander C (2011) Pathway Commons, a web resource for biological pathway data. *Nucleic acids research* **39:** D685-D690

Chan DC (2006) Mitochondrial fusion and fission in mammals. *Annu Rev Cell Dev Biol* **22:** 79-99

Chandran JS, Kazanis I, Clapcote SJ, Ogawa F, Millar JK, Porteous DJ (2014) Disc1 variation leads to specific alterations in adult neurogenesis. *PloS one* **9:** e108088

Cheeseman IM (2014) The kinetochore. *Cold Spring Harbor perspectives in biology* **6:** a015826

Chen F, Wegener G, Madsen TM, Nyengaard JR (2013) Mitochondrial plasticity of the hippocampus in a genetic rat model of depression after antidepressant treatment. *Synapse* **67:** 127-134

Chen LB (1988) Mitochondrial membrane potential in living cells. *Annual review of cell biology* **4:** 155-181

Chubb JE, Bradshaw NJ, Soares DC, Porteous DJ, Millar JK (2008) The DISC locus in psychiatric illness. *Mol Psychiatry* **13:** 36-64

`

Chudal R, Sourander A, Polo-Kantola P, Hinkka-Yli-Salomaki S, Lehti V, Sucksdorff D, Gissler M, Brown AS (2014) Perinatal factors and the risk of bipolar disorder in Finland. *J Affect Disord* **155:** 75-80

Clapcote SJ, Lipina TV, Millar JK, Mackie S, Christie S, Ogawa F, Lerch JP, Trimble K, Uchiyama M, Sakuraba Y (2007) Behavioral Phenotypes of< i> Disc1</i> Missense Mutations in Mice. *Neuron* **54:** 387-402

Collins PY, Patel V, Joestl SS, March D, Insel TR, Daar AS, Bordin IA, Costello EJ, Durkin M, Fairburn C (2011) Grand challenges in global mental health. *Nature* **475:** 27-30

Consortium C-DGotPG (2013) Identification of risk loci with shared effects on five major psychiatric disorders: a genome-wide analysis. *The Lancet* **381:** 1371-1379

Consortium ISG, 2 WTCCC (2012) Genome-wide association study implicates HLA-C* 01: 02 as a risk factor at the major histocompatibility complex locus in schizophrenia. *Biological psychiatry* **72:** 620

Consortium SPG-WAS (2011) Genome-wide association study identifies five new schizophrenia loci. *Nature genetics* **43:** 969-976

Consortium SWGotPG (2014) Biological insights from 108 schizophrenia-associated genetic loci. *Nature* **511:** 421-427

Corcoran C, Walker E, Huot R, Mittal V, Tessner K, Kestler L, Malaspina D (2003) The stress cascade and schizophrenia: etiology and onset. *Schizophrenia bulletin* **29:** 671-692

Corvin A, O'MAHONY E, O'REGAN M, Comerford C, O'CONNELL R, Craddock N, Gill M (2001) Cigarette smoking and psychotic symptoms in bipolar affective disorder. *The British Journal of Psychiatry* **179**: 35-38

Costa RH (2005) FoxM1 dances with mitosis. *Nature cell biology* **7:** 108-110

Couture SM, Penn DL, Roberts DL (2006) The functional significance of social cognition in schizophrenia: a review. *Schizophrenia bulletin* **32:** S44-S63

Coyle JT (2012) NMDA receptor and schizophrenia: a brief history. *Schizophrenia bulletin* **38:** 920-926

Craddock N, O'donovan M, Owen M (2005) The genetics of schizophrenia and bipolar disorder: dissecting psychosis. *Journal of Medical Genetics* **42:** 193-204

Craddock N, Sklar P (2013) Genetics of bipolar disorder. *The Lancet* **381:** 1654-1662

Crosby ME, Almasan A (2004) Review Opposing Roles of E2Fs in Cell Proliferation and Death. *Cancer biology & therapy* **3:** 1208-1211

Cruchaga C, Chakraverty S, Mayo K, Vallania FL, Mitra RD, Faber K, Williamson J, Bird T, Diaz-Arrastia R, Foroud TM (2012) Rare variants in APP, PSEN1 and PSEN2 increase risk for AD in late-onset Alzheimer's disease families. *PloS one* **7:** e31039

`

Cumming G, Fidler F, Vaux DL (2007) Error bars in experimental biology. *The Journal of cell biology* **177:** 7-11

D'Arcangelo G (2014) Reelin in the Years: Controlling Neuronal Migration and Maturation in the Mammalian Brain. *Advances in Neuroscience* **2014**

de Jong S, Boks MP, Fuller TF, Strengman E, Janson E, de Kovel CG, Ori AP, Vi N, Mulder F, Blom JD (2012) A gene co-expression network in whole blood of schizophrenia patients is independent of antipsychotic-use and enriched for brain-expressed genes. *PloS one* **7:** e39498

De Oliveira L, Fraga DB, De Luca RD, Canever L, Ghedim FV, Matos MPP, Streck EL, Quevedo J, Zugno AI (2011) Behavioral changes and mitochondrial dysfunction in a rat model of schizophrenia induced by ketamine. *Metabolic brain disease* **26:** 69-77

Dehay C, Kennedy H (2007) Cell-cycle control and cortical development. *Nature Reviews Neuroscience* **8:** 438-450

Delettre C, Lenaers G, Griffoin J-M, Gigarel N, Lorenzo C, Belenguer P, Pelloquin L, Grosgeorge J, Turc-Carel C, Perret E (2000) Nuclear gene OPA1, encoding a mitochondrial dynamin-related protein, is mutated in dominant optic atrophy. *Nature genetics* **26:** 207-210

Devon RS, Evans KL, Maule JC, Christie S, Anderson S, Brown J, Shibasaki Y, Porteous DJ, Brookes AJ (1997) Novel transcribed sequences neighbouring a translocation breakpoint associated with schizophrenia. *American journal of medical genetics* **74:** 82-90

Di Fiore B, Pines J (2008) Defining the role of Emi1 in the DNA replication-segregation cycle. *Chromosoma* **117:** 333-338

Dowlati Y, Herrmann N, Swardfager W, Liu H, Sham L, Reim EK, Lanctôt KL (2010) A meta-analysis of cytokines in major depression. *Biological psychiatry* **67:** 446-457

Eaton WW, Chen CY, Bromet EJ (2011) Epidemiology of schizophrenia. *Textbook in Psychiatric Epidemiology, Third Edition***:** 263-287

Ehses S, Raschke I, Mancuso G, Bernacchia A, Geimer S, Tondera D, Martinou JC, Westermann B, Rugarli EI, Langer T (2009) Regulation of OPA1 processing and mitochondrial fusion by m-AAA protease isoenzymes and OMA1. *The Journal of cell biology* **187:** 1023-1036

Elmore S (2007) Apoptosis: a review of programmed cell death. *Toxicologic pathology* **35:** 495-516

Engelmann D, Putzer BM (2012) The dark side of E2F1: in transit beyond apoptosis. *Cancer research* **72:** 571-575

Enomoto A, Asai N, Namba T, Wang Y, Kato T, Tanaka M, Tatsumi H, Taya S, Tsuboi D, Kuroda K (2009) Roles of disrupted-in-schizophrenia 1-interacting protein girdin in postnatal development of the dentate gyrus. *Neuron* **63:** 774-787

Etain B, Henry C, Bellivier F, Mathieu F, Leboyer M (2008) Beyond genetics: childhood affective trauma in bipolar disorder. *Bipolar disorders* **10:** 867-876

`

Evans KL, Brown J, Shibasaki Y, Devon RS, He L, Arveiler B, Christie S, Maule JC, Baillie D, Slorach EM, *et al*. (1995) A contiguous clone map over 3 Mb on the long arm of chromosome 11 across a balanced translocation associated with schizophrenia. *Genomics* **28:** 420-428

Eykelenboom JE, Briggs GJ, Bradshaw NJ, Soares DC, Ogawa F, Christie S, Malavasi EL, Makedonopoulou P, Mackie S, Malloy MP, Wear MA, Blackburn EA, Bramham J, McIntosh AM, Blackwood DH, Muir WJ, Porteous DJ, Millar JK (2012) A t(1;11) translocation linked to schizophrenia and affective disorders gives rise to aberrant chimeric DISC1 transcripts that encode structurally altered, deleterious mitochondrial proteins. *Human molecular genetics* **21:** 3374-3386

Fan Y, Abrahamsen G, McGrath JJ, Mackay-Sim A (2012) Altered cell cycle dynamics in schizophrenia. *Biological psychiatry* **71:** 129-135

Farren CK, Hill KP, Weiss RD (2012) Bipolar disorder and alcohol use disorder: a review. *Current psychiatry reports* **14**: 659-666

Fatemi SH, Kroll JL, Stary JM (2001) Altered levels of Reelin and its isoforms in schizophrenia and mood disorders. *Neuroreport* **12:** 3209-3215

Féron F, Perry C, Hirning M, McGrath J, Mackay-Sim A (1999) Altered adhesion, proliferation and death in neural cultures from adults with schizophrenia. *Schizophrenia research* **40:** 211-218

Ferreira MA, O'Donovan MC, Meng YA, Jones IR, Ruderfer DM, Jones L, Fan J, Kirov G, Perlis RH, Green EK (2008) Collaborative genome-wide association analysis supports a role for ANK3 and CACNA1C in bipolar disorder. *Nature genetics* **40:** 1056-1058

Fillman S, Cloonan N, Catts V, Miller L, Wong J, McCrossin T, Cairns M, Weickert C (2012) Increased inflammatory markers identified in the dorsolateral prefrontal cortex of individuals with schizophrenia. *Molecular psychiatry* **18:** 206-214

Fink AL (2005) Natively unfolded proteins. *Current opinion in structural biology* **15:** 35-41

Fletcher JM, Evans K, Baillie D, Byrd P, Hanratty D, Leach S, Julier C, Gosden JR, Muir W, Porteous DJ, *et al*. (1993) Schizophrenia-associated chromosome 11q21 translocation: identification of flanking markers and development of chromosome 11q fragment hybrids as cloning and mapping resources. *American journal of human genetics* **52:** 478-490

Flint J, Kendler KS (2014) The genetics of major depression. *Neuron* **81:** 484-503

Flynn S, Lang D, Mackay A, Goghari V, Vavasour I, Whittall K, Smith G, Arango V, Mann J, Dwork A (2003) Abnormalities of myelination in schizophrenia detected in vivo with MRI, and post-mortem with analysis of oligodendrocyte proteins. *Molecular psychiatry* **8:** 811-820

Folsom TD, Fatemi SH (2013) The involvement of Reelin in neurodevelopmental disorders. *Neuropharmacology* **68:** 122-135

Forbes N, Carrick L, McIntosh A, Lawrie S (2009) Working memory in schizophrenia: a meta-analysis. *Psychological medicine* **39:** 889

`

Frey BN, Martins MR, Petronilho FC, Dal-Pizzol F, Quevedo J, Kapczinski F (2006) Increased oxidative stress after repeated amphetamine exposure: possible relevance as a model of mania. *Bipolar disorders* **8:** 275-280

Frodl T, Carballedo A, Hughes MM, Saleh K, Fagan A, Skokauskas N, McLoughlin DM, Meaney J, O'Keane V, Connor TJ (2012) Reduced expression of glucocorticoid-inducible genes GILZ and SGK-1: high IL-6 levels are associated with reduced hippocampal volumes in major depressive disorder. *Transl Psychiatry* **2:** e88

Fujimoto T, Nakano T, Takano T, Hokazono Y, Asakura T, Tsuji T (1992) Study of chronic schizophrenics using 31P magnetic resonance chemical shift imaging. *Acta psychiatrica scandinavica* **86:** 455-462

Fukuda S, Hashimoto R, Ohi K, Yamaguti K, Nakatomi Y, Yasuda Y, Kamino K, Takeda M, Tajima S, Kuratsune H (2010a) A functional polymorphism in the disrupted-in schizophrenia 1 gene is associated with chronic fatigue syndrome. *Life sciences* **86:** 722-725

Fukuda T, Sugita S, Inatome R, Yanagi S (2010b) CAMDI, a novel disrupted in schizophrenia 1 (DISC1)-binding protein, is required for radial migration. *Journal of Biological Chemistry* **285:** 40554-40561

Garbett K, Gal-Chis R, Gaszner G, Lewis DA, Mirnics K (2008) Transcriptome alterations in the prefrontal cortex of subjects with schizophrenia who committed suicide. *Neuropsychopharmacol Hung* **10:** 9-14

Garcia-Rizo C, Fernandez-Egea E, Oliveira C, Justicia A, Bernardo M, Kirkpatrick B (2012) Inflammatory markers in antipsychotic-naïve patients with nonaffective psychosis and deficit vs. nondeficit features. *Psychiatry research* **198:** 212-215

Gardiner EJ, Cairns MJ, Liu B, Beveridge NJ, Carr V, Kelly B, Scott RJ, Tooney PA (2013) Gene expression analysis reveals schizophrenia-associated dysregulation of immune pathways in peripheral blood mononuclear cells. *Journal of psychiatric research* **47:** 425-437

Gardner A, Johansson A, Wibom R, Nennesmo I, von Döbeln U, Hagenfeldt L, Hällström T (2003) Alterations of mitochondrial function and correlations with personality traits in selected major depressive disorder patients. *Journal of affective disorders* **76:** 55-68

Gerencser AA, Chinopoulos C, Birket MJ, Jastroch M, Vitelli C, Nicholls DG, Brand MD (2012) Quantitative measurement of mitochondrial membrane potential in cultured cells: calcium-induced de-and hyperpolarization of neuronal mitochondria. *The Journal of physiology* **590:** 2845-2871

Gershon ES, Alliey-Rodriguez N, Liu C (2011) After GWAS: searching for genetic risk for schizophrenia and bipolar disorder. *Perspectives* **168**

Gibson G (2012) Rare and common variants: twenty arguments. *Nature Reviews Genetics* **13:** 135-145

Gilmore K, Wilson M (1999) The use of chloromethyl-X-rosamine (Mitotracker Red) to measure loss of mitochondrial membrane potential in apoptotic cells is incompatible with cell fixation. *Cytometry* **36:** 355-358

`

Glahn DC, Bearden CE, Cakir S, Barrett JA, Najt P, Serap Monkul E, Maples N, Velligan DI, Soares JC (2006) Differential working memory impairment in bipolar disorder and schizophrenia: effects of lifetime history of psychosis. *Bipolar disorders* **8:** 117-123

Gogos A, van den Buuse M, Rossell S (2009) Gender differences in prepulse inhibition (PPI) in bipolar disorder: men have reduced PPI, women have increased PPI. *The International Journal of Neuropsychopharmacology* **12:** 1249-1259

Goldstein J, Munoz-Pinedo C, Ricci J, Adams S, Kelekar A, Schuler M, Tsien R, Green D (2005) Cytochrome c is released in a single step during apoptosis. *Cell Death & Differentiation* **12:** 453-462

Goldstein JC, Waterhouse NJ, Juin P, Evan GI, Green DR (2000) The coordinate release of cytochrome c during apoptosis is rapid, complete and kinetically invariant. *Nature cell biology* **2:** 156-162

Gomes LC, Di Benedetto G, Scorrano L (2011) During autophagy mitochondria elongate, are spared from degradation and sustain cell viability. *Nature cell biology* **13:** 589-598

Gomes LC, Scorrano L (2008) High levels of Fis1, a pro-fission mitochondrial protein, trigger autophagy. *Biochimica et Biophysica Acta (BBA)-Bioenergetics* **1777:** 860-866

Gomes LC, Scorrano L (2013) Mitochondrial morphology in mitophagy and macroautophagy. *Biochimica et Biophysica Acta (BBA)-Molecular Cell Research* **1833:** 205-212

Gong Y, Chai Y, Ding J-H, Sun X-L, Hu G (2011) Chronic mild stress damages mitochondrial ultrastructure and function in mouse brain. *Neuroscience letters* **488:** 76-80

Gonzalvez F, D'Aurelio M, Boutant M, Moustapha A, Puech J-P, Landes T, Arnauré L, Vial G, Talleux N, Slomianny C (2013) Barth syndrome: Cellular compensation of mitochondrial dysfunction and apoptosis inhibition due to changes in cardiolipin remodeling linked to Tafazzin gene mutation. *Biochimica et Biophysica Acta (BBA)-Molecular Basis of Disease* **1832:** 1194-1206

Gordon DJ, Resio B, Pellman D (2012) Causes and consequences of aneuploidy in cancer. *Nature Reviews Genetics* **13:** 189-203

Gotlib IH, Joormann J (2010) Cognition and depression: current status and future directions. *Annual review of clinical psychology* **6:** 285

Green MF, Kern RS, Braff DL, Mintz J (2000) Neurocognitive deficits and functional outcome in schizophrenia. *Schizophrenia bulletin* **26:** 119-136

Greene LA, Lee HY, Angelastro JM (2009) The transcription factor ATF5: role in neurodevelopment and neural tumors. *Journal of neurochemistry* **108**: 11-22

Gubert C, Stertz L, Pfaffenseller B, Panizzutti BS, Rezin GT, Massuda R, Streck EL, Gama CS, Kapczinski F, Kunz M (2013) Mitochondrial activity and oxidative stress markers in peripheral blood mononuclear cells of patients with bipolar disorder, schizophrenia, and healthy subjects. *Journal of psychiatric research* **47:** 1396-1402

`

Guidotti A, Auta J, Davis JM, Gerevini VD, Dwivedi Y, Grayson DR, Impagnatiello F, Pandey G, Pesold C, Sharma R (2000) Decrease in reelin and glutamic acid decarboxylase67 (GAD67) expression in schizophrenia and bipolar disorder: a postmortem brain study. *Archives of general psychiatry* **57:** 1061-1069

Guo X, Macleod GT, Wellington A, Hu F, Panchumarthi S, Schoenfield M, Marin L, Charlton MP, Atwood HL, Zinsmaier KE (2005) The GTPase dMiro is required for axonal transport of mitochondria to Drosophila synapses. *Neuron* **47:** 379-393

Hamshere ML, Walters JTR, Smith R, Richards A, Green E, Grozeva D, Jones I, Forty L, Jones L, Gordon-Smith K (2012) Genome-wide significant associations in schizophrenia to ITIH3/4, CACNA1C and SDCCAG8, and extensive replication of associations reported by the Schizophrenia PGC. *Molecular psychiatry* **18:** 708-712

Hansen DV, Loktev AV, Ban KH, Jackson PK (2004) Plk1 regulates activation of the anaphase promoting complex by phosphorylating and triggering SCFbetaTrCP-dependent destruction of the APC Inhibitor Emi1. *Mol Biol Cell* **15:** 5623-5634

Hartmann N, Boehner M, Groenen F, Kalb R (2010) Telomere length of patients with major depression is shortened but independent from therapy and severity of the disease. *Depression and anxiety* **27:** 1111-1116

Hattori T, Shimizu S, Koyama Y, Emoto H, Matsumoto Y, Kumamoto N, Yamada K, Takamura H, Matsuzaki S, Katayama T (2014) DISC1 (Disrupted-in-Schizophrenia-1) regulates differentiation of oligodendrocytes. *PloS one* **9:** e88506

Hattori T, Shimizu S, Koyama Y, Yamada K, Kuwahara R, Kumamoto N, Matsuzaki S, Ito A, Katayama T, Tohyama M (2010) DISC1 regulates cell–cell adhesion, cell–matrix adhesion and neurite outgrowth. *Molecular psychiatry* **15:** 798-809

Hayashi-Takagi A, Takaki M, Graziane N, Seshadri S, Murdoch H, Dunlop AJ, Makino Y, Seshadri AJ, Ishizuka K, Srivastava DP (2010) Disrupted-in-Schizophrenia 1 (DISC1) regulates spines of the glutamate synapse via Rac1. *Nature neuroscience* **13:** 327-332

Head B, Griparic L, Amiri M, Gandre-Babbe S, van der Bliek AM (2009) Inducible proteolytic inactivation of OPA1 mediated by the OMA1 protease in mammalian cells. *The Journal of cell biology* **187:** 959-966

Heiskanen KM, Bhat MB, Wang H-W, Ma J, Nieminen A-L (1999) Mitochondrial Depolarization Accompanies Cytochrome cRelease During Apoptosis in PC6 Cells. *Journal of Biological Chemistry* **274:** 5654-5658

Henquet C, Krabbendam L, de Graaf R, ten Have M, van Os J (2006) Cannabis use and expression of mania in the general population. *J Affect Disord* **95:** 103-110

Henquet C, Murray R, Linszen D, van Os J (2005) The environment and schizophrenia: the role of cannabis use. *Schizophrenia bulletin* **31:** 608-612

Herberth M, Rahmoune H, Schwarz E, Koethe D, Harris LW, Kranaster L, Witt SH, Spain M, Barnes A, Schmolz M, Leweke MF, Guest PC, Bahn S (2014) Identification of a molecular profile associated with immune status in first-onset schizophrenia patients. *Clinical schizophrenia & related psychoses* **7:** 207-215

`

Herzenberg LA, Tung J, Moore WA, Herzenberg LA, Parks DR (2006) Interpreting flow cytometry data: a guide for the perplexed. *Nature immunology* **7:** 681-685

Higginbotham HR, Gleeson JG (2007) The centrosome in neuronal development. *Trends in neurosciences* **30:** 276-283

Hikida T, Jaaro-Peled H, Seshadri S, Oishi K, Hookway C, Kong S, Wu D, Xue R, Andrade M, Tankou S, Mori S, Gallagher M, Ishizuka K, Pletnikov M, Kida S, Sawa A (2007) Dominant-negative DISC1 transgenic mice display schizophrenia-associated phenotypes detected by measures translatable to humans. *Proceedings of the National Academy of Sciences of the United States of America* **104:** 14501-14506

Hill R (2012) Interaction of Sex Steroid Hormones and Brain-Derived Neurotrophic Factor-Tyrosine Kinase B Signalling: Relevance to Schizophrenia and Depression. *Journal of neuroendocrinology* **24:** 1553-1561

Hirokawa N, Niwa S, Tanaka Y (2010) Molecular motors in neurons: transport mechanisms and roles in brain function, development, and disease. *Neuron* **68:** 610-638

Hirokawa N, Noda Y, Tanaka Y, Niwa S (2009) Kinesin superfamily motor proteins and intracellular transport. *Nature reviews Molecular cell biology* **10:** 682-696

Hoek H, Brown A, Susser E (1998) The Dutch famine and schizophrenia spectrum disorders. *Social psychiatry and psychiatric epidemiology* **33:** 373-379

Honda A, Miyoshi K, Baba K, Taniguchi M, Koyama Y, Kuroda Si, Katayama T, Tohyama M (2004) Expression of fasciculation and elongation protein zeta-1 (FEZ1) in the developing rat brain. *Molecular brain research* **122:** 89-92

Horváth S, Mirnics K (2014) Immune system disturbances in schizophrenia. *Biological psychiatry* **75:** 316-323

Howes OD, Kapur S (2009) The dopamine hypothesis of schizophrenia: version III—the final common pathway. *Schizophrenia bulletin* **35:** 549-562

Hroudová J, Fišar Z, Kitzlerová E, Zvěřová M, Raboch J (2013) Mitochondrial respiration in blood platelets of depressive patients. *Mitochondrion* **13:** 795-800

Hudson G, Amati-Bonneau P, Blakely EL, Stewart JD, He L, Schaefer AM, Griffiths PG, Ahlqvist K, Suomalainen A, Reynier P (2008) Mutation of OPA1 causes dominant optic atrophy with external ophthalmoplegia, ataxia, deafness and multiple mitochondrial DNA deletions: a novel disorder of mtDNA maintenance. *Brain* **131:** 329-337

Humbert PO, Rogers C, Ganiatsas S, Landsberg RL, Trimarchi JM, Dandapani S, Brugnara C, Erdman S, Schrenzel M, Bronson RT (2000) E2F4 is essential for normal erythrocyte maturation and neonatal viability. *Molecular cell* **6:** 281-291

`

Hwang Y, Kim J, Shin J, Kim J-I, Seo J, Webster M, Lee D, Kim S (2013) Gene expression profiling by mRNA sequencing reveals increased expression of immune/inflammation-related genes in the hippocampus of individuals with schizophrenia. *Translational psychiatry* **3:** e321

Ibi D, Nagai T, Koike H, Kitahara Y, Mizoguchi H, Niwa M, Jaaro-Peled H, Nitta A, Yoneda Y, Nabeshima T, Sawa A, Yamada K (2010) Combined effect of neonatal immune activation and mutant DISC1 on phenotypic changes in adulthood. *Behavioural brain research* **206:** 32-37

Ichishita R, Tanaka K, Sugiura Y, Sayano T, Mihara K, Oka T (2008) An RNAi screen for mitochondrial proteins required to maintain the morphology of the organelle in Caenorhabditis elegans. *Journal of biochemistry* **143:** 449-454

Insel TR, Landis SC (2013) Twenty-Five Years of Progress: The View from NIMH and NINDS. *Neuron* **80:** 561-567

Ionita-Laza I, Xu B, Makarov V, Buxbaum JD, Roos JL, Gogos JA, Karayiorgou M (2014) Scan statistic-based analysis of exome sequencing data identifies FAN1 at 15q13. 3 as a susceptibility gene for schizophrenia and autism. *Proceedings of the National Academy of Sciences* **111:** 343-348

Ishihara N, Fujita Y, Oka T, Mihara K (2006) Regulation of mitochondrial morphology through proteolytic cleavage of OPA1. *The EMBO journal* **25:** 2966-2977

Ishihara N, Jofuku A, Eura Y, Mihara K (2003) Regulation of mitochondrial morphology by membrane potential, and DRP1-dependent division and FZO1-dependent fusion reaction in mammalian cells. *Biochemical and biophysical research communications* **301:** 891-898

Ishihara N, Nomura M, Jofuku A, Kato H, Suzuki SO, Masuda K, Otera H, Nakanishi Y, Nonaka I, Goto Y-i (2009) Mitochondrial fission factor Drp1 is essential for embryonic development and synapse formation in mice. *Nature cell biology* **11:** 958-966

Jaaro-Peled H, Niwa M, Foss CA, Murai R, Pou S, Kamiya A, Mateo Y, O'Donnell P, Cascella NG, Nabeshima T, Guilarte TR, Pomper M, Sawa A (2013) Subcortical dopaminergic deficits in a DISC1 mutant model: a study in direct reference to human molecular brain imaging. *Human molecular genetics* **22:** 1574-1580

Jacobs PA, Brunton M, Frackiewicz A, Newton M, Cook PJ, Robson EB (1970) Studies on a family with three cytogenetic markers. *Annals of Human Genetics* **33:** 325-336

James R, Adams RR, Christie S, Buchanan SR, Porteous DJ, Millar JK (2004) Disrupted in Schizophrenia 1 (DISC1) is a multicompartmentalized protein that predominantly localizes to mitochondria. *Molecular and cellular neurosciences* **26:** 112-122

Jasinska AJ, Choi O-w, DeYoung J, Grujic O, Kong S-y, Jorgensen MJ, Bailey J, Breidenthal S, Fairbanks LA, Woods RP (2009) Identification of brain transcriptional variation reproduced in peripheral blood: an approach for mapping brain expression traits. *Human molecular genetics* **18:** 4415-4427

Ji B, Higa KK, Kim M, Zhou L, Young JW, Geyer MA, Zhou X (2014) Inhibition of protein translation by the DISC1-Boymaw fusion gene from a Scottish family with major psychiatric disorders. *Human molecular genetics* **23:** 5683-5705

`

Ji B, Kim M, Higa KK, Zhou X (2015) Boymaw, Overexpressed in Brains with Major Psychiatric Disorders, May Encode a Small Protein to Inhibit Mitochondrial Function and Protein Translation. *American Journal of Medical Genetics Part B: Neuropsychiatric Genetics* **168:** 284-295

Jindal RD, Pillai AK, Mahadik SP, Eklund K, Montrose DM, Keshavan MS (2010) Decreased BDNF in patients with antipsychotic naive first episode schizophrenia. *Schizophrenia research* **119:** 47-51

Johansen JP, Cain CK, Ostroff LE, LeDoux JE (2011) Molecular mechanisms of fear learning and memory. *Cell* **147:** 509-524

John GB, Shang Y, Li L, Renken C, Mannella CA, Selker JM, Rangell L, Bennett MJ, Zha J (2005) The mitochondrial inner membrane protein mitofilin controls cristae morphology. *Mol Biol Cell* **16:** 1543-1554

Johnson DG, Schwarz JK, Cress WD, Nevins JR (1993) Expression of transcription factor E2F1 induces quiescent cells to enter S phase. *Nature* **365:** 349-352

Jourquin J, Duncan D, Shi Z, Zhang B (2012) GLAD4U: deriving and prioritizing gene lists from PubMed literature. *BMC genomics* **13:** S20

Kamiya A, Kubo K, Tomoda T, Takaki M, Youn R, Ozeki Y, Sawamura N, Park U, Kudo C, Okawa M, Ross CA, Hatten ME, Nakajima K, Sawa A (2005) A schizophrenia-associated mutation of DISC1 perturbs cerebral cortex development. *Nature cell biology* **7:** 1167-1178

Kamiya A, Tan PL, Kubo K-i, Engelhard C, Ishizuka K, Kubo A, Tsukita S, Pulver AE, Nakajima K, Cascella NG (2008) Recruitment of PCM1 to the centrosome by the cooperative action of DISC1 and BBS4: a candidate for psychiatric illnesses. *Archives of general psychiatry* **65:** 996-006

Kamiya A, Tomoda T, Chang J, Takaki M, Zhan C, Morita M, Cascio MB, Elashvili S, Koizumi H, Takanezawa Y (2006) DISC1–NDEL1/NUDEL protein interaction, an essential component for neurite outgrowth, is modulated by genetic variations of DISC1. *Human molecular genetics* **15:** 3313-3323

Kanehisa M, Araki M, Goto S, Hattori M, Hirakawa M, Itoh M, Katayama T, Kawashima S, Okuda S, Tokimatsu T (2008) KEGG for linking genomes to life and the environment. *Nucleic acids research* **36:** D480-D484

Kang J-S, Tian J-H, Pan P-Y, Zald P, Li C, Deng C, Sheng Z-H (2008) Docking of axonal mitochondria by syntaphilin controls their mobility and affects short-term facilitation. *Cell* **132:** 137-148

Kanki T, Klionsky DJ (2010) The molecular mechanism of mitochondria autophagy in yeast. *Molecular microbiology* **75:** 795-800

Karabatsiakis A, Böck C, Salinas-Manrique J, Kolassa S, Calzia E, Dietrich D, Kolassa I (2014) Mitochondrial respiration in peripheral blood mononuclear cells correlates with depressive subsymptoms and severity of major depression. *Translational Psychiatry* **4:** e397

Kastan MB, Bartek J (2004) Cell-cycle checkpoints and cancer. *Nature* **432:** 316-323

`

Katsel P, Davis KL, Li C, Tan W, Greenstein E, Hoffman LBK, Haroutunian V (2008) Abnormal indices of cell cycle activity in schizophrenia and their potential association with oligodendrocytes. *Neuropsychopharmacology* **33:** 2993-3009

Katsel P, Tan W, Abazyan B, Davis KL, Ross C, Pletnikov MV, Haroutunian V (2011) Expression of mutant human DISC1 in mice supports abnormalities in differentiation of oligodendrocytes. *Schizophrenia research* **130:** 238-249

Kauer-Sant'Anna M, Kapczinski F, Andreazza AC, Bond DJ, Lam RW, Young LT, Yatham LN (2009) Brain-derived neurotrophic factor and inflammatory markers in patients with early-vs. late-stage bipolar disorder. *The International Journal of Neuropsychopharmacology* **12:** 447-458

Kaur P, Jodhka PK, Underwood WA, Bowles CA, de Fiebre NC, de Fiebre CM, Singh M (2007) Progesterone increases brain-derived neuroptrophic factor expression and protects against glutamate toxicity in a mitogen-activated protein kinase-and phosphoinositide-3 kinase-dependent manner in cerebral cortical explants. *Journal of neuroscience research* **85:** 2441-2449

Keller MB (2005) Prevalence and impact of comorbid anxiety and bipolar disorder. *The Journal of clinical psychiatry* **67:** 5-7

Kendler KS, Gatz M, Gardner CO, Pedersen NL (2006) A Swedish national twin study of lifetime major depression. *American Journal of Psychiatry* **163:** 109-114

Kendler KS, Karkowski LM, Prescott CA (1999) Causal relationship between stressful life events and the onset of major depression. *American Journal of Psychiatry* **156:** 837-841

Keryer-Bibens C, Pioche-Durieu C, Villemant C, Souquère S, Nishi N, Hirashima M, Middeldorp J, Busson P (2006) Exosomes released by EBV-infected nasopharyngeal carcinoma cells convey the viral latent membrane protein 1 and the immunomodulatory protein galectin 9. *BMC cancer* **6**: 283

Keshavan MS, Nasrallah HA, Tandon R (2011) Schizophrenia,"Just the Facts" 6. Moving ahead with the schizophrenia concept: from the elephant to the mouse. *Schizophrenia research* **127:** 3-13

Kessler RC, Chiu WT, Demler O, Walters EE (2005) Prevalence, severity, and comorbidity of 12-month DSM-IV disorders in the National Comorbidity Survey Replication. *Archives of general psychiatry* **62:** 617-627

Khatri P, Sirota M, Butte AJ (2012) Ten years of pathway analysis: current approaches and outstanding challenges. *PLoS computational biology* **8:** e1002375

Kim M, Suh J, Romano D, Truong MH, Mullin K, Hooli B, Norton D, Tesco G, Elliott K, Wagner SL (2009) Potential late-onset Alzheimer's disease-associated mutations in the ADAM10 gene attenuate α-secretase activity. *Human molecular genetics* **18:** 3987-3996

Kim Y-K, Kim L, Lee M-S (2000) Relationships between interleukins, neurotransmitters and psychopathology in drug-free male schizophrenics. *Schizophrenia research* **44:** 165-175

`

Kirkpatrick B, Miller BJ (2013) Inflammation and schizophrenia. *Schizophrenia bulletin* **39:** 1174-1179

Kirkpatrick B, Xu L, Cascella N, Ozeki Y, Sawa A, Roberts RC (2006) DISC1 immunoreactivity at the light and ultrastructural level in the human neocortex. *Journal of Comparative Neurology* **497:** 436-450

Klein AB, Williamson R, Santini MA, Clemmensen C, Ettrup A, Rios M, Knudsen GM, Aznar S (2011) Blood BDNF concentrations reflect brain-tissue BDNF levels across species. *The International Journal of Neuropsychopharmacology* **14:** 347-353

Koike H, Arguello PA, Kvajo M, Karayiorgou M, Gogos JA (2006) Disc1 is mutated in the 129S6/SvEv strain and modulates working memory in mice. *Proceedings of the National Academy of Sciences of the United States of America* **103:** 3693-3697

Koopman G, Reutelingsperger C, Kuijten G, Keehnen R, Pals S, Van Oers M (1994) Annexin V for flow cytometric detection of phosphatidylserine expression on B cells undergoing apoptosis. *Blood* **84:** 1415-1420

Koshiba T, Detmer SA, Kaiser JT, Chen H, McCaffery JM, Chan DC (2004) Structural basis of mitochondrial tethering by mitofusin complexes. *Science (New York, NY)* **305:** 858-862

Kowalik TF, DeGregori J, Schwarz JK, Nevins JR (1995) E2F1 overexpression in quiescent fibroblasts leads to induction of cellular DNA synthesis and apoptosis. *Journal of Virology* **69:** 2491-2500

Krogh J, Benros ME, Jørgensen MB, Vesterager L, Elfving B, Nordentoft M (2014) The association between depressive symptoms, cognitive function, and inflammation in major depression. *Brain, behavior, and immunity* **35:** 70-76

Krupczak-Hollis K, Wang X, Kalinichenko VV, Gusarova GA, Wang IC, Dennewitz MB, Yoder HM, Kiyokawa H, Kaestner KH, Costa RH (2004) The mouse Forkhead Box m1 transcription factor is essential for hepatoblast mitosis and development of intrahepatic bile ducts and vessels during liver morphogenesis. *Developmental biology* **276:** 74-88

Küppers R, Engert A, Hansmann M-L (2012) Hodgkin lymphoma. *The Journal of clinical investigation* **122:** 3439-3447

Kuroda K, Yamada S, Tanaka M, Iizuka M, Yano H, Mori D, Tsuboi D, Nishioka T, Namba T, Iizuka Y (2011) Behavioral alterations associated with targeted disruption of exons 2 and 3 of the Disc1 gene in the mouse. *Human molecular genetics* **20:** 4666-4683

Laasonen-Balk T, Kuikka J, Viinamäki H, Husso-Saastamoinen M, Lehtonen J, Tiihonen J (1999) Striatal dopamine transporter density in major depression. *Psychopharmacology* **144:** 282-285

Lagerberg TV, Kvitland LR, Aminoff SR, Aas M, Ringen PA, Andreassen OA, Melle I (2014) Indications of a dose-response relationship between cannabis use and age at onset in bipolar disorder. *Psychiatry Res* **215:** 101-104

`

Lagna G, Nguyen PH, Ni W, Hata A (2006) BMP-dependent activation of caspase-9 and caspase-8 mediates apoptosis in pulmonary artery smooth muscle cells. *Am J Physiol Lung Cell Mol Physiol* **291:** L1059-1067

Lazic SE (2010) The problem of pseudoreplication in neuroscientific studies: is it affecting your analysis? *BMC neuroscience* **11:** 5

Lee I, Pecinova A, Pecina P, Neel BG, Araki T, Kucherlapati R, Roberts AE, Hüttemann M (2010) A suggested role for mitochondria in Noonan syndrome. *Biochimica et Biophysica Acta (BBA)-Molecular Basis of Disease* **1802:** 275-283

Lee J, Park S (2005) Working memory impairments in schizophrenia: a meta-analysis. *Journal of abnormal psychology* **114:** 599

Lee JL, Everitt BJ, Thomas KL (2004) Independent cellular processes for hippocampal memory consolidation and reconsolidation. *Science (New York, NY)* **304:** 839-843

Lee SH, DeCandia TR, Ripke S, Yang J, Sullivan PF, Goddard ME, Keller MC, Visscher PM, Wray NR, Consortium SPG-WAS (2012) Estimating the proportion of variation in susceptibility to schizophrenia captured by common SNPs. *Nature genetics* **44:** 247-250

Legros F, Lombès A, Frachon P, Rojo M (2002) Mitochondrial fusion in human cells is efficient, requires the inner membrane potential, and is mediated by mitofusins. *Molecular biology of the cell* **13:** 4343-4354

Leliveld SR, Bader V, Hendriks P, Prikulis I, Sajnani G, Requena JR, Korth C (2008) Insolubility of disrupted-in-schizophrenia 1 disrupts oligomer-dependent interactions with nuclear distribution element 1 and is associated with sporadic mental disease. *The Journal of neuroscience : the official journal of the Society for Neuroscience* **28:** 3839-3845

Leliveld SR, Hendriks P, Michel M, Sajnani G, Bader V, Trossbach S, Prikulis I, Hartmann R, Jonas E, Willbold D (2009) Oligomer Assembly of the C-Terminal DISC1 Domain (640−854) Is Controlled by Self-Association Motifs and Disease-Associated Polymorphism S704C. *Biochemistry* **48:** 7746-7755

Lencz T, Guha S, Liu C, Rosenfeld J, Mukherjee S, DeRosse P, John M, Cheng L, Zhang C, Badner JA (2013) Genome-wide association study implicates NDST3 in schizophrenia and bipolar disorder. *Nature communications* **4:** 2739

Lev-Ran S, Le Foll B, McKenzie K, George TP, Rehm J (2013) Bipolar disorder and co-occurring cannabis use disorders: characteristics, co-morbidities and clinical correlates. *Psychiatry Res* **209:** 459-465

Lewis DA, Curley AA, Glausier JR, Volk DW (2012) Cortical parvalbumin interneurons and cognitive dysfunction in schizophrenia. *Trends Neurosci* **35:** 57-67

Lewis DA, Hashimoto T, Volk DW (2005) Cortical inhibitory neurons and schizophrenia. *Nature reviews Neuroscience* **6:** 312-324

`

Li W, Zhou Y, Jentsch JD, Brown RA, Tian X, Ehninger D, Hennah W, Peltonen L, Lonnqvist J, Huttunen MO, Kaprio J, Trachtenberg JT, Silva AJ, Cannon TD (2007) Specific developmental disruption of disrupted-in-schizophrenia-1 function results in schizophrenia-related phenotypes in mice. *Proceedings of the National Academy of Sciences of the United States of America* **104:** 18280-18285

Li Z, Wu Y, Baraban JM (2008) The Translin/Trax RNA binding complex: clues to function in the nervous system. *Biochimica et biophysica acta* **1779:** 479-485

Liberzon A, Subramanian A, Pinchback R, Thorvaldsdóttir H, Tamayo P, Mesirov JP (2011) Molecular signatures database (MSigDB) 3.0. *Bioinformatics* **27:** 1739-1740

Lichtenstein P, Yip BH, Björk C, Pawitan Y, Cannon TD, Sullivan PF, Hultman CM (2009) Common genetic influences for schizophrenia and bipolar disorder: a population-based study of 2 million nuclear families. *Lancet* **373:** 234–239

Liesa M, Palacin M, Zorzano A (2009) Mitochondrial dynamics in mammalian health and disease. *Physiol Rev* **89:** 799-845

Lin M-Y, Sheng Z-H (2015) Regulation of mitochondrial transport in Neurons. *Experimental Cell Research* **334:** 35-44

Lipina TV, Zai C, Hlousek D, Roder JC, Wong AH (2013) Maternal immune activation during gestation interacts with Disc1 point mutation to exacerbate schizophrenia-related behaviors in mice. *The Journal of Neuroscience* **33:** 7654-7666

Lipska BK, Deep-Soboslay A, Weickert CS, Hyde TM, Martin CE, Herman MM, Kleinman JE (2006a) Critical factors in gene expression in postmortem human brain: Focus on studies in schizophrenia. *Biological psychiatry* **60:** 650-658

Lipska BK, Peters T, Hyde TM, Halim N, Horowitz C, Mitkus S, Weickert CS, Matsumoto M, Sawa A, Straub RE (2006b) Expression of DISC1 binding partners is reduced in schizophrenia and associated with DISC1 SNPs. *Human molecular genetics* **15:** 1245-1258

Liu X, Kim CN, Yang J, Jemmerson R, Wang X (1996) Induction of apoptotic program in cell-free extracts: requirement for dATP and cytochrome c. *Cell* **86:** 147-157

Lubow R (2005) Construct validity of the animal latent inhibition model of selective attention deficits in schizophrenia. *Schizophrenia Bulletin* **31:** 139-153

Lucassen PJ, Stumpel MW, Wang Q, Aronica E (2010) Decreased numbers of progenitor cells but no response to antidepressant drugs in the hippocampus of elderly depressed patients. *Neuropharmacology* **58:** 940-949

Lucca G, Comim CM, Valvassori SS, Réus GZ, Vuolo F, Petronilho F, Gavioli EC, Dal-Pizzol F, Quevedo J (2009) Increased oxidative stress in submitochondrial particles into the brain of rats submitted to the chronic mild stress paradigm. *Journal of psychiatric research* **43:** 864-869

Lücking CB, Dürr A, Bonifati V, Vaughan J, De Michele G, Gasser T, Harhangi BS, Meco G, Denèfle P, Wood NW (2000) Association between early-onset Parkinson's disease and mutations in the parkin gene. *New England Journal of Medicine* **342:** 1560-1567

`

Ly JD, Grubb D, Lawen A (2003) The mitochondrial membrane potential (Δψm) in apoptosis; an update. *Apoptosis* **8:** 115-128

Ma L, Liu Y, Ky B, Shughrue PJ, Austin CP, Morris JA (2002) Cloning and characterisation of Disc1, the mouse ortholog of DISC1 (Disrupted-in-Schizophrenia 1). *Genomics* **80:** 662-672

Ma TM, Abazyan S, Abazyan B, Nomura J, Yang C, Seshadri S, Sawa A, Snyder SH, Pletnikov MV (2012) Pathogenic disruption of DISC1-serine racemase binding elicits schizophrenia-like behavior via D-serine depletion. *Mol Psychiatry*

MacAskill AF, Kittler JT (2010) Control of mitochondrial transport and localization in neurons. *Trends in cell biology* **20:** 102-112

Macatonia SE, Hosken NA, Litton M, Vieira P, Hsieh C-S, Culpepper JA, Wysocka M, Trinchieri G, Murphy KM, O'Garra A (1995) Dendritic cells produce IL-12 and direct the development of Th1 cells from naive CD4+ T cells. *The Journal of Immunology* **154:** 5071-5079

Machon RA, Mednick SA, Huttunen MO (1997) Adult major affective disorder after prenatal exposure to an influenza epidemic. *Archives of general psychiatry* **54:** 322-328

Maino K, Gruber R, Riedel M, Seitz N, Schwarz M, Müller N (2007) T-and B-lymphocytes in patients with schizophrenia in acute psychotic episode and the course of the treatment. *Psychiatry research* **152:** 173-180

Malaspina D, Harlap S, Fennig S, Heiman D, Nahon D, Feldman D, Susser ES (2001) Advancing paternal age and the risk of schizophrenia. *Archives of general psychiatry* **58:** 361-367

Malavasi ELV, Ogawa F, Porteous DJ, Millar JK (2012) DISC1 variants 37W and 607F disrupt its nuclear targeting and regulatory role in ATF4-mediated transcription. *Human molecular genetics* **21:** 2779-2792

Malhotra D, Sebat J (2012) CNVs: harbingers of a rare variant revolution in psychiatric genetics. *Cell* **148:** 1223-1241

Malka F, Guillery O, Cifuentes-Diaz C, Guillou E, Belenguer P, Lombès A, Rojo M (2005) Separate fusion of outer and inner mitochondrial membranes. *EMBO reports* **6:** 853-859

Manji H, Kato T, Di Prospero NA, Ness S, Beal MF, Krams M, Chen G (2012) Impaired mitochondrial function in psychiatric disorders. *Nature reviews Neuroscience* **13:** 293-307

Manolio TA, Collins FS, Cox NJ, Goldstein DB, Hindorff LA, Hunter DJ, McCarthy MI, Ramos EM, Cardon LR, Chakravarti A (2009) Finding the missing heritability of complex diseases. *Nature* **461:** 747-753

Mao Y, Ge X, Frank CL, Madison JM, Koehler AN, Doud MK, Tassa C, Berry EM, Soda T, Singh KK, Biechele T, Petryshen TL, Moon RT, Haggarty SJ, Tsai LH (2009) Disrupted in schizophrenia 1 regulates neuronal progenitor proliferation via modulation of GSK3beta/beta-catenin signaling. *Cell* **136:** 1017-1031

`

Marcand S, Brevet V, Mann C, Gilson E (2000) Cell cycle restriction of telomere elongation. *Current Biology* **10:** 487-490

Marechal A, Zou L (2013) DNA damage sensing by the ATM and ATR kinases. *Cold Spring Harbor perspectives in biology* **5:** a012716

Marley A, von Zastrow M (2010) DISC1 regulates primary cilia that display specific dopamine receptors. *PLoS One* **5:** e10902

Martinou J-C, Youle RJ (2011) Mitochondria in apoptosis: Bcl-2 family members and mitochondrial dynamics. *Developmental cell* **21:** 92-101

Maurer I, Zierz S, Möller H-J (2001) Evidence for a mitochondrial oxidative phosphorylation defect in brains from patients with schizophrenia. *Schizophrenia research* **48:** 125-136

Mazure CM (1998) Life stressors as risk factors in depression. *Clinical Psychology: Science and Practice* **5:** 291-313

McCurdy RD, Féron F, Perry C, Chant DC, McLean D, Matigian N, Hayward NK, McGrath JJ, Mackay-Sim A (2006) Cell cycle alterations in biopsied olfactory neuroepithelium in schizophrenia and bipolar I disorder using cell culture and gene expression analyses. *Schizophrenia research* **82:** 163-173

McGuffin P, Rijsdijk F, Andrew M, Sham P, Katz R, Cardno A (2003) The heritability of bipolar affective disorder and the genetic relationship to unipolar depression. *Archives of general psychiatry* **60:** 497-502

McNeil TF, Cantor-Graae E, Weinberger DR (2000) Relationship of obstetric complications and differences in size of brain structures in monozygotic twin pairs discordant for schizophrenia. *American Journal of Psychiatry* **157:** 203-212

Mednick S, Huttunen MO, Machón RA (1994) Prenatal influenza infections and adult schizophrenia. *Schizophrenia bulletin* **20:** 263-267

Merikangas K, Yu K (2002) Genetic epidemiology of bipolar disorder. *Clinical Neuroscience Research* **2:** 127-141

Merikangas KR, Jin R, He J-P, Kessler RC, Lee S, Sampson NA, Viana MC, Andrade LH, Hu C, Karam EG (2011) Prevalence and correlates of bipolar spectrum disorder in the world mental health survey initiative. *Archives of general psychiatry* **68:** 241

Meyer KD, Morris JA (2008) Immunohistochemical analysis of Disc1 expression in the developing and adult hippocampus. *Gene Expression Patterns* **8:** 494-501

Meyer U, Feldon J (2012) To poly(I:C) or not to poly(I:C): advancing preclinical schizophrenia research through the use of prenatal immune activation models. *Neuropharmacology* **62:** 1308-1321

Millar J, Brown J, Maule J, Shibasaki Y, Christie S, Lawson D, Anderson S, Wilson-Annan J, Devon R, St Clair D (1998) A long-range restriction map across 3 Mb of the chromosome 11 breakpoint region of a translotion linked to schizophrenia: localization of the breakpoint and the search for neighbouring genes. *Psychiatric genetics* **8:** 175-182

`

Millar J, Christie S, Anderson S, Lawson D, Hsiao-Wei LD, Devon R, Arveiler B, Muir W, Blackwood D, Porteous D (2001) Genomic structure and localisation within a linkage hotspot of Disrupted In Schizophrenia 1, a gene disrupted by a translocation segregating with schizophrenia. *Molecular psychiatry* **6:** 173-178

Millar JK, Christie S, Porteous DJ (2003) Yeast two-hybrid screens implicate DISC1 in brain development and function. *Biochemical and biophysical research communications* **311:** 1019-1025

Millar JK, Christie S, Semple CAM, Porteous DJ (2000a) Chromosomal Location and Genomic Structure of the Human Translin-Associated Factor X Gene (< i> TRAX; TSNAX</i>) Revealed by Intergenic Splicing to< i> DISC1,</i> a Gene Disrupted by a Translocation Segregating with Schizophrenia. *Genomics* **67:** 69-77

Millar JK, James R, Christie S, Porteous DJ (2005a) Disrupted in schizophrenia 1 (DISC1): subcellular targeting and induction of ring mitochondria. *Molecular and cellular neurosciences* **30:** 477-484

Millar JK, Pickard BS, Mackie S, James R, Christie S, Buchanan SR, Malloy MP, Chubb JE, Huston E, Baillie GS (2005b) DISC1 and PDE4B are interacting genetic factors in schizophrenia that regulate cAMP signaling. *Science (New York, NY)* **310:** 1187-1191

Millar JK, Wilson-Annan JC, Anderson S, Christie S, Taylor MS, Semple CA, Devon RS, St Clair DM, Muir WJ, Blackwood DH, Porteous DJ (2000b) Disruption of two novel genes by a translocation co-segregating with schizophrenia. *Human molecular genetics* **9:** 1415-1423

Miller AH, Maletic V, Raison CL (2009) Inflammation and its discontents: the role of cytokines in the pathophysiology of major depression. *Biological psychiatry* **65:** 732-741

Miller BJ, Buckley P, Seabolt W, Mellor A, Kirkpatrick B (2011) Meta-analysis of cytokine alterations in schizophrenia: clinical status and antipsychotic effects. *Biological psychiatry* **70:** 663-671

Miller BJ, Culpepper N, Rapaport MH, Buckley P (2013) Prenatal inflammation and neurodevelopment in schizophrenia: a review of human studies. *Progress in Neuro-Psychopharmacology and Biological Psychiatry* **42:** 92-100

Miller KE, Sheetz MP (2004) Axonal mitochondrial transport and potential are correlated. *J Cell Sci* **117:** 2791-2804

Mironov SL (2007) ADP regulates movements of mitochondria in neurons. *Biophysical journal* **92:** 2944-2952

Mitchell KJ, Porteous DJ (2011) Rethinking the genetic architecture of schizophrenia. *Psychological medicine* **41:** 19-32

Miyoshi K, Asanuma M, Miyazaki I, Diaz-Corrales FJ, Katayama T, Tohyama M, Ogawa N (2004) DISC1 localizes to the centrosome by binding to kendrin. *Biochemical and biophysical research communications* **317:** 1195-1199

`

Miyoshi K, Honda A, Baba K, Taniguchi M, Oono K, Fujita T, Kuroda S, Katayama T, Tohyama M (2003) Disrupted-In-Schizophrenia 1, a candidate gene for schizophrenia, participates in neurite outgrowth. *Molecular psychiatry* **8:** 685-694

Modabbernia A, Taslimi S, Brietzke E, Ashrafi M (2013) Cytokine alterations in bipolar disorder: a meta-analysis of 30 studies. *Biological psychiatry* **74:** 15-25

Moldovan G-L, D'Andrea AD (2009) How the fanconi anemia pathway guards the genome. *Annual review of genetics* **43:** 223

Möller M, Du Preez JL, Viljoen FP, Berk M, Emsley R, Harvey BH (2013) Social isolation rearing induces mitochondrial, immunological, neurochemical and behavioural deficits in rats, and is reversed by clozapine or N-acetyl cysteine. *Brain, behavior, and immunity* **30:** 156-167

Mondelli V, Cattaneo A, Martino Belvederi Murri M, Marta Di Forti M, Hepgul N, Miorelli A, Navari S, Papadopoulos AS, Aitchison KJ, Morgan C (2011) Early Career Psychiatrists. *The Journal of clinical psychiatry* **72:** 1677-1684

Moon HM, Youn YH, Pemble H, Yingling J, Wittmann T, Wynshaw-Boris A (2014) LIS1 controls mitosis and mitotic spindle organization via the LIS1–NDEL1–dynein complex. *Human molecular genetics* **23:** 449-466

Moreno J, Gaspar E, López-Bello G, Juarez E, Alcazar-Leyva S, González-Trujano E, Pavon L, Alvarado-Vásquez N (2013) Increase in nitric oxide levels and mitochondrial membrane potential in platelets of untreated patients with major depression. *Psychiatry research* **209:** 447-452

Morris JA, Kandpal G, Ma L, Austin CP (2003) DISC1 (Disrupted-In-Schizophrenia 1) is a centrosome-associated protein that interacts with MAP1A, MIPT3, ATF4/5 and NUDEL: regulation and loss of interaction with mutation. *Human molecular genetics* **12:** 1591-1608

Mortensen PB, Nørgaard-Pedersen B, Waltoft BL, Sørensen TL, Hougaard D, Yolken RH (2007) Early infections of Toxoplasma gondii and the later development of schizophrenia. *Schizophrenia bulletin* **33:** 741-744

Mortensen PB, Pedersen C, Melbye M, Mors O, Ewald H (2003) Individual and familial risk factors for bipolar affective disorders in Denmark. *Archives of general psychiatry* **60:** 1209-1215

Mortensen PB, Pedersen CB, McGrath JJ, Hougaard DM, Nørgaard-Petersen B, Mors O, Børglum AD, Yolken RH (2011) Neonatal antibodies to infectious agents and risk of bipolar disorder: a population-based case–control study. *Bipolar disorders* **13:** 624-629

Moshe Y, Boulaire J, Pagano M, Hershko A (2004) Role of Polo-like kinase in the degradation of early mitotic inhibitor 1, a regulator of the anaphase promoting complex/cyclosome. *Proceedings of the National Academy of Sciences of the United States of America* **101:** 7937-7942

Motivala SJ, Sarfatti A, Olmos L, Irwin MR (2005) Inflammatory markers and sleep disturbance in major depression. *Psychosomatic medicine* **67:** 187-194

`

Mozdy A, McCaffery J, Shaw J (2000) Dnm1p GTPase-mediated mitochondrial fission is a multi-step process requiring the novel integral membrane component Fis1p. *The Journal of cell biology* **151:** 367-380

Muir W, Gosden C, Brookes A, Fantes J, Evans K, Maguire S, Stevenson B, Boyle S, Blackwood D, St Clair D (1995) Direct microdissection and microcloning of a translocation breakpoint region, t (1; 11)(q42. 2; q21), associated with schizophrenia. *Cytogenetic and Genome Research* **70:** 35-40

Murdoch H, Mackie S, Collins DM, Hill EV, Bolger GB, Klussmann E, Porteous DJ, Millar JK, Houslay MD (2007) Isoform-selective susceptibility of DISC1/phosphodiesterase-4 complexes to dissociation by elevated intracellular cAMP levels. *The Journal of neuroscience : the official journal of the Society for Neuroscience* **27:** 9513-9524

Nagai T, Kitahara Y, Ibi D, Nabeshima T, Sawa A, Yamada K (2011) Effects of antipsychotics on the behavioral deficits in human dominant-negative DISC1 transgenic mice with neonatal polyI:C treatment. *Behavioural brain research* **225:** 305-310

Nagaoka SI, Hassold TJ, Hunt PA (2012) Human aneuploidy: mechanisms and new insights into an age-old problem. *Nature Reviews Genetics* **13:** 493-504

Nahle Z, Polakoff J, Davuluri RV, McCurrach ME, Jacobson MD, Narita M, Zhang MQ, Lazebnik Y, Bar-Sagi D, Lowe SW (2002) Direct coupling of the cell cycle and cell death machinery by E2F. *Nature cell biology* **4:** 859-864

Nakamoto RK, Baylis Scanlon JA, Al-Shawi MK (2008) The rotary mechanism of the ATP synthase. *Arch Biochem Biophys* **476:** 43-50

Nakata K, Lipska BK, Hyde TM, Ye T, Newburn EN, Morita Y, Vakkalanka R, Barenboim M, Sei Y, Weinberger DR (2009) DISC1 splice variants are upregulated in schizophrenia and associated with risk polymorphisms. *Proceedings of the National Academy of Sciences* **106:** 15873-15878

Nanni V, Uher R, Danese A (2012) Childhood maltreatment predicts unfavorable course of illness and treatment outcome in depression: a meta-analysis. *American Journal of Psychiatry* **169:** 141-151

Nestler EJ, Hyman SE (2010) Animal models of neuropsychiatric disorders. *Nature neuroscience* **13:** 1161-1169

Neumüller RA, Knoblich JA (2009) Dividing cellular asymmetry: asymmetric cell division and its implications for stem cells and cancer. *Genes & development* **23:** 2675-2699

Newburn EN, Hyde TM, Ye T, Morita Y, Weinberger DR, Kleinman JE, Lipska BK (2011) Interactions of human truncated DISC1 proteins: implications for schizophrenia. *Transl Psychiatry* **1:** e30

Niwa M, Jaaro-Peled H, Tankou S, Seshadri S, Hikida T, Matsumoto Y, Cascella NG, Kano S-i, Ozaki N, Nabeshima T (2013) Adolescent stress–induced epigenetic control of dopaminergic neurons via glucocorticoids. *Science (New York, NY)* **339:** 335-339

`

Norkett R, Modi S, Birsa N, Atkin TA, Ivankovic D, Pathania M, Trossbach SV, Korth C, Hirst WD, Kittler JT (2016) DISC1-dependent Regulation of Mitochondrial Dynamics Controls the Morphogenesis of Complex Neuronal Dendrites. *Journal of Biological Chemistry* **291**: 613-629

Nosarti C, Reichenberg A, Murray RM, Cnattingius S, Lambe MP, Yin L, MacCabe J, Rifkin L, Hultman CM (2012) Preterm birth and psychiatric disorders in young adult life. *Archives of general psychiatry* **69:** 610-617

O'Brien SM, Scully P, Scott LV, Dinan TG (2006) Cytokine profiles in bipolar affective disorder: focus on acutely ill patients. *Journal of affective disorders* **90:** 263-267

O'Dushlaine C, Ripke S, Ruderfer DM, Hamilton SP, Fava M, Iosifescu DV, Kohane IS, Churchill SE, Castro VM, Clements CC, Blumenthal SR, Murphy SN, Smoller JW, Perlis RH (2014) Rare copy number variation in treatment-resistant major depressive disorder. *Biological psychiatry* **76:** 536-541

Ogawa F, Malavasi EL, Crummie DK, Eykelenboom JE, Soares DC, Mackie S, Porteous DJ, Millar JK (2014) DISC1 complexes with TRAK1 and Miro1 to modulate anterograde axonal mitochondrial trafficking. *Human molecular genetics* **23:** 906-919

Opler M, Charap J, Greig A, Stein V, Polito S, Malaspina D (2013) Environmental risk factors and schizophrenia. *International Journal of Mental Health* **42:** 23-3

Ortiz-Domínguez A, Hernández ME, Berlanga C, Gutiérrez-Mora D, Moreno J, Heinze G, Pavón L (2007) Immune variations in bipolar disorder: phasic differences. *Bipolar disorders* **9:** 596-602

Osbun N, Li J, O'Driscoll MC, Strominger Z, Wakahiro M, Rider E, Bukshpun P, Boland E, Spurrell CH, Schackwitz W (2011) Genetic and functional analyses identify DISC1 as a novel callosal agenesis candidate gene. *American Journal of Medical Genetics Part A* **155:** 1865-1876

Ostacher MJ, Nierenberg AA, Perlis RH, Eidelman P, Borrelli DJ, Tran TB, Ericson GM, Weiss RD, Sachs GS (2006) The relationship between smoking and suicidal behavior, comorbidity, and course of illness in bipolar disorder. *Journal of clinical psychiatry 67*: 1907-1911

Ostacher MJ, LeBeau RT, Perlis RH, Nierenberg AA, Lund HG, Moshier SJ, Sachs GS, Simon NM (2009) Cigarette smoking is associated with suicidality in bipolar disorder. *Bipolar disorders* **11**: 766-771

Overly CC, Rieff HI, Hollenbeck PJ (1996) Organelle motility and metabolism in axons vs dendrites of cultured hippocampal neurons. *Journal of cell science* **109:** 971-980

Ozeki Y, Tomoda T, Kleiderlein J, Kamiya A, Bord L, Fujii K, Okawa M, Yamada N, Hatten ME, Snyder SH, Ross CA, Sawa A (2003) Disrupted-in-Schizophrenia-1 (DISC-1): mutant truncation prevents binding to NudE-like (NUDEL) and inhibits neurite outgrowth. *Proceedings of the National Academy of Sciences of the United States of America* **100:** 289-294

`

Pang D, Syed S, Fine P, Jones PB (2009) No association between prenatal viral infection and depression in later life--a long-term cohort study of 6152 subjects. *Canadian journal of psychiatry Revue canadienne de psychiatrie* **54:** 565-570

Park YU, Jeong J, Lee H, Mun JY, Kim JH, Lee JS, Nguyen MD, Han SS, Suh PG, Park SK (2010) Disrupted-in-schizophrenia 1 (DISC1) plays essential roles in mitochondria in collaboration with Mitofilin. *Proceedings of the National Academy of Sciences of the United States of America* **107:** 17785-17790

Paspalas CD, Wang M, Arnsten AF (2013) Constellation of HCN channels and cAMP regulating proteins in dendritic spines of the primate prefrontal cortex: potential substrate for working memory deficits in schizophrenia. *Cerebral Cortex* **23:** 1643-1654

Peco E, Escude T, Agius E, Sabado V, Medevielle F, Ducommun B, Pituello F (2012) The CDC25B phosphatase shortens the G2 phase of neural progenitors and promotes efficient neuron production. *Development* **139:** 1095-1104

Pendergrass W, Wolf N, Poot M (2004) Efficacy of MitoTracker Green™ and CMXRosamine to measure changes in mitochondrial membrane potentials in living cells and tissues. *Cytometry Part A* **61:** 162-169

Perry W, Minassian A, Feifel D, Braff DL (2001) Sensorimotor gating deficits in bipolar disorder patients with acute psychotic mania. *Biological psychiatry* **50:** 418-424

Pico AR, Kelder T, Van Iersel MP, Hanspers K, Conklin BR, Evelo C (2008) WikiPathways: pathway editing for the people. *PLoS biology* **6:** e184

Plesca D, Crosby ME, Gupta D, Almasan A (2007) E2F4 function in G2: maintaining G2-arrest to prevent mitotic entry with damaged DNA. *Cell cycle (Georgetown, Tex)* **6:** 1147-1152

Pletnikov MV, Ayhan Y, Nikolskaia O, Xu Y, Ovanesov MV, Huang H, Mori S, Moran TH, Ross CA (2008) Inducible expression of mutant human DISC1 in mice is associated with brain and behavioral abnormalities reminiscent of schizophrenia. *Mol Psychiatry* **13:** 173-186, 115

Pletnikov MV, Xu Y, Ovanesov MV, Kamiya A, Sawa A, Ross CA (2007) PC12 cell model of inducible expression of mutant DISC1: new evidence for a dominant-negative mechanism of abnormal neuronal differentiation. *Neuroscience research* **58:** 234-244

Poot M, Pierce RH (1999) Detection of changes in mitochondrial function during apoptosis by simultaneous staining with multiple fluorescent dyes and correlated multiparameter flow cytometry. *Cytometry* **35:** 311-317

Poot M, Pierce RH (2001) Analysis of mitochondria by flow cytometry. *Methods in cell biology* **64:** 117-128

Poot M, Zhang Y-Z, Krämer J, Wells KS, Jones LJ, Hanzel DK, Lugade AG, Singer VL, Haugland RP (1996) Analysis of mitochondrial morphology and function with novel fixable fluorescent stains. *Journal of Histochemistry & Cytochemistry* **44:** 1363-1372

`

Prabakaran S, Swatton J, Ryan M, Huffaker S, Huang J-J, Griffin J, Wayland M, Freeman T, Dudbridge F, Lilley K (2004) Mitochondrial dysfunction in schizophrenia: evidence for compromised brain metabolism and oxidative stress. *Molecular psychiatry* **9:** 684-697

Prut L, Belzung C (2003) The open field as a paradigm to measure the effects of drugs on anxiety-like behaviors: a review. *European journal of pharmacology* **463:** 3-33

Purcell SM, Wray NR, Stone JL, Visscher PM, O'Donovan MC, Sullivan PF, Sklar P (2009a) Common polygenic variation contributes to risk of schizophrenia and bipolar disorder. *Nature* **460:** 748-752

Purcell SM, Wray NR, Stone JL, Visscher PM, O'Donovan MC, Sullivan PF, Sklar P (2009b) Common polygenic variation contributes to risk of schizophrenia and bipolar disorder. *Nature* **460:** 748-752

Qin X-Q, Livingston DM, Kaelin WG, Adams PD (1994) Deregulated transcription factor E2F-1 expression leads to S-phase entry and p53-mediated apoptosis. *Proceedings of the National Academy of Sciences* **91:** 10918-10922

Rakofsky JJ, Dunlop BW (2013) Do alcohol use disorders destabilize the course of bipolar disorder? *Journal of affective disorders* **145**: 1-10

Rang H, Dale MM, Ritter J, Moore P (2003) *Pharmacology* 5th edn. New York: Churchill Livingstone.

Rempel RE, Saenz-Robles MT, Storms R, Morham S, Ishida S, Engel A, Jakoi L, Melhem MF, Pipas JM, Smith C (2000) Loss of E2F4 activity leads to abnormal development of multiple cellular lineages. *Molecular cell* **6:** 293-306

Rezin GT, Cardoso MR, Gonçalves CL, Scaini G, Fraga DB, Riegel RE, Comim CM, Quevedo J, Streck EL (2008) Inhibition of mitochondrial respiratory chain in brain of rats subjected to an experimental model of depression. *Neurochemistry international* **53:** 395-400

Ribeiro-Santos A, Lucio Teixeira A, Salgado JV (2014) Evidence for an immune role on cognition in schizophrenia: a systematic review. *Current neuropharmacology* **12:** 273-280

Richard MD, Brahm NC (2012) Schizophrenia and the immune system: pathophysiology, prevention, and treatment. *American Journal of Health-System Pharmacy* **69:** 757-766

Rimol LM, Nesvåg R, Hagler Jr DJ, Bergmann Ø, Fennema-Notestine C, Hartberg CB, Haukvik UK, Lange E, Pung CJ, Server A (2012) Cortical volume, surface area, and thickness in schizophrenia and bipolar disorder. *Biological psychiatry* **71:** 552-560

Ripke S, O'Dushlaine C, Chambert K, Moran JL, Kähler AK, Akterin S, Bergen SE, Collins AL, Crowley JJ, Fromer M (2013a) Genome-wide association analysis identifies 13 new risk loci for schizophrenia. *Nature genetics* **45:** 1150-1159

Ripke S, Wray NR, Lewis CM, Hamilton SP, Weissman MM, Breen G, Byrne EM, Blackwood DH, Boomsma DI, Cichon S (2013b) A mega-analysis of genome-wide association studies for major depressive disorder. *Molecular psychiatry* **18:** 497-511

`

Robinson TE, Becker JB (1986) Enduring changes in brain and behavior produced by chronic amphetamine administration: a review and evaluation of animal models of amphetamine psychosis. *Brain Research Reviews* **11:** 157-198

Rockstroh M, Müller S, Jende C, Kerzhner A, von Bergen M, Tomm JM (2010) Cell fractionation-an important tool for compartment proteomics. *Journal of Integrated OMICS* **1:** 135-143

Rollins B, Martin MV, Morgan L, Vawter MP (2010) Analysis of whole genome biomarker expression in blood and brain. *American Journal of Medical Genetics Part B: Neuropsychiatric Genetics* **153:** 919-936

Rosenfeld M, Brenner-Lavie H, Ari SG-B, Kavushansky A, Ben-Shachar D (2011) Perturbation in mitochondrial network dynamics and in complex I dependent cellular respiration in schizophrenia. *Biological psychiatry* **69:** 980-988

Rucker JJ, Breen G, Pinto D, Pedroso I, Lewis CM, Cohen-Woods S, Uher R, Schosser A, Rivera M, Aitchison KJ, Craddock N, Owen MJ, Jones L, Jones I, Korszun A, Muglia P, Barnes MR, Preisig M, Mors O, Gill M, Maier W, Rice J, Rietschel M, Holsboer F, Farmer AE, Craig IW, Scherer SW, McGuffin P (2013) Genome-wide association analysis of copy number variation in recurrent depressive disorder. *Mol Psychiatry* **18:** 183-189

Rucker JJ, Tansey KE, Rivera M, Pinto D, Cohen-Woods S, Uher R, Aitchison KJ, Craddock N, Owen MJ, Jones L, Jones I, Korszun A, Barnes MR, Preisig M, Mors O, Maier W, Rice J, Rietschel M, Holsboer F, Farmer AE, Craig IW, Scherer SW, McGuffin P, Breen G (2015) Phenotypic Association Analyses with Copy Number Variation in Recurrent Depressive Disorder. *Biological psychiatry* **79**: 329-336

Ryan M, Lockstone H, Huffaker S, Wayland M, Webster M, Bahn S (2006) Gene expression analysis of bipolar disorder reveals downregulation of the ubiquitin cycle and alterations in synaptic genes. *Molecular psychiatry* **11:** 965-978

Sachs N, Sawa A, Holmes S, Ross C, DeLisi L, Margolis R (2005) A frameshift mutation in Disrupted in Schizophrenia 1 in an American family with schizophrenia and schizoaffective disorder. *Molecular psychiatry* **10**: 758-764

Saetre P, Emilsson L, Axelsson E, Kreuger J, Lindholm E, Jazin E (2007) Inflammation-related genes up-regulated in schizophrenia brains. *Bmc Psychiatry* **7:** 46

Sanchez-Pulido L, Ponting CP (2011) Structure and evolutionary history of DISC1. *Human molecular genetics* **20:** R175-R181

Sawamura N, Ando T, Maruyama Y, Fujimuro M, Mochizuki H, Honjo K, Shimoda M, Toda H, Sawamura-Yamamoto T, Makuch LA (2008) Nuclear DISC1 regulates CRE-mediated gene transcription and sleep homeostasis in the fruit fly. *Molecular psychiatry* **13:** 1138-1148

Sawamura N, Sawamura-Yamamoto T, Ozeki Y, Ross CA, Sawa A (2005) A form of DISC1 enriched in nucleus: altered subcellular distribution in orbitofrontal cortex in psychosis and substance/alcohol abuse. *Proceedings of the National Academy of Sciences of the United States of America* **102:** 1187-1192

`

Schmitt A, Leonardi-Essmann F, Durrenberger PF, Parlapani E, Schneider-Axmann T, Spanagel R, Arzberger T, Kretzschmar H, Herrera-Marschitz M, Gruber O (2011) Regulation of immune-modulatory genes in left superior temporal cortex of schizophrenia patients: a genome-wide microarray study. *World Journal of Biological Psychiatry* **12:** 201-215

Schmitt A, Malchow B, Hasan A, Falkai P (2014) The impact of environmental factors in severe psychiatric disorders. *Frontiers in neuroscience* **8**

Schönbeck U, Libby P (2001) The CD40/CD154 receptor/ligand dyadRID="†" ID="†" Review. *Cellular and Molecular Life Sciences CMLS* **58:** 4-43

Schork NJ, Murray SS, Frazer KA, Topol EJ (2009) Common vs. rare allele hypotheses for complex diseases. *Current opinion in genetics & development* **19:** 212-219

Schultz CC, Koch K, Wagner G, Roebel M, Schachtzabel C, Gaser C, Nenadic I, Reichenbach JR, Sauer H, Schlösser RG (2010) Reduced cortical thickness in first episode schizophrenia. *Schizophrenia research* **116:** 204-209

Schurov I, Handford E, Brandon N, Whiting P (2004) Expression of disrupted in schizophrenia 1 (DISC1) protein in the adult and developing mouse brain indicates its role in neurodevelopment. *Molecular psychiatry* **9:** 1100-1110

Schwarz TL (2013) Mitochondrial trafficking in neurons. *Cold Spring Harbor perspectives in biology* **5:** a011304

Scott J, McNeill Y, Cavanagh J, Cannon M, Murray R (2006) Exposure to obstetric complications and subsequent development of bipolar disorder Systematic review. *The British Journal of Psychiatry* **189:** 3-11

Semple CA, Devon RS, Le Hellard S, Porteous DJ (2001) Identification of genes from a schizophrenia-linked translocation breakpoint region. *Genomics* **73:** 123-126

Shao L, Vawter MP (2008) Shared gene expression alterations in schizophrenia and bipolar disorder. *Biological psychiatry* **64:** 89-97

Shelton R, Claiborne J, Sidoryk-Wegrzynowicz M, Reddy R, Aschner M, Lewis D, Mirnics K (2010) Altered expression of genes involved in inflammation and apoptosis in frontal cortex in major depression. *Molecular psychiatry* **16:** 751-762

Shen S, Lang B, Nakamoto C, Zhang F, Pu J, Kuan SL, Chatzi C, He S, Mackie I, Brandon NJ, Marquis KL, Day M, Hurko O, McCaig CD, Riedel G, St Clair D (2008) Schizophrenia-related neural and behavioral phenotypes in transgenic mice expressing truncated Disc1. *The Journal of neuroscience : the official journal of the Society for Neuroscience* **28:** 10893-10904

Sheng ZH (2014) Mitochondrial trafficking and anchoring in neurons: New insight and implications. *The Journal of cell biology* **204:** 1087-1098

Shenton ME, Dickey CC, Frumin M, McCarley RW (2001) A review of MRI findings in schizophrenia. *Schizophrenia research* **49:** 1-52

`

Sheppard CL, Lee LC, Hill E, Henderson DJ, Anthony DF, Houslay DM, Yalla KC, Cairns LS, Dunlop AJ, Baillie GS (2014) Mitotic activation of the DISC1-inducible cyclic AMP phosphodiesterase-4D9 (PDE4D9), through multi-site phosphorylation, influences cell cycle progression. *Cellular signalling* **26:** 1958–1974

Shi J, Levinson DF, Duan J, Sanders AR, Zheng Y, Pe'er I, Dudbridge F, Holmans PA, Whittemore AS, Mowry BJ (2009) Common variants on chromosome 6p22. 1 are associated with schizophrenia. *Nature* **460:** 753-757

Shimizu S, Matsuzaki S, Hattori T, Kumamoto N, Miyoshi K, Katayama T, Tohyama M (2008) DISC1-kendrin interaction is involved in centrosomal microtubule network formation. *Biochemical and biophysical research communications* **377:** 1051-1056

Shinoda T, Taya S, Tsuboi D, Hikita T, Matsuzawa R, Kuroda S, Iwamatsu A, Kaibuchi K (2007) DISC1 regulates neurotrophin-induced axon elongation via interaction with Grb2. *The Journal of neuroscience* **27:** 4-14

Sipos A, Rasmussen F, Harrison G, Tynelius P, Lewis G, Leon DA, Gunnell D (2004) Paternal age and schizophrenia: a population based cohort study. *Bmj* **329:** 1070

Sklar P, Ripke S, Scott LJ, Andreassen OA, Cichon S, Craddock N, Edenberg HJ, Nurnberger JI, Rietschel M, Blackwood D (2011) Large-scale genome-wide association analysis of bipolar disorder identifies a new susceptibility locus near ODZ4. *Nature genetics* **43:** 977

Smirnova E, Griparic L, Shurland D-L, Van Der Bliek AM (2001) Dynamin-related protein Drp1 is required for mitochondrial division in mammalian cells. *Molecular biology of the cell* **12:** 2245-2256

Smoller JW, Finn CT (2003) Family, twin, and adoption studies of bipolar disorder. *American Journal of Medical Genetics Part C: Seminars in Medical Genetics* **123:** 48-58

Smyth RL, Openshaw PJ (2006) Bronchiolitis. *The Lancet* **368:** 312-322

Snyder JS, Soumier A, Brewer M, Pickel J, Cameron HA (2011) Adult hippocampal neurogenesis buffers stress responses and depressive behaviour. *Nature* **476:** 458-461

Soares DC, Carlyle BC, Bradshaw NJ, Porteous DJ (2011) DISC1: Structure, Function, and Therapeutic Potential for Major Mental Illness. *ACS Chem Neurosci* **2:** 609-632

Soda T, Frank C, Ishizuka K, Baccarella A, Park Y, Flood Z, Park S, Sawa A, Tsai L (2013) DISC1–ATF4 transcriptional repression complex: dual regulation of the cAMP-PDE4 cascade by DISC1. *Molecular psychiatry* **18:** 898-908

Somerville SM, Conley RR, Roberts RC (2011a) Mitochondria in the striatum of subjects with schizophrenia. *World J Biol Psychiatry* **12:** 48-56

Somerville SM, Lahti AC, Conley RR, Roberts RC (2011b) Mitochondria in the striatum of subjects with schizophrenia: relationship to treatment response. *Synapse* **65:** 215-224

Song W, Li W, Feng J, Heston LL, Scaringe WA, Sommer SS (2008) Identification of high risk DISC1 structural variants with a 2% attributable risk for schizophrenia. *Biochemical and biophysical research communications* **367:** 700-706

`

Song Z, Ghochani M, McCaffery JM, Frey TG, Chan DC (2009) Mitofusins and OPA1 mediate sequential steps in mitochondrial membrane fusion. *Molecular biology of the cell* **20:** 3525-3532

Spinazzi M, Casarin A, Pertegato V, Salviati L, Angelini C (2012) Assessment of mitochondrial respiratory chain enzymatic activities on tissues and cultured cells. *Nature protocols* **7**: 1235-1246

St Clair D, Blackwood D, Muir W, Carothers A, Walker M, Spowart G, Gosden C, Evans HJ (1990) Association within a family of a balanced autosomal translocation with major mental illness. *Lancet* **336:** 13-16

St Clair D, Xu M, Wang P, Yu Y, Fang Y, Zhang F, Zheng X, Gu N, Feng G, Sham P (2005) Rates of adult schizophrenia following prenatal exposure to the Chinese famine of 1959-1961. *Jama* **294:** 557-562

Stanford SC (2007) The Open Field Test: reinventing the wheel. *Journal of Psychopharmacology* **21:** 134-135

Steen RG, Mull C, Mcclure R, Hamer RM, Lieberman JA (2006) Brain volume in first-episode schizophrenia Systematic review and meta-analysis of magnetic resonance imaging studies. *The British Journal of Psychiatry* **188:** 510-518

Stefansson H, Ophoff RA, Steinberg S, Andreassen OA, Cichon S, Rujescu D, Werge T, Pietiläinen OP, Mors O, Mortensen PB (2009) Common variants conferring risk of schizophrenia. *Nature* **460:** 744-747

Stöber G, Kocher I, Franzek E, Beckmann H (1997) First-trimester maternal gestational infection and cycloid psychosis. *Acta Psychiatrica Scandinavica* **96:** 319-324

Stowers RS, Megeath LJ, Górska-Andrzejak J, Meinertzhagen IA, Schwarz TL (2002) Axonal transport of mitochondria to synapses depends on milton, a novel Drosophila protein. *Neuron* **36:** 1063-1077

Sugimoto M, Tahara H, Ide T, Furuichi Y (2004) Steps involved in immortalization and tumorigenesis in human B-lymphoblastoid cell lines transformed by Epstein-Barr virus. *Cancer research* **64:** 3361-3364

Sullivan PF, Neale MC, Kendler KS (2000) Genetic epidemiology of major depression: review and meta-analysis. *Genetic Epidemiology* **157:** 1552-1562

Sullivan PF, Kendler KS, Neale MC (2003) Schizophrenia as a complex trait: evidence from a meta-analysis of twin studies. *Archives of general psychiatry* **60:** 1187-1192

Sullivan PF (2005) The genetics of schizophrenia. *PLoS medicine* **2**

Sullivan PF, Fan C, Perou CM (2006) Evaluating the comparability of gene expression in blood and brain. *American Journal of Medical Genetics Part B: Neuropsychiatric Genetics* **141:** 261-268

`

Sun X, Wang J-F, Tseng M, Young LT (2006) Downregulation in components of the mitochondrial electron transport chain in the postmortem frontal cortex of subjects with bipolar disorder. *Journal of Psychiatry and Neuroscience* **31:** 189

Susser E, Neugebauer R, Hoek HW, Brown AS, Lin S, Labovitz D, Gorman JM (1996) Schizophrenia after prenatal famine: further evidence. *Archives of general psychiatry* **53:** 25-31

Susser ES, Lin SP (1992) Schizophrenia after prenatal exposure to the Dutch Hunger Winter of 1944-1945. *Archives of general psychiatry* **49:** 983-988

Swerdlow NR, Weber M, Qu Y, Light GA, Braff DL (2008) Realistic expectations of prepulse inhibition in translational models for schizophrenia research. *Psychopharmacology* **199:** 331-388

Tait SW, Green DR (2010) Mitochondria and cell death: outer membrane permeabilization and beyond. *Nature reviews Molecular cell biology* **11**: 621-632

Tak PP, Firestein GS (2001) NF-κB: a key role in inflammatory diseases. *Journal of Clinical Investigation* **107:** 7-11

Tamminga CA, Stan AD, Wagner AD (2010) The hippocampal formation in schizophrenia. *The American journal of psychiatry* **167:** 1178-1193

Tandon R, Nasrallah HA, Keshavan MS (2010) Schizophrenia,"just the facts" 5. Treatment and prevention past, present, and future. *Schizophrenia research* **122:** 1-23

Taveggia C, Thaker P, Petrylak A, Caporaso GL, Toews A, Falls DL, Einheber S, Salzer JL (2008) Type III neuregulin-1 promotes oligodendrocyte myelination. *Glia* **56:** 284-293

Taya S, Shinoda T, Tsuboi D, Asaki J, Nagai K, Hikita T, Kuroda S, Kuroda K, Shimizu M, Hirotsune S, Iwamatsu A, Kaibuchi K (2007) DISC1 regulates the transport of the NUDEL/LIS1/14-3-3epsilon complex through kinesin-1. *The Journal of neuroscience : the official journal of the Society for Neuroscience* **27:** 15-26

Taylor MS, Devon RS, Millar JK, Porteous DJ (2003) Evolutionary constraints on the Disrupted in Schizophrenia locus. *Genomics* **81:** 67-77

Tennant C (2002) Life events, stress and depression: a review of recent findings. *Australian and New Zealand Journal of Psychiatry* **36:** 173-182

Thomson PA, Malavasi EL, Grunewald E, Soares DC, Borkowska M, Millar JK (2013) DISC1 genetics, biology and psychiatric illness. *Frontiers in biology* **8:** 1-31

Thomson PA, Parla JS, McRae AF, Kramer M, Ramakrishnan K, Yao J, Soares DC, McCarthy S, Morris SW, Cardone L, Cass S, Ghiban E, Hennah W, Evans KL, Rebolini D, Millar JK, Harris SE, Starr JM, Macintyre DJ, McIntosh AM, Watson JD, Deary IJ, Visscher PM, Blackwood DH, McCombie WR, Porteous DJ (2014) 708 Common and 2010 rare DISC1 locus variants identified in 1542 subjects: analysis for association with psychiatric disorder and cognitive traits. *Mol Psychiatry* **19:** 668–675

`

Tkachev D, Mimmack ML, Ryan MM, Wayland M, Freeman T, Jones PB, Starkey M, Webster MJ, Yolken RH, Bahn S (2003) Oligodendrocyte dysfunction in schizophrenia and bipolar disorder. *The Lancet* **362:** 798-805

Traherne J (2008) Human MHC architecture and evolution: implications for disease association studies. *International journal of immunogenetics* **35:** 179-192

Trinchieri G (2003) Interleukin-12 and the regulation of innate resistance and adaptive immunity. *Nature Reviews Immunology* **3:** 133-146

Twig G, Elorza A, Molina AJ, Mohamed H, Wikstrom JD, Walzer G, Stiles L, Haigh SE, Katz S, Las G (2008) Fission and selective fusion govern mitochondrial segregation and elimination by autophagy. *The EMBO journal* **27:** 433-446

Uranova N, Orlovskaya D, Vikhreva O, Zimina I, Kolomeets N, Vostrikov V, Rachmanova V (2001) Electron microscopy of oligodendroglia in severe mental illness. *Brain research bulletin* **55:** 597-610

Vader G, Lens S (2008) The Aurora kinase family in cell division and cancer. *Biochimica et Biophysica Acta (BBA)-Reviews on Cancer* **1786:** 60-72

Valvassori SS, Bavaresco DV, Budni J, Bobsin TS, Gonçalves CL, de Freitas KV, Streck EL, Quevedo J (2014) Effects of tamoxifen on tricarboxylic acid cycle enzymes in the brain of rats submitted to an animal model of mania induced by amphetamine. *Psychiatry research* **215:** 483-487

Valvassori SS, Rezin GT, Ferreira CL, Moretti M, Gonçalves CL, Cardoso MR, Streck EL, Kapczinski F, Quevedo J (2010) Effects of mood stabilizers on mitochondrial respiratory chain activity in brain of rats treated with d-amphetamine. *Journal of psychiatric research* **44:** 903-909

Van De Weerdt BC, Medema RH (2006) Review Polo-Like Kinases. *Cell cycle (Georgetown, Tex)* **5:** 853-864

van Haren NE, Pol HEH, Schnack HG, Cahn W, Brans R, Carati I, Rais M, Kahn RS (2008) Progressive brain volume loss in schizophrenia over the course of the illness: evidence of maturational abnormalities in early adulthood. *Biological psychiatry* **63:** 106-113

Van Laar VS, Berman SB (2013) The interplay of neuronal mitochondrial dynamics and bioenergetics: Implications for Parkinson's disease. *Neurobiology of disease* **51:** 43-55

Volz HR, Riehemann S, Maurer I, Smesny S, Sommer M, Rzanny R, Holstein W, Czekalla J, Sauer H (2000) Reduced phosphodiesters and high-energy phosphates in the frontal lobe of schizophrenic patients: a (31)P chemical shift spectroscopic-imaging study. *Biological psychiatry* **47:** 954-961

Walf AA, Frye CA (2007) The use of the elevated plus maze as an assay of anxiety-related behavior in rodents. *Nature protocols* **2:** 322-328

Wang J, Duncan D, Shi Z, Zhang B (2013) WEB-based GEne SeT AnaLysis Toolkit (WebGestalt): update 2013. *Nucleic Acids Res*

`

Wang Q, Charych E, Pulito V, Lee J, Graziane N, Crozier R, Revilla-Sanchez R, Kelly M, Dunlop A, Murdoch H (2011) The psychiatric disease risk factors DISC1 and TNIK interact to regulate synapse composition and function. *Molecular psychiatry* **16:** 1006-1023

Waxmonsky JA, Thomas MR, Miklowitz DJ, Allen MH, Wisniewski SR, Zhang H, Ostacher MJ, Fossey MD (2005) Prevalence and correlates of tobacco use in bipolar disorder: data from the first 2000 participants in the Systematic Treatment Enhancement Program. *General hospital psychiatry* **27**: 321-328

Wei J, Graziane NM, Wang H, Zhong P, Wang Q, Liu W, Hayashi-Takagi A, Korth C, Sawa A, Brandon NJ (2014) Regulation of N-methyl-D-aspartate receptors by disrupted-in-schizophrenia-1. *Biological psychiatry* **75:** 414-424

Weiss RB, Stange JP, Boland EM, Black SK, LaBelle DR, Abramson LY, Alloy LB (2015) Kindling of life stress in bipolar disorder: Comparison of sensitization and autonomy models. *Journal of abnormal psychology* **124:** 4

Wen Z, Nguyen HN, Guo Z, Lalli MA, Wang X, Su Y, Kim N-S, Yoon K-J, Shin J, Zhang C (2014) Synaptic dysregulation in a human iPS cell model of mental disorders. *Nature* **515**: 414-418

Wender PH, Kety SS, Rosenthal D, Schulsinger F, Ortmann J, Lunde I (1986) Psychiatric disorders in the biological and adoptive families of adopted individuals with affective disorders. *Archives of General Psychiatry* **43:** 923-929

Wenzel RP, Fowler III AA (2006) Acute bronchitis. *New England Journal of Medicine* **355:** 2125-2130

Westermann B (2012) Bioenergetic role of mitochondrial fusion and fission. *Biochimica et Biophysica Acta (BBA)-Bioenergetics* **1817:** 1833-1838

White MK, Pagano JS, Khalili K (2014) Viruses and human cancers: a long road of discovery of molecular paradigms. *Clinical microbiology reviews* **27:** 463-481

Wikgren M, Maripuu M, Karlsson T, Nordfjäll K, Bergdahl J, Hultdin J, Del-Favero J, Roos G, Nilsson L-G, Adolfsson R (2012) Short telomeres in depression and the general population are associated with a hypocortisolemic state. *Biological psychiatry* **71:** 294-300

Wilson-Kubalek EM, Cheeseman IM, Yoshioka C, Desai A, Milligan RA (2008) Orientation and structure of the Ndc80 complex on the microtubule lattice. *The Journal of cell biology* **182:** 1055-1061

Wittmann T, Hyman A, Desai A (2001) The spindle: a dynamic assembly of microtubules and motors. *Nature cell biology* **3:** E28-E34

Wolosker H, Blackshaw S, Snyder SH (1999) Serine racemase: a glial enzyme synthesizing D-serine to regulate glutamate-N-methyl-D-aspartate neurotransmission. *Proceedings of the National Academy of Sciences* **96:** 13409-13414

World Health Organization (1992) *The ICD-10 classification of mental and behavioural disorders: clinical descriptions and diagnostic guidelines.* Geneva: World Health Organization,

`

Xiu MH, Hui L, Dang YF, De Hou T, Zhang CX, Zheng YL, Chen DC, Kosten TR, Zhang XY (2009) Decreased serum BDNF levels in chronic institutionalized schizophrenia on long-term treatment with typical and atypical antipsychotics. *Progress in Neuro-Psychopharmacology and Biological Psychiatry* **33:** 1508-1512

Xu B, Roos JL, Levy S, Van Rensburg E, Gogos JA, Karayiorgou M (2008) Strong association of de novo copy number mutations with sporadic schizophrenia. *Nature genetics* **40:** 880-885

Xu M-Q, Sun W-S, Liu B-X, Feng G-Y, Yu L, Yang L, He G, Sham P, Susser E, Clair DS (2009) Prenatal malnutrition and adult schizophrenia: further evidence from the 1959-1961 Chinese famine. *Schizophrenia bulletin* **35:** 568-576

Xu Y, Sutachan JJ, Plesken H, Kelley RI, Schlame M (2005) Characterisation of lymphoblast mitochondria from patients with Barth syndrome. *Laboratory investigation* **85:** 823-830

Yang ES, Wang H, Jiang G, Nowsheen S, Fu A, Hallahan DE, Xia F (2009) Lithium-mediated protection of hippocampal cells involves enhancement of DNA-PK–dependent repair in mice. *The Journal of clinical investigation* **119:** 1124-1135

Yang J, Liu X, Bhalla K, Kim CN, Ibrado AM, Cai J, Peng TI, Jones DP, Wang X (1997) Prevention of apoptosis by Bcl-2: release of cytochrome c from mitochondria blocked. *Science (New York, NY)* **275:** 1129-1132

Yang Z, Klionsky DJ (2010) Eaten alive: a history of macroautophagy. *Nature cell biology* **12:** 814-822

Yoshino T, Kishi H, Nagata T, Tsukada K, Saito S, Muraguchi A (2001) Differential involvement of p38 MAP kinase pathway and Bax translocation in the mitochondria-mediated cell death in TCR-and dexamethasone-stimulated thymocytes. *European journal of immunology* **31:** 2702-2708

Youle RJ, van der Bliek AM (2012) Mitochondrial fission, fusion, and stress. *Science (New York, NY)* **337:** 1062-1065

Young-Pearse TL, Suth S, Luth ES, Sawa A, Selkoe DJ (2010) Biochemical and functional interaction of disrupted-in-schizophrenia 1 and amyloid precursor protein regulates neuronal migration during mammalian cortical development. *The Journal of Neuroscience* **30:** 10431-10440

Yue W-H, Wang H-F, Sun L-D, Tang F-L, Liu Z-H, Zhang H-X, Li W-Q, Zhang Y-L, Zhang Y, Ma C-C (2011) Genome-wide association study identifies a susceptibility locus for schizophrenia in Han Chinese at 11p11. 2. *Nature genetics* **43:** 1228-1231

Zala D, Hinckelmann M-V, Yu H, da Cunha MML, Liot G, Cordelières FP, Marco S, Saudou F (2013) Vesicular glycolysis provides on-board energy for fast axonal transport. *Cell* **152:** 479-491

Zammit S, Allebeck P, Andreasson S, Lundberg I, Lewis G (2002) Self reported cannabis use as a risk factor for schizophrenia in Swedish conscripts of 1969: historical cohort study. *Bmj* **325:** 1199

`

Zhang B, Kirov S, Snoddy J (2005) WebGestalt: an integrated system for exploring gene sets in various biological contexts. *Nucleic acids research* **33:** W741-748

Zhang B, Schmoyer D, Kirov S, Snoddy J (2004) GOTree Machine (GOTM): a web-based platform for interpreting sets of interesting genes using Gene Ontology hierarchies. *BMC bioinformatics* **5:** 16

Zhou X, Chen Q, Schaukowitch K, Kelsoe JR, Geyer MA (2010) Insoluble DISC1-Boymaw fusion proteins generated by DISC1 translocation. *Mol Psychiatry* **15:** 669-672

Zhou X, Geyer MA, Kelsoe JR (2008) Does disrupted-in-schizophrenia (DISC1) generate fusion transcripts? *Mol Psychiatry* **13:** 361-363

`

Appendix - Relevant Publications

At the time of writing one journal article has been published that is relevant to this thesis. The article was published by Oxford Journals, who grant permission to all authors the "right to include the article in full or in part in a thesis or dissertation, provided this is not published commercially".

Publication details:

"A t(1;11) translocation linked to schizophrenia and affective disorders gives rise to aberrant chimeric DISC1 transcripts that encode structurally altered, deleterious mitochondrial proteins"

Jennifer E. Eykelenboom, Gareth J. Briggs, Nicolas J. Bradshaw, Dinesh C. Soares, Fumiaki Ogawa, Sheila Christie, Elise L. Malavasi, Pravaskevi Makedonopoulou, Shaun Mackie, Patricia M. Malloy, Martin A. Wear, Elizabeth A. Blackburn, Janice Bramham, Andrew M. McIntosh, Douglas H. Blackwood, Walter J. Muir, David J. Porteous, J. Kirsty Millar

Human molecular genetics (2012) **21** (15) 3374-3386

This article contains work described in chapters 3 and 4 of the thesis, including the detection of the *CP1* transcript in t(1;11) lymphoblastoid cell lines and the expression of exogenous der 1 DISC1/DISC1FP1 chimeras in COS-7 cells and primary cortical neurons. With the latter work, neuronal culturing and transfection was carried out by Fumiaki Ogawa. Additionally, the pETG40a-MBP-ΔN597 and pETG40a-MBP-ΔNCP69 constructs I produced were used by Nicolas Bradshaw and Dinesh Soares to perform the biophysical structural analysis and characterisation of the respective truncated species. Jennifer Eykelenboom detected the *CP60* and *CP69* transcripts in t(1;11) lymphoblastoid cell lines and quantified their expression levels. Sheila Christie performed the Western blotting to attempt to detect endogenous chimeric species. The graphics were produced by Kirsty Millar, Nicolas Bradshaw and Dinesh Soares. The article was written by Kirsty Millar with input from David Porteous, Nicolas Bradshaw and Dinesh Soares.

Human Molecular Genetics, 2012, Vol. 21, No. 15 **3374–3386**
doi:10.1093/hmg/dds169
Advance Access published on April 30, 2012

A t(1;11) translocation linked to schizophrenia and affective disorders gives rise to aberrant chimeric *DISC1* transcripts that encode structurally altered, deleterious mitochondrial proteins

Jennifer E. Eykelenboom[1,†], Gareth J. Briggs[1], Nicholas J. Bradshaw[1,‡,¶], Dinesh C. Soares[1,¶], Fumiaki Ogawa[1], Sheila Christie[1], Elise L.V. Malavasi[1], Paraskevi Makedonopoulou[1], Shaun Mackie[1], Mary P. Malloy[1], Martin A. Wear[2], Elizabeth A. Blackburn[2], Janice Bramham[2], Andrew M. McIntosh[1,3], Douglas H. Blackwood[1,3], Walter J. Muir[1,3], David J. Porteous[1] and J. Kirsty Millar[1,*]

[1]Medical Genetics Section, University of Edinburgh Centre for Molecular Medicine, Medical Research Council Institute of Genetics and Molecular Medicine at the University of Edinburgh, Crewe Road, Edinburgh EH4 2XU, UK, [2]Institute of Structural and Molecular Biology, Centre for Translational and Chemical Biology, The University of Edinburgh, King's Buildings, Mayfield Road, Edinburgh EH9 3JR, UK and [3]University Department of Psychiatry, Royal Edinburgh Hospital, Edinburgh EH10 5HF, UK

Received February 16, 2012; Revised and Accepted April 24, 2012

***Disrupted-In-Schizophrenia 1* (*DISC1*) was identified as a risk factor for psychiatric illness through its disruption by a balanced chromosomal translocation, t(1;11)(q42.1;q14.3), that co-segregates with schizophrenia, bipolar disorder and depression. We previously reported that the translocation reduces *DISC1* expression, consistent with a haploinsufficiency disease model. Here we report that, in lymphoblastoid cell lines, the translocation additionally results in the production of abnormal transcripts due to the fusion of *DISC1* with a disrupted gene on chromosome 11 (*DISC1FP1/Boymaw*). These chimeric transcripts encode abnormal proteins, designated CP1, CP60 and CP69, consisting of DISC1 amino acids 1–597 plus 1, 60 or 69 amino acids, respectively. The novel 69 amino acids in CP69 induce increased α-helical content and formation of large stable protein assemblies. The same is predicted for CP60. Both CP60 and CP69 exhibit profoundly altered functional properties within cell lines and neurons. Both are predominantly targeted to mitochondria, where they induce clustering and loss of membrane potential, indicative of severe mitochondrial dysfunction. There is currently no access to neural material from translocation carriers to confirm these findings, but there is no reason to suppose that these chimeric transcripts will not also be expressed in the brain. There is thus potential for the production of abnormal chimeric proteins in the brains of translocation carriers, although at substantially lower levels than for native DISC1. The mechanism by which inheritance of the translocation increases risk of psychiatric illness may therefore involve both DISC1 haploinsufficiency and mitochondrial deficiency due to the effects of abnormal chimeric protein expression.**

GenBank accession numbers: *DISC1FP1* (EU302123), *Boymaw* (GU134617), der 11 chimeric transcript *DISC1FP1* exon 2 to *DISC1* exon 9 (JQ650115), der 1 chimeric transcript *DISC1* exon 4 to *DISC1FP1* exon 4 (JQ650116), der 1 chimeric transcript *DISC1* exon 6 to *DISC1FP1* exon 3a (JQ650117).

*To whom correspondence should be addressed. Tel: +44 1316511044; Fax: +44 1316511059; Email: kirsty.millar@ed.ac.uk
†Present address: Centre for Chromosome Biology, School of Natural Sciences, National University of Ireland, Galway, Ireland.
‡Present address: Department of Neuropathology, Heinrich Heine University Medical School, 40225 Düsseldorf, Germany.
¶These authors made equal contributions to this work.

INTRODUCTION

We identified *Disrupted-In-Schizophrenia 1* (*DISC1*) as a genetic risk factor for major mental illness, through study of a large Scottish family multiply affected with schizophrenia, bipolar disorder and major depressive disorder, that results from inheritance of a balanced t(1;11)(q42.1;q14.3) chromosomal translocation (1). On chromosome 1, the t(1;11) translocation directly disrupts *DISC1* and its non-coding antisense partner *DISC2* (2). Perturbed expression of one or both genes is therefore likely to be directly involved in disease pathogenesis. Independent genetic linkage and association data support the involvement of the *DISC* locus in schizophrenia, schizoaffective disorder, bipolar disorder, recurrent major depression, and most recently autism spectrum disorders, in multiple populations (3,4).

DISC1 is a scaffold protein now known to be essential for many critical brain processes, including regulation of neural precursor proliferation and differentiation (5), migration of newborn neurons within the developing cortex (6) and adult hippocampus (7), integration of newborn neurons into the existing neural circuitry (7), modulation of dendritic spines (8) and synapse formation/composition (7,9). If dysregulated by the t(1;11) translocation through the disruption of *DISC1*, it is conceivable that any or all of these processes could contribute to abnormal brain development and function, thereby triggering psychiatric illness.

Although we have previously provided evidence for haploinsufficiency as the disease mechanism in translocation carriers (10), we now provide evidence for an additional level of complexity. The translocation fuses *DISC1* to a gene on chromosome 11, *DISC1 Fusion Partner 1* (*DISC1FP1*), also known as *Boymaw* (11), resulting in the production of various aberrant chimeric transcripts with novel protein-coding potential. The proteins encoded by these transcripts consist of C-terminally truncated DISC1—in some instances fused to 1, 60 or 69 novel amino acids encoded by the *DISC1FP1* sequence. The 60 and 69 additional amino acids increase the α-helical content of DISC1 *in vitro*, resulting in the formation of abnormally large protein assemblies that exhibit increased thermal stability. When exogenously expressed, these abnormal chimeric proteins are predominantly targeted to mitochondria, where they induce abnormal morphology and abolish mitochondrial membrane potential. Overall, our data suggest that dysregulated mitochondrial function in proliferating cells and neurons may contribute to disease pathogenesis in translocation carriers.

RESULTS

Abnormal chimeric DISC1 transcripts result from the t(1;11) translocation

A gene referred to as *Boymaw* has previously been noted as spanning the chromosome 11 translocation breakpoint in the t(1:11) family (11). Analysis of expressed sequence tags (ESTs) indicates that transcripts produced from this gene (Fig. 1A) are alternatively spliced, utilizing multiple alternative exons and, in exon 5, alternative splice donor sites (Fig. 1B). This gene possesses no significant open reading frames (ORFs) and is therefore most likely a non-coding RNA gene.

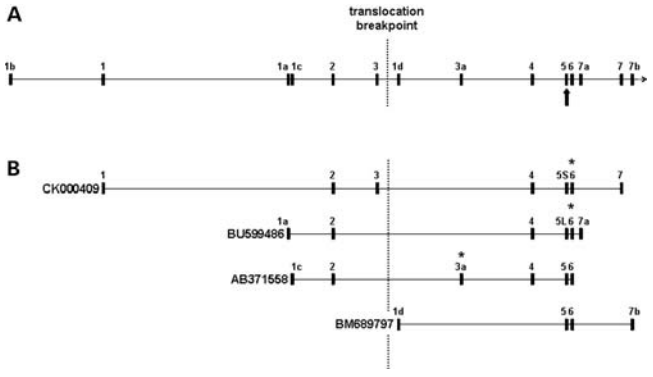

Figure 1. Schematic of *DISC1FP1* (not to scale). (**A**) *DISC1FP1* genomic structure showing all known exons (numbered according to 11 and 34). Arrow indicates alternatively spliced exon 5. (**B**) ESTs from *DISC1FP1*. Asterisks mark positions of translation stop codons predicted to be utilized in chimeric transcripts arising from the der 1 chromosome. CK000409 and BU599486 encode CP60 and CP69, respectively, both terminating within exon 6. AB371558 encodes CP1, which terminates within exon 3a.

DISC1 and the chromosome 11 gene are oriented such that the translocation causes gene fusion. Consequently, in lymphoblastoid cell lines, the derived 1 and 11 chromosomes (der 1 and der 11) may give rise to chimeric transcripts consisting of *DISC1* exons 1–8 fused to breakpoint distal exons of the chromosome 11 gene, or to breakpoint proximal exons of the chromosome 11 gene fused with *DISC1* exons 9–13, respectively (11).

Analysis of chimeric transcript expression using lymphoblastoid cell lines derived from t(1;11) translocation carriers demonstrated that such transcripts are indeed produced (Fig. 2A). Thus, the disrupted gene on chromosome 11 has been officially named *DISC1 Fusion Partner 1* (*DISC1FP1*) (12) to reflect this biological mechanism, although it has also been referred to using the AceView (13) name *Boymaw* (11). Reverse transcription PCR (RT-PCR) analysis using primer pairs designed to amplify chimeric transcripts from both the der 1 and der 11 chromosomes combined with sequencing detected the fusion of *DISC1* exon 9 to *DISC1FP1* exon 3a or exon 4, as well as the fusion of *DISC1FP1* exon 2 to *DISC1* exon 8 in cell lines carrying the translocation (Fig. 2A).

Breakpoint proximal, but not distal, *DISC1* transcript levels are reduced by the t(1;11) translocation

We have previously demonstrated that *DISC1* transcription occurs from the disrupted *DISC1* allele on chromosome 1, and that DISC1 transcript levels, quantified using PCR primers specific for exon 2, are reduced (10). In this extended study, we used SYBR green real-time PCR to quantify *DISC1* expression in lymphoblastoid cell lines derived from t(1;11) family members, utilizing primer pairs designed proximal to the translocation breakpoint, either within exon 2 or spanning exons 4–6 (detecting wild-type *DISC1* transcripts plus transcripts produced from the der 1 chromosome), or distal to the translocation breakpoint, within exon 9 (detecting wild-type

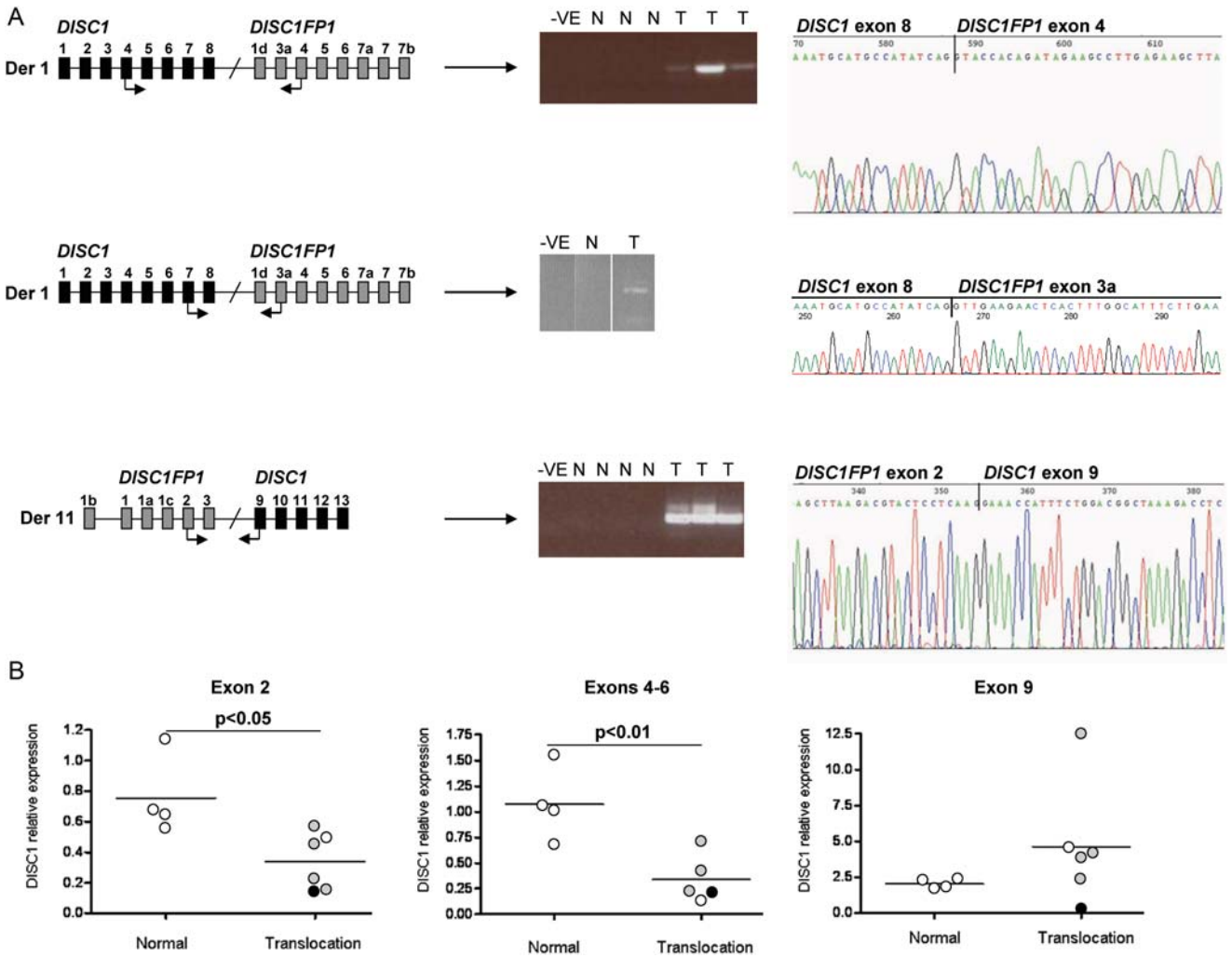

Figure 2. Chimeric transcript expression in t(1;11) family-derived lymphoblastoid cell lines. (**A**) RT-PCR detects chimeric transcripts in translocation cell lines. (Left) Schema of the fused genes on each derived chromosome. Black and grey boxes represent *DISC1* and *DISCFP1* exons, respectively. Arrows denote primers used in this analysis. (Middle) Amplified PCR products. −VE, N and T represent negative controls, normal karyotype cell lines and translocation cell lines, respectively. The *DISC1FP1* exon 2-*DISC1* exon 9 primer pair generated two products corresponding to the inclusion/exclusion of the alternatively spliced *DISC1FP1* exon 3. Data from the *DISC1* exon 7-*DISC1FP1* exon 3a primer pair are shown as three lanes spliced together from a single gel. (Right) RT-PCR products were sequenced to confirm chimeric transcript amplification. (**B**) Real-time PCR quantification of *DISC1* expression levels. Each dot represents a single cell line. Open, black and grey circles represent no diagnosis, schizophrenia and recurrent major depression, respectively. Horizontal lines represent the mean of each group. Statistical significance was determined independently for each primer pair using a two-tailed *t*-test to compare the group mean expression levels.

DISC1 transcripts plus transcripts produced from the der 11 chromosome).

We confirmed the reduction in *DISC1* transcript expression levels using primer pairs proximal to the t(1;11) breakpoint (Fig. 2B, $P < 0.05$ for exon 2 primers, $P < 0.01$ for exon 4–6 primers). In contrast, the exon 9 primers did not detect a decrease in *DISC1* expression in translocation carriers compared with normal karyotype controls (Fig. 2B). Altogether, assuming that DISC1 expression from the non-disrupted allele is unaltered by the translocation, these quantitative data demonstrate that chimeric transcripts produced from the der 1, but not the der 11, chromosome are scarce. The der 1 chimeric transcripts are predicted to have splice junctions downstream of the translation stop codon (Fig. 1B), a feature of aberrant transcripts that marks them for nonsense-mediated mRNA decay (14). These transcripts may therefore be targeted and degraded by this cellular surveillance mechanism and depleted from the cell. In contrast, there are no obvious stability issues for chimeric transcripts from the der 11 chromosome. This interpretation is complicated by the theoretical possibility that the exon 9 primer pair also detects *DISC2* transcripts, which overlap *DISC1* exon 9, although *DISC2* is expressed at unquantifiably low levels in lymphoblastoid cell lines (data not shown).

The translocation-carrying cell lines used in this analysis were derived from one unaffected carrier, and one and four carriers diagnosed with schizophrenia or severe recurrent depression, respectively. Although the sample numbers are low, it is worth pointing out that the quantitative measures

Table 1. Abnormal DISC1 protein species encoded by transcripts produced from the der 1 chromosome

CP1 (*DISC1* exons 1-8 plus *DISC1FP1* exon 3a, EST AB371558)

atgcatgccatatca**gGT**TGA
M H A I S **G** *

CP60 (*DISC1* exons 1-8 plus *DISC1FP1* exons 4-5S, EST CK000409)

atgcatgccatatca**gGT**ACCACAGATAGAAGCCTTGAGAAGCTTACTTTGGTCAGAAATTTTGCCTTTGTCTGCAGGCTTCTACCAGTTCGATT
M H A I S **G** T T D R S L E K L T L V R N F A F V C R L L P V R F

CCATCTGTGGGTCTTAGGTTTCAGTTACCTGAAGTCAAATGTGGTCCAATACACAGACTGGAATAAGAGACATTGGAGACTCCAAAAGAATATTT
H L W V L G F S Y L K S N V V Q Y T D W N K R H W R L Q K N I

TCTGGTAG
F W *

CP69 (*DISC1* exons 1-8 plus *DISC1FP1* exons 4-5L, EST BU599486)

atgcatgccatatca**gGT**ACCACAGATAGAAGCCTTGAGAAGCTTACTTTGGTCAGAAATTTTGCCTTTGTCTGCAGGCTTCTACCAGTTCGATT
M H A I S **G** T T D R S L E K L T L V R N F A F V C R L L P V R F

CCATCTGTGGGTCTTAGGTTTCAGTTACCTGAAGTCAAATGTGGTCCAATACACAGACTGGAATAAGAGACATTGGAGACTCCAAAAG*gtgggca*
H L W V L G F S Y L K S N V V Q Y T D W N K R H W R L Q K V G

*g*AATATTTTCTGGTAGACTGATATATTTCTCCTAA
R I F S G R L I Y F S *

Nucleotide sequences are shown above, and the corresponding translated amino acid sequence below. Der 1-derived chimeric transcripts are predicted to contain DISC1 exons 1–8, encoding amino acids 1–597, but for simplicity only amino acids 593–597 are shown. *DISC1*-derived nucleotides are in lower case, the codon and amino acid (glycine) at the junction are in bold type, lower case italics denote the alternatively spliced region at the 3′ end of *DISC1FP1* exon 5 (the short and long forms of the exon are designated 5S and 5L, respectively) and underlining marks the alternative amino acids within CP60 and CP69.

gave no indication of a relationship between DISC1 transcript levels and diagnosis.

Predicted abnormal DISC1 protein species encoded by the chimeric transcripts

Transcripts fusing *DISC1* exons 1–8 with *DISC1FP1* exons 4-end encode abnormal proteins consisting of DISC1 amino acids 1–597 fused at the C-terminus to novel amino acids encoded by *DISC1FP1*. Alternative splicing of *DISC1FP1* exon 5 induces a frameshift, resulting in the addition of 60 or 69 novel amino acids (Table 1). These proteins will be referred to as Chimeric Protein 60 and 69 (CP60 and CP69). Transcripts fusing *DISC1* exons 1–8 with *DISC1FP1* exon 3a encode DISC1 amino acids 1–597, plus a single glycine derived from the *DISC1FP1* sequence (Table 1). This protein will be referred to as CP1. Since there is normally a glycine at position 598 in DISC1, CP1 essentially corresponds to DISC1 amino acids 1–598.

Chimeric transcripts produced from the der 11 chromosome contain an internal ORF corresponding to amino acids 669–854 of the DISC1 C-terminus. This ORF is unlikely to be translated because *DISC1FP1* is apparently non-coding; therefore, the sequence upstream of the DISC1 ORF is unlikely to provide the signals necessary for translation initiation.

Fusion protein 69 exhibits altered structure and thermal stability

We speculated that the addition of 60 or 69 novel amino acids would alter the properties of the N-terminal DISC1 fragment encoded by the chimeric transcripts. We selected DISC1

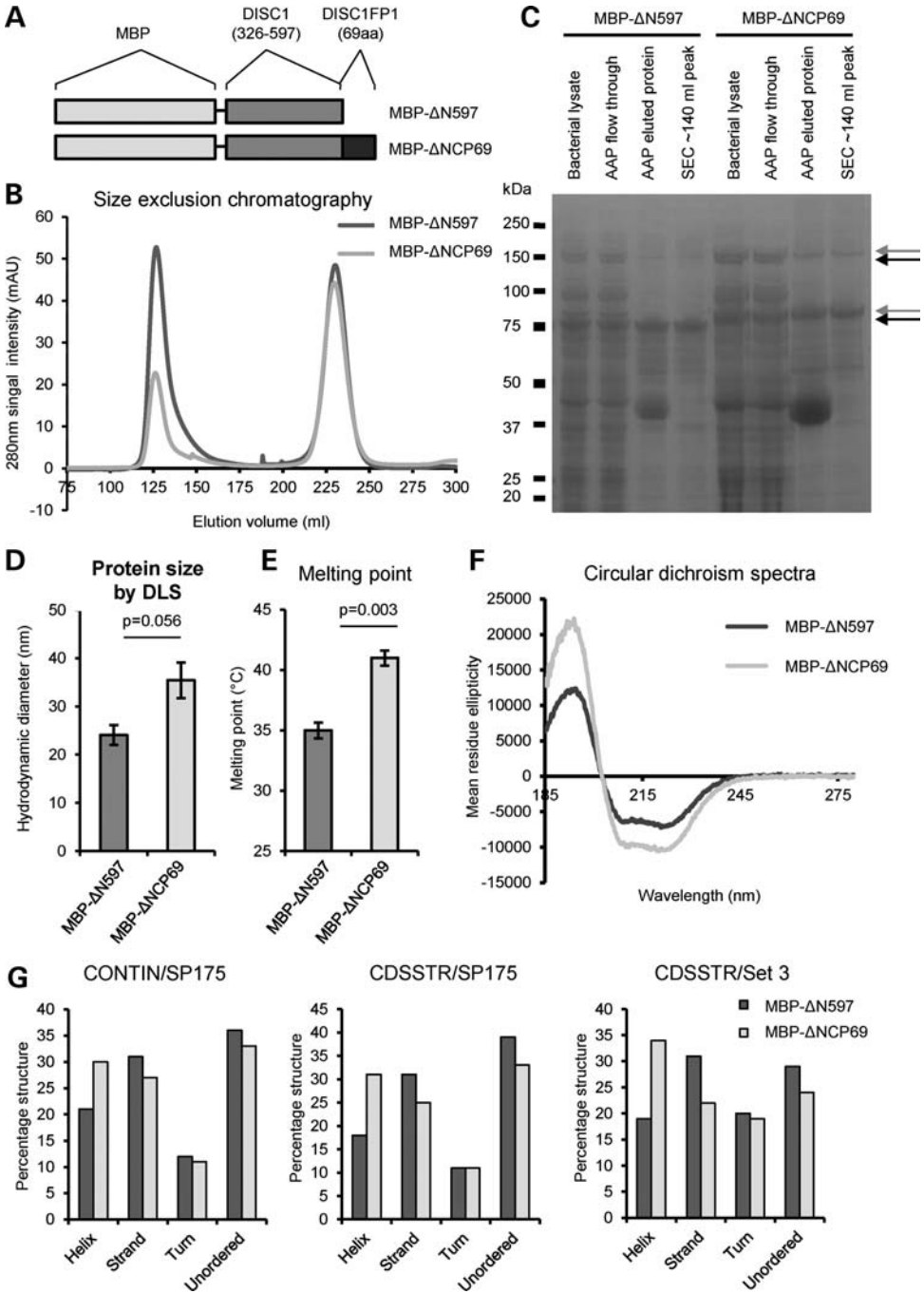

Figure 3. Biophysical characterization of CP69. (**A**) Schematic of the recombinant proteins MBP-ΔN597 and MBP-ΔNCP69, drawn to scale. (**B**) Following amylose affinity purification, size exclusion chromatography separates the recombinant protein (~140 ml peak) from co-purifying contaminants (later peaks); CV: 320 ml. (**C**) SDS–PAGE purification gel of MBP-ΔN597 and MBP-ΔNCP69 proteins. AAP, amylose affinity purification; SEC, size exclusion chromatography. Arrows indicate monomers and dimers. (**D**) Mean hydrodynamic diameters of three independent protein preparations for each of MBP-ΔN597 and MBP-ΔNCP69 determined by DLS. (**E**) Mean melting temperatures of three independent protein preparations for each of MBP-ΔN597 and MBP-ΔNCP69 determined by DLS at increasing temperatures. (**F**) CD spectra of MBP-ΔN597 (0.12 mg/ml) and MBP-ΔNCP69 (0.11 mg/ml) in the far-UV range is shown, with mean residue ellipticity and wavelength (measured from 280 to 185 nm) plotted along the *y*-axis and *x*-axis, respectively. (**G**) Deconvolution of the CD spectra using different algorithms and data sets.

amino acids 326–597 for analysis, fused to maltose-binding protein (MBP) tags, based upon considerations of domain delineation, predicted protein disorder in the N-terminus of native DISC1 and likely consequences for protein expression, purification, and finally on the assessment of secondary structure for the C-terminus of native DISC1 (15). This DISC1 region was expressed both by itself (MBP-ΔN597) or fused to the novel 69 amino acids of CP69 (MBP-ΔNCP69, Fig. 3A),

selected because it is the longest of the chimeric proteins. Following purification from *Escherichia coli*, each product was detectable as two major species (75 and 150 kDa for MBP-ΔN597 and 80 and 160 kDa for MBP-ΔNCP69) on an SDS–PAGE gel (Fig. 3B and C). The molecular weights of these species correspond to the predicted molecular weights of the protein monomers and SDS-resistant dimers (respectively, 76.8 and 153.6 kDa for MBP-ΔN597, and 85.1 and 170.2 kDa for MBP-ΔNCP69). The identities of these species were confirmed by mass spectrometry (Supplementary Material, Figs S1 and S2).

Measurement of native purified protein size (hydrodynamic diameter) using dynamic light scattering (DLS) revealed that MBP-ΔNCP69 forms larger species compared with MBP-ΔN597, although this fell just short of statistical significance ($P = 0.056$, Fig. 3D). In support of this, the initial size exclusion chromatography also suggests that the MBP-ΔNCP69 assembly has a larger hydrodynamic diameter (Fig. 3B). The thermal stability of each protein was then assessed by taking DLS readings at steadily increasing temperatures and measuring the point at which changes in protein structure occur. MBP-ΔNCP69 exhibits a consistently higher melting point than MBP-ΔN597 ($P = 0.003$, Fig. 3E). Altogether, the increased size and higher melting point of MBP-ΔNCP69 suggest that the addition of 69 novel amino acids induces the formation of larger structures with increased stability.

Far-UV circular dichroism (CD) spectra were then recorded to estimate the secondary structure content. Both MBP-ΔN597 and MBP-ΔNCP69 exhibit a pronounced double-negative minimum at ∼208 and ∼222 nm and one positive peak at ∼193 nm in the far-UV range (Fig. 3F), a characteristic of folded proteins with a high α-helical content (16). However, MBP-ΔNCP69 displays significantly more pronounced negative and positive ellipticity centred in these regions, when compared with MBP-ΔN597, implying a greater propensity towards α-helices and indicating that secondary structure variation exists as a result of the novel 69 amino acids. Indeed, upon spectral deconvolution using three combinations of algorithms and reference sets (17–21), the MBP-ΔNCP69 structure is estimated to possess ∼1.4–1.8 times greater α-helical content and lower β-strand composition compared with MBP-ΔN597 (Fig. 3G).

Analysis of the novel 60 and 69 *DISC1FP1* residues shows a strong disagreement between three secondary structure prediction programs (22–24) (Fig. 4); PsiPred predicts several low-confidence β-strands for this region, whereas JPred3 and Porter predict an abundance of α-helices. The CD spectroscopy results revealing elevated α-helical content in MBP-ΔNCP69 are in agreement with the latter predictions. PCoils/Coils (25,26) did not predict any coiled-coil motifs. Although the presence of the MBP tag precludes direct comparison with other CD studies that investigated the C-terminal region of DISC1 (27), altogether these data imply an overall mixed α/β fold for this region.

Thus, it appears that the addition of 69 amino acids from *DISC1FP1* introduces clear differences in secondary structure compared with the control truncated DISC1 protein, resulting in the formation of larger, more stable protein assemblies.

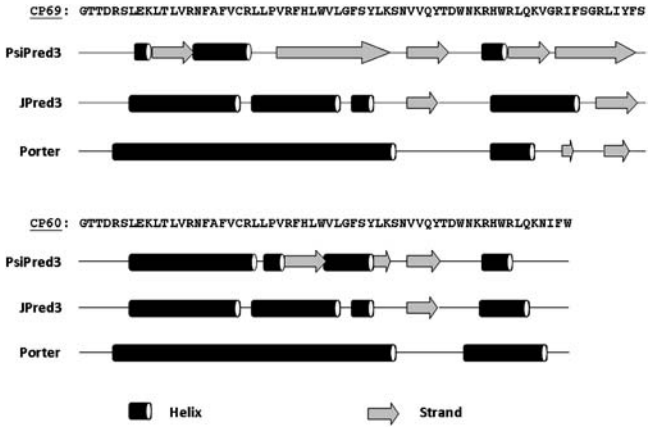

Figure 4. Secondary structure predictions for the *DISC1FP1*-derived amino acids of CP60 and CP69, using three prediction programs: PsiPred3, JPred3 and Porter.

CP60 and CP69 are mitochondrial proteins that induce mitochondrial dysfunction

DISC1 has been detected at multiple subcellular locations, including the centrosome (28), nucleus (29), mitochondria (30), Golgi (31) and synapse (32). C-terminally truncated DISC1 (amino acids 1–597) instead adopts a predominantly diffuse cytoplasmic distribution (Fig. 5A) (6). In COS7 cells, FLAG-tagged CP1 also adopts a diffuse cytoplasmic distribution (Fig. 5A), confirming that these two proteins most likely have highly similar properties.

FLAG-CP60 and FLAG-CP69, however, are strongly targeted to mitochondria in COS7 cells, where they alter mitochondrial morphology from the normal extended tubular structure to abnormal perinuclear clusters (Fig. 5A). Intriguingly, the majority of these abnormal clustered mitochondria do not take up the mitochondrial membrane potential-dependent dye mitotracker (Fig. 5A), indicating that chimeric protein expression inhibits normal mitochondrial function. Importantly, this loss of membrane potential occurs even when the chimeric proteins are exogenously expressed at the lowest levels detectable using this method (Fig. 5A). However, co-staining with the mitochondrial marker cytochrome *c* reveals that the mitochondria remain intact (Fig. 5A). DISC1 has previously been reported to induce mitochondrial dysfunction, including altered mitochondrial NADH activity (33). This enzyme participates in oxidative phosphorylation, a process which generates and maintains the mitochondrial membrane potential, thus the loss of mitochondrial membrane potential in cells expressing CP60 or CP69 possibly indicates a deleterious effect upon mitochondrial NADH activity. In cultured primary cortical neurons from the CD1 mouse strain [days *in vitro* (DIV) 5], or the C57BL/6 mouse strain (DIV 11), FLAG-CP60 and FLAG-CP69 induce the same mitochondrial clustering and the loss of membrane potential (Fig. 5B and Supplementary Material, Fig. S3). Altogether, these data show that the altered biophysical properties demonstrated for CP69, and most likely possessed by CP60 also, correlate with profoundly altered function within proliferating cells and neurons.

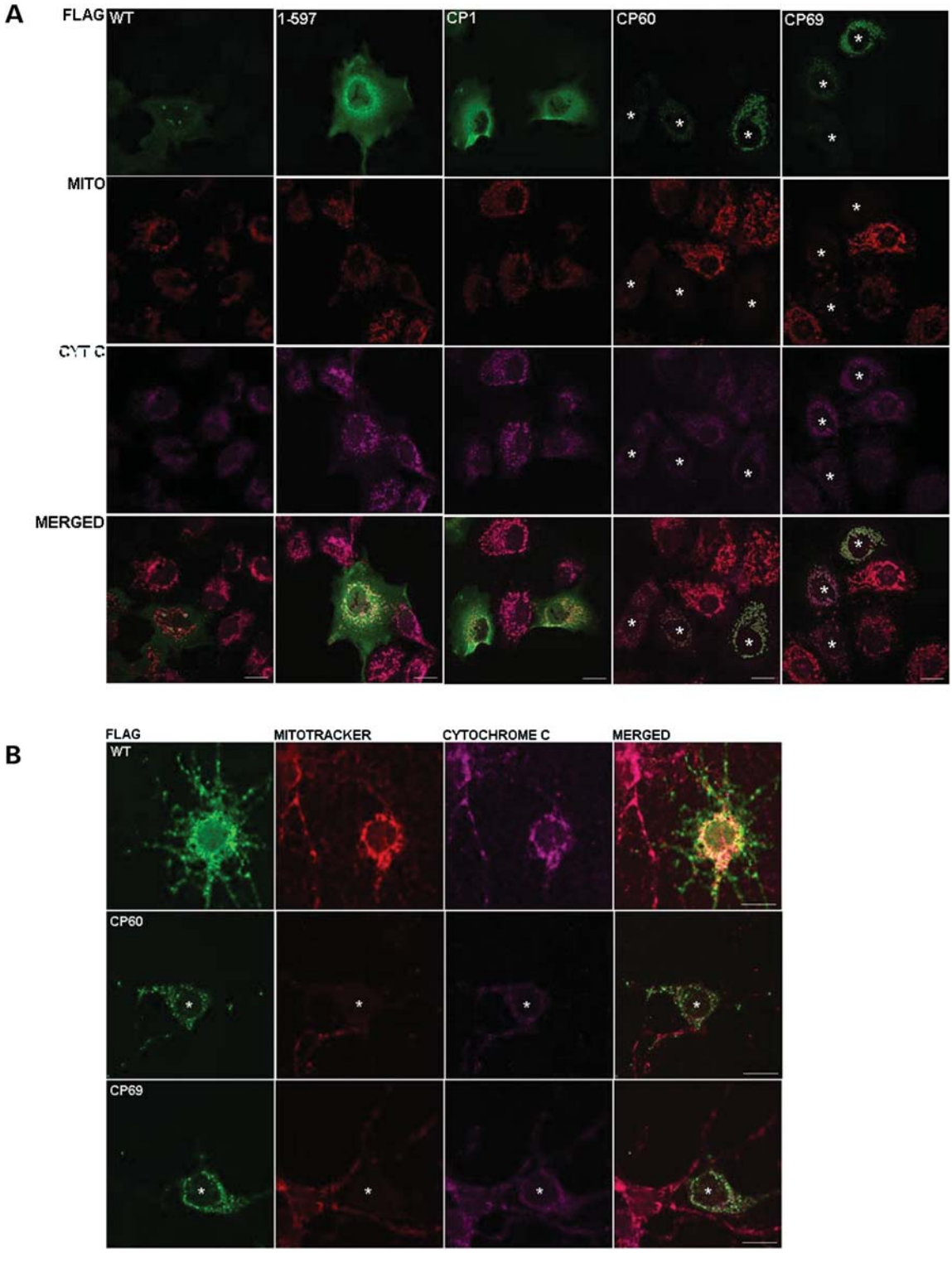

Figure 5. Exogenous chimeric protein expression in COS7 cells and cultured CD1 mouse primary neurons. (**A**) Immunofluorescence detection of FLAG-tagged DISC1 (green), mitochondria (MitoTracker Red CMXRos) and cytochrome *c* (pink) in COS7 cells. Asterisks indicate cells transfected with CP60 or CP69, marking cells with low-, medium- or high-level expression. Scale bars represent 20 μm. (**B**) Immunofluorescence detection, as above, in primary mouse cortical neurons. Asterisks indicate cells transfected with CP60 or CP69. Scale bars represent 10 μm.

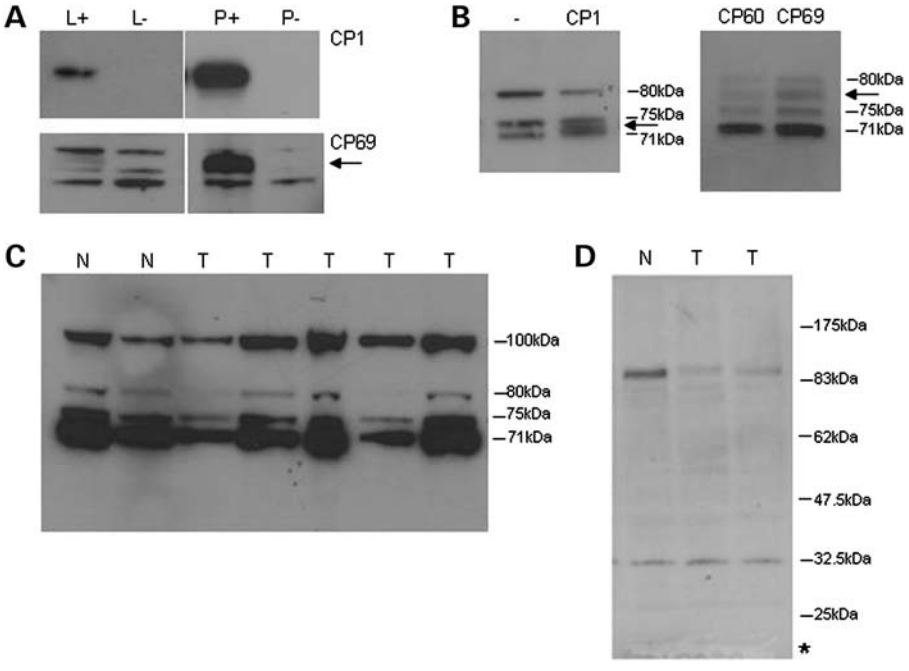

Figure 6. Chimeric protein expression in t(1;11) family-derived lymphoblastoid cell lines. (**A**) Overexpressed untagged CP69 partitions predominantly to pellets from transfected COS7 cells, as detected using antibody R47. L, lysate; P, pellet; +, transfected; -, non-transfected. Arrow marks CP69. CP60 expression is indistinguishable from that of CP69 (data not shown). (**B**) Migration of CP1, CP60 and CP69 with respect to endogenous species expressed in COS7, as detected by R47, shown only in lysates for clarity. Endogenous species sizes are indicated. -, non-transfected. Arrows mark the positions of overexpressed chimeric proteins. (**C**) Detection of endogenous species by R47 in lymphoblastoid cell line pellets. N, normal karyotype. Endogenous species sizes are indicated, including full-length DISC1 at 100 kDa. T, translocation. (**D**) Detection of endogenous species by α-DISC1 in lymphoblastoid cell line lysates. N, normal karyotype; T, translocation. The asterisk marks the predicted size of the hypothetical translation product of chimeric transcripts arising from the der 11 chromosome.

Investigating chimeric protein expression in lymphoblastoid cell lines

Identification of *DISC1* chimeric transcripts prompted us to re-examine our previous report of reduced DISC1 protein expression as a result of the t(1;11) translocation (10). We expressed untagged CP1, CP60 or CP69 in COS7 cells, and investigated isoform expression using DISC1 antibody R47, specific for the N-terminal head domain (30). This demonstrated that CP1 is abundant in soluble lysates, whereas CP60 and CP69 partition predominantly to the pellet produced during cell lysis (Fig. 6A), as has been noted previously for a related DISC1 chimeric protein (34). However, a small proportion of each chimeric protein is also detectable within the soluble lysates. In addition to full-length DISC1, R47 detects a triplet of species of ∼71–80 kDa (30). CP1 (predicted molecular weight of 64.5 kDa) migrates between the 71 and 75 kDa species, whereas CP60 and CP69 (predicted molecular weights of 71.8 and 72.8 kDa, respectively) migrate between the 75 and 80 kDa species, thus each chimeric protein is distinct from the endogenous species detected by R47 on immunoblots (Fig. 6B).

We next examined lymphoblastoid cell lines derived from members of the t(1;11) family. Our previous analysis focused on lysates, and did not detect any abnormal species in translocation cell lines (10). In this study, we examined pellets. The same triplet of bands at 71–80 kDa is detectable in both lysates and pellets, with no additional species detectable in cell lines carrying the translocation (Fig. 6C). The chimeric proteins are thus either not expressed, or are present below the level of detection using this antibody. The latter is consistent with the production, but apparent low expression/predicted short lifespan, of chimeric transcripts from the der 1 chromosome.

We also used α-DISC1 (35), an antibody specific for a translocation breakpoint distal DISC1 epitope that should detect the C-terminal fragment, amino acids 669–854, encoded by chimeric transcripts from the der 11 chromosome. Although the antibody clearly detects full-length DISC1 in the lymphoblastoid cell lines, it failed to detect any novel species in translocation cell lines that could correspond to this fragment (predicted molecular weight of 20.9 kDa, Fig. 6D). Thus, as with the N-terminal chimeric proteins, this fragment is either not expressed, or is present but below the detection limit of the antibody.

DISCUSSION

Although the t(1;11) translocation is a unique genetic event, understanding its molecular consequences in full may help explain the very high penetrance of this mutation and inform on other clinical mutations (15). Aberrant DISC1 proteins putatively arising from the der 1 chromosome lack the final 257 amino acids, required for interaction with a number of important binding partners, including NDE1/NDEL1 (15). C-terminal truncation will thus abolish critical interactions (36), while maintaining others that require amino acids 1–

597, such as GSK3β (5,36). Phosphodiesterase 4 (10) utilizes multiple contact sites within amino acids 1–597 that are sufficient for DISC1/PDE4 interaction (10), but also a C-terminal site that is abolished by the translocation (37), which may consequently dysregulate this complex and dynamic interaction. Altogether, these few examples demonstrate that expression of C-terminally truncated DISC1 is likely to have pleiotropic effects at the cellular level. The importance of this is illustrated by the demonstration that, *in vivo*, expression of amino acids 1–597 by *in utero* electroporation in mice blocks neuronal migration within the developing cortex (6), whereas its transgenic expression in mice induces phenotypes resembling characteristics of human mental illness including enlarged lateral ventricles, and various behavioural deficits (38,39). The shortest aberrant species encoded by transcripts from the der 1 chromosome is CP1, which essentially corresponds to DISC1 amino acids 1–598. CP1 localization is indistinguishable from the aberrant localization of amino acids 1–597 (6); thus, we conclude it is a comparable species that is likely to behave in a similar manner.

Over and above the multiple effects of expressing amino acids 1–597, the additional 60 or 69 novel amino acids in CP60 and CP69 alter the structure of DISC1 amino acids 326–597, leading to the production of larger, more stable protein assemblies. This is intriguing because detergent-insoluble DISC1 aggregates have been detected previously in post-mortem brain samples from psychiatric patients (40,41). Altogether these observations highlight aberrant DISC1 assembly as a possible disease mechanism in psychiatric illness (40,41). The abnormal structure of CP60 and CP69 is predicted to adversely influence protein interactions, and is most likely related to their extreme effects upon mitochondrial morphology and membrane potential, effects which are not induced by amino acids 1–597 alone. However, CP60 and CP69 are very scarce in the translocation-carrying lymphoblastoid cell lines used in this study, if indeed they are expressed at all, so these data must be interpreted with caution. That said, we have demonstrated that even expression of these chimeric proteins at the lowest detectable levels is sufficient to induce mitochondrial dysfunction; thus, it is likely that any endogenous expression of these proteins would be deleterious.

It is not possible to properly assess the contributions of CP1, CP60 and CP69 to disease pathogenesis in translocation carriers until neural material is available for analysis. Induced pluripotent stem cell technology is the most likely route to this, and will be available in the not-too-distant future. Until then, we can only speculate that, because DISC1 is expressed extensively in the developing and adult brain, and expression of CP1, CP60 and CP69 is driven by the *DISC1* promoter, it is likely that at some time chimeric transcripts will be produced at some level in the brain of t(1;11) carriers. Although this specific disease mechanism is unique to translocation carriers, it is notable that C-terminal truncation, addition of GFP tags and the 'ultra-rare' putative causal mutation R37W, identified in a single schizophrenic patient (42), all increase DISC1 mitochondrial targeting and induce abnormal morphology (Ogawa *et al*., manuscript in preparation) (43), whereas the schizophrenia-associated variant L607F influences neuronal mitochondrial transport (44). The psychiatric illness suffered by translocation carriers displays no unique features, thus it likely arises from dysregulation of a pathway common to other unrelated patients. Similarly, the abnormal chimeric DISC1 species, though unique, may act through a common pathway. We propose that this common pathway involves mitochondrial dysfunction. Mitochondria are essential for multiple processes within most cells, due to their role in the provision of energy and calcium homeostasis, as well as their role in apoptosis, either for the clearance of damaged cells or in programmed cell death. In the brain, neurons are particularly sensitive to mitochondrial dysfunction, because mitochondria must be transported to distal dendrites for the supply of energy and calcium buffering to the synapse (45). DISC1 is known to be critical for neural precursor proliferation and differentiation, neuronal migration and integration and synaptic signalling within the developing and adult brain (46). It is conceivable that many, if not all, of these processes would be compromised by mitochondrial dysfunction, if the chimeric proteins CP60 and CP69 are indeed expressed in the brains of t(1;11) translocation carriers, coupled with reduced expression of DISC1 at other subcellular locations, such as the synapse, nucleus and centrosome, due to the loss of normal DISC1 expression from the translocated allele.

MATERIALS AND METHODS

Bioinformatic methods

Chromosome 11 ESTs and DISC1 sequences were examined using the UCSC genome browser (http://genome.ucsc.edu). Predicted cDNA produced by the translocation was evaluated for coding potential, using the ExPASy TRANSLATE tool (www.expasy.org). Molecular weight calculations were also carried out using the ExPASy TRANSLATE tool and the ExPASy Compute Mw tool. Protein secondary structure predictions were made by submitting amino acid sequences independently to PsiPred (23), Jpred3 (22) and Porter (24).

Cell culture and transfection

This study utilized lymphoblastoid cell lines derived from members of the t(1;11) translocation family, either with a normal karyotype or carrying the balanced translocation. Translocation carriers included unaffected family members as well as those diagnosed with either schizophrenia or severe recurrent depression. Lymphoblastoid cell lines were grown in RPMI (Gibco) supplemented with 10% fetal calf serum (Gibco) under standard conditions, with a 75% medium change every 2–3 days. Karyotypes of cell lines used in this study were confirmed by chromosome banding of metaphase spreads. All lymphoblastoid cell lines were grown and harvested concurrently to minimize any effects upon gene expression due to variable growth conditions.

COS7 cells were maintained in Dulbecco's modified Eagle's medium (Invitrogen) containing 10% fetal bovine serum at 37°C in a 5% CO_2 humidified atmosphere. Cortical neuron cultures were prepared from embryonic day (E) 18 mouse fetuses (CD1 or C57BL/6) as described previously (32), grown on cover slips coated with Poly-D-lysine and maintained in Neurobasal medium supplemented with 2% of

B-27 and 2 mM Glutamax (all from Invitrogen) at 37°C with 5% CO_2. Transfection of cultured cells and cortical neurons at 5 or 11 DIV was conducted using Lipofectamine 2000 (Invitrogen) according to the manufacturer's instructions.

RT-PCR analysis

RNA was prepared using the Qiagen RNeasy extraction kit, and cDNA was prepared using the First Strand cDNA synthesis kit (Roche) according to the manufacturer's instructions. PCR, to detect novel *DISC1* chimeric transcripts, was carried out using Thermostart Taq polymerase (Abgene). A typical reaction contains 2 μl of 10× PCR reaction buffer, 1.2 μl of 25 mM magnesium chloride, 0.5 μl of dNTPs (of a 10 mM stock), 0.25 μl of forward and reverse primers (of a 300 ng/μl stock), 0.1 μl of Taq polymerase, 2 μl of DNA template and 13.7 μl of sterile water to a final volume of 20 μl. These reactions were cycled using a touchdown PCR programme as follows: [95°C, 15 min; 94°C, 1 min; 70°C, 30 s (−2°C/cycle); 72°C: 30 s] × 6 cycles, followed by (94°C: 1 min; 60°C: 30 s; 72°C: 30 s) × 34 cycles, or for amplification of transcripts encoding CP1: hot start 95°C: 2 min, followed by (95°C: 30 s; 60°C: 30 s; 72°C: 30 s) × 35 cycles. Products were resolved using standard agarose gel electrophoresis.

For quantitative measurements, *DISC1* expression was measured using the SYBR Green Real-time PCR Detection System (Bio-Rad Laboratories Ltd). For the quantification of *DISC1* in t(1;11) family cell lines, a single reaction contained 7.5 μl of SYBR Green 2× Master Mix (Bio-Rad Laboratories Ltd), 0.25–0.5 μl of forward and reverse primers (stock concentration of 300 ng/μl), 3 μl of template cDNA and distilled water to a final volume of 15 μl. The reactions were cycled using the MyiQ Single-Colour Real-Time PCR Detection System (Bio-Rad Laboratories Ltd) as follows: 95°C: 3 min (1 cycle); 95°C: 10 s; 66°C: 30 s; 72°C: 45 s (40 cycles), followed by melt curve analysis: 55°C: 10 s (+0.5°C per cycle for 80 cycles). Relative *DISC1* expression levels were calculated using the MyiQ Gene expression macro (Bio-Rad Laboratories Ltd), which utilizes the deltaCT method and corrects for primer amplification efficiencies (http://medgen.ugent.be/~jvdesomp/genorm) (47). *DISC1* expression levels were normalized using the geometric mean of *Glyceraldehyde-3-phosphate dehydrogenase* (*Gapdh*) and *Phosphofructokinase* (*PFK*), and the use of each housekeeping gene gave the same results. The same panel of 10 cell lines (four normal, six translocation) was used for each assay. Results were obtained for all cell lines in each assay, with the exception of one translocation cell line when primers specific for *DISC1* exons 4 and 6 were used. This failed assay was not repeatable since the RNA sample in question was spent. Data were analysed by two-tailed *t*-test (GraphPad Prism).

PCR product sequencing

Single PCR products were treated with ExoSAP-IT (GE Healthcare) prior to direct sequencing. Multiple PCR products were resolved by LMP agarose gel electrophoresis and extracted using the QIAquick gel extraction kit (Qiagen) prior to direct sequencing. Alternatively, purified PCR products were cloned using the TOPO TA cloning kit (Invitrogen) according to the manufacturer's instructions. BigDye Terminator sequencing of PCR products or plasmid DNA was carried out using 1 μl of BDv3.1, 1.5 μl of 5× sequencing buffer, 1 μl of DNA template and 6 μl of dH_2O. Reactions were cycled as follows: 96°C: 1 min (1 cycle); 96°C: 10 s; 50°C: 5 s; 60°C: 4 min (25 cycles); 4°C hold. Sequencing chromatograms were analysed using Chromas (version 1.45) (48).

Primer sequences

The primers used to detect *DISC1* expression by real-time PCR in t(1;11) cell lines were as follows: Exon 2 forward 5-GAACGTGGAGAAGCAGAAGG, reverse 5-CAGAGAACTGGAGGAGCCAG; Exons 4–6 forward 5-AGCCTGCACTTTCAACTTCC, reverse 5-AGTTGCTGCTCTTGCTCCTC; Exon 9 forward 5-AGAGAGAGAAGGGCTGGAGG, reverse 5-GTCTCCTGGTGCTCCACTTC.

The housekeeping primers used were as follows: *Gapdh* forward 5-GGGAGCCAAAAGGGTCATCA, reverse 5-GTGGCAGTGATGGCATGGAC; *hPFK* forward 5-AGAGCGTTTCGATGATGCTT, reverse 5-GTGTTCCTCCCAGTCGTCAT.

Primers used to amplify *DISC1* chimeric transcripts were as follows: Derived 1 *DISC1* chimeric transcript: Exon 4 *DISC1* forward 5-AGCCTGCACTTTCAACTTCC, *DISC1FP1* exon 4 reverse 5-AAGACCCACAGATGGAATCG; Derived 1 *DISC1* chimeric transcript: Exon 6/7 *DISC1* forward 5-AAGGAGCCTCCAGGAAAGAA, *DISC1FP1* exon 3a reverse 5-CAAGAAATGCCAAAGTGAGTTC; Derived 11 *DISC1* fusion with BU599486: exon 2 forward 5-GGGACCTGGAATTGAAGAGA, *DISC1* Exon 9 reverse 5-GTCTCCTGGTGCTCCACTTC.

Primers used for the mutagenesis of recombinant *DISC1*/*DISCFP1* chimeric transcripts: forward 5-AAATGCATGCAATTAGCTAATAAGGCACCACCGATCGTAGTCTG, reverse 5-CAGACTACGATCGGTGGTGCCTTATTAGCTAATTGCATGCATTT.

Plasmid constructs

A pcDNA3.1 expression construct carrying full-length N-terminally FLAG-tagged DISC1 has been described previously (37). ORFs encoding human DISC1 amino acids 1–597, plus the 60 or 69 residues from *DISC1FP1* (CP60 or CP69), were synthesized by GeneArt (Invitrogen) and inserted, untagged, in pcDNA3.1. To generate tagged versions of CP60 and CP69, N-terminal FLAG-tags were subsequently added. N-terminally FLAG-tagged DISC1 amino acids 1–597 and 1–598 were also in pcDNA3.1.

An ORF encoding N-terminally His-tagged human DISC1 amino acids 326–597, plus the 69 residues from *DISC1FP1*, was codon-optimized for expression in *E. coli* and synthesized by GeneArt (Invitrogen, Supplementary Material, Fig. S1). The ORF was recombined sequentially into pDONR-221 (Invitrogen) and pETG-40A (A. Geerlof, EMBL) vectors using BP and LR clonase (Invitrogen), adding an N-terminal MBP tag. This construct will be referred to as MBP-ΔNCP69. A control construct, lacking the additional 69-residues (MBP-ΔN597),

was generated by the introduction of two stop codons after the final wild-type DISC1 residue, using a QuikChange II Site-Directed Mutagenesis Kit (Agilent Technology). The cloned constructs were confirmed by sequencing.

Recombinant protein production

Identical expression and purification conditions were used for MBP-ΔN597 and MBP-ΔNCP69. Constructs were first transformed into *E. coli* BL21 Star (DE3) (Invitrogen) and grown in 2XTY medium containing 100 μg/ml carbenicillin to an optical density of ∼0.6 at 37°C (at 600 nm). Protein expression was induced with 1 mM IPTG (isopropyl β-D-thiogalactoside) and cultures were grown at 37°C for 3 h before harvesting by centrifugation (5500*g*, 4°C, 15 min) and pellets snap-frozen and stored at −70°C until required. For purification, bacterial pellets were spun down and resuspended in amylose-affinity purification buffer (AAP buffer: 20 mM Tris/200 mM NaCl/1 mM EDTA/1 mM DTT/10% glycerol, pH 7.4) containing Complete protease inhibitor cocktail (Roche) at 50 ml of buffer per litre of culture pellet. Cells were lysed using a TS Cell Disruptor (Constant Systems, 22 kPsi), centrifuged at 50 000*g* for 1 h and the supernatant filtered through 0.2 μm Whatman cellulose nitrate membrane filters. The lysate was loaded onto an 8 ml amylose-sepharose affinity column (New England BioLabs), using an ÄKTApurifier (GE Healthcare). Non-specific proteins were washed out with 10 column volumes (CV) of AAP buffer and the protein (MBP-ΔN597 or MBP-ΔNCP69) eluted using 10 CV of AAP buffer containing 10 mM maltose. Eluted protein was further purified by size-based separation using a 320 ml HiLoad 26/60 Superdex 200 pg column (GE Healthcare), to which 1.5 CV of storage buffer (25 mM HEPES/200 mM NaCl/10% glycerol, pH 7.4 at 10°C) was applied. The fractions containing proteins (MBP-ΔN597 or MBP-ΔNCP69) were confirmed by SDS–PAGE, and were subsequently concentrated using 10 kDa MWCO Vivaspin Sample Concentrators (Sartorius Stedim Biotech). The identity of individual SDS–PAGE-purified protein bands (MBP-ΔN597 and MBP-ΔNCP69) was confirmed by MALDI-TOF mass spectroscopy, using a Voyager DE-STR MALDI-TOF mass spectrometer (Applied Biosystems). The spectral data were processed using Data Explorer software (Applied Biosystems) and the peptide masses searched using GPMAW 8.0 software (49), after creating a database with the specific modified sequences of MBP-ΔN597 and MBP-ΔNCP69. The identified peptides, found using GPMAW, were cross-checked with the observed peaks in the raw data in Data Explorer and found to match (Supplementary Material, Fig. S2).

Biophysical characterization

The mean hydrodynamic diameter for each protein batch was determined by DLS on a Zetasizer Auto Plate Sampler (Malvern Instruments), with percentage number used as the output format. Each DLS measurement was performed on purified protein that was initially centrifuged for 15 min at 24 000*g* in a desk-top centrifuge and ∼100 μl aliquots loaded into a 384-well plate for analysis with the laser set at 830 nm. Size distribution of each protein construct was determined by performing three independent runs of three measurements (18 × 10 s readings of each sample) at 10°C. DLS is an extremely sensitive tool for detecting the onset of aggregation resulting from protein melting and was thus used to estimate the thermal melting points of the proteins (50) by heating the sample from 10 to 80°C with 2°C increments. Results from three independent batches of each protein (MBP-ΔNCP69 and MBP-ΔN597) were compared by two-tailed, unpaired *t*-tests. To investigate secondary structure, protein was desalted into 10 mM phosphate buffer (8 mM Na_2HPO_4/2 mM NaH_2PO_4, pH 7.4), using pre-equilibrated PD-10 columns (GE Healthcare) and then diluted to 0.11 mg/ml (MBP-ΔNCP69) or 0.12 mg/ml (MBP-ΔN597), as measured using a V-550 UV-VIS spectrophotometer (JASCO) based on absorbance at 280 nm and the theoretical extinction coefficient of the respective protein sequences. CD analysis was performed on a J-810 spectropolarimeter (JASCO) at 25°C, using a 0.1 cm cuvette (Starna), and with wavelengths in the far UV-range of 185–280 nm. Each CD spectrum represents the average of five scans (data pitch: 0.1 nm; scan speed: 10 nm/min; response time: 2 s) and was corrected by subtraction of the respective spectrum obtained for its desalted buffer solution (five-scan average accumulation). The obtained raw spectrum signal was then converted from ellipticity (millidegrees) into mean residue ellipticity (degrees cm^2 per dmol per residue), to allow for concentration and protein size-independent spectrum measurement for comparison purposes, using the Spectra Manager software. The spectra were then submitted to DICHROWEB (21) for deconvolution into secondary structure components utilizing the analysis programs CDSSTR or CONTIN (18–20), with reference sets 'Dataset 3' or SP175 (17).

Immunocytochemistry

To visualize mitochondria, MitoTracker Red CMXRos (Invitrogen) was added to the culture medium at a concentration of 50 nM and incubated for 30 min at 37°C prior to fixation. Cells were fixed in 3.7% formalin for 10 min at room temperature, followed by permeabilization with methanol at −20°C for 5 min. Cells were then blocked in PBS containing 3% bovine serum albumin for 20 min, and incubated with primary antibodies for 2 (neurons) or 1 h (COS7) at room temperature on a platform shaker, followed by incubation with secondary antibodies for 1 h at room temperature. Dilution of primary antibodies is as follows: anti-FLAG rabbit polyclonal (1:5000; Sigma), anti-cytochrome *c* mouse monoclonal (1:2000–3000; Mitosciences/Abcam). Secondary antibodies were Alexa Fluor 488 goat anti-rabbit (A11008) and Alexa Fluor 647 chicken anti-mouse (1:2000; Invitrogen). Confocal images were acquired with a Zeiss LSM510 microscope, and non-confocal images (Supplementary Material, Fig. S3) were captured using a Zeiss Axioskop 2 MOT epifluorescence microscope.

Immunoblotting

Lysates were prepared in ice-cold RIPA buffer containing Complete Protease Inhibitor Cocktail (Roche). Lysates were solubilized by incubation for 1 h at 4°C on a rotary wheel and centrifuged at 24 000*g* for 30 min. Following

centrifugation, pellets were separated from supernatants and sample buffer added to each. 3–8 or 15% polyacrylamide gels were used to separate proteins for analysis with the R47 or α-DISC1 antibodies, respectively. Samples were separated at 150 V and then transferred to PVDF membranes for analysis.

DISC1 R47 (30) and α-DISC1 (35) antibodies were used to analyse DISC1 protein expression. Prior to incubation with the R47 primary antibody, membranes were blocked overnight at 4°C in PBS 0.2% Tween (PBST) containing 5% Marvel. The R47 primary antibody was incubated at a 1:100 dilution in PBST for 1 h at room temperature. Prior to incubation with α-DISC1, membranes were blocked in TBS 0.1% Tween (TBST) containing 1% Marvel for 30 min at room temperature. The α-DISC1 primary antibody was incubated at 1:2000 in TBST/1% Marvel overnight at 4°C. Membranes were washed with either PBST or TBST followed by secondary antibody incubation. Goat anti-rabbit secondary antibodies (HRP conjugates, DakoCytomaten) were incubated at 1:3000 (in PBST or TBST as appropriate) for 20 min at room temperature. Membranes were processed using ECL Plus (GE Healthcare).

SUPPLEMENTARY MATERIAL

Supplementary Material is available at *HMG* online.

ACKNOWLEDGEMENTS

We thank Andrew Cronshaw for advice on mass spectroscopy, Paul Perry for advice on imaging and Professor Tetsu Akiyama for the α-DISC1 antibody.

Conflict of Interest statement. None declared.

FUNDING

This work was supported by grants from the UK Medical Research Council (G0600214, G0902166) and the Wellcome Trust (069300, WT088179MA), and by RCUK fellowship funding for J.K.M. (GR/T27983/01). Use of the Centre for Translational and Chemical Biology facilities was supported by the Wellcome Trust, the Scottish University Life Sciences Alliance and the BBSRC. Funding to pay the Open Access publication charges for this article was provided by the UK Medical Research Council (G0902166) and the Wellcome Trust (069300, WT088179MA).

REFERENCES

1. Blackwood, D.H., Fordyce, A., Walker, M.T., St Clair, D.M., Porteous, D.J. and Muir, W.J. (2001) Schizophrenia and affective disorders—cosegregation with a translocation at chromosome 1q42 that directly disrupts brain-expressed genes: clinical and P300 findings in a family. *Am. J. Hum. Genet.*, **69**, 428–433.
2. Millar, J.K., Wilson-Annan, J.C., Anderson, S., Christie, S., Taylor, M.S., Semple, C.A., Devon, R.S., St Clair, D.M., Muir, W.J., Blackwood, D.H. *et al.* (2000) Disruption of two novel genes by a translocation co-segregating with schizophrenia. *Hum. Mol. Genet.*, **9**, 1415–1423.
3. Bradshaw, N.J. and Porteous, D.J. (2012) DISC1-binding proteins in neural development, signalling and schizophrenia. *Neuropharmacology*, **62**, 1230–1241.
4. Chubb, J.E., Bradshaw, N.J., Soares, D.C., Porteous, D.J. and Millar, J.K. (2008) The DISC locus in psychiatric illness. *Mol. Psychiatry*, **13**, 36–64.
5. Mao, Y., Ge, X., Frank, C.L., Madison, J.M., Koehler, A.N., Doud, M.K., Tassa, C., Berry, E.M., Soda, T., Singh, K.K. *et al.* (2009) Disrupted in schizophrenia 1 regulates neuronal progenitor proliferation via modulation of GSK3beta/beta-catenin signaling. *Cell*, **136**, 1017–1031.
6. Kamiya, A., Kubo, K., Tomoda, T., Takaki, M., Youn, R., Ozeki, Y., Sawamura, N., Park, U., Kudo, C., Okawa, M. *et al.* (2005) A schizophrenia-associated mutation of DISC1 perturbs cerebral cortex development. *Nat. Cell Biol.*, **7**, 1167–1178.
7. Duan, X., Chang, J.H., Ge, S., Faulkner, R.L., Kim, J.Y., Kitabatake, Y., Liu, X.B., Yang, C.H., Jordan, J.D., Ma, D.K. *et al.* (2007) Disrupted-In-Schizophrenia 1 regulates integration of newly generated neurons in the adult brain. *Cell*, **130**, 1146–1158.
8. Hayashi-Takagi, A., Takaki, M., Graziane, N., Seshadri, S., Murdoch, H., Dunlop, A.J., Makino, Y., Seshadri, A.J., Ishizuka, K., Srivastava, D.P. *et al.* (2010) Disrupted-in-Schizophrenia 1 (DISC1) regulates spines of the glutamate synapse via Rac1. *Nat. Neurosci.*, **13**, 327–332.
9. Wang, Q., Charych, E.I., Pulito, V.L., Lee, J.B., Graziane, N.M., Crozier, R.A., Revilla-Sanchez, R., Kelly, M.P., Dunlop, A.J., Murdoch, H. *et al.* (2011) The psychiatric disease risk factors DISC1 and TNIK interact to regulate synapse composition and function. *Mol. Psychiatry*, **16**, 1006–1023.
10. Millar, J.K., Pickard, B.S., Mackie, S., James, R., Christie, S., Buchanan, S.R., Malloy, M.P., Chubb, J.E., Huston, E., Baillie, G.S. *et al.* (2005) DISC1 and PDE4B are interacting genetic factors in schizophrenia that regulate cAMP signaling. *Science*, **310**, 1187–1191.
11. Zhou, X., Geyer, M.A. and Kelsoe, J.R. (2008) Does disrupted-in-schizophrenia (DISC1) generate fusion transcripts? *Mol. Psychiatry*, **13**, 361–363.
12. Seal, R.L., Gordon, S.M., Lush, M.J., Wright, M.W. and Bruford, E.A. (2011) genenames.org: the HGNC resources in 2011. *Nucleic Acids Res.*, **39**, D514–519.
13. Thierry-Mieg, D. and Thierry-Mieg, J. (2006) AceView: a comprehensive cDNA-supported gene and transcripts annotation. *Genome Biol.*, **7**(Suppl. 1), S12 1–14.
14. Wagner, E. and Lykke-Andersen, J. (2002) mRNA surveillance: the perfect persist. *J. Cell Sci.*, **115**, 3033–3038.
15. Soares, D.C., Carlyle, B.C., Bradshaw, N.J. and Porteous, D.J. (2011) DISC1: structure, function, and therapeutic potential for major mental illness. *ACS Chem. Neurosci.*, **2**, 609–632.
16. Greenfield, N.J. (2006) Using circular dichroism spectra to estimate protein secondary structure. *Nat. Protoc.*, **1**, 2876–2890.
17. Lees, J.G., Miles, A.J., Wien, F. and Wallace, B.A. (2006) A reference database for circular dichroism spectroscopy covering fold and secondary structure space. *Bioinformatics*, **22**, 1955–1962.
18. Manavalan, P. and Johnson, W.C. Jr (1987) Variable selection method improves the prediction of protein secondary structure from circular dichroism spectra. *Anal. Biochem.*, **167**, 76–85.
19. Provencher, S.W. and Glockner, J. (1981) Estimation of globular protein secondary structure from circular dichroism. *Biochemistry*, **20**, 33–37.
20. van Stokkum, I.H., Spoelder, H.J., Bloemendal, M., van Grondelle, R. and Groen, F.C. (1990) Estimation of protein secondary structure and error analysis from circular dichroism spectra. *Anal. Biochem.*, **191**, 110–118.
21. Whitmore, L. and Wallace, B.A. (2004) DICHROWEB, an online server for protein secondary structure analyses from circular dichroism spectroscopic data. *Nucleic Acids Res.*, **32**, W668–W673.
22. Cole, C., Barber, J.D. and Barton, G.J. (2008) The Jpred 3 secondary structure prediction server. *Nucleic Acids Res.*, **36**, W197–W201.
23. McGuffin, L.J., Bryson, K. and Jones, D.T. (2000) The PSIPRED protein structure prediction server. *Bioinformatics*, **16**, 404–405.
24. Pollastri, G. and McLysaght, A. (2005) Porter: a new, accurate server for protein secondary structure prediction. *Bioinformatics*, **21**, 1719–1720.
25. Lupas, A. (1996) Prediction and analysis of coiled-coil structures. *Methods Enzymol.*, **266**, 513–525.
26. Lupas, A., Van Dyke, M. and Stock, J. (1991) Predicting coiled coils from protein sequences. *Science*, **252**, 1162–1164.
27. Leliveld, S.R., Hendriks, P., Michel, M., Sajnani, G., Bader, V., Trossbach, S., Prikulis, I., Hartmann, R., Jonas, E., Willbold, D. *et al.* (2009) Oligomer assembly of the C-terminal DISC1 domain (640–854) is controlled by self-association motifs and disease-associated polymorphism S704C. *Biochemistry*, **48**, 7746–7755.

28. Morris, J.A., Kandpal, G., Ma, L. and Austin, C.P. (2003) DISC1 (Disrupted-In-Schizophrenia 1) is a centrosome-associated protein that interacts with MAP1A, MIPT3, ATF4/5 and NUDEL: regulation and loss of interaction with mutation. *Hum. Mol. Genet.*, **12**, 1591–1608.
29. Sawamura, N., Ando, T., Maruyama, Y., Fujimuro, M., Mochizuki, H., Honjo, K., Shimoda, M., Toda, H., Sawamura-Yamamoto, T., Makuch, L.A. *et al.* (2008) Nuclear DISC1 regulates CRE-mediated gene transcription and sleep homeostasis in the fruit fly. *Mol. Psychiatry*, **13**, 1138–1148, 1069.
30. James, R., Adams, R.R., Christie, S., Buchanan, S.R., Porteous, D.J. and Millar, J.K. (2004) Disrupted in Schizophrenia 1 (DISC1) is a multicompartmentalized protein that predominantly localizes to mitochondria. *Mol. Cell. Neurosci.*, **26**, 112–122.
31. Kuroda, K., Yamada, S., Tanaka, M., Iizuka, M., Yano, H., Mori, D., Tsuboi, D., Nishioka, T., Namba, T., Iizuka, Y. *et al.* (2011) Behavioral alterations associated with targeted disruption of exons 2 and 3 of the Disc1 gene in the mouse. *Hum. Mol. Genet.*, **20**, 4666–4683.
32. Bradshaw, N.J., Ogawa, F., Antolin-Fontes, B., Chubb, J.E., Carlyle, B.C., Christie, S., Claessens, A., Porteous, D.J. and Millar, J.K. (2008) DISC1, PDE4B, and NDE1 at the centrosome and synapse. *Biochem. Biophys. Res. Commun.*, **377**, 1091–1096.
33. Park, Y.U., Jeong, J., Lee, H., Mun, J.Y., Kim, J.H., Lee, J.S., Nguyen, M.D., Han, S.S., Suh, P.G. and Park, S.K. (2010) Disrupted-in-schizophrenia 1 (DISC1) plays essential roles in mitochondria in collaboration with Mitofilin. *Proc. Natl Acad. Sci. USA*, **107**, 17785–17790.
34. Zhou, X., Chen, Q., Schaukowitch, K., Kelsoe, J.R. and Geyer, M.A. (2010) Insoluble DISC1-Boymaw fusion proteins generated by DISC1 translocation. *Mol. Psychiatry*, **15**, 669–672.
35. Ogawa, F., Kasai, M. and Akiyama, T. (2005) A functional link between Disrupted-In-Schizophrenia 1 and the eukaryotic translation initiation factor 3. *Biochem. Biophys. Res. Commun.*, **338**, 771–776.
36. Newburn, E.N., Hyde, T.M., Ye, T., Morita, Y., Weinberger, D.R., Kleinman, J.E. and Lipska, B.K. (2011) Interactions of human truncated DISC1 proteins: implications for schizophrenia. *Transl. Psychiatry*, **1**, e30.
37. Murdoch, H., Mackie, S., Collins, D.M., Hill, E.V., Bolger, G.B., Klussmann, E., Porteous, D.J., Millar, J.K. and Houslay, M.D. (2007) Isoform-selective susceptibility of DISC1/phosphodiesterase-4 complexes to dissociation by elevated intracellular cAMP levels. *J. Neurosci.*, **27**, 9513–9524.
38. Hikida, T., Jaaro-Peled, H., Seshadri, S., Oishi, K., Hookway, C., Kong, S., Wu, D., Xue, R., Andrade, M., Tankou, S. *et al.* (2007) Dominant-negative DISC1 transgenic mice display schizophrenia-associated phenotypes detected by measures translatable to humans. *Proc. Natl Acad. Sci. USA*, **104**, 14501–14506.
39. Pletnikov, M.V., Ayhan, Y., Nikolskaia, O., Xu, Y., Ovanesov, M.V., Huang, H., Mori, S., Moran, T.H. and Ross, C.A. (2008) Inducible expression of mutant human DISC1 in mice is associated with brain and behavioral abnormalities reminiscent of schizophrenia. *Mol. Psychiatry*, **13**, **173–186**, 115.
40. Korth, C. (2009) DISCopathies: brain disorders related to DISC1 dysfunction. *Rev. Neurosci.*, **20**, 321–330.
41. Leliveld, S.R., Bader, V., Hendriks, P., Prikulis, I., Sajnani, G., Requena, J.R. and Korth, C. (2008) Insolubility of disrupted-in-schizophrenia 1 disrupts oligomer-dependent interactions with nuclear distribution element 1 and is associated with sporadic mental disease. *J. Neurosci.*, **28**, 3839–3845.
42. Song, W., Li, W., Feng, J., Heston, L.L., Scaringe, W.A. and Sommer, S.S. (2008) Identification of high risk DISC1 structural variants with a 2% attributable risk for schizophrenia. *Biochem. Biophys. Res. Commun.*, **367**, 700–706.
43. Millar, J.K., James, R., Christie, S. and Porteous, D.J. (2005) Disrupted in schizophrenia 1 (DISC1): subcellular targeting and induction of ring mitochondria. *Mol. Cell. Neurosci.*, **30**, 477–484.
44. Atkin, T.A., MacAskill, A.F., Brandon, N.J. and Kittler, J.T. (2011) Disrupted in Schizophrenia-1 regulates intracellular trafficking of mitochondria in neurons. *Mol. Psychiatry*, **16**, **122–124**, 121.
45. Han, X.J., Tomizawa, K., Fujimura, A., Ohmori, I., Nishiki, T., Matsushita, M. and Matsui, H. (2011) Regulation of mitochondrial dynamics and neurodegenerative diseases. *Acta Med. Okayama*, **65**, 1–10.
46. Brandon, N.J. and Sawa, A. (2011) Linking neurodevelopmental and synaptic theories of mental illness through DISC1. *Nat. Rev. Neurosci.*, **12**, 707–722.
47. Vandesompele, J., De Preter, K., Pattyn, F., Poppe, B., Van Roy, N., De Paepe, A. and Speleman, F. (2002) Accurate normalization of real-time quantitative RT-PCR data by geometric averaging of multiple internal control genes. *Genome Biol.*, **3**, RESEARCH0034.
48. McCarthy, C. (1996) *Chromas, version 1.45.* School of Biomolecular and Biomedical Science, Griffith University, Brisbane.
49. Peri, S., Steen, H. and Pandey, A. (2001) GPMAW—a software tool for analyzing proteins and peptides. *Trends Biochem. Sci.*, **26**, 687–689.
50. Nobbmann, U., Connah, M., Fish, B., Varley, P., Gee, C., Mulot, S., Chen, J., Zhou, L., Lu, Y., Shen, F. *et al.* (2007) Dynamic light scattering as a relative tool for assessing the molecular integrity and stability of monoclonal antibodies. *Biotechnol. Genet. Eng. Rev.*, **24**, 117–128.

Annex

Annex table of contents

List of figures

List of tables

Annex A1 - Optimisation of the HSII bioluminescence assay to measure cellular ATP in COS-7 cells and t(1;11) lymphoblastoid cell lines

A1.1 Methods

This annex focuses on the optimisation of a flash luciferase assay, the HSII ATP bioluminescence Kit (Roche), referred to henceforth as the HSII assay. The methods detailed in the annex are supplementary to those listed in the materials and methods (see chapter 2).

A1.1.1 Materials

A1.1.1.1 Reagents

Below are listed the details the chemical reagents used in the production of this annex. The source each chemical reagent is stated alongside, in brackets. Where relevant, the soloution that a reagent is suspended in is stated.

Bicinchoninic Acid (Sigma)

Carbonyl cyanide m-chlorophenyl hydrazone (CCCP) (Tocris) made up in DMSO

Copper II Sulphate (Sigma)

A1.1.2 Cell culture

A1.1.2.1 Cell seeding density

For generation of cells for lysis in the HSII assay with the exogenous expression of DISC1/DISC1FP1 species, $2.5x10^6$ COS-7 cells were seeded and grown overnight in 10cm dishes prior to transfection. In the HSII serum starvation optimisation $3.25x10^6$ COS-7 cells were seeded and grown overnight.

A1.1.2.2 Serum starvation

In the serum starvation of COS-7 cells, the DMEM/10% FCS vol/vol was aspirated and replaced with DMEM/1% FCS vol/vol 18 hours prior to the CCCP treatment. This condition is referred to as the low serum condition while the other parallel COS-7 cultures that remained cultured in DMEM/10% FCS are referred to as the normal serum condition. The following day the COS-7 cells were harvested.

In the serum starvation of the lymphoblastoid cell lines, for two consecutive days the lymphoblastoid cell line media was topped up with an additional 10ml of RPMI/10% FCS vol/vol. On the following day the media was aspirated to leave only 20ml of conditioned media and the flocculated cells. To this 17ml of pre-warmed RPMI/1% FCS vol/vol was added. This condition is referred to as the low serum condition and the other parallel lymphoblastoid cultures that were remained cultured in RPMI/10% FCS are referred to as normal serum condition. The following day the lymphoblastoid cells were harvested.

A1.1.2.3 Drug treatment

CCCP was used as a means to reduce cellular ATP. For the HSII assay, COS-7 cells receiving CCCP treatment were cultured in 10cm dishes to 75-90% confluency. In the method development of the serum starvation/CCCP treatment the cells were untransfected, in experimental assays, the COS-7 cells had been transfected 18-24 houses previously with pcDNA 3.1 (+) empty vector plasmid. The media was aspirated and the cells washed twice in warm PBS. 10ml of pre-warmed media (see table 2.3.A) was then applied to each culture dish. The 100mM CCCP stock was diluted in sterile DMSO (Sigma) to a 1:1000 stock, then delivered to the culture dishes to give final concentrations of 10µM-100µM CCCP. The cells were incubated with CCCP for two hours at 37°C and 5% CO_2. The serum starvation/CCCP treatment method development was produced in parallel with sham treat (DMSO) cells. Following incubation the CCCP or DMSO, the COS-7 cells were harvested and lysed along with the other dishes of COS-7 cells that exogenously expressed protein, for use in the HSII assay.

For immunocytochemistry the CCCP was delivered to 1ml of media (see table 2.3.A) from a 100mM CCCP stock and serial diluted in sterile DMSO (Sigma) to give a final concentration of 20µM CCCP. The cells were incubated with CCCP for two hours at 37°C and 5% CO_2. The serum starvation/CCCP treatment method development was produced in parallel with sham

(DMSO) cells. Following incubation the CCCP or DMSO the COS-7 cells were fixed and permeabilized.

A1.1.2.4 Transfection of plasmids into eukaryotic cells

The FACS analysis in this annex, uses COS-7 cells transiently transfected (see section 2.3.2) with a pMAX-GFP (Lonza) construct which expresses green fluorescent protein (GFP).

A1.1.3 Protein-related methods

A1.1.3.1 Antibodies

The Western blotting in the annex uses an anti-Glyceraldehyde-3-Phosphate Dehydrogenase (GAPDH) antibody (Millipore) raised in mouse, used at 1:100,000 for 1 hour.

A1.1.3.2 Cell lysates

A1.1.3.2.1 COS-7 Harvesting and lysis

In the method development of the HSII assay, three different COS-7 cell harvesting and lysis protocols were trialed. All of the protocols use the HSII lysis buffer (Roche). The following protocol is the method used to harvest and lyse COS-7 cells in the cell seeding optimisation and is the method recommended by Roche. To harvest the COS-7 cells for use in the HSII assay as per manufacturer's instructions the media was aspirated and the cells washed twice with warm PBS. 100µl or 230µl of HSII lysis buffer was then applied per well of COS-7 cells, for the cell seeding and harvesting optimisations, respectively. After five minutes the lysate was removed from the wells and the soluble protein lysate was then separated from the insoluble pellet fraction by pipette. The use of this method in the development of the HSII assay was abandoned following the cell harvesting and lysis optimisation.

The following protocol was only trialed within the cell harvesting and lysis optimisation. The Cell Dissociation Buffer, Hanks Based (Gibco), was seen as a means detach cells for counting prior to lysis with minimal stress during harvesting. The media was aspirated and the cells washed twice in prewarmed PBS. 1ml of prewarmed cell dissociation buffer was aliquoted per well and the cells which were then left to detach at room temperature in the tissue culture hood for 1-2 minutes. 2.5ml of prewarmed media (see table 2.3.A) was then added per well to

resuspend the COS-7 cells. A sample of the resuspended cells was applied to a haemocytometer and the cell number estimated using microscopy. The resuspended cells were then transferred to a 15ml Falcon tube and centrifuged at 1000rpm for five minutes and the supernatant removed. 2.5ml of PBS was then added to the Falcon tube and the cells centrifuged at 1000rpm for five minutes, twice. Following the removal of the supernatant the COS-7 cell pellet was lysed using 230µl of HSII lysis buffer. The whole cell lysate was then transferred to an epindorph and placed a rotary wheel at 20-30rpm for 30 minutes at 4°C and then spun at 13,000rpm by centrifuge for 20 minutes. The soluble protein lysate was then separated from the insoluble pellet fraction by pipette.

The following protocol is the method of cell harvesting and lysis that was adapted to process COS-7 cells in the HSII assay as a result of the cell harvesting and lysis optimisation. This protocol is markedly similar to the production of lysates for Western analysis. The media was aspirated and the cells washed twice with warm PBS. 230µl of HSII lysis buffer was then applied per well of COS-7 cells, and cell lysis was aided with mechanical agitation from a cell scraper. The whole cell lysate was then transferred to an epindorph and placed a rotary wheel at 20-30rpm for 30 minutes at 4°C and then spun at 13,000rpm by centrifuge for 20 minutes. The soluble protein lysate was then separated from the insoluble pellet fraction by pipette. In the final adaption of this protocol, 1ml of HSII lysis buffer was used.

A1.1.3.2.2 Lymphoblastoid harvesting and lysis

The media in a confluent T75 culture was aspirated off to the 5ml mark. The remaining media and flocculated cells were removed into a falcon by pipette and centrifuged at 500rpm for five minutes. The supernatant was then removed and 10ml of PBS added to the cell pellet which was then centrifuged at 500rpm for five minutes. The supernatant was then removed and the cells lysed in 400µl of HSII lysis buffer and the whole cell lysate taken up and down a 25 gauge needle x10 to mechanically aid lysis. A further 100µl of HSII lysis buffer was added to the lysate. The lysate was then placed a rotary wheel at 20-30rpm for 30 minutes at 4°C and then spun at 13,000rpm by centrifuge for 20 minutes. The soluble protein lysate was then separated from the insoluble pellet fraction by pipette

A1.1.3.3 Measuring the protein concentration of cell lysates

The BCA assay was used to determine the protein concentration of both the COS-7 and lymphoblastoid whole cell lysates. Quick Start Bovine Serum Albumin Standards (Bio Rad),

of concntrations 0.125-2.0mg were also assayed to enable sample concentration determination. The master mix of BCA solution was produced from a 50:1 of BCA: Copper II sulphate. For each standard 25ul of protein was added 500ul master mix, for each sample 35ul of protein was added to 700ul master mix. The samples were then vortexed both before and after incubating the reaction at 37°C for 20 minutes.

Following vortexing, 200ul of each solution was loaded by automatic pipette into a 96-well plate. All lysates were loaded in triplicate, all protein standards were loaded in duplicate. The 96-well plate was read on a Synergy 2 (BioTek) plate reader 592nm. The BCA assay data was analysed by linear regression and plotted using the Gen5 software (BioTek). As the assayed protein standards were premade BSA and loaded as duplicate technical replicates, a high R^2 value for the linear regression of 0.998 was aimed for. In the analysis of the whole cell protein lysates assayed, a coefficient of varience (CV%) of 0.1-2 was aimed for, given that these samples were ran as technical replicates in triplicate. As method development progressed and experimental technique developed these levels if accuracy were obtained.

To determine the protein concentration in lymphoblastoid cell lysates, which were often of high protein concentration, 1/3 or 1/5 dilutions of these lysates in HSII lysis buffer were ran on the BCA assay. The readings were then scaled up.

A1.1.3.4 Standardisation of protein concentration

With the determination of the whole cell lysate concentration by the BCA assay, samples of the whole cell lysates were diluted to 0.4mg/ml with additional HSII lysis buffer. This gave 10µg protein per well when 25ul of standardised whole cell lysates was loaded into the 96-well plate. As 5x25ul of experimental replicates were to be ran per lysate in the HSII assay, the production of the standardised protein was scaled accordingly. Initial COS-7 serum starvation experimentation produced less protein per plate (data not shown). To accommodate this, the cell lysates from these experiments were diluted to 0.34mg/ml, with 8.5µg of protein run in 25ul per well.

In the method development for the serum starvation of lymphoblastoid cells, whole cell lysates, were diluted 0.4, 0.8, 1.6mg/ml, using additional HSII lysis buffer. This standardisation gave 10, 20, 40µg of protein per well.

A1.1.4 HSII assay

A1.1.4.1 HSII assay ATP standards

ATP standards of known concentration were run on the HSII assay in order to derive the concentration of ATP in the whole cell lysate assayed. A stock solution of 16.5mM ATP was produced by the solubilisation of lyophilised ATP (Roche) with Dilution Buffer (Roche). A series of serial dilutions using further Dilution Duffer was used to generate ATP standards with a range of concentrations:

ATP standards for the quantification of whole cell ATP in COS-7 cell lysates version 1:

ATP concentrations (µM) 1000, 100, 10, 1, 0.1, 0.01, 0.001, 0.0001

-used in sections A1.3.1-A1.3.6.

ATP standards for the quantification of whole cell ATP in COS-7 cell lysates version 2:

ATP concentrations (µM) 1000, 300, 100, 30, 10, 3, 1, 0.1, 0.01,

Implemented to narrow the range and increase the number of points in the linear part of the curve.

-used in sections A1.3.7 onwards.

ATP standards for the quantification of whole cell ATP in lymphoblastoid cell lysates

ATP concentrations (µM) 100, 30, 10, 6, 3, 1, 0.5, 0.1, 0.01

-used in sections A1.4.1 onwards.

50ul per well of each ATP standard was loaded into the 96-well plate per experiment. The ATP standards were produced on the day of experimentation and kept on ice until the loading of the 96-well plate.

A1.1.4.2 HSII Assay protocol

To run the HSII assay and measure the ATP concentration of whole cell lysates by luciferase luminescence, 25µl of each whole cell lysate was loaded into a black walled 96-well plate in technical replicates of five. To each of the whole cell lysates was added 25µl of Dilution Buffer. Then, 25µl of each ATP standard was loaded in triplicate to the empty wells. To each of the ATP standards 25µl of HSII lysis buffer was added. This gave both the whole cell lysates and the ATP standards contained 50µl of the same stoichiometry of dilution buffer and lysis buffer. A 50µl H_2O sample was loaded as a blank. The loaded plate was left to incubate at room temperature for five minutes following loading. All loading was done by automatic pipette.

The Luciferase reagent was delivered by the Synergy2 (BioTek) plate reader by automated injection. To produce the luciferase, one bottle of luciferase reagent (Roche) was dissolved in 10ml of Dilution Buffer, and then kept on ice, and the vessel wrapped in aluminium foil to minimise exposure to light. The luciferase was connected to the Synergy2 pate reader following the loading of the 96-well plate.

The Synergy2 plate reader was set to detect emission at 562nm. The luciferase was injected at 50µl of per well of the luciferase to the whole cell lysates and the ATP standards. The programming and analysis on the Synergy2 plate reader of the HSII derived ATP concentration data was automated by Gen5 software (BioTek). The whole cell lysate ATP concentrations were derived from the ATP standard curve. A CV% of 0.1-2 was aimed for from the five technical replicate luminescence readings per sample. This would enable the HSII assay to be able to detect differences in whole cell ATP concentrations of 10% between different samples. As method development progressed and experimental technique developed these levels if accuracy were obtained.

A1.2 Introduction

Chapter 4 established that the exogenous expression of the DISC1/DISC1FP1 chimeras, CP60 and CP69, in both COS-7 cells and cortical neurones produces mitochondrial dysfunction. It seems possible, given that CP60 and CP69 display a reduction in the mitochondrial membrane potential, $\Delta\psi m$ as detected by impaired MitoTracker Red staining, that these species may also reduce cellular ATP levels. This is because a sustained mitochondrial membrane potential, $\Delta\psi m$ is required to generate torque to drive F_1F_0 ATP synthase, to generate ATP from ADP (Dimroth *et al*, 2000). The exogenous expression of the third chimera, CP1, may also have a detrimental effect on mitochondrial function. CP1 possesses a highly similar ORF to that of DISC1 aa1-597 (Eykelenboom *et al*, 2012). The exogenous expression of DISC1 aa1-597 in COS-7 cells produces structural mitochondrial changes, with ring mitochondria observed in a sub-population of transfected cells (Millar *et al*, 2005). Bioenergetic activity is also altered with the expression of a truncated murine equivalent to DISC1 aa1-597 being capable of reducing both cellular ATP levels and NADH dehydrogenise (complex I) activity (Park *et al*, 2010). It therefore seems reasonable to investigate whether expression of the DISC1/DISC1FP1 chimeras would impact upon mitochondrial bioenergetic activity in terms of cellular ATP levels.

ATP is the principal metabolic substrate for intracellular metabolic pathways (Schapira, 2006). A constant source of ATP is required for the generation of action potentials in the neurone, with ATP delivered throughout the axon by mobile transported mitochondria (Sheng, 2014). At the synapse, ATP is required for vesicle transport, the recycling of the synaptic membrane and maintenance of the synaptic membrane potential (Ly & Verstreken, 2006). Localised ATP is also essential in the assembly of the synapse at the presynaptic nerve terminal (Lee & Peng, 2008). *In vivo* studies, using 31p-MRS neuroimaging to detect ATP levels in the brains of individuals affected by schizophrenia, have found decreased levels of ATP in both the basal ganglia (Fujimoto *et al*, 1992) and in the frontal lobes (Volz *et al*, 2000).

The optimisation of the HSII assay aimed to firstly detect the cellular ATP level in COS-7 cells exogenously expressing FLAG-tagged CP1, CP60 and CP69. Secondly the HSII assay was to be optimised to quantify cellular ATP in lymphoblastoid cell lines, to enable the measurement of cellular ATP in t(1;11)-family derived lymphoblastoid cell lines.

The overall HSII assay procedure went through a series of optimisation steps. These improvements were rational modifications to the basic HSII assay to aid reproducibility of results. An order of experimentation for the final HSII assay methodology is shown in figure

A1.3.A. The optimisation of the individual experimental protocols will be discussed in the following sections.

This annex comprises the HSII assay method development and refinement of experimental techniques performed to date. Unfortunately experimentation was discontinued due to personal illness and consequently, the final experimental assays to detect the levels of cellular ATP in COS-7 cells exogenously expressing the DISC1/DISC1FP1 chimeras and within t(1;11) lymphoblastoid cell lines were never completed. This research is included in this thesis as a means to discuss the work that was accomplished and to enable the critique of the method developments pursued, addressing both the positive and negative outcomes established.

A1.3 Optimisation of the HSII assay to analyse cellular ATP in COS-7 cells exogenously expressing DISC1/DISC1FP1 chimeras

A1.3.1 Generation of an ATP standard curve to detect cellular ATP in COS-7 cells exogenously expressing DISC1/DISC1FP1 proteins

Initial optimisation of the HSII assay involved the generation of an ATP standard curve from a serial dilution of ATP known standards. A standard curve of ATP bioluminescence was generated following the injection of luciferase reagent into the ATP standards. The ATP standard curve was then used to derive the ATP concentration of the sample lysates assayed following the luciferase catalysed bioluminescence. This initial curve covers a range of standards at concentrations of $1x10^{-4}$ to $1x10^{3}$µM ATP (see figure A1.3.B). As the method development progressed, a standard curve was used that contained a more narrow range of ATP values, with more ATP standards in the exponential phase of the standard curve. This curve covers a range of $1x10^{-2}$ to $1x10^{3}$µM ATP (see figure A1.3.B). These modifications to the standard curve were to improve the accuracy of cellular ATP concentration derivation. This second standard cure was used in HSII assay optimisation from section A1.3.7 onwards.

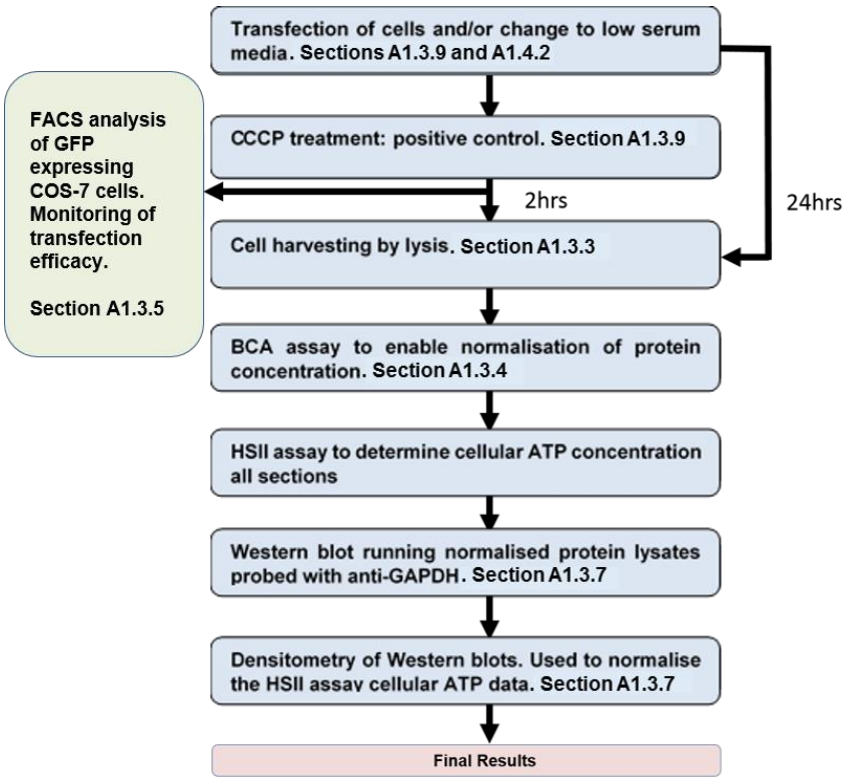

Figure A1.3.A: Flow chart displaying the method developments in the HSII assay optimisation to date.

A1.3.2 Optimisation of COS-7 seeding density for the HSII Assay

Following ATP standard curve generation, the development of the HSII assay progressed to identifying an optimum seeding density of COS-7 cells for lysis. The COS-7 cells were mock transfected 24 hours after seeding to model the final experimental procedure, the cells were then harvested by lysis with the HSII lysis buffer 24 hours post-transfection. To do this, COS-7 cells were seeded in culture dishes at a range of densities, from $1x10^5$ to $5x10^5$ cells in $1x10^5$ increments. The cells were then lysed and run on the HSII assay to identify the cell density that produced a robust cellular ATP concentration that lay on the exponential phase of the ATP standard curve.

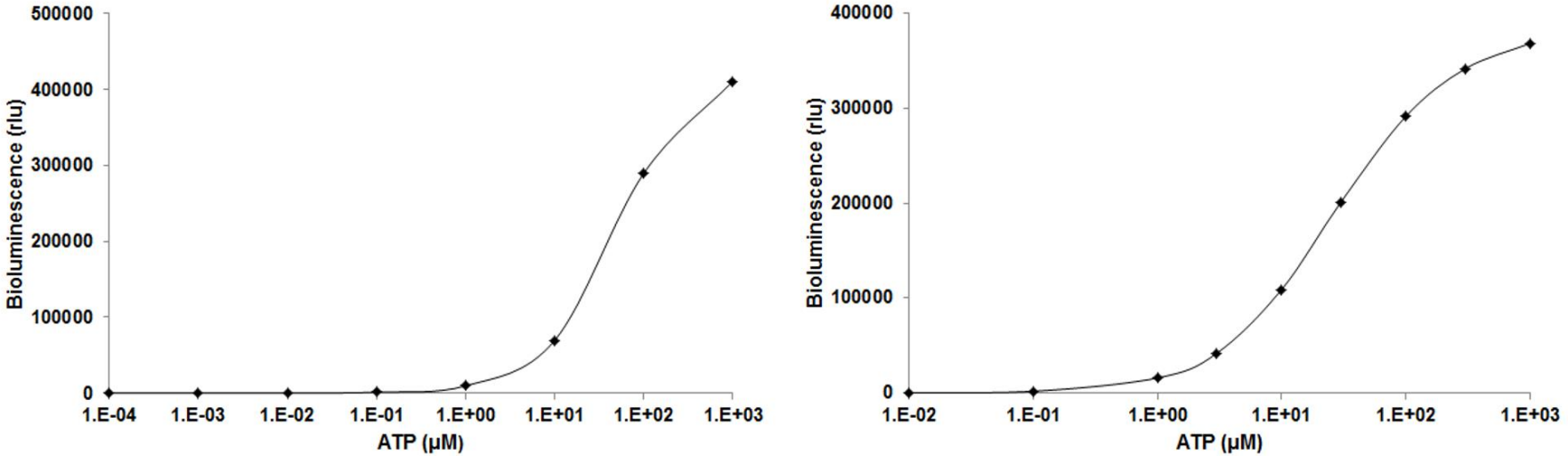

Figure A1.3.B: Development of a standard curve to measure ATP bioluminescence using the HSII assay within COS-7 cells exogenously expressing DISC1/DISC1FP1 chimeric proteins. The initial ATP standards used have a series of redundant ATP standards at the lowest concentrations of ATP assayed and few ATP standards within the exponential phase of the curve (left). To rectify this a standard curve was generated with a narrower rage with a greater number of ATP standards within the exponential phase (see section A1.3.7 onwards). A new standard curve was generated from ATP standards of known concentration per experimental replicate.

The cellular ATP data shows the trend of the ATP concentration increasing along with the COS-7 cell seeding density (see table A1.3.A). The CV% shown is a normalised measure of the variability, here derived from the five technical replicates that make the mean ATP concentration.

COS-7 Cell Seeding Density	Mean Cellular ATP (µM/50µl)	CV%
$5x10^5$	71	13.8
$4x10^5$	61	16.0
$3x10^5$	26	9.3
$2x10^5$	24	2.8
$1x10^5$	11	2.6

Table A1.3.A: Effect of COS-7 cell seeding density on cellular ATP levels. The cellular ATP level increases with the COS-7 seeding density. Note that the CV% also increases with cell seeding density. This is likely present due to unfamiliarity with the protocols at this stage of method development. Mean cellular ATP values are derived from technical replicates (n=5).

The lysates produced from COS-7 cells seeded at densities of $2x10^5$ to $5x10^5$ cells produce cellular ATP concentrations that lie on the linear slope of the ATP standard curve (see figure A1.3.B). However, this optimisation data shows an increase in CV% with cell seeding. The large variation was seen to be tolerable as the observation of a trend was sufficient to drive the optimisation forward at this stage in method development. In light of this variability with the higher cell densities it was decided to focus on $1x10^5$ and $3x10^5$ COS-7 seeding densities for further method design.

A1.3.3 Optimisation of cell harvesting for the HSII Assay

The method of harvesting the COS-7 cells was also optimised. The procedure used to lyse cells may influence both the final concentration of ATP in the lysate and the reproducibility of the HII assay. Here COS-7 lysates were produced from cell seeding densities of either $1x10^5$ or $3x10^5$ cells. These cultures had been mock transfected 24 hours prior to harvesting. The cells were then harvested by three different procedures, all of which used the HSII lysis buffer to lyse cells. These are referred to as: the Cell Dissociation Buffer procedure; the HSII lysis buffer alone procedure; the HSII lysis buffer & scraping procedure.

The Cell Dissociation Buffer (Roche) procedure aimed to see if the number of COS-7 cells could be counted on the day of experimentation, lysed and then run on the HSII assay. This was seen as a means to control variability in culture size that may have occurred between COS-7 seeding and the cell culture growth in the parallel cultures used for experimentation. 48 hours following the initial cell seeding, the Cell Dissociation Buffer was applied to adherent COS-7 cells from culture dishes to dissociate the cells. The total number of cells in each culture was then derived using a haemocytometer. It was calculated that the culture seeded with $1x10^5$ cells now contained $1.9x10^5$ cells and the culture seeded with $3x10^5$ cells contained $5.5x10^5$ cells. These two cultures of COS-7 cells were then lysed with the HSII lysis buffer. This crude lysate was solubilised on wheel, spun down via centrifugation and the solubilised protein was then separated from the pellet. The lysates were then run on the HSII Assay to determine ATP concentration.

The HSII lysis buffer procedure simply involved the lysis of the cells in the culture well with the HSII lysis buffer. These lysates were then run on the HSII Assay. This procedure is similar to Roche guidelines for the HSII Assay.

The HSII lysis buffer & scraping procedure involved the lysis of the COS-7 cells in the culture dish agitated by the use of a cell scraper, without the cells being counted. This procedure also ensured that the lysate produced contained all of the cell debris. The crude lysates produced were then processed in the same manner as the Cell Dissociation Buffer crude lysates, being solubilised on the wheel and the lysate supernatant extracted following centrifugation before being run on the HSII Assay.

Overall, with regard to the initial cell seeding densities, the cell harvesting procedures that produced the highest ATP concentration to those that elicited the lowest ATP concentration were: HSII lysis buffer & scraping; HSII lysis buffer alone; Cell Dissociation Buffer (see table A1.3.B). That the HSII lysis buffer and scraping is more robust in the final cellular ATP concentration produced than the use of the HSII lysis buffer alone is unsurprising, given that, in addition to the cell scraping, the former also involves the protein solubilisation and separation of the soluble from the insoluble protein fraction. For the Cell Dissociation Buffer procedure, it is possible that the extra processing of the COS-7 cells in the procedure and, specifically, the use of the Cell Dissociation Buffer itself results in the lower cellular ATP concentration.

These data generally reveal lower ATP concentrations relative to cell seeding density than the initial seeding density optimisation data (see table A1.3.A). Here, only the cell seeding density

of $3x10^5$ cells harvested with the HSII lysis buffer & scraping lies on the linear part of the ATP standard curve (see figure A1.3.B). However, in this harvesting optimisation data, the coefficient of variance for the conditions is largely within acceptable levels (see A1.3.B) unlike the data on cell seeding density (see table A1.3.A). At this stage of optimising the HSII, it was necessary to acknowledge that there may be problems in using cell seeding density as a means to produce reliability in ATP concentration. It can be concluded, from the harvesting optimisation, that the use of the HSII lysis buffer, in conjunction with the use of a cell scraper, produced the largest cellular ATP concentration of the three procedures tested. The use of the HSII lysis buffer and cell scraper was then implemented for all of the following HSII assay optimisations.

Harvesting Protocol	COS-7 Cell Seeding Density	Mean Cellular ATP (µM/50µl)	CV %
Cell Dissociation Buffer	$1x10^5$	1.71	5.76
Cell Dissociation Buffer	$3x10^5$	3.34	7.61
HSII Lysis Buffer Alone	$1x10^5$	3.59	3.60
HSII Lysis Buffer Alone	$3x10^5$	7.19	5.00
HSII Lysis Buffer & Scraping	$1x10^5$	6.40	4.16
HSII Lysis Buffer & Scraping	$3x10^5$	12.77	3.11

Table A1.3.B: Optimisation of cell harvesting protocol. The cellular ATP level increases with the COS-7 seeding density. In the Cell Dissociation Buffer protocol, the COS-7 cells are disrupted and counted then lysed with HSII lysis buffer. In the HSII Lysis buffer condition, the cells are lysed with no mechanical agitation in contrast to the HSII Lysis buffer & scraping protocol which uses a cell scraper. The HSII Lysis buffer & Scraping protocol produces the greatest cellular ATP levels and was incorporated into the ongoing method development. All protocols were tested using initial seeding densities of $1x10^5$ and $3x10^5$ COS-7 cells. Mean cellular ATP values are from n=2 technical replicates. This involved 2 plates of COS-7 cells.

A1.3.4 Optimisation of protein assays for use in the standardisation of protein concentration in the HSII assay

Concern about the reproducibility of experiments that used seeding density as a means to normalise the cell lysates run on the HSII assay, led to other means of standardisation of the

cell lysates being sought. This involved the initially produced cellular lysates being ran on a protein assay and the protein concentrations then quantified. Following this, the original lysates were all standardised to a single common protein concentration. The uniform protein concentration was used in the standardisation of all future HSII assay lysates, enabling a greater reproducibility in the HSII assay, eliminating errors arising from variation in the size of the COS-7 cultures lysed.

Firstly, for the standardisation of cell lysates to a given protein concentration, optimisation needed to be undertaken to determine which COS-7 lysate protein concentration produced an ATP concentration that lay within the linear part of that standard curve. Initial investigation into a suitable protein assay focused on the Bradford assay (BioRad) as a colorimetric method of protein quantification. However, the results seemed highly variable and did not appear to scale with the experimental conditions used (data not shown). Communication with Roche clarified these problems. The HSII lysis buffer impairs the action of the Bradford assay, preventing effective protein quantification. Roche suggested the use of the BCA assay, another colorimetric method of protein determination.

In the optimisation of protein standardisation using the BCA assay, three dishes of mock transfected COS-7 cells were lysed with HSII lysis buffer and run on the BCA assay against known protein standards (BioRad). For lysate samples 2 and 3, the coefficient of variance was within an acceptable range. However the CV% for sample 1 was extremely large, due to problems with technical replicates (see table A1.3.C). Despite this all three mean protein concentrations were carried forward and used in the next phase of the optimisation.

Each of the three original lysates (see table A1.3.C), were then diluted to produce a range of protein concentrations using additional HSII lysis buffer. The final protein concentrations produced were 0.25mg/ml, 0.30mg/ml, 0.35mg/ml and 0.40mg/ml. This now gave 12 diluted protein lysates, three replicates per lysate at each protein concentration. The HSII assay was then run with standardised protein lysates and the cellular ATP concentration for each of these COS-7 lysates was calculated. The results were pooled by protein concentration and linear regression analysis was performed to look at the relationship between cellular ATP and protein concentration. As the protein concentration of the COS-7 lysates increases so too does the cellular ATP concentration within those lysates, ATP concentration = -11.95 + lysate protein concentration x 124.6, $R^2 = 0.46$ (see figure A1.3.C).

Following this optimisation it was decided to use the BCA assay to quantify the protein in the HSII lysates, enabling the dilution of the HSII lysates to a standard concentration of

0.40mg/ml. At this concentration, the COS-7 lysates contained a mean cellular ATP concentration of 37.9µM (see figure A1.3.C). A cellular ATP concentration of this size adequately falls on the liner phase of the ATP standard curve. A potential source of error in this calculation comes from the carrying over of the original COS-7 lysate sample that had a high coefficient of variance for use in the linear regression. However, in practice, the use of normalising COS-7 cell lysates to 0.40mg/ml in sections A1.3.5-A1.3.7 produced cellular ATP concentrations that lay on the linear phase of the ATP standard curve, irrespective of treatment.

COS-7 Lysate	Protein Conc. (mg/ml)	CV (%)
1	0.426	26.411
2	0.457	1.49
3	0.438	2.841

Table A1.3.C: Determination of the protein concentration in mock transfected COS-7 HSII lysates using the BCA assay. Three parallel 10cm dishes seeded with $2.5x10^5$ COS-7 cells were mock transfected and 24 hours later lysed with HSII lysis buffer. The lysed protein was then incubated with the BCA assay. The absorbance at 562nm due to presence of solubilised protein was then measured. The protein concentration as a mean of (n=3) technical replicates was then derived.

A1.3.5 FACS analysis to monitor the transfection efficacy of exogenously expressed DISC1/DISC1FP1 proteins in COS-7 cells

The transfection efficacy between experimental replicates could be a possible source of variability in the HSII assay ATP data. Consequently, FACS analysis of exogenous GFP expression from COS-7 cells that were transfected in parallel with pMAX-GFP, at the time of the initial experimental DISC1/DISC1FP1 transfections, was used as means to establishing the transfection efficacy of the DISC1/DISC1FP1 chimeras.

The method for detecting transfection efficacy that was developed for use on the day of the running of the HSII assay is as follows: firstly a sample of untransfected COS-7 cells were analysed by FACS to establish the background COS-7 autofluorescence; a subjective gate was then drawn in to capture GFP fluorescing cells. This gate is labelled R1 (see figure A1.3.D).

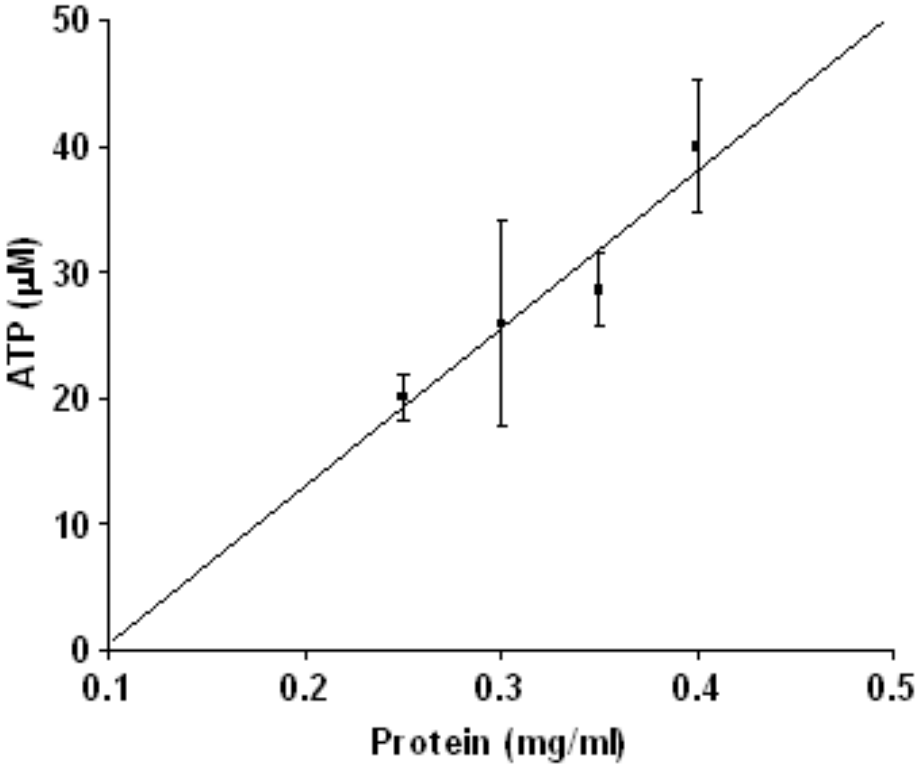

Figure A1.3.C: Effect of protein concentration on cellular ATP in COS-7 cell lysates as measured by the HSII assay following quantification of protein and the standardisation of lysates. Cellular ATP concentration increases with protein concentration, ATP concentration = -11.95 + lysate protein concentration x 124.6, R^2 = 0.46. The mean cellular ATP ± SEM, is derived from (n=3) technical replicates.

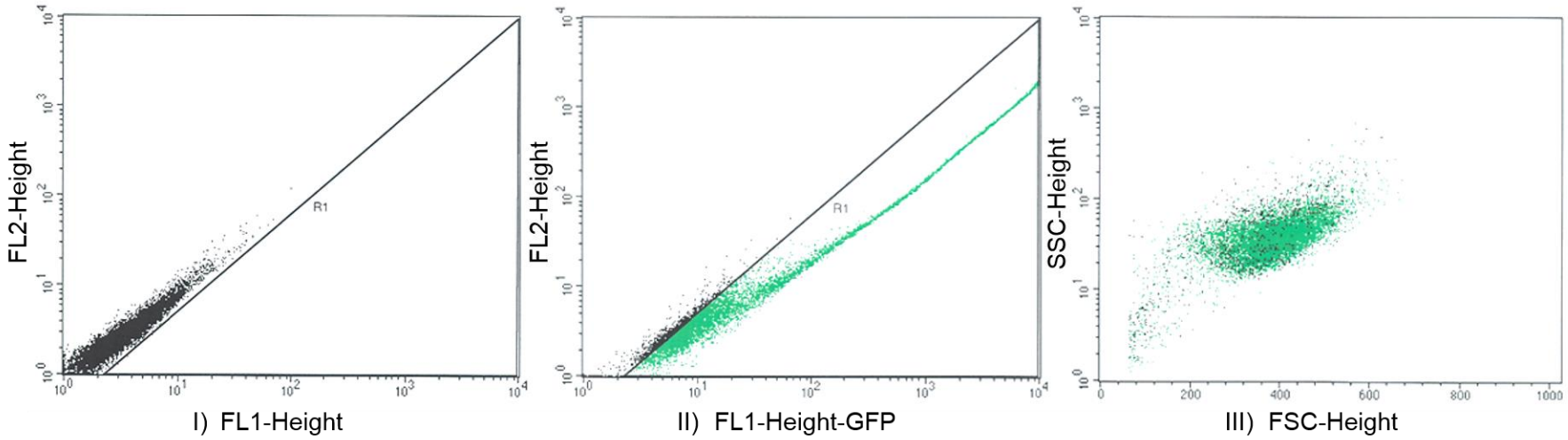

Figure A1.3.D: FACS analysis of fluorescence in COS-7 cells exogenously expressing GFP. The population of COS-7 cells assayed is represented by the black dots. I) The R1 gated region was drawn following the FACS analysis of the unstained cells in order to capture GFP fluorescing COS-7 cells. II) Gating of GFP fluorescing cells GMFI = 139.58. 87.51% of this COS-7 cell sample analysed by FACS are detected in the R1 region, this is taken as a measurement of the transfection efficacy of pMAX-GFP. III) FSC vs SSC analysis of the of COS-7 cells that were expressing GFP. The FCS vs SSC analysis suggests that the sample of COS-7 cells transfected with GFP analysed by FACS does not show signs of early apoptosis which may have occurred as a result of the transfection with pMAX-GFP. Dot plots here depict typical examples of FACS analysis. 10,000 events recorded per dot plot.

A sample of COS-7 cells exogenously expressing GFP, from the same experimental transfection as the FLAG-tagged DISC1/DISC1FP1 chimeras, was then analysed by FACS. The following results are typical for the FACS analysis of the fluorescence of exogenously expressed GFP in COS-7 cells. The percentage of GFP fluorescing cells gated = 87.51, GMFI = 139.58 (see figure A1.3.D.ii). Primarily the focus of this GFP FACS assay was the percentage of GFP fluorescing cells gated, which was taken to be an indicator of the transfection efficacy within the DISC1/DISC1FP1 chimera transfection for use in the HSII assay. The high level of GFP expression observed in figure A1.3.D.ii is not dissimilar to the 99% transfection efficacy stated by Invitrogen for COS-7L cells, for the Lipofectamine 2000 transfection reagent used (Invitrogen, n.d.).

The FSC vs SSC analysis of the COS-7 sample exogenously expressing GFP was run as a simple means to check the integrity of these cells (see figure A1.3.D.iii). The FSC, forward scatter is a measure of cell size, while SSC side scatter is a measure of the complexity and granularity of a cell. It was possible that the transfection process could have stressed the transfected cells. For example, if a series of events were clustered in the upper left side of the plot, with a lower FSC and higher SSC than that seen in figure A1.3.D.iii, this could be an indication of apoptosis occurring within the cell population assayed (Koopman *et al*, 1994).

The use of this method to quantify GFP expression is acknowledged as being an indirect means of assessing the transfection efficacy of the DISC1/DISC1FP1 chimeric protein species. Divergences in the percentage GFP expression between experiments may give cause to exclude HSII experiments from further data analysis.

A1.3.6 Initial whole cell ATP data from the COS-7 lysates exogenously expressing the DISC1/DISC1FP1 chimeras run in the HSII assay with a CCCP positive control

A positive control was required for use in the HSII assay, to reproducibly alter cellular ATP levels and to conclusively establish that the HSII assay had successfully been run to completion. The positive control chosen, CCCP belongs to a class of mitochondrial poisons, uncouplers, which are ionophores that act to uncouple oxidative phosphorylation from ATP synthesis (Benard & Rossignol, 2008). CCCP treatment has a dual action that is concentration dependent. Low concentrations of CCCP cause the collapse of the mitochondrial membrane potential, $\Delta\psi m$ and at higher concentrations the uncoupling of oxidative phosphorylation from

ATP synthesis occurs. The optimum concentration of CCCP to reduce cellular ATP is dependent on the cell line used and the length of treatment. For example, in HeLa cells, 10µM CCCP has been shown to reduce cellular ATP by 20% following a 45 minute incubation (Legros *et al*, 2002). Whereas, 50µM CCCP treatment to Jurkat T-ALL cells reduces cellular ATP by 63% within six hours (de Graaf *et al*, 2002). For use with COS-7 cells it was decided to use a final concentration of 20µM CCCP incubated with COS-7 cells for two hours. The use of this concentration and incubation time was an adaption of the 'CCCP assay' developed by Ishihara *et al*., (Ishihara *et al*, 2006; 2003), which uses CCCP to collapse the mitochondrial membrane potential, $\Delta\psi m$, producing mitochondrial fragmentation, as a means to study mitochondrial fission and fusion.

The following analysis of HSII assay data (n=3) on COS-7 cells exogenously expressing FLAG-tagged CP1, CP60 and CP69 includes a 20µM CCCP treatment as a positive control. FACS analysis was performed on COS-7 cells exogenously expressing GFP that had been transfected in parallel to the experimental constructs to estimate the transfection efficiency of the chimeric species across the HSII assay replicates (see section A1.3.5). The percentage of GFP fluorescing cells gated by FACS was 89.7% ± 2.2; the GMFI 1293.2 A.U. ± 735.5 (data is expressed as mean ± SEM, (n=3)). From this, it was inferred that there was a comparable transfection efficacy across these experimental replicates. The following HSII assay data analysed here were grouped following the exclusion of other experimental runs on the basis of either anomalous FACS or CCCP results.

The grouped cellular ATP data from the HSII assay were normalised to be either: (1) percentage of the FLAG-DISC1 cellular ATP concentration (see figure A1.3.E); (2) percentage of the empty vector cellular ATP (see figure A1.3.E); (3) percentage of the GFP fluorescent COS-7 cells gated by FACS (the transfection efficacy) for statistical analysis (see figure A1.3.E). Irrespective of the means of normalisation used, no significant difference was found between the experimental treatment conditions. One-way ANOVA of the cellular ATP data, from the analysis of COS-7 cellular lysates exogenously expressing the DISC1/DISC1FP1 chimeras normalised to be a percentage of the empty vector cellular ATP (n=3), showed no significant effect of treatment condition, $F(6,14)=0.31$, $p=0.90$. One-way ANOVA of the cellular ATP data from the analysis of COS-7 cellular lysates, exogenously expressing the DISC1/DISC1FP1 chimeras, normalised to be a percentage of the FLAG-DISC1 cellular ATP (n=3) showed no significant effect of treatment condition, $F(6,14)=0.81$, $p=0.57$. One-way ANOVA of the cellular ATP data from the analysis of COS-7 cellular lysates exogenously expressing the DISC1/DISC1FP1 chimeras, normalised to be a percentage of the

GFP stained COS-7 cells gated by FACS (a measure of the transfection efficacy (n=3)), showed no significant effect of treatment condition, F(6,14)=0.12, p=0.99.

The non-normalised data for the three experiments also highlighted that there was substantial inter-experimental variability in the range of the cellular ATP readings (see figure A1.3.E). One-way ANOVA of the cellular ATP data from the analysis of COS-7 cellular lysates,

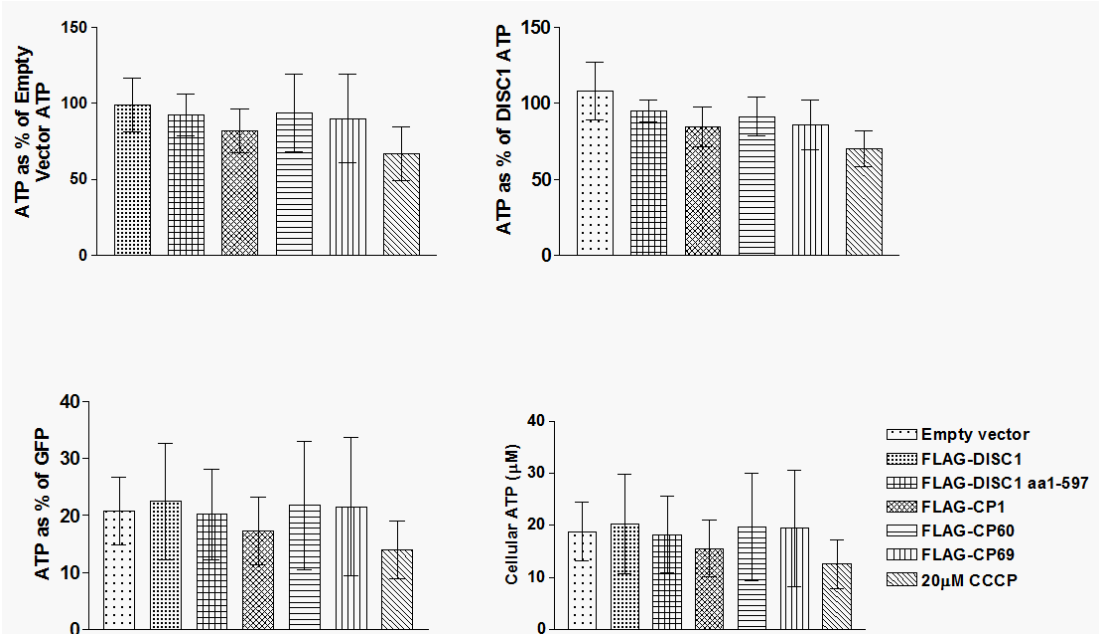

Figure A1.3.E: Initial analysis of the exogenous expression of DISC/DISC1FP1 chimeric species in COS-7 cells on cellular ATP. Cellular ATP data plotted as a percentage of the FLAG-DISC1 cellular ATP. One-way ANOVA shows no significant effect of treatment, p=0.57 (top left). Cellular ATP data plotted as a percentage of the empty vector cellular ATP, pcDNA3.1. One-way ANOVA shows no significant effect of treatment, p=0.90 (top right). Cellular ATP data plotted as a percentage of the GFP cells gated as a measure of transfection efficacy within an independent replication of the HSII assay. One-way ANOVA shows no significant effect of treatment, p=0.99 (bottom left). For the non-normalised cellular ATP data, one-way ANOVA shows no significant effect of treatment, p=0.99 (bottom right). Data is mean ± SEM, (n=3) independent experimental replicates.

exogenously expressing the DISC1/DISC1FP1 chimeras without normalisation (n=3), showed no significant effect of treatment condition, $F(6,14)=0.12$, $p=0.99$. There are interexperimental differences that are up to 8-fold in magnitude within experimental conditions in the non-normalised data. This high level of variability suggests that the HSII assay results was not suited to data normalisation, as such a method produces misleading analysis that suggests a far greater uniformity of results, when the normalised experimental data are pooled.

Given this degree of inter-experimental variation and lack of any significant alterations in cellular ATP between conditions, it was decided to both optimise the CCCP positive control and address means of combating potential sources of error in the HSII assay. In this analysis, the lack of significant alteration in cellular ATP following CCCP treatment is a cause of concern given CCCP has been observed to reduce cellular ATP in highly similar luminescence assays (Legros *et al*, 2002; Migita *et al*, 2007). It may be that the concentration of CCCP used here was too low for the COS-7 cell line and required further optimizing or that the cell culture conditions for incubation required further optimisation. It was necessary to have a positive control within the assay to demonstrate that the assay has run to completion in order to confirm that an alteration in cellular ATP can be detected. Given this, the use of CCCP as a positive control run on the HSII assay to produce a replicable alteration in cellular ATP was further optimised (see section A1.3.9).

This section highlights that there were underlying problems with the HSII assay protocol at this stage of method development that precluded accurate cellular ATP measurement. This may have arisen from error in the normalisation of protein concentration of the sample lysates, or possibly from incorrect loading of the 96-well plate. The normalising of the HSII cellular ATP data by the protein densitometry data derived from the standadised lysates could potentially ameliorate such errors. The densitometry analysis on the resulting bands could then be used in the normalisation of the HSII assay cellular ATP data. The next section will focus on method development for densitometry to normalise HSII assay cellular ATP data.

A1.3.7 The Development of a densitometry analysis method to normalise HSII assay cellular ATP data

The ANOVA analysis for the HSII assay results that ran COS-7 lysates containing exogenously expressed CP1, CP60 and CP69 found no significant differences between conditions when these data were normalised (see figure A1.3.E). Importantly, the HSII assay data had high inter-experimental variability. Consequently, Western blotting and densitometry

were seen as a means to correct some potential sources of experimental error in the HSII assay. This would entail normalising the HSII assay whole cell ATP data to protein levels. To do this, samples of the standardised protein lysates that were run on the HSII assay were analysed by Western blot, using a loading control antibody, GAPDH. The density of the resulting protein bands were quantified by densitometry. These density values were then used to normalise the corresponding cellular ATP data. This method should correct for variation in the number of cells lysed per sample.

The first step was to ensure that the HSII lysis buffer contained protease inhibitors. The use of protease inhibitors is fundamental for the storage of protein in solution prior to analysis by Western blot to prevent protein degradation by proteases. Communication with Roche indicated that the HSII lysis buffer did not contain protease inhibitors. Importantly, Roche were not able to provide information as to how the addition of protease inhibitors to the HSII lysis buffer would impact on the performance of the HSII assay to measure cellular ATP. In order to address this issue, the HSII assay was run with COS-7 lysates produced using two different lysis buffers: the standard HSII lysis buffer, used in all HSII method development up until this section, and the HSII lysis buffer containing a protease inhibitor tablet (PIT) to inhibit protease activity in the lysates.

The performance of the HSII assay does not appear to be impeded by the addition of the Roche PIT to the HSII lysis buffer. There is no significant difference between the cellular ATP levels in HSII buffer lysed COS-7 cells and those lysed with HSII lysis buffer containing a PIT (Student's unpaired two-tailed *t*-test; $t=0.85$, $p=0.44$, ($n=3$), (see figure A1.3.F)**.** The HSII assay lysis buffer containing the PIT was then used for cell lysis in all of the following HSII assay experiments. This enabled protein storage with minimal degradation for subsequent Western blot analysis.

The second step was to attempt to normalise the HSII assay from an experimental replicate with COS-7 cell lysates that exogenously expressed FLAG-tagged CP1, CP60 and CP69 and lysed with the HSII lysis buffer containing the PIT. The aim of this was to test the densitometry protocol. Firstly, the HSII assay was run and the corresponding protein lysates per treatment were assayed in parallel by Western blot. GAPDH was chosen as the initial loading control for use in densitometry as the given anti-GAPDH antibody used is highly potent. This was a precautionary measure to offset any difficulties detecting sufficient quantities of protein for densitometry given that the HSII lysis buffer may be inefficient at protein solubilisation.

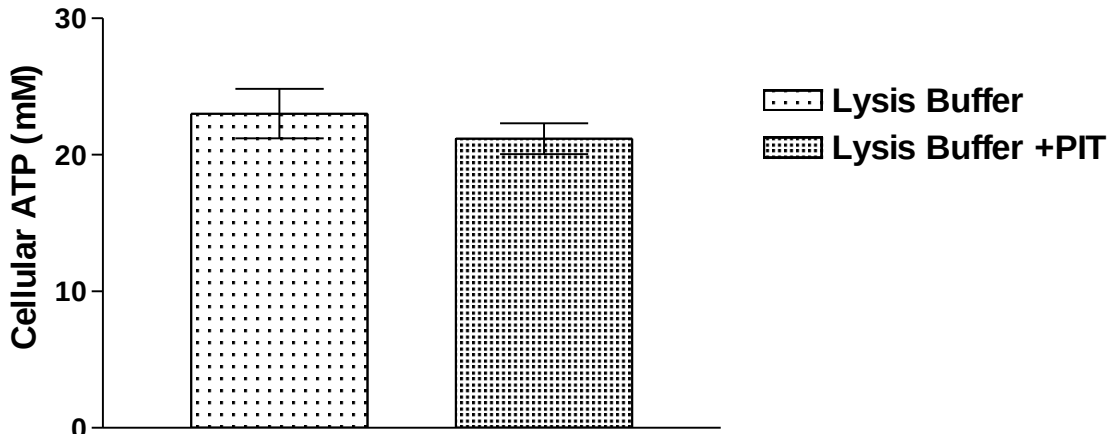

Figure A1.3.F: The addition of a Roche protease inhibitor tablet does not impair the quantification of cellular ATP levels by HSII assay. Student's unpaired two-tailed t-test revealed no significant difference in the cellular ATP levels between COS-7 cells lysed using HSII lysis buffer or HSII lysis buffer containing a PIT, p=0.44. Cellular ATP is expressed as mean ± SEM, (n=3) experimental replicates.

With equal volumes of protein loaded per condition and probing with anti-GAPDH, the anti-GAPDH bands produced appeared to be of appropriate intensity for densitometry analysis (see figure A1.3.G). Two CCCP treatments, 20µM and 50µM, were utilised in this run of the HSII assay to provide ongoing positive control optimisation.

The anti-GAPDH density values appear to be of a similar order of magnitude across the range of treatments. This is expected, given all of the protein loaded was assumed to be of the same concentration, with the same volume loaded for Western blotting (see table A1.3.D).

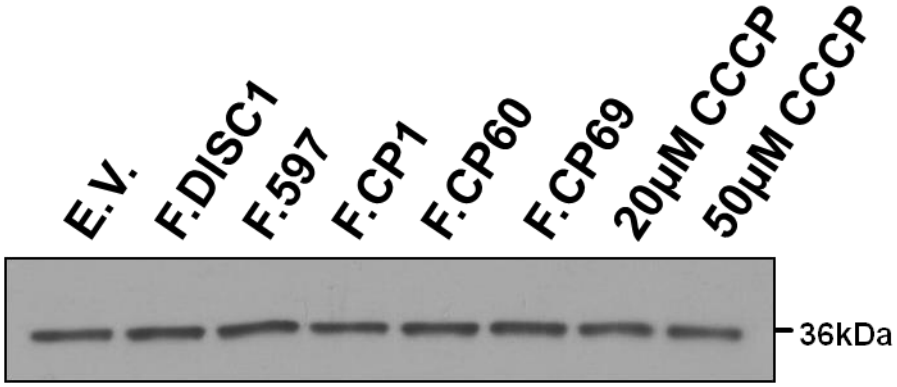

Figure A1.3.G: Detection of GAPDH in COS-7 protein lysates produced using HSII lysis buffer. Lysates are from COS-7 cells exogenously expressing FLAG-tagged DISC1/DISC1FP1 and DISC1 species and CCCP treatments. The HSII protein lysates had been standardised to 0.4mg/ml prior to blotting. The GAPDH protein detected by Western blotting was to be analysed by densitometry as a means to normalise the cellular ATP data. Equal volume of protein was loaded per lane.

The use of three different types of data normalisation demonstrates how densitometry analysis could possibly be applied to normalise an experimental dataset. The data normalisation referred to as Normalised ATP is derived from ATP/(Density/1x10^5) and created values of the same order of magnitude as the cellular ATP. Normalised ATP expressed as a percentage of Empty Vector response, is the cellular ATP normalised to protein density then expressed as a percentage of the normalised ATP level seen for the COS-7 cells treated with pcDNA3.1(+). A similar method of normalisation was used for the normalised ATP as a percentage of FLAG-DISC1. This shows the densitometry normalisation for a treatment as percentage of the normalised ATP level for the COS-7 cells expressing FLAG-DISC1. As these data in table A1.3.D are from a single experiment, no conclusion can be drawn about what the values represent in terms of the effect of the exogenous expression of DISC1/DISC1FP1 in COS-7 cells on cellular ATP. However, the data represented in table A1.3.D and figure A1.3.G serve as examples of how densitometry data could be used as a means of normalising the HSII assay data

Treatment	Density	Cellular ATP (µM/50µl)	Norm. ATP	Norm. ATP as % EV	Norm. ATP as % FLAG-DISC1
Empty vector	11341	24.62	21.71	100	115
F.DISC1	12772	24.08	18.86	87	100
F.DISC1 aa1-597	13261	22.54	17.00	78	90
F.CP1	10624	21.44	20.18	93	107
F.CP60	12181	23.94	19.66	91	104
F.CP69	12598	22.58	17.92	83	95
20µM CCCP	10896	22.80	20.93	96	111
50µM CCCP	10236	27.33	26.70	123	142

Table A1.3.D: Normalisation of cellular ATP data for the exogenous expression of DISC/DISC1FP1 chimeric species in COS-7 cells to anti-GAPDH densitometry intensity. Western blotting of protein lysates corresponding to those run on the HSII assay were used to normalise the HSII assay cellular ATP levels. Normalised ATP is the cellular ATP/density normalisation adjusted to be same order of magnitude as the cellular ATP. Normalised ATP as a percentage of Empty Vector response is the densitometry normalisation for a treatment as a percentage of the normalised ATP level for COS-7 cells treat with pcDNA3.1(+). Normalised ATP as a percentage of DISC1 is the densitometry normalisation for a treatment as percentage of the normalised ATP level for COS-7 cells expressing FLAG-DISC1. Data is (n=1) independent experiment.

The use of densitometry to normalise multiple experimental data sets i.e. (n=3) independent experimental replicates of the HSII assay would need additional critical scrutiny. It is possible that the Western blotting itself could introduce error into data sets. In practice, the initial cellular ATP data, the anti-GAPDH Western blotting, the densitometry data and the final Normalised cellular ATP data for multiple experimental runs of the HSII assay were examined for sources of error before the pooling of data for statistical analysis. A particular source of error in the method covered here is the use of Western blotting with a single antibody. GAPDH, detected here, is itself involved in cellular respiration as part of the glycolytic pathway and is predominantly located in the cytoplasm. However, during stress GAPDH may undergo post-translational modifications and oligomeric state changes (Tristan *et al*, 2011). These structural alterations are associated with GAPDH localising at subcellular structures including the cytoskeleton, mitochondria and nucleus, where GAPDH has dual roles in cell death and cell survival. Due to this, it would be prudent to have antibodies to loading control proteins from a range of cellular compartments to counter bias from using the results gained from a single antibody. The antibodies could have been optimised and used to re-probe blots

for use in densitometry for the normalisation of the cellular ATP data. The development of densitometry analysis as a method to normalise the initial HSII assay cellular ATP data would be used more extensively in the method development for CCCP treatment of COS-7 cells as a positive control for the HSII assay (see section A1.3.9).

A1.3.8 Identification of exogenously expressed FLAG-tagged DISC1/DISC1FP1 species in COS-7 cell lysates produced with HSII lysis buffer

It may have also been necessary post-assay to confirm that the correct exogenously expressed FLAG-tagged chimeric species were present in the lysates that had been run in the HSII assay. To identify that the FLAG-tagged DISC1/DISC1FP1 species transfected had been expressed in the COS-7 cells lysed with the HSII lysis buffer and run in the HSII assay, samples of both the resulting lysate and pellet fractions were analysed by Western blot. The requirement to run pellet fractions, is because CP60 and CP69 proteins are predominantly isolated within this fraction and appear to be insoluble (see section 3.3.1). However, it was likely that CP1, which encodes DISC1 aa1-598, would be predominantly expressed in the lysate fraction. This is because a highly homologous species to CP1, DISC1 aa1-597, is detected in the lysate fraction using the N-terminal DISC1 antibody R47, when exogenously expressed in COS-7 cells (Millar *et al*, 2005).

The Western blot of the COS-7 lysate pellet fraction, produced using the HSII lysis buffer, detects all of the FLAG-tagged DISC1/DISC1FP1 species and also FLAG-DISC1 and FLAG-DISC1 aa1-597. The molecular weights of protein bands in the pellet blot (see figure A1.3.F) are similar to the predicted molecular weight of the given species assayed. FLAG-CP1 and FLAG-DISC1 aa1-597 have bands at molecular weights of ~60kDa, the species predicted molecular weights being 65kDa and 64kDa respectively. The protein bands for FLAG-CP60 and FLAG-CP69 are detected at ~75kDa, this is similar to their respective, predicted molecular weights of 72kDa and 73kDa. In the pellet blot, FLAG-DISC1 protein is observed at ~95kDa, in line with a predicted molecular weight of 94kDa.

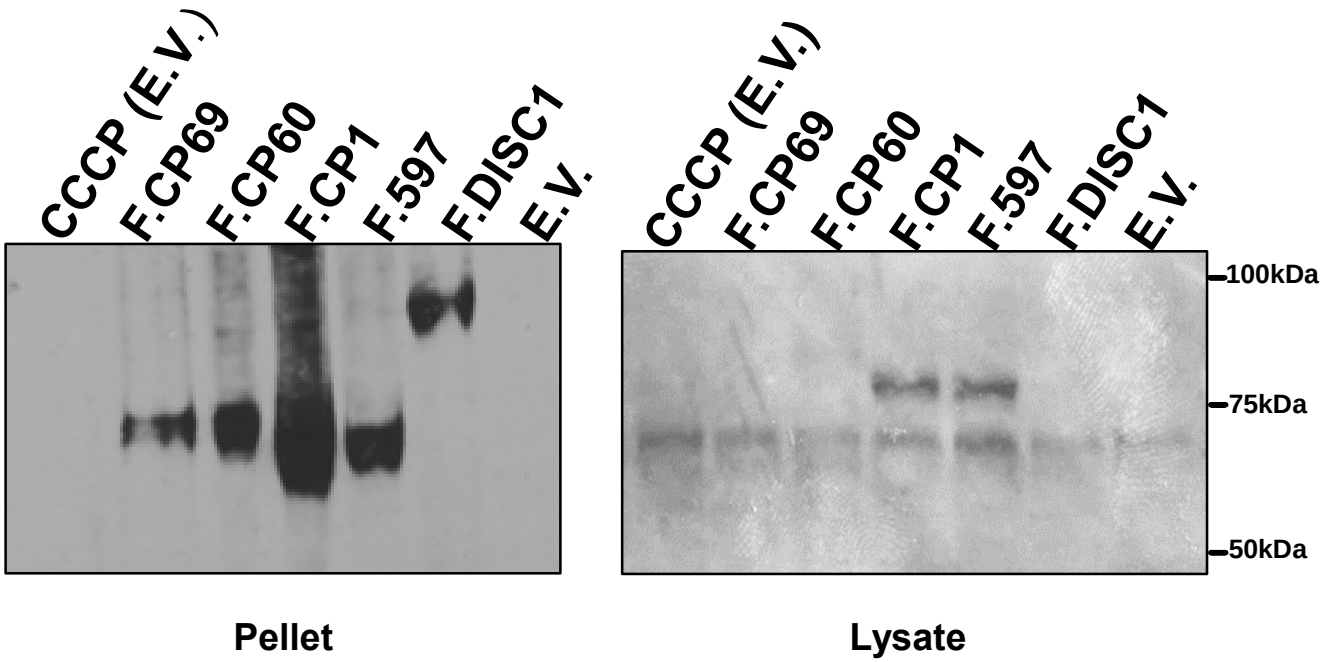

Figure A1.3.H: Detection of exogenously expressed FLAG-tagged DISC1/DISC1FP1 proteins in COS-7 cell pellet and lysate produced using HSII lysis buffer. Only FLAG-CP1 and FLAG-DISC1 aa1-597 are detected in the cell lysate and are indistinguishable (right). The signal intensity for this blot was weak; this is an overnight exposure. Unusually FLAG-DISC1 was not detected in the lysate . The protein bands across all treatments in the lysate, likely represent artefacts, all DISC1 species are detected in the pellet. FLAG-CP60 and FLAG-CP69 protein appear indistinguishable as is FLAG-CP1 from FLAG-DISC1 aa1-597.

The Western blot of the COS-7 lysate lysate fraction produced using the HSII lysis buffer (see figure A1.3.H) was developed overnight as the signal intensity was very weak. Both DISC1 aa1-597 and CP1 species can be isolated in the lysate fraction and the resulting protein bands are indistinguishable, reflecting the high degree of sequence homology between the two proteins. However, both species are detected in the lysate at ~70-75kDa. In line with previous observations (see section 3.3.1), FLAG-CP60 and FLAG- CP69 are not isolated in the lysate fraction. This was further evidence that the additional 60 and 69 amino acids derived for DISC1FP1 that are present in CP60 and CP69 respectively, result in altered localisation of protein compared to that seen with DISC1 aa1-597 alone or the CP1 species.

However, FLAG-DISC1 was not detected in the lysate blot, although FLAG-DISC1 was present in the pellet blot (see figure A1.3.H). Possible explanations for these anomalous observations include: (1) the HSII lysis buffer was not stringent enough to solubilise DISC1 protein; (2) inappropriate antibody dilution (the signal intensity from the protein here was poor); (3) experimental error. In terms of method development, figure A1.3.H should be considered as a means that was tried to detect the FLAG-DISC1 species in COS-7 lysates produced using the HSII lysis buffer, rather than as an experiment principally focussed on the DISC1 species exogenous expression.

The use of Western blot of the pellet fraction of COS-7 lysates run on the HSII assay probed with anti-FLAG was a suitable means to detect the expression of the FLAG-tagged DISC1 species. All of the FLAG-tagged DISC1/DISC1FP1 species can be detected in the pellet fraction (see figure A1.3.H). However, as the pellet fraction produces smeared bands, this method could never be used to quantify FLAG-tagged DISC1 species expression by densitometry (see section A1.3.7). The use of the lysate blot to both qualify and possibly quantify all of the FLAG-tagged DISC1 species expressed is not a viable alternative method. This is because CP60 and CP69 are not present at detectable levels in the soluble fraction (see figure A1.3.H) and is in line with established Western blotting of untagged CP60 and CP69 lysed using RIPA and PBS-Triton (see figure 3.3.A).

A1.3.9 The optimisation of CCCP as a positive control for the HSII assay using a serum starvation procedure

The initial attempts at detecting the effect of the exogenous expression of the DISC1/DISC1FP1 chimeric species on whole cell ATP using the HSII assay, failed to detect any significant difference between the conditions (see section A1.3.6). Importantly, these

assays were run with a 20µM CCCP treatment as a positive control that was expected to reduce whole cell ATP levels, given that CCCP is a potent uncoupler of oxidative phosphorylation (Benard & Rossignol, 2008). To establish that the HSII assay has technically run successfully and can reproducibly detect alterations in cellular ATP levels it would be prudent to further optimise a CCCP treatment for the HSII assay.

CCCP has been successfully used by others to reduce the level of cellular ATP in an assortment of cell lines. For example, the treatment of MDCK cells with 10µM CCCP produced ~ 25% reduction in cellular ATP levels measured using a luciferin-luciferase assay (Migita *et al*, 2007). HeLa cells treated with 10µM CCCP showed ~20% decrease in cellular ATP levels, as detected with a Roche Bioluminescence Assay (Legros *et al*, 2002). The treatment of Jurkat-Bcl-2 cells with 25µM CCCP produced 39% decrease in cellular ATP levels, detected using HPLC (de Graaf *et al*, 2002). This body of work indicates that it is feasible to use CCCP as a positive control to reduce cellular ATP levels in COS-7 cells. However, the optimum CCCP concentration for the treatment of the COS-7 cells still needed to be identified.

Although the treatment of COS-7 cells with 20µM CCCP had not produced a significant reduction in cellular ATP levels so far in the HSII assay (see section A1.3.6), it was of interest to establish the mitochondrial phenotype of these cells. Evidence of fragmentation of the mitochondrial network in CCCP treated COS-7 cells suggested that CCCP treatment was still viable for use as a positive control and that further optimisation was required given the potential structure/function relationships in the mitochondria with the CCCP treatment (Benard *et al*, 2011; Benard & Rossignol, 2008). For example, using immunocytochemistry, mitochondrial fragmentation can be observed in HeLa cells following incubation with 20µM CCCP (Ishihara *et al*, 2006; Ishihara *et al*, 2003).

A similar protocol to that used by Ishihara *et al.*, (2006; 2003) was used to see if mitochondrial fragmentation occurred following the incubation of COS-7 with 20uM CCCP. The anti-CVα stained mitochondria in the CCCP treated COS-7 cells appeared fragmented compared to the tubular mitochondria of the sham (DMSO) treated cells, as visualised with fluorescence microscopy (see figure A1.3.I). This established that 20µM CCCP treatment was capable of inducing mitochondrial fragmentation, a structural alteration, yet the use of this concentration of CCCP had so far failed to produce alterations to cellular ATP levels using the current HSII assay methodology (see section A1.3.6).

To optimise a CCCP positive control for use in the HSII assay both CCCP concentration and culture medium serum concentration were co-varied as treatments to COS-7 cells. This was to identify which combination of conditions would possibly elicit the greatest alteration in cellular ATP as detected by the HSII assay. The CCCP treatment was applied at 20, 50 and 100µM concentrations to COS-7 cells cultured in both high and low serum conditions.

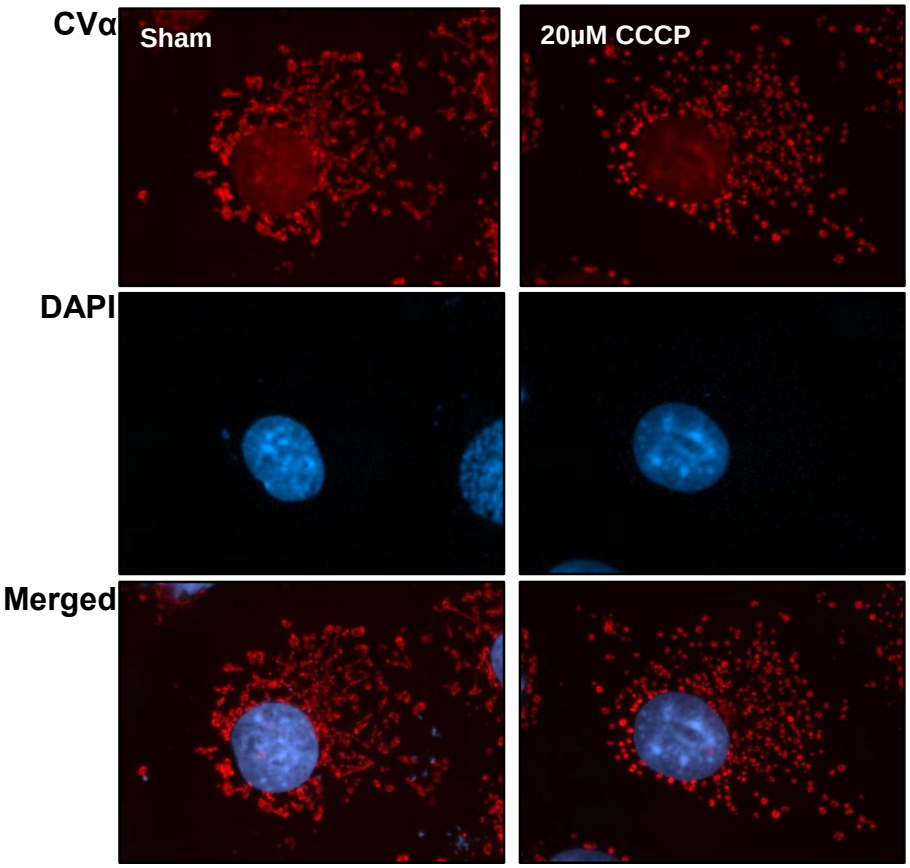

Figure A1.3.I: CCCP treatment of COS-7 cells induces mitochondrial fragmentation. Immunostaining: anti-CVα (Red) and DAPI (blue). The mitochondrial network in sham DMSO treat cells is tubular. Fragmentation of the mitochondrial network was observed following a 2 hour incubation with 20µM CCCP, an uncoupler of oxidative phosphorylation. Protocol adapted from Ishihara *et al.,* (2006; 2003).

The high serum condition discussed in this section is DMEM containing 10% FCS (vol/vol). This is the culture medium used for the DISC1/DISC1FP exogenous expression for both ICC and the HSII assay thus far (see chapter 4 and section A1.3.6). Here, the low serum incubation for the COS-7 cells aimed to reduce any variability in basal ATP levels between the dishes of COS-7 cells used for experimentation. Serum starvation can be used as a means to reduce basal cellular activity (Codeluppi *et al*, 2011).

It was possible that such background variation in basal cellular ATP levels may have contributed to variability of the initial experimental data with the DISC1/DISC1FP1 overexpression in COS-7 cells (see section A1.3.6). The low serum condition discussed in this section is a serum starvation procedure involving the reduction in culture medium FCS, 18hrs prior to lysis. This entailed the COS-7 cell culture medium being changed from DMEM containing 10% FCS (vol/vol) and being substituted with DMEM containing 1% FCS (vol/vol).

The serum starvation data reported here result from the method development in the HSII assay protocol so far. In the optimisation of CCCP as a positive control, (n=3) experimental replicates were performed. This involved the determination of cellular ATP levels using the HSII assay, Western blotting of the protein lysates (see figure A1.3.J) and densitometry analysis on the resulting anti-GAPDH bands. A 3 x 2 (CCCP x Serum) univariate analysis of variance was implemented to assess the effects of FCS serum levels and CCCP concentration on COS-7 ATP level (normalised to the ATP level in sham-treated cells). There was a significant effect of serum level $F(1,15) = 9.90$, $p<0.01$ and of CCCP concentration $F(1,15) = 34.73$, $p<0.001$, as well as a significant interaction between serum level and CCCP concentration $F(1,15) = 9.65$, $p<0.01$, (n=3). Figure A1.3.K shows that, in the low serum condition with the increase in concentration of CCCP, there is an increase in the concentration of cellular ATP. However, the trend for the high serum treatment is less clear. It appears that there is no increase in cellular ATP with increased CCCP dose although this is difficult to interpret due to the high degree of variance seen in the 50µM CCCP/high serum condition. The 50µM CCCP/high serum condition data point may represent an outlier (see figure A1.3.K).

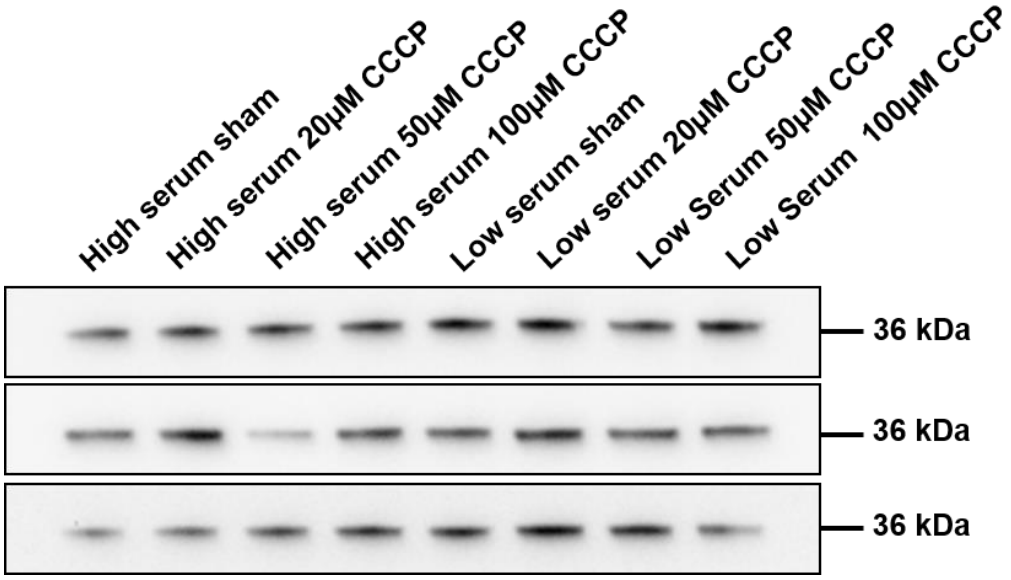

Figure A1.3.J: Anti-GAPDH Western blotting of HSII lysates for COS-7 cells cultured in high/low FCS media and incubated with the mitochondrial poison CCCP. (n=3) independent experiments.

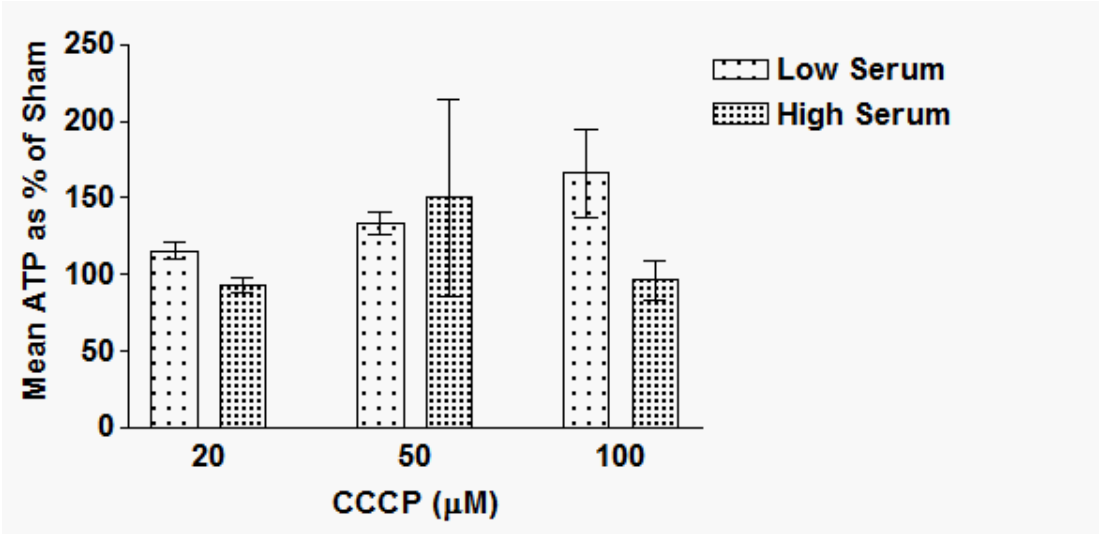

Figure A1.3.K: The CCCP optimisation data normalised using the corresponding anti-GAPDH density intensity and expressed as a percentage of the high/low serum sham (DMSO) normalised ATP concentration. Univariate analysis of variance reveals a significant effect of serum level p<.01, a significant effect of CCCP concentration p<.001 and a significant interaction between serum level and CCCP concentration p<.01 Data is mean ± SEM. (n=3) independent experiments.

For future optimisation, the results indicate that a 100µM concentration of CCCP applied to COS-7 cells cultured in low FCS media would elicit a maximal alteration in the level of cellular ATP. However, the direction in the change of ATP in the low serum/CCCP conditions demonstrates an increase in cellular ATP. This was unexpected. CCCP treatment on cell lines typically results in a reduction in cellular ATP being detected (de Graaf *et al*, 2002; Legros *et al*, 2002; Migita *et al*, 2007). An increase in cellular ATP is observed by de Graaf *et al*., in FL5.12 cells following incubation with 100µM CCCP, although these cells were cultured in IMDM 10% FCS (vol/vol). In this instance it was hypothesised that the increase in cellular ATP arises through upregulation of cytosolic ATP generation via glycolysis. It is possible that the serum starvation in COS-7 cells, in the optimisation of CCCP covered in this chapter, also results in such an upregulation of ATP levels via glycolysis. This could explain the resulting increased cellular ATP levels following addition of CCCP rather than a decrease in cellular ATP as expected. The molecular underpinning of the serum starvation results in this section can be investigated using other drug treatments that affect cellular respiration. The mitochondrial and cytosolic respiratory components could be isolated by the use of drugs specific to each cellular compartment. In this section, the HSII assay methodology is capable of reproducibly detecting an alteration in cellular ATP. Further work is needed to establish why an increase in ATP is observed.

A1.4 Development of a luciferase bioluminescence assay to investigate cellular ATP levels in t(1;11) family derived lymphoblastoid cell lines

The HSII assay needed to be optimised to assay t(1;11)-family derived lymphoblastoid cell lines to observe if the t(1;11) affects cellular ATP levels. The results could then be compared with cellular ATP data for COS-7 cells exogenously expressing DISC1/DISC1FP1 proteins, to determine if any alterations in cellular ATP in translocation cells lines could possibly be attributed to endogenous chimeric proteins.

This lymphoblastoid cell line method development work followed the attempts to optimise CCCP as a positive control for the HSII assay (see section A1.3.9) and included the use of high-10% FCS (vol/vol) and low-1% FCS (vol/vol) serum cultured lymphoblastoid cells. The subsequent HSII assay optimisation cellular ATP data was normalised to anti-GAPDH densitometry from Western blotting of the lymphoblastoid cell lysates (see section A1.3.7).

A1.4.1 Generation of an ATP standard curve to detect cellular ATP in lymphoblastoid cell lines

Initial attempts to measure the cellular ATP level in lymphoblastoid cell lines produced cellular ATP levels that were extremely low compared to the COS-7 cellular ATP optimisation data (data not shown). Consequently, a greater range of ATP standards was used in the lower half of the standard curve than is seen in the COS-7 ATP standard curve. This approach was adopted to improve the accuracy of measuring cellular ATP in lymphoblastoid cell lysates (see figure A1.4.A).

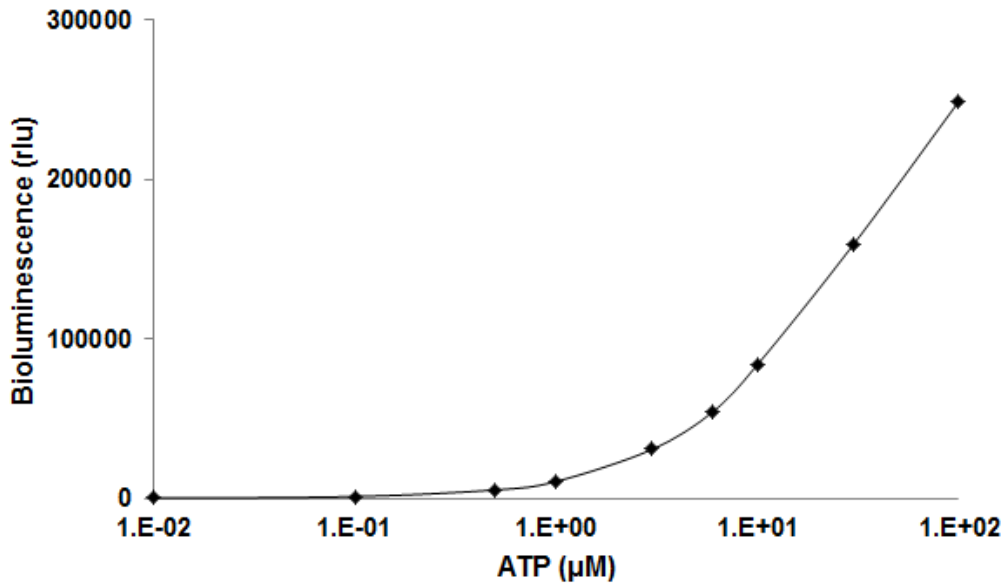

Figure A1.4.A: Development of a standard curve to measure ATP bioluminescence using the HSII assay within t(1;11)-family derived lymphoblastoid cell lines. For the measurement of ATP bioluminescence in lymphoblastoid cell lines, more ATP standards were placed in the lower half of the curve than is seen in the COS-7 ATP standard curve.

A1.4.2 Optimising lymphoblastoid cell line protein lysates for the HSII assay

Following the generation of an ATP standard curve adapted to measure lymphoblastoid cellular ATP (see figure A1.4.A), the identification of a protein concentration that produced a cellular ATP concentration that fell on the exponential phase of the standard curve still needed

to be identified. To optimise the protein concentration loaded into the HSII assay, a normal karyotype control and a translocation lymphoblastoid cell line were lysed. The HSII cell lysates were standardised to protein concentrations of 0.4mg/ml and 0.8mg/ml for kaytoype controls and 0.8mg/ml and 1.6mg/ml for translocation lymphoblastoid cell lines, respectively. The cellular ATP content of these lysates was determined using the HSII assay. Following the Western blotting of the same lymphoblastoid cell lysates (see figure A1.4.B), the HSII assay data was subsequently normalised to GAPDH (see table A1.4.A).

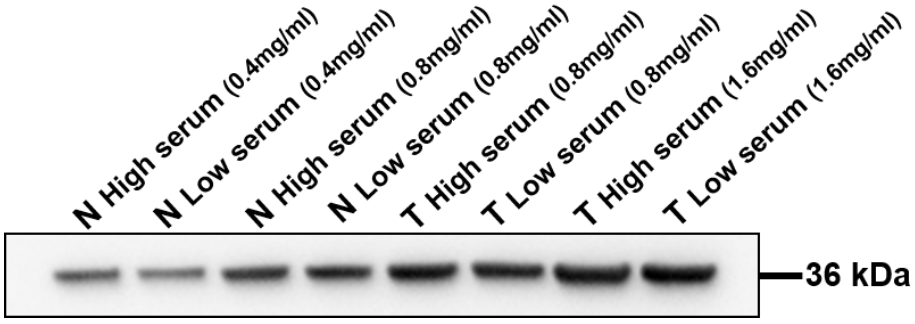

Figure A1.4.B: Anti-GAPDH Western blotting of HSII lysates for lymphoblastoid cell lines cultured in high/how FCS media with cell lysates loaded at different protein concentrations. Blot has 1 normal karyotype control (N) and 1 t(1;11)-family derived lymphoblastoid cell line (T) loaded.

The normal cell line data appears to both show concentration dependent and serum treatment dependent differences in the cellular ATP data (see table A1.4.A). Importantly, all of the normal cell lysate cellular ATP data lie on the exponential phase of the lymphoblastoid ATP standard curve (see section A1.4.1), with the exception of the low serum/0.4mg/ml condition. However, in the translocation cell line, cellular ATP levels were very low in comparison, irrespective of the serum treatment or protein concentration assayed.

Treatment	Density	Cellular ATP (µM/50µl)	Norm. ATP
(N) High serum (0.4mg/ml)	580619	13.90	23.94
(N) Low serum (0.4mg/ml)	472490	5.76	12.20
(N) High serum (0.8mg/ml)	801570	35.09	43.77
(N) Low serum (0.8mg/ml)	830155	11.70	14.09
(T) High serum (0.8mg/ml)	1074385	0.29	0.27
(T) Low serum (0.8mg/ml)	997059	0.94	0.94
(T) High serum (1.6mg/ml)	1290301	0.59	0.46
(T) Low serum (1.6mg/ml)	1345556	2.39	1.77

Table A1.4.A: Normalised cellular ATP level in lymphoblastoid cells cultured in high and low serum media, assayed at a range of protein concentrations. The cellular ATP levels of normal karyotype control (N) and t(1;11)-family derived (T) lymphoblastoid cell lines lysates was determined by the HSII assay. Protein concentration of cell lysate assayed is given in brackets. Anti-GAPDH Western blots of lysates run on the HSII assays were subjected to densitometry analysis and used to normalise the cellular ATP levels. The normal lymphoblastoid cell line shows protein concentration-dependent cellular ATP levels within serum type. The translocation cell line appears not to have been lysed sufficiently for cellular ATP to be detected accurately. One culture of a translocation cell line and one culture of a normal lymphoblastoid cell line were assayed, (n=1) experiment.

These translocation lymphoblastoid results are of a similar order of magnitude to the previous lymphoblastoid HSII optimisation data (data not shown). The translocation anti-GAPDH results were interpreted as being due to the incomplete lysis of the lymphoblastoid cells by the HSII lysis buffer. It is possible that previous attempts to optimise the HSII assay for lymphoblastoid cell lysates also suffered from this problem (data not shown).

The following lymphoblastoid cell HSII optimisation data were generated after the implementation of an attempt to enhance lysis of lymphoblastoid cells by passing the cell lysates up a 25-gauge syringe needle to mechanically enhance lysis. The optimisation featured one normal karyotype control and two t(1;11)-family derived lymphoblastoid cell lines. Given the previous low ATP readings that may have arisen due to incomplete cell lysis, all of the lysate assayed was standardised to a protein concentration of 0.4mg/ml. This concentration was adopted because this was the lowest protein concentration assayed at high serum levels

that lay sufficiently on the standard curve and, because the modification of the lysis protocol was expected to yield a greater concentration of ATP than previous optimisation assays.

The cellular ATP values observed for all the lymphoblastoid cell lines assayed following the use of a syringe needle to enhance lysis ranged from 18.70-28.22µM ATP (see table A1.4.B). These ATP concentrations adequately lie on the exponential phase of the lymphoblastoid ATP standard curve (see figure A1.4.A). This was interpreted as being a consequence of the modified cell lysis protocol. The standadised protein levels used in the HSII assay were analysed by Western blot and probed with anti-GAPDH (see figure A1.4.C).

Treatment	Density	Cellular ATP (µM/50µl)	Norm. ATP
(N) High serum	1677329	23.172	13.81
(N) Low Serum	1356862	18.664	13.76
(T1) High serum	1614640	24.009	14.87
(T1) Low Serum	1539611	18.702	12.15
(T2) High serum	1924628	20.593	10.70
(T2) Low Serum	1361104	28.221	20.73

Table A1.4.B: Normalised cellular ATP level in lymphoblastoid cells cultured in high and low serum media. The cellular ATP levels of normal karyotype control (N) and t(1;11)-family derived (T1) and (T2) lymphoblastoid cell lines lysates was determined by the HSII assay. Protein concentration of the cell lysate assayed is given in brackets. Anti-GAPDH Western blots of lysates run on the HSII assay were subjected to densitometry analysis and used to normalise the cellular ATP levels. All cell lysates were run on the HSII assay at 0.4mg/ml. The cellular ATP concentrations detected here lie on the exponential phase of the ATP standard curve irrespective of culture serum level. One culture of normal and two cultures of differing translocation lymphoblastoid cell line assayed, (n=1) experiment.

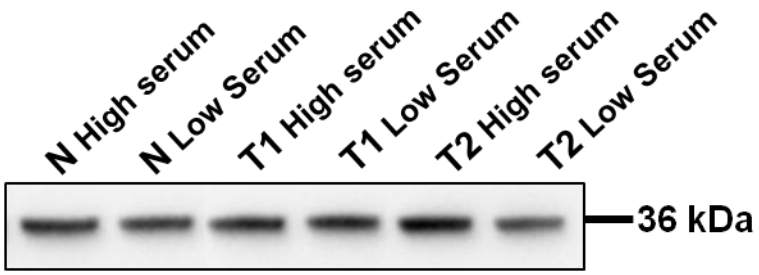

Figure A1.4.C: Anti-GAPDH Western blotting of HSII lysates for lymphoblastoid cell lines cultured in high/low FCS media. Equal volume of protein at 0.4 mg/ml loaded per lane. One normal karyotype control (N) and two t(1;11)-family derived lymphoblastoid cell lines(T) assayed.

The blot bands were then analysed via densitometry and this densitometry data was then used to normalise the HSII assay data (see table A1.4.B). However, no clear serum dependent effect is seen with the cellular ATP or the normalised ATP data. This optimisation appears to show that with the modification to cell lysis lymphoblastoid cell lysates standardised to 0.4mg/ml, with 10ug of protein assayed, produces cellular ATP levels that lie the linear phase of the standard curve for both high and low serum conditions.

An HSII assay optimisation experiment was run with 3 normal karyotype control and 3 translocation lymphoblastoid cell lines. Additionally, one of the lymphoblastoid cell lines was run with both 100µM CCCP and sham (DMSO) treatments. This was a pilot of a possible final experimental design using a CCCP positive control (see section A1.3.9). The cells that received the CCCP treatment were observed to immediately disperse from the flocculated lymphoblastoid cell aggregates. However, when run on the HSII assay, the optimisation experiment itself produced very low ATP values (data not shown). From this it was concluded that further method development was required on the harvesting and lysis of lymphoblastoid cell lines.

A1.5 Discussion

The HSII assay method development was discontinued due to personal illness and, as a result the final experimental assays to detect the levels of cellular ATP in COS-7 cells exogenously expressing the DISC1/DISC1FP1 chimeras and within t(1;11) lymphoblastoid cell lines were never accomplished. However, given that considerable effort went into the research reported in this thesis, it was felt that it should be included with a view to producing a commentary on

the practical issues encountered and the positive and negative outcomes established. The following discussion aims to cover the ongoing method development issues with the HSII assay protocol that needed to be rectified before pursuing such final experiments.

Further normalisation of the HSII assay data is needed using additional loading control antibodies. This would be to explore any issues relating to the use of GAPDH alone as a loading control to generate data for densitometry as a possible source of error. GAPDH protein is expressed in the cytosol and is part of the glycolytic pathway (Tristan *et al*, 2011). As such, it is possible that the anti-GAPDH densitometry used in the COS-7 optimisation of CCCP (see section A1.3.9) may have led to anomalous results if the low serum/CCCP treatments indeed do cause an upregulation of glycolysis. Suitable loading control antibodies to be used in place of anti-GAPDH include anti-β-actin, anti-α-tubulin and anti-β-tubulin.

It is unknown as to how the exogenous expression of the DISC1/DISC1FP1 chimeric species and the resulting impact on mitochondrial function would affect endogenous GAPDH protein levels in the expressing COS-7 cells. In the future, it may also be possible to reprobe blots produced to normalise the HSII assay to look for proteins associated with mitochondrial structure or mitochondrial signalling pathways and enrich the cellular ATP data with this information. For example, it may be worth observing if levels of cytochrome *c* protein are uniform across all transfected DISC1 species given there appears to be no difference in the cytochrome *c* immunocytochemical results (see section 4.4).

An efficient method for the quantification of lymphoblastoid cell line cultures needs to be developed. This is to enable the replicable growth of cultures that are of sufficient size to be lysed effectively. It also likely that the means of lysing the lymphoblastoid cultures also needs to be reviewed given that the use of a 25 gauge syringe to encourage full cell lysis appears to be effective only occasionally. The simplest means to do this would be to heuristically establish the optimal amount of lysis reagent to use with a cell population of given size that in turn produces an acceptable level of cellular ATP released.

At present no means of stopping cellular reactions within the HSII assay has been applied. It is unknown as to whether it is possible that cellular reactions still occur after lysis. However the incorporation of the use of perichloric acid around the time of lysis would ensure that cellular reactions, including ATP synthesis, are stopped, possibly removing a potential source of experimental variation.

Regarding the anomalous CCCP positive control optimisation data, ATP synthesis could be blocked by other means to further investigate the increase in cellular ATP seen with CCCP

treatment in COS-7 cells cultured in low serum media. 2 deoxy glucose (2DG) and oligomycin could be used both separately and together, to block glycolytic, mitochondrial and both glycolytic and mitochondrial ATP synthesis, respectively (Benard & Rossignol, 2008). 2DG is a glucose molecule that cannot undergo glycolysis, and as such, specifically perturbs ATP generation by glycolysis, whereas oligomycin is a potent inhibitor of ATP synthase. A protocol using both of these respiratory active agents could be used in the further optimisation of a low serum condition with oligomycin as a positive control to lower cellular ATP and 2DG as a means to prevent a rise in cellular ATP by glycolytic pathways.

Had the HSII assay been run with COS-7 cell lysates exogenously expressing DISC1/DISC1FP1 chimeric species, the corresponding immunocytochemistry experiments (see chapter 4) would need to be repeated with the cells cultured in low serum conditions. It would be important to phenotypically characterise the effect low serum conditions have on mitochondrial morphology and the distribution of the exogenous chimeric protein when interpreting cellular ATP data. In the low serum treatment, it is possible that mitochondria elongate as an adaption to the increased bioenergetic demand due to the starvation of the cells. Such a change in mitochondrial network shape could be the result of increased mitochondrial fusion (Westermann, 2012).

The starvation of cells by serum (Gomes *et al*, 2011) or nutrient starvation (Rambold *et al*, 2011) results in elongation of the mitochondrial network due to phosphoregulation of mitochondrial fission protein, Drp1. This reduces Drp1 mediated fission, with an increasingly tubular mitochondrial morphology observed. When serum starvation is used in conjunction with starvation of both glycine and glucose there is an increase in the percentage of tubular mitochondria (Rambold *et al*, 2011). Likewise, the mitochondria elongate when mouse embryonic fibroblasts are serum starved by having DMEM/10% FBS media replaced with a Hanks balanced salt solution containing 10mM HEPES (Gomes *et al*, 2011). Of these two different methodologies, the low serum condition reported in this chapter bears greater similarity to that of Rambold *et al*. (2011), though the time frame used for the low serum treatment with COS-7 cells is ~9 times longer. It, therefore, seems possible that serum starvation may change the morphology of mitochondria in culture. This is particularly relevant with regard to what would happen to the clustered mitochondrial shape observed in COS-7 cells exogenously expressing CP60 and CP69.

A further problem with the use of serum starvation protocols is that they can affect signalling pathways in both a temporal and cell line dependent manner. Pirkmajer & Chilbalin (2011) observed, under starvation conditions, that variation is seen in the level of protein

phosphorylation in both the Adenosine Monophosphate-activated Protein Kinase (AMPK) and Extracellular-signal-Regulated Kinase 1/2 (ERK1/2) signalling cascades and, also to a lesser extent in the mTOR pathway. These findings are from both primary cultures and cell lines incubated under absolute serum starvation or serum starvation using 0.5% (wt/vol) BSA. These observations serve to highlight the caution required when interpreting serum starvation data. It is, therefore, possible that serum starvation may affect the signalling pathways in the COS-7 and lymphoblastoid cell lines differently if culturing these cells in low serum conditions was pursued.

Annex A2 - Attempts to detect exogenously expressed CP60 and CP69 in COS-7 lysates by Western blot

A2.1 Exogenously expressed CP60 and CP69 do not partition to the soluble fraction

Upon receipt from GENEART, the untagged CP60 and CP69 constructs housed in a pcDNA3.1(+) vector backbone were transiently transfected into COS-7 cells and the cell lysate analysed using Western blot. The immunoblot was probed with the N-terminal DISC1 antibody R47 (James *et a*l, 2004). Importantly, the positve control, FLAG-DISC1 was detected at a molecular weight of ~100kDa in the 2 minute exposure, as expected. Unfortunately, FLAG-DISC1 expression was somewhat obscured in the overnight exposure. No bands were detected that could be interpreted as being specific CP60 and CP69 protien species in either the 2 minute or overnight exposures. The non-specific bands shared with CP60 and CP69 lysates and the empty vector control (pcDNA3.1(+)) were clearly visible in the overnight exposure. Taken together, these two pieces of pre-experimental data were seen to indicate that CP60 and CP69 protein was not readily detectable in the soluble fraction. It should be noted that all lysates were produced with RIPA lysis buffer, therefore the potency of the lysis buffer was likely not an issue in this instance.

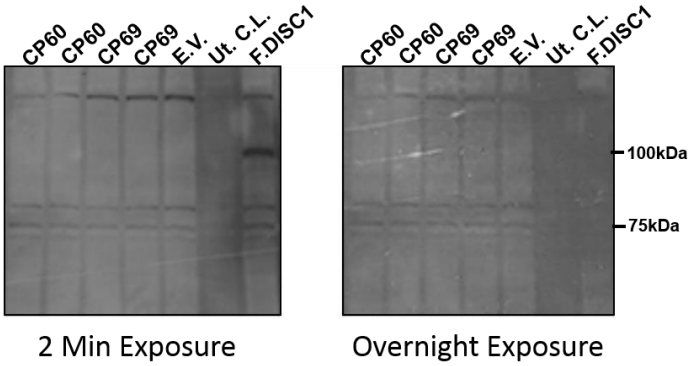

Figure A2.1.A: Attempts to detect exogenous CP60 and CP69 protein in cell lysates. Western blotting detected exogenously expressed FLAG-DISC1 in the soluble fraction at ~100kDa using the N-terminal DISC1 antibody R47 (1:1000), as depicted in 2 minute exposure. Irrespective of exposure length. Lanes ran with untagged CP60 and CP69 only displayed non-specific bands that were also evident in the empty vector (E.V) condition, pcDNA3.1 (+). Irrespective of exposure length. Untransfected cell lysate condition (Ut. C.L.).

References

Benard G, Bellance N, Jose C, Rossignol R (2011) Relationships Between Mitochondrial Dynamics and Bioenergetics. In *Mitochondrial Dynamics and Neurodegeneration*, pp 47-68. Springer

Benard G, Rossignol R (2008) Ultrastructure of the mitochondrion and its bearing on function and bioenergetics. *Antioxid Redox Signal* **10:** 1313-1342

Codeluppi S, Gregory EN, Kjell J, Wigerblad G, Olson L, Svensson CI (2011) Influence of rat substrain and growth conditions on the characteristics of primary cultures of adult rat spinal cord astrocytes. *Journal of neuroscience methods* **197:** 118-127

de Graaf AO, Meijerink JP, van den Heuvel LP, DeAbreu RA, de Witte T, Jansen JH, Smeitink JA (2002) Bcl-2 protects against apoptosis induced by antimycin A and bongkrekic acid without restoring cellular ATP levels. *Biochimica et Biophysica Acta (BBA)-Bioenergetics* **1554:** 57-65

Dimroth P, Kaim G, Matthey U (2000) Crucial role of the membrane potential for ATP synthesis by F (1) F (o) ATP synthases. *Journal of Experimental Biology* **203:** 51-59

Eykelenboom JE, Briggs GJ, Bradshaw NJ, Soares DC, Ogawa F, Christie S, Malavasi EL, Makedonopoulou P, Mackie S, Malloy MP, Wear MA, Blackburn EA, Bramham J, McIntosh AM, Blackwood DH, Muir WJ, Porteous DJ, Millar JK (2012) A t(1;11) translocation linked to schizophrenia and affective disorders gives rise to aberrant chimeric DISC1 transcripts that encode structurally altered, deleterious mitochondrial proteins. *Human molecular genetics* **21:** 3374-3386

Fujimoto T, Nakano T, Takano T, Hokazono Y, Asakura T, Tsuji T (1992) Study of chronic schizophrenics using 31P magnetic resonance chemical shift imaging. *Acta psychiatrica scandinavica* **86:** 455-462

Gomes LC, Di Benedetto G, Scorrano L (2011) During autophagy mitochondria elongate, are spared from degradation and sustain cell viability. *Nature cell biology* **13:** 589-598

Ishihara N, Fujita Y, Oka T, Mihara K (2006) Regulation of mitochondrial morphology through proteolytic cleavage of OPA1. *The EMBO journal* **25:** 2966-2977

Ishihara N, Jofuku A, Eura Y, Mihara K (2003) Regulation of mitochondrial morphology by membrane potential, and DRP1-dependent division and FZO1-dependent fusion reaction in mammalian cells. *Biochemical and biophysical research communications* **301:** 891-898

James R, Adams RR, Christie S, Buchanan SR, Porteous DJ, Millar JK (2004) Disrupted in Schizophrenia 1 (DISC1) is a multicompartmentalized protein that predominantly localizes to mitochondria. *Molecular and cellular neurosciences* **26:** 112-122

Koopman G, Reutelingsperger C, Kuijten G, Keehnen R, Pals S, Van Oers M (1994) Annexin V for flow cytometric detection of phosphatidylserine expression on B cells undergoing apoptosis. *Blood* **84:** 1415-1420

Lee CW, Peng HB (2008) The function of mitochondria in presynaptic development at the neuromuscular junction. *Molecular biology of the cell* **19:** 150-158

Legros F, Lombès A, Frachon P, Rojo M (2002) Mitochondrial fusion in human cells is efficient, requires the inner membrane potential, and is mediated by mitofusins. *Molecular biology of the cell* **13:** 4343-4354

Ly CV, Verstreken P (2006) Mitochondria at the synapse. *The Neuroscientist* **12:** 291-299

Migita K, Zhao Y, Katsuragi T (2007) Mitochondria play an important role in adenosine-induced ATP release from Madin–Darby canine kidney cells. *Biochemical pharmacology* **73:** 1676-1682

Millar JK, Pickard BS, Mackie S, James R, Christie S, Buchanan SR, Malloy MP, Chubb JE, Huston E, Baillie GS, Thomson PA, Hill EV, Brandon NJ, Rain JC, Camargo LM, Whiting PJ, Houslay MD, Blackwood DH, Muir WJ, Porteous DJ (2005) DISC1 and PDE4B are interacting genetic factors in schizophrenia that regulate cAMP signaling. *Science (New York, NY)* **310:** 1187-1191

Park YU, Jeong J, Lee H, Mun JY, Kim JH, Lee JS, Nguyen MD, Han SS, Suh PG, Park SK (2010) Disrupted-in-schizophrenia 1 (DISC1) plays essential roles in mitochondria in collaboration with Mitofilin. *Proceedings of the National Academy of Sciences of the United States of America* **107:** 17785-17790

Pirkmajer S, Chibalin AV (2011) Serum starvation: caveat emptor. *American Journal of Physiology-Cell Physiology* **301:** C272-C279

Rambold AS, Kostelecky B, Elia N, Lippincott-Schwartz J (2011) Tubular network formation protects mitochondria from autophagosomal degradation during nutrient starvation. *Proceedings of the National Academy of Sciences* **108:** 10190-10195

Schapira AH (2006) Mitochondrial disease. *The Lancet* **368:** 70-82

Sheng ZH (2014) Mitochondrial trafficking and anchoring in neurons: New insight and implications. *The Journal of cell biology* **204:** 1087-1098

Tristan C, Shahani N, Sedlak TW, Sawa A (2011) The diverse functions of GAPDH: views from different subcellular compartments. *Cellular signalling* **23:** 317-323

Volz HR, Riehemann S, Maurer I, Smesny S, Sommer M, Rzanny R, Holstein W, Czekalla J, Sauer H (2000) Reduced phosphodiesters and high-energy phosphates in the frontal lobe of schizophrenic patients: a (31)P chemical shift spectroscopic-imaging study. *Biological psychiatry* **47:** 954-961

Westermann B (2012) Bioenergetic role of mitochondrial fusion and fission. *Biochimica et Biophysica Acta (BBA)-Bioenergetics* **1817:** 1833-1838